U.S. Department of Energy
Energy Efficiency and Renewable Energy
Bringing you a prosperous future where energy is clean, abundant, reliable, and affordable

ADVANCED COMBUSTION ENGINE RESEARCH & DEVELOPMENT

Less dependence on foreign oil, and eventual transition to an emissions-free, petroleum-free vehicle

FreedomCAR and Vehicle Technologies Program

2004 ANNUAL PROGRESS REPORT

21ST CENTURY TRUCK PARTNERSHIP

FreedomCAR & Fuel Partnership

Acknowledgement

We would like to express our sincere appreciation to QSS Group, Inc., Oak Ridge National Laboratory, and Argonne National Laboratory for their technical and artistic contributions in preparing and publishing this report.

In addition, we would like to thank all the participants for their contributions to the programs and all the authors who prepared the project abstracts that comprise this report.

U.S. Department of Energy
1000 Independence Avenue, S.W.
Washington, D.C. 20585-0121

FY 2004

Progress Report for Advanced Combustion Engine R&D

Energy Efficiency and Renewable Energy
Office of FreedomCAR and Vehicle Technologies

Approved by Gurpreet Singh

December 2004

CONTENTS

CONTENTS (Continued)

CONTENTS (Continued)

I Introduction

I. INTRODUCTION

Developing Advanced Combustion Engine Technologies

On behalf of the Department of Energy's Office of FreedomCAR and Vehicle Technologies, we are pleased to introduce the Fiscal Year (FY) 2004 Annual Progress Report for the Advanced Combustion Engine R&D Sub-Program. The mission of the FreedomCAR and Vehicle Technologies Program is to develop more energy efficient and environmentally friendly highway transportation technologies that enable Americans to use less petroleum for their vehicles. The Advanced Combustion Engine R&D Sub-Program supports this mission by removing the critical technical barriers to commercialization of advanced internal combustion engines for light-, medium-, and heavy-duty highway vehicles that meet future Federal and state emissions regulations. The primary objective of the Advanced Combustion Engine R&D Sub-Program is to improve the brake thermal efficiency of internal combustion engines from

- 30 to 45 percent for light-duty applications by 2010
- 40 to 55 percent for heavy-duty applications by 2012

while meeting cost, durability, and emissions constraints. R&D activities include work on combustion technologies that increase efficiency and minimize in-cylinder formation of emissions, as well as aftertreatment technologies that further reduce exhaust emissions. Work is also being conducted on ways to reduce parasitic and heat transfer losses through the development and application of thermoelectrics and turbochargers that include electricity generating capability, and conversion of mechanically driven engine components to be driven via electric motors.

This introduction serves to outline the nature, current progress, and future directions of the Advanced Combustion Engine R&D Sub-Program. The research activities of this Sub-Program are planned in conjunction with the FreedomCAR Partnership and the 21st Century Truck Partnership and are carried out in collaboration with industry, national laboratories, and universities. Because of the importance of clean fuels in achieving low emissions, R&D activities are closely coordinated with the relevant activities of the Fuel Technologies Sub-Program, also within the Office of FreedomCAR and Vehicle Technologies.

Research is also being undertaken on hydrogen-fueled internal combustion engines to provide an interim hydrogen-based powertrain technology that promotes the longer-range FreedomCAR Partnership goal of transitioning to a hydrogen-fueled transportation system. Hydrogen engine technologies being developed have the potential to provide diesel-like engine efficiencies with near-zero emissions.

Background

The compression ignition, direct injection (CIDI) engine, an advanced version of the commonly known diesel engine, is the most promising advanced combustion engine technology for achieving dramatic energy efficiency improvements in light- and heavy-duty vehicles. Light-duty hybrid vehicles using CIDI engines are projected to have energy efficiencies that are 80% higher than current gasoline vehicles, though the higher cost of CIDI engines relative to gasoline engines discourages use of this technology in light-duty applications right now. Implementation of the U.S. Environmental Protection Agency's (EPA's) Tier 2 regulations for light-duty vehicles, which took effect in 2004, is imposing another significant barrier to further penetration of CIDI engines in the U.S. This situation is unlike Europe, where diesel vehicles represent just over 50 percent of all new light-duty passenger car sales primarily because gasoline and diesel fuel are more expensive there but also because emission regulations are less stringent.

The CIDI engine is already the primary engine for heavy-duty vehicles because of its high efficiency and outstanding durability. However, the implementation of more stringent heavy-duty engine emission standards, which are to be phased in starting in 2007 (100% implementation in 2010), is predicted to cause a reduction in fuel efficiency due to the exhaust emission control devices needed to meet both the oxides of nitrogen (NO_x) and particulate matter (PM) emissions regulations.

Cut-Away of DaimlerChrysler 3.2 L CIDI Engine that Achieves 30% Better Fuel Economy than its Gasoline Counterpart in Mercedes Light-Duty Vehicles

Given these challenges, the Advanced Combustion Engine Technologies Sub-Program is working toward achieving the following objectives:

- Advance fundamental combustion understanding to enable design of CIDI engines with inherently lower emissions. This will reduce the size and complexity of emission control devices and minimize any impact these devices have on vehicle fuel efficiency.
- Increase overall engine efficiency through fundamental improvements such as advanced combustion processes, reduction of parasitic losses, and recovery of waste heat.
- Improve the effectiveness, efficiency, and durability of CIDI engine emission control devices to enable these engines to achieve significant penetration in the light-duty market and maintain their application in heavy-duty vehicles.

Technology Status

The technology for controlling PM emissions from CIDI engines is highly effective and is entering commercial markets in applications (mostly transit buses) where duty cycles and engine strategies create adequately high exhaust temperatures to ensure regeneration, and where ultra-low-sulfur fuel is available. The current light-duty diesel vehicles for sale in the U.S. (a few passenger car models and one small sport utility vehicle) rely on oxidation catalysts and/or advanced fuel injection and turbocharging to meet the standards for PM emissions. (Full-size pickups with diesel engines are not considered light-duty vehicles.) However, the lowest standard to which these vehicles are certified is Bin 9 (out of a total of 10), which limits their potential market penetration. Light-duty diesel vehicle manufacturers have indicated their desire to employ catalytic PM devices to further lower PM emissions once diesel fuel sulfur levels decrease to 15 ppm nationwide in June 2006. Cost and durability are likely to be the important characteristics for choosing which PM control technology to employ for a given application, though the type of NO_x control device used will also play a role in specifying a PM trap and where it will be placed. Regeneration strategies for light-duty vehicles need further development before these vehicles can be considered market-ready.

Technology for control of CIDI engine NO_x is not nearly as mature as the technology for control of PM. Competing technologies include adsorbers, selective catalytic reduction (SCR), lean-NO_x catalysts (often called hydrocarbon-SCR), and non-thermal plasma (NTP)-assisted catalysis. Of these technologies, SCR using urea as a reductant is the current leader in terms of having the lowest fuel penalty and highest durability. In laboratory testing, Bin 3 emissions have been recorded, though full useful life is yet to be proven with new catalysts. Urea SCR faces the hurdle of requiring a urea distribution infrastructure to supply the vehicles. Heavy-duty vehicle manufacturers in Europe have committed to urea-SCR and are supporting urea distribution and dispensing infrastructure implementation and standards to assure urea quality. Serious discussions of the willingness of U.S. heavy-duty vehicle manufacturers to implement urea-SCR emission control are on-going. Urea-SCR is equally effective on light-duty CIDI vehicles, though development of urea distribution infrastructure is a more daunting prospect than for heavy-duty vehicles that primarily use truck stops for refueling. A system to refuel

light-duty CIDI vehicles with both diesel fuel and urea using one coaxial hose has been demonstrated and shows much promise. However, no proposal has been developed to assure that urea will be available at sufficient numbers of refueling facilities serving light-duty vehicles. Urea can also be stored onboard in solid pellet form, and enough can be stored to allow recharging at each oil change. This approach could make use of the current parts distribution system to recharge vehicles with urea.

Prototype Diesel Fuel/Urea Co-Fueling Dispenser

Development of NO_x adsorbers has shown rapid improvement to the point that they appear to be able to achieve the Tier 2 Bin 5 light-duty vehicle emission levels when new using 4-ppm-sulfur fuel (which is lower than the average sulfur level expected for ultra-low sulfur fuel to be available after June 2006), though not for a full vehicle lifetime. NO_x adsorbers for heavy-duty vehicles are less well-developed based on the size of these units compared with engine displacement (being over twice as large as those required for light-duty vehicles). The durability of NO_x adsorbers is still in question since they are sensitive to even small amounts of sulfur in the fuel or engine lubricant (urea-SCR catalysts are less sensitive to sulfur). The other major concern about NO_x adsorbers is their effect on fuel consumption and cost. NO_x adsorbers use fuel to regenerate instead of urea, and current fuel "penalties" for regeneration are declining but still in the range of five to ten percent of total fuel flow. This is exacerbated by the need to periodically drive off accumulated sulfur by heating the adsorber to high temperatures, again by using fuel. These concerns must be addressed before NO_x adsorbers will be deemed to be commercially viable.

Interest in lean-NO_x catalysis (hydrocarbon-SCR) is making a bit of a come-back for use on both light- and heavy-duty CIDI vehicles. Currently, lean-NO_x catalysts provide only 20-40 percent reduction in NO_x, but this may be sufficient when combined with measures to reduce engine-out NO_x such as exhaust gas recirculation (EGR), low-temperature combustion, or homogeneous charge compression ignition (HCCI). Lean-NO_x catalysis may also be used as an interim step with heavy-duty engines as the 2007 standards are phased in. The advantages of lean-NO_x catalysis include no core engine modifications, no fuel infrastructure requirements as for urea, some reduction of hydrocarbons and carbon monoxide, and being amenable to retrofit applications. Remaining drawbacks include catalyst activity and durability, the need for a broader operating temperature window, and lower selectivity leading to a higher fuel penalty.

Non-thermal plasma NO_x reduction catalysts have not achieved similar progress as competing technologies, and catalyst coking has been identified as a problem. Because of the lack of progress on NTP catalysis and its problems, the Advanced Combustion Technologies Sub-Program has decided to discontinue funding of this technology. Plasmas continue to be explored in reforming processes for generating diesel-fuel-based reductants for use with NO_x adsorbers.

An optimum solution to CIDI engine emissions would be to alter the combustion process in ways that produce emissions at levels that don't need ancillary devices for control, yet maintain or increase the engine efficiency. This is the concept behind new combustion regimes such as HCCI and other models of low-temperature combustion, which result in greatly reduced levels of NO_x and PM emissions (emissions of hydrocarbons and carbon monoxide still exist but are more easily controlled). Significant progress is being made in these types of combustion systems, and performance has been demonstrated over increasingly larger portions of the engine speed/load map. The major issues of this R&D include fuel mixing, combustion control, and extension of the operating range. Control of fuel injection and valve opening independent of piston movement appears to be necessary for HCCI engines to be viable. The optimum HCCI fuel has yet to be determined, though both diesel fuel and gasoline appear to be acceptable.

Complex and precise engine and emission controls will require sophisticated feedback systems employing new types of sensors. NO_x and PM sensors are in the early stages of development and require additional advances to be cost-effective and reliable, but are essential to control systems for these advanced engine/ aftertreatment systems. Much progress has been made, but durability and cost remain the primary issues with these sensors.

Advanced fuel formulations and fuel quality are also crucial to achieving higher energy efficiencies and meeting emissions targets. The EPA rule mandating that sulfur content of highway diesel fuel be reduced to less than 15 ppm starting in 2006 will greatly benefit the effectiveness, durability, and life of emission control devices. The EPA has recently reported that based on pre-compliance reports, 95 percent of all the diesel fuel should be less than 15 ppm sulfur by June 2006.

Future Directions

Internal combustion engines have a maximum theoretical fuel conversion efficiency that is similar to fuel cells; it approaches 100%. The primary limiting factor to achieving high fuel conversion efficiency is the high irreversibility in traditional premixed or diffusion flames. Multiple studies agree that combustion irreversibility losses consume more than 20% of the available fuel energy and are a direct result of flame front combustion. Examples of "new combustion regimes" that might lower the irreversibility losses include dilute combustion with low peak temperatures, higher expansion of combustion gases, and increased reactant temperature. The engine hardware changes needed to execute these advanced combustion regimes include variable fuel injection geometries, methods to produce very high manifold pressures, compound compression and expansion cycles, and improved sensors and control methods.

The other areas where there is large potential for improvements in internal combustion engine efficiency are losses from the exhaust gases and heat transfer losses. Potential ways that these losses might be reduced include compound compression and expansion cycles achieved by valve timing, use of turbine expanders, application of thermoelectric generators, and lean-burn and stratified-charge engines.

Fuels can also play an important role in reducing combustion irreversibility losses. Preliminary analyses show that combustion irreversibility losses per mole of fuel are considerably less for hydrogen than for hydrocarbon fuels. This is consistent with the understanding that combustion irreversibility losses are reduced when combustion is occurring nearer equilibrium (high temperature), since hydrogen has the highest adiabatic flame temperature of the fuels studied to date. This bodes well for the development of highly efficient hydrogen-fueled internal combustion engines.

Goals and Challenges

Quantitative targets have been developed for advanced engines in three major applications: passenger cars, light trucks, and heavy trucks. Light trucks here refer to pickup trucks, vans, and sport utility vehicles that are emissions-certified to the same standards as passenger cars, or generally "light-duty vehicles." Fuel efficiency improvement is the overarching focus of this Sub-Program, but resolving the interdependent emissions challenges is a critical first step. (Penetration of even current technology CIDI engines into the light-duty truck market would reduce fuel use by 30-40% per gasoline vehicle replaced.) The major challenges facing CIDI emission control systems across all three platforms are similar: durability, cost, and fuel penalty (or in the case of urea-SCR, urea infrastructure development). Full-life durability has yet to be demonstrated for either light- or heavy-duty systems. Nor have these systems demonstrated their ability to "bounce back" following exposure to fuel sulfur levels higher than 15 ppm, which could occur periodically due to cross-contamination of fuels and outright fuel substitution mistakes. With significant progress made toward emission controls, attention will be turned more toward engine efficiency improvements by improving combustion and systematically attacking losses such as friction, exhaust energy, heat transfer, and parasitic losses.

The targets for passenger cars, derived primarily by the FreedomCAR Partnership, are shown in Table 1. Achieving emissions compliance for CIDI engines in light-duty vehicles will provide a "quantum leap" (~30%) fuel efficiency improvement over port-fuel-injected spark ignition engines. In the longer term, further advancement of engine efficiency along with reducing the emission control penalty will gain another 15-18% beyond today's technology.

Table 1. Technical Targets for Combustion and Emission Control Activity

Characteristics	Units	Fiscal Year		
		2004	2007	2010
FreedomCAR Goals				
ICE Powertrain				
Peak Brake Thermal Efficiency (CIDI/H_2-ICE) (H_2-ICE)	*%*			*45/45 45 (2015)*
Cost (CIDI/H_2-ICE) (H_2-ICE)	*$/kW*			*30/45 30(2015)*
Reference Peak Brake Thermal Efficiency[a]	*%*	*30*	*32*	*34*
Target Peak Brake Thermal Efficiency/Part-Load Brake Thermal Eff. (2 bar BMEP[b] @1500 rpm)	%	43/29	45/32	46/35
Powertrain cost[c,d]	$/kW	30	30	30
Emissions[e]	g/mile	Tier 2, Bin 5	Tier 2, Bin 5	Tier 2, Bin 5
Durability[e]	Hrs.	5,000	5,000	5,000
Fuel efficiency penalty due to emission control devices[f]	%	<5	<3	<1

[a]Current production, EPA-compliant engine

[b]Brake mean effective pressure

[c]High-volume production: 500,000 units per year

[d]Constant out-year cost targets reflect the objective of maintaining powertrain (engine, transmission, and emission control system) system cost while increasing complexity.

[e]Projected full-useful-life emissions for a passenger car/light truck using advanced petroleum-based fuels as measured over the Federal Test Procedure as used for certification in those years.

[f]Energy used in the form of reductants derived from the fuel, electricity for heating and operation of the devices, and other factors such as increased exhaust back-pressure which reduces engine efficiency.

The light truck diesel engine R&D activity will not be continued past this year. All the 2004 targets listed in Table 2 have been demonstrated to be achievable with the exception of emission controls that have full-useful-life durability. The availability of commercial products having these characteristics depends on manufacturers doing the necessary product engineering and durability testing.

Table 2. Technical Targets for Light Truck Diesel Engine R&D

Characteristics	Units	2004
Engine power	hp	225-325
Fuel economy increase over equivalent gasoline vehicles	%	>50
Engine cost (compared to equivalent gasoline engine)	%	<120
Engine weight (compared to equivalent gasoline engine)	%	<110
NVH[a] (compared to equivalent gasoline engine)	db difference	<1
NO_x emissions[b]	g/mile	<0.07
PM emissions[b]	g/mile	0.01
Durability[c] (on lab dynamometer, computer simulated vehicle miles)	miles (equivalent)	>100,000

[a]Noise, vibration, and harshness

[b]Projected full-useful-life emissions for a SUV (using advanced petroleum-based fuels with 15 ppm sulfur) as measured over the Federal Test Procedure as used for certification in those years.

[c]Projected full-useful-life durability, as measured over the Federal Test Procedure as used for certification.

Heavy truck engine R&D activities are focused on increasing heavy-duty diesel engine efficiency significantly above current levels as well as addressing efficiency penalties resulting from emission control technologies required to meet the increasingly stringent emissions standards. As seen in Table 3, heavy-duty truck engines will need to simultaneously increase thermal efficiency significantly while lowering emissions and doubling durability, all by the end of 2005. To date, all the 2005 targets have been achieved except for emissions systems durability. By 2007, efficiency will need to be increased further while NO_x emissions are reduced and durability doubled over that required to meet the 2005 target. Achieving these technical targets will require sustained R&D activities along several fronts.

Table 3. Technical Targets for Heavy Truck Diesel Engine R&D

Characteristics	Fiscal Year			
	2002 Status	2005	2007	2012
Engine thermal efficiency, %	>40	>45	>50	>55
NO_x emissions,[1] g/bhp-hr	<2.0	<1.2	<0.20	<0.20
PM emissions[1], g/bhp-hr	<0.1	<0.01	<0.01	<0.01
Stage of Development	commercial	prototype	prototype	prototype
Durability, miles (equivalent)	>100,000	>200,000	>400,000	

[1]Using 15-ppm-sulfur diesel fuel

Recovery of energy from the engine exhaust represents a potential for 10 percent or more improvement in the overall engine thermal efficiency. More efficient turbochargers using variable geometry and electric assist are one approach. Turbocompounding and direct thermal-to-electric conversion could also improve the overall thermal efficiency. Semiconductor thermoelectric devices are currently 6 to 8 percent efficient, but recent developments in quantum well thermoelectrics suggest an improvement to over 20 percent is possible. The technical targets for the waste heat recovery R&D activities are listed in Table 4. Significant progress will be needed to meet the 2005 and 2008 targets. Newly awarded projects are focused on achieving this progress.

Table 4. Technical Targets for Combustion and Emission Control Activity

Characteristics	Units	Fiscal Year		
		2003 Status	2005	2008
Electrical turbocompound system				
Light-Duty Vehicles				
Power	kW	<2	>5	>10
Projected component life	Hrs.	<10	>2,000	>5,000
Class 7-8 trucks				
Fuel economy improvement	%	<1	>5	>10
Power	kW	<10	>20	>30
Projected component Life	Hrs.	<10	>5,000	>10,000
Thermoelectric Devices				
Efficiency bulk semiconductor quantum well	%	6-8	-- >10	-- >15
Projected cost @ 250,000 production volume	$/kW	--	500	180

Project Highlights

The following projects highlight progress made in the Advanced Combustion Engine R&D Sub-Program during FY 2004.

Advanced Combustion and Emission Control Research for High-Efficiency Engines

A. Combustion and Related In-Cylinder Processes

The objective of these projects is to identify how to achieve more efficient combustion with reduced emissions from advanced technology engines.

- Argonne National Laboratory (ANL) expanded their x-ray fuel spray measurement technique to inject in atmospheres at pressures of 15 and 20 bar. They also demonstrated for the first time that the x-ray technique can be useful for resolving subtle differences in the sprays based on the internal structure of the nozzle.

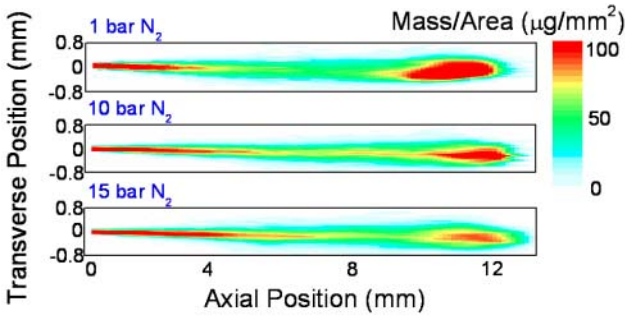

Differences in Fuel Spray Penetration with Pressure Revealed by X-Rays

- Sandia National Laboratories (SNL) experimentally evaluated a late-injection, low-temperature diesel combustion regime for a wide variety of system parameters, including injection pressure, swirl ratio, O_2 concentration (exhaust gas recirculation rate), start of injection, and intake temperature. The optimum swirl level and rate-limiting factors at various stages of the combustion process were identified.
- SNL demonstrated that diesel combustion is soot-free for an ambient gas oxygen concentration of 8% and typical diesel ambient gas temperature (1000 K). They also found that combustion efficiency remains high for mixing-controlled diesel combustion with flame temperatures as low as 1500-1600 K for conditions where the ambient gas temperature is greater than 1000 K.

- Using only high EGR and specific engine operating parameters, Oak Ridge National Laboratory (ORNL) demonstrated rapid transition between conventional combustion and a high-efficiency clean combustion mode in a production light-duty CIDI diesel engine with 90% reduction in engine-out NOx and a 50% reduction in PM emissions under road-load type conditions (20% load, 1500 rpm) without excessive hydrocarbon (HC) emissions.
- Lawrence Livermore National Laboratory (LLNL) extended their combustion multi-zone analysis methodology to make it applicable to analysis of premixed charge compression ignition (PCCI), a generalization of HCCI combustion where the fuel and air mixture may be partially stratified at the moment of ignition.

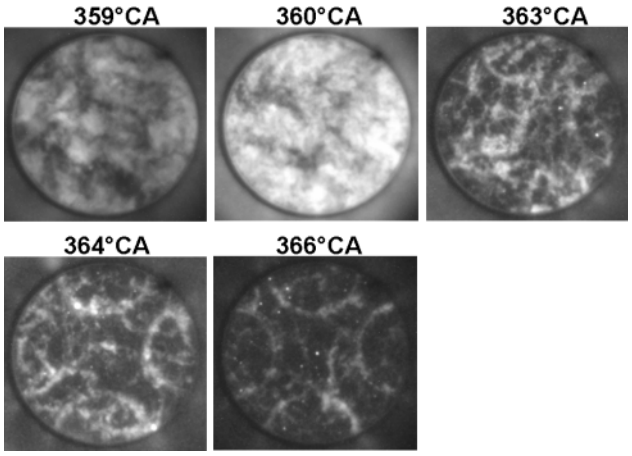

Images of HCCI Combustion Using Laser Imaging

- SNL conducted an investigation of the lowest temperature for complete combustion of hydrocarbon fuels over a wide range of conditions. They showed that the peak temperature must exceed 1500 K at 1200 rpm, regardless of fuel type or combustion timing.
- SNL identified several tracers that improve fuel tracking by better matching the volatility of reference fuels.
- The University of Wisconsin identified diesel HCCI combustion regimes in a Caterpillar 3401 engine using both low-pressure and high-pressure multiple injection strategies. They also developed models that minimize fuel deposition on the walls and provide start-of-combustion control via variable valve timing and variable geometry sprays.
- The University of Michigan experimentally demonstrated potential HCCI engine control methods using valve control and thermal effects and identified that valve control has characteristic response times of 10's of cycles while thermal effects are on the order of 100's of cycles.
- Caterpillar developed a novel HCCI engine system that successfully achieves the proper air-fuel mixture using conventional diesel fuel and achieved 2100+ kPa brake mean effective pressure (BMEP) while meeting future emissions standards. This is the highest known power density in the world achieved using any form of HCCI.
- ORNL demonstrated that HCCI combustion in a gasoline engine could improve fuel economy by an average of 12% while reducing NO_x emissions by 95% compared to conventional combustion.
- ORNL (as part of their CRADA with Detroit Diesel Corporation [DDC]) performed extensive experiments under low and medium load conditions to characterize the effects of EGR rate, rail pressure,

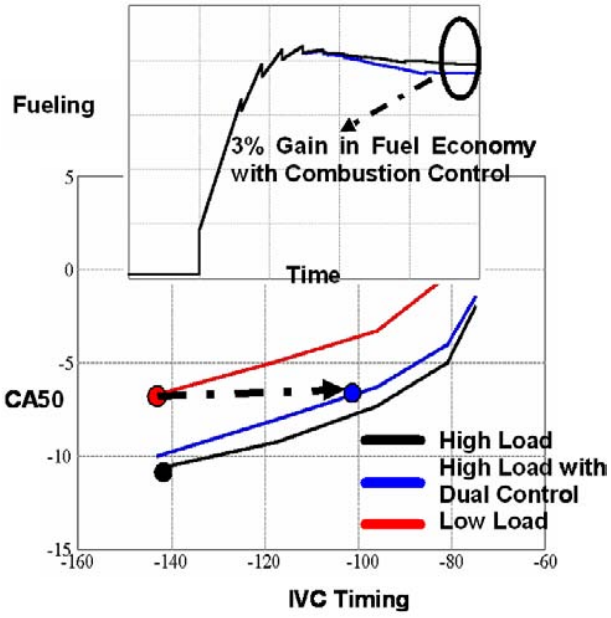

Estimate of Fuel Consumption Reduction with Application of HCCI Combustion

and injection timing on achieving high-efficiency clean combustion operation of a current DDC diesel engine.

- Los Alamos National Laboratory (LANL) modified all subroutines of KIVA-3V to accommodate unstructured grids. A beta version of KIVA-4 has been distributed to the industry Memorandum of Understanding participants.
- LLNL developed models for chemical kinetics of combustion of two major fuel components, toluene and methyl cyclohexane, and for an oxygenated diesel fuel additive, dimethyl carbonate.

B. Energy-Efficient Emission Controls

The following project highlights summarize the advancements made in emission control technologies to both reduce emissions and reduce the energy needed for their operation.

- Pacific Northwest National Laboratory (PNNL) identified cryptomelane, an octahedral molecular sieve based on manganese cations, as a stoichiometric SO_2 absorber having total capacity of approximately 70 wt.% and a breakthrough capacity of 60 wt.% at 325ºC. The capacity of the material is virtually unaffected with realistic feeds under cyclic lean-rich conditions.
- ORNL (as part of a CRADA with International Truck and Engine) developed a strategy for regenerating NO_x adsorbers at rated load (600ºC) to meet the NTE (not-to-exceed) emission standards and achieved 70% NO_x reduction at rated power, with acceptable CO and HC emissions and very low fuel penalty (<2.5%).

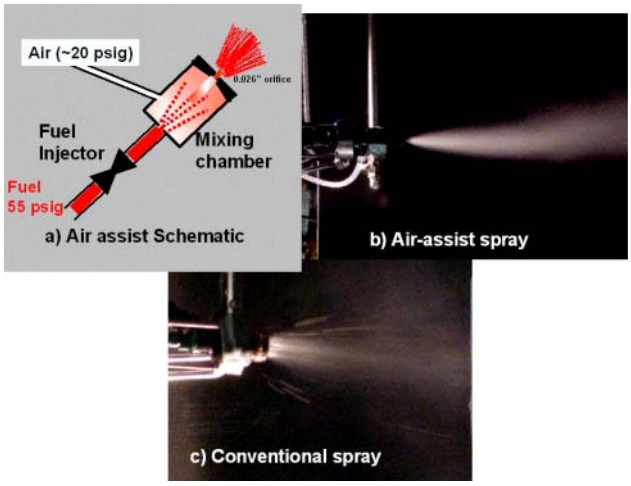

Air-Assisted Fuel Injector for Regenerating NO_x Adsorbers

- ANL demonstrated that paraffins are ineffective as reductants for their deNOx catalyst and that aromatics (toluene and xylenes) are highly effective while selectivity to N_2 still remains near the 100% mark.
- ORNL developed a draft bench characterization protocol for lean NO_x trap (LNT) materials in conjunction with supplier representatives and the LNT Focus Group that is intended to provide the basis of standard kinetic 'maps' (i.e., data templates) for communicating critical simulation properties. ORNL presented the protocol at the 7th CLEERS workshop and posted it on the web.
- Ford achieved low-mileage Tier 2 Bin 5 standards using a fresh catalyst system of oxidation catalysts, urea-SCR and a catalyzed diesel particulate filter (CDPF) in a mid-sized diesel prototype engine designed for a light-duty truck. Engine-out NO_x was lowered by 40% through the use of a cooled, low-pressure EGR system.

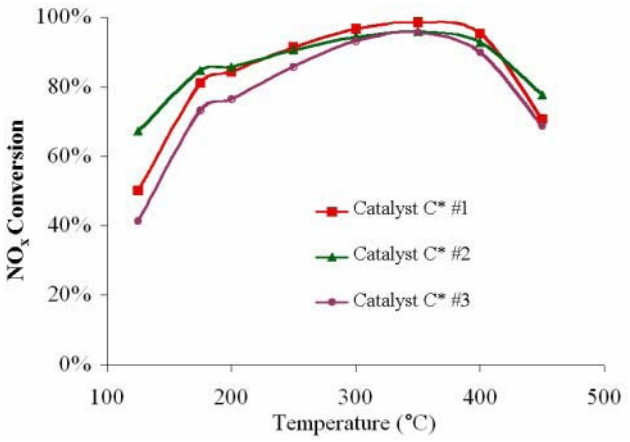

New Catalysts Are Being Discovered that Have High NO_x Conversion Efficiency

- LANL achieved milestone NO_x conversion efficiency of >95% between 160 and 400ºC at a gas hourly space velocity (GHSV) of 30,000 h^{-1} and $NO:NO_2$ = 4:1 using a 'hybrid' dual-bed base metal zeolite catalyst system supported on a monolith.

- PNNL invented a new catalyst material (disclosure filed) that shows excellent activity for hydrocarbon SCR of simulated diesel exhaust without the need for a plasma device.
- ORNL developed a testing procedure for measuring thermal deactivation that simulates 400,000 miles of operation in a 15-hour test. They also demonstrated poisoning effects of sulfur in model LNT catalysts using a test procedure that simulates 126,000 miles of operation.
- Noxtech demonstrated over 94% reduction of NO_x from the exhaust of a high-speed diesel engine under conditions of 30,000 hr^{-1} space velocity while using 50 ppm sulfur fuel.

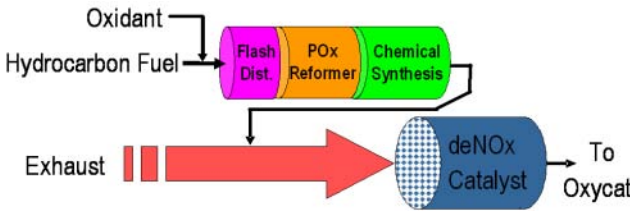

Schematic of a Reductant Preparation System for Lean-NO_x Catalysts

- Using reductants developed from fuel oxygenates, PNNL demonstrated 70% NO_x reduction activity, which is significantly greater than conventional lean-NO_x performance of 40%.
- General Motors tested over 3000 materials for NO_x reduction potential and identified multiple hydrocarbon SCR materials that enable NO_x conversion in excess of 80%.

C. Critical Enabling Technologies

- Sensors, new instrumentation, and advanced catalyst designs are enabling technologies for achieving more efficient engines with very low emissions. The following highlights show the progress made during FY 2004.
- Caterpillar produced prototype metal substrates for catalytic converters that have similar long-term cyclic oxidation resistance as current ceramic-based substrates. Metal substrates are less costly and allow smaller designs with less substrate weight and precious metal content.
- Delphi continued development of a NO_x sensor by improving sinterability of the sensing element, developing a key electrode material, eliminating cross contamination of electrode materials through improved design, and implementing an advanced interconnection design.
- CeramPhysics successfully manufactured capacitor-type combined NO_x and O_2 sensor bodies with two types of porous Rh-based electrodes.
- PNNL developed a ceramic oxygen pumping electrode for an NO_x sensor that is compatible with high sensor processing temperatures, shows very high activity for oxygen pumping, is insensitive to NO_x, and should be less costly than noble metal electrodes.
- ANL developed a portable PM emissions measurement system and successfully demonstrated it onboard an operating diesel vehicle.
- SNL developed a laser-induced incandescence PM measuring instrument and tested it at several industry laboratories as well as at ORNL, demonstrating high accuracy, fast response, and high reliability without the

Prototype NO_x Sensors

Test of Portable Laser-Based PM Measurement Instrument

need for operator oversight. Artium Technologies Inc., in Sunnyvale, California, is commercializing this instrument, and the first commercial sales occurred in the spring of 2004.

- Honeywell established the feasibility of monitoring particulates directly in the exhaust manifold without pretreatment or dilution and without sensor fouling due to accumulation of particulate matter. Concept prototype PM sensors have been fabricated for testing.

Advanced Engine Designs for Improved Efficiency

With the advent of stringent emission standards, it is necessary to design engines as systems to achieve both high efficiency and low emissions. The following project highlights describe the progress made for both light- and heavy-duty engines during FY 2004.

A. Heavy-Duty

- Cummins achieved and demonstrated 45% brake thermal efficiency while meeting 2007 emissions goals. They also demonstrated an advanced recirculated exhaust gas cooling system and evaluated different forms of homogeneous charge compression ignition combustion.
- Caterpillar built a demonstrator truck with 2007 emissions technology that has provided key insight into system integration challenges and real driving cycle performance. They also demonstrated full-load and full-power HCCI operation on a single-cylinder test engine while achieving 2010 emissions levels and demonstrated the potential of NO_x aftertreatment to achieve 2010 emissions levels on a multiple-cylinder engine.

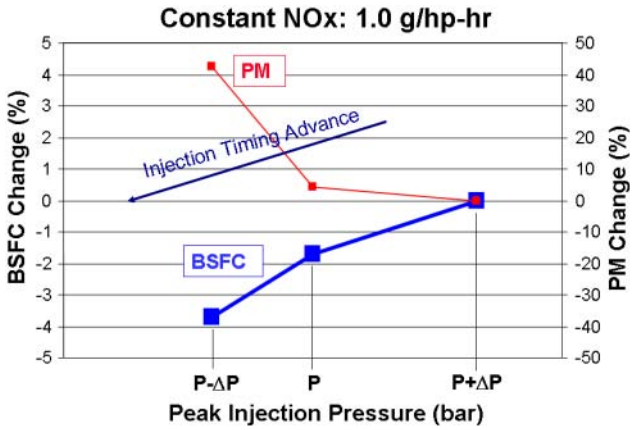

Trade-Off of PM Emissions and Efficiency at Constant Low NO_x Emissions

- DDC achieved 43% brake thermal efficiency in a multi-cylinder engine configuration while demonstrating engine-out NO_x and particulate matter (PM) emissions of 1.1 g/hp-hr and 0.1 g/hp-hr, respectively, over the hot cycle Federal Test Procedure (FTP). They also subsequently demonstrated tailpipe-out NO_x and PM emissions of ~1.0 g/hp-hr and <0.01 g/hp-hr, respectively, with integration of a diesel particulate filter.

B. Light-Duty

- Cummins demonstrated power density of 48 HP/liter on a 4.2-liter V6, and Tier 2 Bin 5 emissions capability through emissions testing at sea level and at altitude with 150,000 mile thermally aged catalyst.
- DDC demonstrated Tier 2 Bin 3 emissions over the FTP75 cycle for a light-duty diesel truck (LDT) equipped with a diesel particulate filter and urea-based selective catalytic reduction (DPF + SCR) system. This aggressive reduction in emissions was obtained without ammonia slip and with a 41% fuel economy improvement compared to the equivalent gasoline engine equipped vehicle. DDC also demonstrated Tier 2 emissions compliance over the US06 cycle.
- Modeling of the Envera variable compression ratio system projected part-load efficiency to be higher than that of the DaimlerChrysler A170 common-rail turbo-CDI current production engine (representative of current design CIDI engines).

Waste Heat Recovery

Two technologies are being pursued to capture waste heat from advanced combustion engines: electricity generation from turbochargers and thermoelectrics. Following are highlights of the development of these technologies during FY 2004.

- Honeywell developed an enhanced version of their e-Turbo™ system. The electricity generated by the turbocharger was shown to lower brake specific fuel consumption at steady-state engine operation by up to 6%. Using the e-Turbo™ system in reverse (i.e., as power assist to the turbocharger) allows low-speed torque to be increased, resulting in potential to reduce engine size by 10-30% with the same vehicle performance. Such engine downsizing could reduce fuel use by 6-17%.
- Hi-Z Technology, Inc. has achieved >530,000 equivalent miles in road tests of their 1-kW diesel truck thermoelectric generator. Post durability test inspection found that the internal resistance increased from 0.6 to 0.75 Ohms. This increase could be partially attributable to electrical contact corrosion. Hi-Z assembled and tested two different single-couple modules, and the conversion efficiency from both tests was in excess of 14% at a temperature differential of 200ºC.
- PNNL scaled up the deposition process for multilayer thermoelectric substrates to 0.5 m^2 in area and demonstrated prototype batch deposition. They also established measurements of thermoelectric properties of thin films at temperatures up to 800ºC.

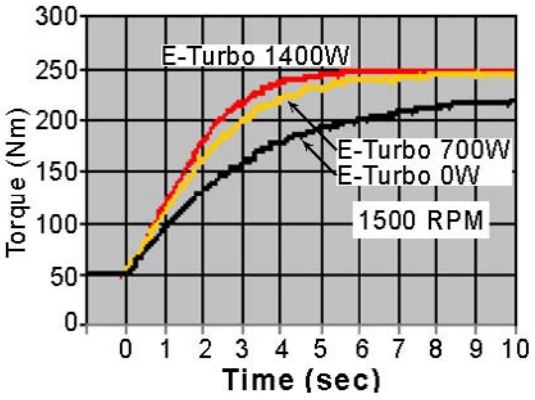

Improved Engine Response from Use of an Electrically-Assisted Turbocharger

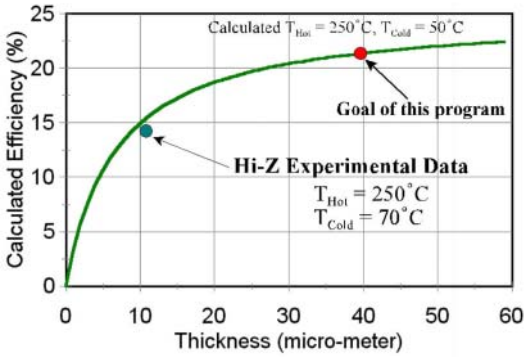

Advancements in Thermoelectric Generator Efficiency

Off-Highway Vehicle Engine R&D

Off-highway vehicles are coming under more stringent emission controls similar to those for highway vehicles. However, their typical duty cycles place unique demands on emission control systems. Following are highlights of off-highway vehicle efficiency improvement and emission control development during FY 2004.

- Cummins designed and optimized engine combustion to achieve compliance with Tier 3 emission levels without the use of EGR and with only a slight degradation in fuel consumption for certain engine models. Work is proceeding on achievement of Tier 4 emission standards.
- John Deere used cooled low-pressure loop EGR and a continuously regenerating diesel particle filter (CR-DPF) to meet Tier 3 emissions with slightly improved fuel consumption.

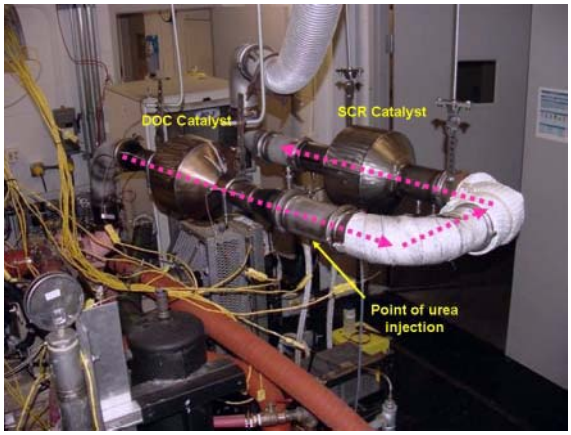

Test Set-Up of Urea-SCR System for Off-Road Engines

- The Electromotive Division of GM completed engine test results showing that their new fuel injection system has the potential to meet locomotive Tier 2 emissions goals with favorable NO_x-BSFC-PM (oxides of nitrogen - brake specific fuel consumption - particulate matter) trade-off characteristics.
- General Electric developed a computational fluid dynamics model to guide development of an advanced fuel injection system. They also designed, built, and tested an electrically assisted turbocharger and evaluated candidate abradable seal materials identified for the turbocharger compressor and turbine shrouds.
- ORNL, in a CRADA with John Deere, demonstrated that a urea-SCR system could meet Tier 4 emissions for off-highway diesel engines. Improved fuel efficiency was also demonstrated through the application of an advanced fuel injection system.

Future Directions

Advanced Combustion and Emission Control Research for High Efficiency Engines

A. Combustion and Related In-Cylinder Processes

- ANL plans to increase the pressure capability of their x-ray fuel spray technique and make upgrades to enable the use of production fuel injector nozzles. They also plan to make improvements in the system including faster data acquisition, processing, and analysis; improved x-ray detector systems; increased x-ray intensity; and greater automation.
- SNL will evaluate alternative low-temperature combustion systems and identify the rate-limiting factors that prevent their application over a wider speed/load range.
- SNL will investigate how very high EGR affects diesel soot formation by performing quantitative measurements for ambient oxygen concentrations ranging from 21% to 10%.
- ORNL plans to investigate techniques for entering and exiting high-efficiency and low-emission combustion modes for CIDI diesel engines and consider potential diagnostic tools for feedback control when transitioning between these modes.
- LLNL will develop combustion analysis tools to accurately predict combustion and emissions under PCCI combustion.
- SNL plans to combine multi-zone Senkin modeling with experimental data to investigate how thermal stratification affects HCCI heat release rates with normal and retarded timing, and to determine the potential for extending the high-load limit with thermal stratification.
- SNL will characterize the charge-preparation process for HCCI engines using alternative injectors and injection strategies, including liquid injection, wall wetting, and fuel-air mixing.
- The University of Wisconsin plans to assess the use of multiple injections for diesel HCCI combustion control.
- The University of Michigan will continue engine control experiments to expand and refine current studies of mode transitions and thermal transients necessary for successful HCCI implementation.
- Caterpillar will focus on identifying and developing a cost-effective method of manufacturing the HCCI engine system they have developed.
- ORNL plans to continue to evaluate and quantify the use of spark augmentation for gasoline HCCI engine control and transition to HCCI combustion.
- ORNL (as part of their CRADA with DDC) will explore the potential of achieving HCCI-like operation and further expanding the range of high-efficiency clean combustion operation of a heavy-duty multi-cylinder diesel engine.

- LANL plans to assemble a KIVA-4 manual, develop a KIVA-3V mesh converter which will convert KIVA-3V meshes to KIVA-4 format, continue validation of KIVA-4 by adding to the existing test suite of engine problems, and develop and begin implementing a grid-generation strategy for KIVA-4 that incorporates commercial grid-generation packages.
- LLNL will extend model capabilities to additional classes of fuel components and continue development of increasingly complex surrogate fuel mixtures.

B. Energy-Efficient Emission Controls

- PNNL will continue studies with metal-modified cryptomelane to further increase SO_2 uptake capacity at 200ºC and below, and develop and characterize alternate SO_2 adsorbents having moderate SO_2 capacity that can be regenerated on the vehicle during the rich cycle.
- ORNL (as part of a CRADA with International Truck and Engine) plans to measure the sulfur compounds that are released from desulfurizing an NO_x adsorber catalyst and re-examine NTE and lower temperature conditions with in-pipe injection of pure compounds.
- ANL will test several optimized deNO_x catalysts on an engine in a test cell using a slip stream of the diesel feed as the reductant. Optimization will include maximizing space velocity while minimizing the catalyst volume.
- ORNL will demonstrate the draft LNT characterization protocol on the ORNL bench-flow reactor and identify needed revisions and technical issues.
- Ford plans to conduct durability testing of their light-duty diesel truck emission control system and continue laboratory testing/development of ammonia sensing technologies to determine their value in a urea-SCR diesel aftertreatment system.
- ORNL will elucidate sulfur-based deactivation mechanisms and chemistry by determining the chemical form of sulfur-based species, identifying the desulfation temperatures for each sulfur species, and evaluating intermediate species formations to determine their chemistry.
- Noxtech plans to use the data generated from the 60-kW engine test to design, build and evaluate a system capable of reducing the NO_x from a 250-kW high-speed diesel engine by over 90%.
- PNNL will investigate additional oxygenates as reductants for lean-NO_x traps and alternate methods of reductant production.
- General Motors plans to continue the discovery of materials with good low-temperature NO_x conversion properties to assist with cold-start emission reduction, and to scale up the promising materials for engine testing.

C. Critical Enabling Technologies

- Caterpillar will complete testing of full-scale current design metal substrate catalyst prototypes with new materials, including hot shake tests; complete modeling of the new design to determine optimum geometry to maximize activity while minimizing backpressure; and produce a full-scale prototype of new design substrate with optimized geometry and new material.
- Delphi plans to evaluate their NO_x sensor subsystem in bench testing and on a running engine.
- CeramPhysics will incorporate NO_x and O_2 sensor bodies into fully assembled NO_x sensors and complete testing of them at an outside laboratory.
- PNNL plans to determine how their NO_x sensor operation is affected by the presence of ammonia in exhaust gases, and investigate pulsed detection methods as a means of enhancing sensor sensitivity and accuracy.
- ANL will complete tests evaluating the sensitivity of their portable PM measuring instrument to the volatile organic fraction of PM, and explore the possibility to incorporate the capability to measure particle aggregate size and number density.

- SNL plans to improve the capabilities of their laser-induced incandescence PM measuring instrument and continue the collaboration with Artium Technologies toward commercialization of instrumentation for PM measurements.
- Honeywell will demonstrate prototype PM sensors and electronics in several end-user facilities.

Advanced Engine Designs for Improved Efficiency

A. Heavy-Duty

- Cummins will perform engine system modeling to predict engine, aftertreatment, and heat recovery system performance and perform test cell testing to verify the models developed and system performance.
- Caterpillar plans to focus on developing supporting engine systems to facilitate full-load HCCI on a multiple-cylinder engine and on developing methods and techniques to overcome NO_x aftertreatment durability problems. Fuel efficiency, cost and manufacturability will also be areas of focus for these technologies.
- DDC will evaluate advanced fuel injection equipment, including hybrid systems, for the potential to enable combustion characteristics that will lead to over 45% thermal efficiency while meeting 2010 regulated emissions.

B. Light-Duty

- A variable compression ratio (VCR) variant of the DaimlerChrysler 1.7L 4-cylinder common-rail turbo-diesel will be used to investigate compression direct injection (CDI) emissions, fuel economy, and advanced combustion benefits that can be attained with VCR.
- The ability to attain 25 percent improvement in spark ignition engine fuel economy with HCCI combustion using VCR and adjustable valve settings for controlled combustion from idle to high load levels will be demonstrated through hardware testing and computer modeling.
- The ability to attain 30 percent improvement in fuel economy with VCR, supercharging, and engine down-sizing at significantly lower production cost than hybrid electric vehicle (HEV) technology (dollars per percent increase in fuel economy) while meeting federal and state emission standards will be demonstrated through hardware testing and computer modeling.

Waste Heat Recovery

- DOE will award new cooperative agreements to develop thermoelectric devices and turbo-compounding units to convert waste heat to electricity.
- Honeywell will develop and demonstrate a 3rd-generation improved prototype e-Turbo design.
- Caterpillar will focus on engine testing of their complete electric turbocompound system.
- Hi-Z plans to accelerate quantum well development with the installation and startup of the 34-inch ID fabrication machine and test 2½-watt and larger modules.
- PNNL will develop $Si/Si_{0.8}Ge_{0.2}$ and B_4C/B_9C multilayer structures on non-crystalline substrates and conduct thermoelectric performance measurements up to 800ºC.

Off-Highway Vehicle Emission Control R&D

- DOE will award new cooperative agreements to improve the efficiency of off-highway engines while meeting future emission standards.
- General Electric will continue to develop advanced fuel injection system and combustion technologies for locomotive application.
- Cummins will develop technologies including engine and aftertreatment solutions to meet the Tier 4 emissions levels at Tier 3 fuel consumption levels.

- John Deere will switch to a 6.8-liter, more advanced diesel engine and reduce the NO_x from 4 to 2 g/kWh to meet the interim Tier 4 (2011) off-highway emission standards. The exhaust aftertreatment will be upgraded to the latest technology for better performance.
- The Electromotive Division of General Motors plans to complete the remaining single-cylinder engine tests and spray imaging experiments at Argonne National Laboratory, and computational fluid dynamics studies on cavitation at Wayne State University.
- ORNL (John Deere CRADA) plans to explore the potential for other NO_x reduction strategies to meet final Tier 4 NO_x and PM emissions, and conduct further urea-SCR studies to optimize NO_x conversion with selected injection control strategies for lower BSFC.

Honors and Special Recognitions

- Chris Powell, et. al, of ANL were awarded "Best Paper" for "Comparison of X-Ray Based Fuel Spray Measurements with Computer Simulation Using the CAB Model" presented at the ASME/CIMAC Congress 2004, Kyoto, Japan, June 2004.
- Chris Powell of ANL received an SAE "Excellence in Oral Presentation" award for presentation of a paper on spray research using x-ray radiography.
- Paul Miles received an SAE "Excellence in Oral Presentation" award for presentation of his paper on low-temperature automotive diesel combustion, SAE Paper 2004-01-1678, in March 2004.
- Paul Miles received a Sandia National Laboratories Employee Recognition Award for Individual Technical Excellence, June 2004, for his work on low-temperature automotive diesel combustion.
- Paul Miles and Richard Steeper of SNL were selected as Co-Vice-Chairs of Combustion for SAE's Fuels and Lubricants Activity.
- The Lawrence Livermore National Laboratory (LLNL) HCCI work was featured in the April 2004 issue of LLNL's "Science and Technology Review."
- Daniel Flowers of LLNL was quoted in the Wall Street Journal (September 28, 2004), discussing the potential benefits of HCCI engines.
- Daniel Flowers delivered an invited lecture at the SAE HCCI TopTech seminar, conducted in Berkeley, California, August 2004.
- John Dec was an invited speaker and panelist for an SAE panel discussion on HCCI at the 2003 SAE Fall Powertrain and Fluid Systems Conference, Pittsburgh, PA, October 2003.
- John Dec was an invited speaker at the SAE Homogeneous Charge Compression Ignition Symposium, Berkeley, CA, August 2004.
- John Dec was invited to present a keynote address on HCCI and advanced combustion at the 2004 SAE Fall Powertrain and Fluid Systems Conference, Tampa, FL, October 2004.
- The paper titled "Lattice-Boltzmann Diesel Particulate Filter Sub-Grid Modeling - a progress report", by George Muntean, D. Rector, D. Herling, D. Lessor and M. Khaleel of PNNL was selected for inclusion into SAE Transactions.
- A 2004 Advanced Combustion Engine R&D Special Recognition Award "For technical excellence and admirable collegiality in inter-laboratory collaborative research" was given to PNNL and ORNL for their work on emission controls for diesel-powered vehicles
- Peter Witze was given the SAE award for "Excellence in Oral Presentation" for his presentation at the SAE 2004 World Congress on high-energy, pulsed laser diagnostics for the measurement of diesel particulate matter.
- Stuart Daw, ORNL, and Dick Bint, GM were recipients of the annual DOE Advanced Combustion Engine Technical Achievement Award for their work in CLEERS.

- Robert Wagner received ORNL's Early Career Award for technical achievement and leadership in 2004.
- Dr. Johney B. Green, Jr., was recognized as one of the "50 Most Important Blacks in Research Science" for 2004. The selection was based on his contributions to automotive research and his highly visible role as a minority scientist and role model to students and others. The "50 Most Important" are featured in the September edition of Science Spectrum magazine.
- John Storey, ORNL, was an invited speaker at the Advanced Collaborative Emissions Study (ACES) Workshop.

Invention and Patent Disclosures

- U.S. Patent 6,736,106 awarded May 2004, "Engine Valve Actuation for Combustion Enhancement," R.D.Reitz, C.J. Rutland, R. Jhavar (University of Wisconsin).
- U.S. Patent 6,716,783 awarded April 6, 2004, "Catalysts for Lean Burn Engine Exhaust Abatement," K.C. Ott, N.C. Clark, M.T. Paffett. [LANL]
- "Novel Catalyst for Selective NO_x Reduction Using Hydrocarbons," C. L. Marshall and M. K. Neylon (European patent application WO 03/031781 A1; April 17, 2003).
- "Novel Catalyst for Selective NO_x Reduction Using Hydrocarbons," C. L. Marshall and M. K. Neylon (U.S. patent application 2003/0073566 A1; April 17, 2003).
- Patent application: "Catalyst and method for reduction of nitrogen oxides," Kevin C. Ott, DOCKET NUMBER: S-100,615. [LANL]
- "A New Concept and Catalysts for Lean-NO_x Reduction", J.-H. Kwak, J. Szanyi and C.H.F. Peden of PNNL (invention disclosure filed December 12, 2003).
- "Sulfur removal via flash separation for on-board fuel utilization," patent pending, May 2004, for the work of Darrell Herling, et.al., of PNNL.
- "Method of generating hydrocarbon oxygenates from diesel, natural-gas and other logistical fuels," patent pending, May 2004, for the work of Darrell Herling, et.al., of PNNL.
- Accelrys filed a provisional patent on 12/01/2003 for inventions that were created while developing the CombiMat 2.5 database. The provisional patent, titled "Method of storing fast throughput experimentation information in a database," refers to four inventions.
- A patent has issued for the oxygen sensor (US 6,592,731) and for the Combined Oxygen and NO_x Sensor (US 6,824,661).
- Portable LII Based Instrument and Method for Particulate Characterization in Combustion Exhaust; US patent No. 6,700,662 awarded to ANL.
- Patent awarded to Cummins Engine Company for an air/oil coalescer with improved centrifugally assisted drainage, Patent No. 6,640,792.
- Patent awarded to Cummins Engine Company for a valve train with a single camshaft, Patent No. 6,390,046.
- A patent has been allowed on a high-performance intake port invented by Charles Mendler. The port exhibits industry-leading flow values, which increases engine torque and reduces boost pressure requirements for engine down-sizing. The port was developed with funding from the U.S. Department of Energy. The publication number and date have not yet been issued.
- Patent application: "Boron carbide films and quantum well structure with improved thermoelectric properties," P. M. Martin and L. C. Olsen of PNNL.
- Patent application: "Integrated self-cleaning window assembly for optical transmission in combustion environments," Michael D. Kass and William P. Partridge Jr., DOE Invention DOCKET NUMBER: S-99,227 (ID1057). [ORNL]

The remainder of this report highlights progress achieved during FY 2004 under the Advanced Combustion Engine R&D Sub-Program. The following 59 abstracts of industry, university, and national laboratory projects provide an overview of the exciting work being conducted to tackle tough technical challenges associated with R&D of higher efficiency, advanced internal combustion engines for light-duty, medium-duty, and heavy-duty vehicles. We are encouraged by the technical progress realized under this dynamic Sub-Program in FY 2004, but we also remain cognizant of the significant technical hurdles that lie ahead, especially those to further improve efficiency while meeting the EPA Tier 2 emission standards and heavy-duty engine standards for the full useful life of the vehicles. In FY 2005, we look forward to working with our industrial and scientific partners to overcome additional barriers that hinder the wide-spread availability of high efficiency clean advanced internal combustion engines.

Gurpreet Singh
Team Leader,
Advanced Combustion Engine R&D
Office of FreedomCAR and Vehicle Technologies

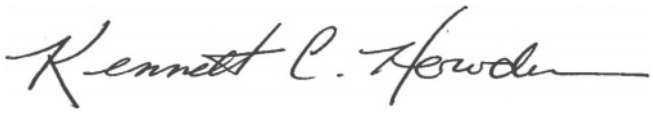

Kenneth Howden
Office of FreedomCAR and Vehicle Technologies

Kevin Stork
Office of FreedomCAR and Vehicle Technologies

John Fairbanks
Office of FreedomCAR and Vehicle Technologies

Roland Gravel
Office of FreedomCAR and Vehicle Technologies

II Advanced Combustion and Emission Control Research for High-Efficiency Engines

II.1 Stretch Efficiency in Combustion Engines with Implications of New Combustion Regimes

Ron Graves (Primary Contact), Stuart Daw, James Conklin, V. K. Chakravarthy
Oak Ridge National Laboratory
NTRC Site
2360 Cherahala Blvd.
Knoxville, TN 37932

DOE Technology Development Manager: Kevin Stork

Subcontractors:
University of Wisconsin, Madison, Wisconsin (Prof David Foster, Mr. Ben Druecke, Prof Sandy Klein)

Objectives

- Analyze and define specific pathways to improve the thermal efficiency of combustion engines from nominally 40% to as high as 60%, with emphasis on opportunities afforded by new low-temperature combustion regimes.
- Establish proof of principle of the pathways to stretch efficiency.

Approach

- Use literature study to reevaluate prior work on improving engine efficiency.
- Exercise appropriate engine models to define the greatest opportunities for further advancement. Develop improvements to those models as needed to address the features of low-temperature combustion. Conduct analyses from the perspective of the Second Law of Thermodynamics as well as the First Law so as to study the large losses inherent in conventional combustion.
- Design and conduct proof-of-principle experiments.

Accomplishments

- Reinforced that the internal combustion engine (ICE) maximum theoretical fuel efficiency approaches 100%, and that a key limiting factor is the high irreversibility in traditional premixed or diffusion flames. These losses, and those from heat transfer during combustion, are the largest losses from a Second Law analysis. The ICE is not a heat engine; hence, direct application of Carnot heat engine principles oversimplifies typical analyses.
- Developed a whitepaper that describes engine loss mechanisms and recommends research paths, and presented it to the FreedomCAR Advanced Combustion and Emission Control Tech Team.
- Initiated modeling and analysis activities at Oak Ridge National Laboratory (ORNL) and the University of Wisconsin to determine whether there are feasible methods to mitigate combustion losses, and to determine whether advanced combustion regimes such as homogeneous charge compression ignition (HCCI) have potential.
- Identified several conceptual pathways to mitigate the losses of thermodynamic availability (exergy) from traditional flames.

Future Directions

- Conduct analysis of data from advanced combustion experiments to determine efficiency implications.
- Develop a protocol to be used in engine experiments that will provide an understanding of where fuel efficiency is being gained/lost when parameters are varied.

- Continue exercising engine and combustion models to identify modifications to the combustion process that would mitigate losses.
- Model and analyze how advanced combustion processes can be best integrated with other engine features for stretching efficiency.

Introduction

Improving engine efficiency is best approached by understanding the losses, then developing ways to mitigate them. Various combinations of analysis and experiments are used in quantifying the thermodynamic losses in engines. A representative distribution of the total available fuel energy to these losses and to useful propulsion (brake) work is shown in Figure 1 [1]. Here we are utilizing a thermodynamic property, availability (or exergy), to study the losses because it gives deeper insight as to the loss mechanisms than a simple energy balance.

The conventional engine combustion process causes the largest losses, which are difficult to mitigate or even explain. These losses are not due to fuel that goes unburned, which is a very small loss. These losses don't even show up on simple "First Law" energy balances for engines. Combustion process losses are associated with the unrestrained chemical reaction of typical combustion processes, and this is where fuel cells gain an advantage over combustion engines. Typical combustion is highly irreversible in the thermodynamic sense and results in destruction of about 20% of the fuel's exergy potential. Most of this irreversibility is associated with so-called 'internal heat transfer' between the products and reactants. Such heat transfer is inevitable in both pre-mixed and diffusion flames,

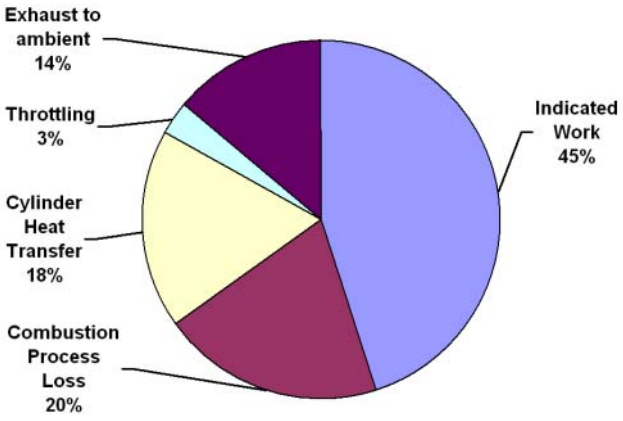

Figure 1. Distribution of Fuel Availability at Full Load, Simulation of Truck Diesel Engine [1]

where highly energetic product molecules are free to exchange energy with unreacted fuel and air molecules [2]. Since these molecules have large energy (i.e., temperature) differences, considerable entropy is generated when they interact. We depict this molecular entropy generation process schematically in Figure 2.

In general, the losses would be mitigated by having the reactions take place nearer equilibrium, bringing reactants to a state closer to the products, reversibly, and by reducing large gradients of temperature or species. These considerations suggest that combustion processes like homogeneous charge compression ignition (HCCI) or low-temperature combustion (LTC) may have some inherent features to reduce combustion reversibility.

Approach

A combination of analyses and experiments will be used to determine the type of engine combustion process that can be devised to reduce the availability destruction in conventional flames. Beginning with an extensive literature review, prior Second Law analyses of engine processes were reviewed for their treatment of this subject. Engine models will be acquired or developed that will perform Second Law calculations and allow introduction of new combustion submodels that address advanced combustion regimes. Commercial codes such as Ricardo WAVE and Gamma Technology GT Power are seen as adequate foundations for this work. Data from various LTC engine experiments at ORNL and elsewhere will be post-processed to determine the exergy losses in the combustion process. Some purposefully designed experiments are likely necessary. Universities will be engaged as appropriate to assist in the development of models and conduct of experiments.

Results

Our literature review of losses associated with typical engine combustion found consistent results that about 20% of the fuel potential is lost in

Table 1. Summary of ICE Efficiency Losses and Pathways to Recover Them

Loss Name	Loss mechanism, description	Potential to improve	Continuous Improvement Path	Breakthrough Path
Combustion process loss	Loss of chemical potential of fuel via unrestrained reaction, dissociation, internal mixing of hot and cool gases.	Large	Higher compression ratio, requiring development in several areas.	"New combustion regimes" dilute combustion with low peak temperatures, high expansion, increased reactant temperature. New thermodynamic strategies and fuel chemistry to lower the temperature of "reversible" combustion. May need variable fuel injection geometries. Methods for very high manifold pressure (boosting). Improved sensors and control methods. Compound compression and expansion cycles.
Exhaust losses	Pressure release and thermal energy.	Large	Miller cycle already has been in commercial use, turbocompounding in limited use in heavy duty diesels.	High expansion ratios achieved by valve timing, turbine expanders, etc. Thermoelectric generators. Lean-NO_x control allowing high compression ratio lean-burn and stratified charge engines. Compound compression and expansion cycles.
Heat transfer loss	Heat transferred to cylinder walls during combustion and expansion.	Large	Improved materials and cooling strategies	Lower temperature combustion, thermal barriers. Downsized engine (low combustion surface area)
Pumping losses	Pressure losses of air and combustion gases. Parasitic engine work to move air and expel combustion products.	Moderate	Improved air management in manifolds and valves.	Fast actuating valves. Improved turbo and air system. Lean-NO_x control to enable unthrottled engines. Variable displacement and compression ratio.
Mechanical friction	Basically rubbing losses.	Moderate	Improved designs for pistons and rings. Rolling contact cam followers in production. Low-friction lubes.	Electromechanical valve system. Lower friction materials and lubes. New component design or engine configuration.
Parasitic losses	Shaft work or fuel consumed to drive auxiliaries and regenerate aftertreatment devices.	Moderate	Electrification of pumps for variable speed and use-on-demand.	New combustion regimes that reduce emissions burden of aftertreatment. Lean-NO_x traps that operate near theorietical requirements of fuel penalty. Combustion regimes that require less fuel pumping

traditional flames. Reference 3 is a good resource for reviewing previous studies. While research and development into other loss mechanisms such as heat transfer and exhaust energy will be very important in improving engine efficiency, progress in reducing combustion irreversibility would be a tremendous and new contribution. A summary of engine losses and technology paths was developed to aid R&D planning for the FreedomCAR Advanced Combustion and Emission Control Tech Team and is shown in Table 1.

Our review also reinforced that the maximum theoretical efficiency of internal combustion engines is oftenunfairly understated by the incorrect application of the Carnot cycle limit. Conventional wisdom holds that internal combustion or reciprocating engines are "heat engines" and are bounded by the maximum theoretical heat engine

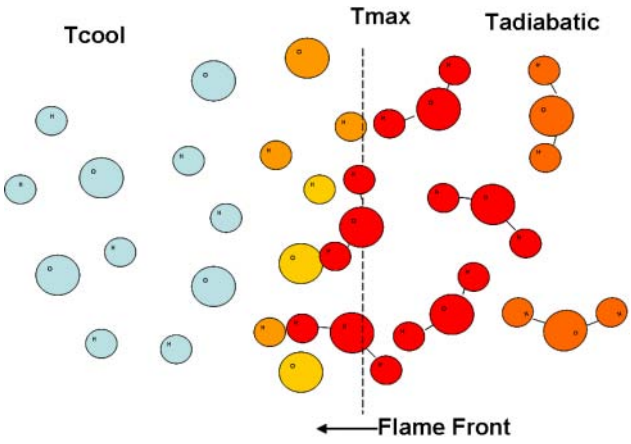

Figure 2. Schematic Depiction of Entropy Generation in a Flame Front (Extremely energetic product molecules dissipate their energy in collisions with surrounding molecules having much lower energy.)

efficiency, known as the Carnot limit. A heat engine, however, has a precise definition: it operates in a thermodynamic cycle, receives heat from a thermal reservoir, produces work from that heat, and rejects heat to a second thermal reservoir. The maximum theoretical efficiency ("Carnot efficiency") of a heat engine is directly related to the temperature difference between the source and sink reservoirs. An internal combustion engine is not a heat engine – there are no thermal reservoirs and the working fluid does not go through a cycle – and thus, its efficiency is not limited to the Carnot cycle efficiency. Moreover, it is widely known that reducing the combustion temperature (as in lean-burn conditions) can increase the engine efficiency, hence departing from the heat engine model. The prevailing notion that all internal combustion engines operate as heat engines in the Otto or Diesel cycle is a simplifying assumption that is useful in education and practical for simple analysis but not theoretically accurate. Both fuel cells and internal combustion engines are subject to the laws of thermodynamics, but neither is bound by the Carnot cycle efficiency. These arguments were articulated in a presentation at the 2004 Diesel Engine Emissions Reduction Conference [4] by Prof. David Foster.

It was recognized, however, that a key tradeoff exists in trying to achieve a more reversible combustion process. Typically, when we configure combustion to occur nearer to equilibrium, we shrink the affinity for reactions to take place and put power density at risk. Paths to mitigate combustion irreversibility were determined to include pre-heating of the reactants (if done reversibly) and better matching of work extraction rate to reaction rate. The latter concept would intuitively approach isothermal combustion.

Analysis of data from a diesel-based LTC experiment at ORNL was started. This engine experiment revealed the interesting situation where peak combustion temperatures were unquestionably lower than conventional due to 90% less NO_x, yet brake thermal efficiency did not decline. This highlights the need for coupling energy and exergy analyses with experiments to track where efficiency is being gained or lost. This will be increasingly important as more emphasis is returned to engine efficiency instead of emission control research, which has been heavily dominant.

The University of Wisconsin was awarded a subcontract to contribute to model development and to study the approach of matching rates of work extraction and combustion reactions. They started with an analysis of availability destruction and Second Law efficiency for constant pressure combustion of hydrogen, methane and octane. In this analysis, the combustion chamber was assumed to be a "black box" in which the properties at the inlet were known and the properties at the outlet were calculated assuming that the fuel-air mixture exited at equilibrium conditions. The purpose of this analysis was twofold. The first reason for this analysis was to compare total availability destruction and Second Law efficiency of octane with the results for hydrogen and methane provided in Dunbar and Lior [2]. The second reason was to provide a precursor to the future study of the distribution of the availability destruction into the underlying mechanisms including heat transfer, chemical reaction and mixing. The analytical results from the University of Wisconsin were very consistent with the earlier work, confirming that the analytical methods are suitable to be exercised further. A notable result is that the exergy destruction per mole of fuel is considerably less for hydrogen than for other fuels. This is consistent with the understanding that exergy destruction is reduced when combustion

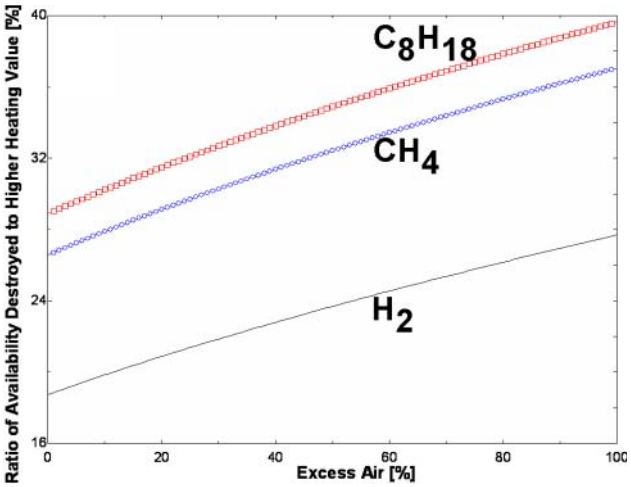

Figure 3. Ratio of Availability Destroyed to Higher Heating Value for Three Fuels at Various Levels of Excess Air

is occurring nearer equilibrium (high temperature) since hydrogen has the highest adiabatic flame temperature of the fuels studied. This is depicted in Figure 3.

Conclusions

- Internal combustion engines have theoretical potential energy conversion efficiency similar to fuel cells (i.e., > 90%).
- The main efficiency losses from current engines are due to combustion irreversibility and heat losses to the surroundings.
- Multiple studies agree that combustion irreversibility losses consume more than 20% of the available fuel energy and are a direct result of flame front combustion.
- The choice of fuel has impact on destruction of availability in combustion, with hydrogen being relatively efficient.
- The potential for volumetric combustion modes, such as HCCI, to reduce combustion irreversibility and wall heat loss has not yet been conclusively determined. Both theoretical and experimental studies focused on Second Law analysis are needed to resolve this issue.

FY 2004 Publications/Presentations

1. Foster, David E., "Are There Practical Approaches for Achieving the Maximum Theoretical Engine Efficiency?," DEER 2004, San Diego, CA, August 2004.
2. Graves, Ron and Murray, Al, "Internal Combustion Engine Efficiency Technology Strategy ('Strawman')," in draft, March 2004.

References

1. Primus, R.J., et al, "An Appraisal of Advanced Engine Concepts Using Second Law Analysis Techniques," Society of Automotive Engineers. SAE 841287, 1984.
2. Dunbar, W.R. and Lior, N., "Sources of Combustion Irreversibility," Combustion Science and Technology, 103, 41-61, 1994.
3. Caton, J.A., "A Review of Investigations Using the Second Law of Thermodynamics to Study Internal-Combustion Engines," Society of Automotive Engineers. SAE 2000-01-1081, 2000.
4. Foster, D.E., "Are There Practical Approaches for Achieving the Maximum Theoretical Engine Efficiency?," DEER 2004, San Diego, CA, August 2004.

II.A Combustion and Related In-Cylinder Processes

II.A.1 Light-Duty Diesel Spray Research Using X-Ray Radiography

Christopher F. Powell (Primary Contact), Jin Wang, Stephen Ciatti
Argonne National Laboratory
9700 S. Cass Ave.
Argonne, IL 60439

DOE Technology Development Manager: Kevin Stork

Objectives

- Study the mechanisms of spray atomization by making detailed, quantitative measurements in the near-nozzle region of sprays from light-duty diesel injectors.
- Perform these measurements under conditions as close as possible to those of modern diesel engines.
- Collaborate with modeling groups, providing them with the results of our unique measurements in order to advance the state of the art in spray modeling.

Approach

- Utilize our unique expertise in both spray measurement and x-ray physics to perform x-ray studies of sprays. Such studies allow quantitative measurements in the near-nozzle region of the spray that is inaccessible with other techniques.
- Measurements are performed at Argonne's Advanced Photon Source, a high-intensity x-ray source that allows us to make quantitative spray measurements with precise position and time resolution. Measurements must be relevant to the engine community while also being compatible with the existing facilities at the x-ray source. Currently, this limits us to performing spray measurements in static pressurized vessels at room temperature.
- Our measurements are designed to study the effects of several different injection parameters of interest to the engine community, such as orifice geometry, injection pressure, and ambient gas density. With our powerful measurement technique, we can quantify the effect of each of these variables on the structure of the spray.
- Using x-ray absorption, we can measure the instantaneous mass distribution of the fuel with very good position and time resolution. This is a unique and unambiguous observation of the structure of the spray. Measurements such as these provide a very stringent test of existing spray models and are crucial for the development of models with improved accuracy and predictive power.

Accomplishments

- Performed and published a series of measurements studying the effects of nozzle geometry on the structure of sprays. These measurements demonstrated for the first time that the x-ray technique can be useful for resolving subtle differences in the sprays based on the internal structure of the nozzle.
- Performed our first measurements at ambient pressures of 15 and 20 bar. This greatly expands our maximum achievable pressure and allows us to operate under ambient density conditions similar to those of a light-duty diesel engine under low-load conditions.
- Acquired a pressure vessel that allows measurements of multi-hole nozzles, and performed our first study of multi-hole valve-covering orifice (VCO) nozzles. This enables us to study nozzles identical to those used in real engines.

- Established a large number of new collaborations with both industrial and academic partners. These collaborations increase the relevance of our work and expand its impact by involving experts in the field from around the world.
- Continued our group's record of a large volume of high-quality publications. We published two peer-reviewed papers and four contributions to conference proceedings, and we presented our results at eight national and international meetings. The quality of this work has been recognized by our peers; one publication was awarded "Best Paper" at the American Society of Mechanical Engineers/International Council on Combustion Engines (ASME/CIMAC) conference, and one presentation received an SAE "Excellence in Oral Presentation" award.

Future Directions

- Increase the relevance of our measurements by studying sprays under conditions closer to those of modern diesel engines. We have made steady progress over the course of the project, continually increasing the ambient pressure and enabling the use of production nozzles. We will continue to pursue the goal of making measurements under conditions that are directly comparable to an operating engine.
- Increase the impact of our work by fostering collaboration with outside groups. Our collaborations with modeling groups allow our work to increase the fundamental understanding of the mechanics of the spray event, while our collaborations with industry enable us to develop a technique that is useful as a diagnostic for injection system manufacturers. Both of these expand the impact of our research and help to meet the Advanced Combustion Technologies Program objectives of decreased emissions and increased efficiency.
- Improve the measurement technique. While we are producing useful results today, improvements to the measurement technique will increase its applicability and accessibility in the future. Such improvements include faster data acquisition, processing, and analysis; improved x-ray detector systems; increased x-ray intensity; and greater automation.

Introduction

Fuel injection systems are one of the most important components in the design of combustion engines with high efficiency and low emissions. A detailed understanding of the fuel injection process and the mechanisms of spray atomization can lead to better engine design. This has spurred considerable activity in the development of optical techniques (primarily using lasers) for measurements of diesel fuel injection systems. Some of these optical techniques have become commercially available and can be readily applied to the testing and development of modern injection systems. Despite significant advances in laser diagnostics over the last 20 years, scattering of light from the large number of droplets surrounding the spray prevents penetration of the light and limits such measurements to the periphery of the spray. This is especially true in the near-nozzle region of the spray, which is considered to be the most important region for developing a comprehensive understanding of spray behavior. Existing models of spray structure have to date only been compared with data acquired in the region relatively far from the nozzle. It is unknown how well these models apply in the crucial near-nozzle region. The limitations of visible light in the near-nozzle region of the spray have led us to develop the x-ray absorption technique for the study of fuel sprays. X-rays are highly penetrative, and measurements are not complicated by the effects of scattering. The technique is non-intrusive, quantitative, highly time-resolved, and allows us to make detailed measurements of the spray, even in the dense droplet region very near the nozzle.

Approach

This project studies the sprays from commercially available light-duty diesel fuel injectors. Our approach is to make detailed measurements of the sprays from these injectors using x-ray absorption. This will allow us to make detailed measurements of the fuel distribution in these sprays, extending the existing knowledge into the near-nozzle region. The x-ray measurements

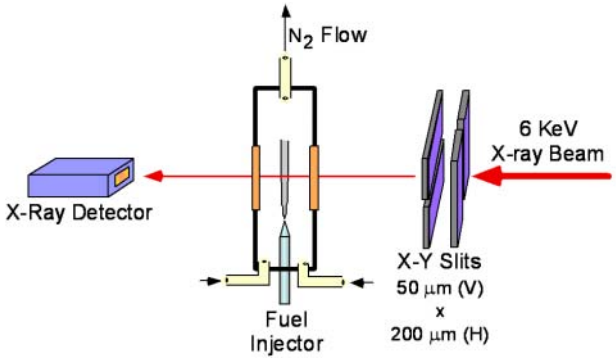

Figure 1. Schematic of the Experimental Setup

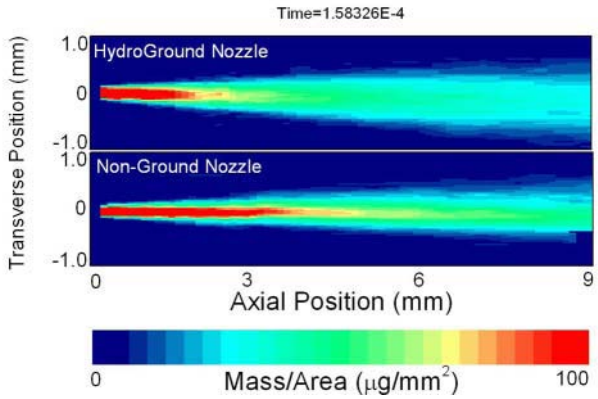

Figure 2. The Effects of Nozzle Geometry on the Structure of Sprays

were performed at the 1BM-C station of the Advanced Photon Source at Argonne National Laboratory. A schematic of the experimental setup is shown in Figure 1; detailed descriptions of the experimental methods are given in [1] and [2]. The technique is straightforward; it is similar to absorption or extinction techniques commonly used in optical analysis. However, the x-ray technique has a significant advantage over optical techniques in the measurement of sprays: because the measurement is not complicated by the effects of scattering, there is a simple relation between the measured x-ray intensity and the mass of fuel in the path of the x-ray beam. For a monochromatic (narrow wavelength bandwidth) x-ray beam, this relation is given by

$$I/I_0 = \exp(-\mu_M M)$$

where I and I_0 are the transmitted and incident intensities, respectively; μ_M is the mass absorption constant; and M is the mass of fuel. The constant μ_M is measured in a standard cell, and the incident and transmitted intensities are measured as a function of time by the x-ray detector. This allows direct determination of the mass of fuel at any position in the spray as a function of time. It is the goal of our work to use the x-ray technique to measure sprays from our light-duty fuel injector at different injection pressures, different ambient pressures, and using different nozzle geometries. This will enable us to quantify how each of these variables affects the structure of the spray. We will also collaborate with spray modelers to incorporate this previously unknown information about the near-nozzle region of the spray into new models. This will lead to an increased understanding of the mechanisms of spray atomization and will facilitate the development of fuel injection systems designed to improve efficiency and reduce pollutants.

Results

A series of x-ray measurements was performed on sprays from a common rail injector manufactured by Robert Bosch Corp. The effects of injection pressure, ambient pressure, and nozzle geometry were explored in these experiments. In previous years, the maximum ambient pressure attainable was 10 bar, and we were limited to performing experiments on single-hole research nozzles. In FY 2004, we were able to expand the scope of our measurements to include multi-hole nozzles and higher ambient pressures. We also established several new collaborations that greatly expand the impact of our work.

In Figure 2, the mass distributions are shown for two sprays from nozzles with different internal geometries; the measurement conditions are otherwise identical. The differences in structure between the sprays are clearly evident; the nozzle without hydrogrinding shows a narrower spray with a denser core extending farther from the nozzle. Such distinct features have never been measured previously in the near-nozzle region; they can provide a stringent test for models attempting to predict the flow of fuel through the nozzle. Researchers at the University of Massachusetts, Amherst have used the geometry of our nozzles to predict the fuel flow and its effect on the fuel distribution outside the nozzle [3]. These results demonstrated the applicability of our measurements

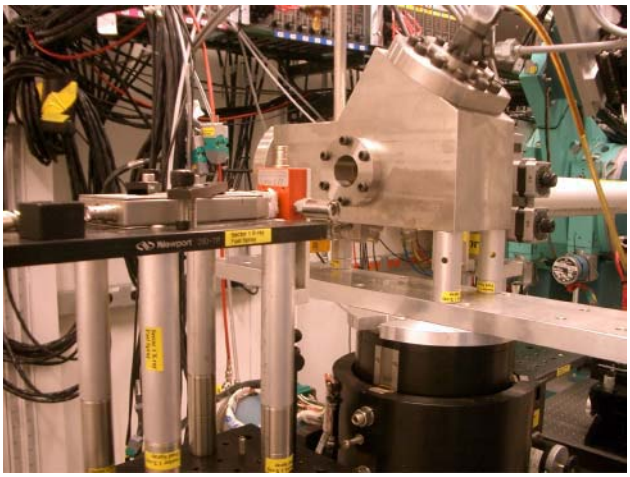

Figure 3. X-Ray Spray Chamber for the Study of Multi-Hole Nozzles

and showed the need for improved position resolution in our measurement technique.

FY 2004 marked the beginning of a long-term collaboration between Argonne, the Engine Research Center at the University of Wisconsin, and General Motors. This partnership proposed and received approval from Advanced Photon Source management for a three-year program of fuel spray studies. This partnership guarantees our group nine weeks of x-ray beam access per year for the next three years. This important achievement prevents us from having to go through the quarterly proposal/ approval cycle, enabling long-term planning for a fixed number of experiments. This partnership also constructed a pressure vessel designed to allow the testing of multi-hole nozzles. The vessel was funded by General Motors and built by the Engine Research Center with guidance from Argonne. The vessel is pictured in Figure 3. Our first experiment using this vessel studying multi-hole VCO nozzles was completed in FY 2004, and we have three weeks of beam time planned for this collaboration in FY 2005.

Figure 4 shows the mass distributions of sprays from the same injector at ambient pressures of 1, 10, and 15 bar at an equivalent penetration of 13 mm from the nozzle. The figure shows the effect that the increasing ambient pressure has on the mass distribution of the spray. As the pressure increases, the spray core shows less expansion perpendicular to the spray axis. This phenomenon has been observed

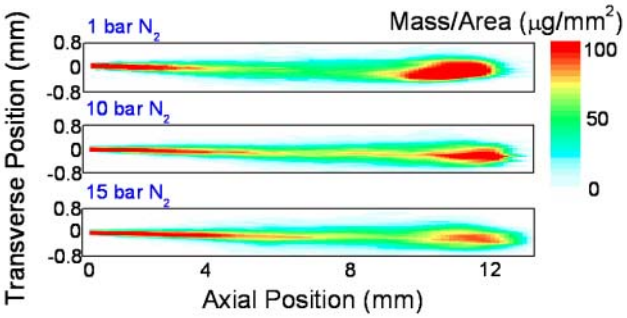

Figure 4. The Effects of Ambient Pressure on the Mass Distribution of the Spray

several times in x-ray experiments but runs contrary to the well-established expansion of the overall spray cone angle with increasing ambient pressure. This apparent contradiction was resolved in a recent publication in collaboration with modelers at Michigan Technological University, which showed that the discrepancy arises because of the fundamental differences between the x-ray and visible light measurements [4,5]. While the x-ray technique measures the fuel distribution of the spray core, visible light techniques are particularly sensitive to individual droplets at the periphery of the spray. Since current spray models have been developed primarily based on the results of visible light measurements, they may accurately simulate the outer regions of the spray while having little predictive power in the core region of the spray which contains the vast majority of the fuel. The quantitative data provided by the x-ray measurements can aid the development of models with the power to accurately simulate the entire spray over a broad range of conditions.

In addition to technical accomplishments, FY 2004 saw the establishment of a number of new collaborations with outside researchers. In addition to those mentioned above, new collaborations were established with Visteon Corp., Helsinki University of Technology, and Caterpillar. We also continued to work with several existing partners, including DaimlerChrysler, Robert Bosch, University of Colorado, and Wayne State University. This increasing list of collaborators keeps us connected to the world's experts in the field and focuses our research on the areas in which it will have the most impact.

Conclusions

- The x-ray technique can be used to observe subtle changes in the spray structure resulting from different nozzle geometries. These changes are not apparent using other imaging techniques. This may be a very useful diagnostic tool to fuel system manufacturers when designing and testing new injection systems.
- Significant differences were discovered in spray penetration and fuel distribution as a function of ambient gas pressure.
- The time-dependent mass measurements provide unique information to spray modelers and allow them to test their models in the near-nozzle region of the spray, something that was impossible previously. This data is crucial for the development of accurate spray models and for the detailed understanding of spray behavior. The quantitative measurements that we have provided may help to elucidate the mechanisms of spray atomization. This could ultimately lead to the design of cleaner, more efficient engines.

Special Honors

1. Chris Powell, et. al, were awarded "Best Paper" for "Comparison of X-Ray Based Fuel Spray Measurements with Computer Simulation Using the CAB Model" presented at the ASME/CIMAC Congress 2004, Kyoto, Japan, June 2004.
2. Received an SAE "Excellence in Oral Presentation" award.

FY 2004 Publications/Presentations

1. "X-Ray Absorption Measurements of Diesel Sprays and the Effects of Nozzle Geometry," C. F. Powell, S. A. Ciatti, S. –K. Cheong, J. Liu, J. Wang, Society of Automotive Engineers, Paper 2004-01-2011.
2. "Dynamics of Diesel Fuel Sprays Studied by Ultra-Fast X-Radiography," S. –K. Cheong, J. Liu, J. Wang, C. F. Powell, S. A. Ciatti, Society of Automotive Engineers, Paper 2004-01-2026.
3. "Analysis of X-Ray-Based Computer Simulations of Diesel Fuel Sprays," F. X. Tanner, K. A. Feigl, S. A. Ciatti, C. F. Powell, S. -K. Cheong, J. Liu, J. Wang., 17th Annual Conference on Liquid Atomization and Spray Systems, May 2004.
4. "Comparison of X-Ray Based Fuel Spray Measurements with Computer Simulation Using the CAB Model," S. A. Ciatti, C. F. Powell, S. –K. Cheong, J. Y. Liu, J. Wang, F. X. Tanner, CIMAC/ ASME Congress 2004; Kyoto, Japan; June 2004.
5. Presentation at DOE National Laboratory Advanced Combustion Engine R&D Merit Review and Peer Evaluation, Argonne National Laboratory, May 2004.
6. "X-Ray Characterization of Diesel Sprays and the Effects of Nozzle Geometry," C. F. Powell, S.-K. Cheong, S. A. Ciatti, J. Liu, J. Wang, DEER Conference, San Diego, CA, August 2004.

References

1. C. F. Powell, Y. Yue, R. Poola, and J. Wang, J. Synchrotron Rad. 7:356-360 (2000).
2. C. F. Powell, Y. Yue, R. Poola, J. Wang, M.-C. Lai, J. Schaller, SAE 2001-01-0531, (2001).
3. D. P. Schmidt and S. Gopalakrishnan, 17th Annual Conference on Liquid Atomization and Spray Systems, Arlington, VA, May 2004.
4. "Analysis of X-Ray-Based Computer Simulations of Diesel Fuel Sprays," F. X. Tanner, K. A. Feigl, S. A. Ciatti, C. F. Powell, S. -K. Cheong, J. Liu, J. Wang., 17th Annual Conference on Liquid Atomization and Spray Systems, May 2004.
5. "Comparison of X-Ray Based Fuel Spray Measurements with Computer Simulation Using the CAB Model," S. A. Ciatti, C. F. Powell, S. –K. Cheong, J. Y. Liu, J. Wang, F. X. Tanner, CIMAC/ ASME Congress 2004; Kyoto, Japan; June 2004.

II.A.2 X-Ray Studies of Heavy-Duty Injector Spray Characteristics

Christopher F. Powell (Primary Contact), Seong-Kyun Cheong, Sreenath Gupta, Essam El-Hannouny, Jin Wang
Argonne National Laboratory
9700 S. Cass Ave.
Argonne, IL 60439

DOE Technology Development Manager: Kevin Stork

Objectives

- Study the mechanisms of spray atomization by making detailed, quantitative measurements in the near-nozzle region of sprays from heavy-duty injectors.
- Provide near-nozzle data that is crucial for the development of accurate spray models.
- Compare the data measured using the x-ray technique with existing data measured using conventional techniques at Sandia National Laboratory.

Approach

- Build a laboratory fuel injection system that is compatible with the x-ray technique based on the design of the existing system at Sandia.
- Test the fuel system for proper operation using visible light imaging techniques.
- Perform x-ray measurements of the fuel sprays generated from several different injector nozzle geometries at several ambient pressures.

Accomplishments

- The fuel system was constructed and the first x-ray measurements were completed in FY 2003. In these studies, we measured the time-resolved mass distribution of sprays from three different nozzle geometries at atmospheric pressure.
- A series of conventional measurements was performed in FY 2004 on the same three nozzles, including rate-of-injection measurements and visible light imaging.
- Two weeks of x-ray experiments were completed in FY 2004. These experiments studied the effects of elevated ambient pressure and injection pressure on the sprays from two different nozzles.
- A collaboration was established between the researchers at Argonne and a modeling group at Helsinki University of Technology.

Future Directions

- Analysis of the measurement results is continuing. Initial results have shown significant differences in the fuel distribution of the sprays at different ambient pressures. Publication of this work is expected in early 2005 and will include the measurement results, comparisons with the conventional spray measurements performed at Sandia, and modeling results from Helsinki University.
- Measurements of the Detroit Diesel heavy-duty injector have been completed, and the funding has been shifted to the X-Ray FuelSpray project and the Caterpillar Cooperative Research and Development Agreement (CRADA). Further x-ray measurements of sprays from heavy-duty injectors will be part of the Caterpillar CRADA and will be performed on modern Caterpillar injection systems.

Introduction

Fuel injection systems are one of the most important components in the design of combustion engines with high efficiency and low emissions. A detailed understanding of the fuel injection process and the mechanisms of spray atomization can lead to better engine design. This has spurred considerable activity in the development of optical techniques (primarily using lasers) for measurements of diesel fuel injection systems. Some of these optical techniques have become commercially available and can be readily applied to the testing and development of modern injection systems. Despite significant advances in laser diagnostics over the last 20 years, scattering of light from the large number of droplets surrounding the spray prevents penetration of the light and limits such measurements to the periphery of the spray. This is especially true in the near-nozzle region of the spray, which is considered to be the most important region for developing a comprehensive understanding of spray behavior. Existing models of spray structure have to date only been compared with data acquired in the region relatively far from the nozzle. It is unknown how well these models apply in the crucial near-nozzle region. The limitations of visible light in the near-nozzle region of the spray have led us to develop the x-ray absorption technique for the study of fuel sprays. X-rays are highly penetrative, and measurements are not complicated by the effects of scattering. The technique is non-intrusive, quantitative, highly time-resolved, and allows us to make detailed measurements of the spray, even in the dense droplet region very near the nozzle.

Approach

This project utilizes a heavy-duty fuel injector designed and built as a prototype by Detroit Diesel Corp. with specially-fabricated single-hole nozzles. The injector and nozzles are similar to those which have been studied at Sandia National Laboratory over a wide range of conditions using a number of different measurement techniques [1,2,3]. Our approach is to make detailed measurements of the sprays from this injector using the x-ray technique. This will allow us to compare the x-ray results with the large body of existing data, and extend the existing knowledge into the near-nozzle region. The

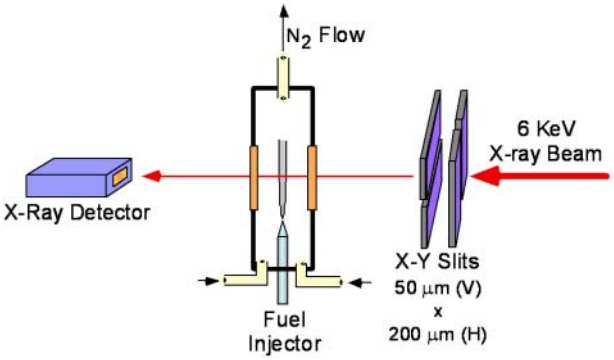

Figure 1. Schematic of the Experimental Setup

x-ray measurements were performed at the 1BM-C station of the Advanced Photon Source at Argonne National Laboratory. A schematic of the experimental setup is shown in Figure 1; detailed descriptions of the experimental methods are given in [4] and [5]. The technique is straightforward; it is similar to absorption or extinction techniques commonly used in optical analysis. However, the x-ray technique has a significant advantage over optical techniques in the measurement of sprays: because the measurement is not complicated by the effects of scattering, there is a simple relation between the measured x-ray intensity and the mass of fuel in the path of the x-ray beam. For a monochromatic (narrow wavelength bandwidth) x-ray beam, this relation is given by

$$I/I_0 = \exp(-\mu_M M)$$

where I and I_0 are the transmitted and incident intensities, respectively; μ_M is the mass absorption constant; and M is the mass of fuel. The constant μ_M is measured in a standard cell, and the incident and transmitted intensities are measured as a function of time by the x-ray detector. This allows direct determination of the mass of fuel at any position in the spray as a function of time. It is the goal of our work to use the x-ray technique to measure sprays from our heavy-duty fuel injector at different injection pressures, different ambient pressures, and using different nozzle geometries. Our work will be compared to the existing data that has been acquired by Sandia National Laboratory using a similar injection system. This will allow us to extend the Sandia database into the region very near the nozzle, and we will be able to determine whether

parameterizations that have been developed based on the Sandia data apply in this region. We will also collaborate with spray modelers to incorporate this previously unknown knowledge of the near-nozzle region of the spray into new models. This will lead to an increased understanding of the mechanisms of spray atomization and will facilitate the development of fuel injection systems designed to improve efficiency and reduce pollutants.

Results

A series of x-ray and conventional measurements was performed on sprays from a prototype common rail injector manufactured by Detroit Diesel Corp. The effects of injection pressure, ambient pressure, and nozzle geometry were explored in these experiments. In FY 2003, we constructed the fuel system and performed a series of x-ray measurements at ambient pressure. In FY 2004, we performed a broader series of measurements designed to study the sprays under a variety of different conditions.

Optical imaging was used to measure the overall spray shape, spray penetration and spray cone angle. These measurements demonstrated the correct performance of the injection system and allow comparison to similar measurements made in the past at Sandia. The nozzle diameter had a strong effect on the spray penetration and angle, as expected from the Sandia work. Additional optical imaging was performed using a microscopic lens, allowing a detailed measurement of the spray boundaries and shape. These images were compared to the images generated from the x-ray measurements; the two techniques showed good agreement in the near-nozzle region.

Another series of conventional spray measurements was made using the Bosch rate-of-injection (ROI) meter. This measurement is the industry standard for determining the fuel flow rate and the overall quantity of fuel injected. These measurements showed good agreement with the momentum method used at Sandia. Also, the mass flow measured in this way can be compared to the mass measurements made using the x-ray absorption method.

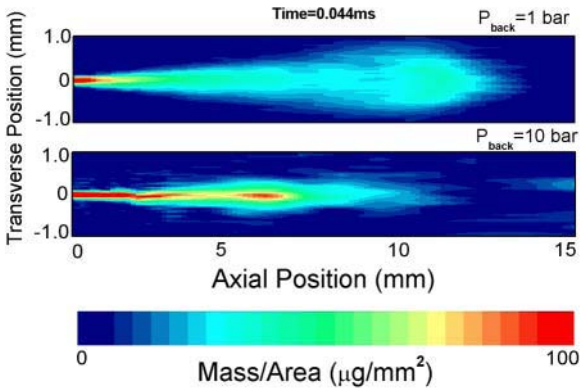

Figure 2. X-ray Image Reconstructions Showing the Effect of Ambient Pressure on the Spray

X-ray measurements were performed on three different nozzles under otherwise identical conditions. The first nozzle had an orifice diameter of 180 μm and orifice length-to-diameter ratio (L/D) equal to four, the second had a diameter of 250 μm and L/D = 4, while the third had a diameter of 250 μm and L/D = 8. The measurements were made at injection pressures of 1000 and 1500 bar, the spray duration was 2.5 ms, and the ambient gas was N_2 at room temperature and pressures of 1 and 10 bar.

The x-ray technique was able to probe the dense region of the spray as close as 0.2 mm (<1.5 nozzle diameter) from the nozzle. Moreover, the x-ray technique provided a quantitative mapping of the mass distribution in two dimensions, which can be used to estimate the volume fraction of the spray as a function of time and space. Several interesting features were observed in the measurements of these nozzles. An interesting breakup process in the high mass density region was observed near the beginning of the injection event between ~ 22-26 s after the start of injection. It was also observed that increasing the ambient pressure from 1 to 10 bar resulted in a narrower and shorter spray than that observed with 1 bar backpressure before 50 s after start of injection (see Figure 2). Later in the spray event, the cone angle at 10 bar ambient pressure gets wider than the spray measured at 1 bar.

All of the measurements made using the x-ray technique are made as a function of time. This allows the dynamic features of the sprays to be

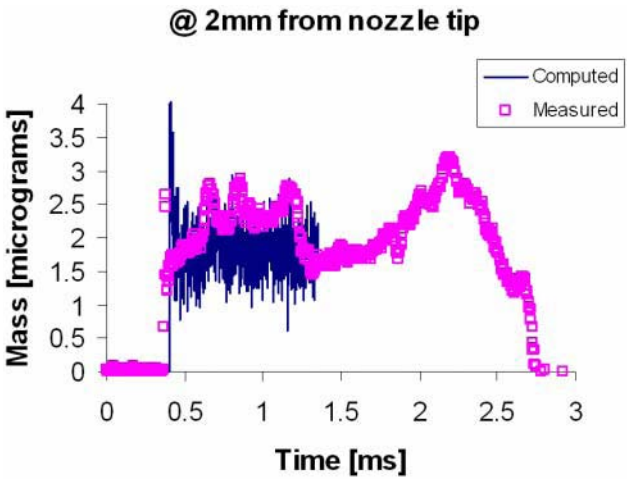

Figure 3. Preliminary Results Comparing the Mass Versus Time Measured Using X-rays and Calculated Using STAR-CD

studied and compared. Changes in the mass flux through the beam were observed as the probe was moved farther from the nozzle. The time-resolved mass 0.2 mm away from the nozzle was nearly flat, while fluctuations developed in the measured mass flux further downstream. This indicates that some physical effect is causing fluctuations to develop in the mass versus time as the spray moves away from the nozzle, and that this is taking place external to the nozzle. Several possible mechanisms could cause this behavior, including air entrainment, variations in speed along the spray axis, and transverse motion of the fuel. Careful theoretical modeling may be able to reproduce the features shown in these plots and would be an important development in the study of the mechanisms of spray atomization.

One very important accomplishment in FY 2004 was the establishment of a collaboration between Argonne and a modeling group at the Helsinki University of Technology. The group from Helsinki has been provided with the results of our measurements and is attempting to reproduce them with modeling using STAR-CD. Preliminary results of the measured and calculated mass flux through the x-ray beam are shown in Figure 3; a full publication of these results is expected in early 2005. This modeling collaboration will increase the impact of our work, since our measurements provide unique information on the structure of sprays that is extremely valuable to modelers.

Conclusions

- Testing has shown that the fuel system which we designed and built is operating as expected and is also compatible with measurements using the x-ray technique.
- The x-ray technique can be used to observe subtle changes in the spray structure resulting from different nozzle geometries. These changes are not apparent using other imaging techniques. This may be a very useful diagnostic tool to fuel system manufacturers when designing and testing new injection systems.
- The time-dependent mass measurements provide unique information to spray modelers and allow them to test their models in the near-nozzle region of the spray, something that was impossible previously. This data is crucial for the development of accurate spray models and for the detailed understanding of spray behavior. The quantitative measurements that we have provided may help to elucidate the mechanisms of spray atomization. This could ultimately lead to the design of cleaner, more efficient engines.

FY 2004 Publications/Presentations

1. "Near-Nozzle Spray Characteristics of Heavy-Duty Diesel Engine", Essam M. EL-Hannouny, Sreenath Gupta, Christopher F. Powell, Seong-Kyun Cheong, Jinyuan Liu, Jin Wang and Raj R. Sekar, SAE, 2003-01-3150.
2. Presentation at DOE National Laboratory Advanced Combustion Engine R&D Merit Review and Peer Evaluation, Argonne National Laboratory, May, 2004.
3. "X-Ray Measurements on Near-Nozzle Spray for Heavy-Duty Diesel Injectors", poster at the DOE National Laboratory Advanced Combustion Engine R&D Merit Review and Peer Evaluation, Argonne National Laboratory, May, 2004.
4. "Lagrangian Diesel Spray Modeling and Near Nozzle X-Ray Measurements", Ari Saarinen, Essam El-Hannouny, and Sreenath Gupta, SAE 2005, to be published.

References

1. D. L. Siebers, SAE 980809, (1998).
2. J. D. Naber and D. L. Siebers, SAE 960034, (1996).

3. B. S. Higgins, C. J. Mueller, and D. L. Siebers, SAE 1999-01-0519, (1999).
4. C. F. Powell, Y. Yue, R. Poola, and J. Wang, J. Synchrotron Rad. 7:356-360 (2000).
5. C. F. Powell, Y. Yue, R. Poola, J. Wang, M.-C. Lai, J. Schaller, SAE 2001-01-0531, (2001).

II.A.3 Low-Temperature Automotive Diesel Combustion

Paul Miles
Sandia National Laboratories, MS9053
P.O. Box 969
Livermore, CA 94551-0969

DOE Technology Development Manager: Kevin Stork

Subcontractors:
University of Wisconsin, Madison, Wisconsin
Wayne State University, Detroit, Michigan

Objectives

- Provide the physical understanding of the in-cylinder combustion processes needed to meet future diesel engine emissions standards while retaining the inherent efficiency and low CO_2 emissions of the direct-injection diesel engine.
- Improve the multi-dimensional models employed in engine design and optimization and validate the model predictions against in-cylinder measurements and tailpipe emissions.
- Investigate the effects of various combustion system parameters on engine performance and emissions, thereby generating a knowledge base for optimization efforts.

Approach

- Obtain measurements of flow and thermophysical properties in an optically-accessible engine using laser-based measurement techniques.
- Measure engine performance, fuel economy, and emissions in a non-optical test engine with the identical geometry.
- Compare in-cylinder measurements and engine emissions and performance to model predictions.
- Refine and improve models and engine operating strategies.

Accomplishments

- Experimentally evaluated a late-injection, low-temperature diesel combustion regime for a wide variety of system parameters, including injection pressure, swirl ratio, O_2 concentration (exhaust gas recirculation rate), start of injection (SOI), and intake temperature. Identified optimum swirl level and rate-limiting factors at various stages of the combustion process.
- Identified the formation of large-scale, mixing-enhancing flow structures as a dominant factor responsible for accelerated late-cycle heat release.
- Constructed a phenomenological picture of the progression of this low-temperature combustion regime in the equivalence ratio-temperature (ϕ-T) plane.
- Analyzed an extensive set of in-cylinder velocity data obtained at various engine speeds, measurement locations, and swirl ratios to establish a data base for comparison with model predictions of the turbulent stresses. Performed a detailed comparison with predictions obtained using the industry standard k-ε model.

Future Directions

- Evaluate alternative low-temperature combustion systems and identify the rate-limiting factors that prevent their application over a wider speed/load range.
- Investigate the mixture formation process in early-injection combustion systems, and evaluate the potential of in-cylinder fluid mechanical process to improve the mixture preparation process.
- Analyze the performance of more advanced turbulence models, including their influence on the prediction of large-scale flow structures, turbulence energy, and anisotropy. Emphasis will be placed on models which utilize minimal computing resources.

Introduction

Direct-injection diesel engines have the highest fuel efficiency and the lowest CO_2 emissions of any reciprocating internal combustion engine technology. This efficiency comes at the cost, however, of NO_x and particulate matter (soot) emissions, which are high in relation to future emission standards. Reduction of these emissions through clean in-cylinder combustion processes is imperative if vehicles powered by these engines are to be available at a competitive cost. Recently, the potential of low-temperature combustion (LTC) regimes to dramatically reduce NO_x and soot emissions has been demonstrated. A key aspect of many LTC systems is reliance on high levels of exhaust gas recirculation (EGR). High EGR levels reduce in-cylinder O_2 concentrations to achieve low combustion temperatures, thereby requiring that a greater mass of ambient fluid be rapidly mixed with the fuel than is needed for conventional diesel combustion. Other LTC systems rely on extensive pre-mixing to overall fuel-lean conditions prior to ignition. In both cases, mixing processes are central to the success of the combustion strategy.

Identifying those aspects of the LTC processes which are dominated by mixing processes, understanding the relevant physics controlling these processes, and developing a predictive modeling capability are thus crucial steps toward the development and optimization of low-emission, fuel-efficient engines utilizing low-temperature combustion systems. Each of these components is represented in the research described below.

Approach

The research approach involves three parallel efforts in a closely coordinated project. Detailed flow and thermochemical property measurements are made in an optically-accessible laboratory test engine; emissions, performance and fuel consumption measurements are made in a traditional single-cylinder test engine; and computer simulations are performed and compared to the data obtained in both the optical and traditional test engines. Natural synergies emerge among these three efforts. For example, detailed measurements of the flow variables permit the evaluation and refinement of the computer models, while the model results can be used to clarify the flow physics—a process that is difficult if only limited measurements are employed. Similarly, traditional test engine measurements serve to identify interesting operating parameter trade-offs that bear further investigation either numerically or experimentally in the optical engine.

Results

The optically-accessible diesel engine facility is depicted in Figure 1. This facility employs a slotted, extended piston assembly with a quartz combustion chamber that permits the progress of combustion to be visualized from below. In addition, the upper region of the cylinder liner is equipped with quartz windows that allow a lateral view of the combustion process to be obtained. This lateral view capability, in a configuration that faithfully maintains the combustion chamber geometry, is a unique aspect of this facility. The engine bowl geometry, bore, stroke, and fuel injection equipment are typical of state-of-the-art direct-injection diesel engines for passenger car applications. Variable cylinder swirl levels can be achieved through throttling of one of the intake ports.

A major thrust of the research performed in FY 2004 was directed towards obtaining a better understanding of late-injection low-temperature

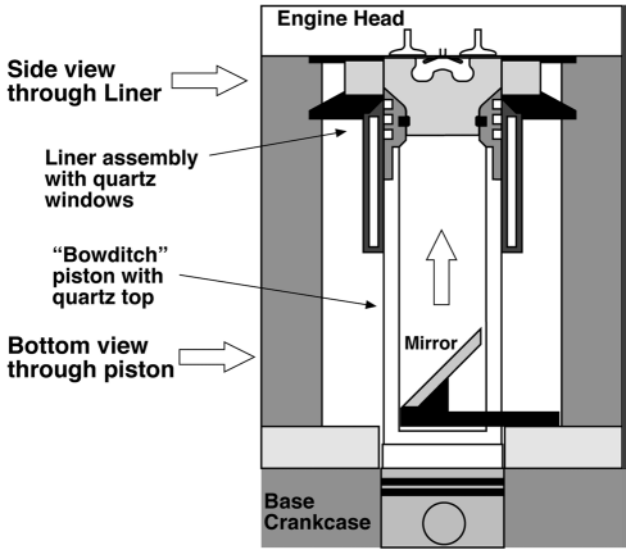

Figure 1. Schematic view of the optical engine, depicting the quartz piston top with a realistic combustion chamber geometry.

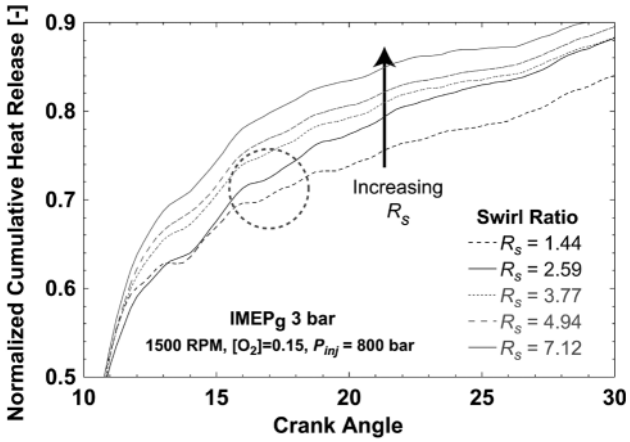

Figure 2. Variation in the cumulative apparent heat release with flow swirl. Accelerated heat release for R_s = 2.59 as compared to R_s = 1.44 (indicated by the dashed circle) corresponds to the formation of the flow structures seen in Figure 3.

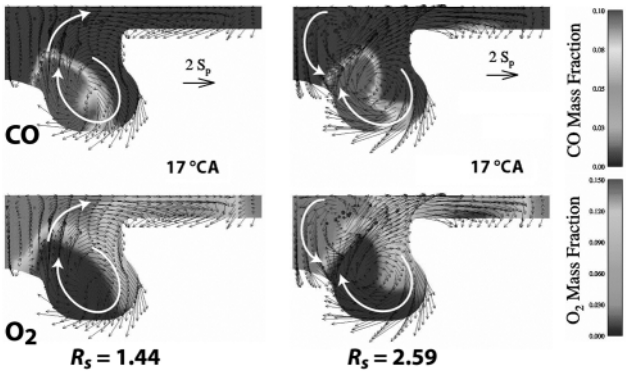

Figure 3. Flow structures formed in the mixing-controlled portion of the combustion process. The double-vortex structure seen for R_s = 2.59 is believed to be the dominant factor responsible for the increased heat release rate observed in Figure 2.

combustion systems, similar to the Nissan "MK"[1] or AVL "HPLI"[2] systems. In these systems, late-cycle mixing processes are key to obtaining acceptable emissions and retaining good fuel economy. Enhanced swirl is one method employed to increase the late-cycle mixing rates. Figure 2 shows the variation in the cumulative apparent heat release as swirl is increased for a typical LTC operating condition. From the divergence of the curves beyond approximately 11 °CA, it is clear that the apparent heat release rate increases with increased swirl. Numerical simulations indicate that this is not associated with increased heat transfer, but rather with increased chemical heat release associated with higher mixing rates. Through examination of the spatial distribution of the unburned fuel and air in the combustion chamber, the probable source of this increased mixing can be identified.

In-cylinder flow fields and distributions of CO and air are shown in Figure 3. The CO serves to mark the locations of the partially-oxidized products of rich combustion produced during the earlier part of the combustion event. The crank angle shown, 17 °CA, is typical of the period during which the cumulative heat release curves (see Figure 2) are diverging rapidly for the two swirl levels shown, R_s=1.44 and 2.59. At the lower swirl ratio, the flow structure in the vertical plane is characterized by a single dominant vortex. Fuel and air thus "follow" each other around the combustion chamber and are only mixed by the random turbulent motions superimposed on the mean flow structure shown. In contrast, at the higher swirl ratio, a double-vortex mean flow structure is formed which greatly enhances the mixing process. The lower vortex transports the partially-burned fuel to an interfacial region which is simultaneously being fed fresh air by the upper vortex. At the interface, high turbulence levels are also generated by sharp gradients in swirl

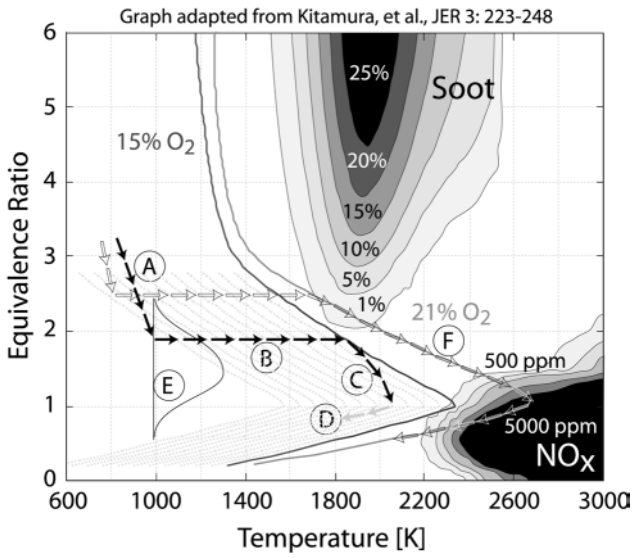

Figure 4. Equivalence ratio-temperature map illustrating the zones of formation of both soot and NO_x, as well as the approximate path taken by a "typical" fuel element during a late-injection low-temperature combustion event.

velocity and by vertical-plane flow deformation associated with the counter-rotating vortices.[3] The bulk transport of fuel and air to a common interface, coupled with high turbulence levels at the interface, results in significantly increased mixing rates. At the higher swirl levels (e.g. R_s=3.77), this interface forms earlier.

A series of tests involving variable swirl ratio, engine speed, injection pressure, SOI, and intake temperature was conducted to better understand the rate-limiting processes that prevent the application of late-injection LTC systems to a wider speed and load range. To illustrate the progress of the combustion event, it is helpful to follow the path of a "typical" fuel element as combustion proceeds (Figure 4). Initially, the fuel and air are premixed near-adiabatically in mixing processes that are dominated by the injection event (path A), resulting in a range of mixture equivalence ratios just prior to ignition, as indicated by the distribution (E). Thermodynamic analysis and in-cylinder soot formation suggest that the mean equivalence ratio of the mixture at ignition is between 1 and 2, and that a significant fraction of the fuel can be found in mixtures with equivalence ratios greater than 2. Ignition and combustion of this mixture are indicated by the idealized path (B), which represents chemical reaction occurring over a short period in which additional mixing is small. This path ends near the adiabatic flame temperature characteristic of the mixture composition prior to ignition, which is indicated by the dark line labeled "15% O_2." The majority of the soot is likely formed near the end of path (B). From this point on, the combustion is limited by mixing (C), much like conventional diesel combustion (F). If the combustion proceeded at constant volume, path (C) would closely follow the adiabatic flame temperature curve. However, due to cylinder volume expansion, the gases are cooling and path C bends downward. Completing the mixing process before falling temperatures quench chemical reaction is critical to the successful application of this LTC system. Even after combustion is complete, additional mixing (D) can be beneficial as it represents a path away from the high temperatures characteristic of NO_x production.

Conclusions

- Mixing rates in the late-cycle period can be significantly enhanced by bulk flow structures that transport fuel and air to a common interface.
- An analysis of the progression of low-temperature, late-injection combustion systems indicates that the late-cycle mixing process is critical to obtaining good fuel economy and low emissions of CO and unburned hydrocarbons.
- The flow development is a multifaceted process involving mutual interactions between intricate combustion chamber geometry, high-pressure sprays, and a complex flow structure. Development of an economical, accurate numerical simulation capability will be key to optimizing low-emission diesel engines of the future.

Special Recognitions & Awards/Patents Issued

1. SAE Award for Excellence in Oral Presentation, for presentation of SAE Paper 2004-01-1678, March 2004.
2. Sandia National Laboratories Employee Recognition Award for Individual Technical Excellence, June 2004.

3. Paul Miles of Sandia National Laboratories was selected as Co-Vice-Chair of Combustion for SAE's Fuels and Lubricants Activity.

FY 2004 Additional Presentations

1. Miles PC. "Low-Temperature Engine Combustion: New Challenges for In-Cylinder Mixing," Keynote address, CECOST and Energy Related Fluid Mechanics Annual Seminar, Gothenburg, Sweden, November 2003.
2. Miles, PC. "Turbulent Flow Structure Development in HSDI Diesel Engines," Invited Seminar, Volvo Car & Volvo Technology Corporation, Gothenburg, Sweden, November 2003.
3. Choi, D. "Heat Release Analysis and Imaging of Combustion Luminosity for MK-like Combustion," DOE OFCVT Advanced Engine Combustion Meeting, Livermore, CA, January 2004.
4. Miles PC. "Recent Progress in the HSDI Diesel Engine Laboratory," DOE OFCVT Advanced Engine Combustion Meeting, Livermore, CA, January 2004.
5. Miles PC. "Engine Turbulence Modeling Support at Sandia National Laboratories" & "Mixing Processes in Swirl-Supported Diesel Engines," Invited Seminars, General Motors Powertrain and R&D, February 2004.
6. Miles PC. "Automotive Low-Temperature Combustion Research," DOE OFCVT Advanced Engine Combustion Peer Review, Argonne, IL, May 2004.
7. Miles PC. "Identification of Dominant Turbulence Generation Mechanisms in Bowl-in-Piston Combustion Chambers," DOE OFCVT Advanced Engine Combustion Meeting, Southfield, MI, June 2004.

FY 2004 Publications

1. Miles PC. "In-Cylinder Turbulent Flow Structure in Direct-Injection, Swirl-Supported Diesel Engines," Ch. 1 in Flow and Comb. in Automotive Engines, C. Arcoumanis, ed. Springer-Verlag, 2004. (*Invited book chapter, final version submitted)*
2. Miles PC, Choi D, Megerle M, RempelEwert BH, Reitz RD, Lai MC, Sick V. "The Influence of Swirl Ratio on Turbulent Flow Structure in a Motored HSDI Diesel Engine –A Combined Experimental and Numerical Study," SAE Paper No. 2004-01-1678, 2004. Also presented at the 2004 SAE World Congress, March 2004. *(Selected for inclusion in 2004 SAE Transactions)*
3. Choi D, Miles PC. "A Parametric Study of Low-Temperature, Late-Injection Combustion in an HSDI Diesel Engine," Paper presented at the 6th Intl. Symp. on Diagnostics and Modeling of Combustion in IC Engines: COMODIA 2004. August 2-5, Yokohama, 2004.
4. Miles PC, Choi D, Pickett LM, Singh IP, Henein N, RempelEwert BH, Yun H, Reitz RD. "Rate-Limiting Processes in Late-Injection, Low-Temperature Diesel Combustion Regimes," Paper presented at Thermo- and Fluid-Dynamic Processes in Diesel Engines: THIESEL 2004. September 8-10, Valencia, 2004.
5. Miles PC. "Light-Duty (Automotive) Diesel Combustion," DOE OFCVT Annual Report, 2003.
6. Zhong L, Henein NA, Bryzyk W. "Effect of Smoothing the Pressure Trace on the Interpretation of Experimental Data for Combustion in Diesel Engines," SAE Paper No. 2004-01-0931, 2004. Also presented at the 2004 SAE World Congress, March 2004. *(Selected for inclusion in 2004 SAE Transactions)*
7. Liu Y, Amr AA, Reitz RD. "Simulation of the Effects of Valve Pockets and Internal Residual Gas Distribution on HSDI Diesel Combustion and Emissions," SAE Paper No. 2004-01-0105, 2004. Also presented at the 2004 SAE World Congress, March 2004. *(Selected for inclusion in 2004 SAE Transactions)*

References

1. Kimura S, Ogawa H, Matsui Y and Enomoto Y. "An experimental analysis of low-temperature and premixed combustion for simultaneous reduction of NO_x and particulate emissions in direct injection diesel engines," Int. J. Engine Res.: vol 3: no 4: pp 249-259, 2002.
2. Weißbäck M, Csató J, Glensvig M, Sams T and Herzog P. "Alternative brennverfahren – ein ansatz für den zukünftigen pkw-dieselmotor," MTZ: vol 64: pp 718-727, 2003.
3. Miles PC, RempelEwert BH, Reitz RD. "Squish-Swirl and Injection-Swirl Interaction in Direct-Injection Diesel Engines," 6th Intl. Conf. on Engines for Automobiles: ICE 2003. Sept. 14-19, Capri, 2003.

II.A.4 The Role of Radiative Heat Transfer on NO_x Formation in a Heavy-Duty Diesel Engine

Mark P. B. Musculus
Combustion Research Facility
Sandia National Laboratories
P.O. Box 969, MS9053
Livermore, CA 94551-0969

DOE Technology Development Managers: Kevin Stork and Gurpreet Singh

Objectives

- The overall objective of this project is to advance the understanding of diesel engine spray, combustion, and emissions formation processes through the application of advanced laser-based and imaging diagnostics in an optically-accessible, heavy-duty, direct-injection diesel engine that is capable of operating under conditions typical of real diesel engines.
- Specific objectives for FY 2004 include:
  - Continue to modernize and upgrade laboratory hardware and capabilities, adding exhaust NO/NO_x measurement capability and upgrading the common-rail fuel injection system to deliver fuel rail pressures up to 2000 bar (30,000 psi).
  - Explore the factors that affect in-cylinder NO_x formation under conditions with large premixed burning. Measure soot temperature/radiation and NO_x as injection timing is retarded and premixed burning becomes significant. Also, investigate the role of soot radiative cooling on NO_x formation as injection pressure, intake temperature, and EGR rates are varied.

Approach

- Optical detection of in-cylinder NO_x is difficult, and quantitative in-cylinder measurements are even more challenging, if not impossible. By contrast, exhaust NO_x measurements are relatively easy, well established, and highly quantitative. Therefore, to provide quantitative insight into in-cylinder NO formation processes, highly quantitative exhaust NO_x measurements were married with in-cylinder optical diagnostics of other measurable phenomena.
  - An exhaust NO_x chemiluminescence analysis capability was implemented in the laboratory to measure NO and NO_x emissions from the optical engine.
  - A soot thermometry diagnostic was developed to measure soot temperature and radiation to measure in-cylinder temperatures for correlation with exhaust emissions.

Accomplishments

- Implemented exhaust NO_x analysis capability in optical engine.
  - Facilitates comparison of quantitative exhaust NO and NO_x measurements with in-cylinder optical diagnostic data.
- Added new higher-pressure (2000 bar) common rail fuel injection pump to optical engine.
  - Part of ongoing hardware upgrade of optical engine facility to reflect new developments in production hardware.
- Developed new soot temperature/heat transfer diagnostic tool.
  - “3-color” soot thermometry using filtered photodiode detectors.

- Examined NO_x formation under large premixed burn conditions.
  - Radiative cooling from hot soot and compression heating of burned gases contribute to increased exhaust NO_x with premixed burning.

Future Directions

- Examine radiation and NO_x emissions with multiple/early injections.
  - Early injections: large, slower premixed burn.
  - Pilot injections: can reduce premixed burning, NO_x.
  - Split injections: affect soot radiation and NO_x.
- Apply other optical diagnostics to low-temperature (exhaust gas recirculation) early injection.
  - Liquid fuel penetration (Mie scatter).
  - Soot formation (laser-induced incandescence and luminosity).
  - Flame development and ignition (planar laser-induced fluorescence of OH and chemiluminescence).

Introduction

In the near future (2007-2010), air quality regulations for new on-road heavy-duty diesel engines in the United States will require a ten-fold reduction in exhaust emissions from current levels. Although aftertreatment technologies to reduce emissions of particulate matter (PM) and oxides of nitrogen (NO_x) in the exhaust are being aggressively pursued, significant improvements must yet be realized before they may be practically utilized, especially for NO_x aftertreatment. Accordingly, reduction of engine-out emissions of NO_x (*i.e.*, prior to aftertreatment) remains an important strategy for regulatory compliance.

Several chemical pathways for NO (and hence, NO_x) formation in combustion systems have been identified. In diesel engines, flame temperatures are high enough that oxygen and nitrogen molecules in the air react to form NO. This pathway, called the "thermal NO mechanism," is expected to be the dominant NO formation pathway in diesel engines. Thermal NO formation increases exponentially with temperature. Hence, NO formation may be reduced significantly by reducing flame temperatures, which can be accomplished by charge dilution, for example, using exhaust gas recirculation (EGR). Indeed, engine-out NO_x has been shown to correlate exponentially with the calculated adiabatic flame temperature as EGR is varied [1]. This degree of success attests to the importance of flame temperature and thermal NO formation in diesel engines. Although flame temperature reduction by EGR has a dominant effect on NO_x, other factors can also affect NO formation significantly.

It has long been recognized that diesel combustion occurs in both premixed modes (immediately following ignition) and non-premixed modes (latter part of combustion). A correlation between diesel premixed burning and engine-out NO_x emissions has been demonstrated in numerous investigations, especially when caused by fuel cetane number effects [2]. The increase in exhaust NO_x with increasing premixed burning often cannot be explained by changes in the calculated adiabatic flame temperature. In some instances, the differences in the energy contents of the fuels and the phasing of combustion may be responsible, but in many other studies, the increase in exhaust NO_x cannot be explained by these factors.

Hence, understanding of the factors that affect NO_x formation for conditions with increased premixed burning is currently incomplete. Many new diesel engine combustion strategies are currently being developed, and many of these strategies employ enhanced fuel premixing prior to combustion, and consequently, increased premixed burning. An improved understanding of the mechanisms responsible for increased NO_x emissions could provide new insight into strategies to mitigate NO_x emissions.

One potential explanation for the increase in NO_x formation with increased premixing is changes in the actual flame temperature caused by changes in radiative heat transfer from hot soot. Previous measurements of radiation for highly sooting diesel conditions show that radiative heat transfer can be significant [3]. As premixed burning is increased, the soot in the jet can decrease, so that radiative heat transfer should also decrease. This could yield higher flame temperatures. Prior to the current study, the magnitude of this effect, and thus its importance on NO formation, had not been quantified.

It is the objective of this study to examine the role of radiative heat transfer on in-cylinder flame temperatures and in-cylinder NO formation. This investigation, and all of the work on this project, is conducted in cooperation with our industrial partners (including Cummins, Caterpillar, Detroit Diesel, Daimler-Chrysler, General Motors, Ford, Mack Trucks, International, John Deere, and General Electric). The results are presented at biannual Advanced Engine Combustion Working Group meetings.

Approach

This project utilizes an optically accessible, heavy-duty, direct-injection diesel engine for in-cylinder measurements of diesel spray, combustion, and pollutant formation processes. A cut-away cross-sectional schematic of the engine is shown in Figure 1. An extended piston with a large window located in the bowl of the piston provides primary imaging access to the combustion chamber. Additional access for imaging and/or laser diagnostics is provided by a window inserted in the cylinder head in place of one of the exhaust valves, and by five windows inserted in the cylinder wall. The engine is capable of operating under fired conditions over the full range of conditions typical of production diesel engines.

In the current study, a soot thermometry diagnostic was developed to measure soot temperature and radiative heat transfer. As shown in Figure 1, the diagnostic utilizes three photodiode detectors and an imaging camera. Narrow bandpass filters, centered at 410 nm, 570 nm, and 900 nm, were placed in front of the photodiodes so that they

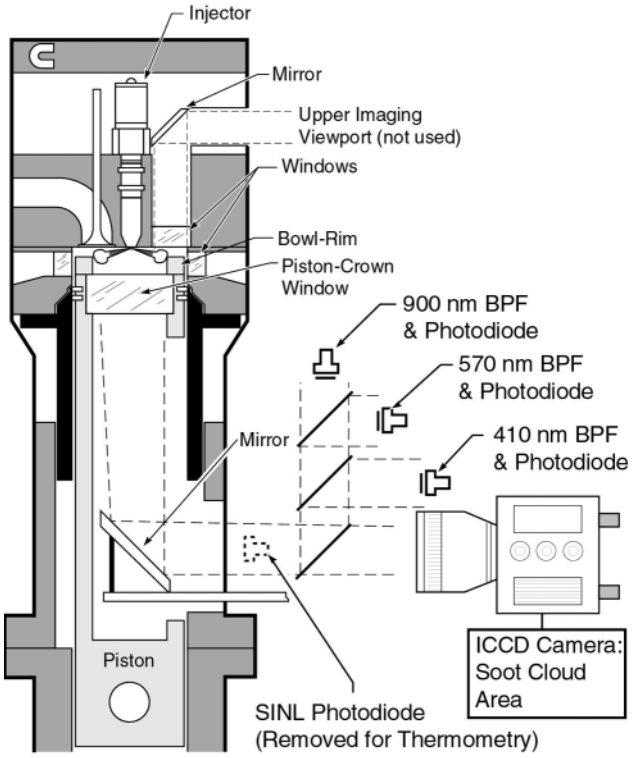

Figure 1. Schematic Diagram Showing Optical Engine and Soot Thermometry Diagnostic

measure the light emitted during combustion at three different colors. Soot particles, formed during combustion and heated to high temperatures, emit light in a broadband spectrum, and the intensities at various colors depend on the temperature and concentration of the soot. Hence, the intensity measurements from the photodiodes at three different colors can be used to determine the soot temperature and concentration. The area of the emitting soot cloud, which is provided by the imaging camera shown in Figure 1, is also necessary to determine the soot temperature and concentration. Other necessary improvements to the laboratory facility include the addition of an exhaust gas chemiluminescence NO_x analyzer and a new higher-pressure fuel delivery system for the common-rail fuel injector.

Results

Shown at the bottom of Figure 2 are exhaust NO and NO_x measurements for a start of injection (SOI) timing sweep from -12 crank angle degrees (CAD) after top dead center (ATDC) to +15.5 CAD ATDC. The emissions index of the exhaust NO_x ($EINO_x$) is

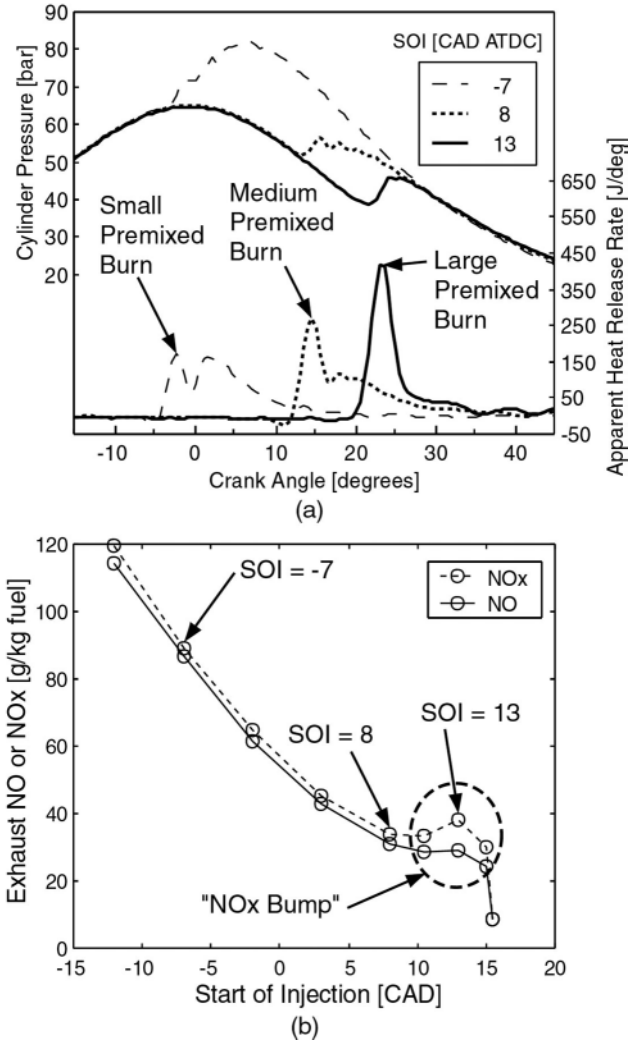

Figure 2. (a) Cylinder pressure and apparent heat release rate for three different SOI timing conditions. (b) Exhaust index of NO and NO_x for a sweep of SOI timings. The circled region indicates the location of the "NO_x bump."

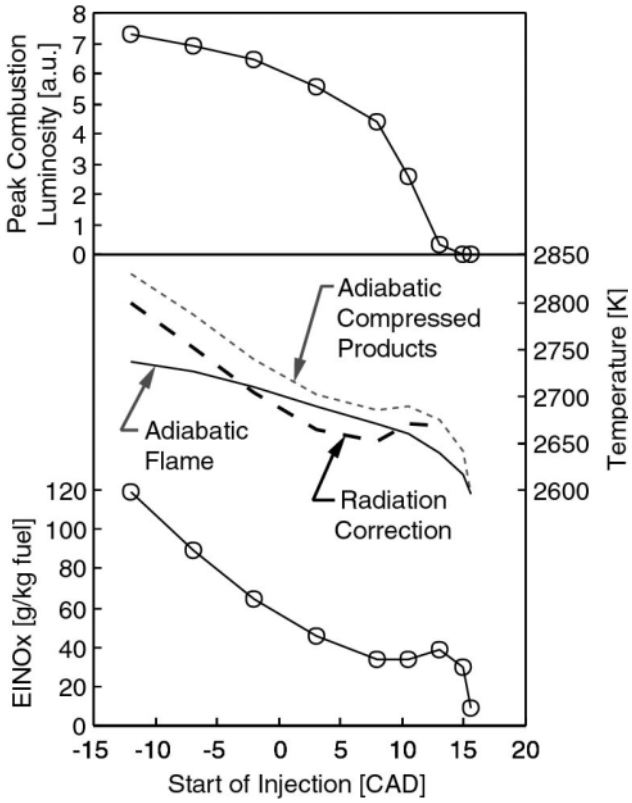

Figure 3. Variation with SOI timing of (top) combustion luminosity, (middle) peak adiabatic flame, adiabatic and radiation-corrected compressed burned gas temperature, and (bottom) measured $EINO_x$.

largest at early SOI and decreases as the SOI is retarded. Near SOI = +8, the $EINO_x$ trend changes, as it begins to increase with further retard of SOI, reaching a peak at SOI = +13. This peak in $EINO_x$ at late SOI is termed the "NO_x bump," as indicated in Figure 2. Shown at the top of Figure 2 are representative cylinder pressure and apparent heat release rates for SOI = -7, +8, and +13. For the early injection conditions, the heat release rate displays a small premixed burn, as typified by the SOI = -7 condition. At SOI = +8, the magnitude of the premixed burn becomes moderate, and at SOI = +13, where the $EINO_x$ increases, the premixed burn becomes large. This observation is an example of the correlation between diesel premixed burning and increased exhaust NO_x emissions.

The peak adiabatic flame temperature for each SOI in Figure 2 is shown in the middle of Figure 3, and the $EINO_x$ data from Figure 2 is shown at the bottom of Figure 3 for reference. As the SOI is retarded, the peak adiabatic flame temperature monotonically decreases, even through the NO_x bump. Hence, the increase in $EINO_x$ at the NO_x bump cannot be explained by changes in the adiabatic flame temperature. A larger premixed burn, however, does increase the compression of burned gases after they pass through the flame. Compression of burned gases for conditions with early injection or large premixed burning can yield gas temperatures even higher than the flame temperature, yielding increased NO formation. Shown as a dotted line in the middle of Figure 3, the

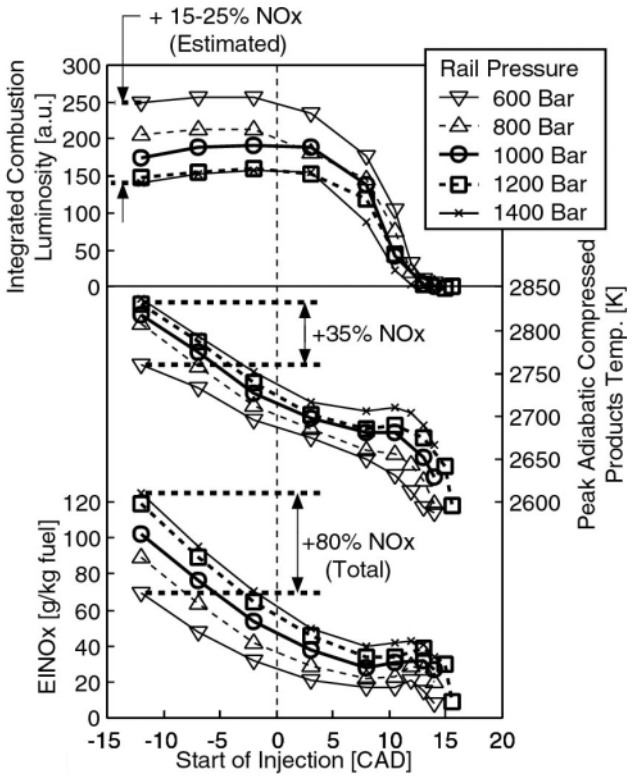

Figure 4. Variation with SOI timing of (top) combustion luminosity, (middle) peak adiabatic compressed burned gas temperature, and (bottom) measured $EINO_x$ for a range of fuel rail pressures, as indicated in the legend.

calculated peak temperature of the compressed burned gases increases slightly near the NO_x bump, but this increase is insufficient to cause the entire NO_x bump.

Concurrent with the $EINO_x$ data, soot luminosity (*i.e,* light emitted by hot in-cylinder soot) was measured with one of the photodiodes in Figure 1, and the peak soot luminosity at each SOI is shown at the top of Figure 3. From SOI = +8 to SOI = +13 where the NO_x bump develops, the combustion luminosity decreases precipitously, suggesting that radiative heat transfer from the soot may also decrease as premixed burning becomes large. If the cooling effect of radiative heat transfer decreased, the gas temperature would increase. Using the soot thermometry diagnostic, the radiative heat transfer from the hot soot was measured, and this was used to correct the compressed burned gas temperature for the cooling effect of soot radiation, as shown in Figure 3 as a dashed line. The radiation correction yields a larger increase in temperature near the NO_x bump and is large enough to nearly account for the entire NO_x bump. Hence, the combination of increasing burned-gas compression and decreasing soot radiative cooling can cause the peak gas temperature to increase as premixed burning becomes large. Based on the data acquired in the current study, these two effects are the primary factors responsible for the correlation between premixed burning and increased exhaust NO_x emissions.

Another practical example of the role of radiation and burned-gas compression on in-cylinder temperatures and NO formation is the well-known increase in exhaust NO_x that accompanies increased injection pressure. Shown in Figure 4 are the $EINO_x$, compressed burned gas temperature, and combustion luminosity for a series of timing sweeps acquired with fuel rail pressures ranging from 600 bar to 1400 bar. As shown at the bottom of Figure 4, as the injection pressure is increased, the $EINO_x$ generally increases with fuel rail pressure. At SOI = -12, for example, the $EINO_x$ increases by 80% from the lowest to the highest fuel pressure. As shown in the middle of Figure 4, the compressed burned gas temperature increases by 75 K, which corresponds to an increase in $EINO_x$ of about 40%. The peak combustion luminosity, shown at the top of Figure 4, decreases by about half, which corresponds to an estimated increase in $EINO_x$ of 15-25%. (Complete soot thermometry data were not acquired for the fuel rail pressure sweep, but soot luminosity data is indicative of changes in radiative heat transfer.) The combination of these two effects predicts that $EINO_x$ should change by a factor of 1.4*1.2 = 1.7, *i.e.*, a 70% increase, compared to the 80% increase that was actually measured. This is good agreement, considering the simplifying assumptions employed in this analysis. With the improved understanding of the factors that affect NO formation provided by this study, other trends in NO emissions observed with advanced diesel operational strategies will be better understood, helping to improve the development process.

Conclusions

Through comparison of exhaust NO_x measurements with in-cylinder soot thermometry,

the influence of soot radiative cooling and burned-gas compression on NO_x formation was studied. Analysis of the data supports the following conclusions:

- For the injection timing sweeps examined in this study, changes in exhaust NO_x with increasing premixed burning cannot be explained by changes in the adiabatic flame temperature.
- As the premixed burn increases in magnitude, the cooling effect of in-cylinder soot radiation decreases, yielding a hotter flame, contributing to the increase in exhaust NO_x.
- Compression of burned gases also yields hotter estimated temperatures, further contributing to the increase in exhaust NO_x.
- Other practical examples of changes in exhaust NO_x that cannot be explained by changes in adiabatic flame temperature, such as the increase of exhaust NO_x with fuel injection pressure, may be explained by these two factors.

FY 2004 Publications/Presentations

1. Musculus, M. P. B., “Effects of the In-Cylinder Environment on Diffusion Flame Lift-off in a DI Diesel Engine,” SAE Paper 2003-01-0074, Accepted for SAE Transactions, June 2004.
2. Musculus, M. P. B. and Pickett, L. M. “Diagnostic Considerations for Soot Extinction Diagnostic in Transient High Pressure Combustion Environments,” submitted to Combustion and Flame, June 2004.
3. Musculus, M. P. B., “On the Correlation between NO_x Emissions and the Diesel Premixed Burn,” SAE Paper 2004-01-1401, SAE International Congress and Exposition, March 2004.
4. Musculus, M. P. B., and Dec., J. E., “Effects of the In-Cylinder Environment and Diffusion Flame Lift-Off in a Heavy-Duty Diesel Engine,” Department of Energy Annual Project Report, November 2003.
5. Musculus, M. P. B., Dec, J. E. and Tree, D. R., “Effects of Fuel Parameters and Diffusion Flame Lift-Off on Soot Formation in a Heavy-Duty DI Diesel Engine,” SAE Paper 2002-01-0889, SAE International Congress and Exposition, Published in SAE Transactions, September 2003.
6. “On the Correlation between NO_x Emissions and the Diesel Premixed Burn,” SAE International Congress and Exposition, Detroit, MI, March 2004.
7. “The Influence of Soot Radiative Heat Transfer on In-Cylinder Temperatures and NO_x Formation,” Advanced Engine Combustion Meeting, Sandia National Laboratories, January 2004.
8. “On NO_x Formation and the Diesel Premixed Burn,” Advanced Engine Combustion Meeting, Sandia National Laboratories, June 2003.

References

1. Plee, S. L., Ahmad, T., Myers, J. P., and Faeth, G. M., "Diesel NO_x Emissions - A Simple Correlation Technique for Intake Air Effects," Proceedings of the Combustion Institute, **19**, pp. 1495-1502, 1982.
2. Lee, R., Pedley, J., and Hobbs, C., "Fuel Quality Impact on Heavy Duty Diesel Emissions: A Literature Review," SAE Paper 982649, SAE Transactions, **107**, No. 4, pp. 1952-1970, 1998.
3. Flynn, P. F., Mizusawa, M., Uyehara, O. A., and Myers, P. S., "An Experimental Determination of the Instantaneous Potential Radiant Heat Transfer Within an Operating Diesel Engine," SAE Paper 720022, SAE Transactions, **81**, No. 1, pp. 95-125, 1972.

II.A.5 Low Flame Temperature Diesel Combustion and Effects of Jet-Wall Interaction

Lyle M. Pickett
MS 9053
Sandia National Laboratories
P.O. Box 969
Livermore, CA 94551-9053

DOE Technology Development Managers: Gurpreet Singh and Kevin Stork

Objectives

- Identify methods for producing low-flame-temperature, soot-free, mixing-controlled diesel combustion to minimize nitrogen oxide (NO_x) and particulate matter (PM) emissions.
- Investigate the minimum flame temperature limits for mixing-controlled diesel combustion.
- Determine how jet-wall interaction affects soot formation. Make the distinction between jet-wall impingement effects and subsequent jet-jet interactions.

Approach

- Utilize advanced optical diagnostics coupled with a unique optically-accessible diesel combustion simulation facility (DCSF) to conduct these investigations.
- Vary flame temperature by adjusting exhaust gas recirculation (EGR) level (ambient gas oxygen concentration).
- Perform quantitative soot and combustion measurements in a plane wall jet and "confined" jet configuration.

Accomplishments

- Demonstrated that diesel combustion is soot-free for an ambient gas oxygen concentration of 8% and typical diesel ambient gas temperature (1000 K). Flame temperatures are also simultaneously low (less than 1800 K), implying that this combustion has minimal NO_x formation.
- Found that combustion efficiency remains high for mixing-controlled diesel combustion with flame temperatures as low as 1500-1600 K for conditions where the ambient gas temperature is greater than 1000 K. This low flame temperature limit is less than that of propagating flame processes in engines but close to that of homogeneous charge compression ignition (HCCI) combustion.
- Showed that the mass of soot downstream of the wall impingement location is approximately a factor of two less in a plane wall jet compared to a free jet. Possible mechanisms for the reduced soot formation include enhanced air entrainment and thermal interaction (cooling) of the jet.
- In a confined geometry that simulates adjacent jet interaction, we found the effect of wall interaction has an opposite effect: soot levels increase compared to a free jet or a plane wall jet. Soot increases when redirected combustion gases shorten the lift-off length, thereby making the fuel-air mixture at the lift-off length more fuel-rich.

Future Directions

- Determine the low temperature limit for soot formation in a reacting diesel fuel jet.
- Investigate how very high EGR affects diesel soot formation by performing quantitative measurements for ambient oxygen concentrations ranging from 21% to 10%.
- Investigate injection rate modulation and orifice geometry effects on diesel combustion and emissions processes.

Introduction

A major objective for experiments in the DCSF this year was to determine what factors affect soot formation during mixing-controlled diesel combustion with flame temperatures less than approximately 2000 K—too low for significant NO_x formation. A second objective was to determine if diesel combustion at temperatures far below 2000 K is possible. These low-temperature combustion regimes are of great interest for diesel combustion because of the potential for engine-out NO_x minimization without the use of aftertreatment. Interest in mixing-controlled diesel combustion is also motivated by the fact that mixing-controlled heat release remains closely coupled to injector controls, and many of the benefits of diesel combustion are inherently connected to this characteristic. The work is further motivated by results from the previous year, which showed that under some conditions it is possible to produce soot-free, low-temperature reacting diesel jets.

The third objective was to identify how realistic engine effects, such as jet-wall interaction, affect diesel combustion and soot formation. The wall has an effect on the mixing and combustion processes of the fuel jet through impingement and redirection of the fuel jet, and the wall also confines the fuel jet such that it turns back on itself and interacts with the adjacent fuel jets. At realistic diesel conditions (high temperature and pressure), a direct comparison of mixing and soot production between a free jet and a plane wall jet or spray has not been addressed experimentally. Moreover, the effect of jet-wall interaction has not been isolated from the ensuing jet-jet interaction. Wall jet experiments at diesel conditions would help the diesel engine community to better understand the basic processes governing soot production. This information, in turn, could help extend results to more complex and realistic engine conditions.

Approach

The research was performed in the DCSF using a common-rail diesel fuel injector. Figure 1 shows a picture of the DCSF in operation. The experimental ambient and injector conditions are carefully controlled in this facility, thereby facilitating investigation of the effects of fundamental parameters on diesel combustion. The DCSF also has full optical access, allowing advanced soot and combustion measurements to be performed.

Diesel flame temperatures were controlled by varying ambient gas oxygen concentration to simulate the effect of EGR in an engine. Combustion

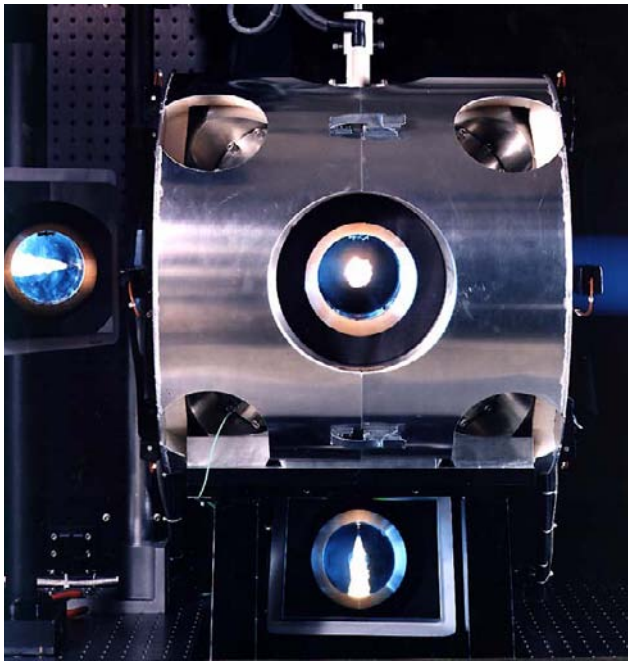

Figure 1. Photograph of the DCSF in operation, demonstrating the optical access to the diesel spray. The bright spot in the center of the front window is a burning diesel spray penetrating toward the viewer. Mirrors at 45° next to the bottom and left-side windows show side views of the burning spray.

was studied after autoignition and premixed burn so that the diesel combustion would be dominated by mixing-controlled combustion [1].

The effects of jet wall interaction were investigated in the DCSF in two experimental configurations: a jet impinging on a plane wall without any additional geometrical constraints and a "confined" jet (a box-shaped geometry simulating secondary interaction with adjacent walls and jets in an engine). In this way, the effects of adjacent geometry and jet interaction were separated from the effects of plane wall interaction. Details of the experimental setup can be found in Reference [2].

Results

Figure 2 shows soot luminosity during the time of injection at various ambient oxygen levels. The figure demonstrates that there is no soot formation with 5% or 8% ambient oxygen, corresponding to very high EGR levels in an engine. The discovery that soot formation is impeded at low oxygen concentration is significant because flame temperatures are also very low. These results were achieved with a conventional injector nozzle (180 μm), as opposed to reports from previous years in which a small injector nozzle (50 μm) was needed to achieve non-sooting, low-temperature combustion.

Summarizing research from this year and last year, a schematic illustrating how the three different methods avoid soot formation and produce low flame temperature is shown in Figure 3. Figure 3 is a plot of equivalence ratio versus temperature, with contours indicating the locations where soot and NO_x formation occur for a diesel-like fuel. Overlaid on the plot are curves (dashed) showing the predicted adiabatic flame temperatures for fuel-air mixtures at the given equivalence ratios for five ambient oxygen concentrations.

The first two methods for low-temperature combustion were discussed last year and involve fast mixing coupled with EGR (1) or fuel-lean mixing-controlled combustion (2) by inducing very high fuel-air mixing prior to the lift-off length. The lean mixture avoids both soot formation and a high-temperature stoichiometric diffusion flame. The third method (3), discovered this year, relies on the use of very high EGR (8% ambient oxygen), resulting in mixtures in the fuel jet that are rich, but with peak adiabatic flame temperatures that are too cool for soot inception at diesel timescales.

Despite the low flame temperature at high-EGR conditions, pressure-rise measurements show that combustion efficiency remains high for flame temperatures as low as 1500-1600 K, as shown in Figure 4. This is true for conditions where the ambient gas temperature is greater than 1000 K. This

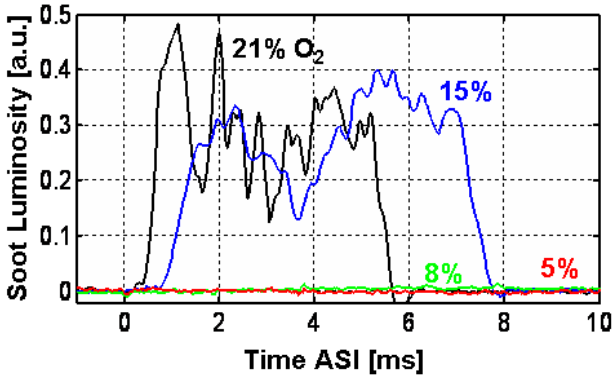

Figure 2. Spatially-integrated natural luminosity for four ambient gas oxygen concentrations. The ambient gas temperature and density were 1000 K and 30.0 kg/m^3, respectively, and the orifice size was 180 μm.

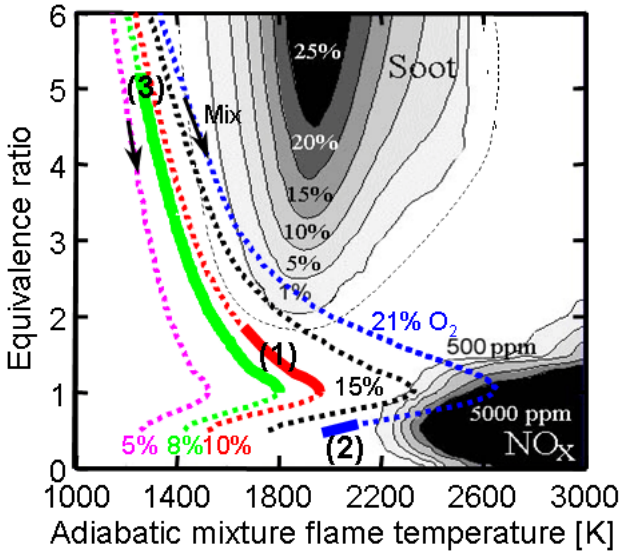

Figure 3. Three methods for soot-free, low-flame-temperature, mixing-controlled diesel combustion shown on a schematic of equivalence ratio versus adiabatic mixture flame temperature.

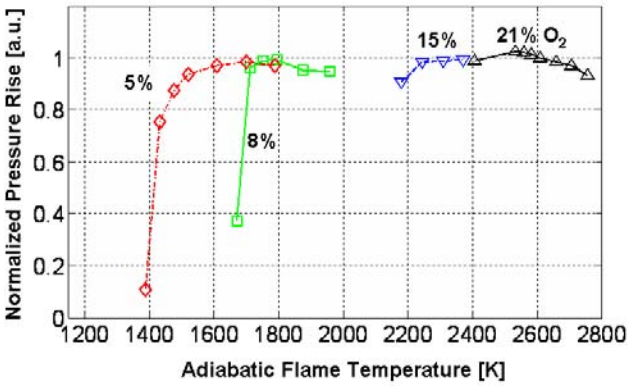

Figure 4. Normalized maximum pressure rise of diesel combustion *versus* flame temperature at four ambient oxygen concentrations.

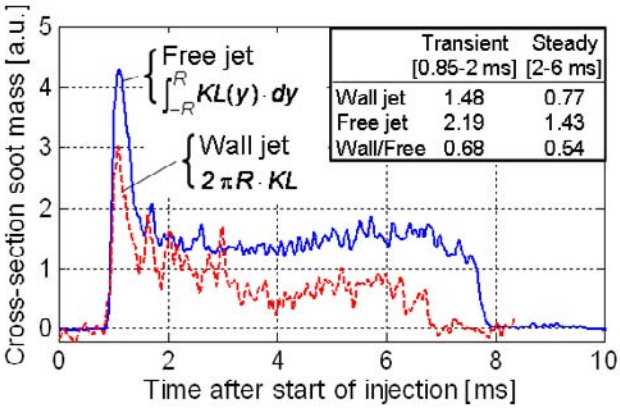

Figure 5. *KL* integral (soot mass) versus time for a free jet and a plane wall jet. Ambient gas temperature and density were 1000 K and 14.8 kg/m^3, respectively. The *KL* measurement positions were x = 70 mm for the free jet and R = 20 mm for the plane wall jet with a wall position of x = 50 mm. Time-integrals of the soot mass profile are indicated in the legend.

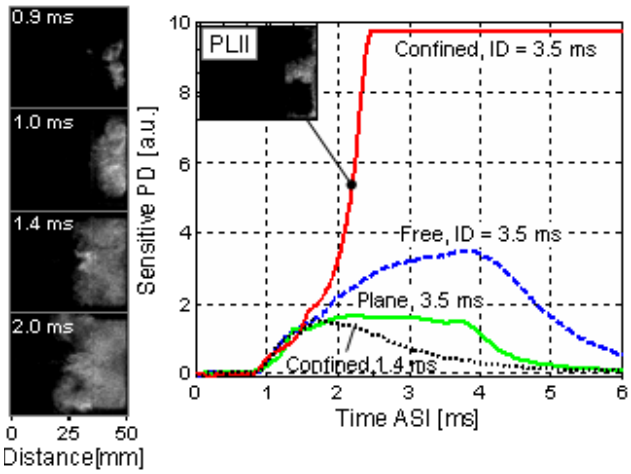

Figure 6. Time sequence of OH chemiluminescence images (left) and flame luminosity emission (right) for various wall configurations. Ambient gas temperature was 900 K. Injection duration (ID) is indicated on the graph. ID was 3.5 ms ASI for the OH chemilu-minescence image sequence. A PLII image showing that soot formation corresponds to a rapid rise in luminous emission is inset on the graph.

low flame temperature limit is less than that suggested for propagating flame processes in engines and is close to that observed for HCCI combustion.

The effects of plane wall interaction on soot formation processes of a diesel fuel jet are shown in Figure 5. The figure shows integrated soot mass measurements in a free jet or plane wall jet at a downstream cross-section of the jet at identical ambient and injector conditions. Soot levels are significantly lower in a plane wall jet compared to a free jet. At other operating conditions, sooting free jets become soot-free as plane wall jets. Possible mechanisms to explain the reduced or delayed soot formation upon wall interaction include an increased fuel-air mixing rate and a wall-jet cooling effect [2].

In a confined-jet configuration, however, there is an opposite trend in soot formation. Figure 6 shows that jet confinement causes combustion gases to be redirected towards the incoming jet, causing the lift-off length to shorten and soot to increase. The figure shows highly sensitive photodiode measurements of fuel jet luminosity at two different injection durations (ID) for various wall-jet configurations. The sensitivity of the photodiode is such that if soot formation occurs, the soot luminosity saturates the detector. Therefore, detectable levels of luminosity for the photodiode are due to chemiluminescence of non-sooting diesel combustion. Images of chemiluminescence are shown at the left for the "confined" jet configuration. The free jet and plane wall jet are non-sooting with an injection duration of 3.5 ms. However, the confined jet is non-sooting only with an injection duration of 1.4 ms. The time-sequence of chemiluminescence for the confined jet shows that combustion gases are redirected back towards the injector for extended injection durations.

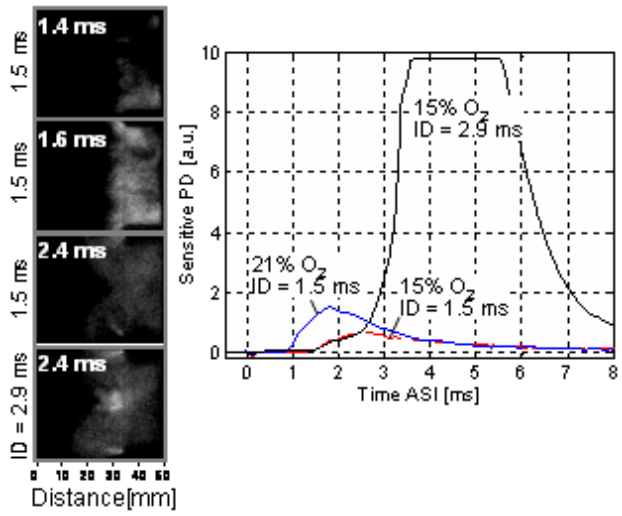

Figure 7. Time sequence of OH chemiluminescence images (left) and flame luminosity emission (right) for a confined jet with an ambient gas oxygen concentration of 15%.

The redirected combustion gases cause the lift-off length to shorten, thereby making the fuel-air mixture at the lift-off length more fuel-rich. The time after the start of injection of soot formation corresponds to the time shortly after this time of jet interaction with redirected combustion gases. The figure also shows that if the injection event is concluded prior to this jet interaction event, soot formation is avoided.

Jet interaction with redirected combustion products may also be avoided using reduced ambient oxygen concentration, as shown in Figure 7. One might suspect that EGR would increase the likelihood of combustion gas interactions at the lift-off length. This is because the lift-off length increases with the use of EGR and also there is less available oxygen in the confined region of the jet. However, Figure 7 shows that the use of EGR did not increase the sooting tendency of a confined jet for similar injection durations. Soot luminosity levels do not saturate the detector for an ignition delay of 1.5 ms, indicating that combustion is non-sooting.

The surprising result that there was no soot formation at 15% ambient oxygen appears to be caused by an increase in the ignition delay. Figure 7 shows that autoignition for the 15% oxygen condition is nearly coincident with the end of injection at 1.5 ms after start of injection (ASI), compared to 0.9 ms ASI for 21% oxygen. The time sequence of OH chemiluminescence for the 15% oxygen condition is consistent with the rise in spatially integrated flame luminosity. At 1.4 ms ASI, ignition kernels are shown within the confines of the box-shape. The OH chemiluminescence quickly fills the box-shape by 1.6 ms ASI. However, because injection has ended, the opportunity for combustion product interaction and its effect on lift-off length is avoided. At 2.4 ms ASI, for example, there is only weak chemiluminescence within the box region. If injection is continued (ID = 2.9 ms), reaction races back towards the injector as shown in the lower left image at 2.4 ms ASI. Soot formation follows shortly thereafter.

Conclusions

A new method for soot-free, low-flame-temperature, mixing-controlled diesel combustion was demonstrated using conventional injector technology. Also, combustion efficiency remains high for flame temperatures as low as 1500-1600 K. The lack of soot formation and low flame temperatures realized suggest that there is a potential for a simultaneous soot and NO_x reduction in an engine, while maintaining a mixing-controlled heat release rate. Jet-wall interaction studies on soot formation show decreased soot formation for plane wall interaction only and increased soot formation when the jet is confined. The identification of important mechanisms affecting combustion and soot formation is expected to be useful for understanding these processes in more complex and realistic diesel engine geometries and also provides guidance to engine designers on directions to proceed to lower soot and NO_x emissions.

Presentations

1. Pickett, L.M., López, J.J., "Jet-Wall Interaction Effects on Soot Formation in a Diesel Fuel Jet," COMODIA 2004, Yokohama, Japan, August 2004.
2. Pickett, L.M., Siebers, D.L., "Low Flame Temperature Limits for Mixing-Controlled Diesel Combustion," 30th International Symposium on Combustion, Chicago, IL, July 2004.
3. Pickett, L.M., "Low Temperature Limits for Soot Formation in Diesel Fuel Jets," AEC meeting, Detroit, MI, June 2004.

4. Pickett, L.M., "Low Flame Temperature Diesel Combustion with Jet-Wall Interaction," DOE Advanced Combustion Engine Annual Review, Chicago, IL, May 2004.
5. Pickett, L.M., Siebers, D.L., "Non-Sooting, Low Flame Temperature Mixing-Controlled DI Diesel Combustion," SAE World Congress, Detroit, MI, March 2004.
6. Pickett, L.M., López, J.J., "Jet-Wall Interaction Effects on Soot Formation in Diesel Fuel Jets," SAE World Congress, AEC meeting, Livermore, CA, January 2004.
7. Pickett, L.M., Siebers, D.L., "Fuel Effects on Soot Processes of Fuel Jets at DI Diesel Conditions," SAE Powertrain and Fluid Systems Conference, Pittsburgh, PA, October 2003.
8. Pickett, L.M., and Siebers, D.L., "Non-Sooting, Low-Flame Temperature, and Mixing-Controlled DI Diesel Combustion," 9th Diesel Engine Emissions Reduction Conference, Newport, RI, August 24-28, 2003.

Publications

1. Pickett, L.M., and López, J.J., "Jet-Wall Interaction Effects on Diesel Combustion and Soot Formation," submitted to SAE World Congress, 2005.
2. Pickett, L.M., "Low Flame Temperature Limits for Mixing-Controlled Diesel Combustion," 30th International Symposium on Combustion, Chicago, IL, July 25-30, 2004.
3. Musculus, M.P.B., and Pickett, L.M., "Diagnostic Considerations for Optical Laser-Extinction Measurements of Soot in High-Pressure Transient Combustion Environments," submitted to Combustion and Flame, 2004.
4. Siebers, D.L., and Pickett, L.M., "Aspects of Soot Formation in Diesel Fuel Jets," THIESEL 2004 Conference on Thermo- and Fluid-Dynamic Processes in Diesel Engines, Valencia, Spain, 2004.
5. Miles, P.C, Choi, D., Pickett, L.M., Singh, I.P., Henein, N., RempelEwert, B.A., Yun, H., and Reitz, R.D., "Rate-limiting Processes in Late-Injection, Low-Temperature Diesel Combustion Regimes," THIESEL 2004 Conference on Thermo- and Fluid-Dynamic Processes in Diesel Engines, Valencia, Spain, 2004.
6. López, J.J., and Pickett, L.M., "Jet/Wall Interaction Effects on Soot Formation in a Diesel Fuel Jet," accepted to COMODIA 2004, Yokohama, Japan, August 2-5, 2004.
7. Pickett, L.M., and Siebers, D.L., "Non-Sooting, Low Flame Temperature Mixing-Controlled DI Diesel Combustion," SAE World Congress, 2004-01-1399 (accepted for Transaction of the SAE 2004).
8. Pickett, L.M., and Siebers, D.L., "Soot in Diesel Fuel Jets: Effects of Ambient Gas Temperature, Ambient Density and Injection Pressure," Combustion and Flame, 138:114-135, 2004.
9. Pickett, L.M., and Siebers, D.L., "Fuel Effects on Soot Processes of Fuel Jets at DI Diesel Conditions," SAE Powertrain and Fluid Systems Conference, 2003-01-3080 (accepted for Transaction of the SAE 2003).
10. Pickett, L.M., and Siebers, D.L., "Non-Sooting, Low-Flame Temperature, and Mixing-Controlled DI Diesel Combustion," 9th Diesel Engine Emissions Reduction Conference, Newport, RI, August 24-28, 2003.

References

1. Pickett, L.M., and Siebers, D.L., "Non-Sooting, Low Flame Temperature Mixing-Controlled DI Diesel Combustion," SAE World Congress, 2004-01-1399.
2. Pickett, L.M., and López, J.J., "Jet-Wall Interaction Effects on Diesel Combustion and Soot Formation," submitted to SAE World Congress, 2005.

II.A.6 Achieving High-Efficiency Clean Combustion (HECC) in Diesel Engines

Robert M. Wagner (Primary Contact), C. Scott Sluder
Oak Ridge National Laboratory
2360 Cherahala Blvd.
Knoxville, TN 37932

DOE Technology Development Manager: Kevin Stork

Objectives

- Explore potential of expanding the HECC speed/load operation range in a light-duty diesel engine while relying on production-like controls.
- Demonstrate HECC operation under road-load type conditions.
- Characterize effect of transition pathway from original equipment manufacturer (OEM) to HECC operation on emissions and performance.

Approach

- Explore potential strategies for achieving HECC operation on a Mercedes 1.7-L diesel engine with reliance only on production-like controls.
- Explore effect of transition pathway from OEM to HECC operation on emissions and performance.
- Perform detailed emissions and combustion characterization to improve understanding of efficient advanced combustion modes.

Accomplishments

- Explored potential of achieving HECC over a range of speeds and loads. Based on these experiments, modifications will be made to the experimental setup in FY 2005 in an attempt to increase the HECC operation window for this engine.
- Demonstrated efficient operation with a 90% reduction in oxides of nitrogen (NO_x) and a 50% reduction in particulate matter (PM) emissions under road-load type conditions (20% load, 1500 rpm) without excessive hydrocarbon (HC) emissions.
- Investigated transition from OEM to HECC operation. Experimental results indicate that the transition pathway has strong impact on achieving efficient operation.

Future Directions

- Upgrade engine control system for greater flexibility in injection timing and frequency as well as improved transient capability.
- Modify experimental setup to include a low-pressure exhaust gas recirculation (EGR) system and a diesel atomizer for partially premixed strategies to explore expanding the effective HECC speed/load range.
- Investigate techniques for entering and exiting HECC modes and consider potential diagnostic tools for feedback control when transitioning between these modes. Methods for transitioning between conventional diesel and HECC operation may have an important role in minimizing harmful emissions and maintaining efficiency.

Introduction

Researchers at Oak Ridge National Laboratory (ORNL) have been exploring the potential of new combustion regimes that exhibit simultaneous low NO_x and PM emissions. An improved understanding of these combustion modes is critical for lowering the performance requirements for post-combustion emissions control devices and meeting future U.S. emissions and efficiency goals. Through proper combustion management, ORNL has achieved significant reductions in NO_x and PM emissions without the decrease in efficiency typically associated with operating in these regimes. This type of operation is commonly referred to as high-efficiency clean combustion (HECC) and was demonstrated at ORNL on a multi-cylinder engine using only production-like hardware. This achievement is dramatically different from other approaches to HECC, which may require expensive hardware modifications or acceptance of significant fuel penalties.

Another important aspect of operating diesel engines in advanced combustion modes is the ability to transition in and out of these modes with minimal adverse effects on emissions or performance. ORNL researchers were able to demonstrate seamless transitions with no significant emissions excursions or effects on performance.

Approach

The overall objective of this activity is to improve the understanding of and the ability to achieve and transition to HECC operation for a range of real-world speed/load conditions with only production-like parameters and controls. A combination of thermodynamic and detailed exhaust chemistry information will be used to dramatically improve the understanding of HECC regimes, which is expected to result in even cleaner and more efficient operation of diesel engines. The thermodynamic and exhaust chemistry information will also be shared with industry and/or other national laboratories for the development and validation of improved combustion models and catalysts.

A Mercedes 1.7-L common rail diesel engine is the experimental platform for this study. This engine is equipped with a rapid-prototype, full-pass engine controller capable of actuating the EGR valve, intake throttle, and fuel injection parameters (timing, duration, fuel rail pressure, and number of injections). HECC operation was achieved on this engine under road-load conditions using a combination of high EGR and specific injection parameters. EGR was used to achieve a low-NO_x, low-PM condition (aka low-temperature combustion, LTC), and injection parameters were used to adjust combustion phasing to recover efficiency. The effect of transition path from the OEM condition to HECC operation using this approach was also investigated using the advanced controller.

Results

Extensive experiments have been performed to develop approaches for achieving HECC operation in a light-duty diesel engine. The results of an example road-load condition are summarized in Table 1. The OEM condition is 1500 rpm at 2.6 bar brake mean effective pressure (BMEP). Results are shown for the OEM condition, the low-NO_x low-PM condition (LTC), and the HECC condition, which may also be referred to as an “efficient LTC” condition. Note that the phrase LTC as used in the literature typically refers to a low-NO_x low-PM condition only and provides no information concerning efficiency. In this document, the LTC condition should be thought of as an intermediate condition which was explored during the search for HECC operation. Comparing the OEM and HECC conditions in Table 1, a 90% reduction in NO_x and a 30% reduction in PM is shown between the two cases with no degradation to engine efficiency or increase in HC emissions. Also note that this was achieved with conventional rail pressures and a single fuel injection event.

The average heat release profiles for the conditions in Table 1 are shown in Figure 1. A significant shift in the heat release profile was observed with increasing EGR, as seen in comparing Figures 1(a) and 1(b). The heat release profile is recovered (or improved) by re-phasing the combustion process with injection timing to achieve HECC operation, as illustrated in Figure 1(c). Recall from Table 1 that the pilot injection was disabled during HECC operation. The 10-50% heat release interval was shorter for HECC operation as

Table 1. Example of HECC Operation at Road-Load Conditions (1500 rpm, 2.6 bar BMEP)

	OEM	LTC	HECC
EGR (%)	21	49	48
BSFC (g/hp-hr)	211	240	209
NO_x (g/hp-hr)	1.2	0.1	0.1
PM (g/hp-hr)	0.38	0.51	0.29
THC (g/hp-hr)	2.68	4.54	2.46
Intake Temp (^oC)	43	129	94
Exhaust Temp (^oC)	205	244	199
Main Timing (BTDC)	2	2	12
Pilot Timing (BTDC)	18	18	Off
Rail Pressure (bar)	320	320	328

compared to OEM operation, indicating a higher fraction of premixed (or kinetically controlled) combustion. Conversely, the 50-90% heat release interval was longer for HECC operation, indicating a slower mixing-controlled combustion phase, potentially due to the increased EGR level under the HECC condition.

HECC operation using high levels of EGR results in a reduction in volumetric efficiency due to the increase in the temperature of the inducted intake charge. For the case summarized in Table 1, the temperature of the intake charge increased from 43°C for the OEM condition to 94°C for the HECC condition, but the thermal efficiency remained unchanged at approximately 30% for the two conditions. Therefore, some form of a reduction in losses occurred during the engine cycle. Further analysis is necessary to determine whether the reduction in losses is due to heat transfer effects or the combustion process. A more detailed first- and second-law thermodynamic analysis will be applied to this and other HECC data during the next phase of this activity. Not shown in the average heat release profiles is the effect of these different operating modes on engine stability. The coefficient of variation (COV) in indicated mean effective pressure (IMEP) increased with EGR level but returned to a comparable OEM level during HECC operation.

Exhaust constituents were analyzed in detail to characterize the production of aldehyde emissions for

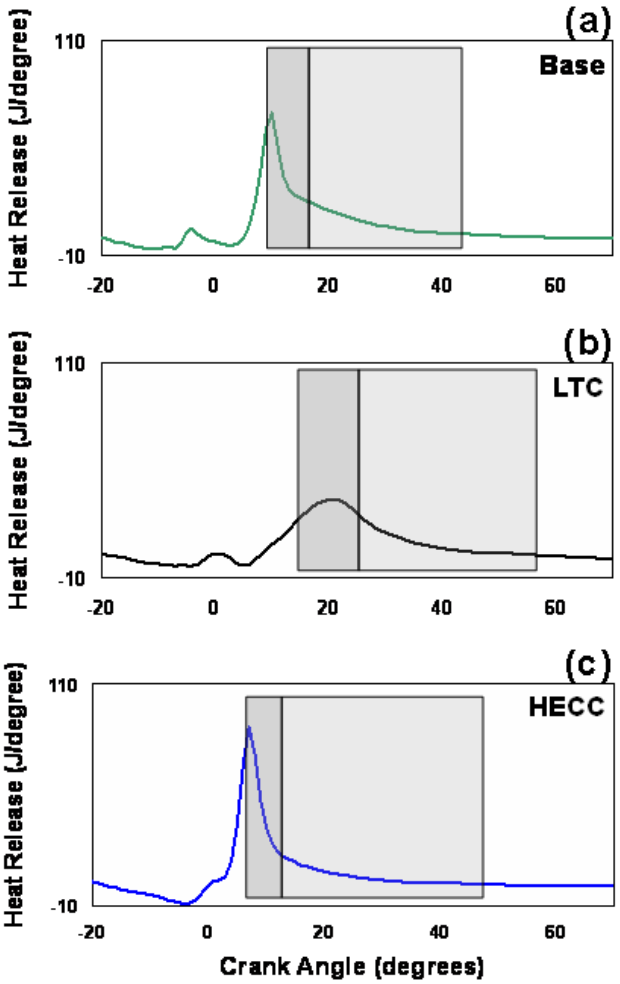

Figure 1. Heat release profiles for OEM (a), LTC (b), and HECC (c) engine operation under road-load conditions. The darker shaded region corresponds to the 10-50% heat release interval and the lighter shaded region corresponds to the 50-90% heat release interval.

Table 1. The results of this analysis are shown in Figure 2 and indicate a sharp increase in aldehyde emissions as EGR is increased to achieve LTC operation. The increase in aldehyde emissions is believed to be the result of slower or delayed combustion and is not necessarily due to increased locally rich combustion. Re-phasing of the combustion process and removal of the pilot injection to achieve HECC operation resulted in a reduction in aldehyde emissions to levels similar to those observed for the OEM condition.

Controlled transition experiments were performed to investigate potential emissions and performance problems which may be associated with

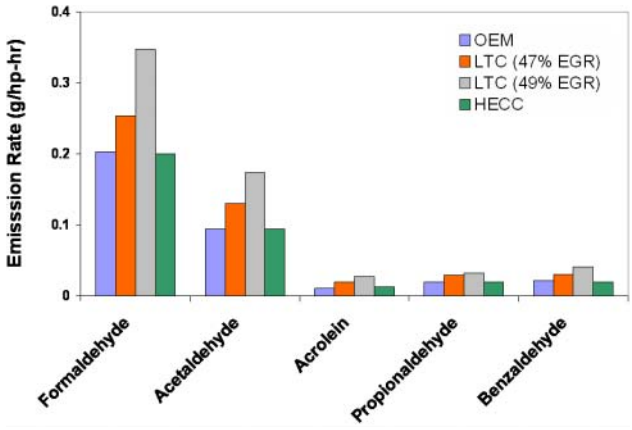

Figure 2. Aldehyde Emissions for OEM, LTC, and HECC Engine Operation under Road-Load Conditions

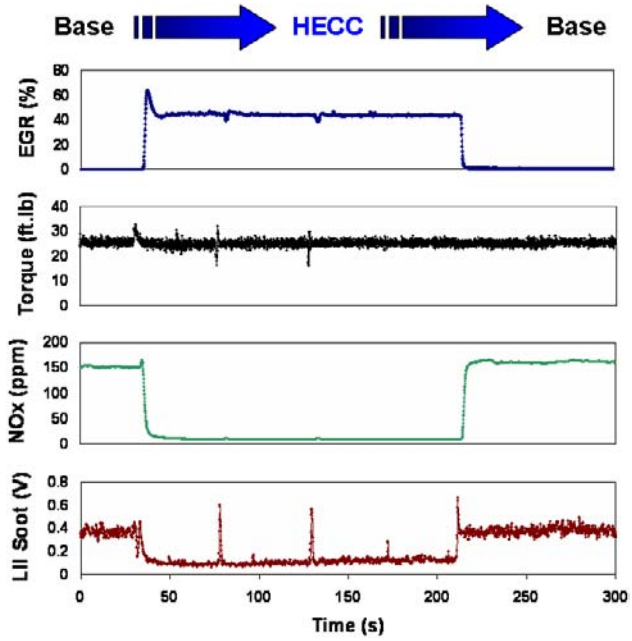

Figure 3. Controlled Transition between OEM and HECC Operation under Road-Load Conditions

transitioning in and out of HECC operation. The results shown in Figure 3 are for conditions similar to those summarized in Table 1. The most significant differences are that the base condition for the transition experiments is 0% EGR and a different engine (though the same model, Mercedes Benz 1.7-L) was used for these experiments. No significant PM or NO_X spikes were observed during transitions in and out of HECC operation. In addition, brake-specific fuel consumption (BSFC) was the same for both modes with no significant excursions in performance.

Summary and Conclusions

- HECC operation under road-load conditions is possible in light-duty diesel engine applications and was achieved with a reduction of engine-out NO_X (90%) and PM (30-50%) without excessive HC emissions and with no efficiency penalty.
- HECC operation is characterized by an increased fraction of premixed combustion.
- Engine-out aldehyde emissions do not increase with HECC operation but are of levels similar to those observed for the OEM condition.
- Transitioning between OEM and HECC conditions does not result in significant PM or performance excursions under road-load conditions.

FY 2004 Publications/Presentations

1. C. S. Sluder, R. M. Wagner, S. A. Lewis, and J. M. Storey, "A Thermal Conductivity Approach for Measuring Hydrogen in Diesel Exhaust," SAE Paper No. 2004-01-2908 and SAE Transactions (Tampa, FL, USA; October 2004).
2. C. S. Sluder, R. M. Wagner, S. A. Lewis, and J. M. Storey, "High Efficiency Clean Combustion in a Direct Injection Diesel Engine," 2004 AFRC/JFRC Joint International Combustion Symposium (Maui, HI, USA; October 2004).
3. R. M. Wagner, C. S. Sluder, S. A. Lewis, and J. M. Storey, "Achieving High Efficiency Clean Combustion in Diesel Engines," 10th Diesel Engine Emissions Reduction Conference (San Diego, CA, USA; August 2004).
4. R. M. Wagner, C. S. Sluder, S. A. Lewis, and J. M. Storey, "Chemical Composition of the Exhaust from Low-NO_X Low-PM Diesel Combustion," 2004 Internal Combustion Division of ASME and the CIMAC World Congress (Kyoto, Japan; June 2004).
5. C. S. Sluder, R. M. Wagner, S. A. Lewis, and J. M. Storey, "Exhaust Chemistry of Low NO_X Low PM Diesel Combustion," SAE Paper No. 2004-01-0114 and SAE Transactions (Detroit, MI, USA; March 2004).

II.A.7 Large Eddy Simulation (LES) Modeling Applied to LT/Diesel/H_2 Combustion Research

Joseph C. Oefelein
Sandia National Laboratories
MS 9051, P. O. Box 969
Livermore, CA 94551-9051

DOE Technology Development Managers: Kevin Stork

Objectives

- New project (as of January 2004) aimed at combining state-of-the-art LES and high-performance computational capabilities with the Advanced Combustion Engine R&D activities and expertise in optical engine experiments at the Sandia Combustion Research Facility (CRF).
- Establish one-to-one coupling of LES with experimental hydrogen-fueled internal combustion engine research:
- Generate baseline time-varying 3D multiblock grid of optical research engine, which is being designed and built simultaneously.
- Begin detailed unsteady analysis of gas injector processes and provide support for pattern optimization.
- Perform progressive verification and validation of fully-coupled model framework for treatment of in-cylinder hydrogen-air combustion processes.

Approach

- Application of unique state-of-the-art software and computational resources.
- Implementation of a sophisticated set of subgrid-scale models that are consistent with the Direct Numerical Simulation (DNS) technique in the limit as the LES grid cut-off is refined toward smaller scales.
- Rigorous validation of models using data acquired from the carefully selected target experiments.
- Detailed characterization of complex turbulent combustion processes through joint-analysis of respective data.

Accomplishments

- Preliminary time-varying 3D multiblock grid that matches the geometry of the Sandia National Laboratories optically assessable hydrogen-fueled research engine has been completed.
- Progressive interdisciplinary verification and validation of model base and boundary conditions are in progress.
- Hydrogen fuel injector analysis and optimization are in progress.

Future Directions

- High-fidelity LES calculations will be synchronized with the development of the hydrogen-fueled internal combustion engine (IC-engine) and homogeneous charge compression ignition engine experiments being developed concurrently at Sandia National Laboratories.
- Detailed analysis of local in-cylinder engine processes will be conducted:
  - Hydrogen fuel injector pattern optimization and analysis.
  - Progressive refinement of grid geometry (valve-port) configuration.

  - Joint experimental-numerical characterization of unsteady mixing and low-temperature combustion process over full engine cycles.
- Work toward critical needs and challenges:
  - Power density limitations and maximum fuel efficiency.
  - NO_x emissions (kinetics-dominated, exhaust gas recirculation alone not sufficient).
  - Flame structure, stability, effects of stratification.

Introduction

This research combines a unique high-fidelity simulation capability based on the large eddy simulation (LES) technique with the Advanced Combustion Engine R&D activities at Sandia National Laboratories (SNL). The objective is to use high-fidelity science-based simulations in a manner that directly complements select optical engine experiments. The simulations will be carried out using a highly specialized state-of-the-art massively-parallel flow solver designed for LES of turbulent reacting multiphase flows that was brought to SNL by J. C. Oefelein. Respective case studies will make use of unique high-performance computational resources available internally and at various DOE facilities such as the National Energy Research Scientific Computing Center. After systematic validation of key processes, quantitative data can be extracted from the simulations that are not otherwise available.

The investment in time and resources will provide two significant benefits. Results from this work will provide both a detailed description of intricately coupled processes not measurable by experimental diagnostics and the information required to better understand the merits and utility of various engineering-based KIVA-like models that provide the fast turn-around times required by industry designers. Significant improvements can then be derived to enhance the accuracy and confidence in these models. The combination of experiments and high-fidelity LES will provide a unique and unparalleled capability to study in-cylinder combustion and transport processes and will facilitate analysis of dynamically coupled processes over the full range of physically relevant time and length scales (i.e., from the largest geometrically dominated turbulence scales to the smallest reactive-diffusive scales). No single approach is capable of achieving this goal.

Approach

The approach involves five key steps: 1) application of unique software capabilities and computational resources that are not typically available in industry and academia, 2) development of fundamental subgrid-scale models that treat turbulence-chemistry interactions and complex thermo-physics in a direct manner consistent with the application of a Direct Numerical Simulation (DNS), 3) adherence to the strict algorithmic requirements that enable LES to effectively eliminate the effects of numerical errors on respective subgrid-scale models, 4) rigorous validation of respective models using data acquired from carefully selected target experiments, and 5) detailed characterization and analysis of key processes by performing tightly coupled joint-analysis of the characteristic unsteady and transient in-cylinder combustion processes associated with a given experiment. Each of the proposed tasks requires considerable high-level expertise, labor, and computational resources. They significantly exceed the time and resources available in industry and academia and are consistent with a National Laboratory's role of using high-performance computing to enable fundamental exploration of complex combustion phenomena.

Results

Given that this project commenced in January of 2004, efforts to date have been focused primarily on establishing a fully synchronized project that is tightly coupled with key target experiments. Figure 1 illustrates the key components. Tasks are being carried out using a unique and unified theoretical-numerical framework developed by Oefelein [1-2]. This framework is currently one-of-a-kind and has been designed for application of both LES and DNS. It solves the fully coupled conservation equations of mass, momentum, total energy and species for complex chemically reacting flows (gas or liquid), in

Figure 1. Sequence of Accomplishments Planned for FY 2004

full geometries. The numerical formulation treats the fully coupled compressible form of the conservation equations but can be evaluated in the incompressible limit. Thus, incompressibility is treated as a limiting extreme. The code is fully modular, self-contained, and written in standard American National Standards Institute (ANSI) Fortran 90.

The theoretical framework handles both multicomponent and mixture-averaged systems, with a generalized treatment of the equation of state, thermodynamics, and transport processes. It can accommodate high-pressure, real-gas phenomena, along with the full range of simplified extremes (such as ideal calorically perfect gas mixtures). This framework has been designed to handle turbulent multiple-scalar mixing processes, finite-rate chemical kinetics and multiphase phenomena (or respective simplifications and modeled approximations) in a fully coupled manner. The overall formulation provides full thermophysical coupling (compressible and incompressible) over a wide range of conditions, and in a fundamental manner.

For LES applications, the instantaneous conservation equations are filtered and models are applied to account for the subgrid-scale (SGS) mass, momentum and energy transport processes. The baseline SGS closure is obtained using the mixed dynamic Smagorinsky model by combining the models of Erlebacher, Hussaini, Speziale and Zang [3] and Speziale [4] with the dynamic modeling procedure [5-9] and the Smagorinsky eddy viscosity model [10]. There are no tuned constants employed anywhere in the closure. The property evaluation scheme is based on the extended corresponding states model [11-12] and is designed to handle full multicomponent systems. This scheme has been optimized to account for thermodynamic nonidealities and transport anomalies over a wide range of pressures and temperatures, and is based on research conducted over many decades [13-21].

Unlike all approaches to date, the filtered energy and chemical source terms are closed directly using an appropriately specified chemical kinetics mechanism and a moment-based reconstruction methodology similar to that of Sarkar et al. [22-23]. The local instantaneous scalar field (p, T, Y_1, …, Y_N) is estimated using an approximate deconvolution operation that requires the statistical filtered moments of respective scalars to match to a specified order. The estimated scalar field is then used as a surrogate for the exact scalar field to calculate the SGS contribution to the filtered chemical source terms. This approach is completely consistent with the dynamic modeling procedure and facilitates simultaneous treatment of multiple-scalar mixing processes and key rate of progress variables associated with the chemical kinetics.

The baseline numerical scheme provides a fully implicit all-Mach-number time advancement using a fully explicit multistage scheme in pseudo-time. A unique dual-time multistage scheme is employed with a generalized (pseudo-time) preconditioning methodology that treats convective, diffusive, geometric, and source term anomalies in an optimal and unified manner. The implicit formulation allows one to set the physical time step based solely on accuracy considerations. This attribute alone typically provides a 2 to 3 order of magnitude increase in the allowable integration time step compared to other contemporary methods, especially in the limit of zero-Mach-number flow.

The spatial scheme is designed using a staggered methodology in generalized curvilinear coordinates that provides non-dissipative spectrally clean damping characteristics and discrete conservation of mass, momentum and total energy. The scheme can handle arbitrary geometric features, which typically dominate the evolution of turbulence in a flow. The differencing methodology includes appropriate switches to handle shocks, detonations, flame-fronts, and contact discontinuities. A Lagrangian-Eulerian formulation is employed to accommodate

particulates, sprays, or Lagrangian-based combustion models, with full coupling applied between the two systems. The numerical algorithm has been designed using a fully consistent and generalized treatment for boundary conditions based on the method of characteristics.

The algorithm is massively-parallel and has been optimized to provide excellent parallel scalability attributes using a distributed multiblock domain decomposition with a generalized connectivity scheme. Distributed-memory message-passing is performed using Message Passing Interface and the Single-Program—Multiple-Data model. It accommodates complex geometric features and time-varying meshes with generalized hexahedral cells while maintaining the high accuracy attributes of structured spatial stencils. The numerical framework has been ported to all major platforms and provides highly efficient fine-grain scalability attributes. Sustained parallel efficiencies above 90 percent have been achieved with jobs as large as 1600 processors.

Conclusions

- Combination of detailed experiments and high-fidelity LES provides unique ability to study key in-cylinder processes.
  - Use of advanced predictive capability to perform both fundamental and applied analysis at relevant conditions.
  - Systematic improvements to KIVA-like engineering models through unique multilayered coupling with key target experiments.
- Tasks specifically address need to resolve intricately-coupled turbulent combustion processes in IC engines.
  - Time-accurate simulations over full range of relevant dynamic scales.
  - Dynamic modeling to evaluate model coefficients, no tuned constants.
  - More universal applicability over broader range of flow regimes.

FY 2004 Publications/Presentations

1. J. C. Oefelein. Large eddy simulation for turbulent combustion and propulsion (invited). *Progress in Aerospace Sciences*, submitted.
2. H. H. Chiu and J. C. Oefelein. Modeling liquid-propellant spray combustion processes (invited). Chapter 6, *Liquid Rocket Thrust Chambers, Aspects of Modeling, Analysis and Design*, in print. Progress in Astronautics and Aeronautics. American Institute of Aeronautics and Astronautics, 2004.
3. J. C. Oefelein. Thermophysical characteristics of shear-coaxial LOX-H2 flames at supercritical pressure. *Proceedings of the 30th International Symposium on Combustion*, 30: in print, 2004.
4. J. C. Oefelein. Hydrogen fuel and lean combustion (invited). *Proceedings of the workshop on Lean Combustion Technology II: Promise and Practice*, Tomar, Portugal, April 25-29, 2004.
5. J. O. Keller, G. A. Richards, J. C. Oefelein and R. W. Schefer. Hydrogen combustion research for gas turbine engines (invited). *Proceedings of the Spring Technical Meeting on Combustion Fundamentals and Applications*, Central States Section of the Combustion Institute, Austin, Texas, March 21-23 2004.
6. J. C. Segura, J. C. Oefelein and J. K. Eaton. Large eddy simulation of turbulence modification by particles. *Proceedings of the Thermal and Fluid Sciences Affiliates Program*, Department of Mechanical Engineering, Stanford University, February 4-6, 2004.
7. J. C. Oefelein. Simulation of combustion and thermophysics in practical propulsion systems (invited). *42nd AIAA Aerospace Sciences Meeting and Exhibit, Paper 2004-0159*, January 5-8 2004. Reno, Nevada.
8. J. C. Oefelein, R. W. Schefer and R. S. Barlow. High-fidelity LES and target flame validation experiments in the Turbulent Combustion Laboratory (invited). *42nd AIAA Aerospace Sciences Meeting and Exhibit, Invited Topical Workshop of the Technical Committees*, January 5-8 2004. Reno, Nevada.
9. J. C. Oefelein. Large eddy simulation for transient analysis of high-pressure combustion devices (invited). *Proceedings of the 39th JANNAF Combustion Subcommittee*, The Aerospace Corporation, Colorado Springs, Colorado, December 1-5 2003. The Johns Hopkins University, Chemical Propulsion Information Agency.
10. J. C. Oefelein. Advances in the application of LES and DNS to gas turbine and liquid rocket combustion processes (invited). *39th AIAA/ASME/SAE/ASEE Joint Propulsion Conference and Exhibit, Paper 2003-5288*, July 20-23 2003. Huntsville, Alabama.

11. J. O. Keller, J. C. Oefelein, R. W. Schefer, and G. A. Richards. Joint program for advanced simulation of fuel flexible gas turbines (invited). *Proceedings of the 1st International Conference on Industrial Gas Turbine Technologies*, Brussels, Belgium, July 10-11 2003.
12. S. V. Apte, K. Mahesh, P. Moin, and J. C. Oefelein. Large eddy simulation of swirling particle-laden flows in a coaxial-jet combustor. *International Journal of Multiphase Flow*, 29 (8): 1311–1331, 2003.

References

1. J. C. Oefelein. *General numerical framework for reacting multiphase flow with complex thermochemistry, thermodynamics and transport*, Copyright 1992-2004 by J. C. Oefelein, All Rights Reserved.
2. J. C. Oefelein. *General package for evaluation of multicomponent real-gas and liquid mixture states at all pressures*, Copyright 1992-2004 by J. C. Oefelein, All Rights Reserved.
3. G. Erlebacher, M. Y. Hussaini, C. G. Speziale, and T. A. Zang. Toward the large eddy simulation of compressible turbulent flows. *Journal of Fluid Mechanics*, 238: 155-185, 1992.
4. C. G. Speziale. Galilean invariance of subgrid-scale stress models in the large eddy simulation of turbulence. *Journal of Fluid Mechanics*, 156: 55-62, 1985.
5. M. Germano, U. Piomelli, P. Moin, and W. H. Cabot. A dynamic subgrid-scale eddy viscosity model. *Physics of Fluids*, 3(7): 1760-1765, 1991.
6. P. Moin, K. Squires, W. Cabot, and S. Lee. A dynamic subgrid-scale model for compressible turbulence and scalar transport. *Physics of Fluids*, 3(11): 2746-2757, 1991.
7. D. K. Lilly. A proposed modification of the germano subgrid-scale closure method. *Physics of Fluids*, 3(11): 633-635, 1992.
8. Y. Zang, R. L. Street, and J. R. Koseff. A dynamic mixed subgrid-scale model and its application to turbulent recirculating flows. *Physics of Fluids*, 5(12): 3186-3195, 1993.
9. B. Vreman, B. Geurts, and H. Kuerten. On the formulation of the dynamic mixed subgrid-scale model. *Physics of Fluids*, 6(12): 4057-4059, 1994.
10. J. Smagorinsky. General circulation experiments with the primitive equations. I. The basic experiment. *Monthly Weather Review*, 91: 99-164, 1963.
11. T. W. Leland and P. S. Chappelear. The corresponding states principle. A review of current theory and practice. *Industrial and Engineering Chemistry Fundamentals*, 60(7): 15-43, 1968.
12. J. S. Rowlinson and I. D. Watson. The prediction of the thermodynamic properties of fluids and fluid mixtures-I. The principle of corresponding states and its extensions. *Chemical Engineering Science*, 24(8): 1565-1574, 1969.
13. J. O. Hirschfelder, C. F. Curtiss, and R. B. Bird. *Molecular Theory of Gases and Liquids*. John Wiley and Sons, Incorporated, New York, New York, 1954.
14. R. B. Bird, W. E. Stewart, and E. N. Lightfoot. *Transport Phenomena*. John Wiley and Sons, Incorporated, New York, New York, 1960.
15. J. O. Hirschfelder, C. F. Curtiss, and R. B. Bird. *Molecular Theory of Gases and Liquids*. John Wiley and Sons, Incorporated, New York, New York, 2nd edition, 1964.
16. S. Gordon and B. J. McBride. Computer program for calculation of complex chemical equilibrium compositions, rocket performance, incident and reflected shocks and Chapman-Jouguet detonations. Technical Report NASA SP-273, National Aeronautics and Space Administration, 1971.
17. S. Takahashi. Preparation of a generalized chart for the diffusion coefficients of gases at high pressures. *Journal of Chemical Engineering of Japan*, 7(6): 417-420, 1974.
18. R. C. Reid, J. M. Prausnitz, and B. E. Polling. *The Properties of Liquids and Gases*. McGraw-Hill, New York, New York, 4th edition, 1987.
19. J. F. Ely and H. J. M. Hanley. Prediction of transport properties. 1. Viscosity of fluids and mixtures. *Industrial and Engineering Chemistry Fundamentals*, 20(4): 323-332, 1981.
20. J. F. Ely and H. J. M. Hanley. Prediction of transport properties. 2. Thermal conductivity of pure fluids and mixtures. *Industrial and Engineering Chemistry Fundamentals*, 22(1): 90-97, 1981.
21. R. J. Kee, F. M. Rupley, and J. A. Miller. Chemkin thermodynamic data base. Technical Report SAND87-8215B, Sandia National Laboratories, 1990. Supersedes SAND87-8215 dated April 1987.
22. C. Pantano and S. Sarkar. A subgrid model for nonlinear functions of a scalar. *Physics of Fluids*, 13(12): 3803-3819, 2001.
23. J. P. Mellado, S. Sarkar, and C. Pantano. Reconstruction subgrid models for nonpremixed combustion. *Physics of Fluids*, 15(11): 3280-3307, 2003.

II.A.8 Nitrogen-Enriched Air for the Reduction of NO_x Emissions in Heavy-Duty Diesel Engines

Steve McConnell (Primary Contact) and Raj Sekar
Argonne National Laboratory
9700 South Cass Avenue
Argonne, Illinois 60440

DOE Technology Development Manager: Kevin Stork

Technical Advisor: Steven Trevitz, Mack Trucks Inc, Hagerstown, Maryland

Objectives

- Evaluate the performance of nitrogen-enriched intake air (NEA) as an alternative to exhaust gas recirculation (EGR) for NO_x reduction in heavy-duty diesel engines.
- Optimise NEA generation system using gas separation membranes.
- Test the NEA generation system installed on a heavy-duty diesel engine using an engine dynamometer.
- Demonstrate the NEA system's durability and effectiveness on a heavy-duty vehicle.

Approach

- Evaluate EGR data for baseline tests and relate target engine requirements to NEA performance.
- Develop parametric membrane model that accounts for bundle volume and fiber size.
- Characterize available gas separation membranes.
- Match membrane to target engine requirements.
- Test prototype on engine test stand (13-mode test).
- Test prototype performance in a vehicle (transient and durability testing).

Accomplishments

- The EGR engine tests (baseline tests) were performed and the data was evaluated. The target engine's requirements were related to engine performance.
- A parametric membrane model that accounts for bundle volume and fiber size was developed and modified to enable comparison of system power requirements.
- A gas separation membrane characterization bench was designed and built to provide data at higher flows and pressures required for heavy-duty diesel engines.
- Six gas separation membrane prototypes have been tested using the new membrane characterization bench.
- Five reports were delivered to Mack Trucks Inc., detailing the characterization results of four gas separation membranes and system power requirements.

Future Directions

- Re-evaluate the membrane characterization test data and optimize the gas separation membranes form factor (fiber dimensions), using the membrane model to more closely determine system power requirements per Mack Truck needs.
- Complete the enhanced, power-enabled model results and build an NEA system for use with heavy-duty diesel engines.
- Conduct a test of the NEA system on a heavy-duty diesel engine using the Environmental Protection Agency's 13-mode test.
- Conduct transient and durability testing on a heavy-duty vehicle.

Introduction

EGR has been used to reduce NO_x emissions for decades in spark-ignited engines. Recently, due to increasingly stringent emissions regulations, diesel engines are beginning to use this technology. EGR reduces NO_x emissions by adding CO_2 as a diluent to lower in-cylinder combustion temperatures. When used in a diesel engine, large quantities of exhaust gas are needed at low loads since the engine operates extremely lean at these points and the exhaust gas has a low percentage of CO_2 (see Figures 1 and 2). Large quantities of EGR must be cooled to keep the volumetric efficiency of the engine at normal levels. This increases the heat load of the radiator. A larger radiator is a problem for heavy-duty diesel vehicles since manufacturers have been trying to reduce the radiator size to lower aerodynamic drag. EGR in diesel engines also introduces particulate matter (PM) and acids into the cylinder which are corrosive and abrasive, increasing engine wear.

A solution to the problems inherent in EGR is to use nitrogen as a diluent. Nitrogen can be used to replace CO_2 to lower in-cylinder combustion temperatures and control NO_x emissions. Gas separation membranes can be used to remove oxygen from the intake air, making it nitrogen-rich. A gas separation membrane works by dividing the air into two streams: one is nitrogen-rich, and the other is oxygen-rich. The higher the driving pressure through the membrane, the higher the purity. Relatively low pressures are needed since the oxygen level only needs to be reduced from 21% to 17% (typical intake oxygen concentrations with EGR). Since exhaust gas is not used, PM is not introduced into the cylinder, decreasing engine wear. Also, since nitrogen is taken directly from the intake air and does not require extra cooling, there is no increased heat load to the engine.

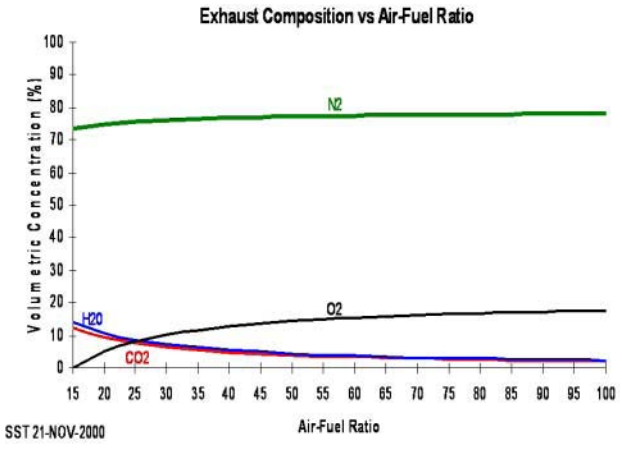

Figure 1. Exhaust Gas Composition at Different Air-Fuel Ratios

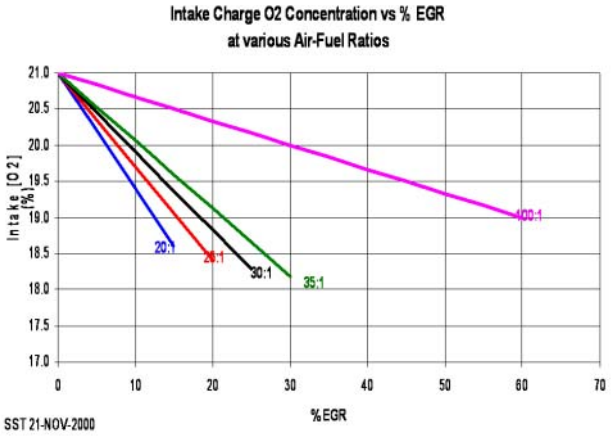

Figure 2. Amount of EGR Required to Lower Intake Air Oxygen Concentration at Different Air-Fuel Ratios

Approach

Typically, the first step in a research project is to develop baseline data to use in evaluating the changes that occur during testing. For a baseline data set, a heavy-duty diesel engine was operated at four different EGR levels and 3 different beginning of injection (BOI) timings over a 13-mode test. The EGR data for baseline tests was evaluated, and target engine requirements were related to NEA performance. This data was used to develop a parametric membrane model that accounts for bundle volume and fiber size.

Previous studies have indicated that the best way to generate nitrogen onboard a vehicle would be to use a gas separation membrane. Several gas separation membrane manufacturers were contacted, and prototype membrane bundles were requested. A new membrane characterization bench was developed since the heavy-duty diesel engine required higher boost pressures that the previous bench could not supply. Four of the six gas separation membranes have been characterized, and the remaining gas separation membranes will be characterized in the near future.

Once the membranes are characterized, the membrane data is evaluated using the model to match the gas separation membrane to target engine requirements. It is perceived that some form factor changes such as membrane thickness or fiber size may have to change to meet the engine requirements. After a suitable membrane is identified, a full-scale NEA unit will be built and evaluated using the 13-mode test on an engine test stand. At the conclusion of the engine tests, the NEA unit will be installed in a heavy-duty vehicle. Transient response and durability will then be evaluated in prototype performance testing.

Results

Originally, four membrane manufacturers were willing to supply prototype membranes for this project. Because some suppliers requested anonymity, the modules will be designated as A, B, C, D, E and F. Analysis done by the membrane manufacturer of A concentrated on three different membrane variants: a high-selectivity membrane, a high-permeability membrane, and a membrane of intermediate performance. The manufacturer's initial conclusion was that their existing membrane technology required more energy than allowed and required more storage volume than available. They reviewed our feedback and concluded that they could develop an alternative module. However, it would have a higher-permeability material with improved separation factor, and it would cost a significant amount of money to produce. They were not willing to spend the money required to produce this module variant due to other product priorities.

Membrane manufacturer B submitted a prototype for evaluation. The prototype was polymeric, consisting of bundled fibers, three elements (bundles) in a single chamber 7 inches in diameter x 40 inches long. These modules had been previously run in a high-contaminant environment. The modules were tested under the following conditions: feed pressures to 40 psig; feed to retentate pressures differential of less than 5 psi; permeate pressure and temperature at ambient conditions; and retentate flows up to 15 SCF/min. During testing, membrane module B achieved target nitrogen enrichment while remaining stable at elevated pressures and after repeated cycles of testing. However, the module required excess power and exceeded the module size limits.

Membrane manufacturer C supplied a low-selectivity, high-permeability, single-element polymeric fiber, bundled in a container 5 inches in diameter x 20 inches long. Test conditions for membrane C were as follows: feed pressures to 50 psig; feed to retentate pressures less than 6 psi; permeate set at ambient pressure and temperatures; and retentate flows up to 25 SCF/min. Membrane C achieved the target nitrogen enrichment while slightly exceeding the power and size limits (see Figures 3 and 4). The membrane was chosen to be resized. Model results showed that if the low-selectivity, high-permeability membrane modules are sized at 18 inches in diameter and the maximum flow is corrected to 70 lb/min, two membrane bundles are needed if the fiber bore diameter is opened to twice its original size. With advanced coatings and optimization, this could be reduced to one bundle. A new bundle has been requested with a larger bore diameter.

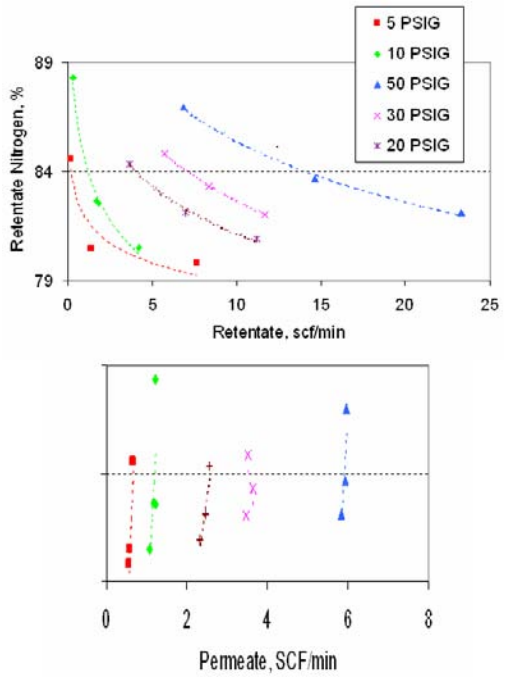

Figure 3. Retentate and Permeate Flows for Membrane C

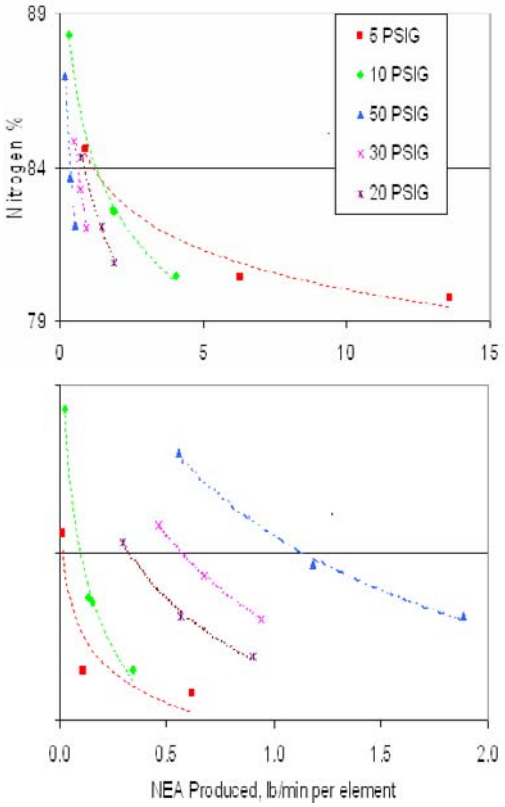

Figure 4. Power and Size Requirements for Membrane C

Modules D, E, and F have been tested. Preliminary results of analysis at low pressures look promising and full analysis is being completed (see Figures 5, 6 and 7).

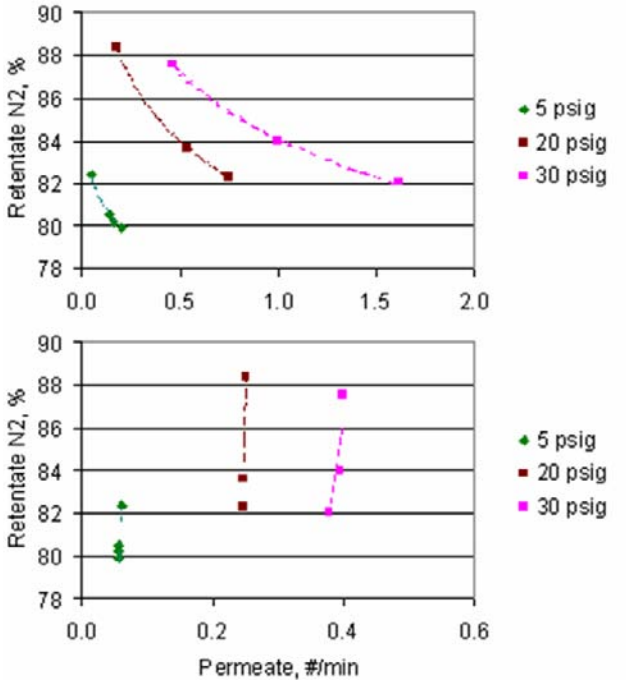

Figure 5. Retentate and Permeate Flows for Membrane D

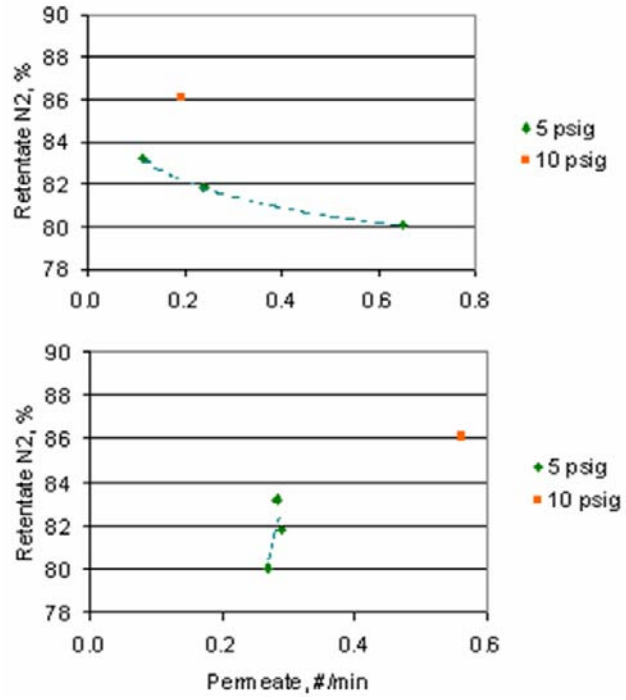

Figure 6. Retentate and Permeate Flows for Membrane E

System power requirements are now more stringent according Mack Truck's needs than originally envisioned. Further analysis of power

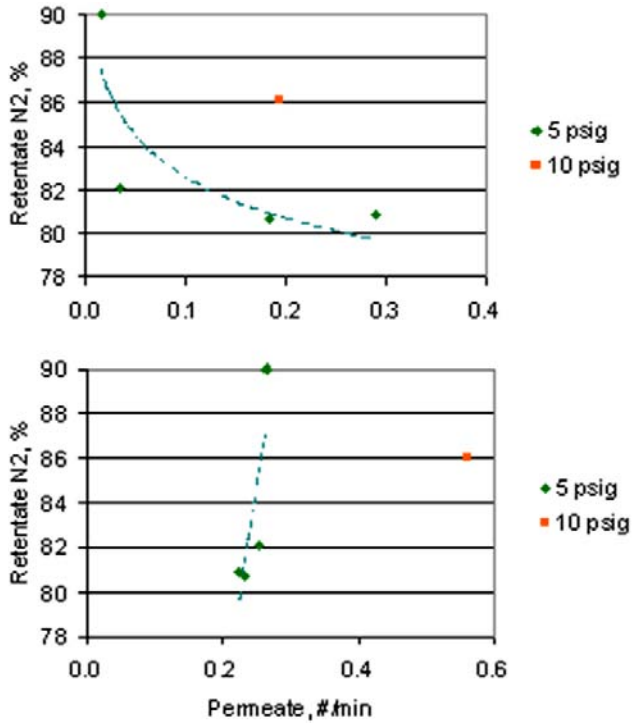

Figure 7. Retentate and Permeate Flows for Membrane F

requirements is in progress as inputs are gathered from Mack Truck (Table 1).

It is projected that an NEA system will be ready for engine testing when it can be placed in Mack Truck's test cell schedule.

Conclusions

- A membrane model was developed and enhanced to incorporate Mack Truck's system power considerations.
- Membrane B achieved the required nitrogen enrichment but exceeded the power and size limits.
- Membrane C achieved the required nitrogen enrichment while slightly exceeding the power and size limits. Using the membrane model, membrane C was chosen to be resized and tested.
- Modules D, E and F have been tested. Preliminary results at low pressures look promising and analysis is in progress.

Table 1. Process Parameters for System Power Analysis

"13-Mode" Test Point	Compressor Flow #/min	Permeate Flow #/min	Retentate Flow #/min	Theoretical Intake N_2, %	Module Feed Pressure, psig	Parasitic Power Loss as % of power
c-100	84	12	72	81	52	5
c-75	68	13	55	82	41	5
c-50	49	14	35	82	25	7
c-25	45	24	21	83	10	9
b-100	72	13	59	82	52	5
b-75	56	12	44	82	36	5
b-50	41	9	32	81	21	4
b-25	28	12	16	84	21	10
a-100	53	7	46	81	40	4
a-75	44	7	37	81	30	4
a-50	29	6	23	81	14	6
a-25	20	7	13	83	15	9

II.A.9 Detailed Modeling of HCCI and PCCI Combustion and Multi-Cylinder HCCI Engine Control

Salvador Aceves (Primary Contact), Daniel Flowers, Joel Martinez-Frias, Francisco Espinosa-Loza, Robert Dibble, Randy Hessel
Lawrence Livermore National Laboratory
7000 East Ave. L-644
Livermore, CA 94550

DOE Technology Development Manager: Kevin Stork

Subcontractors:
University of California Berkeley, Berkeley, CA
University of Wisconsin-Madison, Madison, WI

Objectives

- Obtain low-emissions, high-efficiency operation of homogeneous charge compression ignition (HCCI) and premixed charge compression ignition (PCCI) engines.
- Advance our analysis techniques to learn the fundamentals of HCCI and PCCI combustion and to make accurate predictions of combustion and emissions.
- Conduct experiments to determine strategies to control multi-cylinder HCCI engines. Test new instruments for determining HCCI combustion timing.

Approach

- Develop and use fluid mechanics-chemical kinetics models for analysis of HCCI and PCCI combustion and for evaluation of possible control strategies.
- Conduct experiments on a 4-cylinder Volkswagen TDI engine and on a single-cylinder Caterpillar 3401 engine to evaluate control strategies, develop combustion sensors and validate HCCI fundamentals.

Accomplishments

Part 1. Analysis

- We have developed the most advanced and accurate analysis tools for HCCI combustion. During this year, we have applied this capability to perform a detailed analysis of experiments conducted at Lund Institute of Technology where two different cylinder geometries were considered: a high-turbulence cylinder with a square bowl in piston and a low-turbulence cylinder with a flat top piston. The purpose of the analysis is to determine the role of turbulence during HCCI combustion.
- We have extended our multi-zone analysis methodology to make it applicable to analysis of PCCI combustion. PCCI is a generalization of HCCI combustion where the fuel and air mixture may be partially stratified at the moment of ignition. Examples of PCCI engines include direct injected engines with early injection and controlled autoignition (CAI) engines that use variable valve timing and high residual fraction to control combustion.

Part 2. Experimental

- Experimental and computational work has shown the possibility to use an ion sensor to determine combustion timing in an HCCI engine. This is an important breakthrough, as there is a pressing need for reliable, inexpensive combustion sensors for HCCI combustion control.

Future Directions

- The three fundamental problems of HCCI engines are the difficulty in controlling the engine, the low power achievable, and obtaining consistent timing in the different cylinders of a multi-cylinder engine. In this project, the analytical and experimental work is dedicated to solving these three problems.
- A possible solution to increase the engine power output and balance combustion is to partially stratify the charge (PCCI). We are developing analysis tools to accurately predict combustion and emissions under PCCI combustion.
- Our Volkswagen TDI engine is the ideal test bed for studying combustion balancing between the cylinders of a multi-cylinder engine. We will develop computer controls and inexpensive combustion sensors that will allow us to achieve efficient, controlled HCCI combustion.

Introduction

Homogeneous charge compression ignition (HCCI) engines can have efficiencies as high as diesel engines, while producing ultra-low emissions of oxides of nitrogen (NO_x) and particulate matter (PM). HCCI engines can operate on gasoline, diesel fuel, and most alternative fuels. While HCCI has been demonstrated and known for quite some time, some issues have kept it from widespread commercialization. The main issue is combustion control. Other significant hurdles include low power output, high hydrocarbon and carbon monoxide emissions, and difficulty in starting the engine. In this project we use analytical and experimental approaches to address these issues and assist engine and vehicle manufacturers in producing efficient and clean HCCI engines.

Approach

Our work is a synergistic combination of analysis and experimental work. We have developed advanced analysis methodologies that combine chemical kinetics with fluid mechanics to analyze HCCI and PCCI engines with accuracy never before achievable for other types of engines. We have also developed systems analysis models for HCCI engines that have allowed us to optimize operating conditions to obtain maximum efficiency with minimum emissions. These analysis tools have also been used to guide the experimental effort. In the laboratory, we have tested new control methodologies and developed new combustion sensors for HCCI combustion.

Results

We have applied a sequential fluid mechanics-chemical kinetics model for analyzing HCCI experimental data generated at Lund for two combustion chamber geometries: a flat top piston and a piston with a square bowl [1]. Our model uses a fluid mechanics code to determine temperature histories in the engine as a function of crank angle. These temperature histories are then fed into a chemical kinetics solver, which determines combustion characteristics for a relatively small number of zones (40). The results show that the methodology yields good results for both the flat top piston and the square bowl piston. The model makes good predictions of pressure traces and heat release rates. It is observed that the engine with the highest turbulence level (the square bowl) has longer burn duration than the engine with low turbulence (the flat top). This difference can be explained by our model, which indicates that the cylinder with the square bowl has a thicker boundary layer that results in a broader temperature distribution. This broader temperature distribution tends to lengthen the combustion, as cold mass within the cylinder takes longer to reach ignition temperature when compressed by the first burned gases.

Our multi-zone method has been extended to analysis of PCCI engines when there is some stratification in the air-fuel distribution inside the cylinder at the time of combustion. Our analysis methodology has two stages. First, a fluid mechanics code is used to determine temperature and equivalence ratio distributions as a function of crank angle, assuming motored conditions. The

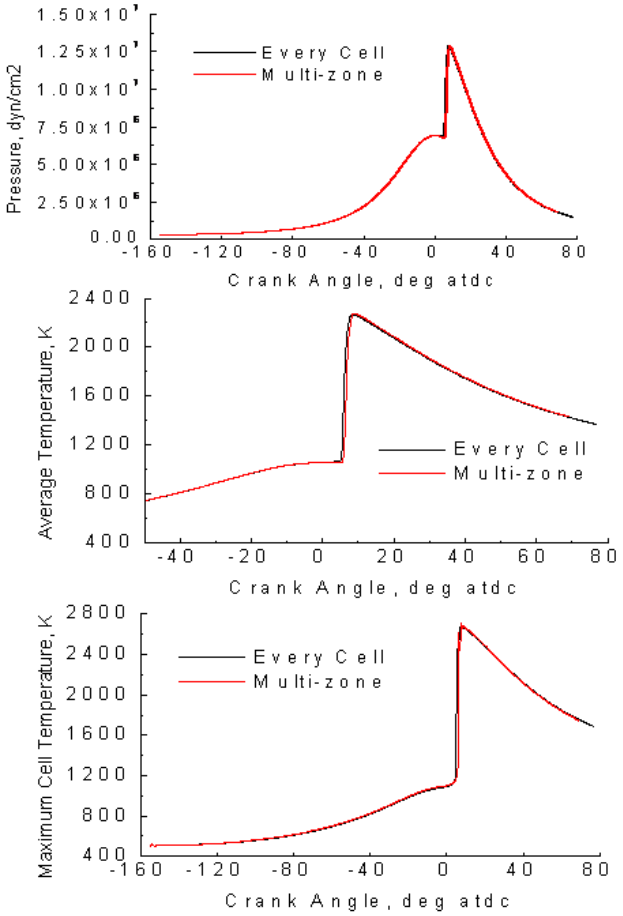

Figure 1. Comparison between results of the multi-zone model and results from an "exact" calculation where the chemical kinetics code is executed at every cell of a fluid mechanics grid. This "exact" solution is labeled "every cell" in the figure.

distribution information is then used for grouping the mass in the cylinder into a two-dimensional (temperature-equivalence ratio) array of zones. The zone information is then handed on to a detailed chemical kinetics model that calculates combustion, emissions and engine efficiency information [2]. We have tested the results for two fuels (methane and n-butane). The results show that the model can accurately predict pressure traces for the fuels being considered.

A second methodology that can be applied to PCCI combustion consists of running the fluid mechanics code for a time step and grouping the many fluid mechanics cells (of the order of

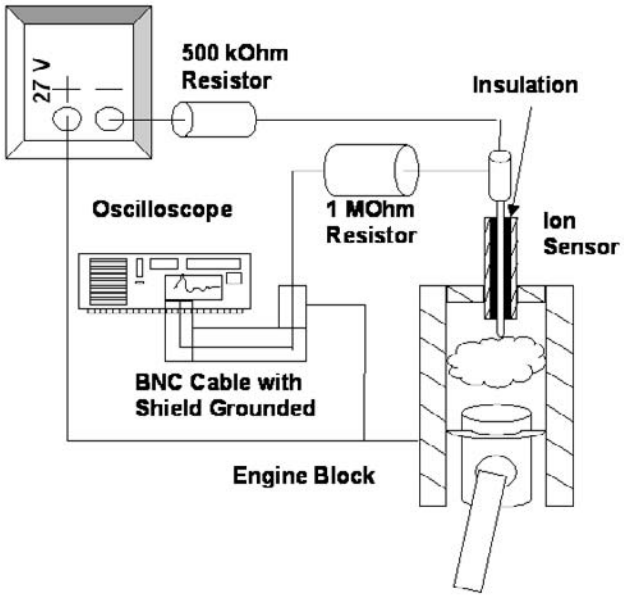

Figure 2. Circuit Used for Detecting Ion Signals in the Volkswagen TDI Engine

~100,000) into a few zones (100 or less). The chemical kinetics code is then run for the 100 zones, and the composition and heat release information obtained from the chemical kinetics code is sent back to the fluid mechanics code to conduct the calculations for the next time step. This method yields accurate results at a much reduced computational cost, since chemical kinetics is the most computationally intensive part of the problem. Our methodology yields accurate results for tested operating conditions (see Figure 1) [3].

We have also studied the ion current signal in HCCI to develop inexpensive combustion sensors [4]. Combustion timing is the key measured quantity used in combustion control systems for HCCI engines. In-cylinder pressure transducers are widely used in the laboratory setting for combustion timing measurement, but these sensors are very expensive and have short life (typically less than 100 hours). A promising alternative means of combustion sensing is to measure electrical current from chemi-ionization that occurs during the combustion event. Ion sensing has great potential as a low-cost and long-life alternative to in-cylinder pressure transducers. An experiment was conducted in the Volkswagen TDI engine, and the circuit used for ion sensing is shown in Figure 2. The results of the

experiments show that a measurable ion current exists even in the very lean combustion (equivalence ratio = 0.35) in an HCCI engine. Numerical models using detailed chemical kinetics for propane combustion, including kinetics for ion formation, support the experimental findings. The effects of the equivalence ratio, the intake mixture temperature, and the applied bias voltage on the ion signal have been studied through a series of experiments. The research shows that an inexpensive ion sensor may replace the expensive pressure transducers currently used in HCCI engines.

Conclusions

Our analytical efforts this year focused on developing numerical techniques for analysis of PCCI combustion. We developed and tested two new methodologies that can be applied for cases where there is some air and fuel stratification at the time of ignition. The two methods yield accurate results. Further development and testing is required to be able to analyze direct injected engines.

Our experimental work has demonstrated the use of inexpensive ion sensors to determine combustion timing in HCCI engines. Determining combustion timing with an accurate and inexpensive sensor is crucial for implementing a successful HCCI engine controller. The experiments show that the ion signal can be successfully applied for determining combustion timing. The experimental results have been evaluated with a chemical kinetics code, and an ion chemical kinetics mechanism has been used to explain the results.

Special Recognitions & Awards/Patents Issued

1. Lawrence Livermore National Laboratory (LLNL) HCCI program was featured in the April 2004 issue of LLNL's "Science and Technology Review."
2. Daniel Flowers was quoted in a recent issue of the Wall Street Journal (September 28, 2004), discussing the potential benefits of HCCI engines.
3. Daniel Flowers delivered an invited lecture at the SAE HCCI TopTech seminar, conducted in Berkeley, California, August 2004.

FY 2004 Publications/Presentations

1. Spatial Analysis of Emissions Sources for HCCI Combustion at Low Loads Using a Multi-Zone Model, Salvador M. Aceves, Daniel L. Flowers, Francisco Espinosa-Loza, Joel Martinez-Frias, John E. Dec, Magnus Sjöberg, Robert W. Dibble and Randy P. Hessel, SAE Paper 2004-01-1910.
2. Investigation of HCCI Combustion of Diethyl Ether and Ethanol Mixtures Using Carbon 14 Tracing and Numerical Simulations, J. Hunter Mack, Daniel L. Flowers, Bruce A. Buchholz, Robert W. Dibble, Proceedings of the Combustion Institute, Vol. 30, 2004.
3. Combustion Timing in HCCI Engines Determined by Ion-Sensor: Experimental and Kinetic Modeling, Parag Mehresh, Jason Souder, Daniel Flowers, Uwe Riedel, Robert W. Dibble, Proceedings of the Combustion Institute, Vol. 30, 2004.
4. Thermal Management for 6-Cylinder HCCI Engine: Low Cost, High Efficiency, Ultra-Low NOx Power Generation, Joel Martinez-Frias, Daniel Flowers, Salvador M. Aceves, Francisco Espinosa-Loza, Robert Dibble, Proceedings of the ASME Internal Combustion Engine Division, 2004.
5. Analysis of Homogeneous Charge Compression Ignition (HCCI) Engines for Cogeneration Applications, Salvador M. Aceves, Joel Martinez-Frias, Gordon M. Reistad, Proceedings of the ASME Advanced Energy Systems Division, 2004.

References

1. Magnus Christensen and Bengt Johansson, 2002, "The Effect of Combustion Chamber Geometry on HCCI Operation," SAE Paper 2002-01-0425.
2. Salvador M. Aceves, Daniel L. Flowers, Francisco Espinosa-Loza, Aristotelis Babajimopoulos, Dennis Assanis, 2005, "Analysis of Premixed Charge Compression Ignition Combustion with a Sequential Fluid Mechanics-Multizone Chemical Kinetics Model," Submitted to the SAE Congress, 2005.
3. Randy P. Hessel, Daniel L. Flowers, Salvador M. Aceves, 2005, "Estimating Combustion with CFD and Detailed Chemistry using an Equivalence Ratio-Temperature Multi-Zone Methodology," Submitted to the SAE Congress, 2005.
4. Parag Mehresh, Jason Souder, Daniel Flowers, Uwe Riedel, Robert W. Dibble, 2004, "Combustion Timing in HCCI Engines Determined by Ion-Sensor: Experimental and Kinetic Modeling," Proceedings of the Combustion Institute, Vol. 30.

II.A.10 HCCI and Stratified-Charge Compression-Ignition Engine Combustion Research

John E. Dec
Sandia National Laboratories
MS 9053, P.O. Box 969
Livermore, CA 94551-0969

DOE Technology Development Managers: Kevin Stork and Gurpreet Singh

Objectives

Project Objective

- Provide the fundamental understanding of homogeneous charge compression ignition (HCCI) combustion required to overcome the technical barriers to development of practical HCCI engines by industry.

FY 2004 Objectives

- Investigate the factors affecting combustion phasing with changes in fueling rate.
- Investigate the relationship between intake temperature and in-cylinder bottom dead center (BDC) temperature, and the factors causing heating/cooling during intake.
- Conduct an initial investigation of the effect of intake pressure boost (for increased power) on HCCI combustion and emissions.
- Acquire chemiluminescence images to investigate the nature of HCCI combustion under various operating conditions.

Approach

- Develop experimental techniques to isolate and evaluate the relative magnitude of each factor that affects HCCI combustion phasing with changes in fueling rate.
- Combine detailed analysis of experimental data with guidance from cycle-simulation modeling to determine the BDC temperature at various operating conditions.
- Design an experimental matrix to evaluate the effects of intake boost and fueling rate on HCCI combustion for various fuel types.
- Bring the optically accessible HCCI engine to full operational status, and establish a capability for low-light-level imaging.
- Work cooperatively with Lawrence Livermore National Laboratory (LLNL) and the University of Michigan on computational fluid dynamics (CFD) and multi-zone modeling of our experiments.

Accomplishments

- Determined the relative magnitude of the factors affecting changes in combustion phasing with changes in fueling rate. Showed how the effect of fuel chemistry on changes in combustion phasing with changes in fueling rate depends on fuel type.
- Established a methodology for computing the in-cylinder BDC temperature from easily obtained parameters.
- Investigated the effect of intake pressure boost on HCCI combustion for gasoline and other representative fuel constituents.

- Conducted an investigation of the lowest temperature for complete combustion of hydrocarbon fuels over a wide range of conditions. Showed that the peak temperature must exceed 1500 K at 1200 rpm, regardless of fuel type or combustion timing.
- Completed installation and shakedown testing of the optically accessible HCCI engine.
- Applied chemiluminescence imaging to investigate the characteristics of well-mixed and mixture-stratified HCCI.

Future Directions

- Evaluate the potential for increasing the naturally occurring thermal stratification by increasing wall heat-transfer rates to extend HCCI operation to higher loads.
- Investigate combustion timing retard as a means to extend the high-load limit of HCCI.
- Combine multi-zone Senkin modeling with experimental data to investigate how thermal stratification affects HCCI heat release rates with normal and retarded timing, and to determine the potential for extending the high-load limit with thermal stratification.
- Conduct detailed exhaust speciation study of HCCI at various operating conditions.
- Set up a high-pressure common-rail diesel fuel injection system for investigations of diesel-fueled HCCI.
- Apply laser-based and other optical imaging diagnostics to investigate the effects of thermal and mixture stratification on HCCI combustion.

Introduction

HCCI engines have significant efficiency and emissions advantages over conventional spark-ignition and diesel engines, respectively. However, several technical barriers must be addressed before HCCI can be implemented in practical engines. Among these, controlling combustion phasing as the fueling rate is varied and extending both the high- and low-load operating limits are some of the most important. As outlined under the accomplishment bullets above, the work conducted for this project during FY 2004 involved several investigations that provide new understanding related to overcoming these technical barriers.

Approach

To obtain the necessary fundamental understanding of HCCI, an HCCI engine laboratory has been established that has been equipped with both all-metal and optically accessible HCCI engines of the same basic design. The majority of the investigations in FY 2004 involved the all-metal engine, which has been fully operational since 2001. These investigations provide substantial information, but it is also advantageous to obtain a detailed understanding of in-cylinder processes through the application of advanced optical imaging diagnostics. Accordingly, installation and shakedown testing of the optically accessible engine was completed, and a low-light-level imaging capability was established.

This HCCI engine research facility is designed to allow operation over a wide range of operating conditions using various fueling techniques. It also has several features to provide precise control of parameters such as combustion phasing and mass flow rates of fuel and air, so that data are repeatable even for relatively small changes in operating conditions. For some investigations, computational modeling was applied to complement the experiments. In most cases this involved single-zone chemical kinetic modeling using the Senkin application of CHEMKIN. In addition, we have worked with LLNL to apply Kiva and multi-zone modeling to our experiment, and a collaborative modeling effort has also been established with the University of Michigan.

Results

Combustion phasing in HCCI engines can be affected by many operating parameters, and two investigations were conducted to provide an understanding of the factors that affect combustion phasing with changes in operating conditions.

For the first investigation, the factors that affect combustion phasing with changes in fueling rate were analyzed. As the fueling rate is increased in an HCCI engine, the combustion phasing, as measured by the 50% burn point (CA50, the engine crankshaft angle at 50% burned), will become more advanced unless the intake temperature is reduced. This occurs for all fuels tested (gasoline, toluene, iso-octane, PRF80 [primary reference fuel, 80 octane], and PRF60), suggesting that fuel autoignition chemistry is faster for all fuels as the mixture becomes richer. However, more careful examination shows that four other factors besides fuel chemistry change as the fueling rate is varied, and each of these can affect the combustion phasing. These factors include changes in the burn duration, wall temperature, residuals, and heating/cooling during induction. To determine the relative importance of these factors, the experiment was altered in a series of steps to sequentially remove each factor, isolating the effects of fuel chemistry.

A sample of the results is shown in Figure 1 (with iso-octane as the fuel). The three curves in this figure show the changes in required intake temperature with changes in fueling for the following scenarios: 1) the base condition with CA50 at top dead center (TDC), 2) with the effect of changes in burn duration with ϕ removed by maintaining constant "ignition" phasing as measured by the 10% burn point, and 3) with the changes in wall temperature and residuals removed by using a novel alternate firing technique, fire 19/1 [1]. For the base condition, the intake temperature must be decreased with increased fueling (equivalence ratio, ϕ), as discussed above, but with the removal of changes in burn duration, wall temperature, and residuals, the curve shows the opposite trend. Analysis of these temperature curves and other data provides the relative magnitude of these factors, as shown in Figure 2. At low loads ($\phi < 0.2$), the change in burn duration is the main reason that the intake temperature must be adjusted to maintain CA50 at TDC, while at higher loads ($\phi > 0.25$), the effect of wall heating is the dominant effect.

With the effects of fuel chemistry isolated, three fuels were examined to determine how the role of fuel chemistry on combustion phasing varied with fuel type. The results showed that for single-stage ignition fuels such as iso-octane and gasoline, the autoignition chemistry is only slightly enhanced by

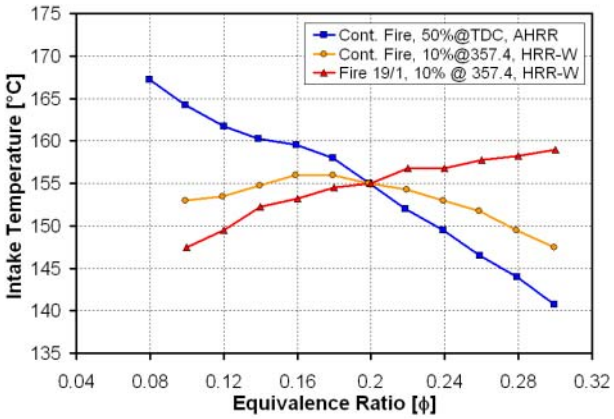

Figure 1. Comparison of the change in required intake temperatures with changes in fueling (ϕ) for three conditions: 1) the base condition with CA50 at TDC, 2) with constant 10% burn point, and 3) with constant wall temperature and residuals.

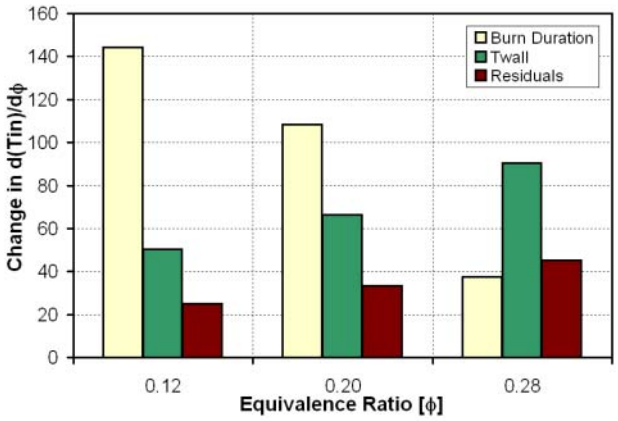

Figure 2. Relative magnitude of the effects of burn duration, wall temperature, and residuals on changes in required intake temperature with changes in fueling rate, at three equivalence ratios.

increased equivalence ratio. Thus, the changes in required intake temperature are dominated by the sum of the other effects. However, for fuels exhibiting two-stage ignition (*i.e.*, cool-flame chemistry), such as PRF80 (or by inference, diesel fuel), the autoignition kinetics are greatly enhanced with increased ϕ, and kinetics are dominant over the other effects [1].

For the second investigation related to factors that affect combustion phasing, the effect of heating and cooling during induction was examined in detail.

In addition, a straightforward algorithm was developed to compute the in-cylinder temperature at the end of induction (T_{BDC}). This investigation showed that are four main effects that cause the T_{BDC} to differ from the measured intake temperature: 1) heat transfer during induction, 2) heating of the charge due to flow dynamics, "dynamic heating", 3) cooling due to fuel vaporization, and 4) mixing with residuals. The technique for estimating T_{BDC} is based on a detailed analysis of experimental data with the dynamic heating being computed for one base condition per engine speed using a cycle-simulation model, as described in detail in Ref. [2].

An example of the application of this technique is shown in Figure 3. As can be seen, the kinetics model (CHEMKIN) predicts that T_{BDC} must be increased with engine speed to maintain the same combustion timing since there is less real time for the autoignition/combustion reactions to occur. In contrast, the required intake temperature for the experiment shows little change above 900 rpm, which seems unrealistic. However, when the experimental T_{BDC} is computed as outlined above, it shows a monotonic increase similar to CHEMKIN. Similar validity of the technique for computing T_{BDC} has been demonstrated for fuel vaporization and wall heat-transfer effects [2].

Boosting the intake pressure can increase the power output of HCCI engines, but it can also affect the autoignition timing and the propensity for knock. To better understand the effects and tradeoffs of intake boosting, tests were conducted over a range of intake pressures for gasoline and several representative commercial-fuel constituents, including: iso-octane, methyl-cyclohexane, toluene, and a mixture of toluene and n-heptane. These studies showed that due to the ignition enhancement with increased intake pressure, the amount of boost is typically limited by the lowest intake temperature that can be achieved or by engine knock. The onset of these limits is strongly related to fuel-type, and for some fuels, boost causes the shift from single-stage to dual-stage ignition, which further reduces the allowable boost before the limits are reached.

In another study, the effect of fuel type was found to be directly related to the minimum fueling

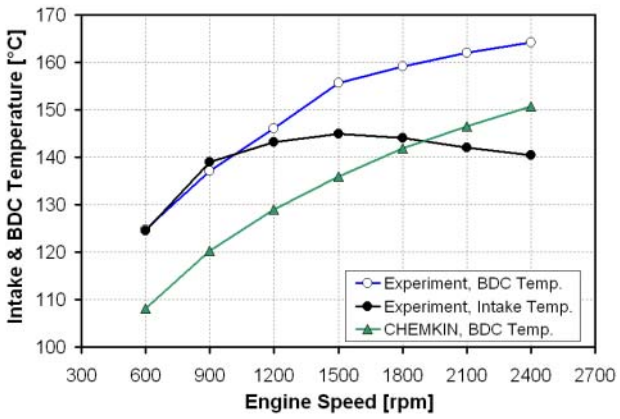

Figure 3. Changes in intake or BDC temperature required to maintain CA50 at TDC as engine speed is varied. The CHEMKIN T_{BDC} is lower that the experimental T_{BDC} because the model is adiabatic.

rate for complete bulk-gas combustion, *i.e.* the low-load limit [3]. This investigation showed that for complete combustion, the peak combustion temperature must exceed 1500 K at 1200 rpm, independent of combustion phasing or hydrocarbon fuel-type. (This required temperature varies from 1460 to 1550 K for engine speeds from 600 to 2400 rpm, respectively.) Thus, for fuels with low ignition temperatures (*e.g.*, PRF80 or diesel fuel), a higher equivalence ratio must be used to reach these required peak temperatures, or some other technique such as charge-mixture stratification must be applied. In addition, a combined computational and experimental study was conducted in cooperation with LLNL [4] that showed how the thermal boundary layer affects the minimum fueling rate for complete combustion.

In order to better understand the nature of HCCI combustion, chemiluminescence images were acquired at various operating conditions using the optically accessible HCCI engine (Figure 4). Figure 5 shows an example of an image sequence with fully premixed intake conditions. Despite the well-mixed intake, the images show significant turbulent structure, and the change in the appearance of the images through the sequence indicates significant thermal stratification. The first image shows ignition/combustion over broad areas, but dark regions suggest colder regions that have not yet ignited. By 363° CA, the first-ignited regions appear

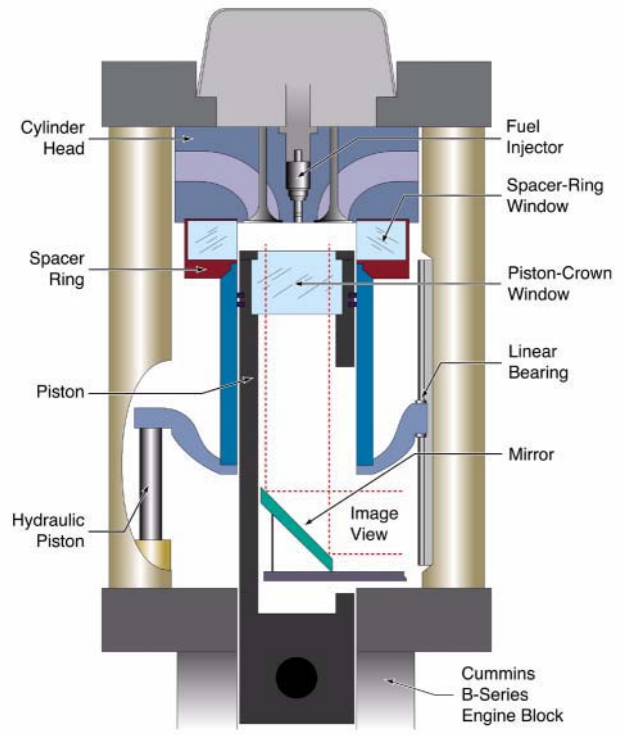

Figure 4. Schematic of the optically accessible HCCI engine.

to have burned out as indicated by the large dark regions. Combustion is now confined to more narrow "string-like" regions, that are thought to correspond to the colder regions that had not yet ignited in the earlier images. Near the end of the heat release (364 - 366° CA), combustion occurs in the valve-pocket crevices where the mixture is even colder. Understanding the nature of thermal stratification in HCCI engines and how it can be affected by operating parameters is a key element for slowing the heat release rate to extend HCCI operation to higher loads.

Conclusions

- In addition to fuel chemistry, several factors affect combustion phasing as the fueling rate is varied. The most important factors are changes in burn duration at low loads ($\phi < 0.2$), and wall heating at higher loads ($\phi > 0.25$).
- The autoignition chemistry is only slightly enhanced by increased fueling for single-stage ignition fuels such as iso-octane and gasoline, but for fuels with two-stage ignition (significant cool-flame chemistry), the enhancement in the autoignition chemistry is substantial and can be dominant over the other factors.
- The in-cylinder temperature at the end of induction (T_{BDC}) is a valuable parameter for analyzing HCCI, and a technique has been developed to estimate T_{BDC} with good accuracy.
- Boosting the intake pressure can significantly increase the power output, but operating range becomes limited by knock and/or the minimum available intake temperature.
- For complete combustion, peak temperatures must exceed 1500 K at 1200 rpm, regardless of combustion phasing or hydrocarbon fuel-type.
- Chemiluminescence imaging was found to provide significant insight into the nature of HCCI combustion and how it is affected by thermal and mixture stratification.

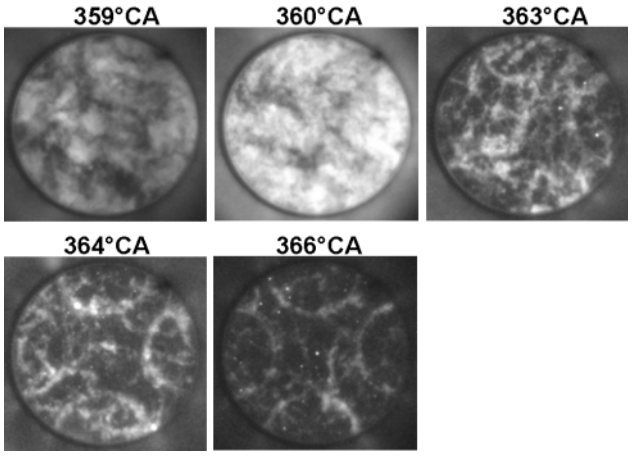

Figure 5. Chemiluminescence images of HCCI combustion for well-mixed intake charge. Fuel is iso-octane, $\phi = 0.24$. Images were acquired through the piston-crown window as shown in Figure 4.

Special Recognitions & Awards/Patents Issued

1. Invited speaker and panelist for SAE panel discussion on HCCI at the 2003 SAE Fall Powertrain and Fluid Systems Conference, Pittsburgh, PA, October, 2003.
2. Invited speaker at the SAE Homogeneous Charge Compression Ignition Symposium, Berkeley, CA, August, 2004.

FY 2004 Publications/Presentations

1. Dec, J. E. and Sjöberg, M., "Isolating the Effects of Fuel Chemistry on Combustion Phasing in an HCCI Engine and the Potential of Fuel Stratification for Ignition Control," SAE Paper 2004-01-0557, 2004.
2. Sjöberg, M. and Dec, J. E., "An Investigation of the Relationship between Measured Intake Temperature, BDC Temperature, and Combustion Phasing for Premixed and DI HCCI Engines," SAE paper 2004-02-1900, 2004.
3. Sjöberg, M. and Dec, J. E., "An Investigation into Lowest Acceptable Combustion Temperatures for Hydrocarbon Fuels in HCCI Engines," presented at and to be published in the proceedings of the 2004 International Combustion Symposium, 2004.
4. Aceves, S. M., Flowers, D. L., Espinosa-Loza, F., Martinez-Frias, J., Dec. J. E., Sjöberg, M. and Dibble, R. W., Hessel, R. P., "Spatial Analysis of Emissions Sources for HCCI Combustion at Low Loads Using a Multi-Zone Model," SAE paper 2004-01-1910, 2004.
5. Sjöberg, M. and Dec, J. E., "Combined Effects of Fuel-Type and Engine Speed on Intake Temperature Requirements and Completeness of Bulk-Gas Reactions for HCCI Combustion," SAE paper 2003-01-3173, 2003, presented at the 2003 SAE Fall Powertrain Conference, October 2003.
6. Dec, J. E. and Sjöberg, M., "The Role of Optical Diagnostics in the Development of HCCI Engines," presented at the SAE 2003 Fall Powertrain and Fluid Systems Conference, October 2003.
7. Sjöberg, M. and Dec, J. E., "An Investigation of the Relationship between Measured Intake Temperature, BDC Temperature, and Combustion Phasing for Premixed and DI HCCI Engines," Advanced Engine Combustion Working Group Meeting, January 2004.
8. Dec, J. E. and Sjöberg, M., "Update on Recent Progress in the HCCI Dual-Engine Laboratory," Advanced Engine Combustion Working Group Meeting, January 2004.
9. Dec, J. E. and Sjöberg, M., "HCCI and Stratified-Charge CI Engine Combustion Research," Advanced Combustion R&D Peer Review, May 2004.
10. Sjöberg, M. and Dec, J. E., "Enhanced Natural Thermal Stratification and Combustion Timing Retard for Smoothing of HCCI Heat-Release Rates," Advanced Engine Combustion Working Group Meeting, June 2004.
11. Dec, J. E. and Sjöberg, M., "Insights into HCCI Combustion Using Chemiluminescence Imaging," Advanced Engine Combustion Working Group Meeting, June 2004.
12. Dec, J. E. and Sjöberg, M., "HCCI Combustion Inefficiency and Potential Solutions," SAE Homogeneous Charge Compression Ignition Symposium, August 2004.
13. Dec, J. E. and Sjöberg, M., "Factors Affecting HCCI Combustion Phasing for Fuels with Single- and Dual-Stage Chemistry," International Energy Agency (IEA) Task Leaders Meeting, August 2004.
14. Dec. J.E. and Sjöberg, M., "Factors Affecting HCCI Combustion Phasing for Fuels with Single- and Dual-Stage Chemistry," presented at and to be published in the proceedings of the 10th Diesel Engine Emissions Reduction Workshop (DEER 2004), San Diego, CA, Aug.-Sept. 2004.

References

1. Dec, J. E. and Sjöberg, M., "Isolating the Effects of Fuel Chemistry on Combustion Phasing in an HCCI Engine and the Potential of Fuel Stratification for Ignition Control," SAE Paper 2004-01-0557, 2004.
2. Sjöberg, M. and Dec, J. E., "An Investigation of the Relationship between Measured Intake Temperature, BDC Temperature, and Combustion Phasing for Premixed and DI HCCI Engines," SAE paper no. 2004-02-1900, 2004.
3. Sjöberg, M. and Dec, J. E., "An Investigation into Lowest Acceptable Combustion Temperatures for Hydrocarbon Fuels in HCCI Engines," to be published in the proceedings of the 2004 International Combustion Symposium, 2004.
4. Aceves, S. M., Flowers, D. L., Espinosa-Loza, F., Martinez-Frias, J., Dec. J. E., Sjöberg, M. and Dibble, R. W., Hessel, R. P., "Spatial Analysis of Emissions Sources for HCCI Combustion at Low Loads Using a Multi-Zone Model," SAE paper no. 2004-01-1910, 2004.

II.A.11 Automotive HCCI Combustion Research

Richard Steeper
Sandia National Laboratories, MS 9053
P.O. Box 969
Livermore, CA 94551-0969

DOE Technology Development Managers: Kevin Stork and Gurpreet Singh

Objectives

The focus of the Automotive HCCI Combustion project is on applying advanced optical diagnostics to characterize homogeneous charge compression ignition (HCCI) fuel injection and fuel-air mixing processes, and to understand how mixture preparation strategies affect the combustion and emission performance of automotive HCCI engines. Objectives for FY 2004 are as follows:

- Benchmark fired operation of the recently completed Automotive HCCI Optical Engine Facility.
- Identify a laser-induced fluorescence (LIF) diagnostic suitable for quantitative equivalence ratio measurements in the HCCI engine.
- Apply selected LIF diagnostics to begin characterizing the fuel-mixture preparation process in the fired HCCI engine.

Approach

- Perform fired tests of the automotive HCCI engine to identify its viable operating range, and benchmark the engine's combustion performance across the range of operating conditions.
- Perform bench-top experiments to match the volatility of LIF tracers to the primary reference fuels (PRF) that they are meant to track in the engine.
- Perform engine experiments to assess the quality of LIF measurements of in-cylinder fuel distribution.
- Apply LIF imaging to characterize the effects of fuel-injection timing on charge preparation.

Accomplishments

- Benchmark tests of the optical HCCI engine were completed using PRF fuels with inlet temperatures up to 220°C, inlet pressures up to 1.75 bar absolute, and loads up to 4 bar indicated mean effective pressure (IMEP). Skip-fired operating conditions viable for optical experiments were identified for PRFs with octane numbers less than 80.
- Bench-top evaporation tests identified several LIF tracers that improve fuel tracking by better matching the volatility of PRF fuels. LIF tracers formulated to co-evaporate well with iso-octane, as shown in prior gasoline direct injection (GDI) work, were shown here to properly co-evaporate with the full range of PRF mixtures.
- The same group of LIF tracers was tested in the fired engine to assess the ability to quantify in-cylinder equivalence ratios. Two co-evaporative tracers with sufficient signal strength at appropriate concentrations were identified. A technical paper describing the results of the bench-top and engine tests of the LIF tracers was submitted to SAE.
- In-cylinder equivalence ratio distributions were measured and converted to probability density function (PDF) statistics to quantify the effects of injection timing on charge preparation.

Future Directions

- Characterize the charge-preparation process for alternative injectors and injection strategies, including liquid injection, wall wetting, and fuel-air mixing.
- Correlate the characterization measurements with combustion and emissions performance as measured using pressure records, combustion-luminosity images, and emissions measurements.

Introduction

Major challenges to the implementation of HCCI combustion—including phasing control, operating-range extension, and emissions control—may well require advanced, non-homogeneous, fuel-air mixing strategies. Alternative injection strategies such as retarded or multiple injections can be used to modify the local equivalence ratios at which combustion takes place, thereby affecting rate of heat release, combustion efficiency, and engine-out emissions. The focus of the current project is the application of in-cylinder optical diagnostics to characterize the fuel-air mixing process and to correlate mixing with the subsequent HCCI combustion.

Approach

Four activities were undertaken in FY 2004. The first activity comprised engine experiments to benchmark the performance of the automotive HCCI engine. Modifications to convert the facility to HCCI operation were completed at the end of the last reporting period. Second, bench-top evaporation experiments tested several LIF tracer/PRF fuel mixtures to determine whether they properly co-evaporate—a necessary condition for quantitative LIF diagnostics. Third, the LIF tracers were tested in the fired engine to assess their signal-to-noise ratios. Finally, measurements of in-cylinder fuel-air mixing were commenced, producing PDF statistics of mixing as a function of injection timing.

Results

Benchmark tests of the optical HCCI engine were performed under the following conditions: compression ratio = 11.8; low residual cams; premixed and direct injection (DI) fueling; fuels = PRF 50, 80, and 100; speed = 1200 rpm; intake temperatures 220°C and intake pressure = 1.75 bar IMEP. A wide range of loads were obtainable using the PRF-50 fuel. For the PRF-80 fuel, the operating range was reduced, with appropriate combustion phasing only possible at elevated intake temperatures and pressures. During tests with PRF 100 (iso-octane) at loads near the limit of the optical engine, phasing near top center was not achievable, even at the limit of our intake temperature and pressure range. Operation with PRF 100 in the future may be possible with residual-enhanced intake temperatures or fuel additives.

The second activity comprised bench-top evaporation experiments to test four selected LIF tracers: 10% 3-pentanone, 9% 3-hexanone + 1% 3-pentanone, 3% toluene, and 1.2% 3-hexanone. Some of these tracers have been previously tested for use with the common GDI surrogate fuel iso-octane, and the current experiments extended the tests to cover the full range of PRF mixtures commonly used as HCCI fuels. Results of the tests for the four tracers are shown in Figure 1. Each graph summarizes data for one of the tracers mixed in four different PRF mixtures: PRF 0, 50, 80, and 100.

The x-axes of the graphs represent the progress variable (remaining liquid mass fraction) during the evaporation of tracer/PRF mixtures, measured using a mass scale. On this axis, time progresses from right (100% mass remaining) to left (zero mass remaining). The open symbols indicate the rate of evaporation of the total mixture, with values read on the left y-axis. The closed symbols, read on the right axis, are derived from LIF measurements of the vapor leaving the evaporation chamber. These data are proportional to the evaporation rate of the tracer alone. By comparing the open and closed symbol data, we can determine if the tracer co-evaporates with the fuel—a necessary condition for the tracer to properly track the fuel during in-cylinder mixing.

The fact that in each graph the open and closed symbols (taken separately) fall on a single curve indicates that the evaporation behavior of all these tracers is the same regardless of the PRF selected as

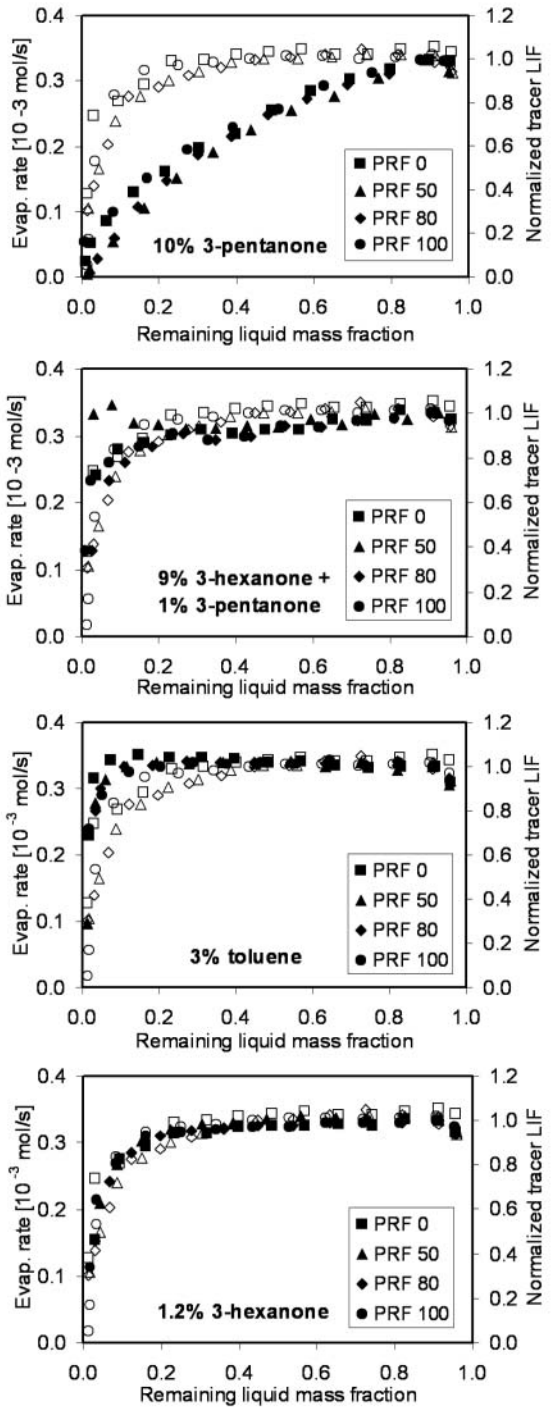

Figure 1. Evaporation histories of mixtures of LIF tracers and PRFs. X-axis: evaporation progress variable = remaining liquid mass fraction, read from left to right; Left axis: total mixture evaporation rate (open symbols); Right axis: normalized vapor-phase tracer LIF signal, proportional to tracer evaporation rate (closed symbols).

fuel. This is due to the close match of the physical properties of the iso-octane and n-heptane components of PRFs. In the top graph, however, it is clear that tracer evaporation (closed-symbol data) does not match the total mixture evaporation rate (open-symbol data). This indicates that 3-pentanone does not properly match the evaporation of the PRFs. In contrast, the other three graphs indicate excellent co-evaporation of tracer and fuel, implying that these tracers will more faithfully track the fuel during in-cylinder evaporation.

Tests of the tracers during LIF imaging in the engine (Activity 3) showed that while signal levels are not as good as 3-pentanone, the 9% 3-hexanone + 1% pentanone signal is satisfactory. The 3% toluene tracer has about the same signal level as the 9% 3-hexanone + 1% pentanone, but the current configuration of our diagnostic is not optimal for this tracer—further gains in signal-to-noise ratio are possible. The fourth tracer, 1.2% 3-hexanone, shows the perfect co-evaporation of an azeotrope mixture, but its signal in the engine tests was too low to be useful for equivalence ratio measurements. The LIF tracer test results will be published in a paper submitted to the 2005 SAE Congress.

The final activity this year comprised engine measurements initiating the characterization of fuel-air mixing in the fired HCCI engine. Using a current-design, 8-holed injector and varying start of injection (SOI) from 300 to 60 crank angle degrees (CAD) before top center of compression, we recorded sets of LIF images to reveal the effect of injection timing on fuel distribution. Data for each SOI timing were reduced to equivalence ratio PDF plots representing the state of mixing in the cylinder just prior to cool-flame ignition. Figure 2 combines PDF plots for the injection timing sweep into a 3-D PDF graph. The rear plane represents early injection, and the narrow PDF peak is characteristic of the resulting homogeneous mixture. As injection is retarded (moving forward in the 3-D graph), the mixture becomes progressively stratified, and the PDF broadens. The goal is to compare these fuel distribution measurements with combustion and emission data to guide the development of mixing strategies that enhance HCCI combustion by, for instance, reducing CO, HC, and NO_x emissions or by moderating heat release rates.

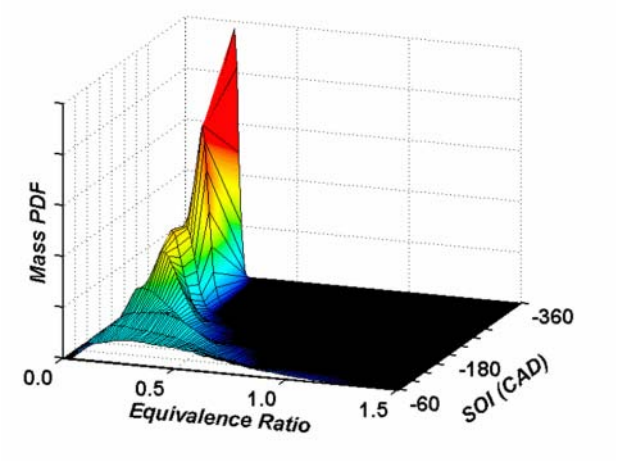

Figure 2. 3-D graph of equivalence ratio PDF curves for a range of SOI timings. Operating conditions: 1200 rpm, 120°C and 1.2 bar intake temperature and pressure, 8-hole injector, PRF-50 fuel, 0.24 equivalence ratio

Conclusions

Following completion of HCCI-enabling modifications to the light-duty optical engine, benchmark tests were performed to map the viable operating range of the automotive HCCI engine. Bench-top comparison of several candidate LIF tracers highlighted three tracers whose evaporation rates match the primary reference fuels far better than 3-pentanone. Tests in the HCCI engine revealed that the signal strength of one of them was too low to be useful. Finally, measurements of fuel-air mixing were commenced in the fired HCCI engine, producing PDF statistics of the effect of injection timing on fuel distribution prior to ignition.

Special Recognitions & Awards/Patents Issued

1. Richard Steeper of Sandia National Laboratories was selected as Co-Vice-Chair of Combustion for SAE's Fuels and Lubricants Activity.

FY 2004 Presentations

1. R. R. Steeper, "HCCI Fuel-Air Mixing Experiments," DOE AEC Working Group Meeting, Sandia National Laboratories, Livermore, January, 2004.
2. R. R. Steeper, "Progress Report: Automotive HCCI Engine Research," Invited seminar, General Motors Research, Detroit, March, 2004.
3. R. R. Steeper, "Automotive HCCI Combustion Research," DOE Advanced Combustion Engine Peer Review, Argonne National Laboratory, Chicago, May, 2004.
4. R. R. Steeper, "Automotive HCCI Engine Progress Report," DOE AEC Working Group Meeting, USCAR, Detroit, June, 2004.

FY 2004 Publications

1. D. Han and R. R. Steeper, "Examination of Iso-octane/Ketone Mixtures for Quantitative LIF Measurements in a DISI Engine," SAE Transactions 111-4: 313-324, 2002.
2. R. R. Steeper, "Automotive HCCI Combustion Research," DOE Advanced Combustion Engine Annual Report, 2003.
3. M. Davy, P. Williams, D. Han, and R. R. Steeper, "Evaporation Characteristics of the 3-Pentanone/ Isooctane Binary System," Experiments in Fluids 35: 92-99, 2003.
4. R. R. Steeper, S. De Zilwa, and A. Fayoux, "Co-Evaporative Tracer-PRF Mixtures for LIF Measurements in Optical HCCI Engines," submitted to 2005 SAE Congress, 2004.

II.A.12 HCCI Engine Optimization and Control Using Diesel Fuel

Profs. Rolf D. Reitz (Primary Contact), Dave Foster, Jaal Ghandhi, Kevin Hoag and Chris Rutland
Engine Research Center
University of Wisconsin-Madison
1500 Engineering Drive
Madison, WI 53706

DOE Technology Development Manager: Kevin Stork

Subcontractor:
Prof. D. Haworth, Penn State University

Objectives

- Develop methods to optimize and control homogeneous charge compression ignition (HCCI) engines, with emphasis on diesel-fueled engines.
- Use engine experiments and detailed modeling to study factors that influence combustion phasing, unburned hydrocarbon (UHC) and carbon monoxide (CO) emissions.
- Provide criteria for transition to other engine operation regimes (e.g., standard diesel and low-temperature combustion).

Approach

- Use two fully-instrumented engines with prototype fuel injection systems and combustion sensors to map and define HCCI combustion regimes, and apply optimization techniques.
- Develop and apply engine performance models, including multi-, zero- and 1- dimensional global models for control system development.
- Use homogeneous and stratified charge Coordinating Fuel Research (CFR) engine and low and high injection pressure heavy-duty engine experiments to document fuel effects on HCCI ignition.
- Develop and apply modeling tools, including multi-dimensional codes (e.g., KIVA with state-of-the-art turbulent combustion and detailed and reduced chemistry models), to reveal combustion mechanisms.

Accomplishments

- Diesel HCCI combustion regimes have been identified on a Caterpillar 3401 engine using both low-pressure and high-pressure multiple injection strategies.
- Evaluated and selected combustion sensors and methodologies for engine control.
- Low-pressure diesel fuel injection has been shown to lead to significant fuel film formation on the cylinder wall that deteriorates engine performance.
- Models have been used successfully to propose methods to minimize wall film fuel and to provide start-of-combustion control via variable valve timing and variable geometry sprays.
- HCCI engine operating limits have been shown to be extended by operation with stratified combustion.
- Detailed combustion computations have been used to identify methodologies to increase mixing prior to ignition for emissions reduction.

Future Directions

- Use of multiple injections for diesel HCCI combustion control will be assessed.
- Guidelines for diesel HCCI will be obtained by experiments and modeling using variable intake valve actuation for combustion phasing control.

- Diesel HCCI will be investigated for fumigated/direct injection configurations including port fuel injection and high-pressure diesel in-cylinder injection systems.
- Efficient methods for including detailed kinetics will be implemented and applied in multidimensional models for more accurate combustion predictions.

Introduction

Advantages of HCCI operation include significantly reduced NO_x and particulate emissions. However, there are significant challenges associated with the successful operation of HCCI engines. One of the major difficulties is controlling the combustion phasing—mainly the assurance of auto-ignition at appropriate timings over a wide range of operating conditions. Another obstacle specific to diesel HCCI engine operation is the fact that the early injection required to provide time for fuel-air mixing can lead to wall impingement and, consequently, poor combustion efficiency. In addition, the formation of relatively high emissions of unburned hydrocarbons (HC) and carbon monoxide (CO) can occur due to incomplete combustion with low-temperature lean burn. The power output of the HCCI engine is also limited since the combustion can become unstable. The present research investigates methods to quantify and overcome these obstacles using a combined experimental and modeling approach.

Approach

In order to control the engine, it is necessary to know what variables to control. The six (6) technical tasks of the present work provide information about HCCI combustion mechanisms for use in knowledge-based engine control schemes. The experiments of Task 1 use a fully instrumented Caterpillar 3401 heavy-duty diesel engine that features electronically controlled fuel injection systems to map combustion regimes. Combustion sensors have been investigated for engine control, including acceleration (knock), ionization and cylinder-pressure detectors. Combustion diagnostics include engine-out particulate, NO_x, HC and other gaseous emissions measurements. Computer modeling, coupled with the engine experiments, is also being used to devise strategies for optimizing and controlling HCCI engine performance and reducing emissions over the speed-load range of interest in applications. The engine performance models include zero- and one-dimensional global models for control system development (Task 2). Task 3, In-cylinder Measurements (removed from the original proposal due to funding limitations, but now included with matching funding from industry), provides detailed validation data for chemical kinetics models. Additional model validation data is obtained using a CFR engine operated with various fuels (Task 4). The influence of turbulence, temperature and mixture inhomogeneity is revealed with highly resolved computational fluid dynamics (CFD) predictions (Tasks 5 and 6).

Results

Task 1: HCCI engine combustion optimization and regime mapping.

The Caterpillar 3401 heavy-duty diesel engine has been tested over a wide range of speeds and loads using low- and high-pressure injection systems and various injection strategies [1]. It was found that to achieve highly premixed combustion (HCCI-like) conditions, optimal dwell between the end of injection and the start of combustion is required to allow sufficient time for fuel-air mixing. The local mixture must be lean for soot/NO_x control [2]. With early injections (e.g., 50 degrees btdc), wall wetting is a significant problem. With high-pressure injection, an injection time earlier than 30 degrees before top dead center (btdc) can cause unacceptably high rates of pressure rise or lead to significant lost fuel due to wall impingement. On the other hand, combustion stability becomes a problem if the fuel is injected late in the cycle (e.g., more than 20 degrees after top dead center [atdc]). With low-pressure injection, the combustion process is complicated by a compromise between vaporization, mixing and ignition that is especially severe with the use of diesel fuel [3, 4]. A real-time control methodology based on a response surface method (RSM) technique has been established that uses a cylinder pressure sensor for feedback control. The methodology has been applied to optimize high

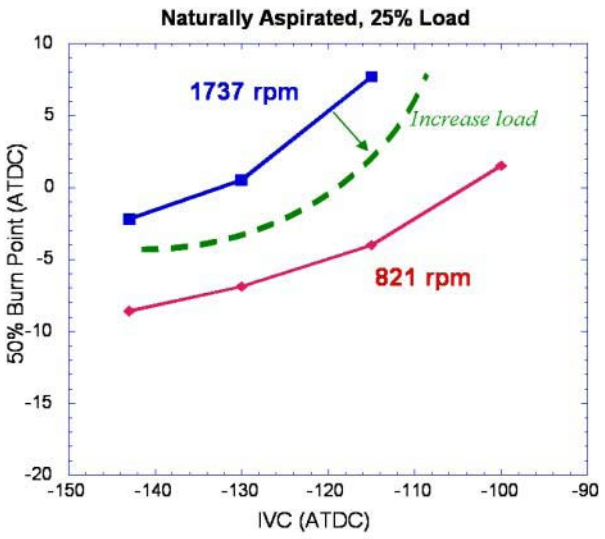

Figure 1. Combustion phasing control with variable valve timing. 50% burn point versus IVC for different engine speeds and loads.

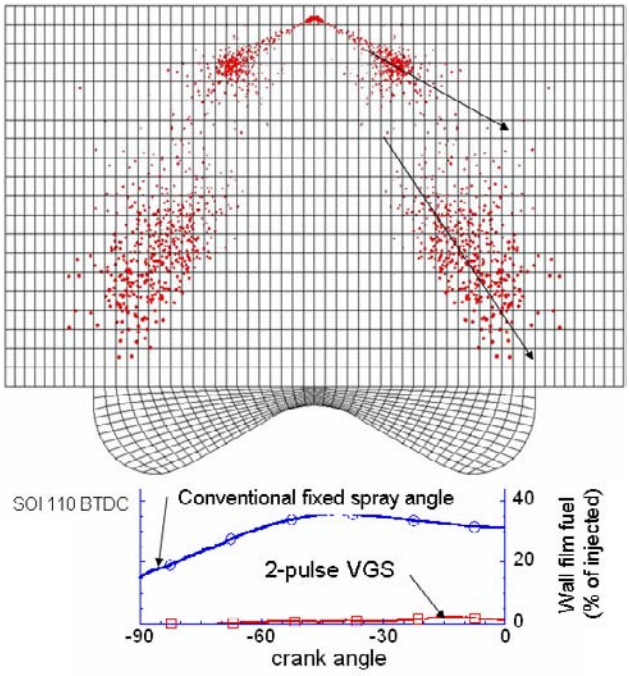

Figure 2. Optimized spray angle in each injection pulse gives improved fuel-air mixing and significantly reduced impinged fuel during the compression and combustion processes.

injection pressure engine operation using a multiple injection strategy [5]. Detailed chemistry models have been developed using an efficient skeletal reaction mechanism to describe diesel fuel oxidation chemistry [6, 7, 8]. NO_x and soot emission models have been integrated into the mechanism such that the model successfully predicts the combustion process, as well as emissions trends. Acetylene is used as the soot formation species in the model formulation. Application of the model has shown that low soot emissions at early start-of-injection (SOI) timings (e.g., 20 btdc) is due to enhanced oxidation, while low soot emissions at late SOI (e.g., 5 atdc) is a result of less soot formation. The model is being further used to study combustion phasing control using variable intake valve camshaft (IVC) timing that has the same effects as varying the compression ratio [9]. Effects of load, boost and engine speed have been investigated, and the results have shown that the 50% burn point is retarded at high engine speed due to the shorter times available for chemical reactions. Combustion phasing can be optimized by increasing the engine load such that the IVC is within a controllable range, as shown in Figure 1. In addition, it is found that the 50% burn point is largely unaffected by boost, which can be used at higher loads to improve indicated mean effective pressure (IMEP). The present CFD models have also been used to explore the benefits of using variable geometry sprays (VGS) on mixture preparation for low-pressure direct in-cylinder injection HCCI operation. The results show that the amount of wall film fuel can be drastically reduced if the included spray angle is allowed to vary from a smaller angle at the beginning to a wider angle at the end of injection, as shown in Figure 2 [10]. Future modeling studies will include the optimization of intake valve timing with the VGS multiple injection strategy and exhaust gas recirculation (EGR). Models will also be used to help set up experimental port fuel injection/direct in-cylinder injection (PFI-DI) conditions to explore diesel HCCI low-emission operation.

Task 2: Combustion modeling and control.

Cycle simulation models are an important tool in understanding and developing viable combustion systems for HCCI operation. However, currently available cycle simulation codes lack advanced models for HCCI combustion. Under this project, advanced system-level modeling tools are being

developed that can accurately predict direct injection diesel-fueled HCCI combustion. These are incorporated into control systems to study the basic time scales and feasibility of various control strategies during transient operations.

Commercially available full-cycle simulation codes are a convenient starting point as they readily model gas exchange processes. Three different approaches were used to couple advanced models with a cycle simulation program to capture the physics of HCCI combustion. The coupled simulations are used to study basic combustion controllers and to analyze fundamental aspects of speed/load transients in direct injection (DI) diesel HCCI operation. In the first approach, the GT-Power engine simulation code was integrated with Chemkin as a single-zone external combustion model to facilitate detailed chemistry calculations. In the second approach, an external cylinder model was developed and implemented into GT-Power. This model incorporates sub-models for fuel injection, vaporization, detailed chemistry calculations (Chemkin), heat transfer, and energy and species conservation. To improve the modeling accuracy, a multi-zone approach was used to account for temperature and fuel stratifications in the cylinder charge [11]. In the third approach, the multi-dimensional ERC-KIVA CFD code was coupled with GT-Power. The primary motivation for this coupling was to more accurately model the fuel injection process since it is critical in DI HCCI operation. To reduce run times, a validated coarse grid version of ERC-KIVA is being used.

The simulation results have been validated with experimental data from the Caterpillar 3401 engine modified for DI diesel HCCI operation. Parametric studies were conducted to identify the variables affecting ignition timing, and the coupled simulation was used to demonstrate transient operations in speed and load to develop closed loop control strategies, as shown in Figure 3. This example shows that a fuel savings of up to 3% is predicted with optimal control of fuel injection and intake valve closure timings. Future work aims at continued model development to make the system-level tools faster and more accurate, better understanding of the physics and relevant time scales for combustion control, and evaluation of relative advantages and disadvantages of various control concepts.

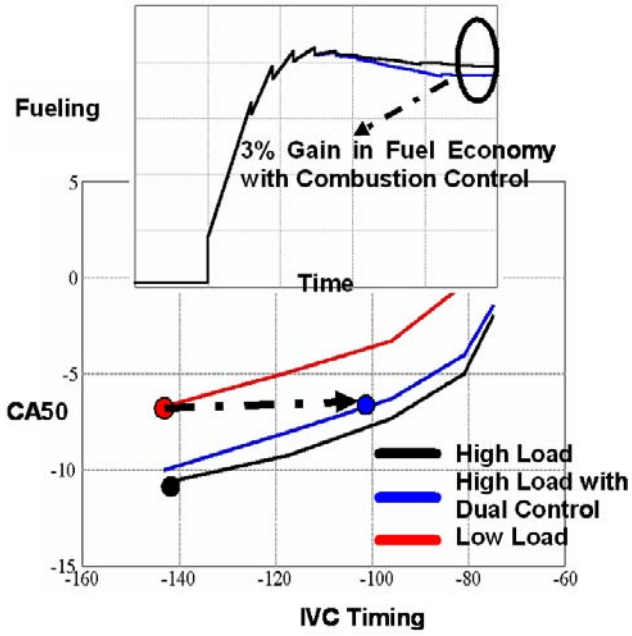

Figure 3. Simulation of load transient using simultaneous closed-loop control of fuel mass injected and variable intake valve closure. The use of variable valve closure demonstrates a 3% improvement in fuel economy.

Task 3: In-cylinder Measurements.

Near-wall planar measurements are being pursued in order to investigate the role of thermal stratification due to the cold cylinder walls. The experiment, however, cannot be performed in the manner of most planar laser-based measurements due to vignetting. [Vignetting is an optical effect that arises when an extended obstruction (e.g., the combustion chamber surface) is between the camera and the image plane, resulting in a reduction of the signal intensity near the obstruction, which is where one desires quantitative intensity information.] To overcome this problem, a through-the-wall illumination technique is being developed. Line-of-sight absorption measurements are being pursued to quantitatively measure the OH concentration as a function of temperature near the lean combustion limit. Presently, the design of the optical system is being undertaken. Finally, a modeless, wavelength-agile laser source has been developed to measure H_2O concentration and temperature. Measurements over a wide range of operating conditions will be pursued next. Wavelength-agile sources that will allow the measurement of other species are also being pursued.

Task 4: Ignition chemistry.

A focus of the research has been experimental engine tests on charge stratification as a means of extending the light-load operating range. The results show that there are operating windows at light-load conditions in which HCCI operation is improved via charge stratification [12]. Under these conditions, if the charge is premixed, the combustion quality is poor and the CO and HC emissions are very high. As the degree of stratification is increased, the CO and HC can be reduced. However, as the stratification is increased further, NO_X starts to increase.

A companion CFD modeling effort has attempted to quantify the threshold stratification for which combustion is improved, yet NO_X stays low. These simulations were conducted as full 3-D calculations that included the intake process, and sample results are shown in Figure 4. Five operating conditions have been simulated at 600 rev/min, compression ratio 16.6, equivalence ratio 0.15, with iso-octane as the fuel used in the simulation (the data are for PRF 91.8, the fuel that enabled us to explore the stratified operating conditions). Except for the premixed homogeneous case, all the fuel was directly injected into the cylinder. The injection profile for each case was created based on a validated spray model.

The trend of NO_X versus time of start of injection (SOI) is shown across the bottom of Figure 4. It is observed that the NO_X stays low when start of injection occurs earlier than 90^o btdc. Also, it was noted that there is significant stratification in both equivalence ratio and temperature right up to start of combustion for all cases investigated, even those in which the NO_X emission from the cylinder is low (see Figure 4). However, when NO_X increases as injection timing is retarded, it increases very rapidly.

Tasks 5 and 6: Multidimensional Modeling.

The impacts of mixing and fuel preparation on HCCI combustion phasing, specifically the study of ignition 'dwell' between end of fuel injection and start of combustion, are being studied using CFD. Temperature is known to have a large and direct impact on the timing and duration of ignition dwell. However, initial fuel-air distribution and mixing can also affect combustion phasing, with the advantage

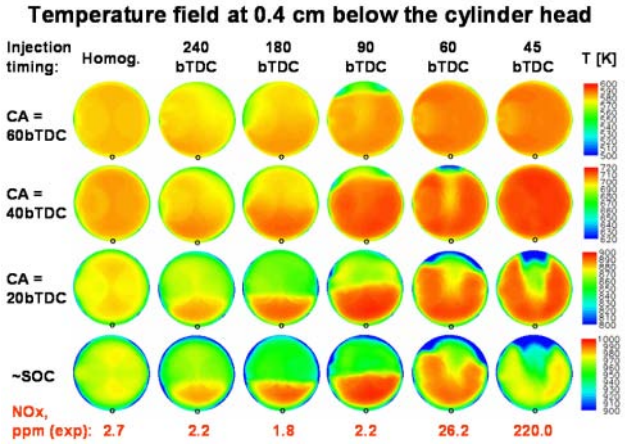

Figure 4. Predicted temperature distributions at different crank angles in a cut plane at the injector location for different SOI. The engine-out NO_X for each operating condition is given at the bottom of each column of images.

of a much faster response time than changes in temperature. To investigate the impact of mixing, variations in EGR percent, fuel injection timing, engine valve actuation and swirl ratio magnitude were simulated. To determine the extent of fuel-air mixing generated by these techniques, the equivalence ratio and temperature distribution, intermediate radical formation, mixing timescales and fuel vaporization were analyzed. The results showed that the initial fuel-air distribution did affect the ignition dwell, although to a smaller extent than changes in temperature [12].

Currently, work is in progress to incorporate several large eddy simulation (LES) models into the study. LES models are more accurate in depicting the large-scale fluid flow structures and will help understand details of mixing in the engine. Figure 5 shows a sample result using the standard Smagorinsky LES model. This image was used to study the details of the flow structure and temperature profiles during the intake stroke. These profiles were compared with earlier profiles from Reynolds Averaged Navier Stokes (RANS) models. It was observed that the LES profiles were able to capture important details of the flow structure. For example, in the top image, eddies are observed downstream of the valve stems in the intake manifold. These are caused by reverse flow at the beginning of the intake stroke and they result in the

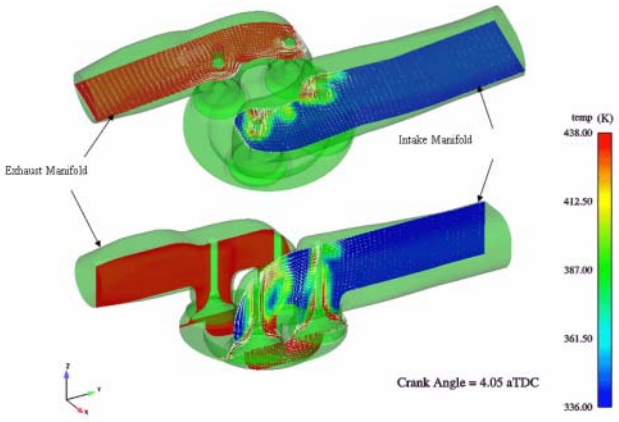

Figure 5. Cut-plane sections showing temperature contours through cylinder, intake and exhaust manifolds close to start of the intake stroke using LES turbulence models.

induction of cooler air into the cylinder later during the intake stroke. This affects the in-cylinder temperature and charge mass so that the LES predictions show a better match with experimental results.

Consistent hybrid particle/finite-volume probability density function (PDF) methods [13], detailed chemical kinetics [14, 15], and chemistry acceleration strategies [8, 16] have been developed for three-dimensional time-dependent simulations of autoignition and emissions in HCCI engines. The resulting model has been compared with experimental measurements in the CFR engine [17, 18], as shown in Figure 6. With no explicit tuning to match these experiments, the model captures the trends with variations in equivalence ratio and other operating conditions.

The influence of turbulence/chemistry interactions (TCI) on autoignition and emissions (CO and unburned hydrocarbons) has been examined by considering the joint PDF of up to 40 chemical species and mixture enthalpy. Variations in global equivalence ratio, wall temperature, swirl level, degree of mixture inhomogeneity (including direct in-cylinder fuel injection), and a top-ring-land crevice (TRLC) have been investigated, and sensitivities to model parameters and engine operating conditions have been established [19, 20]. Key findings are that, for nearly homogeneous reactants with low to moderate swirl and no TRLC,

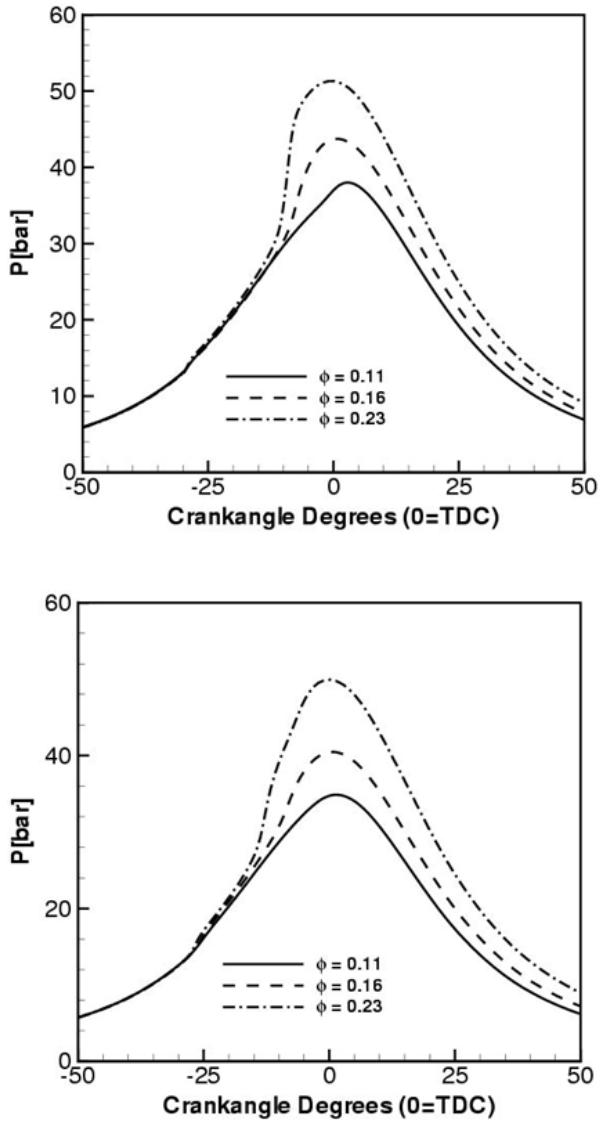

Figure 6. Computed (top) and measured (bottom) in-cylinder pressure with variations in equivalence ratio (Φ) for premixed n-heptane/air in the CFR engine. (From Ref. [18].)

TCI has little effect on ignition timing. However, even in that case, the influence of TCI on emissions is not negligible. In addition, with increasing levels of swirl, higher degrees of mixture inhomogeneity, and for cases that include a TRLC, TCI effects become increasingly important and result in significant changes in ignition timing, global in-cylinder temperature and pressure, and emissions. Finally, unburned fuel is a non-negligible contribution to UHC only in cases with high swirl or where a TRLC has been considered.

Conclusions

The engine tests have shown that operation at both very early and very late start-of-injection timings is effective for low emissions using high-pressure diesel fuel injection. A combustion control criterion based on the ignition/injection time delay has been formulated and has been implemented in a control algorithm for low-emissions operation. With low-pressure fuel injection and early injection for mixing, significant fuel wall impingement occurs and performance deteriorates. Multidimensional modeling has been applied successfully to provide guidelines to minimize wall fuel using variable geometry sprays. In addition, variable intake valve closure timing has been shown to be useful for combustion phasing control in diesel HCCI. Detailed turbulence and chemistry models have been developed and are being applied to study mixing and combustion in diesel HCCI engines. It is concluded that PDF methods are a practical and valuable approach for three-dimensional time-dependent modeling of HCCI autoignition and emissions.

Special Recognitions & Awards/Patents Issued

1. Reitz, R.D., Rutland, C.J., Jhavar, R., "Engine Valve Actuation for Combustion Enhancement", Awarded U.S. Patent 6,736,106, May 2004.

FY 2004 Publications/Presentations

1. UW DOE HCCI Working Group Presentation Meetings: January 29, 2004 (Sandia) and June 24, 2004 (USCAR).
2. Kong, S.-C., and Reitz, R.D., "3-D CFD Tools for PCCI Engine Simulations," SAE Homogeneous Charge Compression Ignition Symposium, Berkeley, CA, August 10-11, 2004.
3. Foster, D.E., "The Impact of Stratification on HCCI Operational Ranges," SAE Homogeneous Charge Compression Ignition Symposium, Berkeley, CA, August 10-11, 2004.
4. Kong, S.-C., Patel, A., and Reitz, R.D., "Development and Application of Detailed Chemistry-Based CFD Models for Diesel HCCI Engine Combustion Simulations," Proceedings of THIESEL 2004 Conference, Valencia, Spain, September 9-12, 2004.
5. Jhavar, R., Rutland C.J., "A Computational Study of the Impact of Mixing on HCCI," Proceedings of THIESEL 2004, Universidad Politecnica De Valencia, Spain, September 2004.
6. Tao, F., Reitz, R.D., Srinivas, S., and Foster, D.F., "Current Status of Soot Modeling Applied to Diesel Combustion Simulations," COMODIA 2004, The Sixth International Symposium on Diagnostics and Modeling of Combustion in Internal Combustion Engines, Yokohama, Japan, August 2-5, 2004.
7. Ra, Y., and Reitz, R.D., "The Role of Vaporization and Mixture Preparation on HCCI Engine Combustion," ILASS-04 Conference, Washington, DC, May 16-19, 2004.
8. Hruby, E.J., Ra, Y., and Reitz, R.D., "Parametric Study of Combustion Characteristics in a Diesel HCCI Engine with a Low Pressure Fuel Injector," ILASS-04 Conference, Washington, DC, May 16-19, 2004.
9. Canakci, M., and Reitz, R.D., "Experimental Optimization of a DI-HCCI-Gasoline Engine's Performance and Emissions Using Split Injections with Fully-Automated Micro-Genetic Algorithms," ASME Journal of Gas Turbines and Power, Vol. 126, No. 1, pp. 167-177, 2004.
10. Juneja, H., Ra, Y., and Reitz, R.D., "Optimization of Injection Rate Shape Using Active Control of Fuel Injection," SAE Paper 2004-01-0530, Presented at SAE Congress, Detroit, MI, 2004.
11. Patel, A., Kong, S.-C., and Reitz, R.D., "Development and Validation of a Reduced Reaction Mechanism for HCCI Engine Simulations," SAE Paper 2004-01-0558, Presented at SAE Congress, Detroit, MI, 2004.
12. 2010 ERC Diesel Emissions Reduction Consortium, Madison, WI, September 21, 2004.
13. Lee, K., and Reitz, R.D., "Investigation of Spray Characteristics from a Low-Pressure Common Rail Injection System for Use in a HCCI Engine," Measurement Science and Technology, Vol. 15, No. 3, pp. 509-519, 2004.
14. Volker, S., Kong, S.C., Foster, D.E., Morikawa, T., Iida, M., "A Computational Investigation into the Cool Flame Region in HCCI Combustion," SAE 2004-01-0552, Transactions, Presented at SAE Congress, Detroit, MI, 2004.
15. Aroonsrisopon, T., Werner, P., Sohm, V., Waldman, J., Foster, D.E., Morikawa, T., and Iida, M., "Expanding the HCCI Operation with Charge Stratification," SAE 2004-01-1756, Transactions, Presented at SAE Congress, Detroit, MI, 2004.
16. Zhang, Y.Z., "Hybrid Particle/Mesh PDF Methods for 3D Time-Dependent Flows in Complex Geometries," Ph.D. Thesis, Department of Mechanical & Nuclear Engineering, The Pennsylvania State University (2004).

17. Zhang, Y.Z., Kung, E.H. and Haworth, D.C., "A PDF Method for Multidimensional Modeling of HCCI Engine Combustion: Effects of Turbulence/Chemistry Interactions on Ignition Timing and Emissions," *Proc. Combust. Institute* **30** (2004), to appear.
18. Veljkovic, Plassmann, P.E. and Haworth, D.C., "Parallel Implementation of Scientific On-line Database for Efficient Function Approximation," *2004 Intern'l. Conference on Parallel and Distributed Processing Techniques and Applications*, Las Vegas, NV (21-24 June 2004).
19. Zhang, Y.Z., Kung, E.H. and Haworth, D.C., "A PDF Method for Three-Dimensional Time-Dependent Computations of HCCI Engine Autoignition and Emissions," *SIAM 10th International Conference on Numerical Combustion*, Sedona, AZ (9-12 May 2004).
20. Haworth, D.C., "A PDF Method for Multidimensional Modeling of HCCI Engine Combustion," *CD-adapco 5th ICE Work-Group Meeting*, London, England (17 March 2004).
21. Haworth, D.C., "Combustion in Internal Combustion Engines," *STAR-CD 12th European User Conference*, London, England (15-16 March 2004).
22. Zhang, Y.Z., Kung, E.H., and Haworth, D.C., "A PDF Method for Multidimensional Modeling of HCCI Engine Combustion: Effects of Turbulence/Chemistry Interactions on Ignition Timing and Emissions," *14th International Multidimensional Engine Modeling Users' Group Meeting*, Detroit, MI (7 March 2004).
23. Veljkovic, I., Haworth, D.C. and Plassmann, P.E., "Parallel Implementation of Scientific On-line Database," *SIAM Conference on Parallel Processing for Scientific Computing*, San Francisco, CA (25-27 February 2004).

References

1. Klingbeil, A., "Particulate and NO_x Reduction in a Heavy-Duty Diesel Engine Using High Levels of Exhaust Gas Recirculation and Very Early or Very Late Start of Injection," MS Thesis, University of Wisconsin-Madison, 2002.
2. Klingbeil, A.E., Juneja, H., Ra, Y. and Reitz, R.D., "Premixed Diesel Combustion Analysis in a Heavy-Duty Diesel Engine," SAE paper 2003-01-0341, 2003.
3. Canakci, M., and Reitz, R.D., "Experimental Optimization of a DI-HCCI-Gasoline Engine Using Split Injections with Fully-Automated Micro-Genetic Algorithms," International Journal of Engine Research, Vol. 4, No. 1, pp. 47-60, 2003.
4. Canakci, M., and Reitz, R.D., "Experimental Optimization of a DI-HCCI-Gasoline Engine's Performance and Emissions Using Split Injections with Fully-Automated Micro-Genetic Algorithms," ASME Journal of Gas Turbines and Power, Vol. 126, No. 1, pp. 167-177, 2004.
5. Von Der Ehe, J., "Closed-Loop Feedback Control of a Heavy-Duty Diesel Engine for Emissions Reduction," MS Thesis, University of Wisconsin-Madison, 2004.
6. Kong, S.-C., and Reitz, R.D., "Use of Detailed Chemical Kinetics to Study HCCI Engine Combustion with Consideration of Turbulent Mixing Effects," ASME Journal of Gas Turbines and Power, Vol. 124 (3), pp. 702-707, 2002.
7. Kong, S.-C., Patel, A., Yin, Q., Klingbeil, A., and Reitz, R.D., "Numerical Modeling of Diesel Engine Combustion and Emissions Under HCCI-Like Conditions with High EGR Levels," SAE paper 2003-01-1087, 2003.
8. Patel, A., Kong, S.-C., and Reitz, R.D., "Development and Validation of a Reduced Reaction Mechanism for HCCI Engine Simulations," SAE Paper 2004-01-0558, 2004.
9. Munnannur, A., Kong, S.-C., and Reitz, R.D., "Performance Optimization of Diesel Engines with Variable Intake Valve Timing via Genetic Algorithms," Submitted to 2005 SAE Congress, September, 2004.
10. Ra, Y., and Reitz, R.D., "The Use of Variable Geometry Sprays with Low Pressure Injection for Optimization of Diesel HCCI Engine Combustion," Submitted to 2005 SAE Congress, October, 2004.
11. Narayanaswamy, K., and Rutland, C.J., "Cycle Simulation Diesel HCCI Modeling Studies and Control," SAE Paper No. 2004-01-2997 (To appear SAE Powertrain Conference, Tampa, FL, October 25-28, 2004).
12. Aroonsrisopon, T., Sohm, V., Werner, P., Foster, D.E., Morikawa, T., and Iida, M., "An Investigation into the Effect of Fuel Composition on HCCI Combustion Characteristics," SAE Paper 2002-01-2830, 2002.
13. Jhavar R., Rutland C.J., "A Computational Study of the Impact of Mixing on HCCI," Proceedings of THIESEL 2004, Universidad Politecnica De Valencia, Spain, September, 2004.
14. Zhang, Y.Z., and Haworth, D.C., "A General Mass Consistency Algorithm for Hybrid Particle/Finite-Volume PDF Method," J. Comput. Phys. 194: 156-193 (2004).

15. Nordin, N., "Numerical Simulation of Non-Steady Spray Combustion Using a Detailed Chemistry Approach," Thesis for the degree of Licenciate of Engineering, Department of Thermo and Fluid Dynamics, Chalmers University of Technology, Goteborg, Sweden, 1998.
16. Pope, S.B., "Computationally Efficient Implementation of Combustion Chemistry Using in Situ Adaptive Tabulation," Combust. Theory & Modelling 1:41-63 (1997).
17. Veljkovic, I., Plassmann, P., and Haworth, D., "A Scientific On-line Database for Efficient Function Approximation," in Computational Science and Its Applications – ICCSA 2003, Lecture Notes in Computer Science (LNCS 2667), Part I, pp. 643-653, Springer Verlag (2003).
18. Aroonsrisopon, T., Werner, P., Waldman, J.O., Sohm, V., Foster, D.E., Morikawa, T., and Iida, M., "Expanding the HCCI Operation Using the Charge Stratification," SAE paper 2004-01-1756, 2004.
19. Zhang, Y.Z., "Hybrid Particle/Mesh PDF Methods for 3D Time-Dependent Flows in Complex Geometries," Ph.D. Thesis, Department of Mechanical & Nuclear Engineering, The Pennsylvania State University, 2004.
20. Zhang, Y.Z., Kung, E.H. and Haworth, D.C., "A PDF Method for Multidimensional Modeling of HCCI Engine Combustion: Effects of Turbulence/Chemistry Interactions on Ignition Timing and Emissions," Proc. Combust. Institute 30 (2004), to appear.

II.A.13 HCCI Engine Optimization and Control Using Gasoline

Dennis Assanis
University of Michigan (UM)
Mechanical Engineering
2045 W.E.Lay Auto. Lab.
1231 Beal Avenue
Ann Arbor, MI 48109-2133

DOE Technology Development Manager: Kevin Stork

Subcontractors:
Massachusetts Institute of Technology (MIT)
Stanford University (SU)
University of California, Berkeley (UCB)

Objectives

- Develop a homogeneous charge compression ignition (HCCI) engine control system.
- Develop full-cycle modeling tools.
- Investigate chemical kinetics for modeling gasoline HCCI combustion.
- Carry out detailed modeling studies of mixing and sprays using computational fluid dynamics (CFD) codes and validate with optical diagnostics.

Approach

- Carry out experimental tests of available HCCI control methods.
- Develop a range of models of HCCI engines, from simple single-zone to complex CFD codes, in order to incorporate and share the knowledge base on HCCI as it develops.
- Investigate critical chemical kinetic rates and mechanisms for gasoline, and develop and validate reduced kinetic mechanisms for computationally efficient use in these engine models.
- Validate models with engine experiments and combine models and experiments to develop a workable engine control system.

Accomplishments

- Experimentally demonstrated potential control methods using breathing and thermal effects on HCCI and identified characteristic times of in-cylinder effects (10 cycles) and thermal effects (100's of cycles).
- Developed controller algorithms and demonstrated them in engine tests.
- Developed a new heat transfer correlation specific to HCCI based on direct heat transfer measurements.
- Constructed a system model based on GT-Power software that integrates experimental data from experiments on heat transfer and kinetics. Validated the model with experimental data including spark ignition (SI)-HCCI transitions. Successfully represented gasoline with the combustion model for isooctane by use of a simple calibration factor.
- Developed an integrated CFD-kinetic model which shows the effect of mixing through the combustion event. Results show significant broadening of the temperature profile throughout the cycle, leading to decreasing burn rate for later combustion events.
- Carried out measurements of ignition delay in isooctane-air mixtures in shocktubes and the UM rapid compression facility. Benchmarked available detailed kinetic models against this data set and identified best performance models.

- Correlated ignition delay data with a simple autoignition integral and successfully integrated the correlation into the engine-vehicle system model.
- Obtained instantaneous and average images of fuel inhomogeneities in an optical engine, and identified effects of swirl and residual levels.
- Performed 0-D and 1-D counterflow reaction simulations to identify fundamental criteria of mixedness (mixture fraction) and rate of mixing (scalar dissipation rate) for different ignition regimes.
- Integrated KIVA-3V with a representative interactive flamelet (RIF) model as an advanced full-cycle simulation strategy.

Future Directions

- Engine control experiments will expand and refine current studies of mode transitions, thermal transients necessary for successful HCCI implementation. Control algorithms will be developed and validated in engine experiments.
- Chemical kinetic and computational studies along with shock tube and Rapid Compression Facility (RCF) experiments will feed improved models of gasoline into the engine simulation tools.
- Detailed kinetics, CFD and mixing models that have been developed will be applied to generate fast semi-empirical models of ignition and HCCI combustion for ongoing incorporation into the engine system model.
- The engine system model will be used to develop and evaluate workable HCCI control strategies, first for an engine alone and then in the full vehicle environment.

Introduction

Homogeneous charge compression ignition (HCCI) has the potential to dramatically reduce NO_x emissions from gasoline internal combustion engines while achieving high thermal efficiencies characteristic of diesels, with lower particulate emissions. Because the ignition is not controlled by a spark plug as in conventional gasoline engines but occurs indirectly as a result of the compression heating of the charge, HCCI has been difficult to implement in practical engines. Therefore, the primary objective of this research project is to develop, through experiments and modeling, the understanding of physical and chemical HCCI processes necessary to develop and apply practical control strategies. To meet the project objectives, we have formed a multi-university research consortium of experts in the areas of engine, optical diagnostics, numerical modeling, gas dynamics, chemical kinetics and combustion research from UM, MIT, SU, UCB.

Approach

Our research project, now in its third year, combines experiments and modeling at various levels of complexity in order to acquire and utilize the knowledge and technology to develop a robust control system for HCCI engines. Both single-cylinder and multi-cylinder engine experiments are addressing issues such as injection strategy, mixture homogeneity, valve timing, exhaust gas recirculation (EGR), intake temperature, fuel properties, cooling strategy, transients and engine mode transitions (e.g. SI-to-HCCI). A range of models of HCCI engines and combustion, from simple single-zone to complex CFD codes, is being used in close coordination with the engine experiments to incorporate the experience gained as it develops. At the same time, extensive studies are underway to develop accurate and reliable chemical kinetic models for practical engine fuels. Together, the kinetics, engine models, and experiments will be used to identify HCCI operating ranges and limits and to develop viable control strategies.

Results

Development of an HCCI engine control system

Potential control methods to handle load changes and mode transitions have been demonstrated at MIT, Berkeley (UCB), and Stanford, on single-cylinder engines employing backpressure valves,

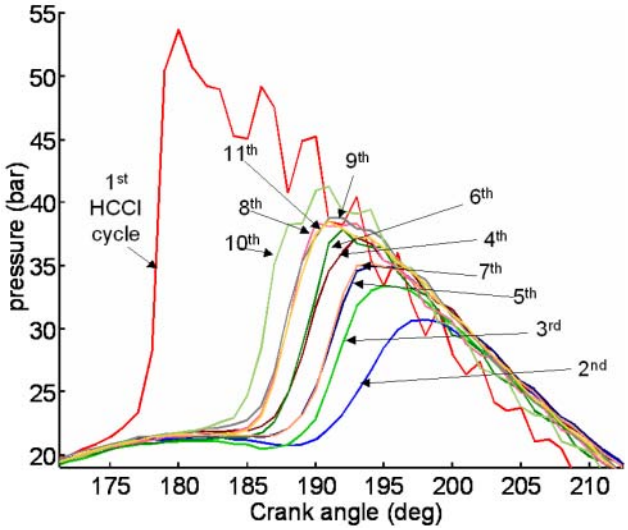

Figure 1. Pressure Traces of the First 10 Cycles During an SI-HCCI Transition (MIT)

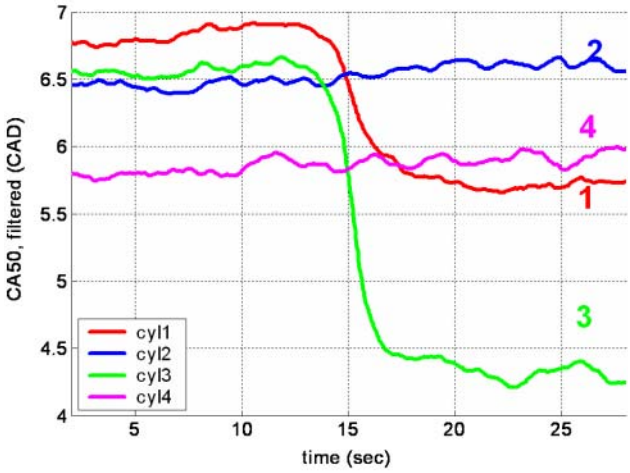

Figure 2. Cylinder-to-Cylinder Cross Talk Observed at UCB (Adjusting combustion phasing by exhaust throttle in Cylinder 1 affects phasing of Cylinder 4.)

inlet heaters, and variable valve actuation (VVA). Figure 1 shows the first HCCI cycle in a SI-HCCI transition using VVA, as well as the following 10 cycles. From this work, the time required for mode and load changes was found to be on the order of ten cycles and is related to prior cycle residual carryover effects. In a multi-cylinder setup at UCB, significant crosstalk was observed between cylinders when exhaust pressure was used for HCCI control (Figure 2). This is expected to present challenges for real-world control, especially for engines that rely on internal EGR for HCCI initiation. Experiments on thermal management at UM determined sensitivities to wall and intake temperature, intake manifold pressure, backpressure, and internal/external EGR. Most significant is the finding that wall temperature is as critical a variable as intake temperature in determining combustion phasing. Work is underway at MIT, Stanford, and UCB to develop controls-oriented models and controller algorithms and to test them in engine experiments. An example of such a control strategy is shown in Figure 3 where Stanford researchers employed a linear reduced-order controller strategy to control peak pressure to desired values.

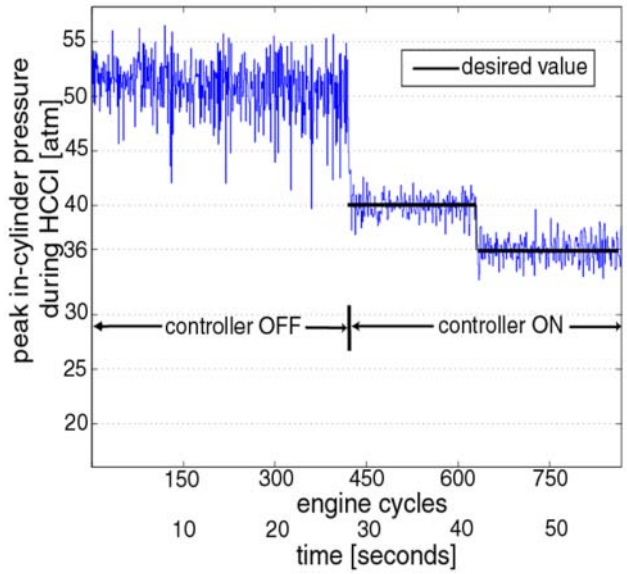

Figure 3. Demonstration of the Effect of a Linear Controller in Combustion Phasing and Load Control Using VVA (Stanford)

Full cycle and system modeling tools

A combined CFD-multizone model was developed at UM and used to explore effects of in-cylinder EGR mixing with different valve strategies. A comparison of negative overlap vs. rebreathing valve profiles showed that the rebreathing strategy provided better EGR mixing, which may be desirable under certain conditions. This approach has been extended with a new integrated CFD-kinetic model developed in collaboration with Lawrence Livermore National Laboratory (LLNL). This allows the CFD computation to be carried out throughout the

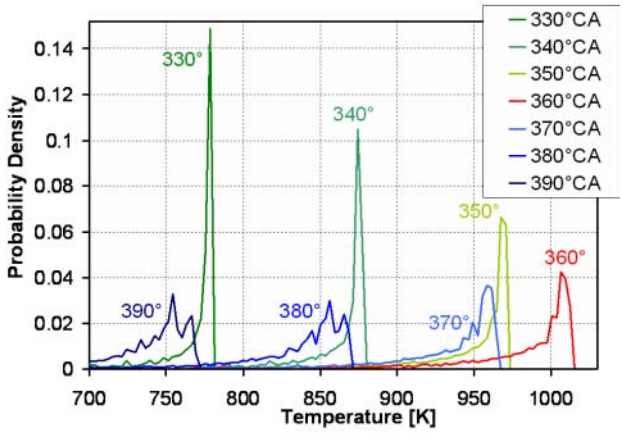

Figure 4. KIVA Results Showing the Broadening of the Probability Density of the Unburned Charge Temperature in the Crank Angle Range 330 - 390°CA (UM-LLNL)

combustion phase. The results in Figure 4 show significant broadening of the temperature profile with crank angle as the piston passes through top dead center and are consistent with the well-known increase in burn duration with later combustion phasing.

A new heat transfer correlation for HCCI was developed at UM based on measured instantaneous heat fluxes. A method was also developed for normalizing kinetic mechanisms for isooctane in order to represent "gasoline" in engine models. Also, a single-zone thermo-kinetic model and an auto-ignition integral model for HCCI combustion were developed.

For the first time, these submodels were incorporated into a GT-Power system environment. The combined system model has been exercised to simulate VVA mode transitions in the MIT experiments. The model results successfully demonstrated the same 10-cycle timescale noted earlier for engine cycle stabilization. Figure 5 shows the experimental SI-HCCI transition achieved by the MIT team compared to the UM modeled results. The system modeling tool was then used in the context of a thermal network of piston, head and cylinder liner to characterize in-vehicle thermal transients for speed and load changes. These transients were found to have timescales on the order of hundreds of engine cycles and will have a major influence on control strategies. Validation work on the model is

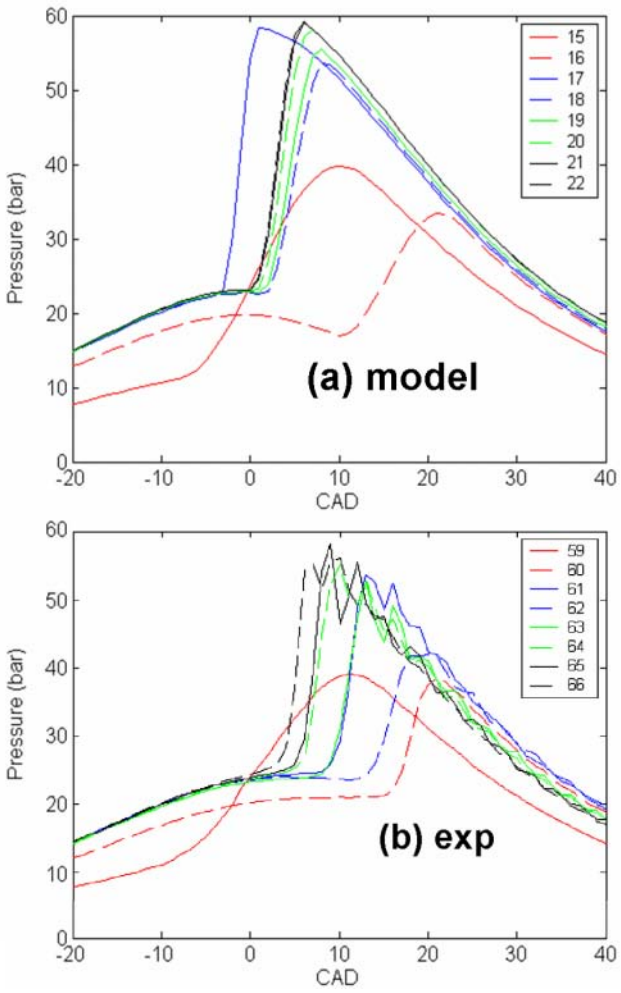

Figure 5. SI-HCCI Transition Simulated by UM System Model (a), and Corresponding Experimental Results from MIT (b)

continuing in preparation for application to a full engine control system simulation.

Investigation of chemical kinetics for gasoline HCCI

Experiments in the UM Rapid Compression Facility (RCF) and shock tube experiments at Stanford have been focused on measuring ignition delay in isooctane air/diluent mixtures. Based on these results, an ignition time correlation was developed quantifying the role of temperature (T), pressure (P), fuel-oxygen equivalence ratio (ϕ_{FO}), oxygen-to-diluent ratio, and EGR on ignition delay. Figure 6 shows the experimental data and the line representing the correlation. The correlation has been successfully used in the engine system

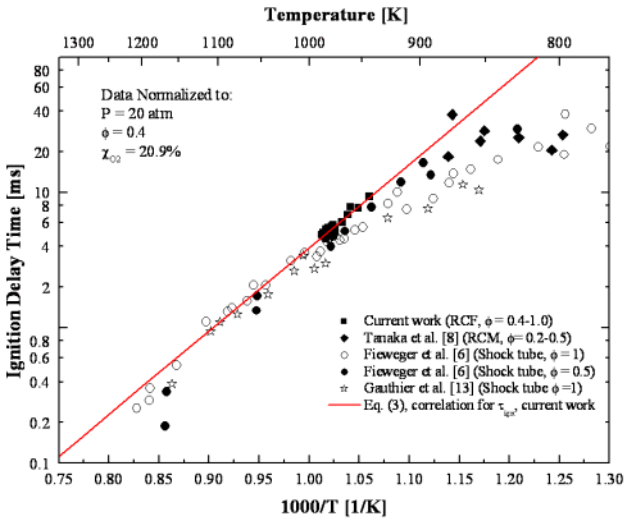

Figure 6. Ignition Delay Data from UM (RCF) and Stanford (shock tube) Along with Correlation Line Developed for Use in Engine System Models

modeling work at UM and has been validated against isooctane engine data and, with a calibration factor, for gasoline data.

On the modeling front, a 258-species skeletal mechanism for isooctane was developed at UCB based on the detailed 857 Curran mechanism. When this mechanism was benchmarked against the data, it was found to perform well near stoichiometric conditions. Under lean conditions, the 84-species reaction scheme of Golovitchev et al. performed better. Both mechanisms significantly reduce the time required for detailed kinetics calculations. At MIT, two software packages have been developed: one automatically constructs detailed chemistry models for any fuel, while the other produces reduced mechanisms from a given detailed mechanism, based on required accuracy over a specified thermodynamic path. Validation is continuing.

Detailed modeling of reaction, mixing and spray dynamics using CFD

Optical engine experiments provided instantaneous and average imaging of fuel disappearance, yielding information about the instantaneous and average mixture inhomogeneities within the engine. The effects of swirl and residual levels on mixture inhomogeneity and combustion phasing have also been investigated. Zero- and one-dimensional counterflow simulations were performed to identify fundamental mixing criterion for different ignition regimes. The parameterization of ignition regimes in terms of mixedness (mixture fraction) and rate of mixing (scalar dissipation rate) was performed to guide an advanced multi-zone modeling effort. KIVA-3V was integrated with a representative interactive flamelet model as an advanced full-cycle simulation strategy. The code integration is complete, and test simulations are currently in progress.

Conclusions

Significant accomplishments have been achieved in FY 2004 through the linked efforts of the multi-university research team:

Control of HCCI operation has been demonstrated on three engines in the consortium, each with a different strategy. Both static (low speed) and dynamic (high speed mode change) control have been achieved. A fourth engine provided detailed heat transfer data and determined sensitivities of combustion to thermal variables. Initial controller algorithms have been developed and tested.

A new heat transfer correlation for HCCI was developed at UM based on measured heat fluxes which were found to be different from gasoline engines. Fundamental combustion data obtained in a rapid compression facility and in shock tube experiments have been used to test available chemical mechanisms for describing HCCI ignition and combustion with isooctane as a surrogate for gasoline. A simple auto-ignition integral correlation with a calibration factor for gasoline was developed for use in engine system models.

These submodels were incorporated into a GT-Power system environment modeling tool. The combined system model has been exercised to simulate VVA experiments and successfully demonstrated the same 10-cycle timescale noted in the experiments for engine cycle stabilization. The system modeling tool was also used in the context of a thermal network to characterize in-vehicle thermal transients for speed and load changes, which were

found to have timescales on the order of hundreds of engine cycles and will have a major influence on control strategies. Validation work on the model is continuing in preparation for application to a full engine control system simulation.

References and FY 2004 Publications/ Presentations

1. Babajimopoulos, A., Lavoie, G.A., and Assanis, D.A. (2003), "Modeling HCCI Combustion with High Levels of Residual Gas Fraction – A Comparison of Two VVA Strategies," SAE Paper 2003-01-3220.
2. Chang, J., et al. (2004), "New Heat Transfer Correlation for an HCCI Engine Derived From Measurements of Instantaneous Surface Heat Flux," SAE Paper No. 2004-01-2996.
3. Chen, J.-Y., Kolbu, J., Homma, R., and Dibble, R.W. (2003), "Optimization of Homogeneous Charge Compression Ignition with Genetic Algorithms," *Combustion Science and Technology*, 175, 373-392, 2003.
4. Chen, J.H., Hawkes, E., Hewson, J.C., Sankaran, R., and Im, H.G. (2003), "The Effect of Turbulent Mixing on Compression Ignition of a Lean Hydrogen/ Air Premixture," Fall Meeting of the Western States Section, The Combustion Institute, University of California, Los Angeles, CA, October 20-21.
5. Choi, Y. and Chen, J.-Y. (2003), "Numerical Modeling of Start-of-Combustion (SOC) in HCCI Engine with Artificial Neural Network (ANN)," Presented at the 2003 Fall Western States Meeting of The Combustion Institute, WSSCI paper 03F-69.
6. Choi, Y. and Chen, J.-Y. (2004), "Fast Prediction of Start-of-Combustion in HCCI with Combined Artificial Neural Networks and Ignition Delay Model," Presented at the 30th Symposium on Combustion, July 2004.
7. Davidson, D.F., Gauthier, B.M., Hanson, R.K. (2004), "Shock Tube Ignition Measurements of Iso-Octane/Air and Toluene/Air at High Pressures," Proceedings of the Combustion Institute 30: in press (2004).
8. Filipi, Z. (2004), "Experimental Insight into Heat Transfer in a Gasoline HCCI Engine," Presented at the SAE Symposium on HCCI, Berkeley, CA, August 10-11, 2004.
9. Flowers, D., Aceves, S., Martinez-Frias, J., Hessel, R., and Dibble, R.W. (2003), "Effect of Mixing on Hydrocarbon and Carbon Monoxide Emissions Prediction for Isooctane HCCI Engine Combustion Using a Multi-Zone Detailed Kinetics Solver," SAE Paper No. 2003-01-1821.
10. Gauthier, B.M., Davidson, D.F., Hanson, R.K., "Shock Tube Ignition Measurements of Iso-Octane and Toluene Ignition at High Pressures," Paper 03F-26, Western States Section/ Combustion Institute Fall Meeting, Los Angeles (2003).
11. Green, W.H., Wijaya, C.D., Yelvington, P.E., and Sumathi, R., "Predicting Chemical Kinetics with Computational Chemistry: Is QOOH = HOQO Important in Fuel Ignition?" *Molecular Physics* 102, 371–380 (2004).
12. Green, W.H., "Computer-Aided Construction of Chemical Kinetic Models," 25th Annual US DOE BES Combustion Research Conference, Airlie, VA, June 2004.
13. Mathews, J., Santoso, H. and Cheng, W.K. (2005), "Load Control for an HCCI Engine," to be presented at SAE Congress, Detroit, MI.
14. Oehlschlaeger, M.A., Davidson, D.F., and Hanson, R.K. (2004), "High-Temperature Thermal Decomposition and Iso-Butane and n-Butane Behind Shock Waves," Journal of Physical Chemistry A108: 4247-4253 (2004).
15. Sankaran, R., Im, H.G., Hawkes, E.R., and Chen, J.H. (2004), "The Effects of Nonuniform Temperature Distribution on the Ignition of a Lean Homogeneous Hydrogen-Air Mixture," Proceedings of The Combustion Institute 30, in press.
16. Sankaran, R. and Im, H.G. (2004), "Characteristics of Auto-Ignition in a Stratified Iso-Octane Mixture with Exhaust Gases under HCCI Conditions," Combustion Theory and Modelling, submitted.
17. Sankaran, R., Oh, T.K., and Im, H.G. (2003), "Ignition and Front Propagation in a Stratified Methane-Air Mixture with Exhaust Gases," Technical Meeting of the Eastern States Section, The Combustion Institute, Pennsylvania State University, University Park, PA, October 27-29.
18. Sankaran, R. and Im, H.G. (2004), "Effects of Mixture Inhomogeneity on the Auto-Ignition of Reactants under HCCI Environment," 42nd Aerospace Sciences Meeting & Exhibit, Paper No. 2004-1328, Reno, NV, January 5-8.
19. Sankaran, R., Im, H.G., Hawkes, E.R., and Chen, J.H. (2004), "A Computational Study on the Ignition of a Lean Hydrogen-Air Mixture with Non-Uniform Temperature Distribution," Spring Technical Meeting of the Central States Section, The Combustion Institute, University of Texas at Austin, Austin, Texas, March 21-23.
20. Santoso, H., Mathews, J. and Cheng, W.K. (2005), "Managing SI/HCCI Dual-Mode Engine Operation," to be presented at SAE Congress, Detroit, MI.

21. Sjöberg M., Dec, J.E., Babajimopoulos, A., and Assanis, D. (2004), "Comparing Enhanced Natural Thermal Stratification against Retarded Combustion Phasing for Smoothing of HCCI Heat-Release Rates," SAE paper 2004-01-2994.
22. Song, J., Sumathi, R., Yu, J., and Green, W.H., "Next Generation Model Construction Software, & New Approaches to Estimating Rates and Thermochemistry for Combustion," American Chemical Society National Meeting (Fuels Division), Philadelphia, PA, August 2004.
23. Tham, Y.F. and Chen, J.-Y. (2003), "Recent Advancement on Automatic Generation of Simplified Mechanisms," Presented at the 2003 Fall Western States Meeting of The Combustion Institute, WSS-CI paper 03F-49.
24. Yelvington, P.E., Bernat i Rollo, M., Liput, S., Tester, J.W., Green, W.H., and Yang, J. (2004), "Predicting Performance Maps for HCCI Engines," *Combustion Science & Technology* 176, 1243-1282.

II.A.14 Diesel HCCI Development

Kevin Duffy (Primary Contact), Gerald Coleman, and George Donaldson
Caterpillar Inc.
PO Box 1875
Peoria, IL 61552-1875

DOE Technology Development Manager: John Fairbanks

Objectives

- Identify a cost-effective engine technology strategy to meet the stringent 2010 heavy-duty and 2014 off-road emissions standards.
- Develop enabling technology to implement the engine technology strategy.

Approach

This research effort focuses on the development of an advanced combustion regime called homogeneous charge compression ignition (HCCI). HCCI holds the potential of meeting future emissions regulatory challenges for internal combustion engines while satisfying the needs of the marketplace. The multi-year development project focuses on the key challenges associated with implementing this technology. Specifically, the challenges are:

- Air-Fuel Mixture Preparation – To date, HCCI using diesel fuel has been largely unsuccessful due to the difficulty of achieving the proper air-fuel mixture. The Caterpillar project has evaluated a number a technical approaches to achieve appropriate mixing.
- Power Density – To date, HCCI demonstrations have been limited to relatively low power density (circa 500 kPa BMEP). Higher power density (1500+ kPa BMEP) is required for a commercially viable technology. The Caterpillar project has evaluated a number of options to increase power density.
- Combustion Phasing and Control – With HCCI, direct control of the combustion event is lost. The Caterpillar project will investigate the parameters that influence the control and identify a means to actively control combustion.

Accomplishments

Caterpillar's project has made significant progress in each of the key technical challenges associated with this technology.

- Caterpillar developed a novel engine system that successfully achieves the proper air-fuel mixture using conventional diesel fuel. This novel engine system overcomes many of the barriers associated with the mixture preparation challenge of diesel HCCI, thereby facilitating the demonstration of engines that achieve future emissions standards. A novel mixed mode injector has been developed and tested which allows for engine operation with unique injection strategies.
- Caterpillar achieved 2100+ kPa BMEP while meeting future emissions standards. This achievement is the highest known power density in the world achieved using any form of HCCI, and specifically diesel-fuelled HCCI. This achievement advances HCCI as a potentially viable approach to meeting future regulatory and marketplace requirements.
- Caterpillar has completed a comprehensive engine test stand evaluation of key performance parameters (boost level, injection event, intake manifold temperature, etc.) to better understand the parameters that impact and control combustion. A novel neural network controls approach has been explored which offers an alternative closed loop feedback controls approach to HCCI combustion phasing control.

Future Directions

The Caterpillar team will utilize best-in-class design practices, advanced combustion modeling techniques, single-cylinder engine testing and multi-cylinder engine testing to advance the technology. Technology development continues in the following key areas:

- With the advent of the novel engine system, the air-fuel mixture issue is largely resolved. Future work will focus on identifying and developing a cost-effective method of manufacturing the engine system.
- Caterpillar will continue to focus on the power density issue to achieve additional breakthrough results. The team will focus on achieving the results with improved engine structure, enhanced air system capabilities, and improved combustion control.
- Additional test stand evaluation, sensor development, and algorithm development are needed to address the challenges associated with controlling this novel combustion approach. Rapid control algorithm development tools will be utilized to expedite the development of this technology. In addition, novel combustion control mechanisms will be designed, analyzed and, if appropriate, evaluated on the engine test stand.

Introduction

Increasingly stringent air quality standards have driven the need for cleaner-burning internal combustion engines. Many emissions reduction technologies adversely affect fuel consumption (and subsequently U.S. dependence on foreign oil). Homogeneous charge compression ignition fundamentally shifts the traditional emissions and fuel consumption trade-off. This breakthrough emissions technology may enable compression ignition engines to compete cost-effectively in the automotive and heavy- duty truck markets, resulting in a dramatic improvement in fuel economy for that market segment. Additionally, this advanced combustion technology will reduce (or eliminate) the need for expensive NO_x aftertreatment devices which rely heavily upon imported precious metals.

Approach

The development team is utilizing a multi-disciplinary approach to resolve this complex engineering challenge. The development team has a unique mix of technical experts from the fields of controls, combustion fundamentals, engine design, engine development, fuel systems development and manufacturing. The team is concurrently developing the analytical tools to model and understand the fundamentals of combustion while delivering novel hardware to the test stand to validate the models, improve our understanding and advance the technology. The unique team is utilizing best-in-class design practices, advanced combustion and engine system modeling techniques, rapid control strategy development tools, single-cylinder engine testing, multi-cylinder engine testing and over 70 years of experience delivering successful compression ignition engine technology to the marketplace.

Results

As stated above, Caterpillar has made significant progress in each of the key technical challenges associated with this technology. Figure 1 shows a prototype fuel system called a mixed mode injector which allows for dual mode operation. The injector can be run in pure HCCI mode, conventional combustion mode or a combination mode. This injector has proven to be a valuable tool for exploring alternative low-temperature combustion modes. Figure 2 shows the power density achieved with HCCI. Caterpillar has made significant progress toward achieving the power levels required for a commercially viable technology. Across the speed range of the engine, over 2000 kPa BMEP was

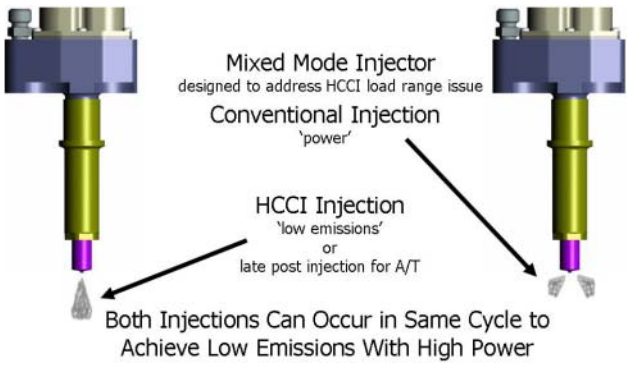

Figure 1. Flexible Injection System

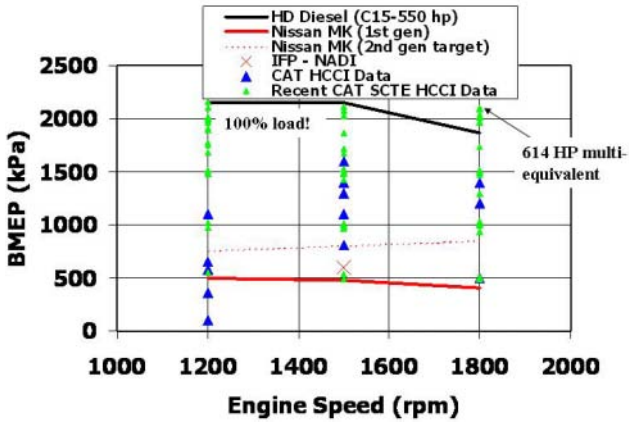

Figure 2. High Power Density

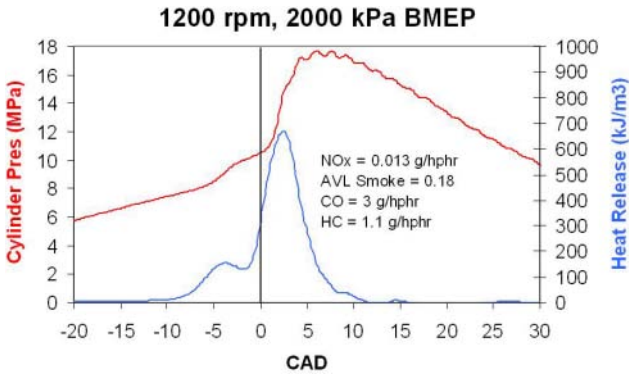

Figure 3. Full Load Diesel HCCI Operation

realized on a single-cylinder test engine. Additional work is needed to translate these results to multi-cylinder platforms; however, the progress to date illustrates the exciting promise that this technology holds. Figure 3 shows the cylinder pressure and heat release curves for a high-load operation point. The cylinder pressure rise rate is significantly higher for HCCI combustion compared to conventional combustion, which suggests engine structural issues cannot be ignored for this concept. NO_x and smoke emissions are very low for this engine operation point. Hydrocarbon (HC) levels at over 1 g/hphr will require the use of an oxidation catalyst to lower them to the 2010 required level of 0.14 g/hphr. Figures 4-6 illustrate the remaining control challenges associated with the combustion process. Figure 4 shows the general effects of injection timing on emissions for diesel HCCI. Both early and late

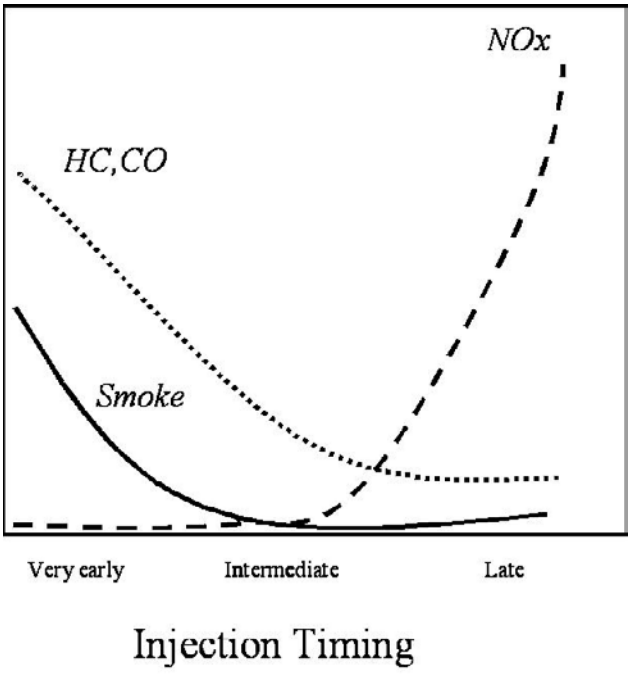

Figure 4. Effect of Injection Timing

injection timings lead to excessive levels of either NO_x, smoke, CO, or HC. An optimum mid-range worktiming exists where NO_x and smoke are low and HC/CO are at moderate levels. As Figures 5-6 illustrate, relatively minor changes in the injection timing and boost level will influence the combustion event, which subsequently affects the fuel consumption and emissions. The combustion phasing must be monitored and a closed loop algorithm used to adjust the appropriate control inputs to arrive at the desired combustion phasing.

Conclusions

Caterpillar's aggressive diesel HCCI development has resulted in significant technical progress against each of the key technical challenges. The progress made by this project has clearly positioned this advanced combustion technology as a potentially viable approach to meeting the regulatory and marketplace challenges of the future. This technology holds the promise of reducing the U.S. dependence on foreign oil and improving the trade balance.

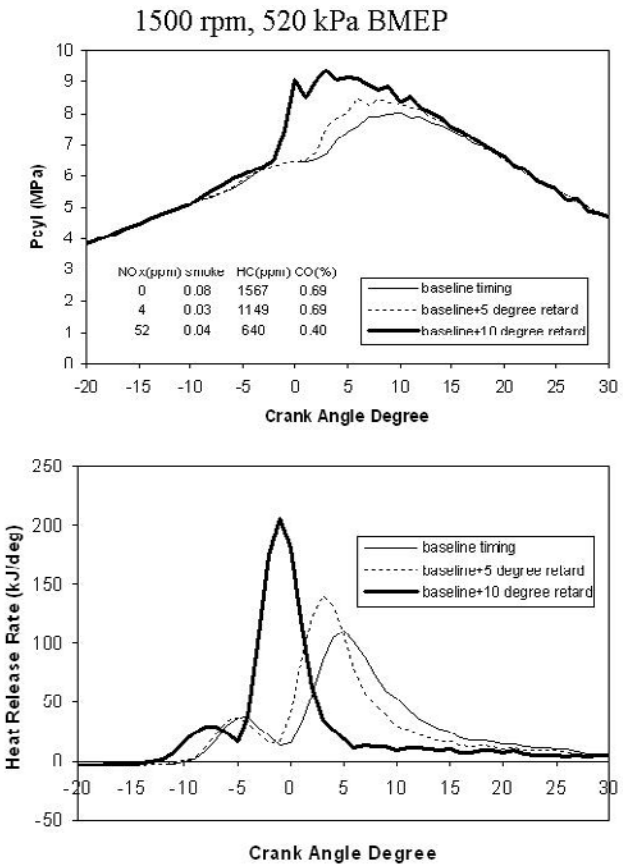

Figure 5. Effect of Injection Timing

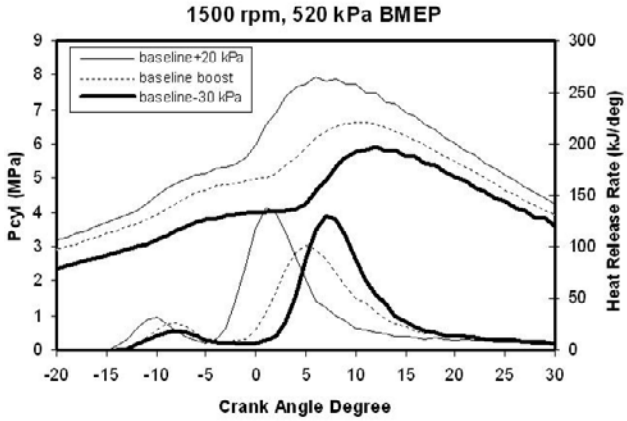

	BL+20kPa	Baseline	BL-30kPa
NO_x (ppm)	1	0	13
Smoke (AVL)	0.01	0.06	0.4
HC (ppm)	890	1605	1514
BSFC (% change)	+5%	baseline	+6%

Figure 6. Effect of Boost

FY 2004 Presentations

1. Duffy, K. "HCCI for Heavy Duty Engines," SAE Powertrain & Fluids Meeting, Pittsburgh, PA, October 2003.
2. Duffy, K. "HCCI for Heavy Duty Diesel Engines," SAE Government-Industry Meeting, Washington, DC, May 2004.
3. Duffy, K. "High Load Diesel HCCI Research,HiH" SAE Homogeneous Charge Compression Ignition Symposium, Berkeley, CA, August 2004.
4. Duffy, K., Fluga, E., Kieser, A. "Heavy Duty HCCI Development Activities," DOE DEER Conference, Coronado, CA, August 2004.
5. Duffy, K., Fluga, E., Faulkner, S., Heaton, D., Schleyer, C., and Sobotowski, "Latest Development in Heavy Duty Diesel HCCI," IFP International Conference on Which Fuels for Low CO_2?, Paris, France, September 2004.

FY 2004 Publications

1. Duffy, K., Fluga, E., Faulkner, S., Heaton, D., Schleyer, C., and Sobotowski, "Latest Development in Heavy Duty Diesel HCCI," IFP International Conference on Which Fuels for Low CO_2?, Paris, France, September 2004.

II.A.15 Spark Augmentation for HCCI Control

Bruce G. Bunting
Oak Ridge National Laboratory
2360 Cherahala Blvd.
Knoxville, TN 37932

DOE Technology Development Manager: Kevin Stork

Subcontractor:
AVL Powertrain, Inc, Plymouth, MI

Objectives

- Demonstrate the effects of spark augmentation for the control of homogeneous charge compression ignition (HCCI) combustion.
- Quantify benefits of HCCI combustion over conventional combustion.
- Determine performance of a rotating arc sparkplug (RASP) compared to a conventional sparkplug for HCCI control.

Approach

- Develop research relationship with subcontractor for access to existing HCCI engine.
- Design test plan and manage test project to achieve research objectives.
- Analyze data obtained relative to HCCI combustion and HCCI combustion control.

Accomplishments

- Demonstrated that HCCI combustion in a gasoline engine could improve fuel economy by an average of 12% while reducing NO_x emissions by 95% compared to conventional combustion.
- Showed that spark augmentation was necessary for successful transition to HCCI and quantified effect of spark after HCCI was achieved.
- Demonstrated that low NO_x is achieved by charge dilution and that HCCI combustion allows the engine to operate in a stable manner at very high exhaust gas recirculation (EGR) rates. This opens the door for combining conventional and HCCI combustion for low NO_x providing good combustion stability can be achieved.
- Compared HCCI control and performance using a conventional sparkplug and the Oak Ridge National Laboratory (ORNL) RASP and found that the conventional sparkplug performed as well or better than the RASP for the conditions tested.

Future Directions

- Continue to evaluate and quantify the use of spark augmentation for HCCI control and transition to HCCI combustion.
- Evaluate the use of combined HCCI and spark augmentation with various fuels and HCCI combustion strategies.

Introduction

In HCCI, fuel and air are pre-mixed prior to combustion and ignition is initiated by kinetic reactions which occur during the compression stroke. Ignition occurs when a threshold temperature is reached, and the timing of ignition is controlled by setting the cylinder conditions at the start of the compression stroke. The cylinder charge of fuel and air is diluted with excess air or with exhaust gas. The purpose of this dilution is to lower the peak flame temperature to reduce NO_x and to regulate the rate of burning after combustion begins. Although HCCI holds the promise of reduced NO_x and smoke emissions combined with improved fuel economy, HCCI stability and control continue to be major barriers to the implementation of HCCI. In addition, HCCI may not be achievable over the entire range of engine operation; conventional operation may be needed at high or light loads, under cold operating conditions, or during transient operation. Spark ignition is often present in gasoline-engine-derived HCCI engines and can be used for engine starting or to assist the transition to HCCI. Results of using the spark during HCCI have been mixed, and various studies have shown different effects. In this study, we explore the use of spark assist during HCCI operation and show the use of spark assist in transitions from conventional to HCCI combustion. In addition, the engine platform is used to evaluate the effect of motor octane number on HCCI combustion characteristics.

Table 1. Specifications for AVL Research Engine as Configured for HCCI Operation

Capable of HCCI, mixed mode, and conventional operation
500 cc, 11.34 C/R
2 valves, naturally aspirated
Gasoline port fuel injection
Spark ignition
Fully variable valve actuation
HCCI currently initiated by early exhaust valve closing
- “negative overlap"
- Retains heat in cylinder
- Retains internal EGR
- Typically operates at > 50% EGR

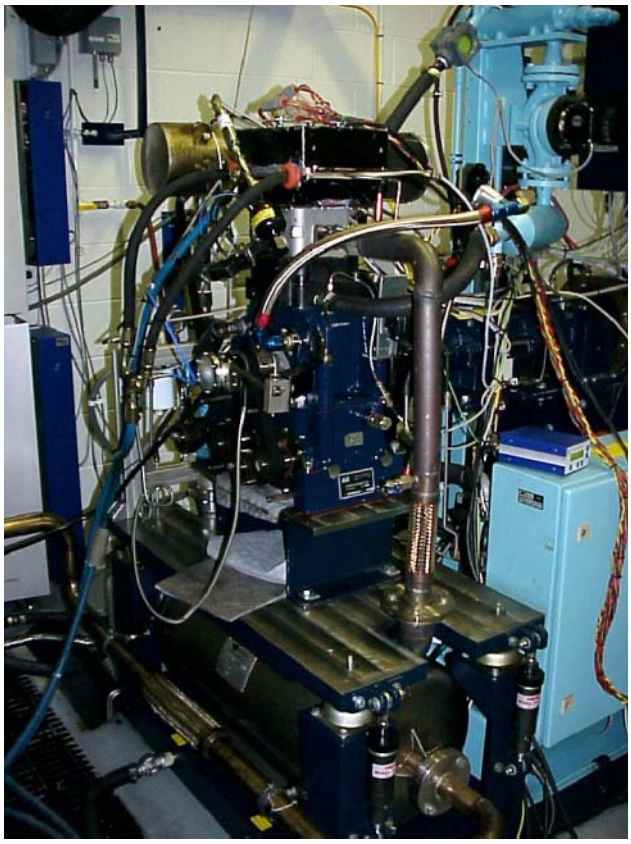

Figure 1. AVL Single-Cylinder Research Engine

Approach

This research was subcontracted to AVL Powertrain in Plymouth, MI, since they already had an existing single-cylinder research engine mapped for HCCI operation. The engine is set up as a 2-valve, naturally aspirated, port fuel injected gasoline engine with 500 cc displacement. HCCI is achieved by a combination of increased compression ratio (11.34:1) and negative valve overlap (early exhaust valve closing). By closing the exhaust valve early, a high residual fraction of the exhaust is retained in the cylinder, which raises compression pressure and temperature to achieve HCCI ignition conditions. Figure 1 shows the engine installed in the lab, and Table 1 lists the important specifications of the engine. A variety of speed-load conditions were run in HCCI with and without spark, and these conditions were also repeated with conventional

combustion. Engine operation was compared based on combustion stability, emissions, fuel efficiency, and ability to operate and transition to other combustion modes.

Results

In a comparison of conventional and HCCI combustion, HCCI combustion has higher peak cylinder pressure and higher rate of cylinder pressure rise but also lower peak combustion temperature. These effects are due to the large amount of exhaust gas retained in the cylinder from the previous cycle due to the valve timing strategy. On the average, retained exhaust was 55% of the cylinder charge in HCCI compared to 12% for the baseline engine configuration. Overall, HCCI operation resulted in a 12% fuel economy gain and a 95% reduction in NO_x compared to conventional combustion. Table 2 compares engine performance in HCCI operation with and without spark and in conventional spark-ignited operation over the range of 1200 to 2400 rpm and 2.0 to 4.5 bar indicated mean effective pressure (IMEP). It is apparent from this data that the spark still exerts an influence on HCCI operation, as indicated by a resulting increase in NO_x. Most probably, the spark initiates a flame kernel which helps pull the remainder of the combustion chamber into HCCI combustion, resulting in earlier or more rapid ignition. In HCCI, the spark can be turned off and the engine will continue to run. If the spark remains on, its influence can be varied by changing the relative timings of exhaust valve closing (% retained exhaust) and spark timing.

Table 2. Comparison of Engine Performance in HCCI and Conventional Combustion

	HCCI no spark high EGR	Spark assisted HCCI high EGR	Conventional throttled low EGR
indicated specific fuel consumption, gm/kw-hr	244	242	277
NOx output, ppm	63	91	1967
coeff of variation of IMEP, %	2.71	2.64	0.98

The engine can be transitioned from conventional to HCCI combustion by progressively earlier closing of the exhaust valve until the pre-flame reaction-initiated combustion preceeds the spark-ignited combustion. This transition is indicated by an improvement in combustion variability (compared to the transition zone), a rise in peak cylinder pressure by up to double, and a shortening of combustion duration from about 20 degrees crank angle (CA) to less than 10 degrees CA. Interestingly, NO_x decreases before this transition to HCCI due to the increasingly large charge dilution from internal EGR. This indicates that low NO_x can be achieved before transition to HCCI and that the main benefit of HCCI is to stabilize combustion with EGR levels above 50%. This finding opens the way to combined combustion modes of conventional and HCCI ignition which may also show acceptable combustion stability while exhibiting low NO_x. Figure 2 shows the transition from conventional ignition to HCCI at 1600 rpm, 3.0 bar IMEP.

The RASP was tested in the engine using a modified cylinder head and compared to a conventional sparkplug for conventional and HCCI combustion behavior. The RASP is an ORNL invention for lean-burn natural gas engines. The plug design imposes a fixed magnetic field on the plug gap area, which causes the spark discharge to rotate. Benefits are a larger spark volume and the continual movement of the spark to new locations on the plug to reduce erosion of the electrodes. Three engine conditions were evaluated for transition from conventional to HCCI combustion. At 1200 rpm, 2.5

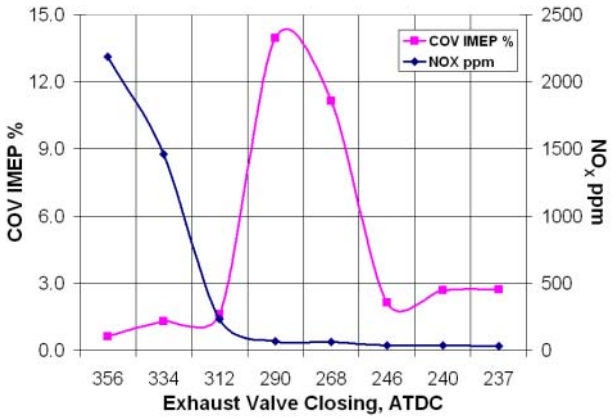

Figure 2. Transition from Conventional to HCCI Combustion at 1600 rpm, 3.0 bar IMEP

bar IMEP, the engine ran with the conventional plug but would not run at all with the RASP plug. At 1600 rpm, 3.0 bar IMEP, the engine ran with both plugs, but the RASP plug showed higher combustion variability. At 2400 rpm, 4.5 bar IMEP, the engine ran with both spark plugs and transitioned to HCCI combustion. Engine performance relative to NO_x emissions, fuel consumption, and combustion variability was about equivalent. Further optimization of the RASP sparkplug is probably needed relative to ignition duration and tip design. The RASP plug has no protrusion into the combustion chamber and may not be reaching a good pocket of fuel/air mixture.

Conclusions

- HCCI combustion provided a 12% fuel economy improvement and 95% NO_x reduction compared to conventional spark ignition in the engine tested.
- The spark addition was needed for transition from conventional to HCCI ignition and was also shown to have an effect on HCCI combustion. This effect could be varied with spark and exhaust valve timing.
- Low NO_x was achieved by charge dilution, and HCCI allowed the engine to operate in a stable manner at EGR rates greater than 50%.
- The RASP did not provide an expected benefit compared to a conventional sparkplug, probably because the RASP ignition system and plug tip configuration were not optimized for the engine.

FY 2004 Publications/Presentations

1. Bruce G. Bunting, COMBUSTION, EFFICIENCY, AND FUEL EFFECTS IN A SPARK-ASSISTED HCCI GASOLINE ENGINE, presented at 2004 DOE DEER Conference, August 31, 2004.
2. Bruce G. Bunting, FUEL EFFECTS ON SPARK ASSISTED HCCI COMBUSTION IN A GASOLINE ENGINE, presented at 2005 annual meeting, American Chemical Society, August, 2004.

II.A.16 Real-Time Control of Diesel Combustion Quality (CRADA with Detroit Diesel Corporation)

Robert M. Wagner (Primary Contact), Eric J. Nafziger
Oak Ridge National Laboratory
2360 Cherahala Blvd.
Knoxville, TN 37932

Craig Savonen (Primary CRADA Contact), He Jiang
Detroit Diesel Corporation (CRADA No. ORNL00-0609)
13400 Outer Drive
Detroit, MI 48239

DOE Technology Development Manager: Kevin Stork

Objectives

- Commission prototype Detroit Diesel Corporation (DDC) heavy-duty diesel engine at Oak Ridge National Laboratory (ORNL).
- Explore operational range of high-efficiency clean combustion (HECC) on DDC engine.
- Perform detailed emissions characterization for improved understanding of the combustion process.

Approach

- Install prototype DDC heavy-duty diesel engine and develop supporting data acquisition and measurement systems at ORNL.
- Determine boundaries of HECC operation on DDC-supplied heavy-duty engine with detailed combustion and emissions characterization.
- Begin construction of physical and statistical-based models for use in evaluating potential control approaches for expanding operational range of HECC.

Accomplishments

- Commissioned DDC engine and supporting infrastructure at ORNL.
- Performed extensive experiments under low and medium load conditions to characterize effects of exhaust gas recirculation (EGR) rate, rail pressure, and injection timing on achieving HECC operation.
- Selected commercially available software package and began development of low-order combustion model for engine simulations.

Future Directions

- Continue analysis and interpretation of recent data.
- Continue model development for multi-cylinder simulations and control.
- Explore potential of achieving homogeneous charge compression ignition (HCCI)-like operation and further expanding HECC operating range on heavy-duty multi-cylinder platform.

Introduction

This CRADA focuses on expanding the operational range of HECC through improved simulation and control with emphasis on the unique dynamics of multi-cylinder engines. Expansion of the stable HECC speed-load range is a key step to operating advanced diesel engines at the regulated emissions levels of 2010 and beyond. Achieving HECC in a diesel multi-cylinder engine requires operation under conditions which are often inherently unstable. These instabilities result in the occurrence of poor or marginal combustion events which cause excessive hydrocarbon and particulate emissions. Practical solutions to the problem are especially difficult to achieve because of the extreme sensitivity of combustion and after-treatment performance to engine parameters as well as "communication" between cylinders on multi-cylinder platforms. The experimental setup has been commissioned this year, and extensive experiments have been performed to understand the potential of achieving HECC operation on the DDC multi-cylinder engine. We have also begun the selection and development of models for future simulations of engine operation and evaluations of potential control approaches.

Approach

The overall objective of this work is to expand the operational range of HECC through improved simulation and control with emphasis on the unique dynamics of multi-cylinder engines. Achieving this objective requires extensive experimentation as well as the development of new low-order models and control strategies. A key target in satisfying this objective will be to minimize the addition of new engine hardware and rely as much as possible on existing actuators, sensors, and signal processors.

The objective is being pursued utilizing a unique multi-cylinder engine provided by DDC to ORNL. The research engine is sized for Class 7-8 heavy trucks, is fully operational, and is installed in a transient-capable dynamometer cell with full instrumentation. The engine is equipped with an electronic control package, exhaust gas recirculation, and other features that are essential for this type of research.

Results

Extensive experiments have been performed to determine the "natural" boundaries of HECC operation in the DDC engine. Engine parameter ranges for these experiments are summarized in Table 1. Note that all of these experiments were carried out using a single injection event to keep the parameter space reasonable for this stage of experiments. The frequency and timing of multiple injection events will be included in the next round of experiments.

The initial exploratory experiments performed on this engine involved studying the effects of load and EGR on emissions and efficiency. Specifically, the purpose of these experiments was to determine whether high EGR is sufficient to cause a simultaneous reduction in oxides of nitrogen (NO_x) and particulate matter (PM), as has been observed on some light-duty diesel engines. An EGR level sweep was performed for the three loads at 1500 rpm with all other engine parameters held constant. The results in Figure 1 show a significant decrease in NO_x and a significant increase in smoke number with increasing EGR level for all three engine loads. The increase in EGR level also results in a decrease in efficiency (increase in brake specific fuel consumption, BSFC) and a significant increase in CO emissions. Although not shown, the 10-50% and 50-90% heat release (HR) intervals increased with EGR level, and the coefficient of variation (COV) in indicated mean effective pressure (IMEP) was relatively constant in the 1-2% range for all conditions.

The effects of beginning of injection (BOI) and fuel pressure were investigated at 20% and 50% load for a fixed speed of 1500 rpm. A summary of the

Table 1. Engine Parameter Ranges Investigated in Recent Experiments

Parameter	Range
Speed, rpm	1500 (fixed)
Torque, % full load	10, 20, 50
EGR rate, %	0 to 65
BOI, deg BTDC	17.5 to 0
Fuel Pressure, bar	600 to 1600

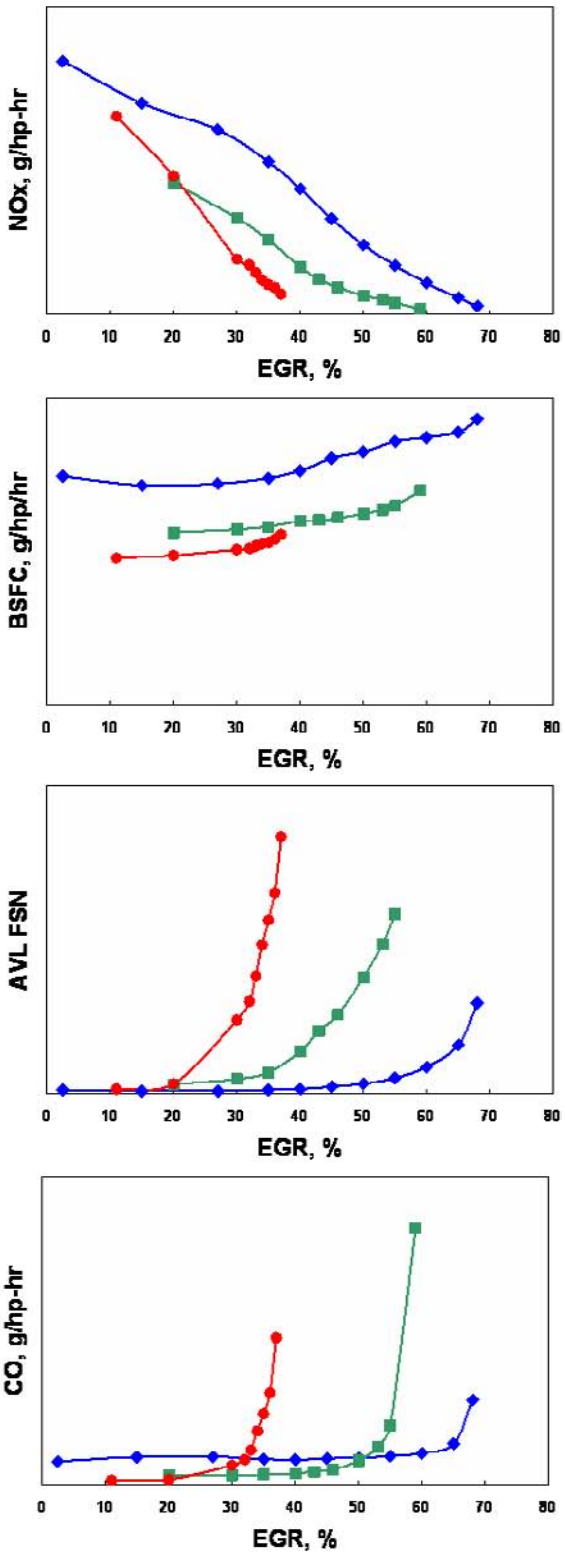

Figure 1. EGR rate sweep at 1500 rpm and 10% (blue diamonds), 20% (green squared), and 50% (red circles) load. All other engine parameters are held constant.

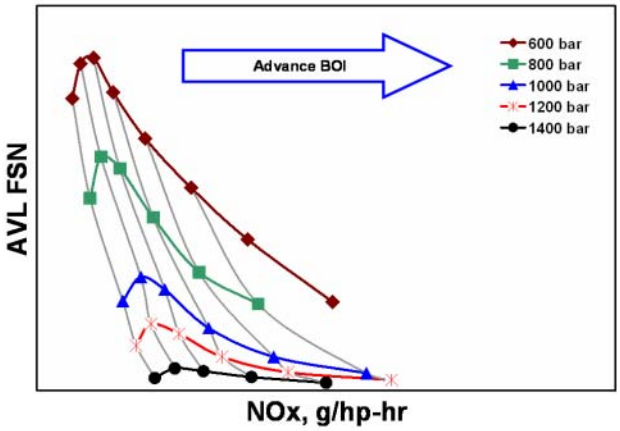

Figure 2. Fuel pressure and injection timing sweep at 1500 rpm, 20% load, and 39% EGR rate. Shaded lines correspond to fixed injection timings.

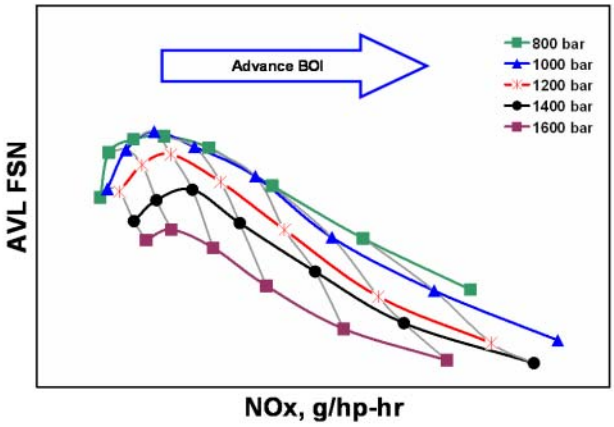

Figure 3. Fuel pressure and injection timing sweep at 1500 rpm, 50% load and 29% EGR rate. Shaded lines correspond to fixed injection timings.

results is shown in Figures 2 and 3 for 20% and 50% load, respectively. EGR rate was held fixed at a slightly elevated level to improve NO_x suppression. In general, smoke number decreased and NO_x increased with increasing fuel pressure. Note that the scales are the same in Figures 2 and 3, and the effect of rail pressure on PM was much stronger for the lower loads. Constant injection timing lines are also shown in Figures 2 and 3 and indicate a decrease in NO_x as injection timing is retarded toward top dead center (TDC). Although not shown, BSFC increased with the later injection timings. Also note that a

simultaneous reduction in NO_x and smoke number was observed for later injection timings. This is opposite of the classic NO_x-PM tradeoff typically observed under conventional operating conditions (see Figure 1). Although not shown, the 10-50% HR interval decreased with fuel pressure, and the 50-90% HR interval decreased with retarding injection. All parameters investigated had little to no effect on stability as indicated by COV in IMEP.

Parameter effects are summarized for the above experiments in Table 2. Note that the effect of each parameter is influenced by a variety of engine conditions including speed and load. For example, the effect of fuel pressure on smoke number appears weaker at high loads. Trends summarized in Table 2 are only for the evaluated parameter combinations.

Table 2. Summar of Parameter Effects Observed in Recent Experiments

Parameter	NOx (g/hp-hr)	PM (g/hp-hr)	BSFC (g/hp-hr)	10-50% HR (deg)	50-90% HR (deg)
EGR Increase	↓	↑	↑	↑	↑
Fuel Pressure Increase	↑	↓	—	↓	
BOI retard	↓	↓↑	↑	–↓	↓

Conclusions

A simultaneous reduction in NO_x and PM emissions was observed with retarded (later) injection timings. A simultaneous reduction was not observed for elevated EGR levels for the conditions investigated in this study but may be possible depending on the settings of other operational parameters such as fuel injection rate and timing. This will be investigated in more detail in the next phase of this study. Increasing fuel pressure appeared to be most effective at reducing PM while maintaining efficiency, particularly at lower loads. This study indicates simultaneous reductions of NO_x and PM emissions (as compared to baseline) are possible with single-injection approaches. More advanced injection strategies involving multiple injections and early injection are expected to provide greater emissions reductions with the ability to maintain efficiency. More advanced injection strategies and their effects on engine emissions and stability will be investigated in the next phase of this activity.

FY 2004 Publications/Presentations

1. CRADA review meeting at ORNL on September 30, 2004.

II.A.17 KIVA-4 Development

David J. Torres
Group T-3, MS B216
Los Alamos National Laboratory
Los Alamos, NM 87544

DOE Technology Development Manager: Kevin Stork

Objectives

- Modify the remaining subroutines in KIVA-3V to accommodate unstructured grids, and call the unstructured version KIVA-4.
- Simulate 3D engines with KIVA-4.
- Distribute KIVA-4 to interested industry and university parties to gain feedback.

Approach

- Implement and validate changes to KIVA-3V subroutines.
- Construct 3D structured and unstructured grids for 3D engine geometries. Compare KIVA-3V results with KIVA-4.
- Perform classification review for KIVA-4. Issue non-commercial licenses to universities interested in KIVA-4.

Accomplishments

- All subroutines of KIVA-3V have been modified to accommodate unstructured grids.
- Calculations have been performed on 3D engines, sector meshes, and a fully tetrahedral mesh. A version of KIVA-4 without allocatable memory is no more than 10% slower than KIVA-3V. A version of KIVA-4 with allocatable memory is about 20% slower.
- A beta version of KIVA-4 has been distributed to the following industry Memorandum of Understanding (MOU) participants: Ford, Caterpillar, Detroit Diesel, and International Truck. Noncommercial licenses have been issued and the code has been distributed to the University of Wisconsin and the University of California at Berkeley. Noncommercial licenses are currently being developed for Massachusetts Institute of Technology (MIT) and Wayne State University.

Future Directions

- Provide support services to KIVA-4 users after its initial distribution in late August 2004.
- Assemble a KIVA-4 manual.
- Develop a KIVA-3V mesh converter which will convert KIVA-3V meshes to KIVA-4 format.
- Continue validation of KIVA-4 by adding to the existing test suite of engine problems.
- Begin parallelization of KIVA-4.
- Develop and begin implementing a grid-generation strategy for KIVA-4 that incorporates commercial grid-generation packages.

Introduction and Approach

Computational fluid dynamics (CFD) computations of engines are increasingly being used as a tool to guide engine design. Most commercial CFD packages use unstructured meshes to grid complex engine geometries because unstructured grids tend to be easier to build and of better quality for complex geometries. Unstructured meshes can use a variety of element types (hexahedra, prisms, tetrahedra and pyramids) to fill up the interior of an engine. Structured meshes generally use only hexahedra. KIVA-3V and all prior versions of KIVA have only accommodated structured meshes. Our objective is to enable KIVA to compute with unstructured as well as structured meshes and to make the grid-generation process easier for KIVA users by developing a new version of KIVA called KIVA-4. KIVA-4 will remain an open source code and thus enable universities and users to interact directly with the code and conduct fundamental research and submodel development.

Results

In FY 2004, Los Alamos National Laboratory finished development of KIVA-4, an unstructured version of KIVA-3V. Simulations were performed on structured and unstructured 3D engine meshes. Simulations were compared with KIVA-3V results to validate the code.

Figure 1 and Figure 2 show vapor fuel (iso-octane) mass fraction contours in a 3D engine simulation with vertical valves performed with KIVA-3V and KIVA-4, respectively. Figure 1 uses a structured grid and Figure 2 uses an unstructured grid. Figure 3 and Figure 4 both show fuel (iso-octane) vapor mass fraction contours in a box with fuel particles currently being compressed by a rising bottom moving surface. Figure 3 only uses hexahedra while Figure 4 only uses tetrahedra. Despite differences in the grids, Figures 1-4 show that KIVA-4 is capable of computing with unstructured grids and producing reliable results.

A beta version of KIVA-4 was distributed in late August, 2004, to interested industry and university parties which included Ford, Detroit Diesel, Caterpillar, General Electric, International Truck,

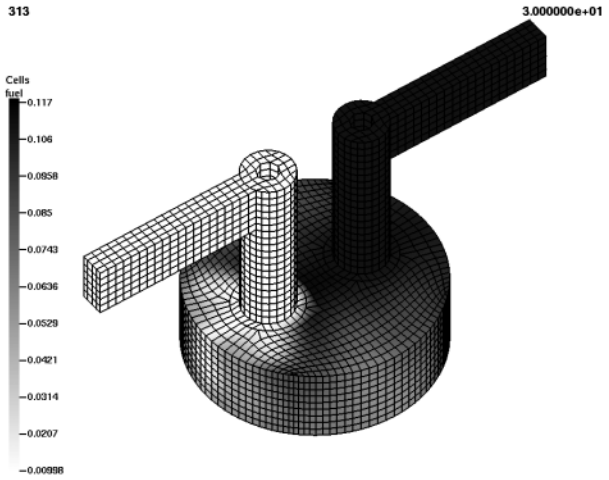

Figure 1. Iso-octane mass fraction vapor contours in a structured mesh. Calculation performed with KIVA-3V.

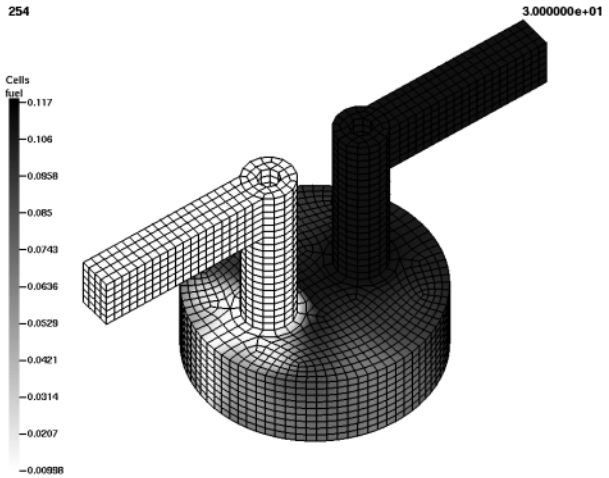

Figure 2. Iso-octane mass fraction vapor contours in an unstructured mesh. Calculation performed with KIVA-4.

University of Wisconsin and the University of California at Berkeley. Noncommercial licenses are being drafted for Wayne State University and MIT.

Conclusions

KIVA-4 (an unstructured version of KIVA-3V) has been developed and tested in several engine geometries. A beta version of KIVA-4 has been distributed to interested industrial members of the MOU and interested university parties. Los Alamos will provide support services for the new KIVA-4

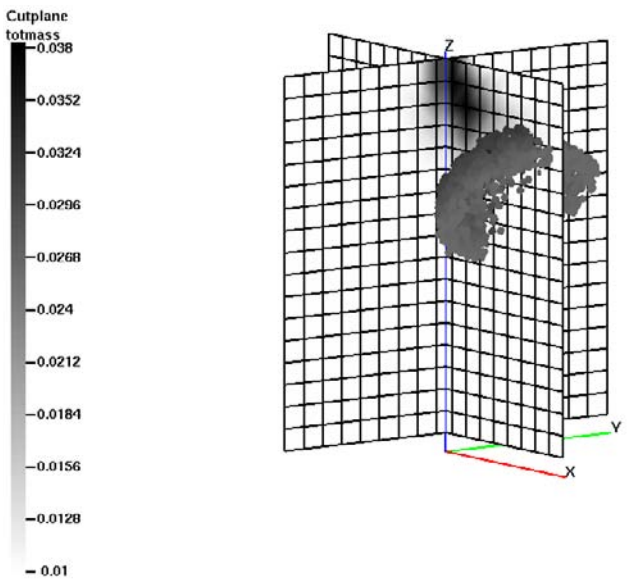

Figure 3. Iso-octane vapor mass fraction contours and particles in a hexahedral structured mesh. Particles are colored according to their temperature (358K- 362K), where the lighter colors designate the cooler particles. Calculation performed with KIVA-4.

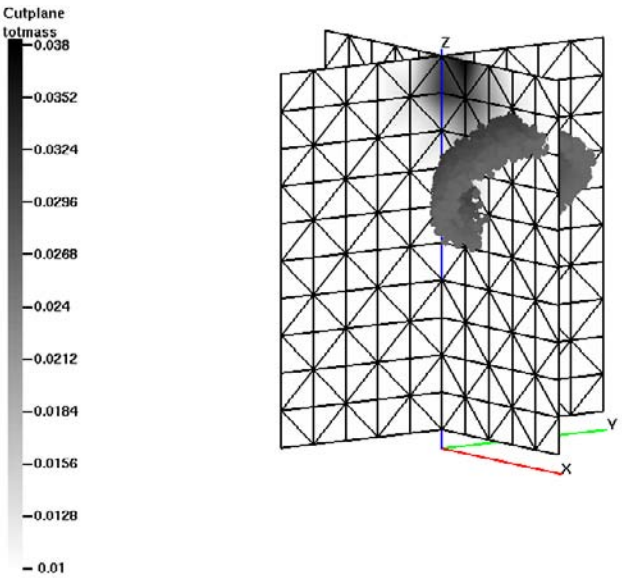

Figure 4. Iso-octane vapor mass fraction contours and particles in a tetrahedral unstructured mesh. Particles are colored according to their temperature (358K- 362K), where the lighter colors designate the cooler particles. Calculation performed with KIVA-4.

code by resolving compiler and run-time issues. We believe the code will be more easily adopted if users can rely on assistance in transitioning from KIVA-3V to KIVA-4. Feedback from users will be incorporated in an updated version of KIVA-4 that will be released after this testing period.

Los Alamos will continue to develop KIVA-4 by beginning to parallelize the code and will use commercial grid packages to create grids for KIVA-4 simulations.

FY 2004 Presentations

1. D. J. Torres, "KIVA-4," Advanced Engine Combustion Meeting, Detroit, MI, June 2004.
2. D. J. Torres, "KIVA-4 Development," DOE National Laboratory Advanced Combustion Engine R&D, Merit Review and Peer Evaluation, Argonne, IL, May 2004.
3. D.J. Torres, "KIVA-4," *International Multidimensional Engine Modeling User's Group Meeting at SAE Congress*, Detroit, MI, March 2004.
4. D. J. Torres, "Unstructured KIVA (KIVA-4)," Advanced Engine Combustion meeting, Livermore, CA, January 2004.

FY 2004 Publications

1. D. J. Torres and P.J. O'Rourke, "KIVA-4," *International Multidimensional Engine Modeling User's Group Meeting Proceedings at SAE Congress*, March 2004.
2. M. F. Trujillo, D. J. Torres and P.J. O'Rourke, "High-pressure multicomponent liquid sprays: departure from ideal behaviour," Int. J. Engine Res., **5**:229-246, October 2003.

II.A.18 Chemical Kinetic Modeling of Combustion of Automotive Fuels

Charles K. Westbrook (Primary Contact), William J. Pitz
Lawrence Livermore National Laboratory
P. O. Box 808, L-091
Livermore, CA 94551

DOE Technology Development Manager: Kevin Stork

Objectives

- Develop detailed chemical kinetic reaction models for components of fuels, including oxygenated species and additives used in diesel, spark-ignition and homogeneous charge compression ignition (HCCI) engines
- Develop surrogate mixtures of hydrocarbon components to represent real fuels and lead to efficient reduced combustion models
- Characterize the role of fuel composition on production of emissions from practical automotive engines

Approach

- Identify individual fuel components and their molecular structures
- Develop kinetic reaction mechanisms for fuel components and additives
- Compute ignition and flame structure for mixtures of fuel components under diesel, spark-ignition and HCCI conditions
- Compute ignition and flame structure for mixtures of surrogate fuel components under diesel, spark-ignition and HCCI conditions

Accomplishments

- Developed models for chemical kinetics of combustion of two major fuel components, toluene and methyl cyclohexane, and for an oxygenated diesel fuel additive, dimethyl carbonate
- Combined various amounts of fuel components and constructed three distinct surrogate mixtures to describe HCCI ignition
- Compared calculated ignition delays under HCCI conditions using surrogate mixtures with experimental results, to provide optimal surrogate
- Continued past studies of mechanisms by which oxygenated diesel fuel components reduce soot production

Future Directions

- Extend model capabilities to additional classes of fuel components
- Continue development of increasingly complex surrogate fuel mixtures
- Increase collaborations with programs outside Lawrence Livermore National Laboratory (LLNL) dealing with automotive fuel issues

---

Introduction

Automotive hydrocarbon fuels consist of complex mixtures of hundreds or even thousands of different components. These components fall largely into a number of rather distinct classes, consisting of n-paraffins, branched paraffins, cyclic and branched cyclic paraffins, olefins, oxygenates, and aromatics (Figure 1). The fractional amounts of these components are quite different in gasoline, diesel

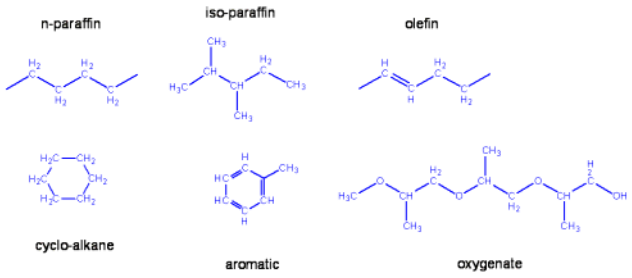

Figure 1. Examples of the major classes of hydrocarbon species present in practical transportation fuels. These specific examples are n-hexane, 2,3-dimethyl pentane, 2-hexene, cyclo-hexane, toluene, and tri-propylene glycol monomethyl ether (TPGME).

fuel and jet fuels, contributing to the very different combustion characteristics of each different type of combustion system.

In order to support large-scale computer simulations of each kind of engine combustion system, there is a need to provide reliable chemical kinetic models for each of the types of fuels. Unfortunately, very few specific hydrocarbon components of these fuels have been modeled, although a few representative components of each type have been simulated. For example, models for benzene and toluene have been developed, although models for few if any larger aromatic compounds currently exist. Similarly, detailed models for small n-paraffins such as propane, n-heptane and n-octane have been developed, but detailed models do not exist for the much larger versions characteristic of diesel fuels, such as n-hexadecane. One solution for this dilemma is to construct a fairly large fuel model, combining one or more representatives of each class of components but not all such components that exist in the real fuels, to serve as a surrogate mixture for which kinetic submodels exist for all of the components. This high-level approach can create realistic substitutes for gasoline or diesel fuel that reproduce experimental behavior of the practical real fuels, and these substitutes, or surrogates, will also then be reproducible in both experiments and modeling studies.

Our recent studies continue our efforts to understand the soot-producing characteristics of diesel fuels. Understanding the kinetics of oxygenated chemical species and their effects on sooting remains a major goal, and we have added several new species to the list of available chemicals, but our current focus is to understand and calculate the separate contributions of the major constituent chemical species on sooting by regular diesel fuels. This will lead to improved understanding of the effects of these diesel fuel components on engine performance and pollutant formation and to development of efficient simplified chemical models for diesel fuel for use in multidimensional computational fluid dynamics (CFD) models of engine combustion. Other applications to ignition and pollutant formation in HCCI engines have also been pursued using a multi-zone spatial model for this type of engine and using suitable surrogates for both diesel fuel and gasoline.

Approach

Chemical kinetic modeling has been developed uniquely at LLNL to investigate combustion of hydrocarbon fuels in practical combustion systems such as diesel and HCCI engines. The basic approach is to integrate chemical rate equations for chemical systems of interest, within boundary conditions related to the specific system of importance. This approach has been used extensively [1-4] for diesel and HCCI engine combustion, providing better understanding of ignition, soot production, and NO_x emissions from these engines in fundamental chemical terms.

The underlying concept for diesel engines is that ignition takes place at very fuel-rich conditions, producing a mixture of chemical species concentrations that are high in those species such as acetylene, ethene, propene and others which are well known to lead to soot production. Some changes in combustion conditions reduce the post-ignition levels of these soot precursors and reduce soot production, while other changes lead to increased soot emissions. The LLNL project computes this rich ignition using kinetic modeling, leading to predictions of the effects such changes might have on soot production and emissions.

Kinetic reaction models were developed for the oxygenated additives proposed by a DOE/industry panel of experts. We then computed diesel ignition and combustion using heptane [5] as a reasonable

diesel fuel surrogate model, mixed with oxygenated additives. The impact of the additive on predicted levels of soot-producing chemical species can then be assessed.

Ignition under HCCI engine conditions is closely related to that in diesel engines since both are initiated by compression ignition of the fuel/air mixtures. Our recent kinetic modeling studies [6] have in fact demonstrated that diesel ignition, HCCI ignition, and spark-ignition gasoline engine knocking are the result of thermal decomposition of the exact same chemical compound, hydrogen peroxide (H_2O_2). However, in very fuel-lean HCCI ignition, the premixing of fuel and air in the gaseous state results in no soot and extremely low NO_x production. Kinetic modeling has proven to be exceedingly valuable in predicting not only the time of ignition in HCCI engines, but also the duration of burn and the emissions of unburned hydrocarbons, CO, NO_x and soot [7].

Results

Our kinetic models assume that soot production in diesel combustion occurs from reactions of chemical species created in fuel-rich ignition near the fuel injection location. Because there is insufficient oxygen in this region to burn the fuel completely, the hydrocarbon species remaining there react instead to produce soot. Our kinetics calculations show that when the fuel itself contains some oxygen, that oxygen helps convert more of the ignition products into chemical species that do not contribute to soot production.

During the past year, the LLNL project has examined additional oxygenated hydrocarbon species that have been proposed as possible diesel fuels or additives, specifically dimethyl carbonate, which includes significant amounts of oxygen imbedded in the primarily hydrocarbon fuel molecule. A detailed chemical kinetic reaction mechanism has been developed for this fuel [8], and the resulting model was used to assess its sooting tendency. The computed soot precursor evolution for this new oxygenated compound was entirely consistent with our previous findings, confirming again that the kinetic analysis of soot production is becoming more and more consistent and reliable. Our recent publication [9] summarizing several years of experimental and kinetic modeling work describes the mechanisms by which oxygenated additives influenced sooting and was just selected as a winner of the Society of Automotive Engineers Arch Colwell Award of Merit for 2005, a prestigious recognition that we previously had received for an earlier (1999) study of diesel engine combustion [3]. We also presented the plenary paper on Computational Combustion [10] at the most recent international Symposium on Combustion.

In addition to the study of oxygenates, we continued numerical studies of soot growth [11-13] from tiny precursors into macroscopic soot particles. The power of this modeling capability is able to relate the chemical properties of these soot particles based on very elementary physical principles.

Basic chemical kinetic studies developing detailed mechanisms for iso-octane [14] and dimethyl ether [15] have been completed recently. The iso-octane model has become an important tool for chemical studies of gasoline in spark-ignition and HCCI engines, and the dimethyl ether (DME) model is a refinement of a previous model that has become heavily used in many studies of DME combustion. DME appears to be a potentially attractive fuel for use in diesel engines and in other applications, since it can be produced relatively inexpensively from natural gas to convert a gaseous fuel to a more convenient liquid fuel.

Finally, we have continued computational studies of HCCI ignition. The multi-zone model [16] has been shown to reproduce nearly all of the important features of engine performance and emissions characteristics when the engines are operated in the normal, fuel-lean regime. We are using the same approach to examine other operating regimes, such as operation with extensive amounts of exhaust gas recirculation or other forms of dilution but with richer fuel/air mixtures. In collaboration with the Combustion Research Facility at Sandia National Laboratories in California, we developed several surrogate gasoline mixtures using representative fuel components from Figure 1 in proportions summarized in Table 1, and compared computationally predicted times of ignition to

Table 1. Three different compositions used as surrogate mixtures for gasoline. Research (RON) and motored (MON) octane numbers for each blend are included for reference.

% Composition	Mix 1	Mix 2	Mix 3
iso-Octane	60	40	40
n-Heptane	8	10	20
Toluene	20	10	10
Methyl Cyclohexane	8	40	30
1-Pentene	4	0	0
RON (blend)	99.2	94	87.6
MON (blend)	94.5	84.8	82

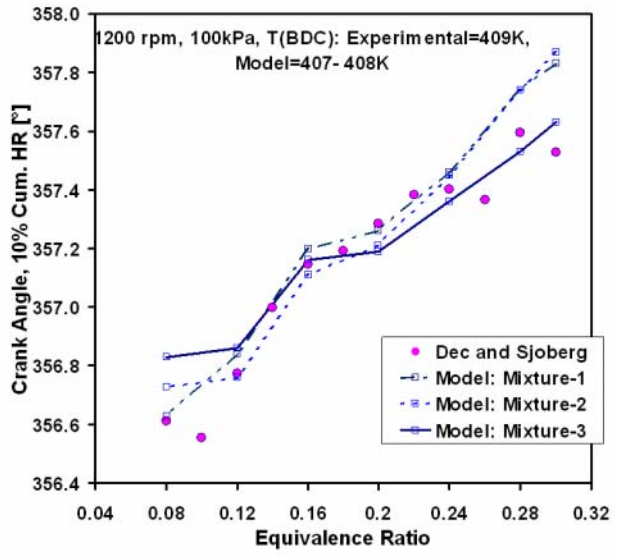

Figure 2. Multicomponent kinetic model for gasoline predictions of ignition timing in Sandia HCCI combustion experiments. Three different multicomponent mixtures with compositions summarized in Table 1.

experimentally measured values under HCCI conditions, as shown in Figure 2.

Conclusions

Kinetic modeling provides a unique tool to analyze combustion properties of diesel, spark-ignition and HCCI engines. A kinetic model can be very cost-effective as an alternative to extended experimental analyses and as guidance for more efficient experimentation, and computations can also provide a fundamental explanation of the reasons for the observed results. LLNL kinetic models are providing this valuable capability for engine research at many university and industrial facilities in the United States and are becoming an essential tool in engine research.

References and Publications

1. Fisher, E. M., Pitz, W. J., Curran, H. J., and Westbrook, C. K., "Detailed Chemical Kinetic Mechanisms for Combustion of Oxygenated Fuels," **Proc. Combust. Inst. 28:** 1579-1586 (2001).
2. Curran, H. J., Fisher, E. M., Glaude, P.-A., Marinov, N. M., Pitz, W. J., Westbrook, C. K., Layton, D. W., Flynn, P. F., Durrett, R. P., zur Loye, A. O., Akinyemi, O. C., and Dryer, F. L., "Detailed Chemical Kinetic Modeling of Diesel Combustion with Oxygenated Fuels," Society of Automotive Engineers paper SAE-2001-01-0653 (2001).
3. Flynn, P. F., Durrett, R. P., Hunter, G. L., zur Loye, A. O., Akinyemi, O. C., Dec, J. E., and Westbrook, C. K., "Diesel Combustion: An Integrated View Combining Laser Diagnostics, Chemical Kinetics, and Empirical Validation," Society of Automotive Engineers paper SAE-1999-01-0509 (1999).
4. Curran, H. J., Fisher, E. M., Glaude, P.-A., Marinov, N. M., Pitz, W. J., Westbrook, C. K., Layton, D. W., Flynn, P. F., Durrett, R. P., zur Loye, A. O., Akinyemi, O. C., and Dryer, F. L., "Detailed Chemical Kinetic Modeling of Diesel Combustion with Oxygenated Fuels," Society of Automotive Engineers paper SAE-2001-01-0653 (2001).
5. Curran, H. J., Gaffuri, P., Pitz, W. J., and Westbrook, C. K., "A Comprehensive Modeling Study of n-Heptane Oxidation," **Combustion and Flame 114**, 149-177 (1998).
6. Westbrook, C. K., "Chemical Kinetics of Hydrocarbon Ignition in Practical Combustion Systems," **Proc. Combust. Inst. 28**, 1563-1577 (2001).
7. Flowers, D., Aceves, S., Westbrook, C. K., Smith, J. R., and Dibble, R., "Detailed Chemical Kinetic Simulation of Natural Gas HCCI Combustion: Gas Composition Effects and Investigation of Control Strategies," **ASME Journal of Engineering for Gas Turbines and Power 123**, 433-439 (2001).
8. Glaude, P.-A., Pitz, W. J., and Thomson, M. J., "Chemical Kinetic Modeling of Dimethyl Carbonate in an Opposed-Flow Diffusion Flame," **Proc. Combust. Inst. 30**, 1111-1118 (2004).

9. Mueller, C. J., Pitz, W. J., Pickett, L. M., Martin, G. C., Siebers, D. L., and Westbrook, C. K., "Effects of Oxygenates on Soot Processes in DI Diesel Engines: Experiments and Numerical Simulations," Society of Automotive Engineers paper SAE 2003-01-1791 and Japan Society of Automotive Engineers paper JSAE 20030193.
10. Westbrook, C. K., Mizobuchi, Y., Poinsot, T. J., Smith, P. J., and Warnatz, J., "Computational Combustion," **Proc. Combust. Inst. 30**, 125-157 (2004).
11. Violi, A., Kubota, A., Truong, T. N., Pitz, W., Westbrook, C. K., and Sarofim, A. F., "A Fully Integrated Kinetic Monte Carlo/Molecular Dynamics Approach for the Simulation of Soot Precursor Growth," **Proc. Combust. Inst. 29,** 2343-2349 (2003).
12. Kubota, A., Mundy, C. J., Pitz, W. J., Melius, C., Westbrook, C. K., and Caturla, M.-J., "Massively Parallel Combined Monte Carlo and Molecular Dynamics Methods to Study the Long-Time-Scale Evolution of Particulate Matter and Molecular Structures Under Reactive Flow Conditions," Proceedings of the Third Joint Meeting of the US Sections of The Combustion Institute, Chicago, March 2003.
13. Kubota, A., Harris, L., Mundy, C. J., Pitz, W. J., Melius, C., Westbrook, C. K, and Caturla, M.-J., "Combined Monte Carlo and Molecular Dynamics Methods to Study the Long-Time-Scale Evolution of Particulate Matter and Molecular Structures Under Reactive Flow Conditions: Hydrocarbon Soot Nanoparticulate Matter Inception, Growth and Aging," Nineteenth International Colloquium on the Dynamics of Explosions and Reactive Systems, Hakone, Japan, July 2003.
14. Curran, H. J., Gaffuri, P., Pitz, W. J. and Westbrook, C. K., "A Comprehensive Modeling Study of iso-Octane Oxidation," **Combustion and Flame 129**, 253-280 (2002).
15. Zheng, X., Lu, T. F., Law, C. K., and Westbrook, C. K., "Experimental and Computational Study of Non-Premixed Ignition of Dimethyl Ether," **Proc. Combust. Inst. 30** (2004).
16. Aceves, S. M., Flowers, D. L., Westbrook, C. K., Smith, J. R., Pitz, W. J., Dibble, R., Christensen, M., and Johansson, B., "A Multi-Zone Model for Prediction of HCCI Combustions and Emissions," Society of Automotive Engineers publication SAE 2000-01-0327, February, 2000. **SAE Transactions**, Section 3, Volume 109, pp. 431-441 (2000).

II.B Energy Efficient Emission Controls

II.B.1 Assessing Reductant Chemistry During In-Cylinder Regeneration of Diesel Lean NO_x Traps

Shean Huff (Primary Contact), James Parks, Stuart Daw, John Storey, Brian West, Bill Partridge, Sam Lewis, Jae-Soon Choi, Todd Toops
Oak Ridge National Laboratory
2360 Cherahala Boulevard
Knoxville, TN 37932

DOE Technology Development Manager: Ken Howden

Objectives

- Enable light-duty diesel market penetration through the development of energy-efficient aftertreatment.
- Establish a relationship between exhaust species and various regeneration strategies on a fully controlled engine.
- Characterize effectiveness of in-cylinder regeneration strategies.
- Develop stronger link between bench- and full-scale system evaluations.
  - Provide data through the Cross-Cut Lean Exhaust Emissions Reduction Simulations (CLEERS) focus group to improve models. Use models to guide engine research.

Approach

- Characterize H_2, carbon monoxide (CO), and hydrocarbons (HCs) generated by the engine.
  - Use Fourier transform infrared (FTIR) spectroscopy, gas chromatography/mass spectrometry (GC/MS), and spatially resolved capillary inlet mass spectrometry (SpaciMS) to characterize engine strategies.
- Characterize candidate lean NO_x traps (LNT) for performance and degradation.
  - Correlate various reductants with catalyst performance.
- Develop and execute rapid sulfation/desulfation experiments.
- Develop experiments for bench-scale work to further characterize LNT monoliths, wafers, and/or powders.

Accomplishments

- Received full-size catalysts (diesel oxidation catalyst and NO_x adsorber) from the Manufacturers of Emission Controls Association (MECA) in August 2003.
  - LNT cores for bench flow (same formulation)
- Defined and procured 2 “model catalysts” (via CLEERS & Emerachem).
  - Engine and bench samples
- Diagnosed engine problem; replaced engine (unplanned).
- Investigated effects of fuel chemistry and regeneration strategy on exhaust species, exhaust species on LNT performance, and regeneration strategy on PM.
- Examined 3 fuels and 2 strategies with full speciation, SpaciMS.
  - Further examine other temperatures.

  - Examine regeneration in the midst of low-temperature combustion (LTC) operation.
- Developed desulfation strategy, desulfurized LNT.
- Coordinating experimental plans with CLEERS and bench reactor teams.

Future Directions

- Conduct similar experiments with catalysts in fresh, heavily sulfated, and desulfated conditions and across a wider temperature range to understand if the conclusions hold for broader cases.
- Further investigate regeneration during "LTC".
- Conduct rapid sulfation/desulfation with speciation and SpaciMS.
- Examine model catalysts and other MECA catalysts.
- Share results and coordinate research plans through CLEERS LNT focus group.

Introduction

NO_x emissions from diesel engines are very problematic, and the U.S. Environmental Protection Agency (EPA) emissions regulations require ~90% reduction in NO_x from light- and heavy-duty diesel engines in the 2004-2010 timeframe. An active research and development focus for lean-burn NO_x control is in the area of LNT catalysts. LNT catalysts adsorb NO_x very efficiently in the form of a nitrate during lean operation, but must be regenerated periodically by way of momentary exposure to a fuel-rich environment. This rich excursion causes the NO_x to desorb and then be converted by more conventional three-way catalysis to N_2. The momentary fuel-rich environment in the exhaust can be created by injecting excess fuel into the cylinder or exhaust and/or throttling the intake air and/or increasing the amount of exhaust gas recirculation (EGR). The controls methodology for LNTs is very complex, and there is no clear understanding of the regeneration mechanisms. NO_x regeneration is normally a 2-4 second event and must be completed approximately every 30-90 seconds (duration and interval dependent on many factors, e.g., load, speed, and temperature).

While LNTs are effective at adsorbing NO_x, they also have a high affinity for sulfur. As such, sulfur from the fuel and possibly engine lubricant (as SO_2) can adsorb to NO_x adsorbent sites (as sulfates). Similar to NO_x regeneration, sulfur removal (desulfation) also requires rich operation, but for several minutes, at much higher temperatures. Desulfation intervals are much longer—on the order of hundreds or thousands of miles—but the conditions are more difficult to achieve and are potentially harmful to the catalyst function. Nonetheless, desulfation must be accomplished periodically to maintain effective NO_x performance. There is much to be learned with regard to LNT performance, durability, and sulfur tolerance.

Different strategies for introducing the excess fuel for regeneration can produce a wide variety of hydrocarbon and other species. One focus of this work is to examine the effectiveness of various regeneration strategies in light of the species formed and the LNT formulation. Another focus is to examine the desulfation process and examine catalyst performance after numerous sulfation/desulfation cycles. Both regeneration and desulfation will be studied using advanced diagnostic tools.

Approach

A 1.7-L Mercedes common rail engine and motoring dynamometer have been dedicated to this activity (Figure 1). The engine is equipped with an electronic engine control system that provides full bypass of the original equipment manufacturer (OEM) engine controller. The controller is capable of monitoring and controlling all the electronic devices associated with the engine (i.e., fuel injection timing/duration/number of injections, fuel rail pressure, turbo wastegate, throttle, and EGR).

Two regeneration strategies [delayed extended main (DEM) and Post80] and three fuel compositions (ECD1, BP15, and DECSE) have been studied with the goal of introducing a broad range of species to the LNT catalysts. The DEM strategy uses intake

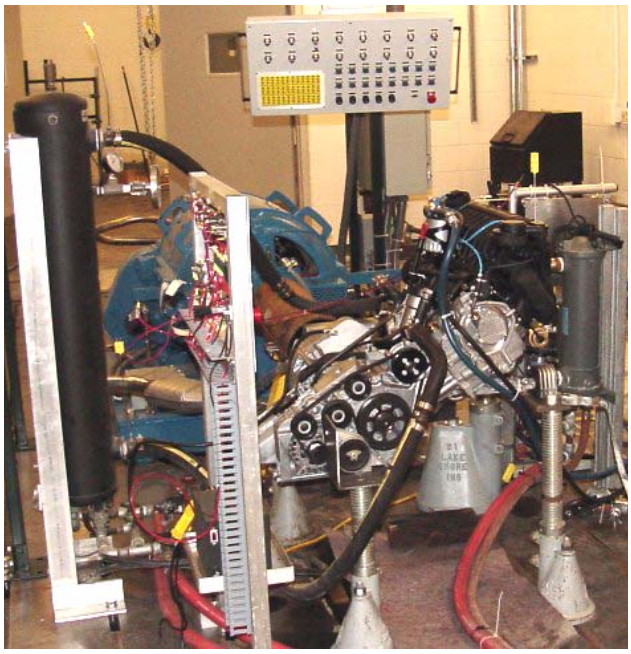

Figure 1. Experimental Setup Including Engine, Control System, Motoring Dyno, and Exhaust System

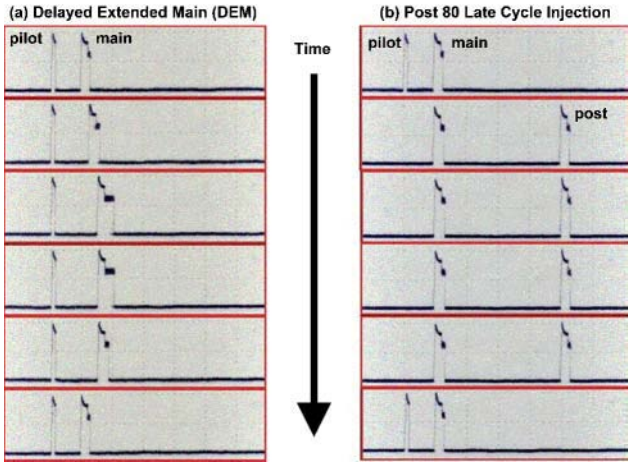

Figure 2. Oscilloscope Traces Showing (a) DEM and (b) Post80 Fuel Injection Strategies

throttling to lower air:fuel ratio. The main injection duration is extended to achieve rich conditions and retarded a few crank angle degrees to reduce the torque increase associated with excess fueling. Figure 2a shows several oscilloscope trace snapshots in time that illustrate the approach. The traces show injector current versus time. Post80 involves adding an injection event after the main injection event to achieve rich operation. The strategy studied here uses a throttle strategy identical to that of the DEM strategy and excess fuel injection at 80 degrees after top dead center (ATDC), as shown in Figure 2b. Note that the pilot is disabled during the post injection. Concerns about injector durability led to the strategy shown in the figure. Catalysts are being studied under quasi-steady conditions, that is, steady load and speed but with periodic regeneration, as shown in Figure 3.

Ultra-low sulfur fuels were used in this study, with sulfur (S) contents at or below the 15 part per million (ppm) limit set by EPA for 2006. Selected properties of the fuels are shown in Table 1. Chromatograms of the 3 fuels are shown in Figure 4. The peaks labeled C10-C25 are normal alkanes. The Diesel Emission Control Sulfur Effects (DECSE) program defined a fuel that has been widely used in diesel emission control research. This fuel is a mix

Table 1. Selected Fuel Properties

Fuel/Property	BP15	ECD-1	DECSE
Cetane No.	50	54	44
Aromatics, % ASTM D1319	29	24	27
Sulfer, ppm ASTM D5453 (as tested)	14	9	<1
H/C Ratio	1.86	1.87	1.84

of refinery streams blended to yield properties representative of 1999 industry average fuel in all respects except for sulfur level. The initial batch of DECSE base fuel was around 3 ppm S; the DECSE fuel used in this study was less than 1 ppm S. The BP15 fuel is a much broader refinery cut and, as shown in the chromatogram, contains a much wider array of HC species than the DECSE fuel. BP15 is a one-time refinery run by BP to produce a “2007-like” fuel, with 15 ppm S (refined for the Advanced Petroleum-Based Fuels – Diesel Emission Control Program). The ECD-1 is a commercially available fuel that has been approved for use in California. As shown in Table 1 and Figure 4, ECD-1 and BP15 are very similar in their HC species, varying only in aromatics, cetane, and S level.

Advanced tools such as H_2-SpaciMS and GC/MS are being used to characterize the species produced in the engine or in upstream catalysts. The H_2-SpaciMS is being used for both in-pipe and in-situ measurements within the catalyst monoliths. In addition, catalysts and exhaust species will be

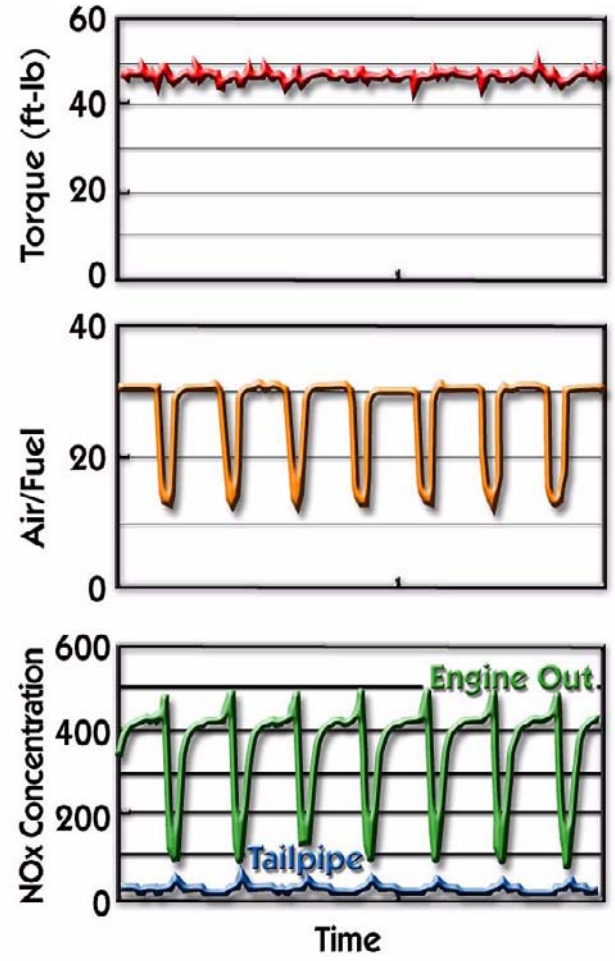

Figure 3. Quasi-Steady-State LNT Regeneration Trace

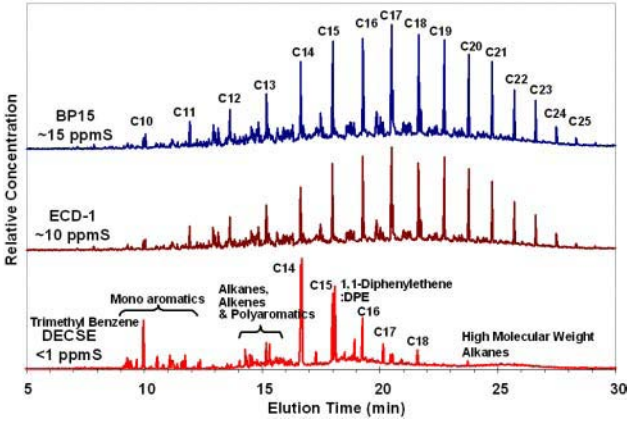

Figure 4. GC/MS Chromatograms Showing Raw Fuel HC Species

characterized after rapid sulfation and during desulfation. LNT catalysts have been provided by some MECA members. "Model" catalysts will also be characterized.

Finally, bench-scale work will be used to further characterize LNT monoliths, wafers, and/or powders using our bench-scale reactor and the diffuse reflectance Fourier transform infrared spectroscopy reactor. Results and characteristics of the engine experiments will be used to help define more meaningful bench-scale studies. In some cases, the exact same catalyst formulation characterized on the engine stand will also be examined in the bench studies.

Results

Summary of Fuel and Strategy Effects

Figures 5a and 5b show the differences in CO and H_2 production for the DEM and Post80 strategies for all three fuels evaluated at the same nominal 1500 RPM, 50 ft-lb_f, 300°C exhaust temperature condition. The DEM strategy produces consistently more CO and H_2 than the Post80, regardless of fuel. The total HC emissions for each strategy and fuel are summarized in Figure 5c. It is interesting to note that while we observed differences in the detailed HC species produced by the strategies and fuels, there appears to be no significant fuel effect on total CO, HC, or H_2 for any given strategy. Figure 5d indicates that the DEM strategy consistently produces better NO_x reduction than the Post80 strategy for all fuels. Moreover, the strategy-dependent LNT efficiency correlates with that of CO and H_2 concentration, but not HC. This result suggests that for the conditions reported here, H_2 and CO have a greater effect on LNT efficiency than do all other HCs present. These results are consistent with bench-scale experiments in the literature that have shown H_2 to be the preferred reductant, followed by CO, then propene.

In-Situ Analysis of H_2 Utilization

In-situ intra-catalyst speciation was used to further investigate the role of reductants in the LNT regeneration process. The H_2-SpaciMS was used to measure transient total NO_x, O_2, and H_2 concentrations at ¼, ½, and ¾ catalyst-length locations within the LNT. These results are combined with conventional LNT-in and -out CO

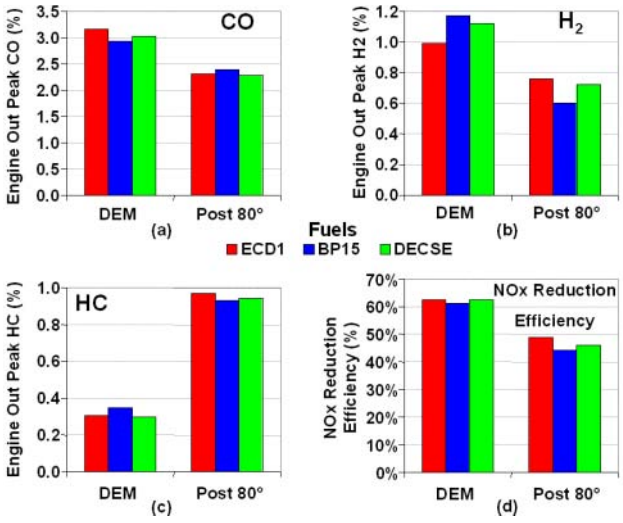

Figure 5. Summary of Fuel and Strategy Effects on CO, H_2, and HC Emissions and Average NO_x Reduction

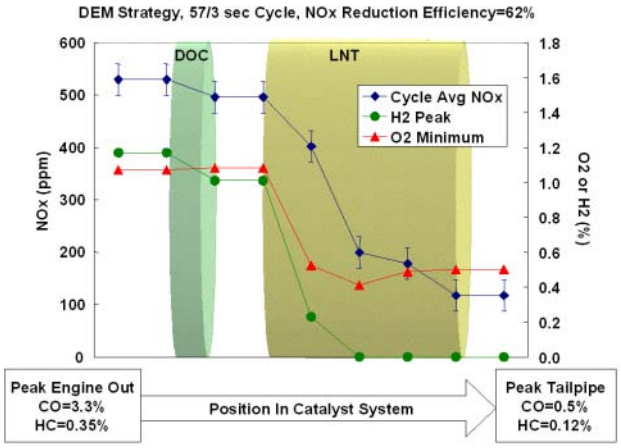

Figure 6. In-Situ Measurements through the Catalyst System for DEM Strategy, BP15 Fuel

and HC measurements from standard bench analyzers and are shown in Figures 6 and 7 for the DEM and Post80 regeneration strategies, respectively. The figures show peak H_2, CO, and HC levels and minimum O_2 during regeneration as well as average NO_x levels over the sorption cycle; similar results were obtained for each fuel studied (data from BP15 fuel is shown).

The data from the DEM strategy (Figure 6) shows little change in exhaust chemistry across the diesel oxidation catalyst (DOC) during regeneration.

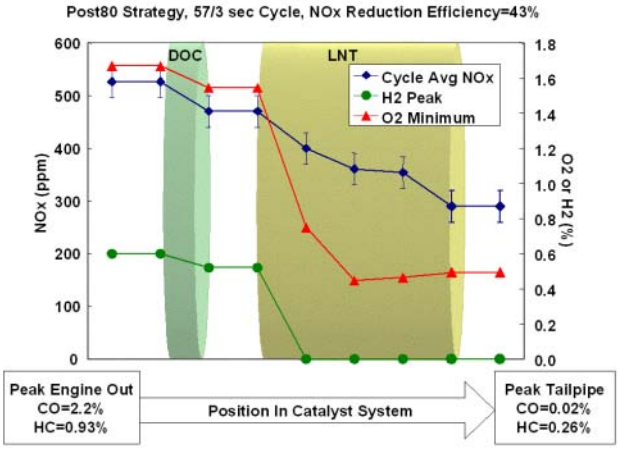

Figure 7. In-Situ Measurements through the Catalyst System for Post80 Strategy, BP15 Fuel

Some decrease in the reductant levels occurs, but the primary decrease in reductant concentration occurs in the LNT catalyst. The strategy is effective in consuming oxygen since engine-out O_2 levels drop to 1.1%; however, the DOC is not effective in completely removing the remaining O_2 since the 1.1% level remains downstream of the DOC. Measured O_2 levels drop to 0.5% at ¼ length inside the LNT and remain at that level throughout the LNT. Oxygen levels of 0% are difficult to measure considering the fact that O_2 levels drop for 2-3 seconds intermittently between lean exhaust O_2 levels of 12.6%; thus, it is assumed that the 0.5% level is representative of O_2 depletion in the catalyst. Note that any remaining O_2 going into the LNT catalyst may influence regeneration since reductants must be consumed to complete the O_2 depletion process. The measured H_2 level drops inside the LNT during the first ½ length of the catalyst, which corresponds with the largest drop in NO_x level. Once H_2 is depleted (during the downstream ½ of the catalyst), little NO_x reduction occurs despite the fact that both CO and HCs are plentiful in the catalyst as evident from measurements at the LNT outlet.

The Post80 strategy data (Figure 7) is similar to the DEM strategy data in terms of O_2 depletion; however, a higher engine-out O_2 level (1.7%) is indicated. Hydrogen depletion occurs earlier in the Post80 case, with H_2 fully consumed by the ¼ length position. The lower available LNT-in H_2 concentration with the Post80 strategy corresponds

with the lower NO_x reduction efficiency shown in Figure 5d. The lower H_2 and CO levels combined with the higher O_2 level at LNT-in may contribute to the degraded regeneration efficiency for the Post80 strategy; less of the apparently preferable reductants are available, and more of these are required for O_2 depletion. Note that in the Post80 case, CO is fully depleted across the LNT. HC levels are greater at both the engine-out and LNT-out positions for the Post80 strategy. The consumption of HCs inside the LNT catalyst may contribute to some NO_x reduction since both CO and H_2 are consumed in the LNT; however, the HCs appear less effective for NO_x reduction since no large drop in NO_x levels was observed in the LNT after the H_2 was consumed.

Conclusions

Two strategies for in-cylinder regeneration have been developed for studying reductant chemistry effects on LNTs. Each strategy was evaluated with three fuels: BP15, ECD-1, and DECSE.

Notable conclusions are the following:

- Fuel chemistry has a definite effect on exhaust HC speciation, but negligible effect on engine-out CO and H_2 emissions for the fuels evaluated.
- For 14:1 minimum indicated air:fuel ratio, the Post80 strategy produces 3 times the HCs, with a much broader mix of HC species than DEM.
- The DEM strategy produces higher engine-out CO and H_2 and lower HC emissions than Post80.
- The DEM strategy produces much higher PM emissions than the Post80 strategy.
- For the conditions studied with a minimum air:fuel ratio of 14:1:
  - DEM yields higher NO_x conversion than the Post80 strategy, implying that CO and H_2 are the key reductants and that HC effects on regeneration are secondary.
  - The correlation between hydrogen depletion and NO_x reduction inside the LNT catalyst indicates H_2 may be the most reactive reductant for LNT regeneration.
  - Although both the DEM and Post80 strategies yield engine-out O_2 levels below 2%, the higher O_2 concentrations for the Post80 strategy may contribute to poorer regeneration performance as reductant supply is consumed to complete depletion of O_2 in the exhaust.

II.B.2 Dedicated Sulfur Trap for Diesel Engine Control

David King (Primary Contact), Liyu Li
Pacific Northwest National Laboratory
P.O. Box 999
Richland, WA 99352

DOE Technology Development Manager: Ken Howden

CRADA Project with Caterpillar Inc.

Objectives

- Develop a low-cost dedicated SO_x trap with capacity exceeding 40 wt.% (SO_2 basis) that can be removed and replaced during periodic vehicle servicing.
- Provide high capacity for both SO_2 and SO_3 removal at temperatures of 200°C and below.
- Demonstrate compatibility with NO_x trap operation (lean-rich cycling).

Approach

- Prepare absorber candidate materials and characterize their properties.
- Test performance with SO_2-containing feedstocks over range of temperatures and with feedstock compositions anticipated under lean-rich cyclic operation.
- Correlate absorbent properties with performance in SO_2 uptake tests.

Accomplishments

- Cryptomelane, an octahedral molecular sieve based on manganese cations, has been identified as a stoichiometric SO_2 absorber having total capacity of approximately 70 wt.% and a breakthrough capacity of 60 wt.% at 325°C. The capacity of the material is virtually unaffected with realistic feeds under cyclic lean-rich conditions.
- Performance of this material has exceeded the 40 wt.% milestone set for SO_2 capacity for the project and is far superior to that of any other reported SO_2 absorber or adsorber. With cryptomelane at 200°C, exit concentration of SO_2 has been maintained at or below 10 ppb until the breakthrough (100 ppb) point, with breakthrough capacity ~2 wt.%.
- A novel metal-modified cryptomelane material has been identified that has resulted in an increase in SO_2 breakthrough capacity to 27 wt.% at 200°C.

Future Directions

- Continue studies with metal-modified cryptomelane to further increase SO_2 uptake capacity at 200°C and below.
- Develop and characterize alternate SO_2 adsorbents having moderate SO_2 capacity that can be regenerated on the vehicle during the rich cycle.
- Demonstrate similar performance of such adsorbers with realistic exhaust conditions and in monolith form.

Introduction

The emission of NO_x from on-road diesel trucks is an important environmental problem. Major efforts are underway to reduce these emissions through the implementation of NO_x conversion devices such as regenerable NO_x traps, which store NO_x as surface nitrates. Sulfur oxides (primarily SO_2) that are present in the diesel exhaust will gradually decrease the effectiveness of NO_x traps. SO_2 is oxidized to SO_3 over the NO_x trap catalyst, and SO_3 reacts to form sulfates that block NO_x adsorption sites. The sulfates are not removed during the rich gas regeneration period that converts adsorbed nitrates to N_2; thus, a high-temperature desulfation step is needed. This results in a gradual degradation of the NO_x trap over the course of many cycles.

One possible approach to improving NO_x trap longevity is to develop a high-capacity, dedicated sulfur oxide-specific trap that is located upstream and can be replaced at regular intervals during engine maintenance. We have identified a promising class of absorbents based on manganese oxide octahedral molecular sieves (OMS). These materials comprise MnO_6 octahedra that are assembled to share faces and edges, resulting in a family of porous absorbents. The most effective of these OMS materials for SO_2 adsorption is the 2x2 member, cryptomelane.

Approach

Following initial results with cryptomelane in which we demonstrated a high SO_2 capacity, we investigated a number of experimental parameters (temperature, space velocity, SO_2 concentration) to further define performance of this material. We then examined the effect of other components in the feed (NO, CO, hydrocarbons) to determine if these species reacted with cryptomelane or were similarly adsorbed. We also examined the performance of other members of the OMS family to compare performance and gain insights into the absorption process. We then studied the capacity and performance of this material under conditions simulating lean-rich cyclic operation. Finally, we examined SO_2 uptake performance at lower temperatures (to 150°C) and developed alternate materials to improve this low-temperature performance.

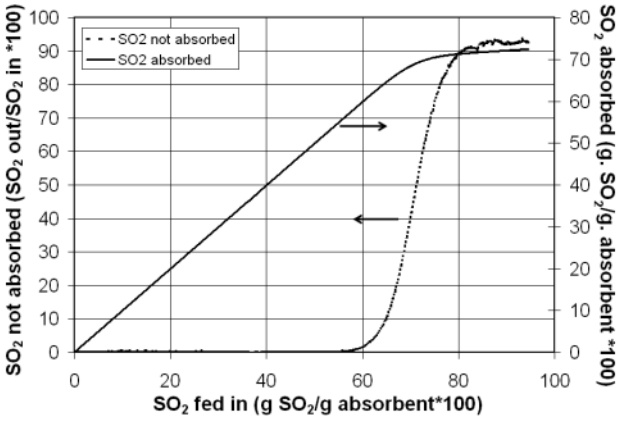

Figure 1. SO_2 Absorption by Cryptomelane at 325 °C at 8000 h^{-1} GHSV

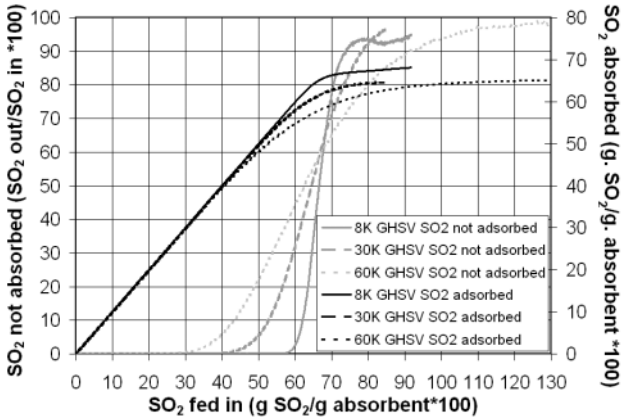

Figure 2. Effect of Feed Gas Space Velocity (GHSV) on SO_2 Absorption by Cryptomelane

Results

Cryptomelane was prepared by the reaction of manganese sulfate with potassium permanganate following a method described by DeGuzman [1]. The adsorption of SO_2 from air (250 ppm SO_2, 325°C, 8000 h^{-1} GHSV) is shown in Figure 1. The figure has plots to show both the instantaneous SO_2 measured in the effluent (SO_2 not absorbed) as well as the cumulative quantity of SO_2 absorbed. The former curve allows clear visualization of the SO_2 breakthrough capacity (approximately 60 wt.%), while the latter curve shows total capacity (approximately 72 wt.%). Such high SO_2 uptake capacities have not been previously described with any material. The effect of space velocity is shown in Figure 2 (250 ppm SO_2, 325°C), indicating that with increasing flow rate the breakthrough capacity

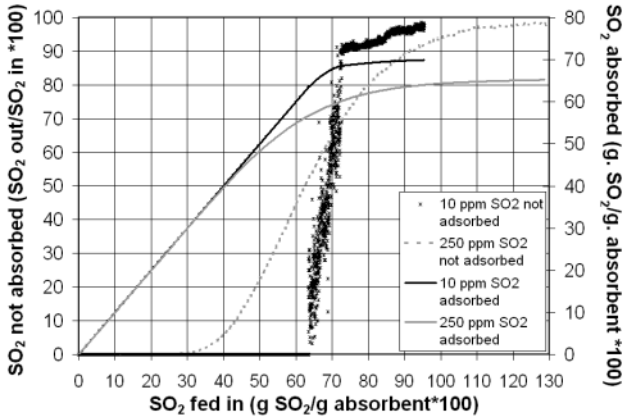

Figure 3. Effect of SO_2 Concentration on Absorption Capacity of Cryptomelane at 325°C and 60,000 h^{-1} GHSV

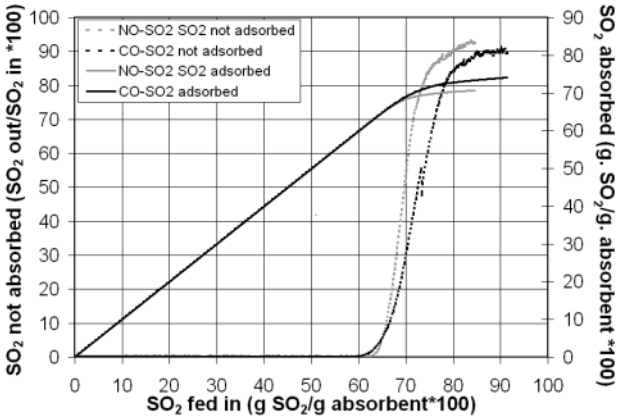

Figure 4. Effect of NO (178 ppm) or CO (250 ppm) on the SO_2 Absorption over Cryptomelane at 325°C and 8000 h^{-1} GHSV

(defined as the point at which SO_2 out = 1% of SO_2 in) shows a significant decrease, whereas the total capacity is affected by only a small percentage. SO_2 concentration in the feed is also an important parameter, as shown in Figure 3. As the SO_2 concentration in the feed is reduced from 250 to 10 ppm (at 325°C, 60,000 h^{-1} GHSV), the breakthrough capacity increases substantially, as does the total capacity. It is clear there are kinetic limitations to the SO_2 uptake process, which we believe proceeds through the following steps: oxidation of SO_2 to SO_3 by the high valent manganese cations in the cryptomelane followed by reaction of SO_3 with the resulting lower valent manganese cations to form manganese sulfate. Since the final product is a bulk manganese sulfate, we refer to this process as absorption rather than adsorption.

For operation in emissions control, the SO_x trap will be exposed to other species such as NO and CO. As was the case with SO_2, it is possible that the cryptomelane can oxidize NO to NO_2 and CO to CO_2, and these reactions could result in loss of oxidizing capacity toward SO_2 and possibly loss of absorption capacity from manganese nitrate and carbonate, respectively. Figure 4 shows that neither NO (178 ppm) nor CO (250 ppm) adversely affects the uptake of SO_2. We have separately demonstrated that cryptomelane does indeed oxidize both NO and CO under the conditions of operation of the test, but they are not absorbed. Since capacity of cryptomelane is maintained, this indicates that the cryptomelane is reoxidized by oxygen in the feedstream and that cryptomelane has catalytic and redox properties.

Cryptomelane is one of a class of octahedral molecular sieves based on manganese. The cryptomelane molecular sieve pore is characterized by a square channel having two manganese octahedra on a side (hence a 2x2 structure). Since there are a number of other members of the OMS family, we investigated their SO_2 absorption properties for comparison with cryptomelane at 325°C. We also investigated for comparison a non-OMS MnO_2 sample that has a high manganese oxidation state similar to that found in cryptomelane. The results are shown in Table 1. Although other OMS materials show high capacity, such capacities are only achieved at low space velocities and low packing densities. These low-density materials would have low volumetric capacity. At comparable packing density, cryptomelane is superior. The non-OMS MnO_2 sample has low SO_2 uptake. It appears that the OMS structure is important for SO_2 absorption, and cryptomelane is the best OMS material for SO_2 adsorption.

A lean-rich cycle experiment was carried out with cryptomelane to determine whether the capacity of the material toward SO_2 could be maintained despite being exposed to periods of reducing gases. Extended exposure of cryptomelane to reducing gases converts the sample to MnO and Mn_2O_3. The cycling treatment employed a lean phase (12% O_2, 10% CO_2, 0.05% NO, 10% H_2O, balance He) for 6

Table 1. SO_2 Absorption Performance of Manganese Oxides OMS Materials at 325 ^oC

Material	Packing density, g/cm^3	SO_2 break-through capacity (100 x g. SO_2/g absorbent)	SO_2 total capacity (100 x g. SO_2/g absorbent)	GHSV[1]
1x1 pyrolusite	1.34	<0.1	2.7	18K
2x2 cryptom-elane A	0.66	59	71	8K
2x2 cryptom-elane B	0.99	50	60	8K
2x3 romanechite	0.29	57.5	70	3.4K
2x3 romanechite	0.43	31	51	5.1K
2x3 romanechite	0.92	12	40	11K
2x4 sodium manganese oxide	0.90	33	42	11K
3x3 torodokite	0.87	1.5	48	11K
EMD MnO_2[2]	0.99	3.5	8.7	12K

1) Feed gas flow for cryptomelane B was 67 sccm, and 100 sccm for all others.

2) EMD MnO_2 is not an OMS material. Source: Comilig, Inc.; BET surface area: 30 m^2/g.

minutes followed by a rich phase (1.5% O_2, 4% CO, 1.3% H_2, 10% CO_2, 10% H_2O, 0.05% NO, 0.4% C_3H_6, balance He) of 30 seconds. The cyclic treatment was carried out at 450°C for 6 hours at 26,000 h^{-1} GHSV. X-ray diffraction showed that the cryptomelane structure remained, although scanning electron microscopy (SEM) showed some coarsening of the particles. The subsequent SO_2 uptake experiment at 325°C and 8000 h^{-1} GHSV showed breakthrough capacity of 45 wt.% and total capacity of 60 wt.%. Although these capacities have decreased somewhat relative to the fresh material, performance remains very good, especially in light of the high temperature of the lean-rich cycling experiment and the duration of the rich period. More realistic conditions of lean-rich cycling (rich period ~10 seconds) are likely to be less detrimental to performance. We believe that the redox properties of the cryptomelane in the presence of oxygen account for its good performance under lean-rich cycling.

Low temperature performance of the SO_2 trap is also critically important under conditions where the diesel exhaust may not attain 325°C or higher. We have evaluated cryptomelane for SO_2 absorption as low as 150°C. The results, provided in Table 2, clearly show that breakthrough capacity decreases significantly with decreasing temperature. This may be a result of lower kinetic activity at lower temperature or a slower rate of diffusion of the manganese sulfate from the surface to the bulk of the material. During the course of this latter investigation, we carried out modification of the cryptomelane by metal modification, and this resulted in an improved low temperature uptake of SO_2, also shown in Table 2. This is a promising lead that may provide guidance to the development of onboard regenerable adsorbents.

Table 2. SO_2 Breakthrough Capacity of Cryptomelane and Metal-Modified Cryptomelane at 60,000 hr^{-1} GHSV as a Function of Absorption Temperature[1]

Absorbent	150°C	200°C	250°C
Cryptomelane	1.54	1.60	2.90
Metal-doped cryptomelane, lower loading	2.20	5.20	38.1
Metal-doped cryptomelane, higher loading	8.75	26.84	33.42

[1]Feed gas: 10 ppm SO_2 in air. Breakthrough capacity (100 x g SO_2/g absorbent) is defined as the point where SO_2-out exceeds 1% of SO_2-in (100 ppb).

Conclusions

The octahedral molecular sieve material cryptomelane is an attractive SO_x absorber for a replaceable trap concept. It possesses the following properties:

- SO_2 total capacity of 70 wt.% and breakthrough capacity of 60 wt.%, which is very high compared to other adsorber materials.
- Capacity is unaffected by the presence of NO or CO in the feedstream.

- Cryptomelane is stable to lean-rich cycling conditions with minimal loss of capacity.
- Breakthrough and total capacity increase as SO_2 concentration is decreased, which is favorable for operation with projected 15 ppm sulfur diesel fuel.
- The breakthrough capacity decreases as temperature decreases from 325°C, but alternate materials show promise for increasing low temperature capacity.

FY 2004 Publications/Presentations

1. Li, L.Y.; King, D.L. Method for Determining Performance of Sulfur Oxide Adsorbents for Diesel Emission Control Using Online Measurements of SO_2 and SO_3 in the Effluent, *Ind. Eng. Chem. Res.*,***2004**, 43, 4452.*
2. Li, L.Y.; King, D.L. High Capacity Sulfur Dioxide Absorbents for Diesel Emissions Control, submitted for publication (*Ind. Eng. Chem. Res.*).
3. Li, L.Y.; King, D.L. Sulfur Oxide Adsorbents and Emissions Control, U.S. patent application, filed January 2004.
4. D.L. King and Liyu Li, "Development of SO_x Trap For Diesel Emissions Control", DOE Annual Review, Argonne National Laboratory, Chicago, May 2004.

References

1. DeGuzman, R.N.; Shen, Y.F.; Neth, E.J,; Suib, S.L.; O'Young, C.K.; Levine,S.; Newsam, J.M. Synthesis and Characterization of Octahedral Molecular Sieves (OMS-2) Having the Hollandite Structure, *Chem. Mater. **1994,** 6, 815.*

II.B.3 In-Pipe Regeneration of NO_x Adsorber Catalysts for Heavy-Duty Applications

Brian H. West (Primary Contact), John Thomas, John Storey, Sam Lewis
Oak Ridge National Laboratory
2360 Cherahala Boulevard
Knoxville, TN 37932

Industrial Partner:
Xinqun Gui, International Truck and Engine Corporation

DOE Technology Development Manager: Kevin Stork

Objectives

- Develop NO_x adsorber regeneration and desulfation strategies for diesel aftertreatment systems (including diesel oxidation catalysts and diesel particle filters).
- Improve understanding of role/fate of different exhaust hydrocarbons in advanced diesel aftertreatment systems for several reductant delivery systems. International Truck and Engine Corporation will focus on in-cylinder strategies while Oak Ridge National Laboratory (ORNL) will examine in-manifold and in-pipe strategies.

Approach

- NO_x adsorber regeneration strategies will be developed for several steady-state conditions. Electronic control of the intake throttle and exhaust gas recirculation (EGR) valve will be used to lower air:fuel ratio prior to reductant (fuel) delivery in-pipe (into exhaust, upstream of catalysts).
- System performance will be measured for a variety of regeneration conditions. Hydrocarbon speciation and other advanced ORNL analytical tools will be used to improve system understanding.

Accomplishments

- Developed PC-based system for transient electronic control of intake throttle, EGR valve, wastegate, and in-exhaust reductant (fuel) delivery.
- Developed strategy for regenerating NO_x adsorber at rated load (600°C) condition for NTE (not-to-exceed); measured hydrocarbon (HC) species entering and exiting the NO_x adsorber for mild, moderate, and aggressive reductant oxidation schemes.
  - Achieved 70% NO_x reduction at rated power, with acceptable CO and HC emissions and very low fuel penalty (<2.5%).
  - Confirmed degree of fuel cracking in oxidation catalysts; observed improved NO_x adsorber performance with aggressive fuel cracking to generate lighter HC species.
  - Showed potential fuel savings with more aggressive in-pipe fuel reforming.
  - Developed air-assisted in-pipe fuel spray for enhanced fuel/air mixing and observed greater degree of fuel cracking.
- Developed strategy for regenerating NO_x adsorber at a road load (400°C) condition; measured hydrocarbon (HC) species entering and exiting the NO_x adsorber with and without an upstream diesel oxidation catalyst (DOC).
  - Demonstrated >80% NO_x reduction at 400°C condition with sulfated catalyst.

Future Directions

- Desulfurize NO_x adsorber catalyst and measure sulfur compounds.
- Re-examine NTE and lower temperature conditions with in-pipe injection of pure compounds.
  - Configure system for multiple in-pipe reductant delivery locations. Reductant upstream of the DOC will consume excess oxygen, while downstream reductant will provide the bulk of HC species for regeneration. This approach will remove any temperature effect of adding or removing the DOC.
  - Speciate hydrocarbons at adsorber inlet and outlet; clarify HC sensitivity as a function of temperature.

Introduction

Heavy-duty emissions standards call for a 90% reduction in NO_x and particulate emissions by 2010, as shown in Figure 1. These new regulations include certification at any and all engine operating conditions, wherein emissions may not exceed 150% of the emissions standard. This regulation is known as not-to-exceed (NTE) and includes steady operation at the rated load condition. The NO_x adsorber catalyst is a promising technology to help meet these stringent new NO_x standards, but there are many open issues that must be resolved prior to commercialization. The (lean-burn) diesel engine does not readily run rich, but rich exhaust conditions are required to regenerate the NO_x adsorber catalyst. With more flexible fueling systems and other advanced engine control schemes, engineers are devising means to run these engines rich during "normal" operation to regenerate NO_x adsorber catalysts. However, the NTE points can include operating conditions at which rich engine operation could be detrimental to the engine and/or aftertreatment system. It is a challenge to produce rich exhaust, and doing so can potentially cause durability problems, excessive fuel consumption, and excess PM, HC, and/or CO emissions.

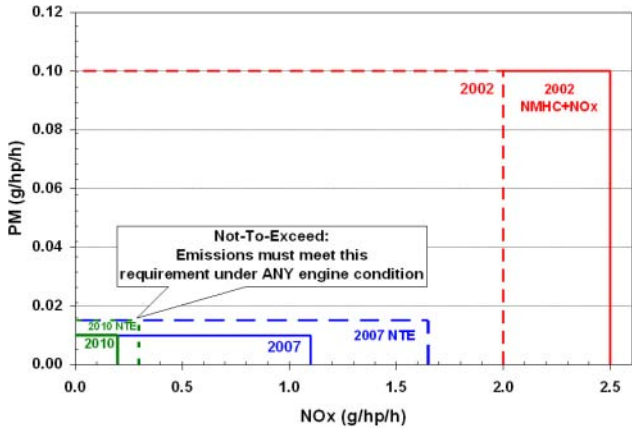

Figure 1. Impending Heavy-Duty Emissions Standards

Additionally, the NO_x adsorber catalyst is very sensitive to sulfur in the exhaust; therefore, effective sulfur management schemes must be developed that will ensure full useful life of the aftertreatment systems. This Cooperative Research and Development Agreement (CRADA) with International Truck and Engine Corporation aims to help resolve some of the problems and unknowns with the NO_x adsorber technology.

Approach and Results

International Truck and Engine is pursuing engine-based (in-cylinder) approaches to adsorber regeneration, while complementary experiments at ORNL are focusing on in-pipe or in-exhaust (after turbo) fuel injection. ORNL has developed a PC-based controller for transient electronic control of EGR valve position, intake throttle position, and actuation of fuel injectors in the exhaust system (Figure 2). Aftertreatment systems consisting of different diesel oxidation catalysts in conjunction with a diesel particle filter and NO_x adsorber are

Figure 2. In-Pipe Fuel Injection for NO_x Adsorber Regeneration

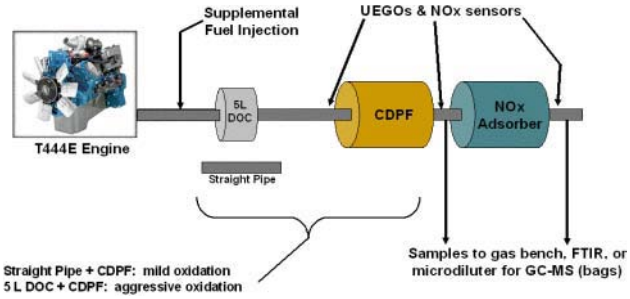

Figure 3. Aftertreatment System Schematic Diagram

being evaluated under quasi-steady-state conditions with sampling for HC species at multiple locations in the exhaust system.

A catalyzed diesel particulate filter (CDPF) was installed just upstream of the NO_x adsorber catalyst for all experiments, as shown in Figure 3. Fuel cracking upstream of the 14.0 liter NO_x adsorber was examined by using the CDPF alone and in conjunction with a 5.0 liter oxidation catalyst. Gas chromatograph mass spectrometry (GC-MS) and Fourier transform infrared spectroscopy (FTIR) were used to speciate the hydrocarbons entering and exiting the NO_x adsorber catalyst for the rated load condition (450 ft-lb, 2300 RPM, ~600°C catalyst temperatures) and for a lower-temperature "road load" condition (200 ft-lb, 1800 RPM, ~400°C catalyst temperatures).

GC-MS and FTIR are used to identify and quantify the various HC species in the exhaust. With the DOC upstream of the CDPF, we find many cracked HC compounds (cracked HCs that are not prevalent in raw fuel) at the NO_x adsorber inlet during regeneration. The apparent benefits of fuel cracking in the diesel oxidation catalyst for the rated load condition (600°C) are shown in Figure 4. The fuel penalty on the x-axis is the amount of fuel used for regeneration, expressed as a fraction of the fuel used for normal lean operation. It is clear in this figure that for an equivalent level of NO_x reduction, 10-20% less fuel is needed for regeneration when an oxidation catalyst is added upstream of the CDPF. From these data we presume that the lighter HC species are more effective reductants than the heavier HC compounds in raw diesel fuel. The GC-MS data indicate that the light alkenes (propene, butenes, pentenes) and mono-aromatics are more readily consumed, whereas a larger fraction of the branched

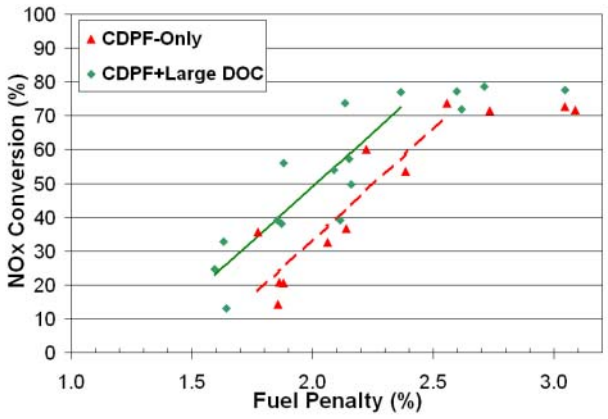

Figure 4. NO_x Conversion Versus Fuel Penalty for Rated Load Condition, CDPF-Only vs. CDPF+DOC (600°C catalyst temperature)

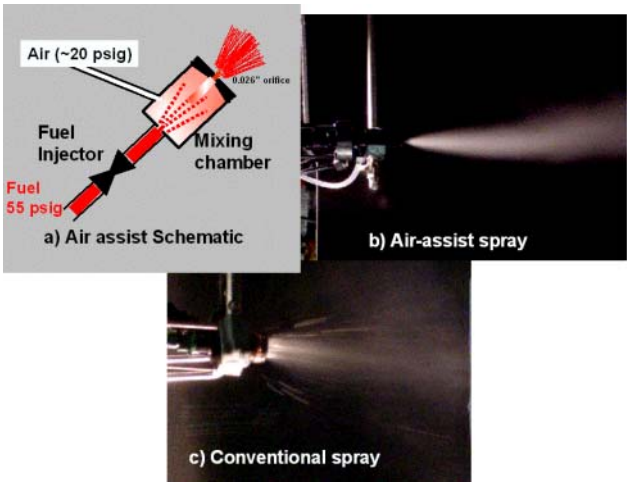

Figure 5. a) Schematic of Air-Assist Injection, b) Air-Assisted Fuel Spray, c) Conventional Injector Spray

alkanes pass through the NO_x adsorber catalyst. The experiments represented in Figure 4 used a conventional automotive fuel injector for delivering excess fuel (reductant) into the exhaust (shown in Figure 2). Concerns about fuel evaporation and mixing, particularly at the lower-temperature road load condition, led to development of an air-assist fuel injector, shown in Figures 5a and 5b. As the schematic (5a) shows, the conventional injector sprays into an air chamber, which then sprays into the exhaust through an orifice, assisted by compressed air. As shown in Figure 5b, atomization was greatly improved as compared to the conventional spray in Figure 5c.

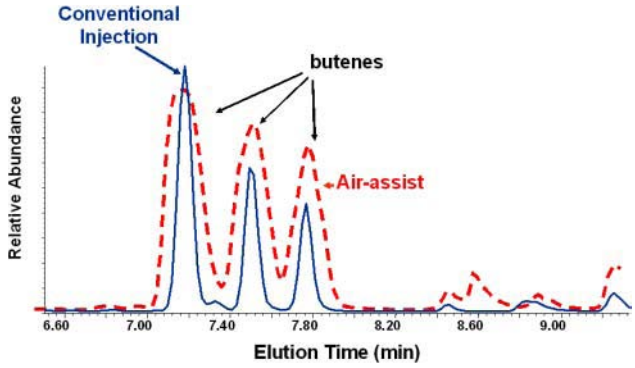

Figure 6. Gas Chromatogram Showing Butene Peaks at NO_x Adsorber Inlet During Regeneration for Conventional and Air-Assist Injection (rated load condition)

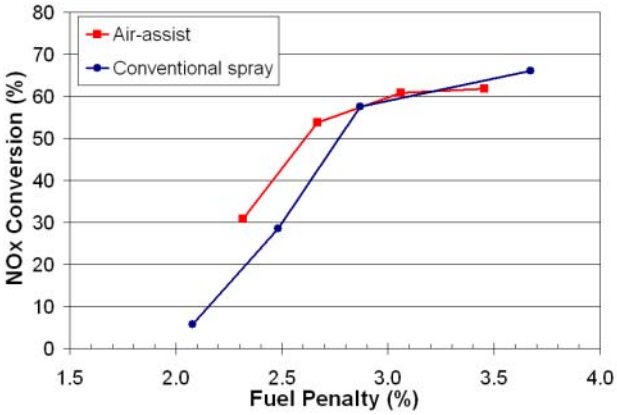

Figure 7. NO_x Conversion Versus Fuel Penalty for Rated Load Condition, Conventional vs. Air-Assist Injection (600°C catalyst temperature)

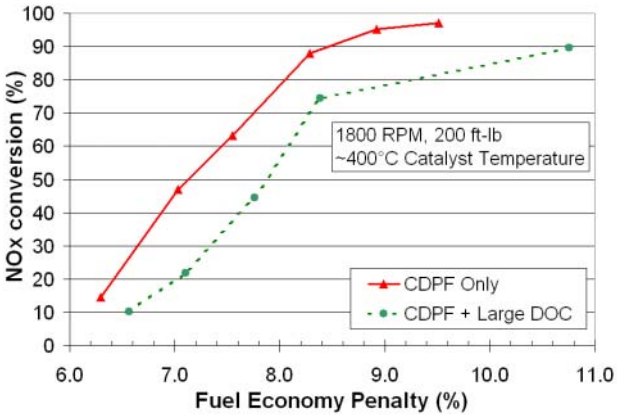

Figure 8. NO_x Conversion Versus Fuel Penalty for Road Load Condition, CDPF-only vs. CDPF+DOC (~400°C catalyst temperature)

The use of the air-assist injector improved the fuel cracking in the upstream DOC, as indicated in Figure 6. The figure shows butene peaks at the NO_x adsorber inlet from GC-MS for regeneration using the air-assist and the conventional injector at the rated load condition (600°C). Note that the butene area counts with the air-assist injector are over double the area counts with the conventional injector, and these higher counts are saturated (above the maximum detection), so the concentration ratio is much higher than 2. Similar results were noted for other species as well, including propene. For the 600°C rated load condition, the improved fuel cracking with the air-assist injector resulted in a small improvement in NO_x conversion; perhaps 5-8% less fuel nets the same NO_x reduction, as shown in Figure 7. The NO_x conversions shown in Figure 7 are not as good as those shown in Figure 4 due to sulfur poisoning of the NO_x adsorber. Exhaust sulfur (largely SO_2) is readily stored on the NO_x storage sites in the NO_x adsorber catalyst as a sulfate. These sulfated sites are rendered ineffective for NO_x storage until they are "desulfurized" by a process similar to regeneration, except with higher temperatures and longer times required. The NO_x adsorber was sulfur-poisoned through the normal course of running the engine on an ultra-low sulfur fuel containing 10 ppm (parts per millon) sulfur.

Figure 8 summarizes the results of experiments at the road load condition. In contrast to the rated load condition (Figure 4), note that this figure implies that the "CDPF Only" case actually provides equivalent NO_x reduction at a lower fuel penalty than the "CDPF + DOC" case. While GC-MS and FTIR data indicate that the DOC also enhances fuel cracking at this lower temperature, thereby providing lighter HC species to the NO_x adsorber, any benefits of these lighter species on NO_x adsorber regeneration are confounded by other differences in the two cases. The variations in the NO_x adsorber temperature, as shown in Figure 9, probably contribute to some of this difference. Note (in the top half of the figure) that with the DOC present, the exotherms in the NO_x adsorber catalyst are very small, resulting in a fairly steady temperature of 385-390°C. When the DOC is removed, the regeneration event produces a large exotherm in the front core of the NO_x adsorber

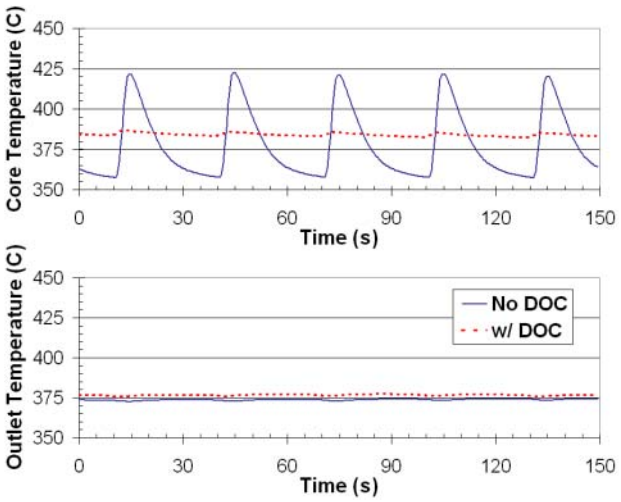

Figure 9. NO_x Adsorber Temperatures for Road Load Condition (Top: NO_x Adsorber Core Temperature; Bottom: NO_x Adsorber Outlet Temperature)

(previously in the DOC), causing the NO_x adsorber temperature to climb rapidly to over 420°C, then cool to a minimum temperature below 360°C before the next cycle. This core temperature is measured with a 0.020 inch diameter thermocouple at the center of the front 3-inch monolith of the NO_x adsorber catalyst, which is composed of four 3-inch monoliths. The actual surface temperature swings inside the catalyst could be more pronounced due to the relatively slower transient response of the thermocouple. As the bottom half of the figure shows, the temperatures out of the NO_x adsorber are very similar for either case; thus, on a net basis, the same amount of energy is deposited into the catalyst system during regeneration even though the position of energy deposition (heat release) differs. For the case with no upstream DOC, the higher thermal dynamics may contribute to improved NO_x conversion. Catalytic activity varies with temperature, and these effects can be different for various processes. For example, HC oxidation rates and NO_x reduction rates increase with increasing temperature, while nitrate stability and, thereby, NO_x storage is improved at lower temperatures. One theory derived from the observed data follows: the higher temperature during regeneration improves reaction rates for HC utilization and/or nitrate decomposition (which leads to more NO_x storage sites recovered) and the lower temperature during lean operation improves nitrate stability and/or NO oxidation (which leads to more NO_x storage site utilization). Thus, temperature modulations in the NO_x adsorber catalyst can alter NO_x reduction performance.

The exotherm is caused by oxidation of a portion of the reductant (fuel) in depleting any remaining engine-out oxygen. This oxidation reaction must occur before the chemical reduction can take place in the NO_x adsorber. If this oxidation takes place in the DOC, then the NO_x adsorber temperature is more constant. If the DOC is not in place, the bulk of this oxidation and exotherm occurs in the NO_x adsorber, generating the temperature swings noted in Figure 9. This interesting result highlights another challenge in designing and operating these complex systems. While lighter HC species are probably more desirable under any regeneration condition, the presence of a small amount of oxygen during regeneration may also enhance NO_x reduction by momentarily increasing temperature. In addition, with the DOC removed, a small amount of engine-out CO (800-900 ppm) was present at the NO_x adsorber inlet during regeneration. With the DOC installed, this CO and remaining exhaust gas oxygen were largely consumed while also cracking the raw fuel HC into lighter species. Follow-on experiments in FY 2005 will examine desulfation and attempt to clarify the HC species sensitivity as a function of temperature.

Conclusions

Cracking of raw fuel with DOCs can provide the NO_x adsorber catalyst with HC species not present in raw fuel. Observations from experiments to date include the following:

- Providing the NO_x adsorber with preferred HC species can lower the fuel penalty associated with NO_x adsorber regeneration for a given level of NO_x reduction, shown at the rated load condition.
- Mono-aromatics and light alkenes have been found to be readily consumed in the NO_x adsorber catalyst, while a large fraction of the branched alkanes are passed through.
- The heavy-duty not-to-exceed (NTE) regulations are extremely demanding. For 70% NO_x reduction to be adequate in the 2010 timeframe, engine-out NO_x emissions will have to be reduced to below 1.0 g NO_x/(hp•h).

- Momentary exotherms from oxidation of raw fuel in the NO_x adsorber catalyst during regeneration can improve NO_x conversion, overwhelming any benefit associated with cracking the fuel in an upstream DOC.

Publications/Presentations

1. West, Brian H., John F. Thomas, Mike Kass, John Storey, and Sam Lewis, "NO_x Adsorber Regeneration Phenomena in Heavy-Duty Applications," U.S. Department of Energy Advanced Combustion Engines Merit Review, May 13-15, 2003, Argonne, IL.
2. West, Brian H., John F. Thomas, Mike Kass, John Storey, and Sam Lewis, "NO_x Adsorber Regeneration Phenomena In Heavy Duty Applications: ORNL/ ITEC CRADA," presented at 9th Diesel Engine Emissions Reduction Workshop, August 2003.

II.B.4 Hydrocarbon-Based NO_x Catalysts for Diesel Applications

Christopher L. Marshall
Chemical Engineering Division
Argonne National Laboratory
9700 South Cass Avenue, CMT/205
Argonne, IL 60439-4837

DOE Technology Development Manager: Ken Howden

Objectives

- Test the use of deNO_x catalysts developed for stationary source applications for use in diesel vehicle emission reduction. Use realistic feeds and conditions typical of diesel emissions (temperature, space velocity, oxygen content) to appraise the ability of the catalyst to work under these conditions.
- Optimize the deNO_x catalyst and processing conditions for high conversion and selectivity to N_2 as the desirable nitrogen product.
- Demonstrate the integration of the catalyst system to work onboard a diesel vehicle.
- Set up a formal Cooperative Research and Development Agreement (CRADA) between Argonne National Laboratory (ANL) and a diesel manufacturer and a catalyst manufacturer. The goal of the CRADA will be to complete commercialization of the catalyst package for onboard NO_x reduction using diesel fuel as the reductant.

Approach

- **Task 1.** Work with a diesel engine manufacturer and a catalyst manufacturer to develop catalyst testing protocols and conditions that will both adequately test the range of the catalysts and properly simulate realistic diesel conditions. These conditions will include the proper hydrocarbon, space velocity, and fuel-to-air ratio.
- **Task 2.** The current catalyst testing system will be optimized to test catalysts using the protocols developed under Task 1. In addition, under this task we will construct a combinatorial screening unit that will allow us to test as many as 12 catalysts per day. Such a unit will speed the optimization of catalyst parameters and feed considerations to be tested in Tasks 3 and 4.
- **Task 3.** Continue the synthesis of new catalyst materials begun for stationary source applications. The catalyst formulations will be optimized for use in diesel applications. Variables to be studied include zeolite type, exchange metal type and amount, and additive composition and means of addition.
- **Task 4.** Catalyst formulations developed under Task 3 will be tested for NO_x conversion under simulated diesel conditions using the protocols developed under Tasks 1 and 2. Product yields will be recorded, concentrating not just on the conversion levels (as reported) but also on the exact composition of the exhaust stream. We are especially interested in the makeup of the nitrogen compounds and will concentrate on complete conversion of all nitrogen to N_2. Composition of CO_x will also be studied under this task.
- **Task 5.** Utilize the in situ characterization tools developed for testing the stationary source catalysts. These include in situ extended x-ray adsorption fines structure spectroscopy/x-ray adsorption near edge spectroscopy (EXAFS/XANES) and Fourier transform/infrared (FT/IR) techniques, which reveal the state of the metals and the adsorbed species on the surface of these metals under true reaction conditions. The Heterogeneous Catalysis Group at ANL has worked to develop both the techniques and the reactor cells that can examine the working catalysts under realistic conditions (see, e.g., “In Situ EXAFS Analysis of

the Temperature Programmed Reduction of Cu-ZSM--5," M. K. Neylon, C. L. Marshall, A. J. Kropf, J. Amer. Chem. Soc., 124(19), p 5457 [2002]).

- **Task 6.** Catalysts being tested under Tasks 3 and 4 will also be studied using ex situ temperature-programmed techniques such as temperature-programmed reduction (TPR) and temperature-programmed oxidation. TPR has been especially effective in monitoring the ease of reduction of the metals, which is directly related to both the activity and selectivity of the catalyst.
- **Task 7.** Report results to DOE and collaborators. The project progress reporting procedure will conform to the requirements of the Office of FreedomCAR and Vehicle Technologies.

Accomplishments

- Catalytic tests showed that when using feeds containing only paraffins (~70% of diesel fuel), the current catalyst was ineffective in converting NO_x to N_2. $DeNO_x$ activity was not achieved below the hydrocarbon combustion temperature. Nitrogen selectivity still remained near 100%. These results suggest that the paraffinic portion of diesel fuels cannot be effectively used as the reductant.
- Tests with aromatic feeds (toluene and xylenes) were very effective in converting NO_x to N_2 over the current catalyst. $DeNO_x$ light-off activity was achieved far below the hydrocarbon combustion point. Nitrogen selectivity to N_2 still remained near the 100% mark. These results suggest that the aromatic fraction of diesel fuels (~20%) is a prime candidate as the reductant for $deNO_x$ catalysts.
- The data from the bullet above was extended to low-sulfur jet fuel (JP-8). JP-8 was tested as a reductant for the CeO_2/Cu-ZSM-5 catalyst, both neat and with added aromatics. The catalyst converted 80% of the NO_x to N_2 at a 40,000 hr^{-1} space velocity (Figure 1). JP-8 also improved the high-temperature activity of the catalyst. The activity improvement over using propylene as a feed is 195% at 400°C and 212% at 450°C (Figure 2). Spiking studies with xylenes show that the improvements are related to the wider variety of boiling points of the JP-8 fuels. This wider temperature range meets the industry needs for both low-temperature $deNO_x$ for low- and normal-load operations and high-temperature $deNO_x$ for higher-temperature, high-load operations.

Future Directions

- The results with JP-8 will be extended to low-sulfur diesel (e.g., BP-15; 15 ppm sulfur).
- Conduct tests with BP-15 and JP-8 under high O_2 concentrations in order to optimize the processing conditions under realistic feed conditions.
- Coat several optimized materials and test the activity with BP-15 and JP-8, with the aim to optimize process conditions towards making a working catalyst.
- Coat the best material onto a large monolithic support and test on an engine using a slip stream of the diesel feed as the reductant. Optimization will include maximizing space velocity while minimizing the catalyst volume.

Introduction

The oxide forms of nitrogen (NO, NO_2, and N_2O, collectively called NO_x) are some of the most difficult but important pollutants yet to be eliminated from exhaust streams. A key problem is that the most active commercial catalysts use ammonia to convert NO_x to nitrogen in the exhaust. Not only is ammonia difficult to store, but if conversion is not complete, ammonia can be released to the atmosphere - a problem worse than the release of NO_x. Catalysts are needed that will convert NO_x using a more readily available, more environmentally benign reductant.

One of the most promising catalysts is a metal-exchanged form of the zeolite ZSM-5. In the copper (Cu) exchanged form (Cu-ZSM-5), this catalyst shows a significant ability to reduce NO_x to N_2 using hydrocarbons such as propylene as the reductant.

Many published studies have shown that Cu-ZSM-5 has high selectivity for NO_x conversion with very low hydrocarbon slippage. A major disadvantage to Cu-ZSM-5 is that it is effective only when the exhaust stream is dry. The addition of water (a common component in all exhaust streams) renders the catalyst inactive. For this reason, most commercial development of Cu-ZSM-5 has been stopped.

We have been working on new additives to extend the life of catalysts such as Cu-ZSM-5. One of these additives (cerium oxide, CeO_2) has not only proven effective in eliminating the water stability problem for Cu-ZSM-5, but actually improves its activity.

Approach

The Heterogeneous Catalysis Group at Argonne National Laboratory has developed a series of additives that significantly lower the effective temperature for hydrocarbon-based NO_x reduction. These same catalysts have been recently examined under conditions closer to diesel engine applications and have shown great promise. The conditions used were around 500 ppm NO, a C:N ratio of 6:1, and a high O_2 concentration (8%). These conditions were suggested to us during discussions with diesel engine manufacturers. Tests were performed using n-hexane as the reducing gas for the deNO_x catalyst. The Argonne catalyst selectively converted NO_x (NO/NO_2) into N_2 (95+% selectivity) at temperatures of 300°C and higher. Throughout these tests, no coking was observed on the catalyst material and no catalyst deactivation was observed.

These catalysts can reduce NO_x emissions from diesel engines while saving energy. The energy savings come about from using hydrocarbons already "on-board" the diesel vehicle rather than manufacturing urea off-line which requires secondary storage, shipping, and delivery systems.

In FY 2004, we examined the further development of these catalysts for diesel engine applications. Development included improving means of adding the oxidation additive, investigating the effects of space velocity and air/fuel mixture changes, and determining the effects of potential poisons such as sulfur. Reaction kinetics was examined in order to optimize the stoichiometries of the fuel, air, and water.

Results

The CeO_2/Cu-ZSM-5 system shows significant activity for NO to N_2 conversion when JP-8 fuel is used as reductant (Figure 1). The unusual enhancement in activity observed in C_3H_6-SCR by the addition of water to the feed is also observed with this type of reductant. JP-8 improves the high-temperature activity of the catalyst. Unlike the C_3H_6 system, the middle distillate fuels increase the temperature window of activity while exhibiting no NO_2 breakthrough. The activity improvement over using propylene as a feed is 195% at 400°C and 212% at 450°C (Figure 2). It is proposed that in the CeO_2/Cu-ZSM-5 system, the aromatic components of the fuel are responsible for the greater part of the NO conversion.

Conclusions

The use of onboard fuel as the reductant for NO_x abatement in diesel and lean-burn engines is an attractive alternative to adding a reductant requiring additional onboard storage, as in the case of urea or light hydrocarbon selective catalytic reduction (SCR). The work has shown JP-8 to be effective and preferable for high-temperature (high-load) operation of the catalyst. Work will continue to investigate the use of low-sulfur diesel as a reductant.

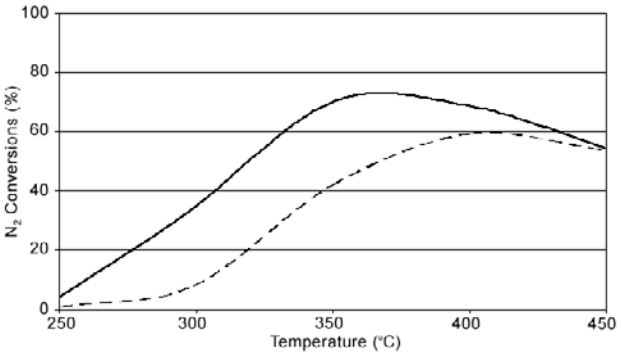

Figure 1. NO to N_2 Conversion for CeO_2/Cu-ZSM-5 with JP-8 as Reductant [Solid line: 10% water in stream. Dashed line: Dry stream. Conditions: 1000 ppm NO, 2% O_2, 2000 ppm JP-8 (based on average molecular weight). GHSV: 32,000 hr^{-1}.]

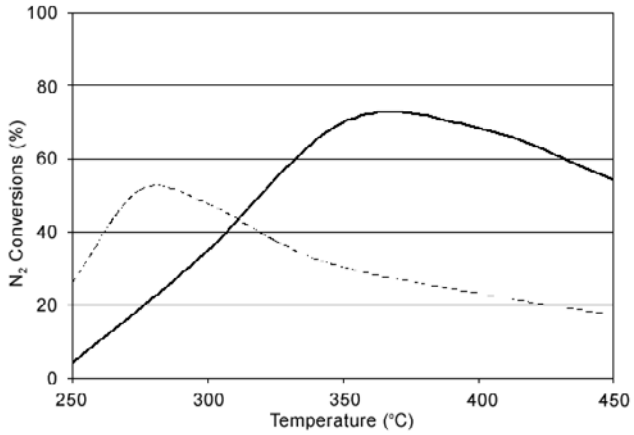

Figure 2. NO to N_2 Conversion for CeO_2/Cu-ZSM-5 with JP-8 or Propylene as the Reductant (Solid line: JP-8 as the reductant. Dashed line: Propylene as the reductant. Conditions: 1000 ppm NO, 2% O_2, 32,000 hr^{-1}.)

Special Recognitions & Awards/Patents Issued

1. "Novel Catalyst for Selective NO_x Reduction Using Hydrocarbons," C. L. Marshall and M. K. Neylon (European patent application WO 03/031781 A1; April 17, 2003).
2. "Novel Catalyst for Selective NO_x Reduction Using Hydrocarbons," C. L. Marshall and M. K. Neylon (U.S. patent application 2003/0073566 A1; April 17, 2003).

FY 2004 Publications/Presentations

1. "Coated Bifunctional Catalysts for NO_x SCR with C_3H_6 - Part I: Water-Enhanced Activity," Michael K. Neylon, Mario J. Castagnola, Norma B. Castagnola and Christopher L. Marshall, Catalysis Today, **96** (2004) 53-60.
2. "Coated Bifunctional Catalysts for NOY SCR with C_3H_6 - Part II: In situ Spectroscopic Characterization," Mario J. Castagnola, Michael K. Neylon, A. Jeremy Kropf and Christopher L. Marshall, Catalysis Today, **96** (2004) 61-70.
3. "Bifunctional Catalysts for the Selective Catalytic Reduction of NO by Hydrocarbons," C. L. Marshall, M. K. Neylon, M. J. Castagnola, and A. Jeremy Kropf, Annual Peer Review Meeting, Argonne National Laboratory, Argonne, IL, May 18, 2004.
4. "Bifunctional Catalysts for the Selective Catalytic Reduction of NO by Hydrocarbons," C. L. Marshall, M. K. Neylon, M. J. Castagnola, and A. Jeremy Kropf, 10th Diesel Engine Emissions Reduction Conference, San Diego, CA, August 31, 2004.

References

1. Shimizu, K., Shibata, J., Yoshida, H., Satsuma, A., Hattori, T. Appl. Catal. B: Environmental, 30, 151 (2001).
2. Klingstedt, F., Eranen, K., Lindfors, L. E., Andersson, S., Cider, L., Landberg, C., Jobson, E., Eriksson, L., Ilkenhans, T., Webster, D. Topics Catal. 30-31, 27 (2004).
3. Neylon, M. K., Castagnola, M. J., Castagnola, N. B., and Marshall, C. L. Catal. Today, 96, 53 (2004).
4. Castagnola, M. J., Neylon, M. K, and Marshall, C. L. Catal. Today, 96, 61 (2004).

II.B.5 Crosscut Lean Exhaust Emission Reduction Simulation (CLEERS)

Stuart Daw
Oak Ridge National Laboratory (ORNL)
National Transportation Research Center (NTRC)
2360 Cherahala Boulevard
Knoxville, TN 37932-6472

DOE Technology Development Manager: Ken Howden

The following report is for three separate activities that are included under CLEERS:

- Administrative support (Stuart Daw and Sreekanth Pannala)
- Joint development of benchmark kinetics (Stuart Daw, Kalyana Chakravarthy, Katey Lenox, Jae-Soon Choi, and Jim Parks)
- Micro-scale catalyst modeling for performance and durability (Bill Shelton and Sreekanth Pannala)

Objectives

Administrative Support

Provide coordination of the CLEERS activity for the Diesel Crosscut Team in accomplishing the following:

- Promote development of improved computational tools for simulating realistic full-system performance of lean-burn engines and the associated emissions control systems.
- Promote development of performance models for emissions control components such as exhaust manifolds, catalytic reactors, and sensors.
- Provide consistent framework for sharing information about emissions control technologies.
- Help identify R&D needs and priorities.

Joint Development of Benchmark Kinetics

- Coordinate ORNL's collaboration with Pacific Northwest National Laboratory (PNNL) and Sandia National Laboratories (SNL) in the development of kinetics information needed for aftertreatment component simulation.
- Provide benchmark laboratory measurements of NO_x reduction chemistry and reaction rates.
- Coordinate laboratory measurements of lean NO_x trap (LNT) materials with ongoing test-stand/vehicle studies in the NTRC facility.
- Develop and validate global chemistry and (low-order) models for LNT kinetics.

Micro-Scale Catalyst Modeling

- Develop a simplified computational model that relates the effects of catalyst surface morphology on the chemistry and performance of critical aftertreatment components.
- Utilize this model in combination with experimental performance data and microscopic surface characterizations to correlate and predict trends in aging, sulfur poisoning, and component regeneration.

Approach

Administrative Support

- Set up and coordinate meetings of the CLEERS Planning Subcommittee;
- Co-lead the LNT Focus Group.

- Provide overall coordination and secretarial assistance in planning and carrying out the CLEERS public workshops.
- Maintain the CLEERS website on an ORNL server accessible via the internet.
- Provide periodic status updates and summary reports to the Crosscut Team.
- Respond to general requests and inquiries about CLEERS from the public and technical community.

Joint Development of Benchmark Kinetics

- Maintain regular interactions with PNNL and SNL through the Focus Groups and direct meetings.
- Conduct experimental measurements of LNT chemistry and reaction rates using the pre-competitive adsorber materials in the ORNL bench-flow and diffuse reflectance infrared spectroscopy (DRIFTS) reactors.
- Analyze test-stand/vehicle LNT data collected at the NTRC facility, and compare this data with the laboratory bench-flow and DRIFTS measurements.
- Write and validate simplified computer LNT codes that can be used to evaluate the laboratory and test-stand rate measurements.
- Publish and post experimental/modeling results from ORNL in journals and on the website.

Micro-scale Catalyst Modeling

- Develop a computer code that uses a simplified rule-based Monte Carlo process to simulate surface morphology changes in supported catalysts as they age and the impact of those changes on reaction conversion efficiency.
- Initially apply the code to simulating LNT aging and sulfur poisoning.
- Validate the code predictions with experimental data.
- Apply the results of the Monte Carlo simulations to global LNT performance models.

Accomplishments

Administrative Support

- Co-led the CLEERS Planning Committee.
- Assisted in completing organization and implementation of the Selective Catalytic Reformer (SCR) Focus group.
- Co-led LNT Focus Group, and provided assistance as needed for diesel particulate filter (DPF) and SCR Groups in their regular meetings.
- Provided regular update reports to the DOE Diesel Crosscut Team.
- Held 7th CLEERS workshop at Detroit Diesel Corporation on June 16 and 17.
- Collaborated with supplier representatives and LNT Focus Group to develop a draft bench characterization protocol for LNT materials that is intended to provide the basis of standard kinetic ‘maps’ (i.e., data templates) for communicating critical simulation properties. Presented the protocol at the 7th CLEERS workshop and posted on the website.
- Expanded website functionalities, security, and data to facilitate web meetings and serve Focus Group interactions.

Joint Development of Benchmark Kinetics

- Developed LNT kinetic map characterization protocol in conjunction with the LNT Focus Group and collaborating suppliers.
- Acquired first available commercial LNT material from Umicore as a standard benchmark material and initiated degreening and detailed chemical analysis.
- Acquired Toyota DPNR (Diesel Particulate NO_x Reduction, combined LNT and DPF aftertreatment) and LNT samples from Ford and initiated chemical analysis and bench testing.

- Completed simplified global models of LNT capture and regeneration. Described models in public presentations and publications. Posted MATLAB code that implements these models on the website.
- Extensively upgraded the ORNL bench-flow reactor to ensure compliance with key requirements of the draft characterization protocol.

Micro-Scale Catalyst Modeling

- Developed rules-based Monte Carlo code that better simulates sintered Pt particle distributions within Pt islands as well as the distribution of the Pt islands.
- Implemented and tested a new rules-based NO_x chemistry module interfaced with the Pt sintering code.

Future Directions

Administrative Support

- Continue co-leading CLEERS planning committee.
- Continue co-leading the LNT Focus Group and support the DPF and SCR Focus Groups as needed.
- Continue providing standard reference LNT materials and data for Focus Group evaluation.
- Organize 8th CLEERS workshop sometime after March 2005.
- Continue maintenance and expansion of CLEERS website.
- Continue providing regular update reports to the DOE Diesel Crosscut team.

Joint Development of Benchmark Kinetics

- Complete improvements to the ORNL bench-flow reactor.
- Demonstrate draft LNT characterization protocol on ORNL bench-flow reactor and identify needed revisions and technical issues.
- Complete bench reactor measurements, DRIFTS reactor measurements, chemical analysis, and microscopic characterization of Umicore LNT reference material. Transmit these results to the LNT Focus Group as they become available.
- Update and post revised global LNT model with input from SNL, literature, and ORNL experimental data as these become available.
- Complete chemical analysis, powder and bench-flow reactor measurements, and microscopic characterization of the Toyota DPNR and LNT samples.
- Coordinate kinetic and microscopic characterization measurements with LNT durability tests developed under the rapid aging protocol.

Micro-Scale Catalyst Modeling

- Derive mean-field approximations that can be used to speed up simulations.
- Refine the Pt particle coarsening rules to correlate with microscopy measurements of the LNT model and reference materials.
- Include explicit steps for sulfur poisoning in aging simulation.
- Use combined Monte Carlo code to produce relative rate parameters that can be used in global performance models for studying the impact of different operating and control strategies.

Introduction

Improved catalytic emissions controls will be essential for utilizing high-efficiency lean-burn engines without jeopardizing the attainment of the U.S. Environmental Protection Agency heavy-duty engine emission standards scheduled to take effect in 2007. Simulation and modeling are recognized by the DOE Diesel Crosscut Team as essential capabilities needed to achieve this goal. In response to this need, the CLEERS activity (Crosscut Lean Exhaust Emissions Reduction Simulation) was

initiated to promote development of improved computational tools for simulating realistic full-system performance of lean-burn engines and the associated emissions control systems. While CLEERS does not directly support the development of extensive full-emissions-system performance simulation codes, it does provide explicit support for the following activities:

- Public workshops on key emissions control topics;
- Collaborative interactions among and between Crosscut Team members, emissions control suppliers, universities, and national laboratories under specially organized topical focus groups;
- Development of experimental data, analytical procedures, and computational tools that are directly useful for understanding component performance and the behavior and durability of catalytic materials;
- Development of consistent frameworks for sharing information about emissions control technologies; and
- Development of explicit recommendations to DOE and the Diesel Crosscut Team regarding the most critical emissions control R&D needs and priorities.

ORNL is involved in three separate DOE-funded tasks that support CLEERS:

- Overall administrative support;
- Joint development of benchmark LNT kinetics with SNL and PNNL; and
- Micro-scale catalyst modeling for performance and durability.

In the administrative task, ORNL staff members coordinate the CLEERS Planning Committee, the CLEERS Focus groups, the public workshops, and the CLEERS website (www.cleers.org). The joint kinetics development task involves collaboration among ORNL, SNL, and PNNL to produce key kinetics information needed for predicting the performance of lean NO_x adsorbers and catalyzed particulate filters. The results of this work are discussed with the LNT and DPF Focus groups prior to publication to provide technical review and guidance to the labs. The collaboration is structured to build on the strengths of each lab and leverages against other DOE-funded activities to maximize benefits. The micro-scale modeling task is intended to help improve understanding of catalyst morphology, how changes in that morphology relate to aging, and how those changes affect practical component performance.

Approach

Administrative Support

In FY 2004 ORNL has continued acting as the lead coordinator of the overall functions of the CLEERS Planning Committee and Focus Groups. Stuart Daw of ORNL is responsible for providing general assistance to each of the Focus Groups and is a co-leader (with Dick Blint of General Motors) of the LNT Focus Group. George Muntean and Darrell Herling from PNNL are co-leaders of the DPF and SCR Focus Groups, respectively, and report on their activities elsewhere. ORNL organizes and implements the public workshops under guidance from the Focus Groups and Planning Committee, providing both technical and secretarial support. The CLEERS website is maintained (under direction of Sreekanth Pannala) on an ORNL server accessible via the internet. Both public and restricted areas have been set up on this website to facilitate distribution of technical information, workshop information and presentations, and interactive web meetings. Stuart Daw provides assistance to Dick Blint (GM) in presenting periodic status updates and summary reports to the Crosscut Team. Both Stuart and Sreekanth Pannala at ORNL respond to general requests and inquiries about CLEERS from the public and the technical community.

Joint Development of Benchmark Kinetics

ORNL's responsibility in this activity is to set up and conduct experimental measurements of LNT chemistry and reaction rates that will help to define the critical physical characteristics of LNT materials responsible for determining practical performance (i.e., NO_x emissions reduction and energy efficiency). In this function, ORNL utilizes reference non-competitive adsorber materials in the ORNL bench-flow and DRIFTS reactors. Where possible, these bench measurements are also supplemented with other specialized measurement

capabilities such as high-resolution microscopy at the ORNL High Temperature Materials Laboratory (HTML). ORNL maintains regular interactions with PNNL and SNL and the industry collaborators through the LNT Focus Group in order to maximize the value of the data generated and provide feedback that can be considered in planning future experiments. Where possible, laboratory results are compared with and analyzed in the context of test-stand/vehicle LNT measurements generated in parallel projects at ORNL's NTRC facility. For assistance in interpreting trends, ORNL has been writing and validating simplified computer LNT codes that can be used to evaluate the laboratory and test-stand data. Results are published in peer-reviewed journals, presented in public meetings, and/or posted on the CLEERS website.

Micro-Scale Catalyst Modeling

In this activity, ORNL is applying previously developed methods for rule-based Monte Carlo simulations to construct a computer code that can capture the key physics of surface morphology changes that occur in supported catalysts (initially specifically for LNTs) as they age. In addition to reflecting the changes in morphology, the code is designed to reflect the impact of these changes on NO_x conversion efficiency and reductant consumption in terms of global rate parameters that can be used in system simulations. The target phenomena at this stage are Pt particle sintering (coalescence) and sulfur poisoning. Validation of the predicted trends with experimental data is an important aspect of the approach (as data become available). In regard to the latter, we have begun to closely coordinate with the rapid aging protocol development started in FY 2004.

Results

Administrative Support

The seventh CLEERS workshop was held June 16 and 17 at the Detroit Diesel Corporation training facility in Detroit. All three emissions control technology areas (LNTs, DPFs, and SCR) were covered, but the greatest emphasis was on DPFs and SCR. The complete technical program, meeting summary, and most of the presentations are available on the website (www.cleers.org). More detailed summaries were also provided to the Diesel Crosscut Team. This was the largest workshop to date, with a total of 90 registrants. This attendance also included very large participation from emissions control suppliers as well as original equipment manufacturers (OEMs).

The LNT and DPF Focus Groups have been holding regular phone/web meetings throughout the year, and summary reports of the meetings have been provided to the Diesel Crosscut Team. Darrell Herling from PNNL and Joe Bonadies from Delphi agreed to serve as co-leaders for the SCR Focus Group, and this group began meeting in May.

One of the main activities of the LNT Group has been the development of standard kinetic "maps" or "templates" that can be transferred between suppliers and users. Direct involvement of the suppliers was initiated with assistance from Joe Kubsch at Manufacturers of Emission Controls Association (MECA). Supplier representatives from Delphi, Johnson Matthey, Engelhard, 3M, Tenneco, and Arvin Meritor have participated in meetings with a subcommittee from the LNT Group composed of Dick Blint (GM), Neal Currier (Cummins), Ed Jobson (Mack/Volvo), and Stuart Daw (ORNL). As a result, considerable progress was made in defining a set of 74 bench flow reactor conditions to be used as the basis for the kinetic maps. This list of specified conditions was publicly distributed at the seventh CLEERS workshop and on the website in June. It is expected that the standard conditions can be used to define a minimal characterization of the key features of each LNT sorbent material being considered by OEMs. With this information, OEMs should be able to obtain reasonably accurate performance predictions using their in-house LNT models. Field demonstrations of the feasibility and applicability of the LNT bench reactor characterizations at multiple LNT Focus member sites are now underway.

The LNT Group has agreed to concentrate initial testing of the protocol on LNT samples provided by Umicore of their European commercial product intended for gasoline direct injection (GDI) applications. Because these samples are commercial, complete physical and chemical characterizations

can be made to correlate with the bench measurements. ORNL will also make comparisons between this material and other LNT materials being tested at ORNL in other activities, including standard Ba-type model materials made at ORNL and prototype MECA materials (for which detailed physical and chemical characterizations are unavailable). Ford has also supplied a sample of DPNR material from the Toyota Avensis vehicle to ORNL for evaluation. Results from this material will be shared with the LNT Group as they become available.

The DPF Group has been using the experience of the LNT Group as a guide for developing their own concept of DPF performance 'maps'. They have decided to consider both defining a test matrix of characterization procedures for the DPF materials as well as developing actual performance trends from model simulations to help guide the analysis and understanding of DPF function. George Muntean provided a presentation summarizing these approaches at the March Diesel Crosscut Meeting. One of the major technical difficulties with DPFs will be to decouple filter loading and regeneration since loading affects soot distribution and cake properties, which then influence regeneration. The question has been raised whether engine tests can be minimized for DPFs as they were in the LNT test matrix. Engine tests may be necessary to obtain realistic soot loading. Engine operating conditions, such as steady state vs. dynamic, can affect soot quality (ash content, organic carbon/elemental carbon ratio) via changing oil consumption. It was suggested that a filter might be loaded on an engine and then regenerated in a reactor. Other practical issues under consideration are the observations that soot seems to age and that filter regeneration properties may vary over time (i.e., vary with time after loading). The DPF Group has formed a subcommittee charged with defining the objectives and general approach needed to characterize particulate filters. One emerging conclusion thus far is that DPF characterizations are likely to require a significant amount of testing on actual engines as opposed to laboratory bench reactors. This will be a significant departure from the LNT and SCR protocols, which are mainly focused on bench reactor measurements.

In the SCR Group, Ford has proposed their list of characterization protocol measurements for urea-SCR materials as a starting point. Measurements such as those proposed by Ford would appear to be relatively simple because they are made at steady-state conditions without the need to resolve detailed dynamic transients. The Group has also found a supplier that appears willing to supply a commercial zeolite-type SCR catalyst that can be used as a shared reference by the group (similar to the Umicore material used by the LNT Group). The SCR Group has also spent considerable time defining the performance features that need to be captured by the characterization protocol and simulations.

Joint Development of Benchmark Kinetics

Early in 2004, the ORNL bench flow reactor was modified to include a higher-speed switching system that allowed more rapid transitions between lean and rich conditions. Experience has shown that the observed breakthrough profiles can be strongly affected by the lean/rich transition time, with the optimal time being as fast as possible. Even with these changes, the transition between lean and rich states took as long as two seconds to be completed. The spatially resolved capillary inlet mass spectrometry (SpaciMS) instrument has turned out to be very useful for determining this response time. Example results illustrating this fast response for hydrogen breakthrough are shown in Figure 1.

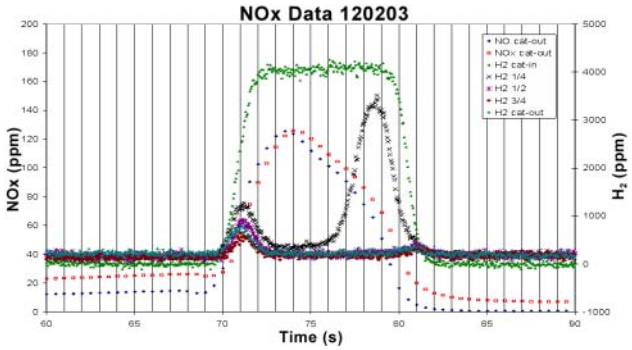

Figure 1. Hydrogen breakthrough profiles for a SCONOx-type (SCONOx is the brand name of a lean NO_x trap catalyst containing potassium made by Emerachem) catalyst in the bench flow reactor as measured by SpaciMS. NO_x breakthrough profiles measured by conventional gas analyzers are shown for comparison.

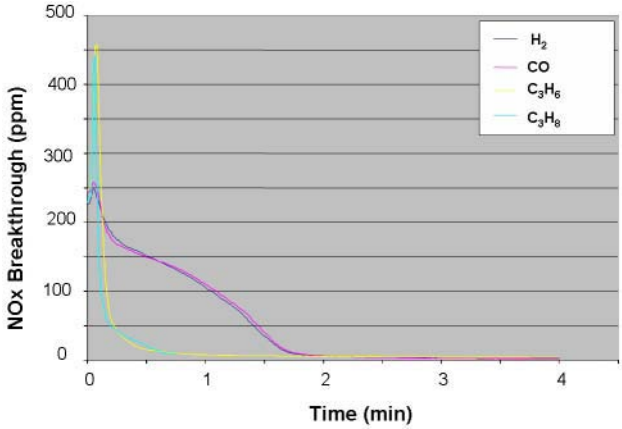

Figure 2. NO_x breakthrough for regeneration of the first model sorbent with different reductant species. The capture and regeneration times were set very long in these experiments to accentuate differences.

Two different model sorbents containing barium as the primary alkali sorbent species were produced in monolith form, both as full bricks and as core samples for the bench reactor. Bench testing of these materials is still underway, and engine testing of the full bricks is planned for next year. Preliminary bench flow results for different reductant species (hydrogen, CO, propane, and propylene) have shown large differences in response for the first model sorbent. Example breakthrough profiles illustrating these results are shown in Figure 2. These differences illustrate the importance of having reliable methods for characterizing and defining the different species effects in accurate simulation models.

Direct comparisons are now being made between the bench flow characteristics of the candidate sorbents and the engine/dyno performance seen in the DaimlerChrysler 1.7-liter LNT tests. Using the high-speed switching system to transition between lean and rich conditions on the bench reactor, we are now able to nearly reproduce the cycling conditions of the engine tests. In addition to the model barium-containing sorbents described previously, we have also begun experiments with sorbents supplied by MECA. Such comparisons between the laboratory and bench scale measurements have been extremely helpful in improving our understanding and models of capture and regeneration.

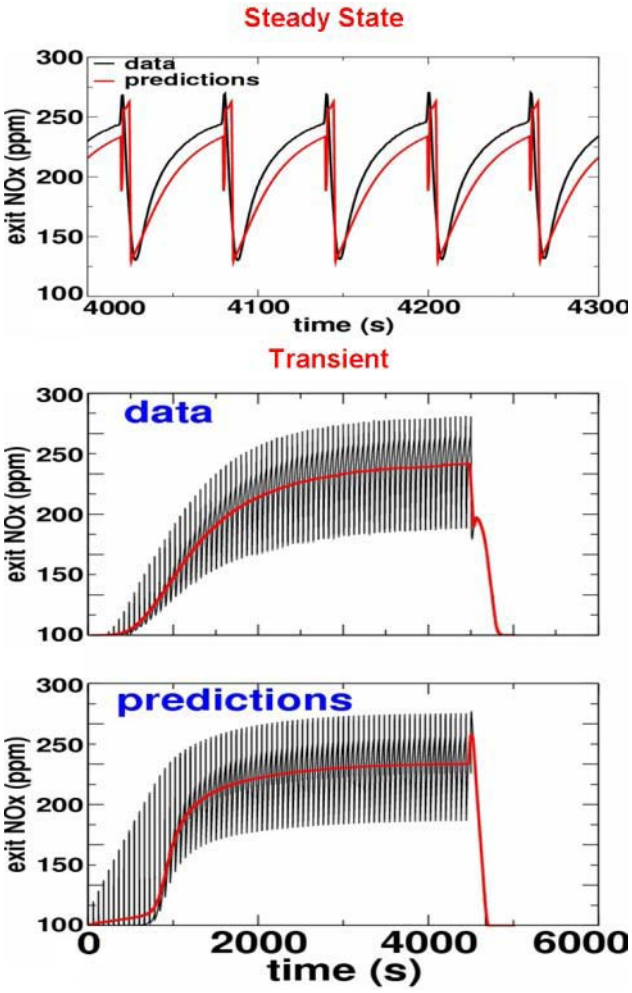

Figure 3. Observed and predicted NO_x breakthrough profiles for a MECA catalyst in the bench flow reactor during fast lean/rich cycling (55 s lean/ 5 s rich). The reductant in this case is 0.2% hydrogen, and the inlet NO concentration is 300 ppm during the lean period. The sorbent is clean (no stored NO_x) at the beginning of the experiment. The transient plots compare the predicted and observed long-term NO_x breakthrough trends as the sorbent loads up, while the steady-state plot compares the details of NO_x breakthrough for individual cycles.

By estimating the thermodynamic properties and global kinetics from the bench reactor measurements and then implementing them in an integral reactor model, we are able to quite closely reproduce the observed sorbent performance for all the materials evaluated. For example, Figure 3 illustrates the NO_x breakthrough observed in the bench reactor under fast cycling conditions and compares the observation

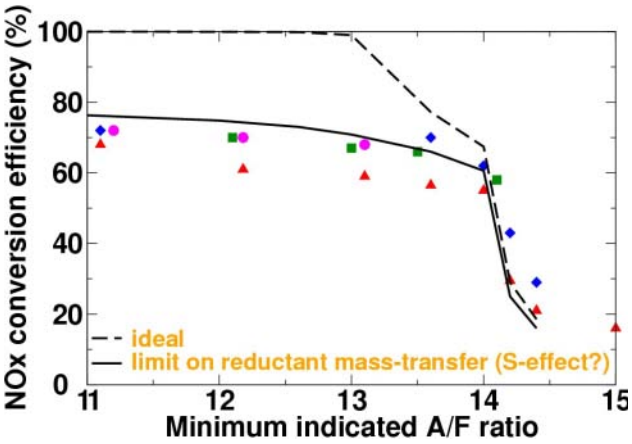

Figure 4. Observed and predicted engine/dyno LNT NO_x conversion (overall) as a function of the level of richness during regeneration. The MECA sorbent in this case was heavily sulfated. Richness is indicated in terms of the engine-out universal exhaust gas oxygen sensor indicated air/fuel ratio. Note the limit in performance at increasing richness. This can be replicated by the model only by adding a finite limiting rate for reductant diffusion during regeneration.

with corresponding predictions from our global kinetics model.

The global kinetics and integral reactor models have also provided guidance in interpreting the observations from the engine/dyno experiments. Essentially, these models are based on the differential mass balances for NO_x, O_2, and reductant species, which are then integrated along the reactor over time. For example, in Figure 4, the conversion performance of a highly sulfated LNT is shown as a function of the richness of the regeneration pulse produced by in-cylinder fuel modulation (as indicated by the engine-out universal exhaust gas oxygen sensor). Note that as the richness is increased (lower as-indicated air/fuel ratio), a definite limit in overall NO_x conversion of 60-70% is reached. Further increases in richness with this regeneration strategy did not improve conversion and succeeded only in wasting fuel. By applying our integral global kinetics model, we have been able to determine that the performance limit is the result of a zeroth-order rate limit on the reduction reaction. This limit appears to be significantly reduced by the high degree of sulfur poisoning. Now that this limit has been recognized, the specific physical causes and correlation with sulfur poisoning can be more effectively investigated.

Additional details of the global kinetics model have been summarized in publications and posted on the CLEERS website. We are also using the insights provided by the model and bench and engine/dyno experiments to help improve the effectiveness of the standard characterization matrix for LNT characterization being developed by the CLEERS LNT Focus Group. The latter is intended as a minimal set of reference data that can be provided by suppliers to OEMs for each sorbent material. It is expected that OEMs will be able to use this data with their in-house models to estimate performance trends for candidate materials and evaluate options for emissions control system designs and control strategies.

Meetings were held in March between ORNL and SNL staff to further define the details of our collaboration for modeling the multiple reaction steps involved in determining the observed global rates for capture and regeneration. One particular area of interest is in the loss of reactive surface area on the Pt-group metals in the sorbent. Bench reactor data at ORNL suggests that there may be a gradual surface oxide formation (i.e., oxygen poisoning) that limits NO_x storage during the lean period. Likewise, it may be possible that NO_x reduction may become limited by a similar surface sulfide formed during regeneration. Tony McDaniel is investigating how previous kinetics studies of oxide and sulfide formation on Pt may be applied to the LNT context.

Additional hardware modifications were made later in the year to the ORNL bench flow apparatus in order to accommodate the expected requirements of the standard LNT protocol. Specifically, a faster valve was added for the lean/rich cycling mechanism, and inlet and outlet couplings for the quartz reactor tube were redesigned to reduce the potential for leaks. Considerable effort is also being spent on calibrating the dynamic responses of the NO, NO_x, CO, O_2, and Fourier transform infrared (FTIR) analyzers in order to be able to make the needed measured breakthrough corrections. Recent studies have included extensive use of SpaciMS measurements of NO_x, O_2, and H_2 breakthrough profiles at 5 axial locations.

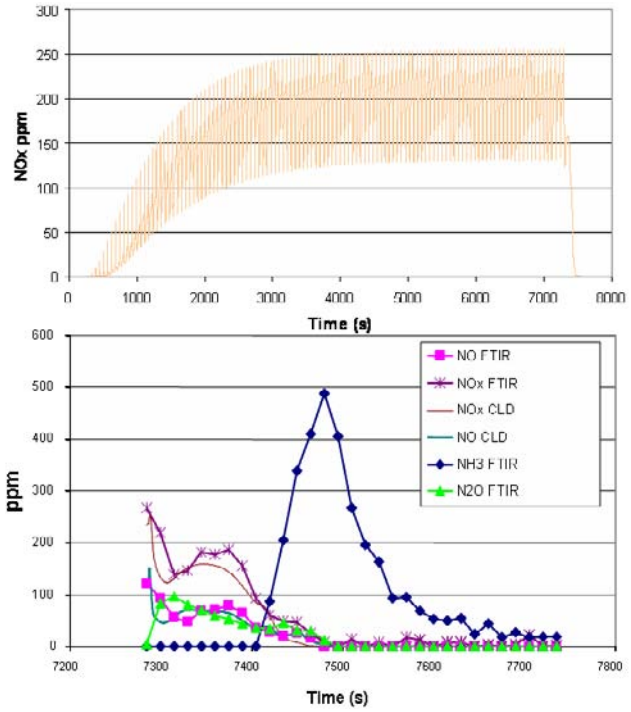

Figure 5. Observed breakthrough profiles for a MECA candidate sorbent during fast cycling followed by a deep regeneration. The fast cycling conditions were 55 s lean (with 300 ppm NO in simulated exhaust) and 5 s rich (with 0.5% H_2). At the end of fast cycling, the 0.5% H_2 condition was continued without interruption. The lower plot is an enlargement of the measurements for the latter period.

A simplified MatLab version of the global NO_x breakthrough model that has been used to successfully match the observed bench reactor performance so far is now posted on the CLEERS website for public downloading. While it has many shortcomings, we believe this model can serve as a basis for sharing information and developing improved methods for reconciling protocol data from different bench flow reactors (e.g., reactors with different space velocities and length/diameter ratios). It also may be possible in the future to utilize this or a similar model to serve as a basis for 'compressing' the standard protocol measurements (i.e., fitting the measured breakthrough profiles to the global model with a relatively small number of global rate parameters that can then be used in place of the original data). Perhaps more generally, it may be possible to use these parameters to compare the responses of different materials.

Although the global LNT model appears to be useful for correlating overall NO and NO_2 breakthrough, recent observations indicate that N_2O and NH_3 can also be produced in significant quantities during NO_x regeneration. This can be observed in Figure 5 for a fast cycling case with the MECA prototype sorbent where a 'deep' reduction condition is imposed at the end of a large number of repeated lean/rich cycles. Under these conditions, we observe both a large pulse of N_2O and a large pulse of NH_3, indicating that there is some type of long-timescale, complex storage of nitrogen compounds on the sorbent surface leading to a significant and unexpected loss in NO_x conversion to N_2. This general behavior has been observed for both H_2 and CO reductants, indicating that it is not specific to regeneration strategies that favor either species. Recent discussions in the LNT Focus Group have confirmed that others have seen similar releases of N_2O and NH_3 even during fast cycling. Clearly, these byproduct species will be of great importance in realistic applications and need to be included in subsequent versions of the LNT model.

During the summer, post-doc Jae-Soon Choi was able to complete extensive use of SpaciMS measurements of NO_x, O_2, and H_2 breakthrough profiles at 5 axial locations. Figure 6 illustrates the kind of information made available by the SpaciMS measurements; specifically, it is possible to observe the transitions in the shape of the concentration profiles as the species fronts move axially down the channel. This type of information is extremely useful in improving and validating LNT models that address the effects of reactor length on performance.

Micro-Scale Catalyst Modeling

The development of a continuously distributed NO_x storage site model that includes the effects of precious metal coarsening is necessary to understand the aging process and interpret microscopy experiments. This year we developed a model that better captures the realistic particle distribution within a Pt island as well as distribution of the islands. This new approach better represents the experimentally observed behavior. This process also

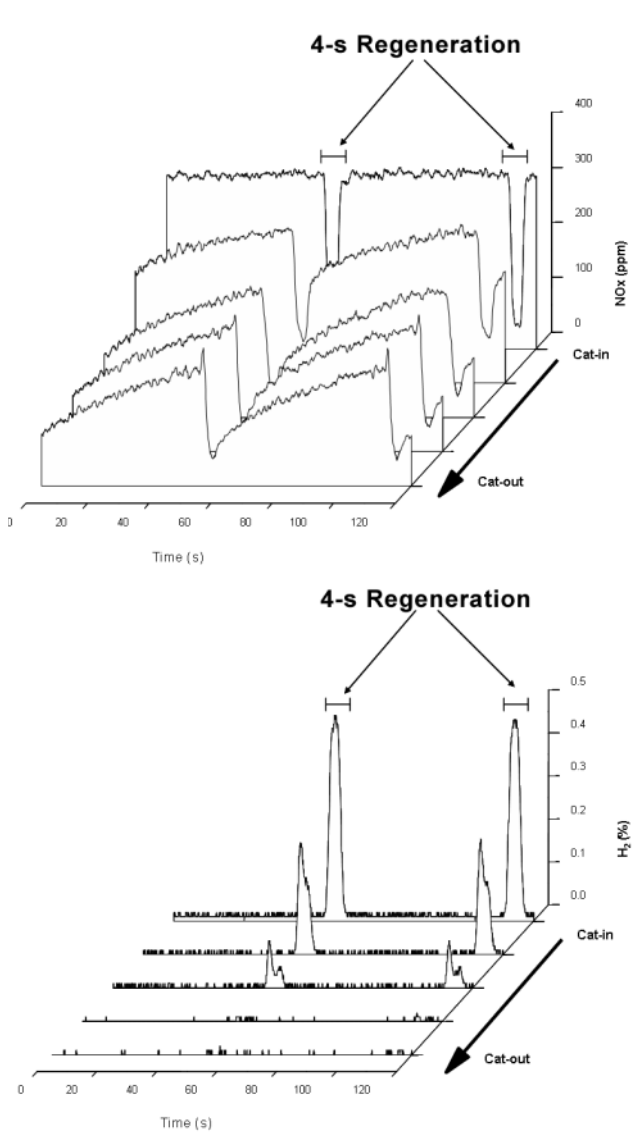

Figure 6. Plots illustrate the transient breakthrough of NO_x and hydrogen at different axial locations in a potassium sorbent LNT monolith as measured with SpaciMS. The LNT sample is mounted in the ORNL bench reactor and is being cycled for 56 s under lean conditions (12% O_2, 5% H_2O, 300 ppm NO) and 4 s under rich conditions (0% O_2, 5% H_2O, 0 ppm NO, 0.5% H_2) at a space velocity of 25000 h^{-1} and 200°C.

includes two competing coarsening and de-coarsening steps. Currently, the rule used in the de-coarsening step is based on a probability distribution that scales inversely with particle size, and additional distributions are being explored.

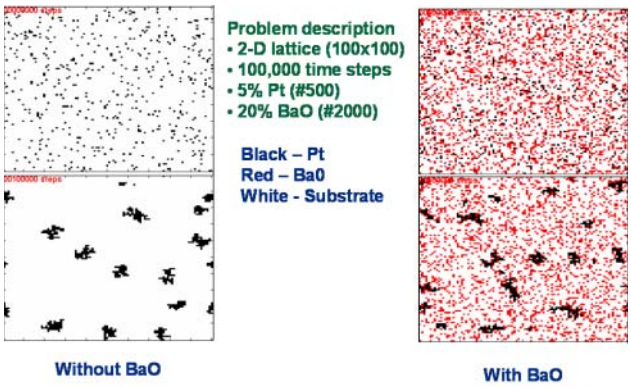

Figure 7. Platinum Coarsening With and Without BaO

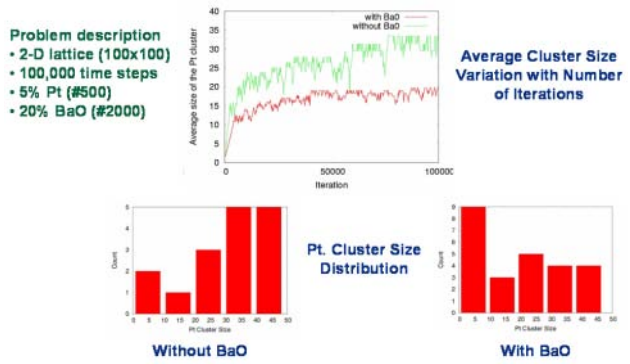

Figure 8. Platinum Cluster Size Distribution and Evolution of Average Size of the Pt Cluster With and Without BaO

In addition, post-processing tools have been added to visualize the coarsening effects and also to track the particle size distribution with time. To validate the code, we are performing both small-scale (10,000 cells) and large-scale (500,000 cells) systems simulations for long timescales and comparing to available experimental data. This work has been presented at the 7th CLEERS workshop held in Detroit, and sample results are shown in Figures 7 and 8. In Figure 7, Pt coarsening with and without BaO are plotted (the upper plots are the initially dispersed condition, the lower plots are after 100,000 Monte Carlo iterations). The simulations reproduce the experimentally observed behavior that Pt coarsening is inhibited by the presence of BaO. In Figure 8, both average cluster size variation with time and probability density function of Pt size are plotted. The simulations do reach a statistically stationary state after 100,000 iterations, as can be seen in Figure 8, and the average cluster size occurs

for the case with BaO as expected. In addition, the cluster size distribution indicates that the BaO case has a different distribution than the case without BaO, and the presence of BaO oxide inhibits formation of large clusters.

We have implemented and tested a new rules-based NO_x chemistry module. We are in the process of performing long-timescale simulations of NO_x chemistry with coarsening. Furthermore, we are interacting with the microscopy group at the HTML of ORNL, where several experiments have been identified that would produce data that can be compared with simulation. Thus, our simulation results would assist in interpreting ongoing experimental efforts at the NTRC and HTML facilities on Pt coarsening and its effect on NO_x chemistry. Equally important, the results will be used to determine the correlation of atomistic effects to aging and efficiency that will be incorporated into the CLEERS LNT database. A key aspect of this work is that it will help bridge the gap between the microscopy experiments and translating their results through simulation into usable performance numbers and criteria.

Conclusions

Administrative Support

The CLEERS Planning Committee and LNT, DPF, and SCR Focus Groups are now fully functioning as intended and have successfully facilitated collaborations among the Diesel Crosscut Team members. ORNL, PNNL, and SNL are providing special expertise, equipment, and facilities that are not readily available otherwise to the OEM members. The CLEERS activity allows OEMs and suppliers to cooperate with each other, national labs, and universities on non-competitive issues. These types of collaborations are important for leveraging limited resources.

The seventh CLEERS workshop was held June 16 and 17 at the Detroit Diesel Corporation training facility in Detroit. All three emissions control technology areas (LNTs, DPFs, and SCR) were covered, but the greatest emphasis was on DPFs and SCR. The complete technical program, meeting summary, and most of the presentations are available on the website (www.cleers.org). This was the largest workshop to date, with a total of 90 registrants and considerable participation from emissions controls suppliers as well as OEMs.

A key achievement has been the development of an experimental protocol for characterizing LNT materials in bench-flow reactors. This protocol is intended to provide the basis of standard kinetic 'maps' (i.e., data templates) for communicating critical simulation properties. It is anticipated that such maps will be useful to OEMs in generating LNT performance parameters for their individual user models and systems simulations. The current protocol was reached as a consensus among the LNT Focus Group with considerable interactions from collaborating supplier representatives.

Joint Development of Benchmark Kinetics

The ongoing experimental bench-reactor studies at ORNL contributed significantly to the development of the LNT characterization protocol. These experimental studies have evaluated model LNT materials fabricated locally as well as samples obtained through MECA and now commercial LNT samples from Umicore. The model and Umicore samples are currently being analyzed for their detailed chemical composition and microscopic features. Ford has also provided Toyota DPNR and LNT samples that will be included in the ORNL studies. The ORNL bench-flow reactor is undergoing extensive modifications to ensure compliance with key requirements of the draft characterization protocol. Simplified global models of LNT capture and regeneration have been completed and documented in publications and on the CLEERS website.

Micro-Scale Catalyst Modeling

A rules-based Monte Carlo code has been created that better captures the realistic particle distribution within a Pt island as well as distribution of the islands. This new approach better represents the experimentally observed behavior. Post-processing tools have been added to visualize the coarsening effects and also to track the particle size distribution with time. The code is being validated for both small-scale (10,000 cells) and large-scale systems (500,000 cells) for long timescales and compared to available experimental data.

Presentations

1. A simple limiting-case LNT model, K. Chakravarthy, Sixth Department of Energy Crosscut Workshop on Lean Emissions Reduction Simulation, GM R&D Center, Warren, Michigan, September, 2003.
2. A bench-scale study of NO_x capture in $Pt/K/Al_2O_3$ NSR (LNT) catalysts, K.
3. Chakravarthy, K. Lenox, S. Daw, W. Partridge, T. Miller, J.-S. Choi, DOE National Laboratory Catalysis Conference, Oak Ridge, Tennessee, October, 2003.
4. Global modeling of NO_x storage, K. Chakravarthy, C. S. Daw, K. Lenox, T.
5. Miller, J. Choi, T. Toops, W. Partridge, Seventh CLEERS Workshop on Lean Emissions Reduction Simulation, Detroit, Michigan, June, 2004 (www.cleers.org).
6. Assessing reductant chemistry during in-cylinder regeneration of diesel lean NO_x traps, B. H. West, S. P. Huff, J. E. Parks, S. A. Lewis, J.-S. Choi, W. P. Partridge, and J. M. Storey, 2004 SAE Powertrain & Fluid Systems Conference & Exhibition, Tampa, Florida, 2004.
7. Regeneration behavior of NO_x storage-reduction catalysts under simulated or realistic diesel exhaust, J.-S. Choi, T. Miller, W. S. Epling, S. P. Huff, K. Chakravarthy, K. E. Lenox, W. P. Partridge, C. S. Daw, 4th Department of Energy National Laboratory Catalysis Conference, Oak Ridge, Tennessee, 2003 (poster).

Publications

1. "Phenomenology of NO_x adsorber catalysts", C. S. Daw, K. E. Lenox, K. Chakravarthy, W. E. Epling, and G. Campbell, International Journal of Chemical Reactor Engineering, Vol. 1 (A24), 2003.
2. "Global modeling of NO_x breakthrough from lean NO_x traps", K. Chakravarthy, S. Daw, T. Miller, A. Strezlec (under preparation, to be submitted to International Journal of Chemical Reactor Engineering).
3. "Adsorption isotherm based modeling of NO_x storage in lean NO_x traps", K. Chakravarthy, S. Daw, T. Miller, K. Lenox, A. Strezlec (under preparation, to be submitted to Applied Catalaysis B : Environmental).
4. "Key characteristics of the sorption process in lean NO_x traps", K. Chakravarthy, C. S. Daw, K. E. Lenox, SAE 2003-01-3246, SAE Powertrain & Fluid Systems Conference & Exhibition, Pittsburgh, Pennsylvania, October, 2003.
5. "Assessing reductant chemistry during in-cylinder regeneration of diesel lean NO_x traps", Brian H. West, Shean P. Huff, James E. Parks, Sam A. Lewis, Jae-Soon Choi, William P. Partridge, and John M. Storey, SAE Technical Paper 2004-01-3023 (2004).
6. "Spatially-resolved in situ gas-phase speciation during the cyclic operation of monolithic NO_x storage-reduction catalyst based on $Pt/K/Al_2O_3$: comparison between H_2 and CO in regeneration step", Jae-Soon Choi, William P. Partridge, and C. Stuart Daw, Applied Catalysis A : General, to be submitted.
7. "Intra-channel evolution of carbon monoxide and its implication on the regeneration of monolithic NO_x storage-reduction catalyst based on $Pt/K/Al_2O_3$", Jae-Soon Choi, William P. Partridge, William S. Epling, and Neal W. Currier, in preparation.

II.B.6 Cross-Cut Lean Exhaust Emissions Reduction Simulations (CLEERS) Diesel Particulate Filter (DPF) Modeling

Mark Stewart, Gary Maupin, George Muntean (Primary Contact)
Pacific Northwest National Laboratory
P.O. Box 999, MSIN: K5-22
Richland, WA 99352

DOE Technology Development Manager: Ken Howden

Objectives

- Develop improved modeling capabilities for diesel particulate filtration
  - Create improved models of the local properties of the soot filter, e.g., cake permeability, density, morphology
  - Develop improved sub-grid representations of the local soot oxidation reactions in diesel soot filters, e.g., oxidation mechanisms, detailed kinetics, global rates
- Coordinate and lead the CLEERS DPF sub-team activities (see www.cleers.org for sub-team minutes and updates)
  - Provide project updates to the industry sub-team, solicit feedback, and adjust work scope accordingly
  - Lead technical discussions, invite distinguished speakers, and maintain an open dialogue on DPF modeling issues
  - Lead working group formed to create a “DPF standard map”

Approach

- Map the substrate microstructure to create a computational “physical” domain
- Apply a lattice-Boltzmann flow field solution
- Incorporate soot particle motion and deposition in two manifestations
  - As a discrete particle model
  - As a continuum representation
- Incorporate soot oxidation mechanism(s)
- Validate models with experimental results
- Perform parametric analysis with the detailed model
- Develop low-dimensional sub-models from the parametric data

Accomplishments

- Full-flow single particle deposition model has been developed
- Partial differential equation based continuum soot cake model has been developed
- Employing single-channel experimental technique for model validation
- Coordinated and led monthly telecoms for DPF sub-team
  - Formed a “DPF mapping” working group
  - Developed an initial “short cycle” test matrix

Future Directions

- Quantitative studies of filter performance metrics
  - Capture efficiency as a function of time/soot loading
  - Measure pressure drop as a function of time/soot loading
- Parametric studies with
  - Varying Darcy resistance for deposited particle regions
  - Adjustable capture probability
- Smaller-scale models including
  - Realistic particle size distribution
  - Complex irregular particle shapes
  - Agglomeration of moving particles
- Particle deposition with simultaneous filter regeneration
  - Incorporation of oxidation mechanism(s)

Introduction

Diesel particulate filters (DPFs) are the leading candidate technology for control of diesel engine particulate emissions. While this technology appears very promising, it is still not sufficiently mature for commercial implementation in heavy-duty trucks. Considerably more research and development will be needed to address the numerous unresolved issues [1,2,3,4]. Of particular concern is the potential for a significant degradation in fuel efficiency of diesel-powered vehicles employing DPF. This degradation is due to two inherent features of DPFs:

- They increase engine backpressure, and
- They require energy input for active regeneration.

Minimization of both of these items is linked to the fundamental properties of soot capture and oxidation on the nano/micron-length scales. It is becoming increasingly apparent that modeling and simulation are essential aspects of the needed R&D because exhaustive experimental evaluation of each possible system configuration is simply too costly and too time-consuming to be practical. In particular, both industry and DOE need access to the ability to accurately simulate trends and make objective comparisons of the various options for system materials and designs so that empirical experimentation can be minimized.

Through several technical workshops sponsored by the DOE Diesel Crosscut Team under CLEERS, the diesel emissions control stakeholder community (including automotive and engine companies, national labs, and universities) has identified the most pressing un-addressed needs for modeling and simulation. For DPF, the modeling parameters of greatest concern are those associated with

- Local properties - cake permeability, density, morphology
- Kinetics - oxidation mechanisms, detailed kinetics, global rates
- Simple 1-D models (using the information from the first two bullets) for systems modeling
- Detailed 3-D models for understanding capture and oxidation phenomenon (for design and optimization of devices)
- Flow distribution - packing, anisotropic regenerations (for practical engineering considerations)

Of the above, the current project focuses on the first two bullets – local properties and kinetics – and how these interact with the physical distribution of particles to determine peak regeneration temperature, backpressure and capture efficiency.

Approach

A computer program has been developed to predict the nature and location of soot deposits within porous filter substrates by simulating the flight and deposition of individual soot particles. The lattice-Boltzmann method is used to solve for the flow field

of exhaust through the substrate microstructure as soot deposits form. The motion of simulated soot particles is derived from the exhaust flow field and includes random Brownian motion. Predicted soot deposits within the substrate and on the filter wall surface are being validated with various experimental approaches.

Once the fine-scale lattice-Boltzmann models are created and validated, they will be used to run parametric tests. The results of these tests will then be used to create improved sub-models (algorithms) which can be incorporated into standard device-scale DPF models.

Results

The lattice-Boltzmann method is an increasingly popular alternative to traditional computational fluid dynamics (CFD). For most CFD approaches, the three-dimensional Navier Stokes equations are discretized in time and space, and a global pressure field is solved for at each time step. With the lattice-Boltzmann method, the Boltzmann equation for local velocity probability distributions is discretized in time, space, and direction. The pressure field evolves and the Navier Stokes equations are recovered as lattice nodes relax toward equilibrium velocity distributions. For the DPF substrate model, an incompressible formulation of the lattice-Boltzmann method was used similar to that described by He and Luo [He, X. and Lou, L. S. "Lattice Boltzmann Model for the Incompressible Navier-Stokes Equation", Journal of Statistical Physics, Vol. 88, Nos. 3/4, 1997.].

In order to resolve the exhaust flow field and particle capture mechanisms at the scale of individual pores, it was first necessary to construct an accurate three-dimensional map of a DPF substrate microstructure. A Corning EX-80 filter was sectioned to provide several 1-cm samples of the substrate wall, which were potted in an acrylic epoxy microscope mount. The samples were then ground to the filter wall surface and polished flat. An automatic polishing station was used to remove additional material in approximately 6-micron increments. After each 6-micron layer was removed, a micrograph was taken of the sample. This procedure of polishing and imaging was repeated 25 times and produced a series of 25 surface images of the porous filter wall structure. The images were then processed with image analysis software and converted into digital representations of the solid filter material and void space. Once a physical domain was created, the lattice-Boltzmann technique was applied to simulate the exhaust flow field.

The formation of soot deposits has been simulated by the motion and capture of individual particles in the work of Konstandopoulos and others [Konstandopoulos, A.G. "Deposit Growth Dynamics: Particle Sticking and Scattering Phenomen", Powder Technology, 109, pp. 262-277, 2000. Konstandopoulos, A.G., Saperdas, E., and Masoudi, M. "Microstructural Properties of Soot Deposits in Diesel Particulate Traps", SAE Technical Paper Series, 2002-01-1015.]. Aggregate particles in these models were represented as mono-sized spheres with an aerodynamic diameter of 100 nm. The soot particles in this approach moved in a linear trajectory and either rebounded or were captured upon impact. The effect of the fluid motion on that of the particles was not included directly. Since particles could not be carried around corners by the flowing fluid, applicability to the depth filtration mode was limited. The work described here represents an effort to extend this type of modeling approach by adding the effects of the flowing exhaust on soot particle motion.

For the sake of simplicity and easy comparison with previous models, soot particles in the lattice-Boltzmann model were considered to have a single aerodynamic diameter of 100 nm. Future work will examine the effects of particle size distributions on filter behavior. Particles with an aerodynamic diameter of 100 nm are essentially inertia-less at the time and length scales examined. For larger aggregates, however, particle momentum may become significant, in which case particle acceleration must be calculated from drag forces.

Local fluid velocities are estimated from the eight surrounding lattice sites using tri-linear interpolation. Each particle is then displaced in the direction of this average velocity according to the particle time step. A particle time step of $3x10^{-7}$ seconds was used for this initial study.

Brownian motion is super-imposed on the motion caused by the local average fluid velocity. The

average magnitude of random Brownian motion determines the particle diffusivity, which is calculated according to

$$D_p = \frac{k_B \cdot T}{3\pi \cdot \mu \cdot d_{particle}} \cdot \left(1 + Kn\left(1.257 + 0.4e^{1.1/Kn}\right)\right)$$

where k_B is Boltzmann's constant, T is the absolute exhaust temperature, is the dynamic fluid viscosity, $d_{particle}$ is the aerodynamic diameter, and Kn is the Knudsen number calculated as

$$Kn = \frac{2\lambda}{d_{particle}}$$

where is the exhaust mean free path [5].

A perfectly inertia-less particle with no Brownian motion would follow the fluid through the filter substrate and would be unlikely to touch the solid walls. Inertial deposition is important for large particles, wherein the particle's momentum causes it to skid between curving streamlines and thus increases its likelihood of contact with obstructions. For smaller particles, Brownian motion becomes the important effect by bouncing the particles between streamlines and allowing them to interact with the solid substrate walls.

For simplicity, and to reduce the number of particle motion calculations, particles were dealt with in "clouds" or "bundles" having a diameter of 1 micron. The individual bundles can have any aerodynamic diameter and can therefore behave as agglomerates of any specified size with respect to momentum and Brownian motion. The 1 micron diameter is used only to test for contact with the solid substrate regions or previously deposited particles. Since the controlling substrate pores can have diameters of many tens of microns, the bundle approach allows soot deposit shapes to be sufficiently resolved with a tractable number of particle motion calculations.

Particles are assumed to be deposited immediately upon contact with solid substrate walls or with previously deposited particles. The resistance of soot deposits to exhaust flow is modeled by assigning deposited particles to the nearest lattice site. Resistance to flow through that lattice site is then included as an additional Darcy force term in the lattice-Boltzmann solution. The Darcy resistance at a lattice site is incrementally increased as more particles deposit near it, or in other words as the porosity of the soot deposit in that lattice volume decreases. The current discrete particle model does not consider passive regeneration, re-entrainment, or mechanical restructuring of the soot deposits as they form.

Table 1 lists conditions modeled for the simulation results shown here. Almost a million particle bundles were introduced during the model run, 98.5% of which were captured by the filter.

Table 1. Parameters for Model Run

Wall flow velocity	3.6 cm/s
Particulate concentration	0.02 g/scm
Exhaust temperature	300°C
Loading time modeled	3.3 hours

Figure 1 shows a cross-section of the filter wall as the soot deposits form. Solid substrate regions are shown in white and soot deposits in black. Note the extent of depth filtration in the early stages of loading. Bottlenecks in the pore structure within the substrate wall quickly become blocked by soot deposits. As pores near the surface become blocked, growth of deposits deeper within the substrate slows and then stops. The total loading at the end of the simulation would correspond to about 3.9 g/m^2 of filter area. A Corning EX-80 5.66 x 6 inch cordierite

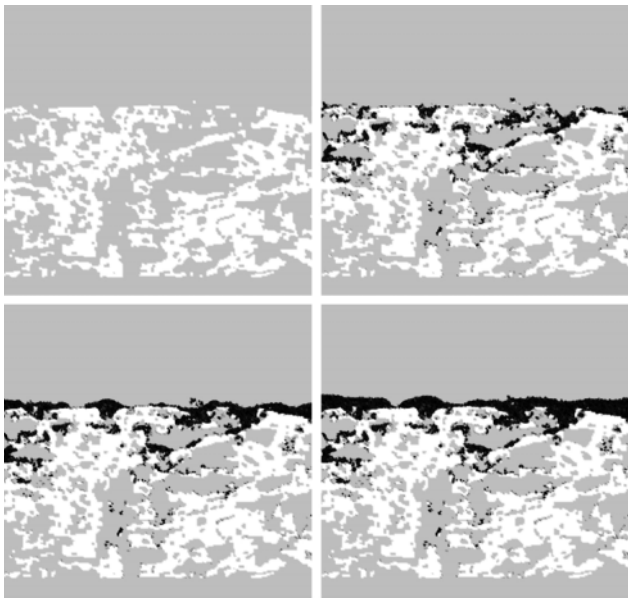

Figure 1. Cross Section of Filter during Loading Shown at Time = 0, 66, 132, and 198 Minutes

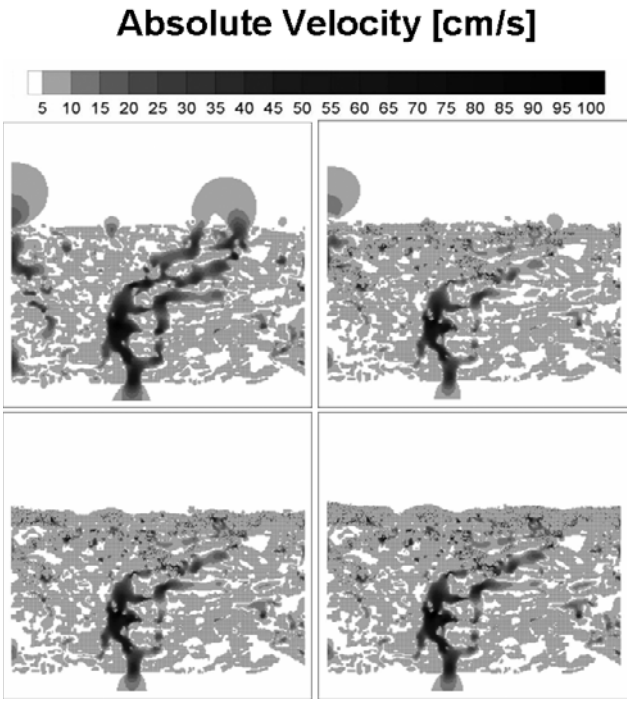

Figure 2. Cross Section of Filter Showing Absolute Velocity at Time = 0, 66, 132, and 198 Minutes

filter has a filtration area of 1.66 m^2 and a maximum soot loading of roughly 15 g [8]. For this filter, the end of the simulation would correspond to about 6.5 g of total loading or 43% of capacity.

Figure 2 shows exhaust velocity contours at the same cross-section over the same time period. Solid substrate regions are shown in a mesh pattern. Exhaust velocity near the surface of the clean substrate is highly non-uniform, with high velocities near the entrances to important flow paths and stagnation regions elsewhere. Since the soot aggregates modeled are inertia-less, they are all swept into these flow paths and have opportunities to deposit anywhere along the exhaust routes through the filter material. The formation of deposits in key bottlenecks quickly begins to redistribute the flow near the surface. Even after surface deposits begin to form, the exhaust velocity is still greater over the entrances to important flow paths. This results in mounds of soot forming over large pores while some locations on the substrate wall are still bare. Eventually, the accumulating soot distributes the exhaust flow evenly over the deposit surfaces, and the few remaining stagnation areas shrink as the

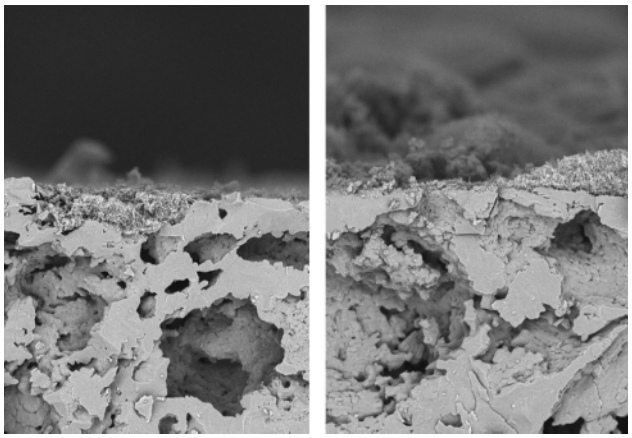

Figure 3. Scanning Electron Micrographs of Soot Deposits

deposits grow and blend together. Flow patterns deep within the substrate are relatively unaffected by the degree of soot loading.

Several qualitative similarities can be observed between real soot deposits and those predicted by the model. Figure 3 shows pictures of actual soot deposits near the surface during early stages of loading. The micrographs show examples of shallow pore mouths at the substrate surface filling with soot while other areas on the surface remain bare. As loading progresses, mounds of soot tend to form in some locations. Sizable soot deposits are occasionally seen deep within the substrate wall, as shown in Figure 4, but most of the void space within the substrate is clear of soot, even after a significant layer has formed on the surface.

Conclusions

Discrete particle modeling with realistic flow field effects is providing insight into the way soot deposits form with respect to substrate microstructure. Soot deposits predicted by the simulation have been found to share many qualitative features with those observed in real filter substrates. Quantitative validation of the model is in progress using a variety of approaches. Improving the fidelity of the model by adding effects such as the aerodynamic size distribution of real soot particles could lead to accurate predictions of pressure drop versus soot loading for new or hypothetical substrate microstructures.

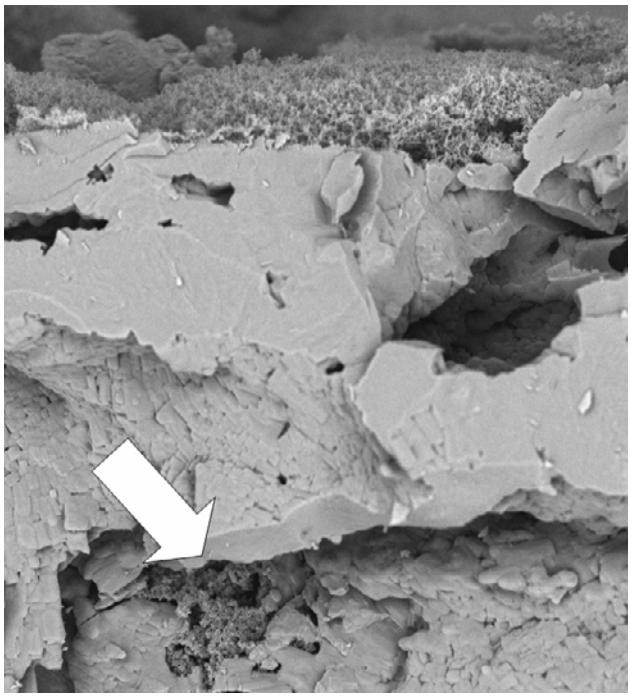

Figure 4. Micrograph Showing Soot Deposit Within Substrate Wall

To date, the lattice-Boltzmann method has been found to be:

- versatile and easy to use
- proven effective for extruded ceramic structures with tortuous pores
- able to qualitatively reproduce several structural features of soot deposition
- easily implemented with incremental improvements
- able to address macroscopic phenomena such as particulate capture efficiency and pressure drop
- supportive of continuum modeling of the soot layer

Special Recognitions & Awards/Patents Issued

1. The paper SAE 2003-01-0835 was selected for inclusion into SAE Transactions.

2004 Publications/Presentations

1. G. Muntean, D. Rector, D. Herling, D. Lessor and M. Khaleel, "Lattice-Boltzmann Diesel Particulate Filter Sub-Grid Modeling – a progress report", SAE 2003-01-0835, February, 2003.
2. G. Muntean, "CLEERS DPF SUBTEAM", presented at the CLEERS workshop, September 2003.
3. G. Muntean, D. Rector, and D. Lessor, "Modeling Diesel Soot Filtration at the Smallest Length Scales: A Lattice-Boltzmann Approach", presentation at the American Filtration Society conference, September 2003.
4. G. Muntean, and M. Stewart, "Characterization of Cordierite Substrates for Particulate Filtration Using Lattice Boltzmann Techniques and Experimental Measurements", presentation at the American Ceramics Society conference, January 2004.
5. G. Muntean, "CLEERS DPF Sub-team Update", presented to the diesel crosscut team, March 2004.
6. G. Muntean, M. Stewart, and G. Maupin, "CLEERS DPF Modeling", presentation at the DOE Combustion and Emission Control Review, May 2004.
7. M. Stewart, "Discrete Particle Modeling of Diesel Soot Filtration", presented at the CLEERS workshop, September 2004.

References

1. Konstandopoulos, A. G. and Kostoglou, M. "Microstructural Aspects of Soot Oxidation in Diesel Particulate Filters", SAE Technical Paper Series, 2004-01-0693.
2. Konstandopoulos, A. G. "Deposit Growth Dynamics: Particle Sticking and Scattering Phenomena", Powder Technology, 109, pp. 262-277, 2000.
3. Konstandopoulos, A. G., Skaperdas, E., and Masoudi, M. "Microstructural Properties of Soot Deposits in Diesel Particulate Traps", SAE Technical Paper Series, 2002-01-1015
4. Konstandopoulos, A. G., Kostoglou, M., Skaperdas, E., Papaioannou, E., Sarvalis, D., Kladopoulou, E., "Fundamental Studies of Diesel Particulate Filters: Transient Loading, Regeneration and Aging", SAE Technical Paper Series, 2000-01-1016.
5. He, X. and Lou, L. S. "Lattice Boltzmann Model for the Incompressible Navier-Stokes Equation", Journal of Statistical Physics, Vol. 88, Nos. 3/4, 1997.
6. Park, K., Feng, C., Kittelson, D. B., and McMurray, P. H. "Relationship Between Particle Mass and Mobility for Diesel Exhaust Particles," Environ. Sci. Technol., 37, pp. 577-583, 2003.
7. Friedlander, S. K. "Smoke, Dust, and Haze: Fundamentals of Aerosol Dynamics", Oxford University Press, New York, 2000.

8. Merkel, G. "Relationship Between Pressure Drop and Microstructure for Diesel Particulate Filters from Experimentation and Capillary Pore Modeling", Cross-Cut Lean Exhaust Emissions Reduction Simulations Workshop 7, June 16, 2004, Detroit, MI.

II.B.7 Advanced CIDI Emission Control System Development

Christine Lambert and Robert Hammerle (Primary Contact)
Ford Research & Advanced Engineering
P.O. Box 2053, MD 3179, SRL
Dearborn, MI 48121

DOE Technology Development Manager: Ken Howden

Subcontractors:
FEV Engine Technology, Inc., Auburn Hills, MI
ExxonMobil Research and Engineering Company (EMRE), Paulsboro, NJ

Objective

- Develop and demonstrate a highly efficient exhaust emission control system for light-duty compression ignition direct injection (CIDI) engines to meet 2007 Tier 2 emissions standards (0.07 g/mi NO_x, 0.01 g/mi PM [particulate matter]) with minimal fuel economy penalty and 120,000 mile durability.

Approach

- Conduct parallel engine dynamometer and vehicle testing.
- Continue research to identify the most active and durable catalysts and catalytic diesel particulate filters (CDPFs).
- Continue research to determine the most selective and durable exhaust gas sensors.
- Use a very low-sulfur diesel fuel to represent U.S. fuel of 2007 and beyond.
- Assist in the development of a feasible aqueous urea delivery system for diesel vehicles.

Accomplishments

- Low-mileage Tier 2 Bin 5 standards were achieved using a fresh catalyst system of oxidation catalysts, urea selective catalytic reduction (SCR) and CDPF in a mid-sized diesel prototype engine designed for a light-duty truck. Engine-out NO_x was lowered by 40% through the use of a cooled, low-pressure exhaust gas recirculation (EGR) system. An additional 90% reduction of NO_x by the urea SCR system resulted in a tailpipe NO_x level of 0.04 g/mi.
- A rapid warm-up procedure was developed for use during the cold-start portion of the Federal Test Procedure for light-duty vehicles (FTP-75), decreasing the time for the urea SCR system to begin operating at high efficiency by almost a minute. Fuel economy was reduced by less than 1%.
- Hydrocarbons (HC) and carbon monoxide (CO) were converted at or above 97% cycle efficiency, resulting in 0.08 g/mi HC and 0.3 g/mi CO.
- Improvements were made to the durability of the urea SCR system, including modifications to the urea dosing system to eliminate clogging. The SCR catalyst was improved for greater thermal durability to withstand CDPF regeneration conditions.
- A separate vehicle equipped with a urea SCR system maintained 80% FTP-75 NO_x conversion after 35,000 miles of on-road driving. Due to limited access to engine calibration, there was no rapid warm-up procedure; therefore, 80% was the maximum NO_x conversion expected.
- A co-fueling dispenser for urea and diesel fuel was tested successfully to minus 20°F. Heaters were used in the urea tank and delivery system to prevent freezing. A potential nozzle durability issue was discovered that caused leakage of aqueous urea into the diesel fuel line.

- The economics of an aqueous urea infrastructure for light-duty (LD) service stations in the U.S. was studied. The cost of co-fueled urea was high in the short-term during introduction and was greatly dependent on the number of LD diesel vehicles that would require urea.

Future Directions

- Begin durability testing of the emission control system on the engine dynamometer.
- Continue laboratory testing of improved SCR catalyst formulations.
- Continue laboratory and vehicle testing of NO_x sensors, with the aim of developing a better model of their response.
- Continue laboratory testing/development of ammonia sensing technologies and determination of their value in a urea SCR diesel aftertreatment system.
- With a major nozzle supplier, improve the durability of the co-fueling nozzle to prevent leakage of aqueous urea into the diesel fuel line.

Introduction

Particulate matter (PM) and NO_x emissions are primary concerns for diesel vehicles required to meet 2007 Federal Tier 2 and California LEVII emission standards (Table 1). These standards represent a 90-95% reduction from current Federal Tier I diesel standards.

Table 1. 2007 Emission Standards* (passenger cars and light-duty vehicles)

	50,000 miles		120,000 miles	
Standard (g/mi)	**NO_x**	**PM**	**NO_x**	**PM**
California LEVII	0.05	----	0.07	0.01
Federal Tier 2, Bin 5	0.05	----	0.07	0.01
*Supplemental Federal Test Procedure standards not included.				

The high oxygen content of diesel exhaust makes onboard NO_x control complicated. The available technologies for high NO_x reduction in lean environments include selective catalytic reduction (SCR), in which NO_x is continuously removed through active reductant injection over a catalyst; and lean NO_x traps (LNT), which are materials that adsorb NO_x under lean conditions and require periodic regeneration under rich conditions to reduce NO_x to N_2. The technology with the most potential to achieve 90+% NO_x conversion with minimal or no fuel economy penalty is SCR with an ammonia-based reductant such as aqueous urea. Ammonia-SCR has been used extensively for stationary source NO_x control [1]. Its high selectivity and reactivity with NO_x in high-O_2 environments makes SCR attractive for diesel vehicle use. The main reactions are shown below:

urea decomposition:

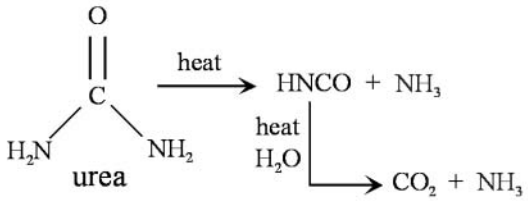

NO_x reduction:

$$4NO + 4NH_3 + O_2 \longrightarrow 4N_2 + 6H_2O$$
$$6NO_2 + 8NH_3 \longrightarrow 7N_2 + 12H_2O$$
$$2NH_3 + NO + NO_2 \longrightarrow 2N_2 + 3H_2O$$

Compared to ammonia, aqueous urea is much safer for onboard vehicle use. Feasibility has been proven by past work at Ford [2,3], Volkswagen [4], Mack Truck [5] and DaimlerChrysler [6].

Control of diesel PM is accomplished with a periodically regenerated ceramic filter. The filter may be washcoated with precious metal to help oxidize HC and collected soot. A diesel oxidation catalyst (DOC) may also be placed upstream of the filter to further aid in filter regeneration.

Approach

At Ford, supplier catalysts were tested in a laboratory flow reactor and ranked for fresh and aged

conversion levels. Full-size monoliths of the most promising formulations were installed in the engine dynamometer and onboard the vehicle and tested in parallel. Modeling was used to help choose the catalyst configuration with the highest potential to meet the emission standards. Since cold-start plays an important role in emission control system functionality, special emphasis was placed on rapid warm-up strategies. Appropriate exhaust gas sensors and control strategies were used for durable system function. The economics of delivering aqueous urea to LD diesel vehicles was explored.

A 14,000 gallon batch of ultra low sulfur (<15 ppm S) diesel was manufactured for use in the optimization and long-term durability portions of the project. Fuel properties were selected to approximate the product quality anticipated in the 2006 market. The resultant fuel also met the Environmental Protection Agency (EPA) certification fuel standards for 2007.

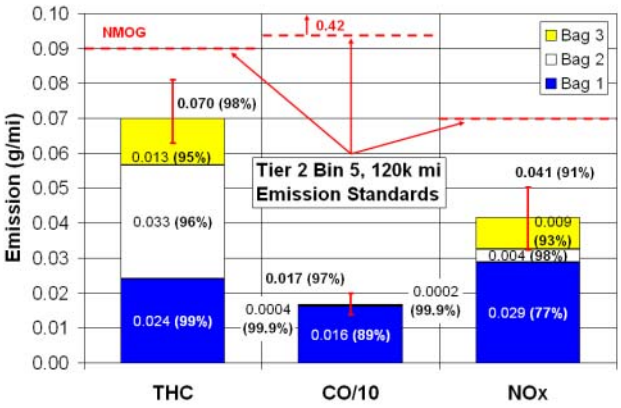

Figure 1. Average tailpipe emissions and system efficiencies from four cold-start FTP-75 simulations with fresh catalysts on the engine dynamometer. Enhanced mixing of reductant in the exhaust gas and additional EGR resulted in a low mileage tailpipe NO_x level below Tier 2 Bin 5. THC results are shown while the standard does not include methane (NMOG).

Results

Over 90% NO_x conversion was achieved with fresh catalysts on a simulated FTP-75 on the engine dynamometer. The urea injector was pointed against the exhaust flow. A spray target, developed for this program at FEV, was added to the system, resulting in enhanced mixing of reductant in the exhaust gas. Engine-out NO_x was reduced approximately 40% through the use of higher EGR levels. A rapid warm-up procedure was used during the cold-start portion of the test cycle. Tailpipe emissions and system efficiencies from four simulated FTP-75 tests were averaged, as shown in Figure 1. Emissions of THC (total hydrocarbon) were below the non-methane standard. Tailpipe NO_x was below the Tier 2 Bin 5 (120,000 mile) level of 0.07 g/mi NO_x, and PM levels were approximately 1 mg/mi.

Several improvements were made to the SCR system for more durable conversion of NO_x. The urea dosing system clogged due to collection of solid urea in the urea/air mixing chamber located downstream of the urea injector. A new design eliminated any dead volume that might collect urea. The system was tested successfully for 10,000 miles on a 2.4L European Ford Transit, with no need for interim cleaning of the mixing chamber, transfer tube or nozzle.

The thermal durability of the SCR catalyst was tested extensively in the laboratory because it will be exposed to high temperatures during regeneration of the CDPF. Catalyst cores were aged at high temperature for 20 h in 14% O_2, 4.5% H_2O, 5% CO_2, balance N_2, at 30k h^{-1}. Sulfur was not added because low sulfur diesel fuel was assumed. High NO_x conversion was maintained over a wide window after aging at 700, 725 and 750°C. A significant drop in performance occurred after aging at 800°C when the feedgas NO_x consisted mainly of NO. As the amount of NO_2 relative to NO in the feedgas was increased, the performance improved. These results indicated that the SCR catalyst should be able to withstand exposure to high temperatures during CDPF regenerations, especially if the upstream oxidation catalyst retains high activity for NO_2 production.

Both NO_x and NH_3 sensors were studied in the laboratory and onboard the project vehicle. A pre-production NO_x sensor was used upstream of the underbody oxidation catalyst to ensure that the correct amount of urea solution was injected during transient operation. Several prototype NH_3 sensors were tested downstream of the SCR catalyst to monitor NH_3 slip for possible feedback control of urea dosing. Laboratory tests demonstrated good sensitivity to NH_3 with some sensitivity to H_2O.

Figure 2. Prototype Co-Fueling Dispenser

Making the use of urea completely transparent to the customer would facilitate introduction. A way to do this is through the use of a concentric nozzle that "co-fuels" urea and diesel fuel simultaneously [7]. A prototype dispenser was fabricated using a modern diesel dispenser and off-the-shelf parts as shown in Figure 2. The dispenser was successfully tested to minus 20°F with heating where necessary. Durability testing of the nozzle indicated a small, intermittent leak of urea (0.5%) into the fuel within the nozzle/insert seal.

An economics study was conducted to understand the costs associated with providing aqueous urea to LD diesel vehicle customers. Model inputs were derived from existing data when possible. The number of service stations used in the model matched the current number of about 167,571 stations in the U.S., with approximately 1/3 selling diesel fuel. Trends in LD diesel vehicle population growth and fuel consumption were derived from DOE's Energy Information Administration 2003 Annual Energy Outlook [8], and vehicle distribution and mileage accumulation by age came from EPA's MOBILE6 model [9]. It was assumed that a solution of 32.5 wt% urea in deionized water would have a wide usage among heavy-duty (HD) diesel vehicles with an established pathway from the manufacturing plant to distribution facilities. The capital payout period for the investment in co-fueling dispensers was assumed to be three years, at a 15% rate of return. The urea consumption was estimated to be 2% of the diesel fuel consumption on average. Results did not include profit markup or taxes, and all estimates were in constant dollars.

The estimated cost of aqueous urea to the customer at the service station was calculated by the following equation:

Estimated Urea Cost at the Service Station ($/gal) = (Manufacture + Distribution Cost) + Storage Cost + Delivery Cost + Service Station Cost.

The estimated urea cost, not including service station costs, was found to be about $1.20/gal.

Service station costs included the capital investment and operating expenses divided by the urea volume throughput for that station. The capital cost of a single co-fueling dispenser was estimated to be about $26,500, and the annual operating expenses, with full heating in winter, were calculated to be about $1,777/yr. The resulting cost for co-fueled urea was therefore highly dependent on the number of dispensers installed and the urea demand.

The lowest-cost scenario for an aqueous urea infrastructure was determined to be the use of bottled urea during the introduction of urea SCR vehicles in 2007, with co-fueling dispensers preferentially installed at the highest-throughput light-duty diesel stations as demand for urea increases. The cost of bottled urea was estimated at $3.66/gal. For 2010, it was estimated that co-fueled urea would be cost-competitive with bottled urea if installed at the top 1% of service stations (based on volume throughput of diesel fuel). After the cost recovery period, the long-term cost of co-fueled urea was about $1.50/gal.

Conclusions

- The objective of emissions reduction to 0.07 g/mi NO_x and 0.01 g/mi PM based on engine

dynamometer testing over the FTP drive cycle was met with a fresh emission control system of urea SCR and CDPF. System improvements were required to lower engine-out NO_x and enable rapid exhaust system warm-up.

- Durability of the urea dosing system was improved after redesign of the mixing chamber.
- In the laboratory flow reactor, the SCR catalyst withstood temperatures in excess of those typically associated with CDPF regeneration, and NO_x conversion was high assuming the upstream oxidation catalyst had high activity for NO_2 production.
- Laboratory and in-vehicle testing of pre-production NO_x and prototype NH_3 sensors was successful.
- A co-fueling dispenser for urea and diesel fuel was tested successfully to minus 20°F, and a potential nozzle durability issue was discovered.
- The cost of co-fueled aqueous urea for LD diesel vehicles is projected to be high in the short-term during introduction. Costs are minimized when bottled urea is used initially and co-fueling is phased in gradually. The long-term cost of co-fueled aqueous urea is estimated to be $1.50/gal.

References

1. R.M. Heck and R.J. Farrauto, *Catalytic Air Pollution Control*, Van Nostrand Reinhold, NY, 1995.
2. H. Luders, R. Backes, G. Huthwohl, D.A. Ketcher, R.W. Horrocks, R.G. Hurley, and R.H. Hammerle, "An Urea Lean NO_x Catalyst System for Light Duty Diesel Vehicles," SAE 952493.
3. P. Tennison, C. Lambert and M. Levin, "NO_x Control Development with Urea SCR on a Diesel Passenger Car," SAE 2004-01-1291.
4. W. Held, A. Konig, T. Richter, L. Puppe, "Catalytic NO_x Reduction in Net Oxidizing Exhaust Gas," SAE 900496.
5. W.R. Miller, J.T. Klein, R. Mueller, W. Doelling, J. Zuerbig, "The Development of Urea-SCR Technology for US Heavy Duty Trucks," SAE 2000-01-0190.
6. W. Mueller, H. Ölschlegel, A. Schäfer, N. Hakim and K. Binder, "Selective Catalytic Reduction - Europe's NO_x Reduction Technology," SAE 2003-01-2304.
7. M.B. Levin, R.E. Baker, "Co-fueling of Urea for Diesel Cars and Trucks," SAE 2002-01-0290.
8. "Annual Energy Outlook 2003 With Projections to 2025," DOE Energy Information Administration, January 2003, http://www.eia.doe.gov/oiaf/archive/aeo03/index.html
9. MOBILE6 Vehicle Emission Modeling Software, US EPA, http://www.epa.gov/otaq/m6.htm
10. http://www.bts.gov

FY 2004 Publications/Presentations

1. Christine Lambert, Robert Hammerle, Ralph McGill, Magdi Khair and Christopher Sharp, "Technical Advantages of Urea SCR for Light-Duty and Heavy-Duty Vehicle Applications," SAE 2004-01-1292.
2. C. Lambert, et al., "Urea SCR and DPF System for Diesel Sport Utility Vehicle Meeting Tier 2 Bin 5," 2004 DEER Conference.

II.B.8 Development of Improved SCR Catalysts

Eric N. Coker
Sandia National Laboratories (SNL)
Ceramic Processing and Inorganic Materials
P.O. Box 5800, MS 1349
Albuquerque, NM 87185-1349

John M. Storey
Oak Ridge National Laboratory (ORNL)
National Transportation Research Center
P.O. Box 2008 MS 6472
Oak Ridge, TN 37831-6472

Kevin C. Ott
Los Alamos National Laboratory (LANL)
Chemistry Division
Actinides, Catalysis, and Separations Group
MS J514
Los Alamos, NM 87545

CRADA Partners
Low Emissions Technologies Research and Development Partnership (LEP)
(Member Companies: DaimlerChrysler Corporation, Ford Motor Company, and General Motors Corporation)

DOE Technology Development Manager: Ken Howden

Technical Advisors:
John Hoard (Ford Motor Company)
Christine Lambert (Ford Motor Company)
Richard Blint (General Motors)

Objectives

- Develop new catalyst technology to enable compression ignition direct injection (CIDI) engines to meet EPA Tier II emission standards with minimal impact on fuel economy.
- Optimize catalyst formulations for activity, stability, and resistance to poisoning.
- Obtain mechanistic information to support catalyst discovery efforts.
- Demonstrate feasibility for scale-up of preparation of promising catalysts.
- Transfer technology of most promising formulations to catalyst suppliers via original engine manufacturers.
- Evaluate emissions from a CIDI engine utilizing prototype selective catalytic reduction (SCR) system technology.
- Elucidate effects of urea decomposition on performance.

Approach

- Design and develop new non-vanadia catalyst materials for reducing NO_x emissions in lean-burn exhaust environments using ammonia as a reductant.

- Using identical protocols, compare and contrast the efficacy of two catalyst types:
  - Hydrous metal oxide (HMO) or other oxide-supported catalysts;
  - Microporous materials-supported catalysts, including zeolites.
- Test catalyst formulations under realistic laboratory conditions using protocol developed with LEP input.
- Where appropriate, transfer successful powder catalyst formulations to monolith platform and re-evaluate.
- Evaluate short-term durability under hydrothermal conditions and in the presence of SO_2/SO_3.
- Characterize catalysts using a variety of techniques to gain understanding of critical parameters related to activity and aging phenomena.
- Scale up synthesis and processing of promising catalyst formulations to enable fabrication of prototype catalytic converters for CIDI engine dynamometer testing.
- Conduct technology transfer of the most promising catalyst formulations and processes to designated catalyst suppliers *via* the LEP.
- Utilize prototype supplier SCR catalysts and a light-duty CIDI engine to study emissions reductions that can be achieved with the SCR technology.
- Measure both regulated and unregulated emissions, focusing on temperatures lower than 300°C.

Accomplishments

- SNL verified that powder catalyst data acquired under appropriate conditions can be used to predict monolith performance.
- SNL switched catalyst testing system to include testing of powders at higher space velocities to mimic anticipated monolith performance.
- SNL developed control strategy for tuning HMO-supported catalyst surface area during synthesis; catalyst activity was found to vary with surface area in non-linear fashion.
- SNL demonstrated tunability of activity to high-temperature or low-temperature regime by simple catalyst component concentration variation.
- SNL catalyst performance unaffected by aromatic hydrocarbon co-feed.
- SNL monolith development and optimization underway, including novel “Robocast” structured materials.
- SNL has filed one technical advance for new catalyst materials.
- LANL mechanistic work has led to the discovery of a ‘hybrid’ dual bed catalyst system, for which a patent application has been filed.
- LANL achieved milestone of NO_x conversion efficiency of >95% between 160 and 400°C at a gas hourly space velocity (GHSV) of 30,000 h^{-1} and $NO:NO_2$ = 4:1 using a ‘hybrid’ dual-bed base metal zeolite catalyst system supported on a monolith. By 'tuning' the catalyst configuration, >95% NO_x conversion can be obtained to temperatures above 500°C.
- ‘Hybrid’ portion of LANL catalyst system was tested at Ford on a 1” core. Ford results were consistent with LANL’s small core tests.
- LANL optimized one of the NO-oxidizing function compositions of the LANL ‘hybrid’ catalyst.
- LANL determined that the ‘hybrid’ catalyst with potent oxidation function is tolerant to high steady-state concentrations of hydrocarbons by way of a ‘self-cleaning’ mechanism.
- Potent oxidation capacity of LANL’s ‘hybrid’ catalyst was shown to convert ammonia (500 ppm) to 80% N_2, 20% NO_x. At lower concentrations, little or no NO_x is detected; this material may make a good ammonia clean-up catalyst.
- LANL had two patents issued on lean NO_x catalysts using hydrocarbon reductants.

- Through collaboration with faculty and a student at New Mexico Tech, LANL has submitted a paper on ^{15}NMR of NO_x and NH_3 adsorbed on lean NO_x catalysts.
- Over the life of the Lean NO_x Cooperative Research and Development Agreement (CRADA), LANL synthesized, tested, and characterized well over 1000 different formulations of lean NO_x catalysts for use with hydrocarbons or ammonia reductants.
- ORNL demonstrated low-temperature storage and release of urea and ammonia on an SCR-equipped light-duty diesel engine.
- ORNL showed that ammonia storage and SCR performance are adversely impacted by urea decomposition on the catalyst surface in the first 3 inches of length of the SCR catalyst.

Future Directions

- SNL will continue to synthesize, characterize, and evaluate new catalyst compositions as ammonia SCR catalysts.
- SNL will continue to optimize most promising catalysts.
- SNL hydrothermal and sulfur durability tests on most promising catalysts will be continued.
- SNL will continue to give samples to CRADA partners for comparison testing.
- SNL will transfer the most promising candidates to suppliers via LEP.
- LANL and ORNL CRADAs have ended; no future directions apply for this program. However, there are still many opportunities and a significant number of issues that could be addressed by additional work at all three laboratories. These include:
  - Evaluate a diversity of compositions of 'hybrid' catalysts that take advantage of their dual role in NO oxidation and subsequent reduction. This work has barely scratched the compositional surface – many promising compositions are untested.
  - Evaluate additional dual-bed configurations to effectively tune the NO_x conversion window.
  - Explore possibility of using 'hybrid' catalysts as potent oxidation catalysts for
    - Dual ammonia/hydrocarbon clean-up applications
    - NO oxidation for low-temperature lean NO_x trap applications
- Define mechanisms of interactions of NO_x species with adsorbed NH_3; define mechanisms of the oxidation of NH_3; and elucidate the influence of water, SO_x and hydrocarbons on these mechanisms.

Introduction

This multi-partner effort has been continued under Office of FreedomCAR and Vehicle Technologies (OFCVT) sponsorship and involves separate CRADAs between three national laboratories [Los Alamos National Laboratory (LANL), Oak Ridge National Laboratory (ORNL), and Sandia National Laboratories (SNL)] and the Low Emissions Technologies Research and Development Partnership (LEP, composed of DaimlerChrysler Corporation, Ford Motor Company, and General Motors Corporation). The CRADAs with LANL and ORNL ended in 2004; the SNL CRADA is operating on carry-over funds due to short staffing in FY 2003. SNL's FY 2004 funds were not received until the end of June, 2004, and the project was without funds (closed) for five months; a time-only extension has been granted allowing continuation until April 29th, 2005.

The project addresses reduction of CIDI engine NO_x emissions using exhaust aftertreatment – identified as one of the key enabling technologies for CIDI engine success. The overall CRADA efforts are currently focused on the development of urea/ammonia selective catalytic reduction (SCR) processes for reducing NO_x emissions, specifically targeting the selection of appropriate catalyst materials to meet the exhaust aftertreatment needs of light- and medium-duty diesel engines (SNL and LANL) and the understanding of urea-catalyst

interactions as well as factors influencing urea decomposition (ORNL). Infrastructure issues notwithstanding, the SCR process has the greatest potential to successfully attain the >90% NO_x reduction required for CIDI engines to meet the new EPA Tier II emission standards scheduled to be phased in starting in 2004.

Reports from the three national laboratory groups are given separately below.

A) Sandia National Laboratories (SNL)

Approach

SNL continues to develop catalysts supported on hydrous metal oxides (HMOs) and other oxides. We have been investigating new catalyst formulations as well as optimization of catalyst compositions to allow maximization of low-temperature activity. During FY 2004, we have focused on testing catalysts under more stringent testing conditions, with particular attention paid to the development of catalysts with high activity for a wide range of $NO:NO_2$ ratios. We have also investigated the effects of residual aromatic hydrocarbons (combined with paraffinic and olefinic hydrocarbons) on catalytic activity. During un-planned bench reactor down-time, we focused on optimization of catalyst synthesis parameters.

Results

In FY 2003, we reported on a catalyst (Catalyst C) that showed excellent activity, hydrothermal stability, and tolerance to SO_2 with $NO:NO_2$ = 1:1. This catalyst also exhibited good performance over a wide range of $NO:NO_2$ ratios in the feed. In FY 2004, we have continued to optimize this catalyst formulation and its transfer to monolith platform, and we have continued catalyst discovery efforts.

Standard experimental details for catalyst evaluation are summarized in Table 1 together with performance targets under each set of conditions.

A series of monolithic Catalyst C units was prepared using a slurry-coating technique where the catalyst loading was systematically increased up to a maximum of 28 wt.-% (mass of catalyst powder / mass of final monolith). Monolith performance was tested with both $NO:NO_2$ = 1:1 and $NO:NO_2$ = 4:1.

Table 1. Standard conditions used in bench reactor evaluation of SCR catalyst performance, and performance targets developed in conjunction with the LEP.

	Standard Test Conditions I ($NO:NO_2$ = 1:1)	**Standard Test Conditions II** ($NO:NO_2$ = 4:1)
Temperature	450 - 125 °C	450 - 125 °C
GHSV (h^{-1}) [monolith]	30,000	30,000
GHSV (h^{-1}) [powder]*	120,000 - 140,000	120,000 - 140,000
NO (ppm)	175	280
NO_2 (ppm)	175	70
NH_3 (ppm)	350	350
O_2 (%)	14	14
CO_2 (%)	5	5
H_2O (%)	4.6	4.6
Balance	He or N_2	He or N_2
NO_x conversion target, 200°C (%)	90	50
NO_x conversion target, 200 – 400°C (%)	90	N/A

*Powders tested at standard flow rate of 3.125 Liters (g catalyst)$^{-1}$ min^{-1}; GHSV varies depending on catalyst density.

At the highest loading, monolith activity at a GHSV of 30,000 h^{-1} was found to be close to that of the Catalyst C powder operated at ~140,000 h^{-1} (3.125 L g^{-1} min^{-1}); see Figure 1. This verifies that screening of powder catalysts under appropriate conditions allows prediction of monolith catalyst performance. This is important since the preparation of monolith catalyst cores can be time-consuming and lead to uncertainties in sample homogeneity and reproducibility; screening powders allows a faster turnaround and good reproducibility.

In addition to hydrothermal durability and sulfur tolerance, it is important that catalysts in lean NO_x environments maintain activity in the presence of residual hydrocarbons. In the FY 2003 report, we presented data showing that addition of a mixture of

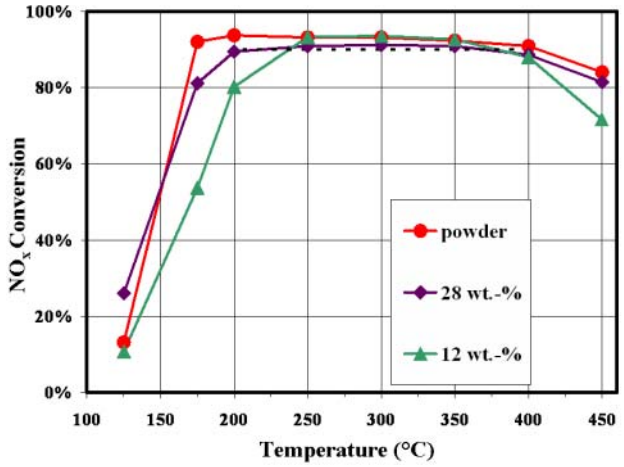

Figure 1. Comparison of powder performance with monoliths of various catalyst loadings. Experimental conditions as in Table 1, with $NO:NO_2$ = 1:1. Powder evaluated at GHSV = 140,000 h^{-1}; monolith at 30,000 h^{-1}.

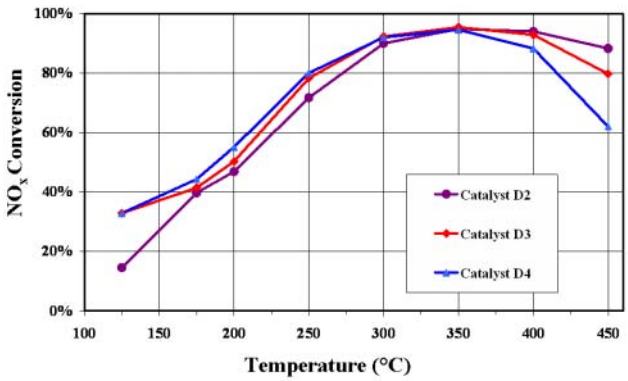

Figure 2. Performance of three powder catalysts based on SNL Catalyst C. Concentrations of active components were varied within +/- 1 wt.-% to enhance low- or high-temperature performance. Experimental conditions as in Table 1, with $NO:NO_2$ = 4:1.

olefins and paraffins (390 ppm C_1 equivalent) to the reactor gas upstream of the catalyst had minimal effect on the SCR performance of Catalyst C, i.e., only 10% drop in NO_x conversion, and only above 300°C. In FY 2004, we investigated the effect of toluene (aromatic hydrocarbon), in addition to olefins and paraffins, on the catalyst's performance and found that 60 ppm toluene co-fed for >12 hours has no effect above that of the other hydrocarbons. This result is significant because aromatic hydrocarbons are known to interact more strongly with catalyst surfaces than do olefins or paraffins and thus could be expected to be more potent poisons.

In a separate study, the components of Catalyst C were systematically varied in concentration in an attempt to optimize the performance of the catalyst at low temperature. By varying the concentrations of two components over a small range (e.g., +/- 1 wt.-% from "baseline" composition), catalysts could be tuned for operation at low temperature (achieving the target of 50% NO_x conversion at 200°C with $NO:NO_2$ = 4:1) or at high temperature; see Figure 2.

Hardware servicing and repair issues following the 5-month closure of this project due to late arrival of funds resulted in SNL bench reactor down-time in excess of 16 weeks; during this time efforts were directed to optimizing catalyst synthesis parameters (see below) and troubleshooting reactor performance. After new mirrors and a new laser had been installed in the Fourier transform infrared (FTIR) by the manufacturer, and the FTIR and bench reactor apparatus had been re-calibrated, it was found that results obtained previously, including results verified through independent testing by LEP collaborators, could not be reproduced. Catalyst activity measurements by the recently serviced and re-calibrated system were systematically lower than those found before, even though the system had been regularly re-calibrated before the servicing. This led to several weeks of troubleshooting and further servicing and repairs to the system. Partial recovery of perceived catalyst performance was achieved; however, further investigation is underway to identify the causes of this step change. Results reported from this point forward were all recorded after the reactor down-time; while they are self-consistent, comparison to earlier data may not be valid. It is our belief that the earlier data is correct (independent testing verified that); catalysts which met the targets given in Table 1 before reactor down-time typically failed to meet the targets afterward.

Several novel catalyst formulations based on SNL Catalyst C and containing additional metal components, chosen based on information in the scientific literature and prior experience, were screened in powder form under standard conditions (Table 1). The principal aim was to boost low-temperature performance by introducing additional

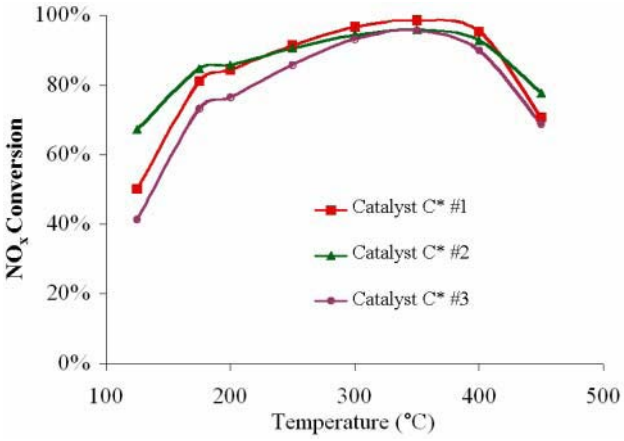

Figure 3. Performance of three powder catalysts based on SNL Catalyst C with additional metal components included in formulation. Experimental conditions as in Table 1, with $NO:NO_2$ = 4:1.

NO oxidation functionality and/or oxygen storage capability so that under conditions of low NO_2 concentration in the feed, the catalyst would generate sufficient NO_2 to bring the $NO:NO_2$ ratio close to unity, which is beneficial because the SCR reaction involving equimolar quantities of NO and NO_2 has the fastest rate. None of the compositions were found to be significantly better than Catalyst C, although some slight enhancement of low-temperature performance (<200°C) was observed in some cases. Figure 3 shows NO_x conversion data for three variants of Catalyst C (with additional metal components). Note that this data was recorded after the step-change in measured performance was observed and cannot be compared directly with earlier data (see previous paragraph).

During the un-planned bench reactor down-time, modifications were made to the catalyst synthesis procedure in search of materials possessing higher catalytic activity. These modifications included alteration of HMO (support) synthesis conditions and compositions, and alternative techniques for incorporation of active components into the final catalyst. HMO synthesis typically proceeds through hydrolysis of an alcohol-soluble sodium-silicotitanate precursor (derived from alkoxides of silicon and titanium) in a water/acetone mixture; the HMO precipitates as a white powder.

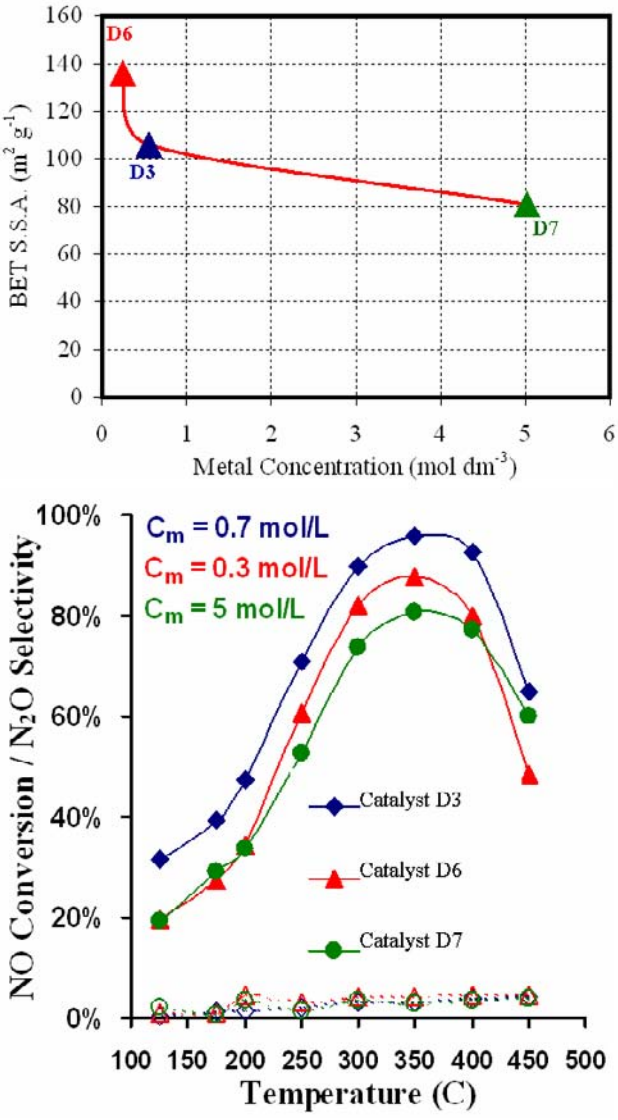

Figure 4. Variation of catalyst surface area (left) and corresponding NO_x conversion profiles (right) as a function of metal concentration used during HMO synthesis.

HMOs prepared with lower concentrations of sodium-silicotitanate in the ultimate hydrolyzed solution yielded both supports and catalysts with approximately 20% greater surface area (as measured using the Brunauer, Emmett and Teller, or B.E.T. method) than that obtained with the original synthesis procedure. The relationship between surface area and catalytic activity was found to be non-linear, and an optimum surface area for catalytic activity was defined (Figure 4).

Additional studies performed but awaiting catalyst evaluation include alteration of the ratio of Ti:Si to impact the surface properties of the HMOs, and variation in the method of introduction of metal oxide into the catalyst to improve the distribution of active sites.

Conclusions

- A powder catalyst operated at a high GHSV of 120,000 to 140,000 h^{-1} is a reliable predictor for how that catalyst would perform as a monolith with ~25 wt.-% loading at 30,000 h^{-1}. This allows faster, more reproducible catalyst screening to be performed by using powder formulations.
- SNL Catalyst C is resistant to poisoning by toluene (60 ppm, >12 hours at steady state).
- Small changes in the loadings of active components of SNL Catalyst C can enable the NO_x conversion performance to be tuned for low-temperature or high-temperature operation.
- Modest improvements in low-temperature NO_x conversion may be achieved by incorporation of other oxidation components into the formulation of Catalyst C; however, further work is needed to optimize such systems.
- Catalyst support (HMO) synthesis parameters can be adjusted in order to increase the surface area of the resultant catalyst. The HMO surface area for optimum NO_x conversion was defined.
- Bench reactor servicing and repair issues, as well as project closure for 5 months, have slowed progress this fiscal year. With the carryover funds remaining, we will address all outstanding milestones.

B) Los Alamos National Laboratory (LANL)

Approach

During FY 2004, work on the Lean NO_x Catalyst CRADA was brought to a close. During this time, the focus of the work at LANL was on completing studies on our recently discovered 'hybrid' and dual-bed catalyst systems that have proven so effective at the reduction of NO_x across a broad range of operating temperatures and in the presence of potential catalyst poisons. Some mechanistic work on the NO:NO_2 ratio was also performed and is illuminating, but it is far from complete.

A special focus of LANL's research has been the discovery of catalysts that are effective at lean NO_x reduction at low temperatures, low being below 200°C. Over 1000 compositions have been studied at LANL in this undertaking over the course of the CRADA. The LANL approach to catalyst discovery has been to apply whatever mechanistic insights are available to design materials that could have potentially high activity for the reduction of lean NO_x with ammonia as reductant. There is a good deal of empirical evidence that the rate of reduction of NO_x with ammonia is a strongly peaked function of the NO:NO_2 ratio fed to the lean NO_x catalyst. The highest rates of NO_x reduction are achieved with a NO:NO_2 ratio of 1 (some mechanistic data to address this appears later in this report). The major problem in achieving high conversions of NO_x at low temperatures (<200°C) lies in the fact that the exhaust gas NO_x speciation has a composition of NO_2 << NO. In most proposed aftertreatment systems, an upstream diesel oxidation catalyst will be used to remove unburned hydrocarbons and soot; this oxidation catalyst will also oxidize some of the NO to NO_2, which will clearly help the NO_x conversion, but even some of the best Pt-based oxidation catalysts generate 1:1 NO:NO_2 ratio only at temperatures greater than 200°C.

To achieve high activities of NO_x reduction at low temperature, LANL set out to find non-precious metal catalysts that were able to oxidize NO to NO_2 to approach the ratio of 1 at temperatures lower than 200°C, and supply the NO_x reduction function as well. This strategy has led to the invention of new so-called 'hybrid' catalysts that consist of a potent oxidation catalyst coupled with a competent NO_x reduction catalyst. Because these are potent oxidation catalysts, their excellent low-temperature NO_x conversion is countered by the oxidation of ammonia (mainly to N_2!) at higher temperature, thereby reducing the amount of ammonia available for the reduction of NO_x – i.e., the conversion of NO_x falls off at high temperature. Our recent research has explored a strategy to counter this problem of over-oxidation of ammonia. This has led to the invention of a dual-bed catalyst system that is capable of operating at unusually high NO_x

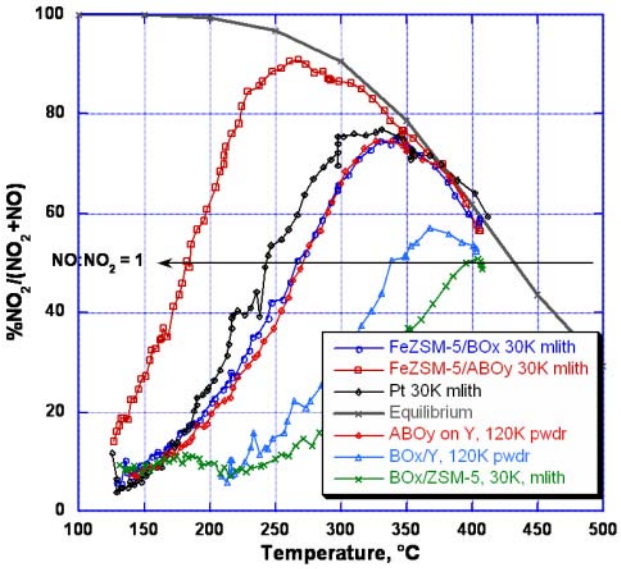

Figure 5. NO oxidation to NO_2 as a function of temperature is plotted for a number of base metal zeolite catalyst types having variable oxidation capability. The plot shown in red is the NO oxidation capability of a typical 'hybrid' catalyst. Conditions: 190 ppm NO, 12% O_2, 5% CO_2, balance He, GHSV = 30,000 h^{-1}.

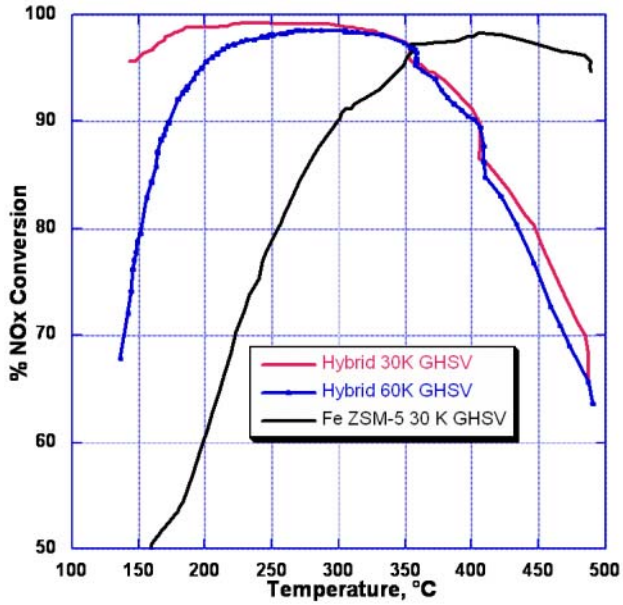

Figure 6. NO_x conversion as a function of temperature for a typical 'hybrid' monolith catalyst based upon Fe ZSM-5 for various space velocities. Conditions: 280 ppm NO, 70 ppm NO_2, 360 ppm NH_3, 5% CO_2, 12% O_2, 5% steam.

conversions over a broad temperature range. This invention is an additional subject of a patent application filed this year.

Results

Research accomplished during FY 2003 at LANL led to the discovery of 'hybrid' lean NO_x catalysts that have extraordinary activity at temperatures below 200°C, and we have followed up on these catalysts during FY 2004 but with reduced funding. These catalysts are comprised of a potent oxidation function to convert a significant fraction of NO to NO_2 even at low temperatures, and a second component that is competent at converting the resulting NO/NO_2 mixture with ammonia to nitrogen and water. For these studies, this second component is a conventional, well-studied base metal zeolite catalyst, Fe ZSM-5. Most of our studies that we will describe below were conducted by supporting catalysts on cordierite monolith of 400 cpi. The conditions selected and agreed upon by the CRADA partners for the testing of these catalysts are specified in Table 1. The studies at LANL focused on the $NO:NO_2$ = 4:1 mix to best simulate the NO_x mixture anticipated to be generated at low temperatures downstream of the diesel oxidation catalyst in a proposed emission control system. Conversion data on monolith catalysts were obtained at a GHSV of 30,000 h^{-1}. Data on powder catalysts were obtained at a GHSV of 120,000 h^{-1} in an attempt to make a realistic comparison of activities between monolith and powder catalysts (Figure 1 provides some justification for this).

It is now well known that the highest rates of NO_x conversion are obtained when the ratio of $NO:NO_2$ = 1:1. Figure 5 shows data regarding the capability of some zeolite-based lean NO_x catalysts to oxidize NO to NO_2. Note that most catalysts are not able to appreciably oxidize NO to NO_2 to a ratio of 1 below temperatures of 250°C. A catalyst of 5% Pt/ZSM-5 supported on cordierite also does not oxidize NO to the desired ratio of 1 below about 240°C. LANL 'hybrid' catalysts that contain a potent base metal oxidation component do oxidize to the desired ratio of 1 at temperatures as low as 175°C. The impact this has on NO_x conversion is shown in Figure 6, which shows the marked

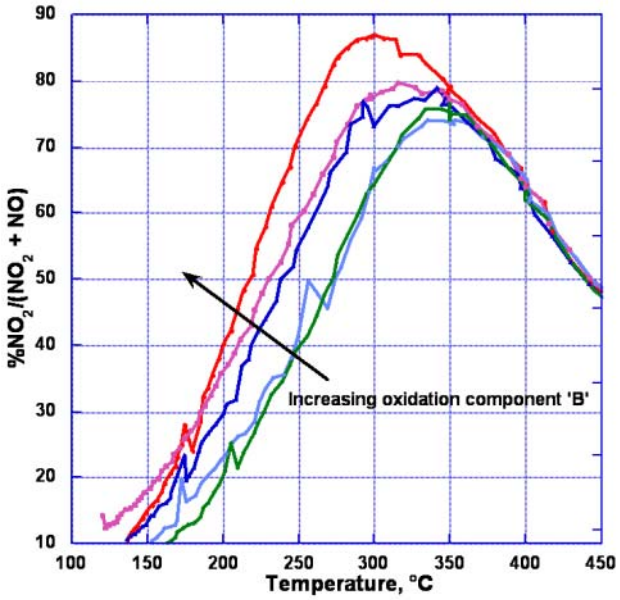

Figure 7. NO oxidation as a function of the added components 'A' and 'B' to Fe ZSM-5 supported on monolith. Conditions as are given in Figure 5.

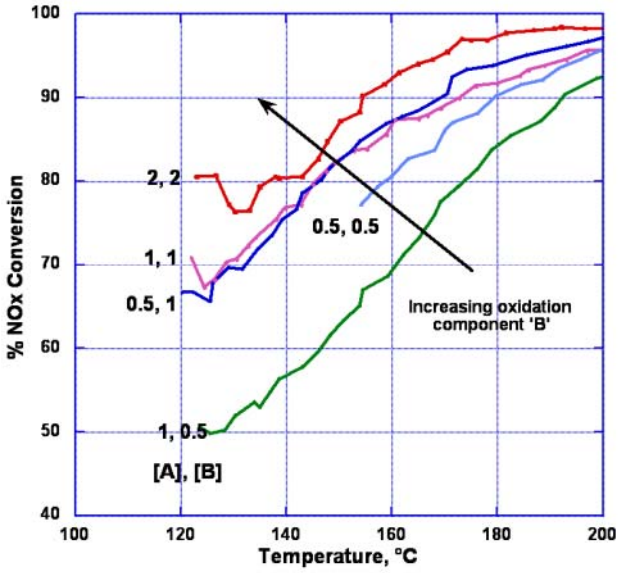

Figure 8. NO_x conversion as a function of added components 'A' and 'B' to Fe ZSM-5 supported on monolith. Conditions are as given in Figure 6.

improvement of NO_x conversion when the oxidation component is added to Fe ZSM-5. For Fe ZSM-5 supported on monolith, NO_x conversion amounts to approximately 60% at 200°C; upon addition of the oxidation component to form the 'hybrid' catalyst, conversion improves to >98%. Figure 6 also shows the influence of space velocity on NO_x conversion occurring below 300°C, with NO_x conversion dropping from >98% to approximately 95% at 200°C upon doubling the GHSV from 30,000 to 60,000 h^{-1}.

An attempt at optimizing the composition of the oxidizing component was made by varying the quantities of components 'A' and 'B' that were added to the conventional lean NO_x catalyst Fe ZSM-5 supported on monolith. Varying the ratio and the amounts of these components and obtaining reactivity data both on NO oxidation (Figure 7) and NO_x reduction (Figure 8), it is concluded that component 'B' is most important, but that components 'A' and 'B' interact synergistically, probably through compound formation. We attempted to identify the phase composition of the presumed 'ABO_x' oxidation component by powder X-ray diffraction (XRD) (data not shown); whatever the oxidation component is, it appeared by XRD to be amorphous or of very small particle size, and no phase information was obtained by this technique.

The LANL 'hybrid' catalysts are exceedingly active for the conversion of lean NO_x at low temperatures as compared to currently available catalysts. Above about 350°C, however, these 'hybrid' catalysts begin to exhibit poorer NO_x conversion relative to other catalysts. The source of this loss of NO_x conversion was explored experimentally by examining the oxidative conversion of ammonia in the absence of NO_x. It was anticipated that these 'hybrid' catalysts that contain a potent oxidation function were simply oxidizing the ammonia to NO_x, leading to apparent loss of NO_x conversion with increasing temperature. What we found, however, was that while ammonia was being converted oxidatively, it was mostly being converted to N_2. At 450°C, conversion of 500 ppm NH_3 in excess oxygen at a GHSV of 30,000 h^{-1} yielded a selectivity to N_2 of 80% and selectivity to NO_x of only 20%, indicating that while ammonia is oxidized to NO_x, the NO_x generated is largely reduced to N_2 by the remaining ammonia. But this still indicates that ammonia is being removed from the system, leaving not enough reductant to convert the NO_x.

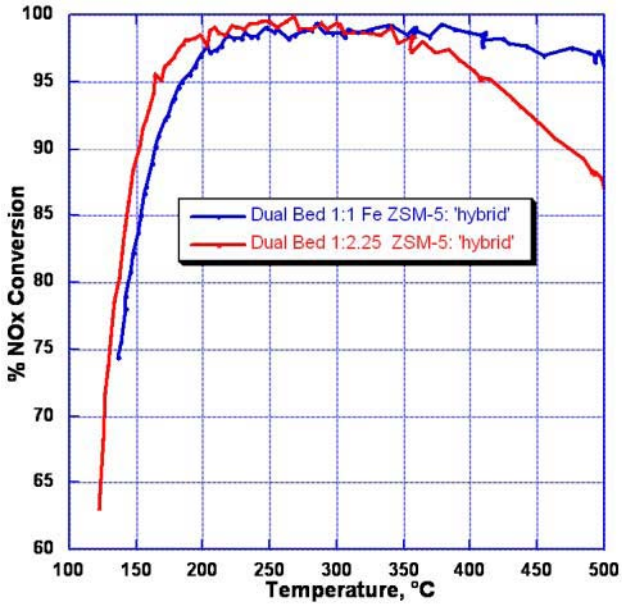

Figure 9. NO_x conversion of two dual-bed configuration catalysts. Conditions are as given in Figure 6.

The LANL approach to solving this problem arose from the realization that at high temperatures above 300°C, most base metal zeolite catalysts such as Fe ZSM-5 are competent NO oxidation catalysts. The added oxidation component in the 'hybrid' catalysts is not only not needed, but is deleterious at higher temperatures because of the oxidation of ammonia. This realization led to the invention of 'hybrid' dual-bed catalysts, where a competent lean NO_x catalyst such as Fe ZSM-5 is placed upstream from a bed of 'hybrid' catalyst. Consider a dual bed where the upstream half of the bed volume is Fe ZSM-5 and the downstream half is a LANL 'hybrid' catalyst, with a GHSV through the entire bed of 30,000 h^{-1} (this, of course, yields effectively 60,000 h^{-1} GHSV through each individual piece). At low temperatures, e.g., 150°C, where Fe ZSM-5 can only convert <50% of the NO_x, the majority of the un-reacted NO_x and ammonia will flow to the downstream 'hybrid' catalyst, which under these conditions can readily convert 80% of the NO_x at 60,000 h^{-1}, as shown in Figure 6. At higher temperatures above 350°C, the upper bed of Fe ZSM-5 is expected to readily convert nearly all the NO_x and ammonia, so there would be no ammonia left in the gas stream to enter the lower 'hybrid' catalyst bed and become oxidized.

This, in fact, is what is observed in a dual-bed configuration. The NO_x conversion of a dual bed, where the upstream bed is Fe ZSM-5 and the downstream bed is a LANL 'hybrid' catalyst, is shown in Figure 9. The NO_x conversion is quite similar to what would be anticipated from the simple addition of the activities of the individual beds at twice the GHSV. The relative volumes of the upper and lower beds can be adjusted to 'tune' the catalyst activity to favor better low-temperature activity or better high-temperature activity, as shown in Figure 9.

Mechanistic insight led to the invention of the 'hybrid' catalysts; understanding of the various reaction pathways then led to the demonstration that dual-bed approaches result in tunable activity for lean NO_x conversion over broad temperature ranges. The 'hybrid' catalysts have been shown to have acceptable hydrothermal stability, and they recover from poisoning by SO_x. Because of their exceptional oxidation activity, the 'hybrid' catalysts are also resistant to poisoning by toluene. Injection of 100 ppm of toluene upstream of the catalyst during a ramp-down, ramp-up cycle resulted in no loss of NO_x conversion. Increasing the toluene concentration to 1000 ppm does result in temporary deactivation, but all activity is recovered upon cycling the catalyst to above 250°C. Pulses of large concentrations of toluene (10 microliters toluene/1 cc catalyst) injected and vaporized upstream from the catalyst held at 177°C result in a few percent diminution in activity. Even at 177°C, the activity recovers fully over a period of minutes; return to full activity is very fast above 250°C. Carbon dioxide and water are detected as products of toluene oxidation. There may be other products as well, but attempts were not made to identify them.

Because of the oxidation capacity of the 'hybrid' catalysts, they may also find utility in other aftertreatment applications. Because they can readily oxidize hydrocarbons, and ammonia is mainly converted to nitrogen, they may find utility as clean-up catalysts downstream of the lean NO_x catalyst. Because they are potent NO oxidation catalysts, the LANL 'hybrid' catalysts may find application as non-platinum-group-metal catalysts upstream of lean NO_x trap (LNT) catalysts, which also require NO to

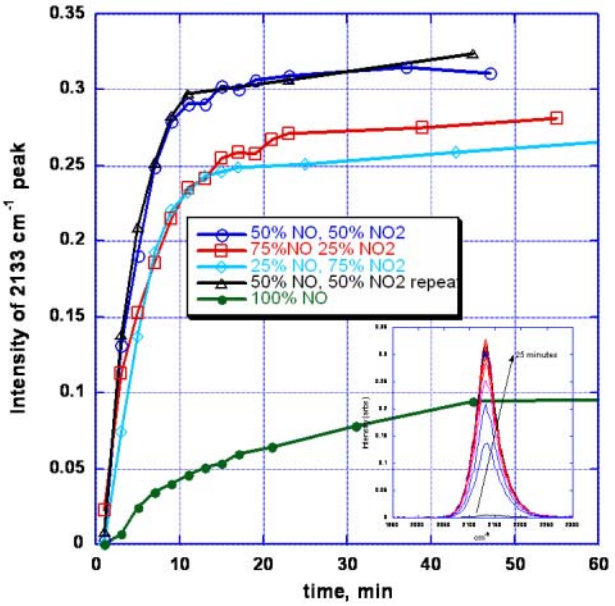

Figure 10. Appearance of the 2133 cm^{-1} feature as a function of time and $NO:NO_2$ ratio. Total concentration of NO_x = 1050 ppm, temperature = 100°C. Inset is an example of the growth of the 2133 cm^{-1} peak with time with $NO:NO_2$ = 1:1.

NO_2 oxidation to enable efficient trapping of NO_x. Higher LNT efficiency at lower temperatures would be beneficial, and obtaining that activity without the use of Pt would be desirable.

A small part of our effort has been to understand in more detail the role of oxidation of NO in the overall scheme of NO_x reduction, and to use this information to develop better catalysts. During this last year of the project, LANL focused on examining the speciation of NO_x adsorbed on zeolite supports. While zeolites without metal cations exchanged within their pores are not highly effective catalysts, they are still moderately catalytically active, and so are useful and simple model systems to study using spectroscopic techniques. Using FTIR spectroscopy, a preliminary examination of the NO_x species adsorbed on the zeolite as a function of $NO:NO_2$ ratio was undertaken.

These experiments were performed using a diffuse reflectance FTIR (DRIFT) cell where the catalyst atmosphere and temperature may be accurately controlled. A commercial sample of NH_4^+ ZSM-5 was calcined (to generate the H^+ form of the zeolite) and placed in the DRIFT cell heated to 100°C. At this temperature, various ratios of $NO:NO_2$ of total concentration 1050 ppm NO_x were passed through the sample. The $NO:NO_2$ ratios used were 1:3; 1:1; 3:1; and 1:0. Other researchers have previously observed a variety of bound NO_x species on zeolite catalysts at higher concentrations of NO_x; the studies discussed here were intended to examine the bound species under realistic concentrations.

At all ratios of 1050 ppm NO_x, a strong absorbance at around 2133 cm^{-1} is observed to grow with time of exposure, as shown in Figure 10. This feature has been previously assigned to zeolite-adsorbed NO^+, consistent with the substantial blue shift relative to gas-phase NO, and the observed absorption of known 'free' nitrosonium cations which have infrared transitions at around 2200 cm^{-1}.

The growth of the 2133 cm^{-1} band exhibits saturation kinetics and reaches a plateau that is a function of $NO:NO_2$ ratio. As shown in Figure 11, a plot of the fraction of NO in the feed (blue curve) results in a peaked curve with a maximum at a ratio of $NO:NO_2$ = 1:1 – the same functional form as is observed in plots of NO_x conversion with ammonia as a function of NO in the feed. Because NO (formally N(II)) and NO_2 (formally N(IV)) are in rapid equilibrium with N_2O_3 (formally N(III)), the concentration of N_2O_3 is directly related to the product of the concentration of NO with the concentration of NO_2, i.e., $[N_2O_3] = K_{eq}[NO][NO_2]$. It is highly likely that N_2O_3 dissociatively adsorbs on the zeolite surface as NO^+ and NO_2^-. This suggests an explanation for the plot of $[NO]x[NO_2]$ vs. surface coverage of NO^+ (directly related to the concentration of N_2O_3) being a straight line (red plot, Figure 11). A similar relationship should hold for adsorbed NO_2^-, but this species is likely to give rise to infrared bands in the same region as the framework of the zeolite, making observation difficult under the low-concentration conditions used for these studies. The NO^+ and NO_2^- species, when reacted with water, give rise to nitrous acid HONO; nitrous acid is known to react rapidly with ammonia to form ammonium nitrite, NH_4NO_2. Ammonium nitrite is known to rapidly decompose to nitrogen and water at temperatures above 50°C. These spectroscopic observations of NO^+, tracking the rate of lean NO_x conversion, and the known and observed

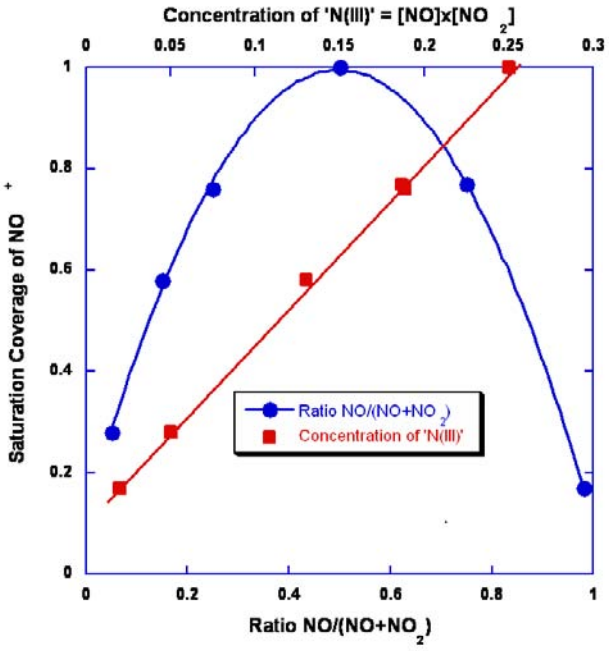

Figure 11. Plots of normalized intensity of the 2133 cm^{-1} infrared feature as a function of fraction of NO in the feed and the product of the NO and the NO_2 concentrations.

reactions of NO_x with ammonia are consistent with the following reaction scheme:

$NO + NO_2$	→	N_2O_3
N_2O_3 + zeolite	→	zeol-NO^+ + zeol-NO_2^-
H_2O + zeol-NO^+ + zeol-NO_2^-	→	2 zeol-HONO
Zeol-HONO + NH_3	→	NH_4NO_2
NH_4NO_2	→	$N_2 + 2H_2O$

Conclusions

Requirements for active lean NO_x catalysts are that they must be able to oxidize NO to NO_2 at a rate such that a 1:1 ratio of NO:NO_2 is generated. This results in the maximum concentration of reactive N(III) intermediates such as NO^+ and NO_2^- having nitrogen in the formal oxidation state of +3, which are the species that are known to most rapidly react with ammonia via transient formation of highly unstable ammonium nitrite, which subsequently decomposes rapidly to nitrogen and water. The catalyst should also provide a reservoir of ammonia to provide the highest rate of reaction of the N(III) intermediates to ammonium nitrite. Zeolite catalysts are particularly suited to this latter role, as they provide a large reservoir of bound ammonium ions through interaction of gas-phase NH_3 with a high concentration of Brønsted acid sites in the zeolite channel structure. The necessary oxidation function must be added to the zeolite structure; our recent work on 'hybrid' catalysts for lean NO_x conversion indicates that one path to doing this is to form a potent oxidation catalyst on the zeolite itself. This is not without tradeoffs, however, as even though these catalysts are highly active at low temperatures, they suffer from over-oxidation of ammonia at higher temperatures. We have solved this problem by preparing tunable dual-bed configurations, where the low-temperature active 'hybrid' catalyst is placed below a lean NO_x catalyst that has reactivity only at the higher temperatures.

There is still much to do to understand the interplay of water, ammonia, NO_x, SO_x, and hydrocarbon fragments with the ammonia storage component and the oxidation function of these zeolite-based lean NO_x catalysts. The structural stability of these various components appears good, but particularly the oxidation function is not well-studied at this point, and further work is required to better define the ultimate stability of this class of catalysts.

C) Oak Ridge National Laboratory (ORNL)

Approach

A Mercedes 1.7-liter displacement direct-injection diesel engine at ORNL was utilized for the engine portion of this research. A catalyst supplier provided prototype non-vanadia zeolite catalysts as well as a diesel oxidation pre-catalyst to provide NO-to-NO_2 conversion and to remove hydrocarbons which can damage SCR catalysts. A second industry partner provided some of the urea injection hardware. Engine experiments were run at typical light-duty temperatures (from 165-260°C) while maintaining flow and NO_x as constant as possible. A 3"-long monolith was used to obtain a GHSV of 50,000 hr^{-1} and to speed up equilibration. In addition

to NO_x conversion performance measurements, exhaust samples were taken before and after the catalyst to look specifically for urea decomposition products. Care was taken to clean off the catalyst thoroughly between runs and to allow NO_x conversion to stabilize, which could often take more than an hour at low temperatures.

Results

Overall, NO_x conversion of the catalyst occurred as low as 165°C, with conversions close to 90% at 250°C. Most of the study was focused on storage and decomposition of urea on the monolith. Under typical light-duty temperatures (T < 250°C), there was little or no decomposition of the urea in the gas phase prior to catalyst introduction. The urea decomposes after it contacts the monolith. At temperatures around 200°C, ammonium nitrate is the likely form of urea storage.

Koebel and co-workers reported these likely reactions for ammonium nitrate formation and release.

$2NH_3 + 2NO_2$	→	$NH_4NO_3 + N_2 + 3H_2O$	(1)
NH_4NO_3	→	$NH_3 + HNO_3$	(2)
$2HNO_3 + NO$	→	$3NO_2 + H_2O$	(3)

Figure 12 shows the results for nitrate measurement downstream of the catalyst as a function of temperature. Note that nitrate can be a significant faction of the total NO_y species, which include NO, NO_2, and NO_3^- . In Figure 12, it is likely that the storage sites on the monolith were full and that the equilibrium in Eq. 2 and the slow reaction in Eq. 3 resulted in emissions of nitrate.

Figure 13 reports on the behavior of the catalyst during "burn-off' release of stored species. The catalyst is equilibrated at 165°C, and then the urea injection is turned off and load is applied to the engine to raise the exhaust temperature to 190°C. An FTIR is used to monitor the resulting catalyst-out species. Note that for the first 100 seconds, SCR continues despite the lack of urea injection. The NO then goes up and later drops. Ammonia, despite the urea being turned off, also goes up before

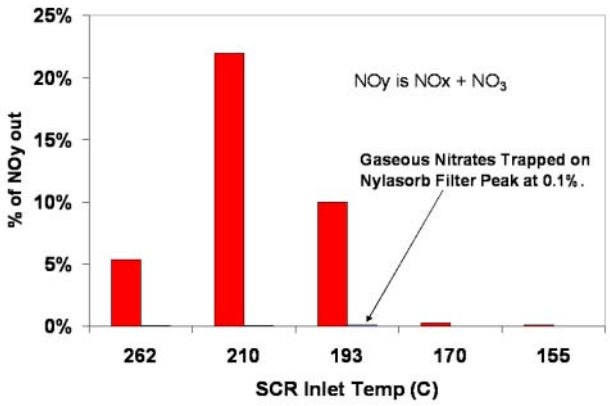

Figure 12. High nitrate formation was observed (relative to NOy) post-SCR for some temperatures.

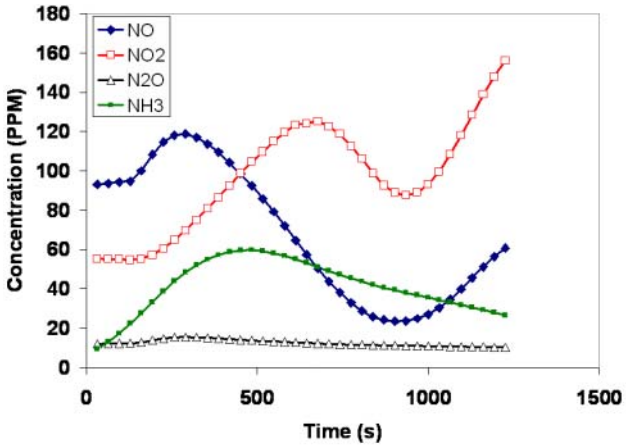

Figure 13. FTIR measurements of species resulting from catalyst burnoff shows complex interactions between species. Urea SCR was equilibrated at 165°C, then urea was shut off at time = 0 sec and exhaust temperature increased to 190°C.

disappearing, indicating that a desorption and/or release mechanism similar to Eq. 2 is occurring. The subsequent decrease in NO may be due to reaction of NO with nitric acid, as in Eq. 3. Finally, after 20 minutes, the NO and NO_2 values are approaching the "catalyst-in" values.

Clearly, there is significant complexity associated with transient operation at low temperatures. This study identified issues with urea decomposition and storage. For vehicle applications, model-based controls for urea injection will require knowledge of the storage and release functions of particular catalyst formulations, as well as keeping

track of how much urea has been injected and stored on the catalyst.

Conclusions

Significant storage of urea and urea decomposition appear to occur on a light-duty SCR catalyst.

Special Recognitions & Awards/Patents Issued

1. US Patent 6,716,783, April 6, 2004, "Catalysts for lean burn engine exhaust abatement," K.C. Ott, N.C. Clark, M.T. Paffett. [LANL]
2. Patent application: "Catalyst and method for reduction of nitrogen oxides," Kevin C. Ott, DOCKET NUMBER: S-100,615. [LANL]

FY 2004 Publications/Presentations (SNL, LANL and ORNL; chronological)

1. "Development of Ammonia SCR Catalysts for NO_x Reduction in Lean-Burn CIDI Engines," E.N. Coker, D.A. Peña, R.S. Sandoval and J.E. Miller, *4th National Laboratory Catalysis Conference*, Oak Ridge, TN, October 22-24, 2003. [SNL]
2. "Development of Ammonia SCR Catalysts for NO_x Reduction in Lean-burn Light-duty Diesel Engines," D. Peña, E. Coker, R. Sandoval and J. Miller, *15th Rio Grande Symposium on Advanced Materials*, Albuquerque, NM, October 27, 2003. [SNL]
3. "Selective Catalytic Reduction and Sulfur Management Issues in Vehicle Emission Control," E.N. Coker, D.A. Peña, S. Hammache and J.E. Miller, *28th Int'l Cocoa Beach Conference and Exposition on Advanced Ceramics & Composites*, Cocoa Beach, FL, January 25-30, 2004. [SNL]
4. "Mobile Diesel Exhaust Treatment: Lean-NO_x Reduction by Ammonia," D.A. Peña, E.N. Coker, R.S. Sandoval and J.E. Miller, *18th Annual Western States Catalysis Club Meeting*, Provo, UT, February 27, 2004. [SNL]
5. "Development of Improved SCR Catalysts; LEP CRADA," E.N. Coker, D.A. Peña, R.S. Sandoval and J.E. Miller, *DOE National Laboratory Advanced Combustion Engine R&D Merit Review and Peer Evaluation*, Argonne National Laboratory, May 18-20, 2004. [SNL]
6. "Experimental Speciation of Urea SCR Exhaust," J. Storey, *CLEERS Workshop 7*, Detroit, MI, June 17, 2004. [ORNL]
7. "Decomposition Phenomena of Urea in SCR Systems," J. Storey and S. Sluder, *10th Diesel Engine Emission Reduction Conference*, Coronado, CA, August 29-September 2, 2004. [ORNL]
8. "Development of a Durable Low-Temperature Urea-SCR Catalyst for CIDI Engines," D.A. Peña, E.N. Coker, R.S. Sandoval and J.E. Miller, *10th Diesel Engine Emission Reduction Conference*, Coronado, CA, August 29-September 2, 2004. [SNL]
9. "Selective Catalytic Reduction of NO_x with Ammonia on Gallium-exchanged Ferrierites", M. Mecárová, N.A. Miller, N.C. Clark, K.C. Ott, and T. Pietraß, *Appl. Catal. A.*, in review. [LANL]

References

1. M. Kleemann, M. Elsener, M. Koebel and A. Wokaun, *Ind. Eng. Chem. Res.*, **39(11),** 4120-6, (2000)

II.B.9 Plasma Catalysis for NO_x Reduction from Light-Duty Diesel Vehicles

Stephan Barlow, Ja-Hun Kwak, Chuck Peden (Primary Contact), Janos Szanyi, and Russ Tonkyn
Pacific Northwest National Laboratory
P.O. Box 999, MS K8-93
Richland, WA 99353

DOE Technology Development Manager: Ken Howden

CRADA Partner:
Low Emissions Technologies Research and Development Partnership (LEP – Member Companies: Ford Motor Company, General Motors, and DaimlerChrysler Corporation)
John Hoard (Primary Contact), Ford Scientific Research Labs; Byong Cho and Steven Schmieg, General Motors R&D Center; and David Brooks, DaimlerChrysler Technology Center

This project also included a plasma-reactor materials development effort with the following personnel:
Steve Nunn, Oak Ridge National Laboratory, Oak Ridge, TN
This portion of the project was funded and managed by:

DOE Technology Development Manager: Patrick Davis

Objective

- Develop a novel plasma/catalyst NO_x reduction and particulate matter (PM) aftertreatment system that will achieve 90% NO_x reduction using less than 5% of the engine power on a compression ignition direct injection (CIDI) engine.

Approach

- Synthesize and characterize new catalysts. A highly active and stable plasma catalyst material is critical to meeting the project goals.
- Measure plasma/catalyst activity in simulated and real exhaust.
- Through more fundamental mechanistic studies, identify the important reaction intermediates and the rate-limiting reactions in a plasma/catalyst system. Use this information to guide the catalyst synthesis efforts.
- Design and construct prototype plasma/catalyst reactor systems.
- Evaluate prototype reactor systems for emissions (NO_x and PM) reduction performance, energy efficiency, and durability.
- Utilize Oak Ridge National Laboratory (ORNL) ceramic processing capabilities to simplify the design of the plasma reactor portion of the emission control device.

Accomplishments

- Detailed studies of HCN oxidation over Pt-based oxidation catalysts were completed. This project had previously identified HCN as an unfortunate byproduct of hydrocarbon SCR in the plasma-catalyst process, but Pt oxidation catalysts were found to be effective for its removal. In fact, HCN oxidation is found to provide additional NO_x reduction 'capacity' to the overall system. Three journal publications have been submitted describing this work.

- A new catalyst material has been invented (disclosure filed) that shows excellent activity for hydrocarbon selective catalytic reduction (SCR) of simulated diesel exhaust without the need for a plasma device. This catalyst formulation was based on the mechanistic understanding provided in prior years' studies.
- The project received national recognition with the 2004 Advanced Combustion Engine R&D Special Recognition Award.
- Since the inception of this project, a total of 49 reports have been published, most of which are in peer-reviewed publications such as Catalysis Today, SAE proceedings, Journal of Applied Physics, Applied Catalysis B, Journal of Advanced Oxidation Technologies, etc. In addition,
- 58 presentations have been given, including talks at SAE World Congress and Fuels and Lubes Meetings, American Chemical Society, DEER, North American Catalysis Society, Future Car Congress, etc.

Future Directions

This project ended in January of 2004. Despite this, several important areas for continued R&D can be identified:

- More consistently available engine dynamometer time for realistic testing that should include studies of transient performance (e.g., Federal Test Procedure cycles);
- Improved methods to prepare realistic coated monoliths with laboratory-synthesized catalyst materials for fair testing of performance;
- Continued and focused (e.g., resistance to coking) development of catalyst materials and plasma reactors; and
- Continued fundamental studies of NO_x adsorption and reaction on and deactivation (e.g., coking) of oxide catalyst materials (zeolite- and alumina-based catalysts for plasma-enhanced hydrocarbon SCR, NO_x adsorber materials, urea SCR catalysts).

Introduction and Approach

The control of NO_x (NO and NO_2) emissions from so-called 'lean-burn' vehicle engines remains a challenge. In this project, we have been developing a novel plasma/catalyst technology for the remediation of NO_x under lean (excess oxygen) conditions, specifically for compression ignition direct injection (CIDI) diesel engines that have significant fuel economy benefits over conventional stoichiometric gasoline engines. Project efforts included (1) improving the catalyst and plasma reactor efficiencies for NO_x reduction, (2) studies to reveal important details of the reaction mechanism(s) that can then guide our catalyst and reactor development efforts, (3) evaluating the performance of prototype systems on real engine exhaust, and (4) studies of the effects of the plasma on particulate matter (PM) in real diesel engine exhaust. Figure 1 is a conceptual schematic of a plasma/catalyst device which also shows our current best understanding of the role of the various components of the overall device for reducing NO_x from the exhaust of a CIDI engine. When this program was initiated, it was not at all clear what the plasma was doing and, as such, what class of catalyst materials might be expected to produce good results. With the understanding of the role of the plasma (as depicted in Figure 1) obtained in this project, faujasite zeolite-based catalysts were developed and shown to produce high activity for NO_x reduction of plasma-treated exhaust in a temperature range expected for light-duty diesel engines. These materials are the subject of a pending patent application and were recognized with a

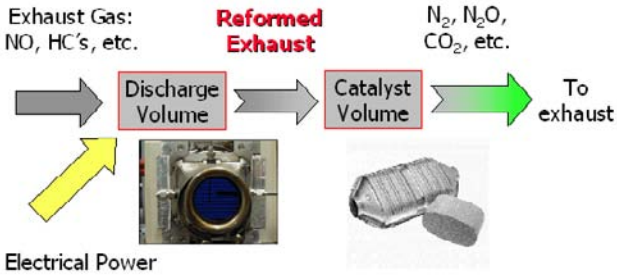

Figure 1. Schematic of Two-Step Discharge/Catalyst Reactor

prestigious R&D100 Award in 2002. In addition, Pacific Northwest National Laboratory (PNNL) staff were awarded a Federal Laboratory Consortium (FLC) Award in 2003 "For Excellence in Technology Transfer". The project also received the DOE's 2001 CIDI Combustion and Emission Control Program Special Recognition Award and 2004 Advanced Combustion Engine R&D Special Recognition Award.

Results

Our studies have shown that a plasma device combined with a catalyst can reduce as much as 90% or more of NO_x in simulated diesel and other 'lean-burn' exhaust. In the case of propylene-containing simulated diesel exhaust, the beneficial role of a plasma treatment is now thought to be due to oxidation of NO to NO_2 and the formation of partially oxidized hydrocarbons that are more active for the catalytic reduction of NO_2 than propylene. *Thus, the overall system can be most usefully described as hydrocarbon selective catalytic reduction (SCR) enhanced by 'reforming' the exhaust with a non-thermal plasma* (NTP) *device.* For plasma-enhanced catalysis, both zeolite- and alumina-based materials have shown high activity, albeit in somewhat different temperature ranges, when preceded by an NTP reactor. Various alkali- and alkaline earth-cation-exchanged Y zeolites have been prepared, their material properties have been characterized, and they have been tested as catalytic materials for NO_x reduction in laboratory NTP-catalysis reactors. Interestingly, NO_2 formed in the plasma and not subsequently removed over these catalysts will back-convert to NO, albeit to varying extents depending upon the nature of the cation. On this basis, a new "cascade" reactor process was invented. Besides measuring comparative reactivity, we also developed a number of synthesis strategies for enhancing the performance of these zeolite-based catalyst materials. A particularly important result from our mechanistic studies was the observation that aldehydes, formed during the plasma treatment of simulated diesel exhaust, are the important species for the reduction of NO_x to N_2. Indeed, acetaldehyde has been found to be especially effective in the *thermal* reduction of both NO and NO_2 over Ba- and Na-Y zeolite catalysts. This knowledge led to the invention of a new, highly active catalyst that does not need the plasma device in the last year of the project.

Special Recognitions and Awards/Patents Issued

1. 2004 Advanced Combustion Engine R&D Special Recognition Award "For technical excellence and admirable collegiality in inter-laboratory collaborative research".
2. "A New Concept and Catalysts for Lean-NO_x Reduction", J.-H. Kwak, J. Szanyi and C.H.F. Peden (invention disclosure filed December 12, 2003).

FY 2004 Presentations

1. C.H.F. Peden, S.E. Barlow, J.W. Hoard, D.-H. Kim, J.-H. Kwak, M.L. Balmer-Millar, A.G. Panov, S.J. Schmieg, J. Szanyi, and R.G. Tonkyn, "Selective Reduction of NO_x in Oxygen Rich Environments with Plasma-Assisted Catalysis: Catalyst Development and Mechanistic Studies", presentation at the 9th DEER Workshop, Newport, RI, August, 2003.
2. J.W. Hoard, D.J. Brooks, S.J. Schmieg, C.H.F. Peden, S.E. Barlow, R.G. Tonkyn, and F. Beier, "Dynamometer Evaluation of Plasma-Catalysis for Diesel NO_x Reduction", presentation at the 9th DEER Workshop, Newport, RI, August, 2003.
3. J. Szanyi, J.-H. Kwak, and C.H.F. Peden, "Non-thermal Plasma Assisted NO_x Reduction over Na- and Ba-Y,FAU: A Mechanistic Study by FTIR Spectroscopy", presentation at the 4th DOE National Laboratory Catalysis Conference, Oak Ridge, TN, October, 2003.
4. J.-H. Kwak, J. Szanyi, and C.H.F. Peden, "TPD and in-situ FTIR Studies of NO_2 on NaY and BaY Zeolites", presentation at the 4th DOE National Laboratory Catalysis Conference, Oak Ridge, TN, October, 2003.
5. K.G. Rappé, C.L. Aardahl, and C.H.F. Peden, "Broad Temperature Coverage for Plasma-Facilitated NO_x Reduction via Combination of Low and High Temperature Catalytic Materials", presentation at the 4th DOE National Laboratory Catalysis Conference, Oak Ridge, TN, October, 2003.
6. H. Zhao, R.G. Tonkyn, S.E. Barlow, B.E. Koel, and C.H.F. Peden, "Reactions of HCN with NO_x over a Platinum Catalyst under Lean Conditions", presentation at the 4th DOE National Laboratory Catalysis Conference, Oak Ridge, TN, October, 2003.

7. J. Szanyi, J.-H. Kwak, and C.H.F. Peden, "Non-thermal Plasma Assisted Catalytic NO_x Reduction over Na- and Ba-Y,FAU: Mechanistic Studies", presentation at the 13th International Congress on Catalysis, Paris, France, July, 2004.
8. C.H.F. Peden, H. Zhao, R.G. Tonkyn, S.E. Barlow, and B.E. Koel, "Kinetics and Mechanism of HCN Oxidation over Pt/Al_2O_3", presentation at the 13th International Congress on Catalysis, Paris, France, July, 2004.
9. C.H.F. Peden, J. Szanyi, and J.-H. Kwak, "Non-thermal Plasma Assisted Catalytic NO_x Reduction over Na- and Ba-Y,FAU: Mechanistic Studies", presentation at the Isotopes in Catalysis Workshop, Poitiers, France, July, 2004.

FY 2004 Publications

1. S. Barlow, J.-H. Kwak, C. Peden, J. Szanyi, R. Tonkyn, G. Singh, K. Stork, J. Hoard, B. Cho, S. Schmeig, D. Brooks, S. Nunn, P. Davis, "Plasma Catalysis for NO_x Reduction from Light-Duty Diesel Vehicles", Combustion and Emission Control for Advanced CIDI Engines, FY 2003 Progress Report (2003) 129-136.
2. J. Szanyi, J.-H. Kwak, and C.H.F. Peden, "The Adsorption and Reaction of NO_2 and the $NO+O_2$ Reaction on Na-Y,FAU: An *in-Situ* FTIR Investigation", Physical Chemistry and Chemical Physics **5** (2003) 4045-4051.
3. J.-H. Kwak, J. Szanyi, and C.H.F. Peden, "Non-thermal Plasma-Assisted Catalytic NO_x Reduction over Ba-Y,FAU: The Effect of Catalyst Preparation", Journal of Catalysis **220** (2003) 291-298.
4. C.H.F. Peden, S.E. Barlow, J.W. Hoard, D.-H. Kim, J.-H. Kwak, M.L. Balmer-Millar, A.G. Panov, S.J. Schmieg, J. Szanyi, and R.G. Tonkyn, "Selective Reduction of NO_x in Oxygen Rich Environments with Plasma-Assisted Catalysis: Catalyst Development and Mechanistic Studies", Proceedings of the 9th DEER Workshop, Newport, RI, August, 2003.
5. J.W. Hoard, D.J. Brooks, S.J. Schmieg, C.H.F. Peden, S.E. Barlow, R.G. Tonkyn, and F. Beier, "Dynamometer Evaluation of Plasma-Catalysis for Diesel NO_x Reduction", Proceedings of the 9th DEER Workshop, Newport, RI, August, 2003.
6. K.G. Rappe, J.W. Hoard C.L. Aardahl, P.W. Park, C.H.F. Peden, and D.N. Tran, "Combination of Low and High Temperature Catalytic Materials to Obtain Broad Temperature Coverage for Plasma-Facilitated NO_x Reduction", Catalysis Today 89 (2004) 143-150.
7. J.-H. Kwak, J. Szanyi, and C.H.F. Peden, "Non-thermal Plasma-Assisted Catalytic NO_x Reduction over Alkali and Alkaline Earth Ion Exchanged Y,FAU Zeolites", Catalysis Today **89** (2004) 135-141.
8. T.M. Orlando, A. Alexandrov, A. Lesbak, J. Herring, M. Saxon, and J.W. Hoard, "The Reactions of NO_2 and CH_3CHO with Na-Y Zeolite and the Relevance to Plasma-Activated Lean-NO_x Catalysis", Catalysis Today **89** (2004) 151-158.
9. S.J. Schmieg, B.K. Cho, and S.H. Oh, "Selective Catalytic Reduction of Nitric Oxide with Acetaldehyde over NaY Zeolite Catalyst in Lean Exhaust Feed", Applied Catalysis B **49** (2004) 113-125.
10. J. Szanyi, J.H. Kwak, C.H.F. Peden, "The Effect of H_2O on the Adsorption of NO_2 in Na- and Ba-Y,FAU Zeolites: A Combined FTIR and TPD Investigation", J. Phys. Chem. B **108** (2004) 3746-3753.
11. J. Szanyi, J.H. Kwak, R. Moline, C.H.F. Peden, "Adsorption, Coadsorption and Reaction of Acetaldehyde and NO_2 on Na-Y,FAU: An *in situ* FTIR Investigation", J. Phys. Chem. B **108** (2004) 17050-17058.
12. H. Zhao, R.G. Tonkyn, S.E. Barlow, C.H.F. Peden, and B.E. Koel, "Fractional Factorial Study of HCN Removal over a 0.5% Pt/Al_2O_3 Catalyst", Chemical Engineering Journal, submitted for publication.
13. H. Zhao, R.G. Tonkyn, S.E. Barlow, B.E. Koel, and C.H.F. Peden, "Removal of HCN by Oxidation over a 0.5% Pt/Al_2O_3 Catalyst. Part 1: N_2O, NO, NO_2, and HCN Adsorption and Co-Adsorption on Pt/Al_2O_3", Journal of Catalysis, submitted for publication.
14. H. Zhao, R.G. Tonkyn, S.E. Barlow, B.E. Koel, and C.H.F. Peden, "Removal of HCN by Oxidation over a 0.5% Pt/Al_2O_3 Catalyst. Part 2: Reaction between HCN and O_2 on Pt/Al_2O_3 and Effects of Co-Feeding C_3H_6, Water, NO, and NO_2", Journal of Catalysis, submitted for publication.
15. J. Szanyi, J.H. Kwak, S. Burton, J.A. Rodriguez, C.H.F. Peden, "Characterization of NO_x Species in Dehydrated and Hydrated Na- and Ba-Y,FAU Zeolites Formed in NO_2 Adsorption", J. Electron. Spectrosc. Rel. Phenom., submitted for publication.
16. J. Szanyi, J.H. Kwak, C.H.F. Peden, "The Catalytic Chemistry of $HCN+NO_2$ over Na- and BaY,FAU: An *in situ* FTIR and TPD/TPR Study", J. Phys. Chem. B, submitted for publication.

II.B.10 Mechanisms of Sulfur Poisoning of NO_x Adsorber Materials

Do Heui Kim, Ya-Huei Chin, George Muntean, Chuck Peden (Primary Contact)
Pacific Northwest National Laboratory
P.O. Box 999, MS K8-93
Richland, WA 99352

DOE Technology Development Manager: Ken Howden

CRADA Partners:
Cummins Engine Company - Randy Stafford, John Stang, Alex Yezeretz, Bill Epling, Neal Currier Johnson Matthey - Hai-Ying Chen, Howard Hess, Oferi Kresnawahjuesa, Dave Lafyatis

Objectives

- Develop and apply characterization tools to probe the chemical and physical properties of NO_x adsorber catalyst materials for studies of deactivation due to sulfur poisoning and/or thermal aging. Utilize this information to develop mechanistic models that account for NO_x adsorber performance degradation.
- Develop protocols and tools for failure analysis of field-aged materials.
- Provide input on new catalyst formulations; verify improved performance through materials characterizations and laboratory and engine testing.

First Year Goals

- Identify which Pacific Northwest National Laboratory (PNNL) characterization tools can be most useful to study catalyst material property changes that result from:
  - Thermal aging
  - Sulfur adsorption and removal
- Develop capability for performance testing of materials exposed to specific 'aging' conditions.
- Correlate characterization and performance testing data to identify different behavior of model and representative catalysts as a function of the thermal and sulfur 'aging'.
- Initiate preparation of some catalyst materials with known history to baseline above results.

Approach

- In collaboration with Johnson Matthey researchers, synthesize and process (via various thermal aging and SO_2 treatment protocols) model and representative NO_x adsorber materials.
- Utilize PNNL's state-of-the-art surface science and catalyst characterization capabilities, such as x-ray diffraction (XRD), transmission electron microscopy (TEM)/energy dispersive spectroscopy (EDS), x-ray photoelectron spectroscopy (XPS), temperature-programmed desorption (TPD)/thermal gravimetric analysis (TGA), and Brunauer-Emmett-Teller (BET)/pore size distribution, as well as performance testing facilities to examine the NO_x storage chemistry and deactivation mechanisms on the model and more representative materials.

Accomplishments

- Initiated project with two catalyst samples provided by Johnson Matthey. These materials were a 'model' $Pt/BaO/Al_2O_3$ material and a more 'representative' sample. The catalysts were further 'aged' at PNNL at high temperatures and by exposure to sulfur (SO_2).
- Constructed a laboratory microcatalytic reactor for measuring NO_x storage activity and for following detailed kinetics under transient lean-rich cycling conditions.

- Have applied a considerable number of catalyst characterization techniques, including XRD, TEM/EDS, XPS, and TPD and temperature-programmed reaction (TPRX), to the two catalysts 'as received' and 'processed'.
- Considerable differences were noted in the material properties of the 'model' and 'representative' samples with respect to high-temperature and sulfur 'aging'.
- A considerable amount of 'cyclic' NO_x performance data has been obtained, and these results are being correlated with catalyst material properties.

Future Directions

- A detailed, proprietary milestone schedule for the second year of the project has been developed and agreed to by the CRADA participants. These milestones relate to planned experiments aimed at understanding sulfur poisoning and thermally-induced deactivation.
- Identify the mechanisms of sulfur poisoning by investigating the amount and type of sulfur deposited on the catalyst surface as a function of exposure time using the characterization techniques established in the first phase of the project.
- Investigate de-sulfation processes for effects on performance and materials properties.
- Identify the mechanisms of thermal degradation of Johnson Matthey supplied materials by correlating performance measurements with changes in the material properties.
- Quantify the kinetics of thermal deactivation as measured by changes in the material properties.

Introduction

The NO_x adsorber (also known as lean-NO_x trap – LNT) technology is based upon the concept of storing NO_x as nitrates over storage components, typically barium species, during a lean-burn operation cycle and then reducing the stored nitrates to N_2 during fuel-rich conditions over a precious metal catalyst. This technology has been recognized as perhaps the most promising approach to meet stringent NO_x emission standards for heavy-duty diesel engines within the Environmental Protection Agency's (EPA's) 2007/2010 mandated limits. However, problems arising from either or both thermal and SO_2 deactivation must be addressed to meet durability standards. Therefore, an understanding of these processes will be crucial for the development of LNT technology.

This project is focused on the identification and the understanding of the important degradation mechanism(s) of the catalyst materials used in LNTs. A model $Pt/BaO/Al_2O_3$ sample and more representative samples are being investigated. In particular, the changes in physicochemical properties related to the reaction performances of these LNT materials, due to the effects of high-temperature operation and sulfur poisoning, are the current focus of the work.

Approach

In a newly built microcatalytic reactor system, LNT performance is evaluated in a fixed bed reactor operated under continuous lean-rich cycling. In addition, material treatments such as SO_2 aging and post mortem catalyst characterizations are conducted in the same test stand without exposing the catalyst sample to air. We have established a reaction protocol which evaluates the performance of samples after various thermal aging and sulfation conditions. In this way, we are able to identify optimum de-sulfation treatments to rejuvenate catalyst activities.

In addition, state-of-the-art catalyst characterization techniques such as XRD, XPS, TEM/EDS, BET/pore size distribution, and TPD/TPRX were utilized to probe the changes in physicochemical properties of the catalyst samples under deactivating conditions, *e.g.*, thermal aging and SO_2 treatment. Specifically, H_2 TPRX (temperature-programmed reaction), NO_2 TPD and XPS methods were used extensively to quantify the levels, speciation and distribution of sulfur on the adsorber material as a function of exposure time.

By comparing model $Pt/BaO/Al_2O_3$ with representative materials, we try to understand the role of various additives on the deactivation processes. However, this report covers only the results obtained to date on the model $Pt/BaO/Al_2O_3$ materials for proprietary reasons. In addition, in order to investigate the thermal properties of barium species in detail, we made a reference BaO/Al_2O_3 sample and applied it to many established techniques.

Results

Reactor and Performance Measurement Protocols

Figure 1a is a schematic of a newly constructed microreactor developed for performance measurements on LNT materials for this project. Rapid lean-rich switching is enabled just prior to the elevated temperature zone (furnace) where the LNT materials are contained in quartz tubing. After removing water, the effluent of the reactor can be analyzed by mass spectrometry, gas chromatography, and by a chemiluminescent NO_x analyzer. A typical baseline performance testing protocol is illustrated in Figure 1b. In this case, the sample is heated to a reaction temperature in flowing He, the feed switched to a 'lean-NO_x' mixture containing oxygen and NO as well as CO_2 and/or H_2O. After an extended period (15 minutes or more), multiple rich/lean cycles of 1- and 4-minute duration, respectively, are run, and NO_x removal performance is assessed after at least three of these are completed. In the LNT technology, the state of the system is constantly changing so that performance depends on when it is measured. As such, we measure NO_x removal efficiencies in at least three different ways as illustrated in Figure 1b. "Lean conversion (4 minutes)" and "lean conversion (30 minutes)" measure NO_x removal efficiencies for the first 4 minutes and first 30 minutes of the lean period, respectively. "Overall conversion" measures NO_x removal efficiencies for the 1-minute rich period plus the first 4 minutes of the lean period.

Effect of Thermal Aging and SO_2 Aging

The results obtained in the first year of this project indicated that thermal aging gave rise to the formation of a $BaAl_2O_4$ phase, formed from a

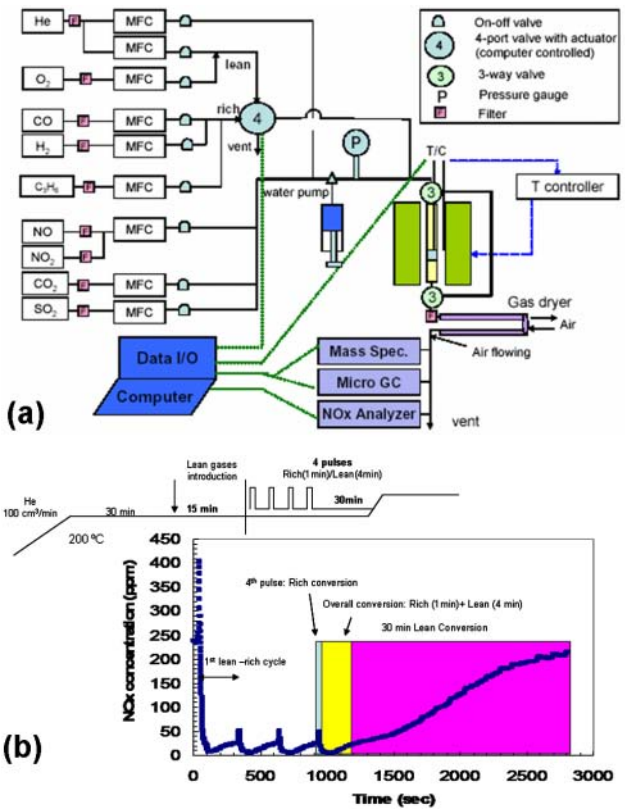

Figure 1. (a) A schematic of the microreactor constructed for this project's studies, and (b) a common reaction protocol used here along with example data where the performance assessments are defined.

dispersed BaO or $BaCO_3$ phase, and a dramatic increase in the size of Pt metal particles. These conclusions were based on detailed XRD and TEM studies. Moreover, the extent of the physicochemical changes varied as a function of the formulation of the samples. Figure 2 shows the NO_x conversion as a function of temperature for the model $Pt/BaO/Al_2O_3$ samples calcined at 500°C for 3 hrs (as-calcined) and 900°C for 10 hrs (900°C). Compared with as-calcined sample, which exhibits high activities over a wide range of temperatures between 300°C and 450°C, the thermally aged sample displays a dramatic decrease in activity (by more than 50%). A "representative" sample showed higher conversion than the "model" one after the same thermal aging process (data not shown in this report).

After SO_2 'aging' of the catalyst, sulfur exists in the form of sulfate based on XPS analysis. NO_x storage activity measurements indicate a strong suppression of performance with increasing amounts

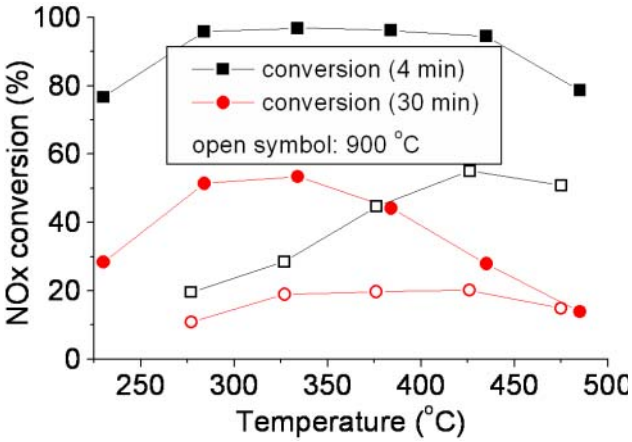

Figure 2. NO_x conversion of model $Pt/BaO/Al_2O_3$ catalysts calcined at 500°C for 3 hrs (as-calcined) and 900°C for 10 hrs (900°C). Lean (4 min) and lean (30 min) conversions are defined in Figure 1.

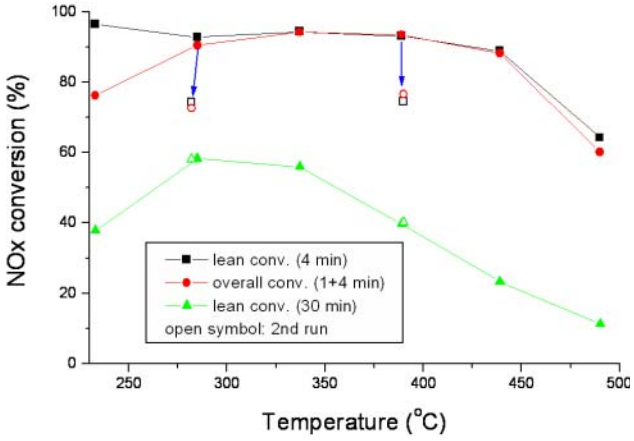

Figure 3. NO_x conversion of model $Pt/BaO/Al_2O_3$ catalysts after light sulfation. The open symbol indicates a 2nd performance measurement at the indicated temperature after completing a 1st set of measurements from 200°C to 450°C.

of SO_2. Figure 3 shows the NO_x conversion of the "model" sample after being lightly sulfated. The 1st run indicates little, if any, change in the conversion. However, remeasuring performance after completing a first set of runs from 200°C to 450°C reveals a significant decrease in activity, perhaps caused by a redistribution of sulfur species during the reaction. Similar to thermal aging, a "representative" sample displayed higher conversions than the "model" one after SO_2 'aging' (not shown).

Our studies are aimed at identification of the mechanisms of sulfur poisoning for the LNT catalysts. After sulfating the catalyst with different amounts of sulfur, H_2 TPRX, NO_2 TPD and XPS were used to obtain information about levels, speciation and distribution of sulfur, and their effects on NO_x adsorption/desorption chemistry as a function of sulfur exposure. Depending on the degree of sulfation, the sulfur species are present in a combination of both easily desorbed weakly bound and strongly bound forms, both most likely in the form of sulfates. The relative concentration of each species and the recovery of NO_x conversion performance after de-sulfation were found to depend on the SO_2 exposure time.

Segregation of BaO/Al_2O_3 upon H_2O Contact

Recently, a group at Ford research labs [1] reported that Ba^{2+} ions in a $BaAl_2O_4$ phase, formed by high-temperature calcination, leached out from the alumina support material to form a crystalline $BaCO_3$ phase upon contact with H_2O, probably due to an interaction of carbonic ions dissolved in liquid H_2O. However, as shown in the XRD patterns of Figure 4, we find that, irrespective of the initial barium phase (highly dispersed BaO and/or $BaCO_3$, or $BaAl_2O_4$), liquid H_2O treatment at room temperature facilitates segregation of Ba from the Al_2O_3 support to produce large crystallites of $BaCO_3$. The segregation process at the microstructural level is clearly demonstrated in the TEM micrographs of Figure 5, where two distinctly different and distinguishable phases exist. EDS analysis indicates that two phases are aluminum oxide (A) and barium-containing (B), respectively. This finding may have considerable relevance to the practical NO_x trap system, since H_2O condensation is known to regularly occur in exhaust systems during start-up and shut-down of the engine [1].

Another important implication of our findings is relevant to the synthesis of NO_x trap catalysts. Commonly, the conventional incipient wetness impregnation method is used to sequentially add Pt to alumina-supported baria [2,3]. During the Pt deposition step from an aqueous solution, the $BaO-Al_2O_3$ material is unavoidably in contact with liquid water, leading to formation of Ba species that are different from Pt-free Ba samples.

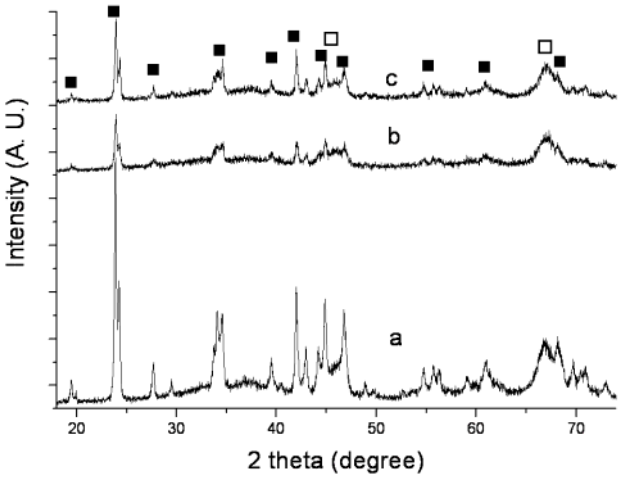

Figure 4. XRD patterns of H_2O-treated 20 wt% BaO/Al_2O_3 samples pre-calcined at 500 °C (a), 900 °C (b) and 1000 °C (c). (solid squares: $BaCO_3$, open squares: γ-Al_2O_3)

New Reaction Protocol to De-couple the Thermal Aging and De-sulfation

In order to regenerate the LNT catalysts to remove sulfate species that poison the material, a high-temperature de-sulfation process is required. Physical and chemical property changes in the material due to removal of sulfates and/or due to the required high temperatures of de-sulfation are unavoidable. Thus, there is a trade-off in regenerating activity by removing the sulfur species while, on the other hand, potentially decreasing it due to thermal deactivation. Furthermore, it becomes difficult to distinguish what is responsible for deactivation in this case. Therefore, a reaction protocol was established to de-couple these two effects. After running the reaction in the presence or absence of SO_2, the catalyst was treated at higher temperature, followed by a 2nd evaluation of the activity without SO_2. Comparison of the activities with/without SO_2 and before/after the heat treatment allowed us to estimate the contribution to the activity changes from the two potential sources of deactivation. In addition, post-reaction analysis gave important clues to understand the deactivation process in more detail. Importantly, it was found that SO_2 poisoning and thermal treatment deactivated the catalyst to different extents depending on the catalyst formulation.

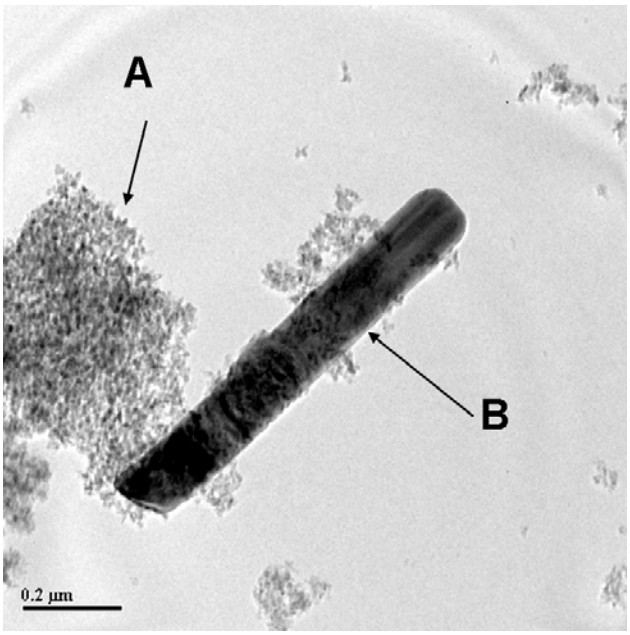

Figure 5. TEM micrograph of a H_2O-treated BaO/Al_2O_3 sample calcined at 1000°C. The particle labeled "A" contains predominantly Al while the "B" particle is Ba rich.

Conclusions

PNNL and its CRADA partners from Cummins Engine Company and Johnson Matthey have undertaken a project to study the mechanisms of deactivation of the materials proposed for use in lean NO_x traps arising from thermal aging and SO_2 poisoning. Results demonstrate that thermally aged and heavily sulfated representative samples showed higher activities than aged model materials, and these differences in performance could be correlated with changes in their respective material properties. H_2O treatment gave rise to the segregation of barium carbonates from the alumina support irrespective of the initial phase (e.g., highly dispersed barium carbonate and barium aluminate). The observed phenomena imply that special care must be taken during catalyst synthesis and during realistic operation of $Pt/BaO/Al_2O_3$ NO_x trap catalysts since both processes involve potential exposure of the material to liquid H_2O. An experimental protocol to decouple de-sulfation and thermal deactivation was developed. By using the protocol, it was found that sulfur poisoning and thermal treatment both led to deactivation of the studied LNT materials, but to different extents depending on the formulation.

Special Recognitions and Awards/Patents Issued

1. 2004 Advanced Combustion Engine R&D Special Recognition Award "For technical excellence and admirable collegiality in inter-laboratory collaborative research".

FY 2004 Publications/Presentations

1. D.H. Kim, Y.-H. Chin, G.G. Muntean, and C.H.F. Peden, "Effect of Thermal Aging and SO_2 Treatment on the Physicochemical Properties of NO_x Adsorber Materials, presentation at 2003 National Laboratory Catalysis Conference, Oak Ridge, TN, October, 2003.
2. D.H. Kim, Y.-H. Chin, G.G. Muntean, C.H.F. Peden, N. Currier, B. Epling, R. Stafford, J. Stang, A. Yezerets, H.-Y. Chen, H. Hess, and D. Lafyatis, "Mechanisms of Sulfur Poisoning of NO_x Adsorber Materials", presentation at the DOE Combustion and Emission Control Review, Argonne, IL, May, 2004.
3. Y.-H. Chin, D.H. Kim, G.G. Muntean, C.H.F. Peden, L.C. Broering, R.J. Stafford, J.H. Stang, H. Chen, B. Cooper, H. Hess, and D. Lafyatis, "Mechanisms of Sulfur Poisoning of NO_x Adsorber Materials", in *Combustion and Emission Control for Advanced CIDI Engines: 2003 Annual Progress Report*, pp. 141-145.
4. D. H. Kim, Y.-H. Chin, J.-H. Kwak, J. Szanyi, and C.H.F. Peden, "Segregation of Ba Phase in BaO/Al_2O_3 upon H_2O Treatment", Gordon Conference on Catalysis, New London, NH, June 2004.

References

1. G.W. Graham, H.-W. Jen, J.R. Theis, R.W. McCabe, Catal. Lett. 93 (2004) 3.
2. L. Olsson, E. Fridell, J. Catal. 210 (2002) 340.
3. G.E. Arena, A. Bianchini, G. Centi, F. Vazzana, Topics in Catal. 16/17 (2001) 157.

II.B.11 Characterization of Adsorber Chemistry for LNT Catalysts, DOE Pre-Competitive Catalyst Research

Todd J. Toops (Primary Contact), D. Barton Smith, W. William Partridge, Jim E. Parks
Oak Ridge National Laboratory
2360 Cherahala Blvd.
Knoxville, TN 37932

DOE Technology Development Manager: Ken Howden

Objectives

- Quantify model lean NO_x trap (LNT) catalyst storage behavior between 150 and 400C to identify key reaction steps for simulation and engine optimization.
- Investigate regeneration behavior of model LNT catalysts.
- Inspect thermal deactivation effects with respect to NO_x capacity, surface area losses, and precious metal sintering.
- Investigate the poisoning effects of sulfur, the desulfation requirement of each model catalyst, and the relationship between desulfation and thermal deactivation and overall catalyst aging.

Approach

- Effort is pre-competitive for easy dissemination of results to industry.
- Test model powder catalysts indicative of LNT technology.
  - $Pt/K/Al_2O_3$: 1% Pt, 8% K_2CO_3 on Al_2O_3
  - $Pt/Ba/Al_2O_3$: 1% Pt, 20% BaO on Al_2O_3
  - 50-100 g Pt/ft^3 equivalent
- Analyze surface species for validation of chemical behavior using Oak Ridge National Laboratory's (ORNL's) powerful barrel ellipse diffuse reflectance infrared Fourier-transform spectroscopy (DRIFTS) reactor.
- Measure aging effects with respect to Pt size, catalyst surface area, and NO_x capacity using high-temperature treatments up to 900C while cycling between characteristic lean and rich conditions.
- Disseminate results openly to guide and validate modeling efforts and to immediately affect engine controls.

Accomplishments

- Conducted full investigation of storage behavior at 150-450C; the results were immediately applied to ORNL's global model.
  - Quantified DRIFT spectroscopy at all temperatures.
  - Identified kinetic limitations for LNTs at 150C.
  - Characterized thermodynamic limitations above 400C.
- Identified limitations during catalyst regeneration and verified the importance of including H_2O in all valid simulated exhaust experiments.
- Developed unique reactor for simultaneous surface observation and kinetic measurements, which will be used to elucidate key steps of NO_x reduction to benign N_2.

- Developed testing procedure for measuring thermal deactivation that simulates 400,000 miles of operation in a 15-hour test.
  - Demonstrated 65% less storage capacity for model catalysts at 760C.
  - Demonstrated 50-90% loss in capacity at 900C.
- Demonstrated poisoning effects of sulfur in model LNT catalysts using a test procedure that simulates 126,000 miles of operation.
  - Observed complete loss of capacity for both model catalysts.
  - Desulfurization under rich conditions recovered 75% of capacity.

Future Directions

- Elucidate chemistry of catalyst regeneration with unique flow-through DRIFTS reactor. Include O_2 as a variable in regeneration investigation (2003 feedback).
- Elucidate sulfur-based deactivation mechanisms and chemistry.
  - Determine chemical form of sulfur-based species.
  - Elucidate the desulfation temperatures for each species.
  - Evaluate intermediate species formations to determine chemistry.
- Establish DRIFTS reactor system to axial analyze washcoated substrate samples *in-situ*. Work with Englehard to use realistic systems that model a working channel of a catalyst.

Introduction

Under future vehicle regulations, the efficiency of a diesel engine system will be correlated to the efficiency of the catalyst system since a fuel penalty is sustained to achieve the emissions requirements. Therefore, it is essential to have an efficiently functioning catalyst system in operation with a diesel engine. Modeling/simulating processes is an effective way to develop efficient systems, and basing the model on fundamental chemistry is critical for it to be transportable and broadly useful to industry; parametric-based models will not fill the need.

The emphasis of this project is to improve detailed understanding of mechanisms limiting catalyst performance by working closely with catalyst industry representatives to identify and investigate pre-competitive catalyst performance issues of broad relevance across the catalysis industry. A specific objective is to improve the fundamental understanding of adsorption, reduction, poisoning processes and the influence of catalyst morphology. The objectives of this project are consistent with those of the Diesel Cross-Cut Team regarding details of sulfur poisoning and catalyst morphology effects.

Approach

Several efforts previously investigated under the Cummins/ORNL Cooperative Research and Development Agreement (CRADA) which are pre-competitive have been transferred to this project. This allows open dissemination of those research results without confusing issues of CRADA-protected information and frees up CRADA funds to investigate protected topics. The transferred efforts are primarily in the optical spectroscopy areas. Nevertheless, the two projects will continue to work closely to address both competitive and pre-competitive research issues.

ORNL will perform analysis of selected model catalyst samples with a focus on in-situ measurements in bench-scale reactors to elucidate catalyst chemistry. Emerachem will provide in-kind support to the project including catalyst sample preparation and personnel to co-direct the project.

Results

Based on the full analysis of DRIFTS data between 150 and 400C, a storage mechanism has been proposed. NO can adsorb onto K-LNT only through the initial formation of a nitrite (NO_2^-) on a

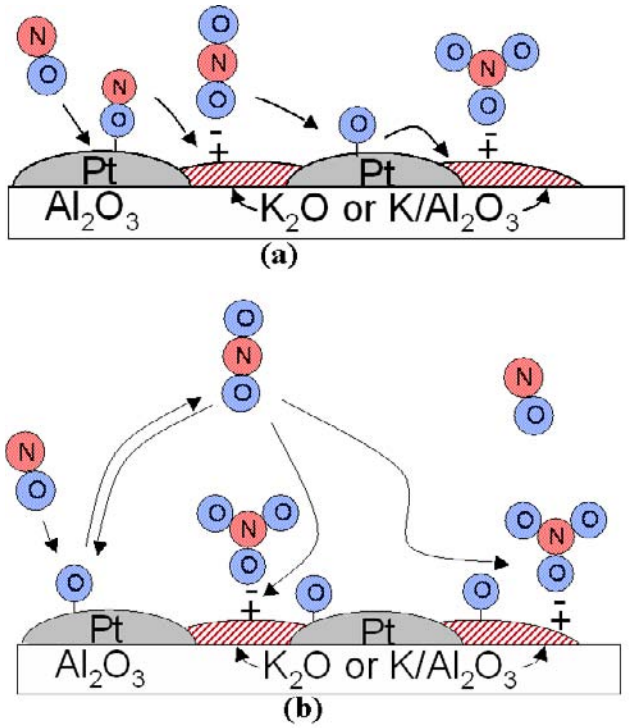

Figure 1. Key Steps in $Pt/K/Al_2O_3$ Storage (a) Route of adsorption for NO that is not oxidized to NO_2, but requires an adjacent Pt site; typically only significant below 200C. (b) Route of adsorption for NO_2 through either a "spillover" mechanism where it is adsorbed adjacent to a Pt site, or a disproportionation reaction where two molecules from a nitrate desorb an NO molecule; these routes dominate above 200C.

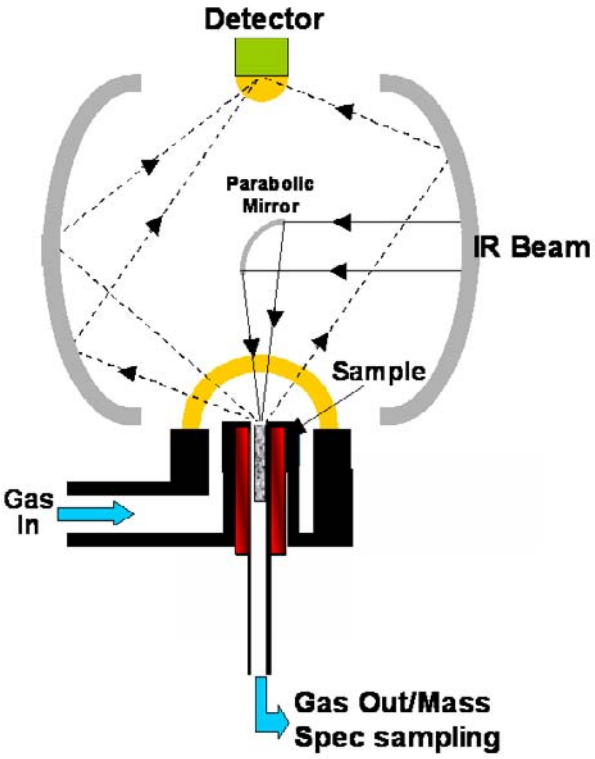

Figure 2. Newly Developed Flow-Through Packed Bed/ Plug Flow DRIFTS Reactor

K site near Pt. This nitrite can be further oxidized to form an ionic nitrate (NO_3^-). The NO storage route is only of significance below 200C, where Pt activity for NO oxidation to NO_2 is low. This is graphically depicted in Figure 1a. Once NO is oxidized to NO_2, it can adsorb readily on K-LNT through a "spillover" step near a Pt site or through a two-step disproportionation reaction on the K-phase. Both of these steps are depicted in Figure 1b. These results have been used in the model being developed at ORNL.

To better understand the chemistry that occurs during the regeneration of the catalyst, the DRIFTS system was modified to allow meaningful kinetic information to be gathered at the same time as surface spectra. The reactor is equipped with 3 inches of heated length exposed on the front edge for DRIFTS measurements, as depicted in Figure 2. The plug flow reactor is a classical kinetic regime with well-defined rate equations. The combination of this reactor with the surface measurements provided by DRIFTS offers a powerful and unique tool for fundamental studies.

A full array of thermal deactivation experiments was performed. Model K- and Ba-based LNTs were studied to determine the effects associated with exposing the catalyst to elevated temperatures. The catalysts were sequentially heated to 500C, 600C, 760C, and 900C with catalyst evaluation after each temperature. A 15-h test at 760C represents approximately 400,000 miles of driving. The test procedure was based on the initial feedback of the industrial survey for the Rapid-Aging Protocol. The results of these experiments are shown in Figure 3a for the K-LNT and Figure 3b for Ba-LNT. It is evident that catalyst function can be maintained at a significant level after heating up to 760C for both catalysts, but the catalysts, the Ba-LNT in particular, incur dramatic losses after 900C.

A complete series of sulfur poisoning experiments on model $Pt/K/Al_2O_3$ and $Pt/Ba/Al_2O_3$ catalysts was fully quantified and analyzed. The

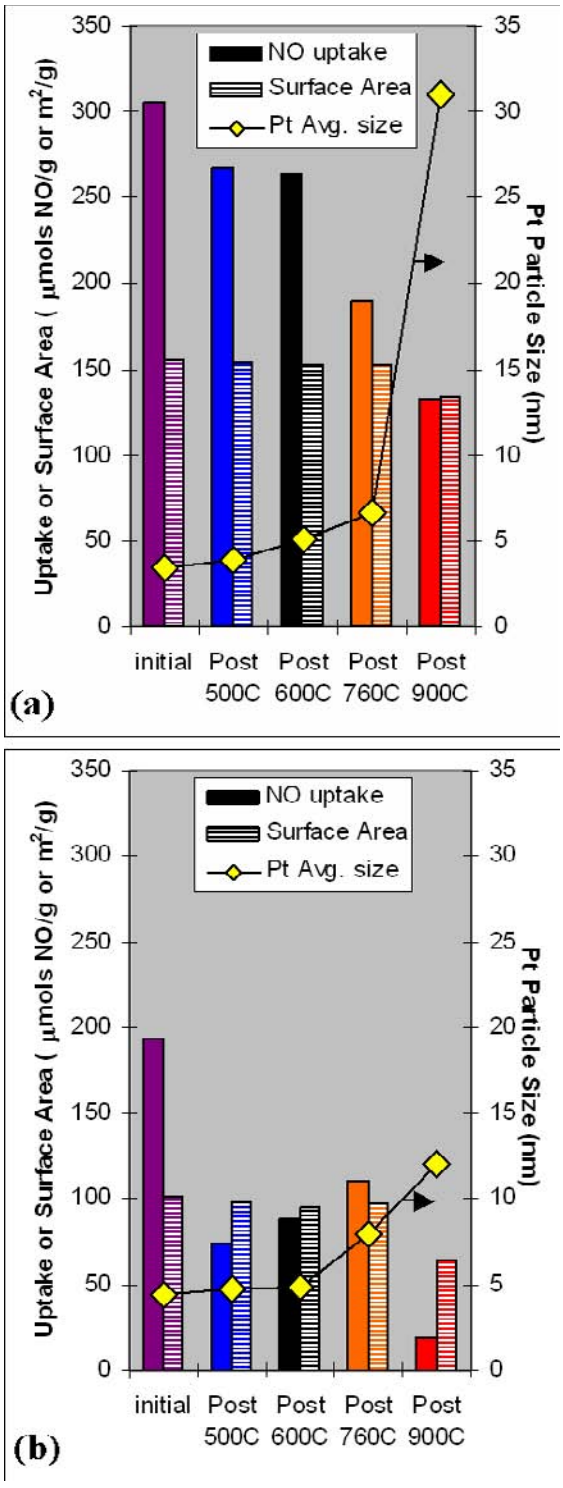

Figure 3. Thermal Deactivation Effects Associated with Operating (a) a K-based LNT and (b) a Ba-based LNT. NO uptake experiments were performed at 250°C, total surface area was determined using liquid N_2 BET, and average Pt size was estimated with H_2-O_2 titration experiments at 25°C.

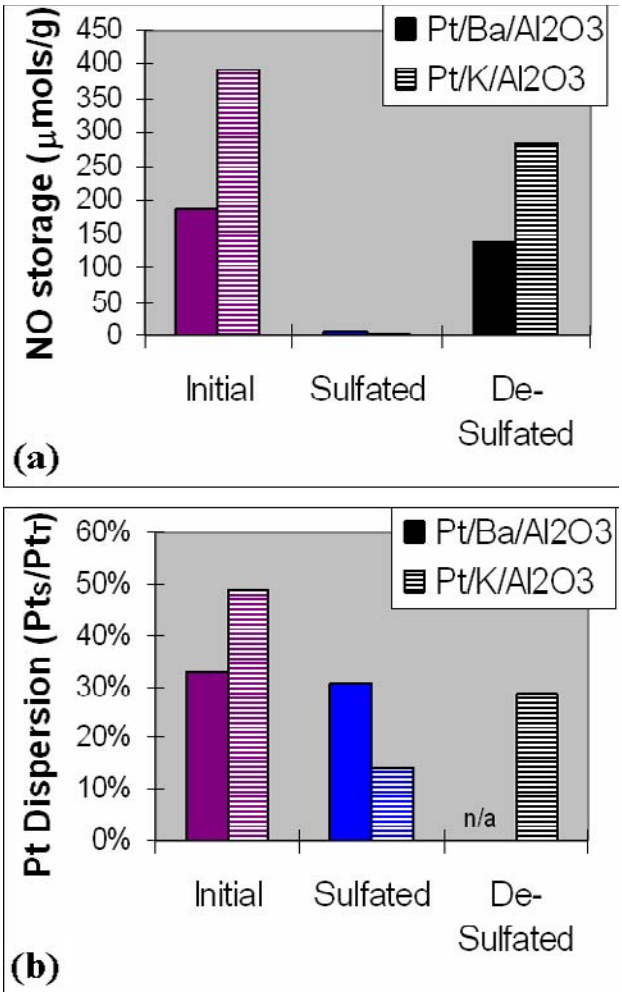

Figure 4. Effect of SO_2 and Its Subsequent Desulfation at 760C with Respect to (a) NO_x Storage Capacity at 250C and (b) Exposed Pt Surface Atoms

catalysts were poisoned with 140 ppm SO_2 at 250C for 24 hours, and then desulfated up to 760C. This is an extreme sulfur condition but represents an LNT that has been fully poisoned after approximately 100,000 miles of driving. Figure 4a shows that the sulfur treatment causes the NO_x storage capacity to diminish by 97% and 99% for Pt/Ba/Al_2O_3 and Pt/K/Al_2O_3, respectively. Effects on Pt were also monitored (Figure 4b), and interestingly, the Pt on the K-based LNT was affected by SO_2 but not the Pt on the Ba-based LNT. This suggests that the potassium sulfate phase may grow to the point that it covers some of the Pt that is on the Pt/K/Al_2O_3 catalyst. Future DRIFTS experiments will help to elucidate this phase-change effect.

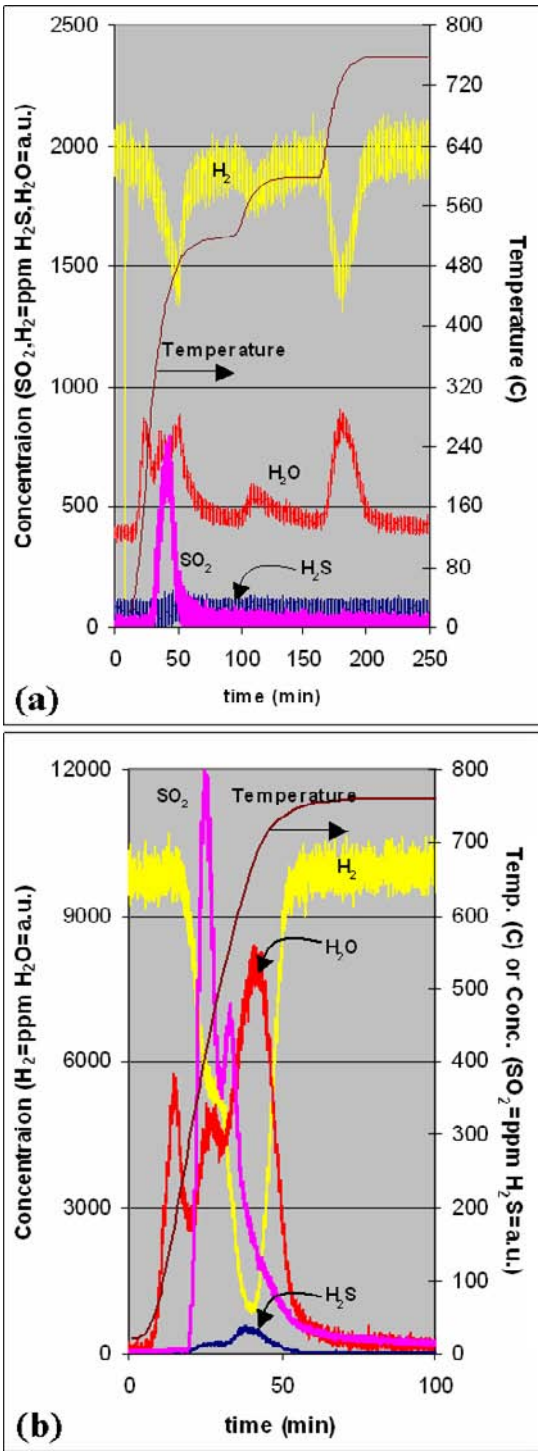

Figure 5. Desulfation of (a) $Pt/Ba/Al_2O_3$ and (b) $Pt/K/Al_2O_3$ for Heating up to 760C

Desulfation under rich conditions of the $Pt/Ba/Al_2O_3$ released a significant amount SO_2 between 250 and 500C, but virtually no H_2S was observed, as shown in Figure 5a. Post desulfation, the storage capacity was 25% less than the initial measurement.

Desulfation of the $Pt/K/Al_2O_3$ occurred in two phases, as indicated in Figure 5b. Most of the S was removed as SO_2 with peak at 435C, but a second release of SO_2 was also observed between 500 and 760C, with a peak at 575C. In conjunction with the release of SO_2 was the formation of H_2S, with an initial peak at 400C and a second, more substantial peak at 650C. Post desulfation, the storage capacity for $Pt/K/Al_2O_3$ has also decreased by 27% of the initial measurement.

These results from the deactivation studies correspond well with the observations from engine work. This suggests that a detailed kinetic and chemical analysis of the model catalysts will correspond well with real catalyst-engine combinations. The continuing effort in FY 2005 will focus on identifying the pathway that leads to deactivation of these representative model catalysts.

Conclusions

- DRIFTS measurements at 150-450C led to significant mechanistic findings for NO_x storage.
  - NO is only significantly adsorbed on sites near Pt.
  - NO_2 is not adsorbed as a nitrite.
  - NO_2(g) can adsorb readily with/without Pt present.
- At an equivalence of 400,000 miles, exposure of the catalyst at 760C results in a 65% loss in capacity and about a 50% loss in precious metal surface area.
- A temperature of 900C must be avoided due to extreme degradation of capacity (50-90%) and a 90% loss of precious metal surface area.
- Sulfur is a severe catalyst poison that, if unchecked, may render the catalyst inoperable after 100,000 miles.
- Extreme thermal treatments in rich conditions can reverse the poisoning effects of sulfur, but losses will be incurred as demonstrated in the thermal deactivation experiements.

FY 2004 Publications/Presentations

1. TJ Toops, DB Smith, WS Epling, JE Parks, WP Partridge, "Quantification of the *in-situ* DRIFT Spectra of Pt/K/gamma-Al_2O_3 NO_x Adsorber Catalysts", Applied Catalysis B Environmental, in print.

2. TJ Toops, DB Smith, WS Epling, JE Parks, WP Partridge, "Quantified NO_x Adsorption on Pt/K/gamma-Al_2O_3 and the Effects of CO_2 and H_2O", Applied Catalysis B Environmental, in print.
3. TJ Toops, DB Smith, WP Partridge, "NO_x Adsorption of Pt/K/Al_2O_3 in the Presence of CO_2 and H_2O: an *in-situ* DRIFTS Study", National Laboratory Catalysis (NLCat) Conference, Oak Ridge, Tennessee, October 22-24, 2003.
4. TJ Toops, DB Smith, WS Epling, JE Parks, WP Partridge, P6-076: "Lean NO_x Trap Chemical Behavior and Thermal Deactivation Effects", 2004 DOE Advanced Combustion Review, May 18-20, 2004.
5. TJ Toops, DB Smith, WP Partridge, "Lean NO_x Trap Chemical Behavior and Thermal Deactivation Effects", Seventh DOE Crosscut Workshop on Lean Emissions Reduction Simulation (CLEERS), June 16-17, 2004.
6. TJ Toops, DB Smith, WS Epling, JE Parks, WP Partridge, P6-076: "*In-situ* DRIFTS Study of NO_x Storage on Pt/K/Al_2O_3", 13th International Congress on Catalysis, Paris, France, July 11-16, 2004.

II.B.12 Plasma-Facilitated NO_x Reduction for Heavy-Duty Diesel Emissions Control

Chris Aardahl (Primary Contact), Ken Rappe, Bob Rozmiarek, Donny Mendoza, Nathan Bauman, Jamie Holladay
PNNL
Process Science and Engineering Division
Box 999 MS K6-28
Richland, WA 99352

DOE Technology Development Manager: Ken Howden

Objectives

- Assess the ability of plasma reformers to produce oxygenates for lean NO_x catalysis from diesel-type hydrocarbons.
- Design and construct a catalyst test system capable of simulating diesel transient test cycles.

Approach

- Couple plasma reformer to lean NO_x catalyst bench.
- Run series of experiments with propene to assess correlation to plasma-catalysis data.
- Run experiments with dodecane to assess plasma reformer for diesel-like hydrocarbons.
- Assemble transient testing bench and assess ability to simulate thermal transients like those found in the heavy-duty Federal Test Procedure (FTP) cycle.
- Conduct transient experiments on NO_x catalysts to determine impact of transients on performance.

Accomplishments

- Reformation of propene coupled to a lean NO_x catalyst (Ag_xO/Al_2O_3) was consistent with prior results on plasma-catalysis indicating that formation of oxygenate species aside from the exhaust was possible. Results indicated similar fuel penalty to plasma-catalysis.
- Results on dodecane were completed, but no benefit was observed with plasma reformation. Post mortem characterization of the catalyst showed heavy coking and deactivation.
- A transient catalyst test bench was constructed and was shown capable of reproducing heavy-duty FTP thermal transients.
- NO_x reduction experiments using the transient system show good cycle average NO_x conversions, but NO_x slip is shown with rapid increases in the catalyst temperature.

Future Directions

- Project ended in FY 2004, so no further work will be undertaken.
- Work with heavy hydrocarbons shows that coking issues are the main factor limiting plasma lean NO_x. Any future efforts should focus on reduction of coking problems.
- The transient testing capability is applicable to all forms of diesel aftertreatment and will be used to support NO_x and other emissions work at Pacific Northwest National Laboratory (PNNL).

Introduction

Non-thermal plasma-assisted catalysis (PAC) is an effective method for reducing NO_x emissions in diesel exhaust; however, further advances in plasma system efficiency and catalyst development are needed for vehicle applications. Research in FY 2004 focused on the process modification where the plasma is decoupled from the exhaust. Here, plasma reformation (partial oxidation) of hydrocarbons is used to produce oxygenates and other more reactive molecules for NO_x aftertreatment catalysis in a side stream apart from the exhaust. Figure 1 shows the differences in configuration between traditional plasma-assisted catalysis and reformer (plasma)-enhanced catalysis.

A second task focused on developing an apparatus to simulate transient thermal cycles in catalysts that are representative of qualification cycles such as the FTP. This apparatus was used to characterize catalysts in transient operation, which is much more demanding than steady-state conditions.

Approach

Plasma-catalysis for NO_x reduction is a two-step process. First, the exhaust is treated in a non-thermal electrical discharge. Such treatment facilitates the conversion of NO to more reactive NO_2. In addition, a portion of hydrocarbon that is added to the stream is partially oxidized to form oxygenated species. In the second step, the plasma-treated exhaust is passed over a lean NO_x catalyst. In FY 2004, PNNL focused on a modification of traditional PAC

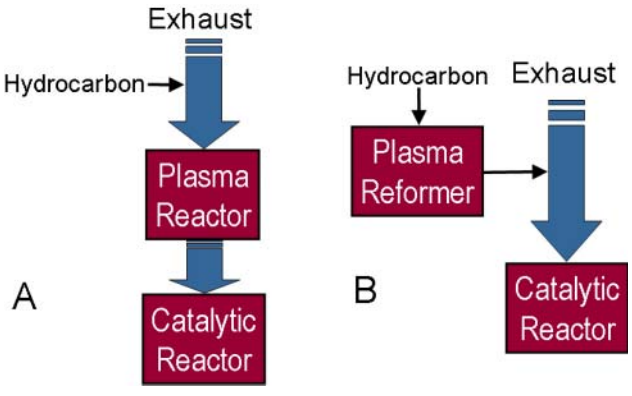

Figure 1. Configurations of the Plasma-Assisted Catalysis (A) and Plasma-Reformer Catalysis (B) Systems

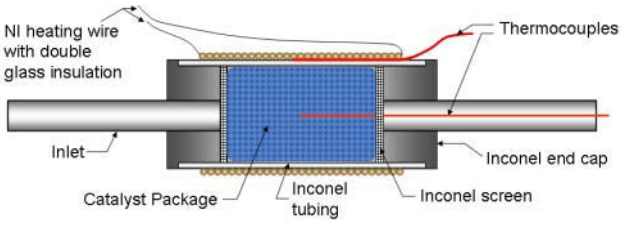

Figure 2. Transient System Test Catalyst Test Package and Accompanying Thermal Control Peripherals

(Figure 1A). In the alternate setup (Figure 1B), the plasma was removed from the exhaust line and used to treat the hydrocarbon separate from the exhaust. This treated hydrocarbon was then fed into a simulated exhaust and passed over a Ag_xO/Al_2O_3 catalyst to assess NO_x reduction levels.

For the characterization of transients in NO_x catalysts, the system in Figure 2 was designed and constructed, which enabled rapid thermal cycling of catalyst powders. The design was based on embedding a catalyst powder in a nickel or carbon foam material in a small pellet. This *catalyst package* was housed in an Inconel tube and wrapped with glass-coated nickel heating wire that was attached to a DC power supply. Thermocouples were used to monitor temperature and provide feedback to the control system for the DC supply. The small dimension and open porosity of the catalyst package allowed effective heating and reasonable pressure drop, respectively.

Results

Figures 3 and 4 present the results of plasma-reformer-assisted lean NO_x catalysis for propene and dodecane hydrocarbon feeds, respectively. In each figure, baseline refers to lean NO_x alone with no reformer assist. Curves with a ratio indicate the carbon to oxygen ratio in the reformer operating at an energy density of 6 kJ/L. Figure 3 shows substantial enhancement of NO_x conversion at lower temperatures, indicating that propene is at least partially reformed to oxygenated species. This was confirmed by independent gas chromatography-mass spectrometry (GC-MS) measurements where a variety of lighter oxygenates were produced. From the GC-MS data, it was estimated that roughly 20% of the propene was converted in the reformer. The

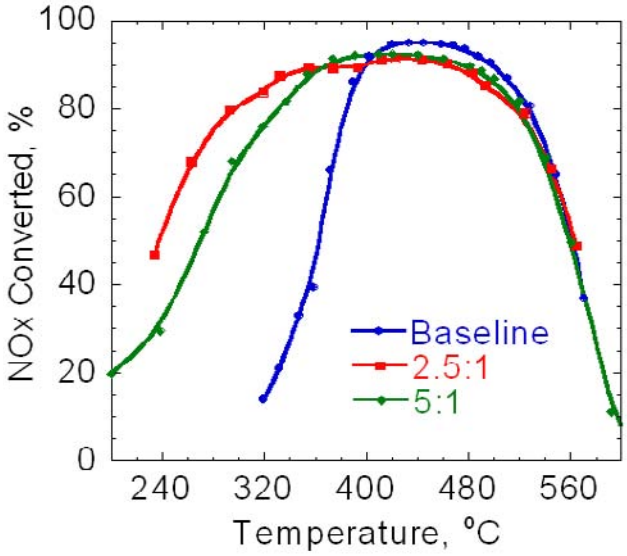

Figure 3. Results from Plasma-Reformer-Assisted Lean NO_x Catalysis with Propene

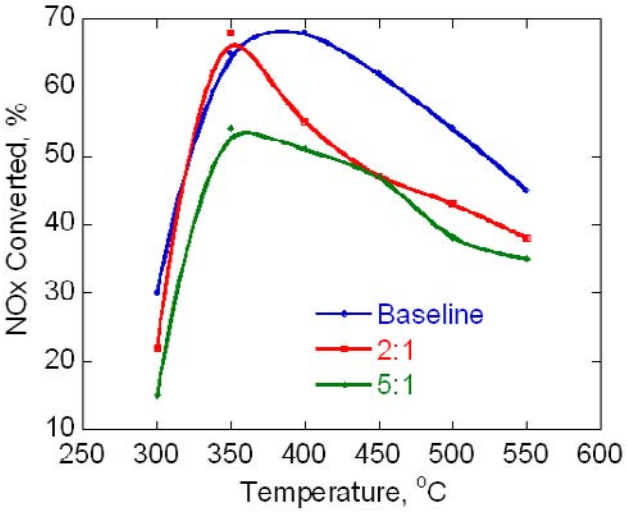

Figure 4. Results from Plasma-Reformer-Assisted Lean NO_x Catalysis with Dodecane

only penalty is that the maximum conversion (*ca.* 470°C) suffers. This is due to the fact that reformers are not perfectly selective, and the overall C_1:NO_x ratio drops compared to the baseline lean NO_x catalysis. Results on dodecane were significantly different from propene. Figure 4 shows that there is essentially no enhancement of NO_x reduction when the dodecane is reformed with plasma. GC-MS data showed that only olefins were being produced, and oxygenates were not evident. In addition, numerous

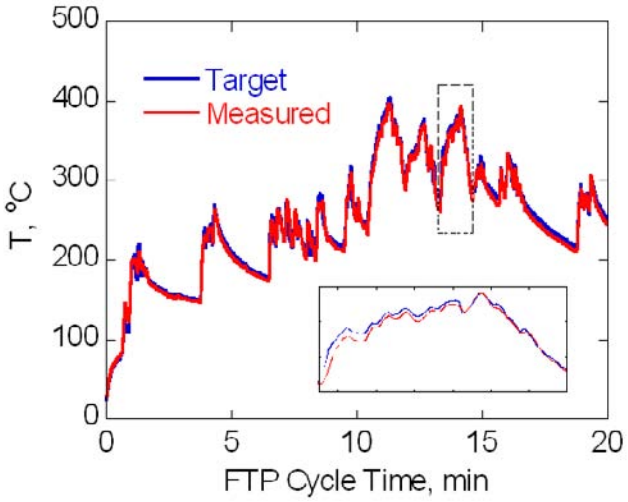

Figure 5. Typical Data Set from Transient Characterization Bench Showing Correlation of Target Temperature with Actual Temperature (Inset shows a small section of the data to indicate typical offsets)

condensation products such as aromatics and polyaromatics were produced in the plasma reformer. This fact coupled with the imperfect selectivity of the reformer explains the drop in activity. In addition to low activity levels, post mortem inspection of the catalyst showed severe coking, which was likely due to incomplete decomposition of some of the heavier species produced in the reformer.

The transient system was successfully assembled and tested. Results of the thermal matching obtained are shown in Figure 5. The target temperature was obtained from the thermal history of a typical heavy-duty FTP cycle. The internal temperature was taken from the thermocouple placed in the catalyst package. Notice the good matching across the entire FTP cycle. The inset of Figure 5 shows a close-up of the data indicating that temperature offset can be up to 5-10°C. Such small deviations from the target temperature may affect NO_x conversion slightly; however, the impact of transients on NO_x adsorption/desorption behavior should be representative. Figure 6 shows a sample of the data obtained on transient performance of the Ag_xO/Al_2O_3 catalyst. When the catalyst is heated significantly over a short duration of time, NO_x is desorbed from the surface, resulting in spikes of NO_x on the outlet of the catalyst. This is prominent in the first half of the cycle, where the

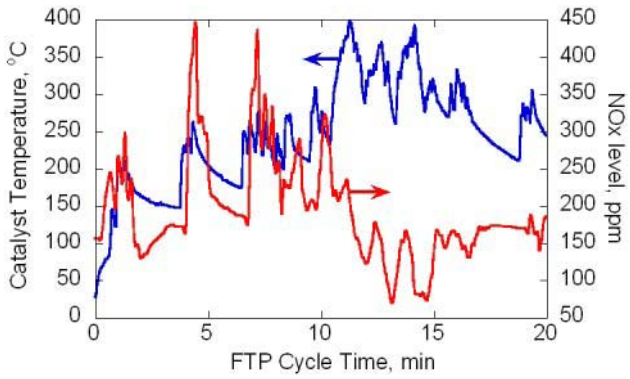

Figure 6. Impact of Transient Catalyst Operation on NO_x Reduction (Inlet NO_x concentration was 500 ppm; C_1:NO_x = 9 as propene)

catalyst temperature is lower. In the second half of the FTP, the catalyst temperature is sufficient to increase activity for NO_x reduction to the point where these spikes are diminished. Figure 6 illustrates that bench-scale transient experiments can be useful in understanding dynamic phenomena in aftertreatment catalysts.

Conclusions

Plasma-reformer lean NO_x catalysis was unsuccessful with diesel-like hydrocarbons. This was the main avenue available to lower the fuel penalty from levels of traditional plasma-catalysis. Better reformation technology for heavier hydrocarbons and development of coking-resistant catalysts could enable additional development of the technology. Development of the transient catalyst characterization capability was successfully performed. Test data show that higher temperature excursions result in NO_x desorption from the catalyst surface and eventual NO_x slip. The transient capability is applicable to many aftertreatment problems and will be used in the future on other aftertreatment projects.

FY 2004 Publications/Presentations

1. KG Rappe, JW Hoard, CL Aardahl, PW Park, CHF Peden, DN Tran (2004) Combination of low and high temperature catalytic materials to obtain broad temperature coverage for plasma-facilitated NOx reduction. *Catalysis Today* **89** 143.
2. DN Tran, CL Aardahl, KG Rappe, PW Park, CL Boyer (2004) Reduction of NO_x by plasma-facilitated catalysis over In-doped γ-alumina. *Appl. Catal. B* **48** 155.
3. CL Aardahl. PNNL-Caterpillar CRADA on Lean NO_x Catalysis. Poster presented at the Advanced Combustion Engine Peer Review, Argonne, IL, May 2004.
4. CL Aardahl, RT Rozmiarek, KG Rappe, DP Mendoza, PW Park. Reformer-assisted lean NO_x catalysis for diesel emissions control. Presentation given at the 13th International Congress on Catalysis, Paris, France, July 2004.

II.B.13 The Use of Ceramic Catalysts and Tailored Reductants for NO_x Reduction

Ralph Slone
Noxtech, Inc.
1939 Deere Ave.
Irvine, CA 92606

DOE Technology Development Manager: John Fairbanks

Subcontractors:
Analytical Engineering, Inc., Columbus, Indiana

Objectives

- The overall objective of this project is to quantify the performance of Noxtech's plasma-assisted catalyst (PAC) system for achieving the cost-effective, customer-transparent, reliable, and industry-acceptable control of emissions from both light- and heavy-duty diesel engines.
- Achieve over 90% reduction of the NO_x from the exhaust of high-speed diesel engines at a space velocity of 50,000 hr^{-1} and 200-500 deg C.
- Scale up technology for engines of greater than 200 kW from the current size suitable for engines only up to 60 kW.

Approach

- Optimize the performance, cost, ease of fabrication, operating range, and efficiency of the PAC components and integrated system, and improve understanding of the controlling mechanisms for PAC systems.
- Use the data and component enhancements/improvements to design, build and quantify the performance of the PAC system on the exhaust from a 60-kW diesel-powered generator.
- The data from the improved components and the 60-kW field test will be thoroughly analyzed and modeled to enhance and improve the design of an advanced PAC system.

Accomplishments

- Demonstrated over 94% NO_x reduction (Figure 1, single temperature) from the exhaust of a high-speed diesel engine under these conditions:
  - 30,000 hr^{-1} space velocity
  - Temperature range: 175-550 deg C
  - 50 ppm sulfur fuel
- Improved the performance and durability of system components:
  - Increased space velocity, improved selectivity and low-temperature activity of the NO_x catalyst
  - Refined reductant formation/composition and compatibility with the NO_x catalyst surface
  - Reduced the size and improved the efficiency of the plasma device by moving it external to the main exhaust flow
- Determined that high levels of NO_x reduction could be achieved without an in-line plasma and identified promising NO_x and reductant-forming catalysts that could be developed to optimize this new approach.

Future Directions

- Complete the 60-kW engine test after resolving these issues:
  - Eliminate formation of polymer/carbon deposits on the NO_x catalyst
  - Refine reductant formation over the cracking catalyst
  - Enhance catalyst performance and increase space velocity
- Use the data generated from the 60-kW engine test to design, build and evaluate a system capable of reducing over 90% of the NO_x from a 250-kW high-speed diesel engine.
- Continue to improve the performance, cost, ease of fabrication, operating range, and efficiency of the system components and integrated system.

Introduction

Emission standards in the U.S. will require reduction of diesel emissions for light- and heavy-duty diesel-powered vehicles by as much as 90% from current levels in the 2005-2010 time frame. Achieving these reductions with acceptable durability will be very difficult. NO_x reduction approaches presently being developed present many problems and difficulties. Catalyst poisoning, thermal cycling and the generation of a practical reductant make achieving acceptable performance and life of NO_x adsorbers and lean-NO_x catalysts problematic. Selective catalytic reduction devices (SCRs) require that a reductant be carried onboard the vehicle and a national distribution system be developed. Combustion control technologies such as exhaust gas recirculation (EGR), high injection pressures, variable geometry turbochargers and other similar mechanisms used to control NO_x emissions from diesel engines add complexity and cost and reduce reliability and efficiency. Noxtech's PAC system is a promising alternative for exhaust aftertreatment of NO_x from diesel engine exhaust since it does not have the sensitivity to fuel sulfur levels and operating temperature excursions as do typical catalyst-based systems. At the same time, it offers the potential for significantly improving fuel efficiency and reducing emission control system complexity at much lower cost than other systems being investigated, i.e., SCRs, NO_x adsorber catalysts, and combustion modifications.

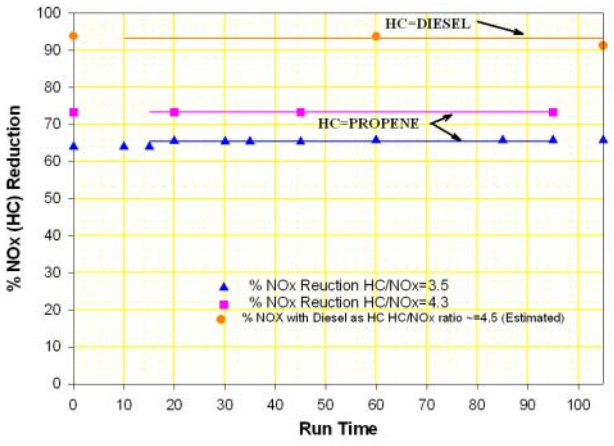

Figure 1. Steady-State NO_x and Hydrocarbon Reduction for the PAC System on a 1988 Cummins 80 HP Engine

Approach

It became clear after 2003 that an in-line plasma system, even though proven to be technically feasible, was not practical. It was determined that the function of the in-line plasma device (conversion of $NO \rightarrow NO_2$ and the decomposition of the reductant hydrocarbon) could be achieved through an external device that was smaller and more efficient. Alternatively, it was shown that the plasma system was not needed at all and its functions could be performed by a combination of catalyst systems. The focus of this project is to determine the optimum combination of these components to produce the most practical and commercially viable system.

All of the components of the Noxtech PAC must be improved in order to produce a viable integrated system that can be used to meet the performance goals of the 60-kW diesel engine demonstration test. Needed component improvements include the following:

- Expand temperature range: The effective low temperature for the PAC NO_x catalyst (Figure 2) must be reduced from 200 deg C to 150 deg C to demonstrate over 90% NO_x reduction over the

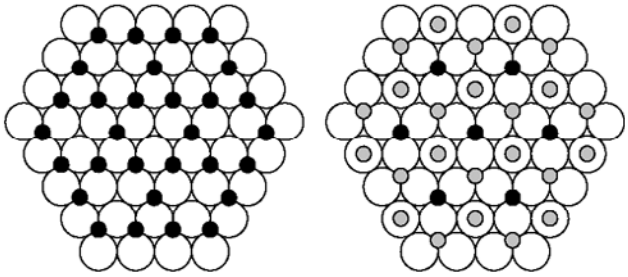

Figure 2. Gamma Alumina Crystal Structure

150-500 deg C range observed from the 60-kW demonstration test. Experimental zeolites are being evaluated because they offer higher surface areas per unit mass and the ability to control selectivity of species through cage size/ cage surface properties (substituting doping metals into the cage structure). The basic crystal structure of these materials can be optimized to make them more active at lower temperatures (Figure 3). High-surface-area doped Al_2O_3 catalysts are also being designed and evaluated to enhance low-temperature activity and selectivity for NO_x reduction. It should be noted that achieving the activity goals over the designated operating temperature range for this project will require the optimization and matching of the reductant species and the species to be reduced (NO/NO_2) in addition to the catalysts.

- Increase operating space velocity to 50,000 from 30,000: The ultimate goal of this project is to demonstrate 94% NO_x reduction from the exhaust of a diesel engine at 50,000 hr^{-1}space velocity. The immediate realistic goal for the 60-kW prototype is 30,000 hr^{-1}. Catalyst effectiveness, or efficiency per unit mass of catalyst, can be improved through increasing normalized surface areas and making the catalyst more selective. This project is enhancing surface area by customizing zeolite catalysts to maximize surface areas (over 900 m^2/gm) and by optimizing pore sizes and surface binding capabilities through doping of the basic zeolite crystals. In addition, doped Al_2O_3 catalysts are being optimized for selectivity and increased surface area per unit mass (300-600 m^2/gm) to create higher surface efficiencies and effectiveness.

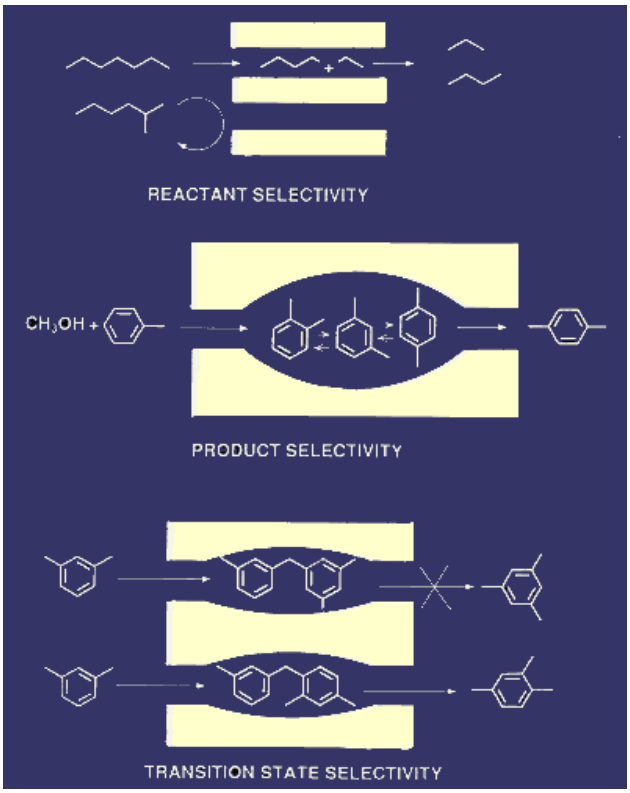

Figure 3. Zeolite Structure

- Enhance catalyst durability: NO_x catalyst durability is determined by its thermal and chemical stability when exposed to the exhaust of a diesel engine. The durability of the PAC NO_x catalysts has been enhanced and assured by selecting and enhancing ceramic-based materials, including zeolites and aluminas, that are inherently very thermally stable but also have a minimum of metals (no precious metals). Metals are undesirable because they can react with poisons (sulfur in particular) in the exhaust to form stable, inactive compounds that deactivate the catalyst, or they can produce SO_x compounds that are undesirable. The doping metals in the ceramic catalysts being used in the PAC are not available to react with the sulfur compounds in the diesel exhaust nor to react thermally to grow into larger crystallites, reducing the active surface of these catalysts.
- Generate reductant: Viable generation of a reactive reductant from diesel fuel is a critical requirement for the project in order to eliminate the need for carrying an additional fluid on

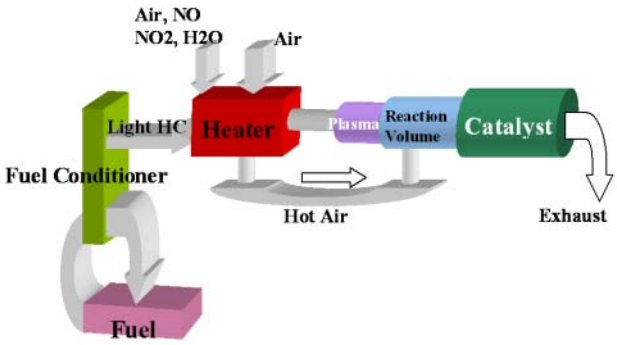

Figure 4. Component Schematic of the Bench Test Unit

vehicles and because diesel fuel is commercially available with properties that are familiar to and accepted by the general public. However, generating a functional reductant that will react efficiently and effectively on the surface of the PAC catalyst without producing undesirable by-products (solid or gaseous) is a challenging task. Reductants for the NO_x catalysts in this project are being produced using proprietary cracking catalysts and zeolitic cracking catalysts. In addition, the use of an external non-thermal plasma (NTP) in combination with cracking catalysts to tailor the formation of partially oxidized reductant species is being investigated. The reductant formation process must be refined and controlled to produce the optimum species for reaction with NO_x from the NO_x catalysts but also to prevent the formation of solids on the catalyst surface and/or noxious gaseous species.

- Plasma system: The plasma system will be located external to the exhaust in this project to produce ozone and/or chemical reductants for the NO_x catalyst (see Figure 4). The plasma system will be a small, very efficient corona discharge NTP based on the design of the larger in-line system already demonstrated in this project. It will be used to generate ozone to convert NO→NO_2 in order to determine which species, NO or NO_2, is the most viable and practical to remove from the exhaust. This will be accomplished by determining the most practical and optimum catalyst and reductant combination.
- The plasma system will be investigated (as previously described) for use in combination with a cracking catalyst to form reductant species from diesel fuel.

A PAC system will be designed, fabricated, and installed in-line in the exhaust of a 60-kW, high-speed diesel engine. This system will use component and system improvements needed to assure it will be able to achieve over 90% NO_x reduction over a representative temperature range (150-500 deg C). The improvements will assure that the issues encountered during past similar tests do not recur:

- Carbon/polymer accumulation on NO_x catalyst
- Catalyst active temperature range too narrow
- Control of reductant composition not sufficient
- In-line plasma system converted to external unit to avoid sensitivity to particulate fouling and lack of robust construction
- Catalysts must retain their resistance to sulfur poisoning while maintaining their ability to reduce exhaust NO_x by over 90%

A third party will conduct performance evaluation/testing of Noxtech's PAC system for the removal of NO_x from the exhaust of a 60-kW, high-speed diesel engine. These tests will be conducted at three steady-state load points that cover the load and exhaust temperature ranges for this engine. Thorough measurements will be made of all operating parameters for this system, including exhaust emissions, temperatures, reductant flows, and engine loads. The Hoard Test (an informal test developed by John Hoard of Ford Motor Company) will be conducted using an oxidation catalyst to test the treated exhaust downstream from the NTP aftertreatment system for false positive NO_x reduction as a result of potential complexing of NO_x with hydrocarbons during the PAC treatment process. The efficiency goal for the Noxtech NTP is 2.5-3.0% of the total engine fuel consumption.

The PAC system that will be used to demonstrate over 90% NO_x reduction by treating the exhaust from a 60-kW diesel engine will have a modular design that will allow the component configuration to be optimized using the results from the component improvement work.

In the basic system, the inlet exhaust flow will be injected with a partially oxidized hydrocarbon stream formed from diesel fuel using a cracking catalyst and/or an external plasma reactor. Ozone may also be injected at this point to oxidize NO to NO_2 in the

exhaust (based on the optimum catalyst/reductant/ reactant species). The injected species will flow into a mixing chamber to assure a homogenous species mix. This exhaust mixture will then flow over a doped ceramic NO_x reduction catalyst.

The results from the component development effort and the 60-kW demonstration test will be used to design and demonstrate the next generation of PAC systems. The next-generation PAC system will be scaled to treat the exhaust from a 250-kW diesel engine and will not involve an in-line plasma.

Results

It has been clearly shown in this project that an in-line plasma coupled with an NO_2/NO_x reduction catalyst could produce high levels of NO_x reduction. However, it also became clear that the in-line plasma system was going to require a major level of funding to make the plasma unit robust and reasonable to fabricate. The system would, in addition, require significant integration efforts with the control system and pulser to produce a viable, practical unit.

After analyzing this issue, Noxtech decided to pursue an alternative course. It was determined and confirmed with bench data that significant levels of NO_x reduction in diesel exhausts could be achieved in a simpler and more practical manner by using a catalyst or external plasma in the presence of a catalyst.

Ceramic catalysts were developed to crack diesel fuel to produce reductants active enough to react over ceramic NO_x catalysts. Ceramic NO_x catalysts were developed to reduce NO and/or NO_2, making the system more versatile. The use of a catalyzed external plasma to produce injectable ozone and modified diesel fuel is also being investigated and is much more practical and cost-effective than an in-line system. The active components in ceramic catalysts are integrated into a crystal matrix and are not available for reaction with sulfur that would deactivate these catalysts. In addition, this same matrix makes these catalysts much more thermally stable.

The new system is still experiencing problems with polymer and carbon formation on the NO_x catalyst surface and inadequately controlled production of reductants from the diesel fuel modification catalysts. Noxtech believes these issues are solvable.

Conclusions

The development of an in-line plasma system for the reduction of NO_x from a diesel engine does not appear to be a cost-effective approach to emission control.

An alternative system design using plasma to generate ozone and catalysts to prepare reductants from diesel fuel was designed and proven to be viable on a bench scale. The plasma and catalyst are located outside of the exhaust stream.

While this alternative system has proven to be more practical and potentially more viable than the in-line plasma system, it needs improvements to eliminate polymer/deposit formation on the NO_x catalyst and to optimize the efficiency and life of both the reductant-producing and NO_x catalysts.

II.B.14 NO_x Control and Measurement Technology for Heavy-Duty Diesel Engines

Bill Partridge[1] (Primary Contact), Tom Yonushonis[2], John Stang[2], Mike Ruth[2], Neal Currier[2], Bill Epling[2], Sam Geckler[2], Norberto Domingo[1], Sam Lewis[1], Jae-Soon Choi[1]
Oak Ridge National Laboratory
Fuels Engines and Emissions Research Center
2360 Cherahala Blvd.
Knoxville, TN 37932

[1]ORNL
[2]Cummins Inc.

DOE Technology Development Manager: Ken Howden

Objectives

- Improve diesel engine-catalyst system efficiency through detailed characterization of chemistry and degradation mechanisms. This objective is based on bench-scale research.
- Work with industrial partner to develop full-scale engine-catalyst systems to meet efficiency goals while complying with emissions regulations.

Approach

- Develop improved analytical techniques for characterizing combustion and catalyst chemistry.
- Evaluate reaction order and contribution and deactivation-method effects based on bench-scale studies.
- Evaluate the effectiveness/efficiency of select engine-system parameters (e.g., operation strategies, fuel formulations and catalyst) to realize efficiency goals on full-scale engine-catalyst systems.

Accomplishments

- Developed minimally invasive analytical technique for in-situ intra-catalyst measurement of transient temperature distributions.
- Improved hydrogen-spatially resolved capillary inlet mass spectrometer (H_2-SpaciMS) to provide better temporal response for measurement of polar species concentrations.
- Evaluated timing, priority and significance of various detailed reactions involved in reactor chemistry relevant to the Cooperative Research and Development Agreement (CRADA) objectives.
- Quantified select effects of deactivation mechanisms on the efficiency of reactors relevant to the CRADA objectives.
- Quantified engine-out species pools associated with engine-managed reductant-generation strategies at various engine conditions.
- Supported CRADA objectives through two separate campaigns involving field application of the H_2-SpaciMS and Phosphor Thermography (PhosphorT) instruments at the industrial partner's research facilities.

Future Directions

- Quantify select effects of additional deactivation mechanisms on the efficiency of reactors relevant to the CRADA objectives.

- Additional reforming reactions will be studied. As with the FY 2004 work on different reactions, this work will evaluate the timing, priority and significance of various detailed reactions involved in reactor chemistry relevant to the CRADA objectives.
- Investigate variations in reaction effectiveness with reaction parameters. The purpose of this task is correlate reaction efficiency with fuel penalty and to better define an optimum strategy.
- Full engine-systems research will characterize the engine-out and catalyst(s)-out species pools resulting from engine-managed operation with different low-sulfur fuels. This will help guide fuel selection for follow-on work. The primary research goal for FY 2005 is to identify pathways for improved fuel economy.

Introduction

Increasing expectations for efficiency, fuel economy, and low emissions from heavy-duty vehicles require corresponding improvements in system design. The realm of expectation is now sufficiently high to require carefully integrated engine-catalyst-control systems working in precise concert. This level of design and control requires detailed knowledge of the combustion and catalyst chemistry; i.e., what reactants make the catalyst most efficient, what is the order and significance of reactions throughout the system, and how can the engine/system be controlled to enhance catalyst efficiency? This CRADA takes a parallel approach with highly controlled bench-scale and more final-product-indicative full-engine-scale research to address these issues.

Approach

The big-picture approach that has been used in this CRADA is to combine the unique resources available at Cummins Inc. and Oak Ridge National Laboratory (ORNL) to improve the efficiency of the target diesel-engine systems. The approach uses parallel bench-component and full-engine-scale investigations. The goal of such studies is to establish a more detailed understanding of the component and system operation so that pathways to efficiency improvements and technology barriers can be identified. Technology limitations include analytical technique deficiencies that limit the detail with which the system can be characterized. As suggested by the project title, developing advanced measurement technology when necessary to improve characterization ability is also a central purpose of this project. Continual refinement of detailed system knowledge and the analytical techniques used to establish that knowledge enhances the team's ability to correspondingly improve the efficiency, fuel economy and emissions of the diesel-engine system.

Results

Development of advanced measurement technologies continues to be an area of success for this CRADA. This success builds on that of the spatially resolved capillary inlet mass spectrometer, or SpaciMS, which allows for minimally invasive intra-catalyst measurement of transient species distributions. A later version of this instrument, the H_2-SpaciMS, allowed for quantifying the concentration of hydrogen, which is a very active and important species in catalyst function. Further improvements to the H2-SpaciMS in FY 2004 provided improved temporal resolution for measurement of polar compounds. The SpaciMS allows measurement of a broad range of species and, hence, detailed characterization of the evolution of the various chemical reactions ongoing within the catalyst reactor. In addition to species, transient temperature distributions are critical to understanding catalyst chemistry. In FY 2004, a new instrument, PhosphorT, for providing the requisite temperature measurements was developed and field demonstrated. The PhosphorT instrument is based on phosphor thermography and uses optical fiber physical probes to provide intra-reactor minimally invasive temperature measurements. Both the H_2-SpaciMS and PhorphorT instruments were applied along with conventional analytical techniques at the Cummins Technical Center in FY 2004 to study detailed chemistry relevant to the CRADA objectives. This work allowed the priority of the various reactions to be ranked. More specifically, via the intra-catalyst measurements, we have quantified the phase of the various reactions; the reaction phase

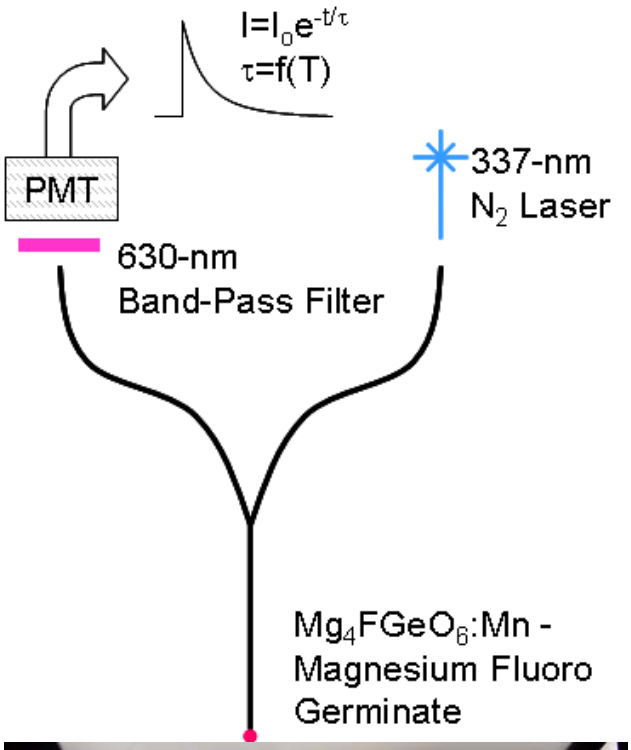

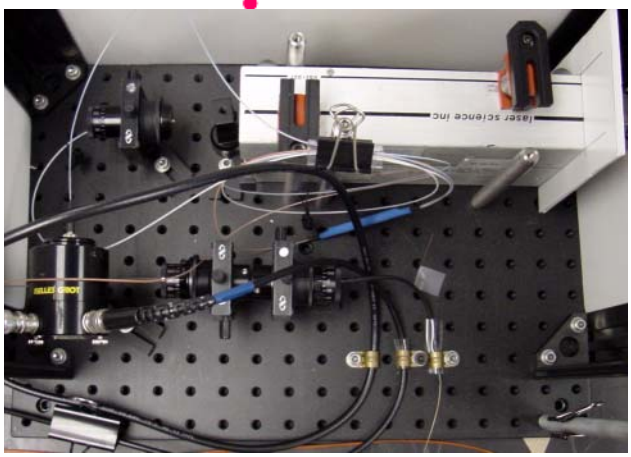

Figure 1. Schematic (top) and Photograph (bottom) of the Phosphor Thermography Instrument

is consistent with step-wise completion of the various reactions in the order of their priority. This detailed understanding is relevant to optimizing the efficiency of systems defined in the CRADA objectives.

The Phosphor Thermography instrument was developed to quantify transient temperature distributions throughout an operating catalyst. Figure 1a shows a schematic of the instrument, and Figure 1b shows a photograph of a version of the instrument suitable for use in the field. The

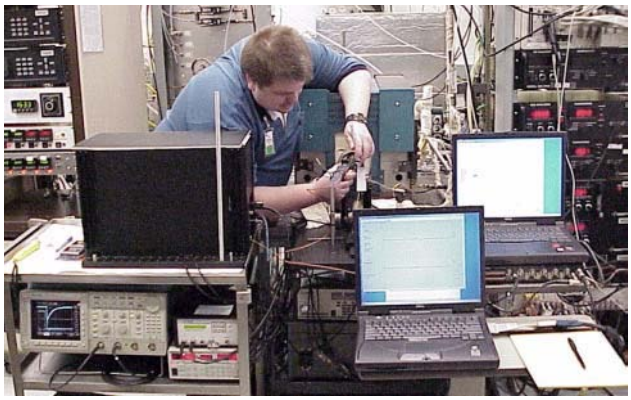

Figure 2. Bench-Reactor Experiments to Measure In-Situ Intra-Catalyst Transient Temperature and Species Distributions via PhorphorT and H_2-SpaciMS

instrument is based on the temperature-dependent phosphorescence lifetime of rare-earth-doped ceramic phosphors. A 337-nm laser is injected into one (pump) leg of a fiber coupler to excite a phosphor deposited on the tip of a gold-coated fiber. The gold coating allows for high-temperature applications up to 750°C. The phosphor is laser-promoted to long-lived excited states which decay via phosphorescence in the 650-nm range. Some of the phosphorescence is captured by the same optical fiber used to deliver the pump light and is directed to a second (detection) leg of the fiber coupler. The light emitted from the detection leg is filtered to reject pump light and is detected via a photomultiplier tube (PMT). The phosphorescence signal displays an exponential decay with a time constant, τ, proportional to temperature. The PMT signal is monitored at 400 kHz and analyzed via a LabView program to actively determine the phosphorescence time constant. The time constant can be measured and converted to temperature at rates up to ca. 2 Hz. Temperature gradients are resolved by translating the fiber's phosphor tip.

Figure 2 shows the PhosphorT instrument (black box on the cart) being used for bench-scale catalyst measurements at a Cummins Technical Center laboratory. Post Doc Shawn Goedeke is leaning on a tube furnace containing the catalyst core sample and inserting the phosphor-tipped optical fiber into the reactor outlet. The silver box behind the tube furnace in Figure 2 is the H_2-SpaciMS, which sampled at five

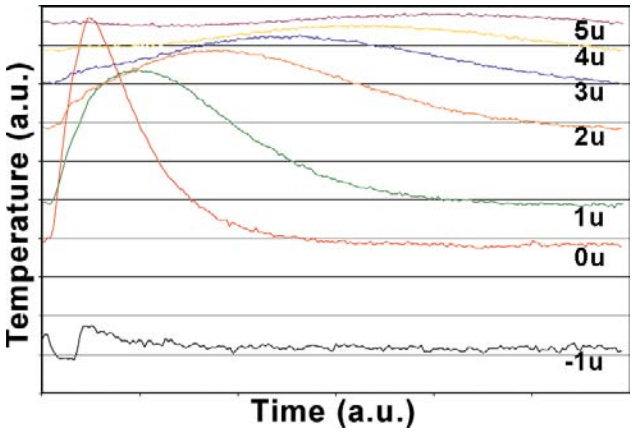

Figure 3. Intra-Catalyst Transient Temperature Distributions Associated with Dynamic Catalyst Operation

positions throughout the reactor via capillaries inserted in the reactor inlet. Some of the conventional analyzers used for additional analysis can be seen in Figure 2. Figure 3 shows intra-catalyst transient temperature distributions measured via the PhosphorT instrument. Temperature dynamics are shown for seven positions within the reactor and indicated by ju, where j is a unit multiple; 0u is the catalyst inlet face, -1u is one unit before the inlet face, and positive j values are corresponding unit multiples into the catalyst. The temperature values for the various curves are absolute; i.e., the curves are not offset. Sharp or high-frequency temperature transients are indicative of exothermic reactions, and lower-frequency temperature transients are indicative of bulk heat transfer. It is apparent from Figure 3 that the 0u position is actually just inside the catalyst, rather than at the catalyst face, or that exothermic reactions occur at the catalyst face. The detailed nature of the thermal wave's progression through the catalyst is characterized by the data of Figure 3 for certain catalyst conditions and reactants. These results show that at many positions within the catalyst, the peak temperature occurs at times significantly removed from the initial exotherm; i.e., the time of the leading exotherm edge is at the 0u position. Such delayed heating is inefficient to some catalyst processes, suggesting that alternate parameters might provide improved efficiency. Figure 3 indicates that exothermic reactions occur at positions 0u through 4u at early times. By correlating the PhosphorT measurements with corresponding H_2-SpaciMS measurements, more detail of the catalyst chemistry is revealed. For instance, the exotherms apparent in Figure 3 at positions 1u through 4u are attributable to a different reaction than causes the exotherm at the 0u position; i.e., exothermic reaction A occurs very fast and at the very front of the catalyst. Once reaction A is complete, a second exothermic reaction B occurs. This type of detail is being used by the CRADA team to improve the efficiency and reduce fuel use of diesel catalyst systems.

In the Engine Systems section of the CRADA, a full engine system was used to assess the reductant pool resulting from engine-managed reductant generation when using Diesel Emission Control Sulfur Effects (DECSE) and Chevron Phillips (CP) 2007 Ultra-Low-Sulfur (ULSD) fuels. The CP 2007 ULSD fuel is what Chevron Phillips anticipates providing at the pump in 2007. The species pool was characterized using a range of analytical techniques available at ORNL to measure several species including CH_4, total (non-CH_4) hydrocarbon (HC), detailed HC speciation via gas chromatography/mass spectrometry, NO, NO_2, O_2, CO, CO_2, H_2 (via H_2-SpaciMS) and smoke number. The engine performance, emissions and reductant pool generation were found to be similar for DECSE and the CP 2007 ULSD fuels. Based on these results, an overview of the basic fuel compositions was prepared for a range of fuels being studied at ORNL including Pump, BP-15, ECD1, Certification, CP 2007 ULSD, 10% Aromatic and DECSE. Figure 4 a, b and c show the base fuel chromatogram for ECD1, CP 2007 ULSD and DECSE fuels, respectively. The distinct features in Figure 4 are straight-chain saturated compounds, alkanes, while the broad envelop is composed of a soup of other compounds including branched alkanes, alkenes, aromatics, etc. It is apparent from Figure 4 that ECD1 has a much broader range of straight-chain alkanes compared to both CP ULSD and DECSE fuels. The CP fuels have a bimodal HC envelope; the high-molecular-weight alkanes and alkenes that make up one lobe of the HC envelope are apparent in the combustion exhaust. The aromatic content of the CP fuels is apparently comprised of a smaller number of aromatics, which are primarily confined to lower-molecular-weight compounds. These are some of the distinct differences in the CP fuels (Certification, CP ULSD,

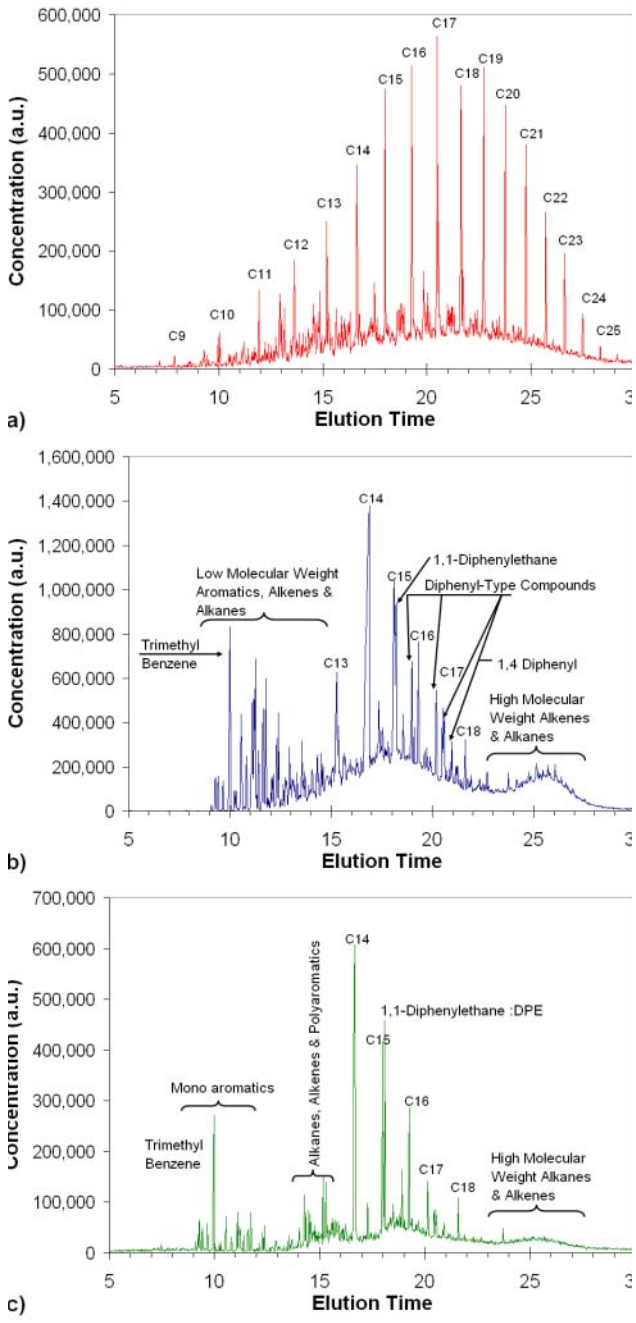

Figure 4. Base Fuel Chromatogram for ECD1 (a), Chevron Phillips 2007 ULSD (b) and DECSE (c) Fuels

10% Aromatic and DECSE) and both the BP (BP-15, ECD1) and pump fuels; both BP fuels are similar in terms of base-fuel chromatogram to current pump diesel. There are dramatic differences in the slated 2007 fuel intended by BP (ECD1) and CP (ULSD). Ongoing and future work will further characterize the fuel differences, specifically in terms of aromatic content. The fuels-effects research is co-supported by the Fuel Technologies activity in the Office of FreedomCAR and Vehicle Technology. In light of the similarities in the DECSE and CP ULSD fuels, the similarities in the engine-managed performance resulting from these fuels may not be unexpected. FY 2005 work will investigate engine-managed performance with a very different fuel such as ECD1 to highlight fuel effects.

Conclusions

A new analytical technique for quantifying transient temperature distributions within operating reactors was developed and demonstrated. This diagnostic was used in parallel with the H_2-SpaciMS to quantify detailed intra-catalyst species and temperature dynamics in experiments at both the Cummins Technical Center and ORNL. That work has established a new understanding of reaction order, priority and distribution within the catalyst and is allowing engine/catalyst system improvements as defined in the CRADA objectives. Full-scale engine-system experiments compared the engine-out reductant pool associated with engine-managed reductant generation for two fuels. We have found that the composition of the 2007 diesel fuels proposed by BP and Chevron Phillips are dramatically different, and we expect corresponding differences in the combustion product species pools. Follow-on experiments will detail the species pools associated with engine-managed reductant generation throughout the engine-catalyst system for the two 2007 fuels.

FY 2004 Publications/Presentations

1. Jae-Soon Choi, Trevor Miller, William S. Epling, Shean P. Huff, Kalyana Chakravarthy, Katey E. Lenox, William P. Partridge, C. Stuart Daw, "Regeneration behavior of NO_x storage-reduction catalysts under simulated or realistic diesel exhaust," poster presentation at the 4th Department of Energy National Laboratory Catalysis Conference, Oak Ridge, Tennessee, October 2003.

II.B.15 Advanced NO_x Control for Off-Road Diesel Engines Based on Hydrocarbon Oxygenates as Active Reductants over Lean-NO_x Catalysts

Darrell Herling (Primary Contact), Chris Aardahl, Ken Rappe, Bob Rozmiarek
Pacific Northwest National Laboratory
P.O. Box 99, MS: K2-03
Richland, WA 99352

DOE Technology Development Manager: Ken Howden

Objectives

Provide fuel-efficient and economical aftertreatment options that will enable the use of lean-burn, energy-efficient diesel engines in the off-highway industries.

- Demonstrate 70% NO_x conversion for off-road diesel
- Utilize hydrocarbon-based (diesel fuel) reductant
- Obtain <1.5% fuel consumption increase
- Accommodate high fuel-sulfur levels of up to 3000 ppm
- Achieve NO_x reduction targets at high exhaust flow rates (>10 lbs/sec) and with NO_x concentrations of 500-1000 ppm

Approach

- Employ lean-NO_x catalysis aftertreatment, assisted by a fuel reformation system that produces specific hydrocarbon oxygenates on-board for lean-NO_x
- Use of proper oxygenates as reductant can potentially increase lean-NO_x performance to acceptable levels
- Convert hydrocarbon fuel to oxygenates:
  - Distill light hydrocarbon (HC) fraction from diesel fuel and remove sulfur
  - Reform light HC fraction to syngas by partial oxidation (POx) method
  - Synthesize alcohols and ethers from syngas for active reductant
- Use combinatorial catalysis to screen and select novel catalyst formulations

Accomplishments

- Demonstrated 70% NO_x reduction activity, which is significantly greater than conventional lean-NO_x performance of 40%
- Identified four specific oxygenates that work well with conventional lean-NO_x catalysts
- Screened over 200 specific catalyst formulations and variations – have strong leads on catalyst-reductant pairs
- Designed and constructed experimental apparatus for fuel reforming-synthesis process
- Initiated evaluation, product speciation, and process parameter development of partial oxidation method
- Started compiling a database for conversion and selectivity of products possible using reductant synthesis process

Future Directions

- Introduce high-volume catalyst production into testing cycle
- Expand screening of multi-metal mixed oxides and perovskites with multiple oxygenate reductants

- Optimize current NO_x catalyst leads to improve activity at high flow rates
- Optimize catalyst tolerance to poisons
- Continue process parameter development and speciation for oxygenate production: 1) flash distillation; 2) POx; 3) reductant synthesis
- Investigate additional oxygenates as reductants and alternate methods of production as necessary
- Combine three fuel processing steps together and demonstrate continuous operation
- Improve fuel processing system design, operation and catalysts

---

Introduction

The diesel engine is the dominant power source for heavy-duty off-road vehicles worldwide due to its relatively high thermal efficiency, reliability, and ability to deliver power under extended high-load conditions. Despite its attractive operating cost and power delivery features, diesel combustion is under challenge due to significant NO_x and particulate emissions in the exhaust.

Aftertreatment technology often comes at the price of fuel efficiency. For aftertreatment technology to be successfully introduced, it must be robust, retrofittable to older platforms, tolerant of higher sulfur levels (especially for off-road vehicles), and it must have a minimal impact on fuel efficiency. Experience with automobile aftertreatment has shown that a successful catalytic system can have a high degree of commercial viability. The case for catalytic aftertreatment in off-road applications is not different except for the additional technical challenges inherent in the diesel fuel source and powertrain system.

Several technologies are being examined for on-road applications, including selective catalytic reduction (SCR) with urea, active lean-NO_x catalysis, regenerative lean-NO_x traps (LNT), and plasma-facilitated lean-NO_x catalysis. A survey of the off-road industry shows a strong bias to avoid carrying urea on-board the vehicle. In addition, off-road fuel does not currently allow the use of LNT technology because of the relatively high level of sulfur typically found in fuel used for off-road. The relatively steady-state exhaust temperatures of most off-road applications (~350-450°C) make lean-NO_x catalysis a judicious choice for developing a durable approach, without the need to carry an additional reagent such as urea. Over the past few years, several -alumina-based catalysts have been discovered that show promise for active lean-NO_x catalysis in temperature ranges applicable to off-road diesel exhaust. Results have also shown that use of hydrocarbon oxygenates as reducing agents significantly improves the NO_x reduction selectivity and decreases the sensitivity to fuel sulfur.

Approach

The research focus for this project is development of a process to transform diesel fuel to active reagents that are highly selectable for lean-NO_x catalysis. An additional focus is on catalyst investigation and discovery of enhanced formulations that work synergistically with specific alcohol, ether, and aldehyde reducing agents to reduce NO_x. The scope of work involves building the necessary understanding of HC reforming to execute design and testing of catalytic reactors capable of converting diesel fuel HCs into oxygenated species, such as methanol or acetaldehyde. Such oxygenates are known to be active reagents for lean-NO_x catalysis. This process will then be demonstrated on a bench-scale lean-NO_x system, followed by slip-stream engine testing.

Results

At the project inception, several approaches for HC reformation were considered before down-selection to a two-step method involving the conversion of diesel fuel to syngas, followed by a synthesis process to form dimethyl ether (DME) and methanol (MeOH) utilizing the syngas feedstock. Partial oxidation (POx) reforming is the most attractive approach for reforming fuels with high sulfur levels, primarily due to high process temperatures where sulfur compounds are less likely to absorb. Hybrids of POx with steam reformation (SMR) (pseudo autothermal reforming) can yield a

more appropriate CO/H_2 ratio for downstream processing through the water-gas shift reaction and the SMR reaction. However, it was determined that the availability of a water source on-board is a limiting factor for implementation of SMR. It may be possible to perform pseudo autothermal reforming, but these systems may result in unacceptable coking and sulfur poisoning levels due to lower-temperature operation.

The final concept selected for hydrocarbon fuel treatment and conversion to oxygenates contains three specific steps:

- Distillation of diesel fuel to separate light HC fractions ($<C_{12}$) from heavy HCs which contain the majority of sulfur components
- Reforming of light HC fraction by POx to produce syngas
- Synthesis of DME/MeOH mixture at pressure from syngas feedstock

Oxygenate products are then injected upstream of the lean-NO_x catalyst for subsequent deNO_x chemistry and enhanced lean-NO_x performance. A schematic of the system is shown in Figure 1.

In order to assist in the POx and synthesis process development, dedicated bench-scale POx and synthesis apparatus were designed and constructed. The POx system design is based on a short-contact-time, catalytic reactor similar to the ones used by Krummenacher, Schmidt and others. Figure 2 shows a schematic of the bench-scale POx reactor apparatus used for the experimental work, from which the effluent then feeds into the chemical synthesis system. These systems are used for the evaluation, product speciation, and process parameter development of POx and reductant synthesis methods.

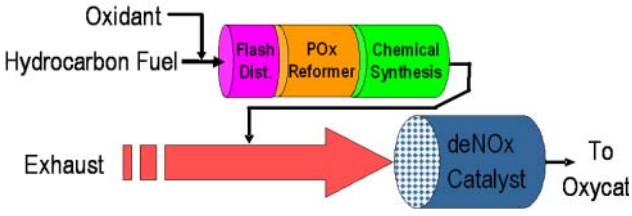

Figure 1. Conceptual Schematic of Fuel Processing System and Integration with Lean-NO_x Catalyst Aftertreatment

Flash Distillation of Fuel

Lean-NO_x catalysts and the synthesis catalysts utilized for DME/MeOH production are susceptible to sulfur poisoning. Therefore, a method to reduce the level of sulfur in the fuel is necessary prior to fuel reforming, in order to meet system performance and durability goals. The method employed for this system consists of separating the light hydrocarbon fraction ($<C_{12}$) from a slip-stream of diesel from the fuel tank. A schematic of the system function is shown in Figure 3. Thermodynamic calculations predict that approximately two-thirds of the sulfur in the full fuel stream are not included in this light fraction, as indicated by the data in Figure 4. This data was generated by ChemCad utilizing a normal distribution of alkanes from C_{10} to C_{18} as the inlet fuel. Subsequent calculations were performed using an alkane distribution representative of Diesel#2, shown in Figure 5, with similar sulfur removal results.

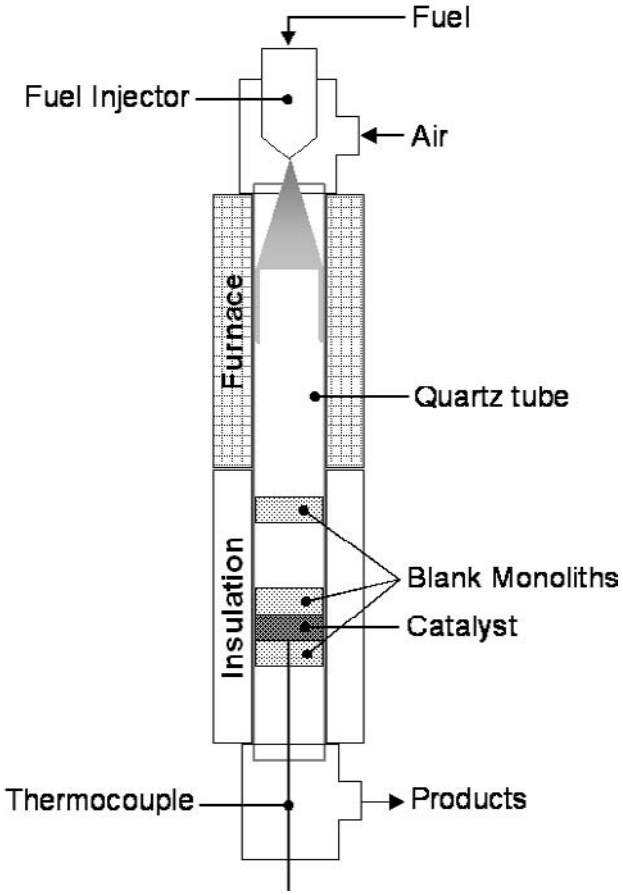

Figure 2. Schematic of the Experimental PO_x Reactor Design

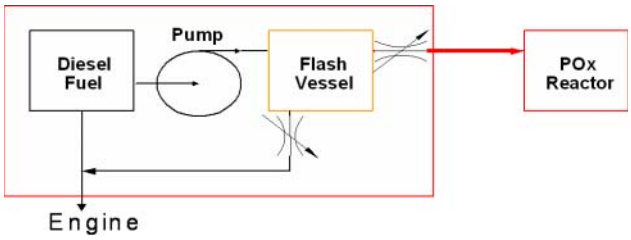

Figure 3. Schematic of the Flash Distillation Unit Operation

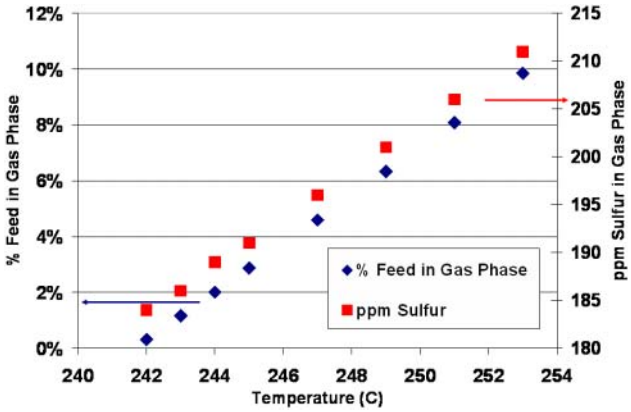

Figure 4. Thermodynamic calculation of remaining sulfur in reagent stream after flash distillation. Results obtained using ChemCad and based on normal distribution of C_{10} to C_{18} alkanes, and fuel-sulfur level of 500 ppm of dibenzothiophene. Fuel was flashed from 20 atm to 1 atm.

The low-sulfur fuel fraction in a gas phase is then used for reforming to syngas, while the remaining liquid fraction of the fuel that retains most of the sulfur is returned to the engine for combustion. No significant effect on the combustion process is expected; the slight shift in the cetane number can be effectively managed by adjusting fuel timing as necessary. Since this approach means only a specific portion of the fuel is utilized for the aftertreatment reagent (production of oxygenates), and the heating value of the remaining liquid portion is retained for combustion, it is anticipated that the fuel penalty impact can be significantly reduced compared to the more conventional approach of post-injection of the diesel in-cylinder or into the exhaust.

By employing this method, along with the expected better selectivity when using oxygenates as the reagent, there is a potential for less than a 1.5%

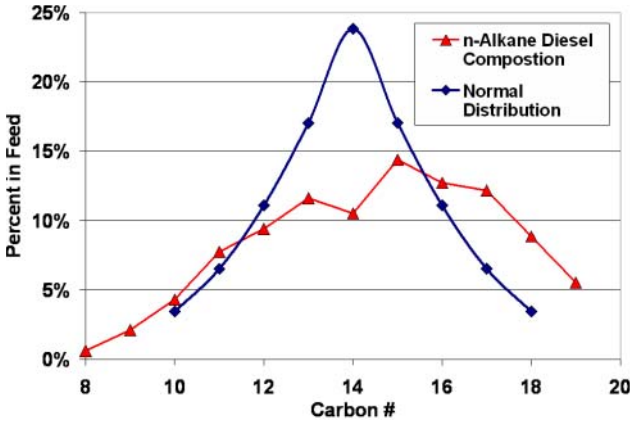

Figure 5. Alkane Distributions Used For Flash Distillation Thermodynamic Calculations

fuel economy penalty. Experiments will be conducted in order to validate the expectations.

Partial Oxidation of Fuel

The gas-phase HC from the distillation step is then fed into the POx step to be converted to syngas. For the conversion of diesel fuel to syngas, the approach must of course be sulfur tolerant, be resistant to coking, and have good selectivity to CO and H_2. The ideal ratio of CO/H_2 in the products is 2:1 for use as the feedstock into the chemical synthesis process and for the production of DME and MeOH. Because POx is an exothermic reaction, and temperatures range from 700°C-900°C, the process is expected to be resistant to sulfur poisoning and coking. However, since it is not necessarily an equilibrium-controlled process, there is a relatively low degree of control over product distribution beyond selecting the proper C/O inlet ratio, reforming catalyst formulation, and catalyst contact time (space velocity, SV).

Initial investigations of diesel POx used n-decane as a surrogate fuel. This was chosen for ease in trouble-shooting, process shakedown, and parameter development, and because it makes up the lighter end of diesel fuel composition. The reactor pressure was maintained at 1 atm, at which the combustion ratio (C/O) for n-decane is 0.323. An experimental protocol was established where the inlet C/O ratio was varied between 0.7 and 2.5 to avoid operating in the flammable mixture range. Experiments were conducted at two discrete flow rates, equivalent to contact times of 12 ms and 6 ms.

The reforming catalyst was comprised of an 80-ppi (pores per square inch) reticulated -alumina monolith used for the catalyst support, which was washcoated with -alumina and doped with 4-6 wt% Rh metal.

The experimental focus was on chemical characterization of POx reactor products and oxidation catalyst evaluation. This was achieved using a customized sampling/chromatographic assembly on-line, which allows accurate characterization of the following: unburned fuel; cracking and incomplete oxidation products; C, H, and O balances. This analytical method is essential, as accurate product stream analysis will provide direction on POx reactor operation and performance. Multiple experiments with the POx reactor alone (i.e. not coupled to the chemical synthesis reactor) have been conducted. Results of H_2 and CO production are shown in Figure 6. Initial experiments were conducted without reducing the catalyst, which was detrimental to POx performance. Subsequent experiments were conducted with varying degrees of reduction as shown in the figure.

Future plans call for follow-on experiments to understand the system performance and reproducibility, catalyst performance and formulation optimization, catalyst deactivation potential, and byproduct distribution. Investigations of lower contact times with n-decane and diesel fuel will also be conducted.

DME/MeOH Synthesis

The catalytic chemical synthesis of DME/MeOH was chosen for production of reductants due to the decrease in operating pressure required versus MeOH synthesis alone. DME/MeOH synthesis from syngas is an exothermic process that is equilibrium favored at relatively low temperatures (240-280°C) and relatively high pressures (200-600 psig). Syngas conversion to DME/MeOH is equilibrium hindered by nitrogen dilution (from the POx reaction) via a decrease in the partial pressure of H_2 and CO.

The syngas stream produced from the fuel POx reformer is pressurized to 200-300 psig and passed over a Cu/Zn catalyst, which is physically mixed with a 1:1 ratio of an acidic -Al_2O_3 at 240-280°C to form a mixture of DME, MeOH, hydrogen, carbon monoxide, carbon dioxide, and nitrogen. The current

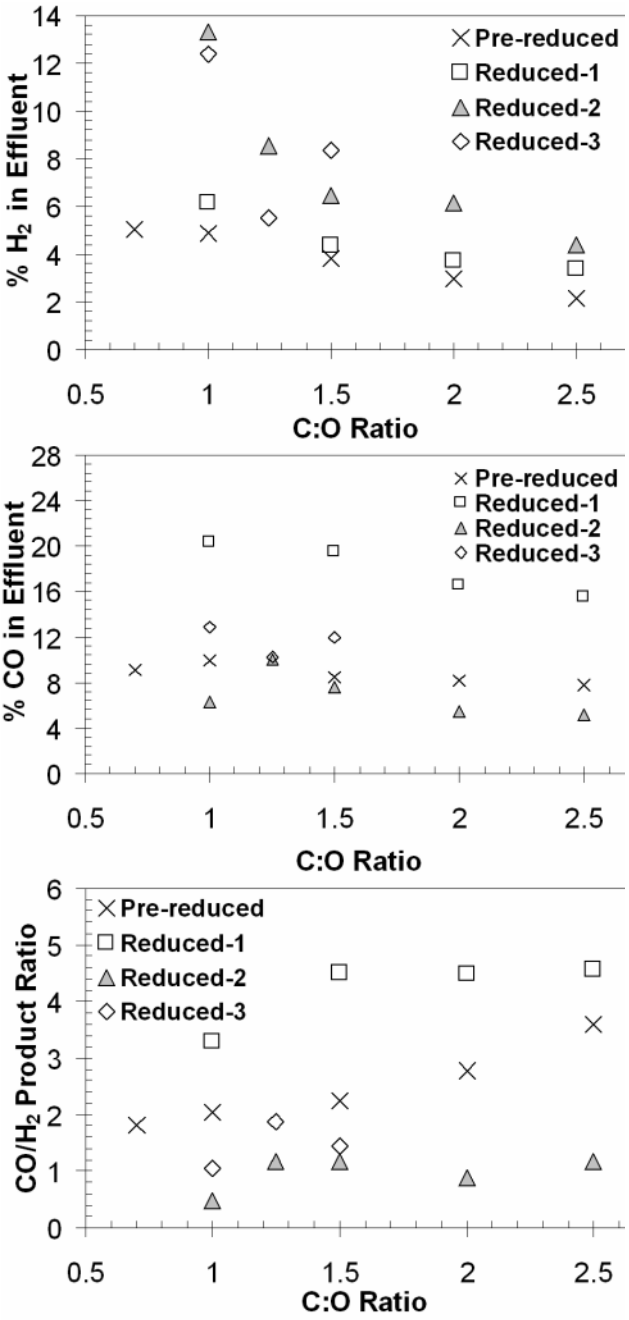

Figure 6. H_2 and CO Production and CO/H_2 Product Ratio at 8 SLPM Flow in POx Reactor (varying fuel/air feedstream ratios)

testing apparatus utilizes simulated syngas delivered via Brooks mass flow controllers. The simulated syngas is pre-heated before entering an oil-heated catalytic reactor at the desired reaction pressure (100-300 psig). The product gas mixture from the reactor is then chilled to remove condensable constituents (H_2O and MeOH) prior to analysis via an Agilent

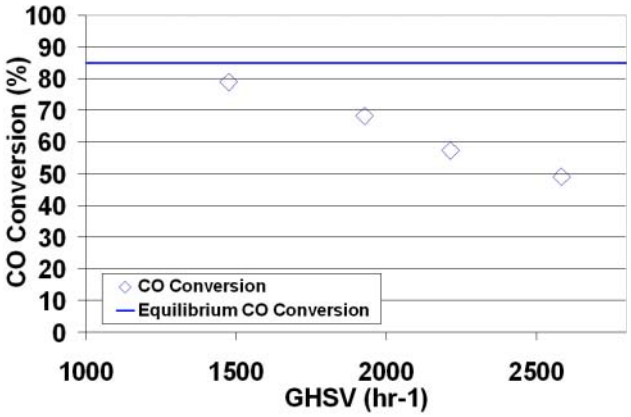

Figure 7. CO Conversion as a Function of GHSV with a 2:1 H_2/CO Ratio with 4% CO_2 at 300 psig and 260°C

four-column micro-GC which utilizes thermal conductivity detectors.

Initial experimental investigations of reductant synthesis focused on variables including temperatures, pressures, syngas ratios, syngas compositions, dehydration catalyst selection and contact time. Equilibrium CO conversions can be reached at a SV of ~1450/hr at a temperature of 260°C and 300 psig with a feed synthesis gas composition of 2:1 H_2/CO, as shown in Figure 7. The product selectivity (on a carbon basis) breakdown is generally 60% to DME, 30% to CO_2, and 10% to MeOH. Acidic -Al_2O_3 was found to deliver an ideal dehydration function to DME versus ZSM-5, which was found as an over-active dehydration element. Increased pressure (100-300 psig) and temperature (240-280°C) were found to increase CO conversion and maintain product selectivity.

Future plans call for follow-on experiments to understand the system variables in relation to performance, catalyst performance and formulation optimization, catalyst deactivation potential, effect of H_2O and integration with POx effluent.

Lean-NO_x Catalyst Formulation

The benefits of using fuel oxygenates for lean-NO_x catalysis are better selectivity and higher activity, which result in the ability to reduce the C_1:NO_x ratio necessary for adequate conversion. The enhanced selectivity also means that higher space velocities can be achieved, which results in smaller catalysts and more efficient on-vehicle packaging. In addition, the use of certain oxygenates has been shown to help the sulfur tolerance of common lean-NO_x catalysts.

Initial screenings of catalyst families were performed using a synthetic gas mixture based on the lean-burn engine conditions for typical off-road diesels, and expected reagents produced by a fuel reformer system. Catalysts for testing were selected from a group of several supported multi-metal oxide catalysts recently discovered that show promise for active lean-NO_x catalysis. Specific formulations were chosen based on process conditions determined by the diesel exhaust stream composition, as well as resilience to anticipated deactivation processes (competing reactions with water and/or sulfur species). Due to the relatively high temperature of the exhaust, efforts are focused on high-temperature catalyst substrates such as -alumina, initially in a powder form, and the key points of acidity, dispersion and coupling to a reductant of the active species identified and optimized.

High-throughput screening techniques are being used to accelerate testing of numerous variables within the catalyst design space while facilitating the high-risk, innovative experiments that would be too costly and time-consuming in a conventional reactor system. To date, screening of over 200 multi-metal mixed oxide catalyst formulations has been completed using four specific reductants, two of which were DME and MeOH. Results from this screening study are shown in Figure 8 for proprietary catalyst-reagent combinations.

In addition, thermal-bench testing of Ag/-Al_2O_3, a commonly known lean-NO_x catalyst for heavy-duty diesels, was conducted using DME as the reagent. This study revealed that DME is an excellent reducing agent for NO_x, with higher selectivity compared to using propene as the reductant. However, the higher activity, as shown in Figure 9, was achieved with very low or no amount of silver in the catalyst. Silver is typically used in lean-NO_x catalysts as a promoter for the possible oxidation of light HCs to intermediate species, such as DME or MeOH, and subsequent oxydehydrogenation to products like formaldehyde,

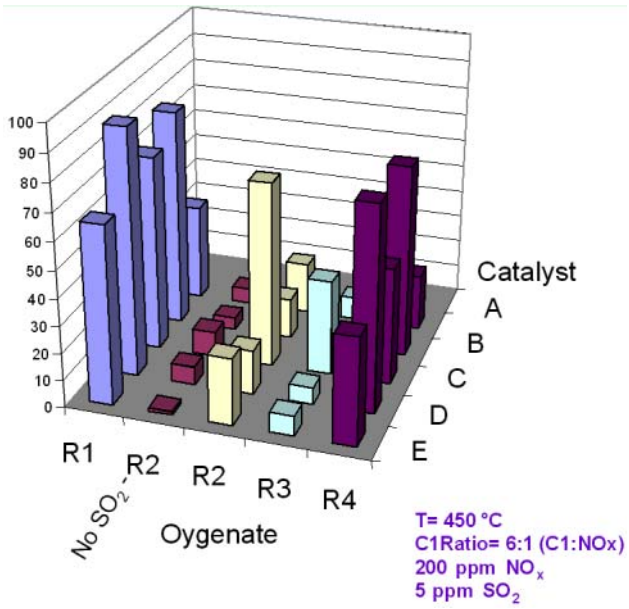

Figure 8. Screening Study Results for Proprietary Catalyst-Reagent Combinations

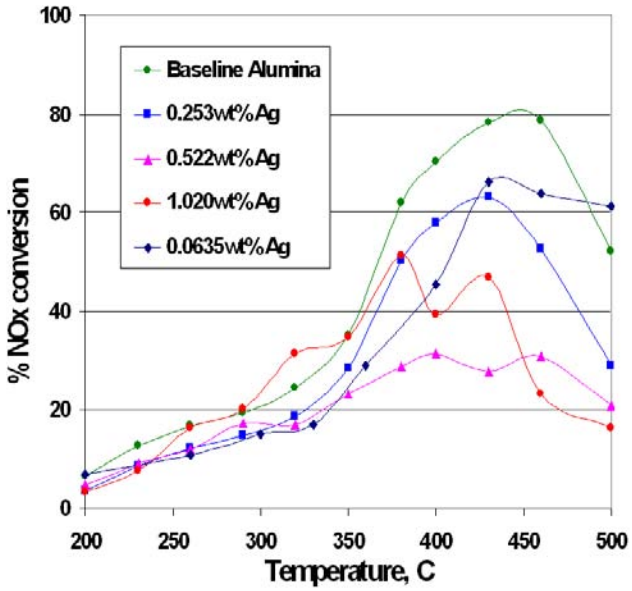

Figure 9. Thermal Bench Test Results for NO_x Reduction Using DME as a Reagent and Varying Concentrations of Ag on the Alumina Catalys

which is thought to be the actual active reducing agent for NO_x. Significant work is still needed on the mechanistic understanding of the reaction sequence and on understanding why DME and formaldehyde are good reagents.

The leading catalyst candidates will be scaled up to a fixed bed reactor with a synthetic gas stream to simulate a diesel emission stream, and tested along with the laboratory-generated stream of the reagents.

Conclusions

High NO_x reduction activity of >70% was demonstrated using lean-NO_x catalysis with DME and MeOH as the reagent. These validation experiments were conducted using a micro-reactor synthetic gas bench and undoped –alumina. This reflects a performance increase of over 30% relative to using the same catalyst formulation with diesel or propene as the reagent. In addition, two other specific oxygenates were identified to work well with conventional lean-NO_x catalyst, and also exhibited enhanced performance when used in conjunction with specific multi-metal mixed oxide catalyst formulations. Over 200 specific catalyst formulations and variations were screened using combinatorial catalysis methods, which has produced some strong leads on catalyst-reductant pairs.

A bench-scale POx reactor experimental apparatus was designed and constructed for fuel reforming process development. In addition, an alcohol synthesis reactor was updated to process syngas for the production of DME and MeOH. Experimental work was initiated to develop a database on selectivity and activity of products possible using the reductant synthesis process from syngas feedstock. To date, the concept of reforming a diesel fuel surrogate to syngas, followed by DME synthesis has been demonstrated at the bench scale.

Special Recognitions & Awards/Patents Issued

1. "Sulfur removal via flash separation for on-board fuel utilization," patent pending, May 2004.
2. "Method of generating hydrocarbon oxygenates from diesel, natural-gas and other logistical fuels," patent pending, May 2004.

FY 2004 Publications/Presentations

1. Chris Aardahl, "Reformer-Assisted Lean NO_x Catalysis for Diesel Emissions Control," 13th International Congress on Catalysis, Paris, France, July 2004.
2. Darrell Herling and Chris Aardahl, "Reformer Assisted Lean-NO_x," 10^{th} Diesel Engine Emissions Reduction (DEER) Workshop, San Diego, CA, August 2004.

Acknowledgments

The authors would like to thank Diana Tran, Jamie Holliday, Gary Maupin, Novella Bridges, and Donny Mendoza, all of the Pacific Northwest National Laboratory, for their work in designing and fabricating the test systems, and well as conducting the experiments.

References

1. Tran, D.N.; Aardahl, C.L.; Rappe, K.G.; Park, P.W.; Boyer, C.L.; "Reduction of NO_x by plasma-facilitated catalysis over In-doped -alumina," Applied Catalysis B: Environmental, Vol: 48, Issue: 2, March 18, 2004, pp. 155-164.
2. Rappé, K.G.; Hoard, J.W.; Aardahl, C.L.; Park, P.W.; Peden, C.H.F.; Tran, D.N.; "Combination of low and high temperature catalytic materials to obtain broad temperature coverage for plasma-facilitated NO_x reduction," Catalysis Today, Vol: 89, Issue: 1-2, February 29, 2004, pp. 143-150.
3. Angelidis, T.N.; Kruse, N.; "Promotional effect of SO_2 on the selective catalytic reduction of NO_x with propane/propene over Ag/-Al_2O_3," Applied Catalysis B: Environmental, Vol: 34, Issue: 3, November 15, 2001, pp. 201-212.
4. Satokawa, S.; Shibata, J.; Shimizu, K.; Satsuma, A.; Hattori, T.; "Promotion effect of H_2 on the low temperature activity of the selective reduction of NO by light hydrocarbons over Ag/Al_2O_3," Applied Catalysis B: Environmental, Vol: 42, Issue: 2, May 8, 2003, pp. 179-186.
5. Krummenacher, J.J.; West, K.N.; Schmidt, L.D.; "Catalytic partial oxidation of higher hydrocarbons at millisecond contact times: decane, hexadecane, and diesel fuel," Journal of Catalysis, Vol: 215, Issue: 2, April 25, 2003, pp. 332-343.
6. Hartmann, et.al., Power Sources, 2003.
7. Ng et al. *Chem Eng Sci* **54** (1999) 3587-3592.

II.B.16 Discovery of New NO_x Reduction Catalysts for CIDI Engines Using Combinatorial Techniques

Richard J. Blint (Primary Contact, GM), Gerald Koermer (Engelhard Corporation), George Fitzgerald (Accelrys, Inc.), Charles Gough (GM)
General Motors Corporation
Research and Development Center
Mail Code 480-106-185
30500 Mound Road
Warren, MI 48090-9055

DOE Technology Development Manager: Ken Howden

Subcontractors:
Engelhard Corporation, Iselin, NJ
Accelrys, Inc., San Diego, CA

Objectives

Develop new NO_x selective catalytic reduction (SCR) catalysts that operate in the lean combustion of diesel or in lean gasoline engines. The catalysts should:

- Utilize the onboard fuel (i.e., hydrocarbon SCR) as the reductant.
- Have NO_x conversion activities in excess of 80%.
- Span the operating range (e.g., temperature and flow rate) for these lean engines.
- Have sufficient durability and resistance to poisoning to meet the 120k mile emission standard.

Approach

- Use fast-throughput techniques to synthesize and measure the activities of a large range of materials for NO_x reduction properties (Engelhard).
- Use design of experiment (DoE) and statistical analysis to predict optimum compositions from materials identified in the discovery (fast-throughput) phase of materials evaluation using the CombiMat 2.5 database developed for this project (Accelrys and GM).
- Scale up, evaluate and do a feasibility analysis of potential NO_x reduction catalysts identified from the discovery phase of the project.
- Test the most promising materials on an engine.

Accomplishments

- Identified multiple hydrocarbon (HC) SCR materials that have in excess of 80% NO_x conversions.
- Tested over 3000 materials for NO_x reduction potential.
- Developed an ANX line interconnected database system that enables the use of data mining techniques to optimize the materials discovered in this project.
- Coated the most promising materials on monolith cores for reactor testing and feasibility analysis.

Future Directions

- Continue the discovery phase of the project to identify materials with good low-temperature NO_x conversion properties to assist with cold-start emission reduction.
- Continue the development of trend analysis techniques to systematize the search for new NO_x reduction materials.
- Scale up the promising materials for engine testing.

Introduction

This General Motors (GM) project was initiated on August 16, 2002. Its goal is to develop new NO_x reduction catalysts for lean combustion systems such as both light- and heavy-duty diesels and for stratified charge gasoline engines. These new catalysts are needed to enable these engines to meet the Tier II NO_x standards for the North American markets that are being phased in over the time period between 2007 and 2010.

Approach

Selective catalytic reduction (SCR) with reductants from the fuel is the technology that is the development focus of the new catalytic materials. The approach is to use fast-throughput technology to develop the new materials (Engelhard), informatics to mine the data arising from the fast-throughput experimentation (Accelrys and GM) and classic reactor evaluation to determine the suitability of the new materials for automotive applications (GM and Engelhard). Figure 1 shows the structure of the responsibilities within the project.

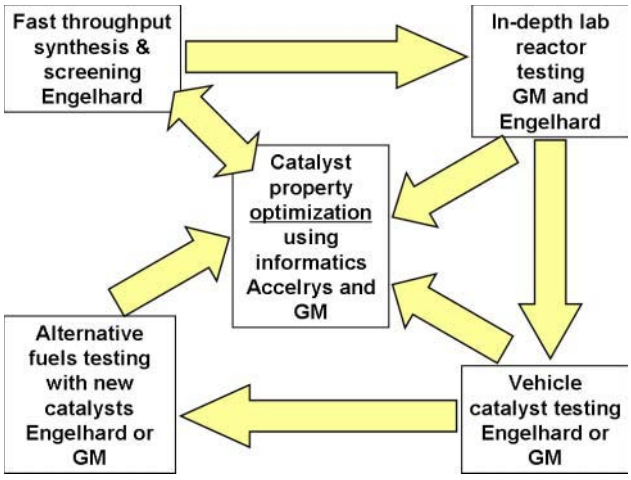

Figure 1. Schematic of the NO_x Discovery Project and the Separation of the Tasks Within the Project

Results

To date, over 3000 new materials have been evaluated on the discovery system (at Engelhard). Even with such a large number, this turns out to be a very sparsely populated space if one considers all the possible combinations of 3-5 components and their separate concentrations. The activity characteristics identified with each of the materials include the peak to peak (P2P) ratio (the ratio of the peak activity of the new material to the peak activity of our reference material), FWHM temperature range (the full width at half the maximum activity as a function of temperature) and the LO temperature (the lowest temperature at which half the peak activity is measured). Typically we are getting 'hits' for approximately 10% of the materials tested, where a 'hit' is identified as a P2P value for a material of 0.8 or greater. The informatics database (Accelrys's CombiMat 2.5, which was specially tailored for this project) incorporates all the synthesis, analytical and activity data and is being used to optimize the compositions to develop viable lean SCR catalysts.

A typical extract from the database might look like the results shown in Table 1. This characteristic activity data is extracted from a discovery experiment such as that in Figure 2. The extract shows the mass % composition of the individual material and the activity information. The P2P value has a range from 0.95-1.46 and the light-off temperature (defined here as the temperature at 50% of the maximum conversion, not 50% of total conversion) ranges between 150-400°C for this A/B combination with a range of mass compositions for A and B of 0.1-2% as a set of supported catalysts.

The workflow for this project has evolved into the following steps:

- Widely dispersed initial scan of component space to identify "hits".

Table 1. An Extract from the Database Showing the Activity Characteristics of a Two-Component Supported Catalyst System, Where the Two Components are Coded as A and B

Sample Number	A	B	FWHM	LO	P2P
1	0.575	1.525	318	182	1.46
2	0.1	1	325	175	1.43
3	1	1	238	212	1.37
4	2	0.1	190	310	1.31
5	0.1	2	350	150	1.3
6	2	2	35	165	1.28
7	0.575	0.575	325	175	1.14
8	0.1	0.1	100	400	1.02
9	1	0.1	200	300	0.95

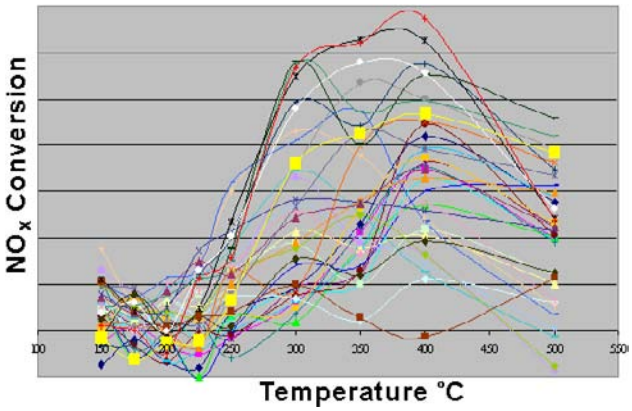

Figure 2. Representative discovery experiment for a range of materials shows the type of data from which the P2P, FWHM and LO data are extracted. The yellow line with the large square symbols is the standard material from which the P2P ratio is calculated.

- Focused design of experiment (DoE) in the neighborhood around a hit to optimize the composition.
- Scale-up of a representative composition in the range of the initial "hit" for GM reactor analysis. This scale-up initially was a powder-like material (extrudate with the support); however, most scale-ups are now being done on wash-coated monolith cores similar to the technology that would be used on a full-size monolith brick.

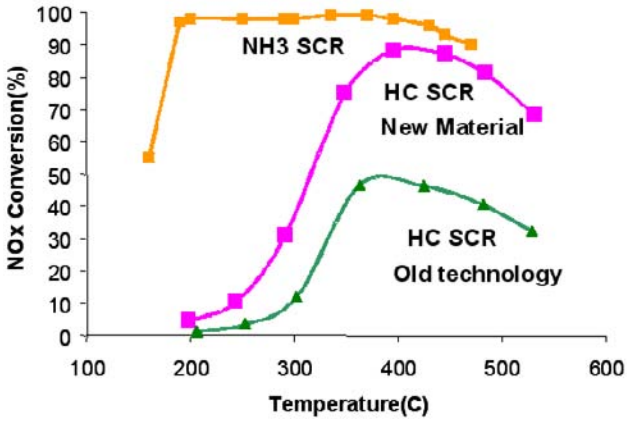

Figure 3. Comparison of Urea SCR, HC SCR old technology and the fast-throughput technology (new material). The HC SCR materials are coated on monoliths.

- Decision to downselect for feasibility analysis and possible engine testing or do another DoE for a finer scale of optimization.

To date, the results from this approach have identified at least two materials that have been downselected for feasibility analysis. Figure 3 compares the activity of one of the new materials to urea SCR and older hydrocarbon SCR technologies. As can been seen, significant strides have been made. Since this is a publicly funded project, there is no restriction on Engelhard sales of catalyst products developed under this project.

Conclusions

- Instrumental approaches for fast-throughput experimentation on NO_x reduction catalysis have been implemented and are working successfully.
- Informatics techniques have been developed that are effective in data mining the NO_x reduction "hits" from a large range of compositional materials.
- Successful materials with possible commercial application have already been identified in this project.

Special Recognitions & Awards/Patents Issued

1. Accelrys filed a provisional patent on 12/01/2003 for inventions that were created while developing CombiMat. The provisional patent, titled "Method of storing fast throughput experimentation information in a database," refers to four inventions.

FY 2004 Presentations

1. "High Throughput Program for the Discovery of NO_x Reduction Catalysts", Seventh DOE Crosscut Workshop on Lean Emissions Reduction Simulation (CLEERS), June 16th and 17th, 2004, Detroit, MI.
2. "High Throughput Program for the Discovery of NO_x Reduction Catalysts", 2004 DEER Conference, August 29th-September 2nd, 2004, Coronado, CA.

II.B.17 Demonstration of Integrated NO_x and PM Emissions Control for Advanced CIDI Engines

Houshun Zhang
Detroit Diesel Corporation (DDC)
13400 Outer Drive, West
Detroit, MI 48239-4001

DOE Technology Development Manager: Ken Howden

Subcontractor:
Engelhard Corporation

Objectives

- Demonstrate technologies that will achieve future federal Tier 2 emissions targets.
- Achieve production-viable technical targets for engine-out emissions, efficiency, power density, noise, durability, production cost, aftertreatment volume and weight.

Approach

- Develop and utilize emerging combustion technologies combined with advanced aftertreatment technologies to pursue achievement of integrated engine, aftertreatment and vehicle system technical targets.
- Develop aftertreatment simulation models and integrate them with engine simulation tools for emissions prediction, engine control and total system design.
- Select and evaluate system(s) (vehicle + engine + aftertreatment) using an integrated experimental and simulation methodology.
- Conduct system performance, emissions and limited durability evaluations.

Accomplishments

- Further consolidated DDC's integrated compression-ignition direct-injection (CIDI) engine and emissions control system [diesel particulate filter (DPF) + selective catalytic reduction (SCR)] for light-duty truck applications.
- Demonstrated Tier 2 Bin 3 emissions target over the FTP75 cycle on a light-duty truck utilizing a DPF + SCR system, synergizing efforts with another DOE-DDC project. This aggressive reduction in tailpipe-out emissions was achieved with no ammonia slip and a 41% fuel economy improvement, compared to the equivalent gasoline engine equipped vehicle. Tier 2 Bin 3 emissions were demonstrated earlier on a Partnership for a New Generation of Vehicles (PNGV)-type mule passenger car application as well.
- Demonstrated Tier 2 near-Bin 9 emissions compliance without active NO_x aftertreatment devices on a light-duty truck, in synergy with another DOE-DDC project.
- Developed a practical DPF regeneration strategy using DDC's virtual lab toolbox, allowing DPF active regeneration to be triggered in a controlled manner at any desired operating condition.
- Characterized SCR performance through well-designed representative aging cycles, demonstrating that there was minimal impact on SCR performance over 1000 hours.
- Characterized diesel oxidation catalyst (DOC) performance through a reactor test bench. Data will be utilized for DOC model calibration. The calibrated model will be utilized for precious metal screening and optimization, thus resulting in an efficient and shortened development cycle of a robust and optimized aftertreatment system.

Future Directions

The project has successfully achieved the aggressive emissions objectives. No more technical activities are planned in 2005, and the project will be concluded at the end of the 2004 calendar year. A comprehensive final report is being prepared and will be submitted to DOE in early 2005.

Introduction

DDC is conducting the Low Emissions Aftertreatment and Diesel Emissions Reduction Program under a DOE project entitled "Research and Development for Compression-Ignition Direct-Injection Engines (CIDI) and Aftertreatment Subsystem." The project objective is to develop emissions control technologies on vehicle platforms and demonstrate scalability to various vehicle classes. The ultimate objective is to achieve the aggressive vehicle emissions targets for 2007 and beyond.

Approach

DDC has developed a proven concept and methodology of combining experimental and analytical tools (Figure 1) to facilitate an integrated engine, aftertreatment and vehicle development roadmap. This system development approach benefits substantially from an integrated experimental and analytical approach to technology development, resulting in a shortened developmental cycle and substantial emissions and fuel economy improvement in both engines and vehicles. The core of this integrated system approach features DDC's CLEAN Combustion© strategy for engine combustion development, and state-of-the-art analytical tools including 0-D for real-time control, 1-D for system integration and 3-D for component optimization.

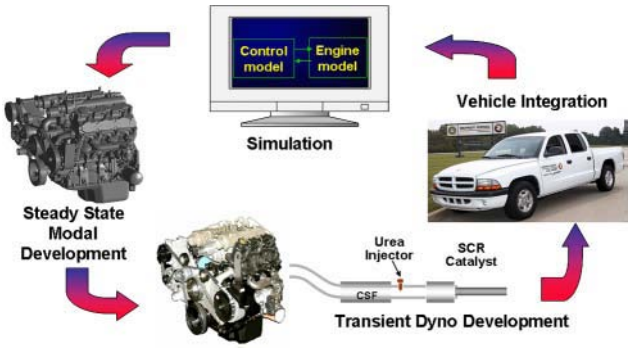

Figure 1. DDC "System Development" Methodology

Results

The DDC team first demonstrated Tier 2 Bin 3 emissions goals in 2002 on a PNGV-type Neon passenger car using an integrated aftertreatment (DPF + SCR) system (Bolton et al, 2002[1]). Building upon this technology demonstration and with increased emphasis on system integration, Tier 2 Bin 3 results were demonstrated on the light truck platform (Aneja et al, 2003[2]). A 41% fuel economy improvement compared to the baseline gasoline engine equipped vehicle was obtained. This aggressive reduction in tailpipe-out emissions can be attributed to successful integration of advanced combustion, aftertreatment and control technologies. Figures 2 and 3 present DDC's roadmap for light-duty truck (LDT) FTP75 emissions. This approach targets Tier 2 Bin 10 emissions levels engine-out, i.e., without the use of any aftertreatment device, and Tier 2 near-Bin 9 emissions levels via integration of engine technologies and passive aftertreatment devices.

Having successfully met the emission objectives of this project, the focus this year included increased emphasis on developing a robust integrated engine, aftertreatment and vehicle system that is capable of achieving the project performance and emission

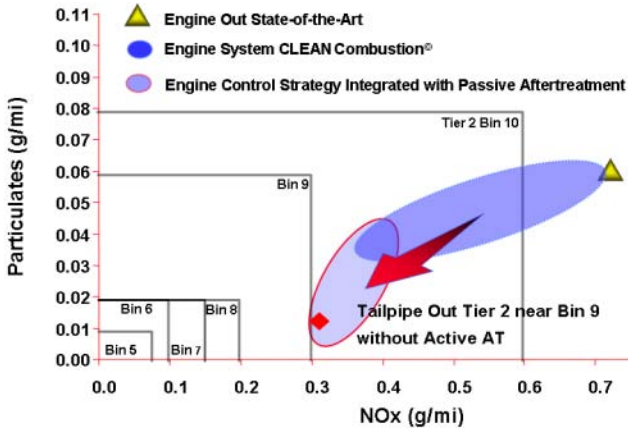

Figure 2. Achieved Tier 2 Near-Bin 9 Emission without Active Aftertreatment; Light Truck Chassis Dynamometer Results

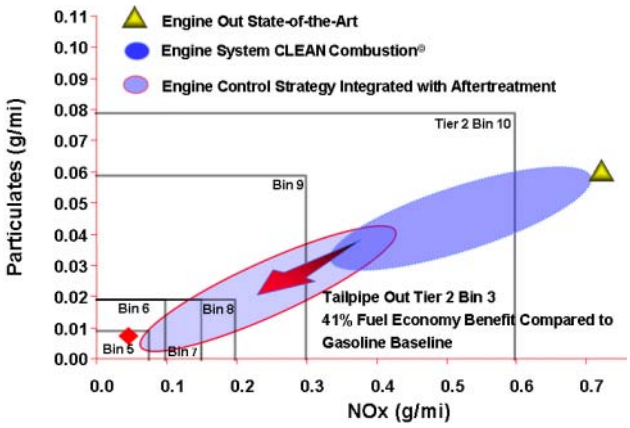

Figure 3. Road Map to Achieve Tier 2 Bin 3 Emissions; Light Truck Chassis Dynamometer Results

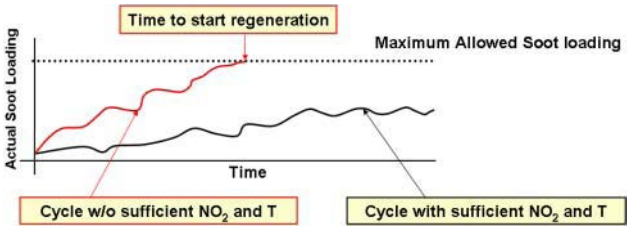

Figure 4. DPF Regeneration Control Concept

targets under diverse driving and operational conditions. A few specific examples of this effort include development of a comprehensive DPF regeneration control strategy, characterization of the impact of aging on DPF and SCR performance, and DOC performance characterization.

The DDC team developed a comprehensive DPF regeneration control strategy that allows regeneration to occur in a controlled manner at any desired operating condition. Figure 4 shows the concept of this strategy, which utilizes a comprehensive algorithm to track the actual soot loading over time and compares it to the maximum allowable soot loading. The outcome of this comparison is one of the parameters that can be used to trigger regeneration.

SCR and DPF characterization was conducted through well-designed representative aging cycles. As an example of the results obtained, Figure 5 shows the NO_x conversion performance characteristics of the SCR as a function of time and normalized stoichiometric ratio (NSR), which is a measure of the ratio of actual urea injection rate to

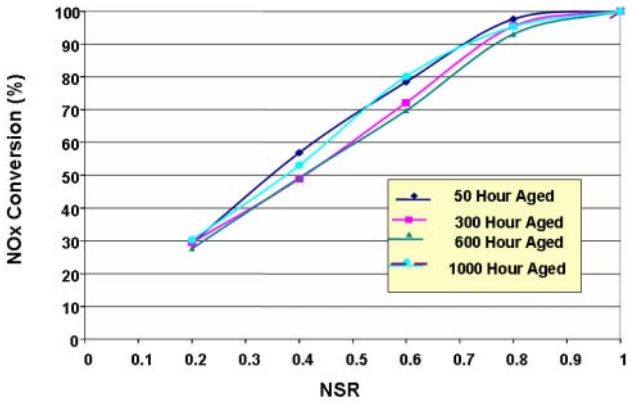

Figure 5. NO_x Conversion Comparison of Aged SCR Devices at 2000 rpm and 260 Nm

required urea injection rate. Interestingly, while a slight degradation in SCR performance was observed over 300 hours and 600 hours, the performance characteristics were recovered over 1000 hours.

Reactor bench tests were conducted to characterize DOC performance at diverse conditions. The data generated from these tests will be utilized to calibrate DDC's state-of-the-art DOC models. The calibrated models would be used to perform precious metal screening and optimization, thus resulting in an efficient and shortened development cycle of a robust and optimized aftertreatment system.

Conclusions

Integration of advanced combustion, aftertreatment and vehicle technologies allowed the DDC team to demonstrate state-of-the-art performance and Tier 2 Bin 3 emissions levels for both passenger car and SUV/LDT applications. Having successfully met the emissions objectives of this project, the focus this year included increased emphasis on developing a robust integrated engine, aftertreatment and vehicle system that is capable of achieving the performance and emission targets under diverse driving and operational conditions.

Publications

1. Brian Bolton, Anthony Fan, Kayhan Goney, Zornitza Pavlova-MacKinnon, Kevin Sisken, Houshun Zhang, "Analytical Tool Development for Aftertreatment Sub-Systems Integration, 2003," 9th DEER Workshop, Newport, Rhode Island, August 24-28, 2003.

2. Houshun Zhang, "Aftertreatment Modeling Status, Future Potential and Application Issues," 10th DEER Workshop, San Diego, California, August 29-September 3, 2004.

References

1. Brian Bolton, Nabil Hakim and Houshun Zhang, "Demonstration of Integrated NO_x and PM Emissions for Advanced CIDI Engines," FY 2002 Progress Report for Combustion and Emission Control for Advanced CIDI Engines, U.S. Department of Energy, November, 2002.
2. Rakesh Aneja, Brian Bolton, Bukky Oladipo, Zornitza Pavlova-MacKinnon, and Amr Radwan, "Advanced Diesel Engine and Aftertreatment Technology Development for Tier 2 Emissions," 2003 Diesel Engine Emissions Reduction (DEER) Conference, August 24-28, 2003.

II.B.18 Microwave Regenerated Diesel Particulate Filter Using Selective Spot Particulate Matter Ignition

Mr. Eugene Gonze (Primary Contact), Dr. Richard Blint, and Dr. Kevin Kirby (HRL)
General Motors Corporation

Subcontractors:
Hughes Research Laboratories (HRL)
Emerachem
Michigan Technological University

Objectives

- Develop and produce an energy-efficient microwave regeneration system for the removal of carbon particulates from diesel particulate filters (DPFs).
- Evaluate candidate microwave-absorbing materials coated onto coupons and full-size DPF samples.
  - Through cavity modeling and testing, develop an optimized laboratory microwave system for DPF regeneration.
  - The laboratory version of the microwave system will next be transitioned into a prototype suitable for vehicle dynamometer evaluation.
  - Regeneration strategies developed during laboratory or dynamometer testing will be implemented in a full vehicle demonstration.
  - Analyze the performance and feasibility.

Approach

- Utilize high-frequency structure simulator (HFSS) microwave modeling as a tool to achieve selective uniform low power heating of a DPF.
- Use full-system DPF models to develop a regeneration control strategy(ies), and determine the optimal heating configurations before building prototype hardware.
- Assure that the microwave system is designed to operate within standard automotive catalytic converter shapes and sizes.
- Use selective heating of the DPF to reduce electrical power consumption.
- Maintain a simple engine control strategy.

The core of this technical project is the use of modeling tools to evaluate multiple regeneration architectures. Based on model predictions generated, the objective of the project team is the construction of a microwave regeneration system that efficiently heats spots within the DPF and then leverages the particulate matter's exothermic energy to cascade the cleaning process throughout the filter.

Accomplishments

At completion of the first year of this two-year project, highlights of the completed tasks and/or tasks in progress include:

- Developed microwave cavity for material absorption measurement.
- Two candidate microwave-absorbing materials were identified and evaluated: an electric field absorber and a magnetic field absorber.
- Microwave materials successfully coated onto DPFs. Different coating positions and sizes were evaluated.

- HFSS cavity model developed. Validation experiments reveal a high degree of correlation with the experimental results. The model is now being utilized to refine cavity heating patterns.
- Prototype microwave cavity built, and operating with microwave coated DPFs.
- Prototype microwave cavity actively regenerating soot-loaded DPFs.
- Developed full-system DPF model with variable heat deposition.
- Utilized DPF model to predict optimal heating locations within the DPF.
- DPFs loaded using Federal Test Procedure (FTP) driving schedules on a vehicle dynamometer.

Future Directions

- Develop a new heating strategy that reduces power consumption by minimizing soot interaction with the microwave field.
- Investigate applicability of higher magnetic cut-off temperature materials.
- Evaluate microwave DPF regeneration on a diesel demonstration vehicle.
- Evaluate microwave system costs and competitive alternative systems.

Introduction

This General Motors Corporation (GM) project was initiated on September 29, 2003. The goal is to develop and produce an energy-efficient microwave regeneration system for effective and efficient removal of carbon particulates from DPFs. The project team is investigating a new approach to microwave-initiated soot combustion. The approach involves selective heating within a cordierite DPF to achieve controlled and uniform soot combustion during a regeneration cycle. Since only a small section of the DPF is being heated, the energy inputs required to start the particulate matter combustion process are smaller. Most of the energy required to thermally combust the soot comes from the particulate matter exotherm imitated by the microwave spot heating. GM is the prime contractor and is supplying vehicle integration and exhaust emission expertise. GM is also responsible for the full-system DPF modeling, as well as the detailed system analyses. Hughes Research Laboratories (HRL) is supplying the expertise in microwave systems. HRL is responsible for evaluating dielectric and magnetic absorbing materials and optimizing a model-based microwave delivery system. Emerachem is a monolith coating sub-contractor that is doping the microwave-absorbing materials on DPFs under study within the project. Michigan Technological University is enhancing its existing DPF modeling software to comprehend microwave heat insertion. The task integration for all of the project partners is described in Figure 1.

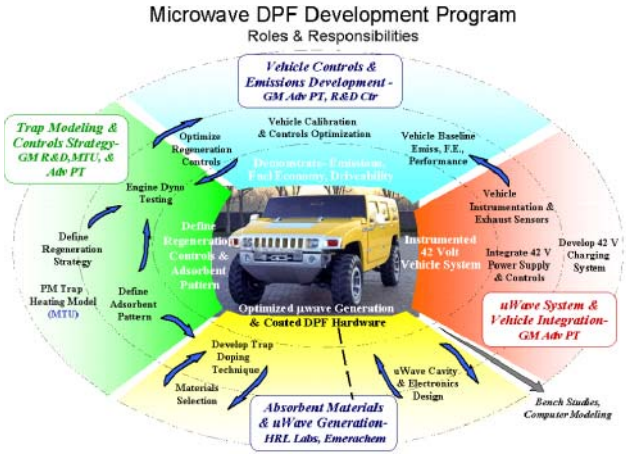

Figure 1. Microwave DPF Development Program

Approach

The first phase of this project concentrated on the microwave heating of a DPF. HRL has identified highly microwave-absorbent materials that efficiently absorb microwave energy. DPFs were coated with these materials and inserted into a microwave cavity. The microwave cavity was designed to utilize the size and shape of the basic automotive catalytic converter. The converter shape was optimized for exhaust flow and under-floor vehicle packaging rather than microwave field simplicity. Another design guideline was to leverage existing high-volume magnetron hardware to reduce overall system costs. Within these design guidelines, a HFSS microwave cavity model was developed to optimally predict the best locations and shape of the power input antenna. This model is helping the

project team refine the microwave cavity design to achieve selective heating that maximizes heating uniformity while reducing input power within this complex microwave field.

The second phase of the development was testing the strategy of leveraging the exothermic energy of particulate matter to complete the DPF regeneration. The model was designed to predict operating times, position, and size of the heating spots that produced the highest probability of successfully regenerating the DPF. Based on experimental results and DPF model predictions, the team designed a new microwave cavity. This cavity was designed to limit the parasitic power effects and the microwave field disruptions caused by the particulate matter. This newly developed design contemplated the results of the model output.

Results and Conclusions

The team completed the project milestones for the first year. The microwave-absorbing materials were defined, and the heating performance of the various candidates has been evaluated using an infrared camera. A full-size microwave-regenerated DPF unit was lab demonstrated at the yearly project review. Model-based predictions correlate closely with the experimental lab demonstration. A model prediction DPF regeneration is described in Figure 2.

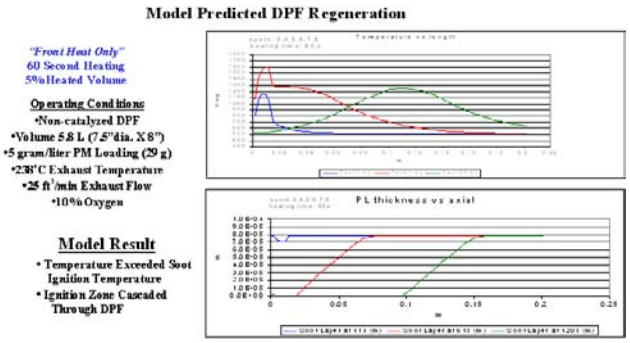

Figure 2. Particulate Matter Regeneration as it Progresses through a DPF Channel

This project is now in full discovery mode. The HFSS and full exhaust DPF model predictions have led to the evaluation of new hardware configurations that should improve the efficiency and robustness of regenerating a DPF. Full-scale vehicle tests will begin upon completion of these studies and implementation of the results.

II.C Critical Enabling Technologies

II.C.1 Development of Metal Substrate for $DeNO_x$ Catalysts and Particulate Traps

Michael Pollard (Primary Contact), Craig Habeger, Paul Park, Amy Fluharty
Caterpillar Inc. Technical Center
Advanced Materials Technology Department
P.O. Box 1875
Peoria, IL 61656-1875

DOE Technology Development Manager: John Fairbanks

Objectives

- Evaluate materials that would suffice as metallic substrates for catalytic converters. Materials must have a lower cost than the current material used with properties sufficient for off-highway diesel applications.
- Evaluate alternate substrate designs that increase catalyst performance to allow smaller designs with less substrate weight and precious metal content.
- Successfully implement these material and design changes into off-highway production units.

Approach

- Material Identification and Testing: New and existing materials will be identified which meet the current requirements of coating adhesion, strength, and oxidation resistance at the lower temperatures experienced in diesel engines. Material testing will compare these to the current material.
- Alternate Design Testing: Alternate designs will be evaluated that increase catalyst performance with minimal change in backpressure.
- Implementation: Durability testing will be performed to ensure that design and material changes do not lower the useful life of the converter.

Accomplishments

- The long-term cyclic oxidation resistance of the candidate alloys was tested and found to be comparable to the current material up to 900°C.
- Prototype production of converters with candidate materials was completed. In producing prototypes, the coatability of these alloys was confirmed.
- Both new materials were formed into the new design substrate in the annealed condition.
- Small prototypes with the new design were produced.

Future Directions

- Complete testing of full-scale current design prototypes with new materials, including hot shake tests.
- Complete modeling of the new design to determine optimum geometry to maximize activity while minimizing backpressure.
- Produce full-scale prototype of new design substrate with optimized geometry and new material.
- Complete hot shake and engine testing of new design substrate.

Introduction

To meet estimated Tier 2 and Tier 3 Environmental Protection Agency emission limits for off-highway vehicles, it may be necessary to add exhaust aftertreatment devices. Two technologies under consideration are $DeNO_x$ catalysts and particulate traps that utilize a packaged cordierite honeycomb catalyst support. This package performs well in on-highway applications; however, off-highway applications are much harsher. Ceramic material properties are not expected to be adequate for the severe conditions found in off-highway applications, such as high-vibration loads (>10 x gravity). Additionally, the ceramic matrix requires relatively thick walls between cells, causing high flow resistance, which translates to increased engine exhaust backpressure and approximately a 2-3% fuel consumption increase. Because metallic substrates have superior mechanical properties over ceramics in this application, they are a possible solution to both durability and flow resistance issues. Metallic substrates are expected to be a key enabler for durable, commercially viable off-highway exhaust aftertreatment devices.

Approach

The development of the metal catalyst substrate is focused in two areas: materials and design. The materials focus includes investigating metals that are more applicable to the diesel exhaust environment. Current metallic catalyst substrates are made from higher-cost alloys that have properties that are necessary for the automotive market. Since diesel engine applications are less demanding in terms of maximum temperature than the automotive market, the search for a less costly material was a major driver. The material selected must have a few key qualities: good oxidation resistance at diesel exhaust gas temperatures, catalyst coatability and adhesion, and good formability.

On the design side, the investigation is moving to alternative design shapes and packages. Current commercially available catalyst supports have straight channel passages. The current work looks to optimize the flow path, thereby increasing catalyst efficiency and potentially reducing necessary catalyst volume. The approach relies on computation methods to give design direction. The package shape is also critical since off-highway vehicles have severe space limitations on additional equipment. The work will also investigate the applicability of package shapes alternative to cylindrical or rectangular.

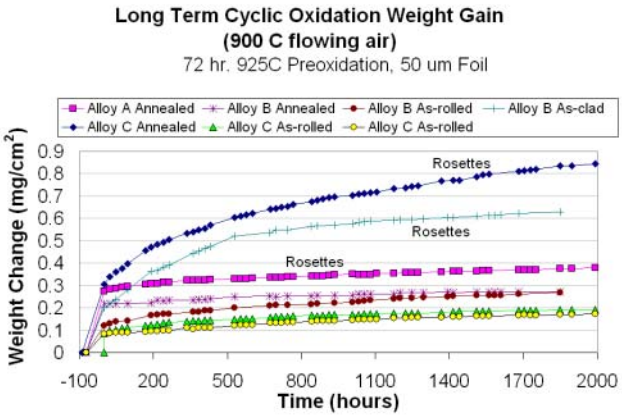

Figure 1. 900°C Flowing Air Cyclic Oxidation Data for Alloys A, B, and C (The material condition and pretreatment are shown in the legend. Each data point represents a cycle from 900°C to room temperature back to 900°C.)

Results

The long-term cyclic oxidation testing of the current alloy (Alloy A), Alloy B, and Alloy C was completed (see Figure 1). The alloys were tested with different pre-treatments to create different types of oxide scale to assess their relative oxidation resistance. They were cycled by heating at 900°C followed by a rapid air cool to room temperature five times per week. It appears from these results that the oxide morphology tends to drive the oxidation rate as much as the alloy chemistry. The three samples with the highest oxidation rates (Alloy A annealed, Alloy C annealed, and Alloy B clad) all formed a rosette structure of alumina on the surface (see Figure 2). This structure provides excellent mechanical adhesion of the washcoat, but it apparently is not good at protecting the metal from further oxidation. The oxide structure of the samples with lower oxidation rates was found to have a “nodular” structure of Al, Cr, and Fe oxides (see Figure 2). This structure is a flatter, more protective oxide. Regardless of the oxide structure, it should be noted that all of these samples displayed very low oxidation

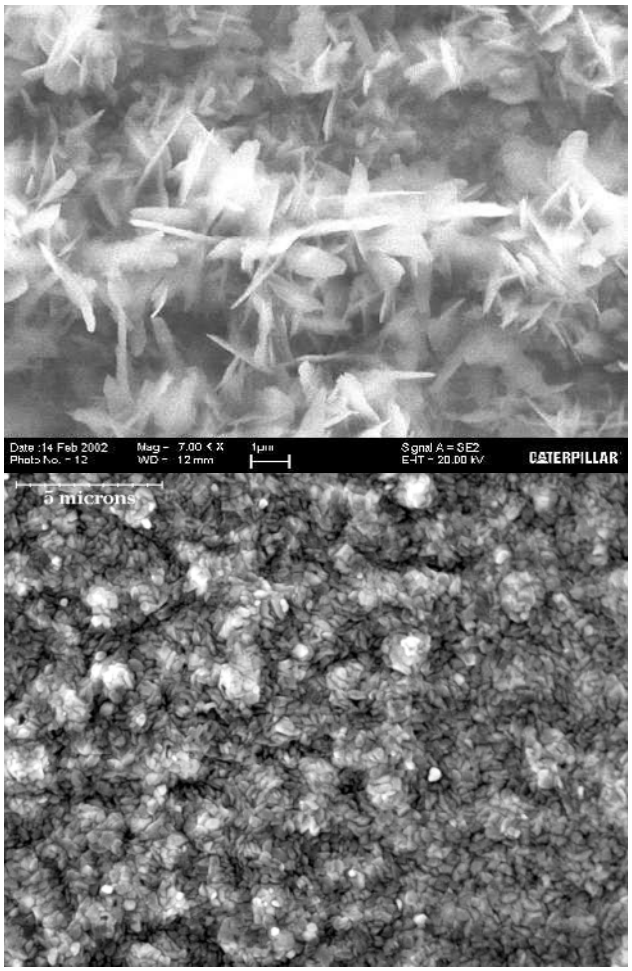

Figure 2. SEM Images of the Alumina Rosette Structure (a) and the Nodular Oxide Structure (b)

rates and are considered acceptable for long-term exposure in diesel engine exhaust.

Is was originally assumed that an alumina rosette structure was necessary for optimum washcoat adherence due to good mechanical bonding in addition to any chemical bonding. This was a drawback to these new alloys, as their lower aluminum contents caused more difficulties in forming the rosette structure over the nodular structure. However, based on discussions with suppliers, as well as prototype production with the new materials (see Figure 3), it was determined that the washcoat adherence is very robust. The nodular structure provides sufficient washcoat adherence. Vibration testing of the full-scale prototype samples showed less than 1% weight loss on all samples

Figure 3. Example of 13" Diameter Prototype Substrate with Alloys B and C and a Straight-Channel Design

tested, which is well within the acceptance range for the supplier's test.

For the new substrate design, it was necessary to determine if the different foil materials in various conditions could be easily corrugated with the new, more complex design. Alloy C annealed, with the lowest aluminum content, was easily formed into the new design at production speeds. Alloy B annealed was satisfactorily formed into the new design. However, there were some small crimps and pinholes. Alloy B has an aluminum content only slightly lower than Alloy A. When in the as-rolled condition, both Alloys B and C had extensive splitting of the foil. Therefore, an annealed foil is necessary for the improved design because there is some tensile deformation of the foil during the corrugation.

Conclusions

The two candidate alloys have passed the minimum requirements thus far for oxidation resistance and coating adherence, and are useful for the new design in the annealed conditions. Assuming both alloys pass the durability and emissions testing, we will be able to choose the most cost-effective alloy.

II.C.2 NO_x Sensor for Direct Injection Emission Control

David B. Quinn (Primary Contact), Earl W. Lankheet (Principal Investigator)
Delphi Corporation
MC 485-220-065
1601 N. Averill Ave.
Flint, MI 48556

DOE Technology Development Manager: Roland Gravel

Subcontractors:
Electricore, Inc., Indianapolis, IN
Delphi Electronics and Safety, Kokomo, IN
SRI International, Menlo Park, CA

Objectives

- Develop an electronics control circuit for the NO_x sensor.
- Develop the packaging for the electronic controller.
- Develop the sensing element structure based on integrating zirconia and alumina ceramics and planar element technology.
- Develop the interconnection method to carry power and signal to and from the NO_x measurement device.
- Develop the necessary materials and process refinements in support of the ceramic sense element.

Approach

- Use alumina and zirconia ceramic tapes and thick film screen-printed pastes to form the necessary control and measurement cells. Integrate the heater on the co-fired substrate. Initiate development using simple configuration test samples and coupons. Continue to evolve the design and test samples into a fully functional NO_x measurement sense element.
- Confirm the operation of the sense element using bench and engine testing.
- Use set-based concurrent engineering to develop at least 2 different techniques to interconnect the power and signal wires to the sense element substrate. Use accelerated engine and environmental testing to establish the optimum interconnection approach.
- Use existing sensor packaging technology to house and protect the sense element.

Accomplishments

- Improved sinterability of a highly complex NO_x sense element.
- Developed process for key electrode material.
- Eliminated cross contamination of electrode materials through improved design.
- Implemented and improved an advanced interconnection design.
- Proved operation of the prototype electronic controller.
- Initiated electronics control parameter refinement.

Future Directions

- Evaluate the NO_x sensor subsystem in bench testing and on a running engine.
- Continue sensor technology refinements.

- Complete testing and characterization of the advanced interconnect.
- Investigate enhancements to the controller and associated algorithms.
- Continue process and materials developments.

Introduction

This project continues to develop the remaining technologies needed to deliver a robust NO_x sensor for use in closed-loop control of NO_x emissions in lean-burn engine technologies, particularly compression ignition, direct injection (CIDI) engines. At least two applications for NO_x sensors have been identified: (1) for measuring engine-out NO_x, requiring a high NO_x range of zero to 1500 ppm NO_x, and (2) for aftertreatment control and diagnostics, requiring a low NO_x range of less than about 100 ppm NO_x.

This activity builds on existing and developing Delphi technology in multi-layer and exhaust sensor ceramics, as well as work performed under a separate CRADA with Pacific Northwest National Laboratory (PNNL). Electricore, Inc., a 501c3 advanced technology development consortium, administers this project.

Approach

The Delphi-led team continues to leverage the electrochemical planar sensor technology that has produced stoichiometric planar and wide-range oxygen sensors as the basis for development of a NO_x sensor. Zirconia cell technology with an integrated heater will provide the foundation for the sensor structure. Proven materials and packaging technology will help to ensure a cost-effective approach to the manufacture of this sensor.

The electronics technique and interface are considered to be areas where new strategies need to be employed to produce higher signal-to-noise (S/N) ratios of the NO_x signal with emphasis on signal stability over time for robustness and durability. Both continuous-mode and pulse-mode control techniques are being evaluated.

Packaging the electronics requires careful design and circuit partitioning so that only the necessary signal conditioning electronics are coupled directly in the wiring harness, while the remainder are situated within the electronic control module (ECM) for durability and cost reasons.

The sense element is based on the amperometric method utilizing integrated alumina and zirconia ceramics. Precious metal electrodes are used to form the integrated heater as well as the cell electrodes and leads. Inside the actual sense cell structure, it is first necessary to separate NO_x from the remaining oxygen constituents of the exhaust, without reducing the NO_x. Once separated, the NO_x is measured using a measurement cell. Development or test coupons have been used to facilitate material selection and refinement as well as cell, diffusion barrier, and chamber development.

The sense element currently requires elaborate interconnections. To facilitate a robust, durable connection, mechanical as well as metallurgical connections are under investigation. Materials and process refinements continue to play an important role in the development of the sensor.

Results

A differential pulse voltammetry (DPV) electronic control strategy was investigated. Significant oxygen cross sensitivity was observed, as shown in Figure 1. Analytical modeling revealed that diffusion of NO_x on the electrode surface is a controlling function. Future work needed to understand the underlying phenomena and their influential factors have been outlined, and it has been

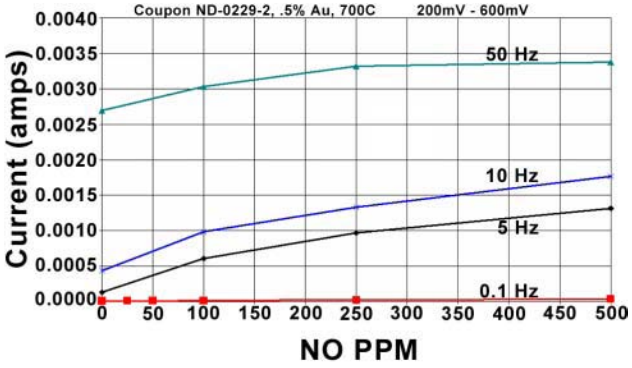

Figure 1. Differential Pulse Voltammetry vs. Frequency

Figure 2. NO_x Sensor Development Controller

decided to focus on continuous-mode control. A prototype electronic controller has been developed based on the continuous-mode control and is pictured in Figure 2. This controller will allow the use of the sensors for initial performance and durability studies.

The NO_x sense element is a device comprised of layers of alumina and zirconia ceramics that are processed to achieve the desired structure. Via's (small holes which are punched through the ceramic tape, later to be filled with precious metal) are used to bring the power and signal from the interior of the element to the exterior. Other features in the device are diffusion ports, chambers, electrodes, leads, contact pads, and air channels. The structure is built layer by layer and then "stacked" in the correct orientation and alignment. The layers are then consolidated using a lamination process, which applies both pressure and heat to mold the layers together. The sensors are each cut from the larger "tile" into individual sense elements prior to sintering.

The ceramic tapes have a significant portion of binders, plasticizers, and organics that require careful removal during the initial stages of sintering. Removal of the organics can cause delamination of the layers and formation of macro and/or micro cracks in the device. In the past, success was achieved through a slow binder removal process in argon to avoid ignition of the organics during the

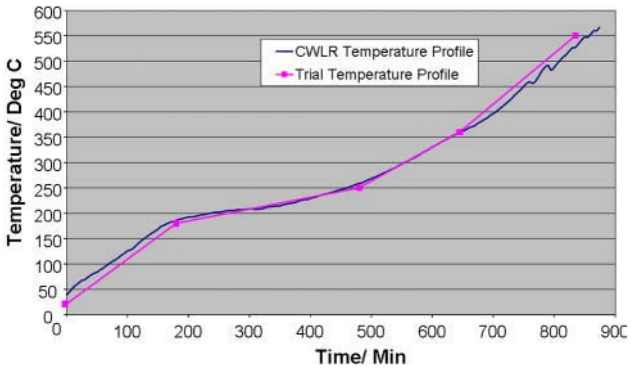

Figure 3. Constant Weight Loss Rate Temperature Profile

Figure 4. NO_x Sensor Packaged Assemblies

removal step. An alternative solution has recently been achieved through the use of a constant weight loss rate of the organics in air, as exemplified in Figure 3. This technique has allowed the successful sintering of the complex-shape NO_x sense elements. The majority of sense elements fabricated are free from defects that would interfere with the performance or structural integrity of the device. Post-sintering techniques and optimization of the chamber-electrode orientations were combined with additional materials development to significantly improve the sensing element.

Once the sense elements are processed and post treated, they are packaged in an exhaust sensor package such as those shown in Figure 4. This involves complex interconnects that require a parallel development activity to ensure robustness and

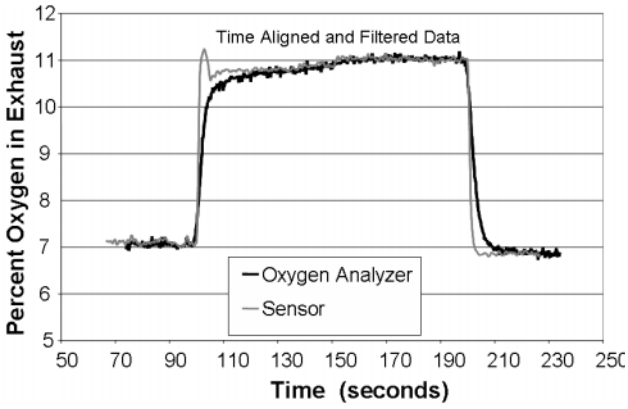

Figure 5. Time-Aligned Oxygen Measurement on the Dyno

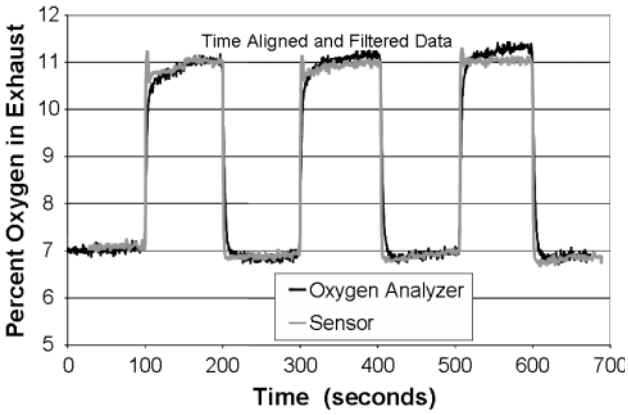

Figure 6. Oxygen Measurement over Several Cycles

enhance the potential for production viability. Mechanical interconnection technology has progressed to the point where it has been chosen as the primary connection technique.

Results of initial testing of the NO_x sensor system on a running diesel engine are shown in Figure 5. This figure compares the sensor oxygen concentration signal at the engine-out location to an oxygen analyzer. It can be seen that the processed oxygen concentration signal from the NO_x sensor correlates well with that from the analyzer. Figure 6 shows six engine exhaust oxygen step changes with similar results from the oxygen concentration signal of the sensor.

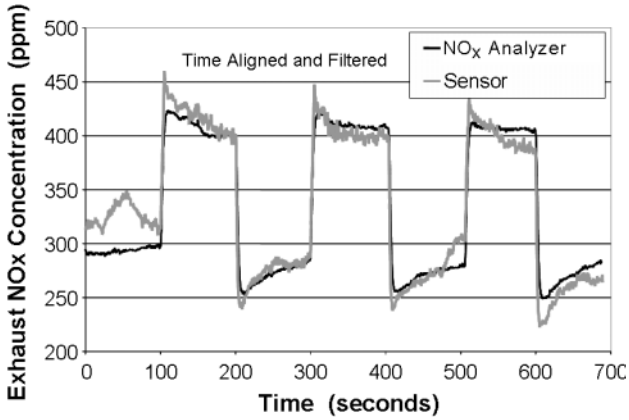

Figure 7. NO_x Measurement on the Dyno

Figure 7 shows the NO_x response with time through six step changes. The NO_x levels varied from about 250 ppm to about 450 ppm. In general, the NO_x sensor correlates very well with the NO_x analyzer.

Conclusions

The development needs of the DPV control approach have been identified, and continuous-mode control electronics have been developed and demonstrated.

NO_x sense elements have been fabricated successfully using a constant weight loss rate profile for the debindering stage of sintering.

NO_x sensors have been successfully packaged using a promising robust interconnection technique.

NO_x sensors have been tested on a diesel engine, with both the oxygen and NO_x concentration signals having a reasonable correlation to analyzer data.

II.C.3 Small, Inexpensive Combined NO_x and O_2 Sensor

W. N. Lawless, C. F. Clark (Primary Contact)
CeramPhysics, Inc.
921 Eastwind Drive, Suite 110
Westerville, Ohio 43081

DOE Technology Development Manager: Roland Gravel

Subcontractors:
MRA Laboratories, Adams, MA
RJS Electronics, Columbus, OH

Objectives

- Demonstrate miniature, amperometric, inexpensive NO_x sensor body in the form of a multilayer ceramic capacitor.
- Incorporate NO_x sensor body with a similar oxygen sensor body in a zirconia tube as a fully assembled NO_x sensor.
- Demonstrate microprocessor-based measuring electronics.
- Supply sensors and measuring electronics for testing at Rosemount Analytical and other outside institutions.

Approach

- Measure NO_x sensing characteristics of a matrix of sensor bodies manufactured from stabilized zirconia in the form of multilayer capacitors with porous, Rh-based electrodes.
- Determine optimum electrodes, operating temperature range, and long-term stability of NO_x sensor bodies.
- Design and breadboard microprocessor-based measuring electronics and characterize.
- Prepare sensors and measuring electronics and supply these to Rosemount and others for testing.

Accomplishments

- Capacitor-type sensor bodies successfully manufactured with two types of porous Rh-based electrodes.
- Solved, but have not optimized, technical hurdle of rhodium oxidation.
- Large NO_x sensitivity demonstrated with sensor bodies having both types of Rh-based electrodes.
- Operating temperature range and voltage determined.
- Measuring electronics designed, built and tested successfully.

Future Directions

- Optimize Rh-based electrodes.
- Continue characterizations and long-term testing of NO_x sensor body.
- Develop electronic control of pO_2 inside assembled sensor and its temperature.
- Incorporate NO_x and O_2 sensor bodies into fully assembled NO_x sensors.
- Complete testing at outside institutions.

Introduction

The need exists for an inexpensive, reliable, on-board sensor to monitor NO_x emissions of vehicles to meet state and federal regulations. This NO_x-sensor project builds on a recent successful project supported by DOE to develop a miniature, amperometric *oxygen sensor* manufactured from stabilized zirconia as a multilayer ceramic capacitor with porous Pt electrodes which catalyze oxygen molecules to oxygen ions. The basic concept of the oxygen (and NO_x) sensor is illustrated in Figure 1. Oxygen ions are "pumped" from the (-) to the (+) electrodes across the zirconia ceramic layers under an applied voltage, and this amperometric current provides a measure of the oxygen partial pressure in the surrounding gas. The porosity of the Pt electrodes provides the necessary diffusion limitation, and there is no need for a reference gas. The sensitivity of this oxygen sensor is shown in Figure 2, and the output current is in the milliamp range. The sensor body contains eleven active ceramic layers and is approximately 2 mm x 3 mm x 5 mm. The established manufacturing methods for ceramic capacitors make this a very low-cost sensor body (~ $1).

It is well known that Rh catalyzes NO_x to nitrogen and oxygen. If porous *Rh electrodes* are substituted for the porous Pt electrodes above, the resulting sensor will have an amperometric current output due to the oxygen released from the NO_x and will thereby provide a NO_x measurement. A schematic illustration of a *combined* oxygen and NO_x sensor is shown in Figure 3. The oxygen sensor

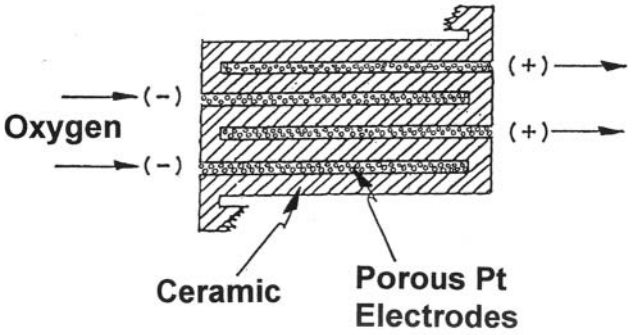

Figure 1. Schematic illustration of the capacitor-type amperometric sensor body showing the porous electrodes. The ceramic layers are stabilized zirconia and the electrodes are Pt in this example.

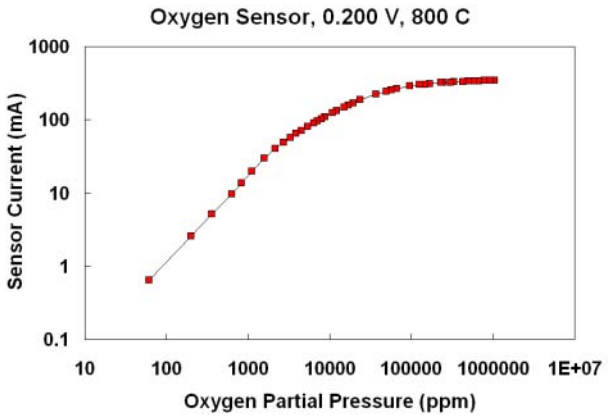

Figure 2. Oxygen sensitivity of the previously developed amperometric oxygen sensor (0.1 VDC applied).

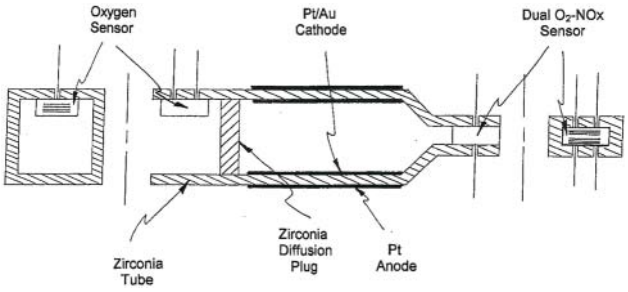

Figure 3. Schematic illustration of the combined sensor for measuring both the oxygen partial pressure and NO_x content of an exhaust gas. The exhaust gas diffuses through the zirconia diffusion plug, and the oxygen level in the inner chamber is pumped to a small, residual level by applying a voltage to the Pt/Au cathode and Pt anode electrodes.

is mounted in the open end of the zirconia tube to measure the oxygen in the exhaust gas, and bonded oxygen and NO_x sensors are mounted in the closed end. Exhaust gas diffuses through a diffusion plug into the inner chamber, where the oxygen in the gas is pumped to a low, residual level by a voltage applied across the Pt anode and the Pt/Au cathode. The oxygen sensor measures only the oxygen content of the gas. The NO_x sensor measures both the oxygen and NO_x contents. The difference in these two measurements is then a measure of the NO_x content of the exhaust gas. It is estimated that this combined sensor would be about 2.5 cm long and 1.3 cm in diameter, and parts cost would be $5-10.

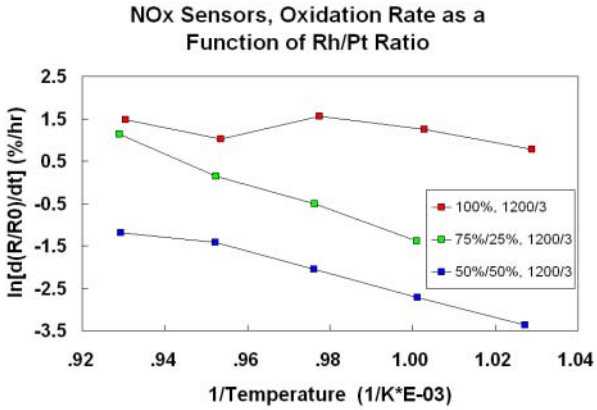

Figure 4. Arrhenius plot of the rate of change of resistance versus temperature for various electrode alloy materials.

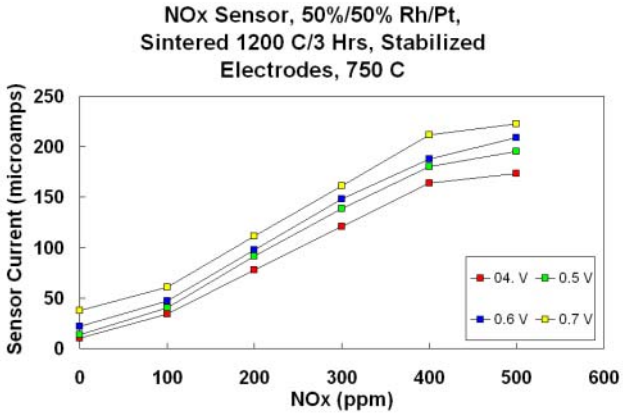

Figure 5. Typical NO_x sensitivity curves for NO_x sensor bodies with three electrodes and 50%/50% Rh/Pt electrodes as a function of applied voltage.

Approach and Results

The capacitor manufacturer made zirconia sensor bodies with Rh electrodes and three active ceramic zirconia layers, each 0.008 cm thick. The first step involved measuring the NO_x sensitivity as a function of sintering temperature because, as with the oxygen sensor, the important porosity of the electrodes decreases with increasing sintering temperature. Sintering temperatures in the range 1200-1300°C were used, and the optimum temperature is 1200°C. The basic concept of sensing NO_x was demonstrated in these tests.

However, a fundamental problem arose in that the Rh slowly *oxidizes* in the 600-800°C operating range, and the amperometric current degrades with time. As the oxidation goes to completion, the volume change causes the sensor body to delaminate. Therefore, the emphasis shifted to using Rh-Pt alloys for the electrodes to inhibit electrode oxidation, and the manufacturer made sensor bodies with two alloys, 75%/25% and 50%/50% Rh/Pt electrodes. The alloying significantly decreased the rate of oxidation without affecting the NO_x sensitivity. The rate of oxidation was measured by monitoring the change in resistance of the electrodes as a function of time at various temperatures. Typical results are shown in Figure 4, which is an Arrhenius plot of the change in resistance with time versus temperature. The 50%/50% Rh/Pt electrodes reduce the oxidation rate significantly compared to the pure Rh electrodes.

Typical NO_x sensitivity is shown in Figure 5 as a function of the voltage applied to the sensor. In order to keep testing costs down, all these measurements have been made using sensor bodies with only three active layers (refer to Figure 1). The final sensor bodies will have up to 30 electrodes, which will increase the response shown in Figure 5 by a factor of ten.

The basic electronic hardware has been designed, built, and tested successfully. This instrument has three outputs for each of the three sensors shown in Figure 3. Each output holds the voltage constant at the sensor while providing for independent measurement of the current through that sensor.

Conclusions

The basic concept of a miniature, inexpensive, amperometric NO_x sensor *has been demonstrated*, and this is the *key* element in the combined oxygen and NO_x sensor illustrated in Figure 3 (the accompanying oxygen sensor has been developed previously). The prospect of achieving a small, inexpensive NO_x + oxygen sensor that does not require a reference gas is now very promising, and such a sensor would serve an important diagnostic function onboard trucks and other vehicles for emissions control.

The Pt-Rh alloy for the electrodes of the NO_x sensor body has not yet been optimized, but the methods for determining this alloy are straightforward, although time-consuming and expensive.

Patents

1. A patent has issued for the oxygen sensor (US 6,592,731) and for the Combined Oxygen and NOx Sensor (US 6,824,661). Both patents were based on patent disclosures filed with the Patent Office prior to the receipt of the corresponding DOE contract.

II.C.4 Development of an Advanced Automotive NO_x Sensor

L. R. Pederson (Primary Contact), G. W. Coffey, and E.C. Thomsen
Pacific Northwest National Laboratory
902 Battelle Boulevard
Richland, Washington 99352

DOE Technology Development Manager: Ken Howden

Technical Advisor:
David B. Quinn, Delphi Corporation

Objectives

- In collaboration with Delphi Corporation, develop an electrochemical NO_x sensor that meets performance targets for sensitivity, range, accuracy and resolution, transient response, cross-sensitivity, lifetime and cost.
- Develop active, selective and stable oxygen roughing pump, oxygen finishing pump, and NO_x sensing electrode compositions and structures.
- Address materials processing issues in producing multistage ceramic sensor structures.

Approach

- Establish rates of electrochemical decomposition for oxygen and NO_x for selected electrode/electrolyte combinations as a function of temperature and partial pressures of oxygen, NO_x and other exhaust gases.
- Explore the suitability of non-noble metal-based compositions for use as the oxygen pump and NO_x sensing electrodes.

Accomplishments

- A ceramic oxygen pumping electrode was developed that is compatible with high sensor processing temperatures, shows very high activity for oxygen pumping, is insensitive to NO_x, and should be less costly than noble metal electrodes.
- Precise control of the oxygen partial pressure in the NO_x sensing stage has been shown to be essential to accurate and stable sensor performance.
- Reactions of carbon monoxide with NO_x over the NO_x sensing electrocatalyst can be suppressed by maintaining the oxygen partial pressure over a critical level.

Future Directions

- Determine how sensor operation is affected by the presence of ammonia in exhaust gases.
- Investigate pulsed detection methods as a means of enhancing sensor sensitivity and accuracy.

Introduction

A reliable NO_x sensor is an important part of advanced diesel exhaust gas treatment systems. The NO_x sensor is necessary to evaluate the efficacy of after-treatment approaches, which include the use of selective catalytic reduction, NO_x absorbers, and/or plasma-based catalytic reactor systems. Sensors that can accurately assess NO_x slip from NO_x reduction devices are a necessary part of any exhaust treatment strategy. An increase in fuel economy related to the use of a NO_x sensor in a closed loop control mode is

estimated to be between 0.5 and 1%. A particularly challenging requirement for NO_x sensors is that they must continue to function properly even during such operations as trap regeneration, when pulses of reducing gases are introduced.

NO_x sensors were identified in the 2000 DOE Sensor Workshop as a high-priority need for compressed ignition/spark ignition direct injection (CIDI/SIDI) engines (Glass, Milliken, Sullivan and Howden 2000). Performance requirements for a NO_x sensor were recommended: 20-300±5 ppm sensitivity range for diesel fuel; 100-200±20 ppm sensitivity for gasoline; 600-1000°C operating range; 10 year lifetime (150K miles for autos, 500K miles for trucks); 1 second response time; provide separate measurements for NO and NO_2; and be immune to soot, sulfur, and ammonia. The need for improvements with respect to sensor durability, cost, response time, drift, and ammonia interference were noted.

Approach

The purpose of this project is to collaborate with the Delphi Corporation in the development of a reliable NO_x sensor. A multi-stage, amperometric approach is being followed, shown schematically in Figure 1, and consists of an oxygen roughing pump, an oxygen finishing pump, and a NO_x sensing stage, in addition to one or more reference cells. An amperometric design, as opposed to an approach based on mixed potentials, is believed to provide superior sensitivity, selectivity, and durability. Research and development performed at Pacific Northwest National Laboratory (PNNL) focuses on electrochemical response of the oxygen pump and NO_x sensing electrodes under a wide range of exhaust gas conditions, evaluation of alternative metal oxide electrode compositions, investigations of exhaust gas reactions that may affect the accuracy and sensitivity of the sensor, and evaluation of pulsed potential methods as a means of improving sensor response. These activities support Delphi Corporation's efforts to design and develop sensor elements, packages, and associated electronics; building of prototype sensors on a pilot scale; dynamometer and vehicle testing of prototype sensors; and evaluation of degradation processes.

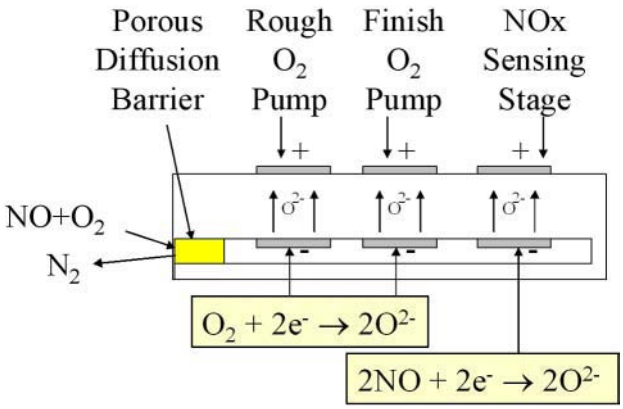

Figure 1. Functional diagram of an amperometric NO_x sensor being developed by the Delphi Corporation.

Results

Alternative ceramic electrode compositions were evaluated for use in oxygen pumping and NO_x sensing cells. One family of ceramic composite compositions is a promising candidate for use as the oxygen roughing pump electrode. The composite is compatible with high processing temperatures used in fabricating the multilayer sensors, provides a good thermal expansion match to other sensor components, shows excellent activity for oxygen pumping, is insensitive to NO_x, and should be less costly than noble metal-based electrode materials. The performance of this electrode is not affected by possible redistribution of gold from the oxygen finishing pump electrode, a dilute Au alloy with Pt. Pumping currents for this ceramic composite versus cell potential for a constant oxygen partial pressure and varied NO_x concentrations are given in Figure 2, which shows virtually no sensitivity to NO_x below an applied potential of 0.4 volts – approximately the operating potential of the roughing pump. Some small response to NO_x was found for higher potentials, but this behavior is unimportant for sensor operation.

Lanthanum strontium chromite compositions were also screened for use as oxygen pumping and NO_x sensing electrodes. The chromites are quite refractory materials with excellent electrical conductivity, and thus would be compatible with many sensor processing and operational requirements. Unlike results for the ceramic

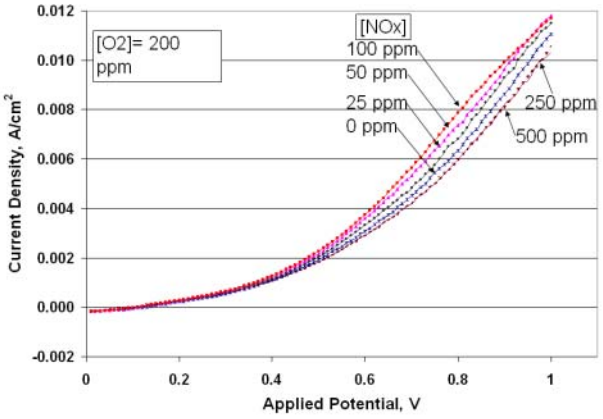

Figure 2. Oxygen pumping current density versus applied potential for an alternative ceramic composite electrode for a constant oxygen partial pressure of 200 ppm and NO_x concentrations ranging from 0 to 500 ppm. The ceramic composite electrode showed no sensitivity to NO_x below ~0.4 volts, approximately the operating potential of an oxygen roughing pump.

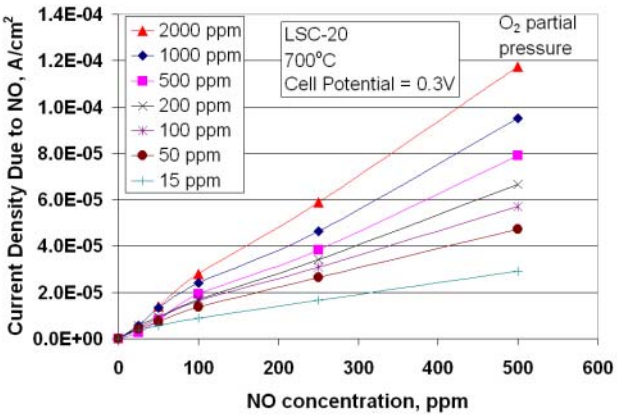

Figure 3. Current density versus NO_x concentration for oxygen concentrations ranging from 15 to 2000 ppm. Unlike the ceramic composite electrode, lanthanum strontium chromite electrodes were sensitive to NO_x. Further, the response depended on the partial pressure of oxygen in the test mixture.

composite described above, the chromite electrode showed high sensitivity to NO_x. Further, the NO_x response was sensitive to the partial pressure of oxygen, as is shown in Figure 3. This material quite clearly is not appropriate for use in the oxygen roughing pump, but may be appropriate as the NO_x sensing electrode. Further testing showed the limitations of chromites for that purpose, however.

Lanthanum strontium chromite, and by inference most other metal oxide compositions, can be partially reduced under the conditions of the NO_x sensing stage. The applied electrical potential and low oxygen partial pressure in the NO_x sensing stage combine to create a locally very reducing environment. For the chromites, electrical conductivity is enhanced by partial substitution of Sr^{2+} for La^{3+}, which causes an approximately equal quantity of Cr^{3+} to be converted to Cr^{4+}. These introduced electron holes provide sites for electronic conduction. In a reducing environment, Cr^{4+} is converted back to Cr^{3+}, as follows:

$$La_{0.8}Sr_{0.2}Cr^{3+}_{0.8}Cr^{4+}_{0.2}O_3 \rightarrow La_{0.8}Sr_{0.2}Cr^{3+}_{1.0}O_{2.9} + 0.05\ O_2 \quad (1)$$

Oxygen that is produced by partial reduction contributes to an enhanced pumping current, which could be mistaken for the presence of NO_x. As shown in Figure 4a, this effect is important for cell potentials greater than ~0.4 volts for chromite electrodes. The transient nature of this enhanced cell current is shown in Figure 4b, which describes changing pumping currents following a potential step. Because the chromites are among the more stable perovskite-based electronic ceramics originally developed for use in solid oxide fuel cells, others are expected to show similar trends. As such, use of metal oxide as the NO_x sensing electrode could complicate signal interpretation.

Response of the NO_x sensing electrode was found to be sensitive to oxygen partial pressure. Incremental current densities due to the presence of NO_x are given as a function of the oxygen partial pressure in Figure 5 for a platinum composite electrode and a constant NO_x concentration of 25 ppm. When the oxygen concentration was held very low, the sensitivity to NO_x was likewise low. An important mechanism for the electrochemical pumping of NO_x appears to involve the oxidation of nitric oxide by adsorbed oxygen, followed by the decomposition of nitrogen dioxide:

$$NO(ads) + O(ads) \rightarrow NO_2(ads) \quad (2)$$

$$NO_2(ads) + 4e^- \rightarrow \tfrac{1}{2}\ N_2 + 2\ O^{2-} \quad (3)$$

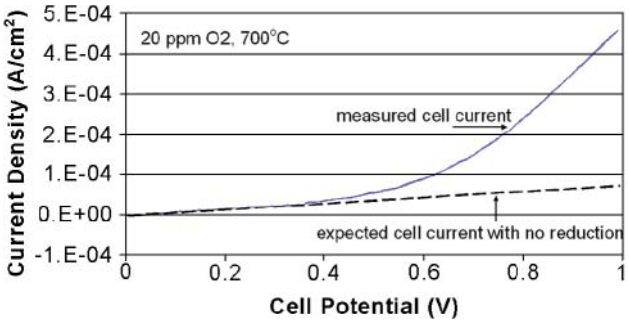

Figure 4a. Current densities arising from the use of a lanthanum strontium chromite electrode versus applied cell potential for low oxygen partial pressures. The partial reduction of the chromite results in higher cell currents than expected.

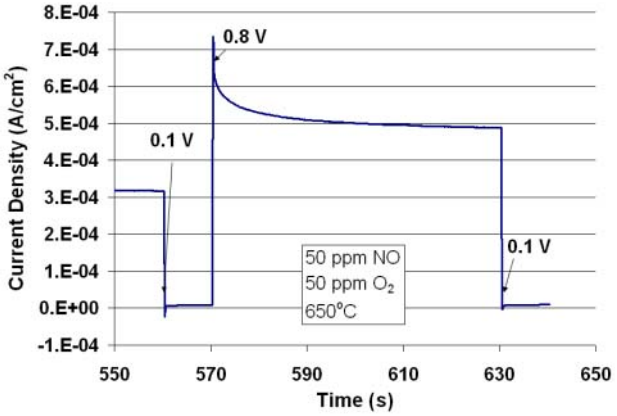

Figure 4b. Application of a voltage step results in a transient cell current for lanthanum strontium chromite electrodes, due to partial reduction of that electronic ceramic.

Mass spectrometer fragmentation patterns for nitrogen and oxygen support the above mechanism. Control of the oxygen partial pressure in the NO_x sensing stage to a constant non-zero level will therefore be necessary to maintain good sensitivity to NO_x.

Carbon monoxide was observed to quantitatively reduce NO_x over a platinum electrocatalyst for very low oxygen partial pressures, as follows:

$$CO(ads) + NO(ads) \rightarrow CO_2 + \tfrac{1}{2} N_2 \quad (4)$$

Because lean diesel exhaust contains low levels of carbon monoxide, nominally 30 ppm, this reaction

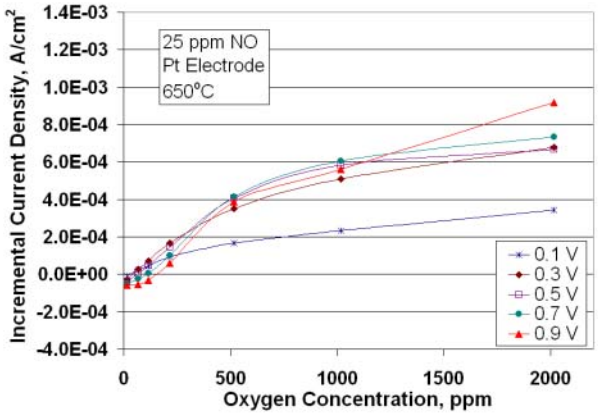

Figure 5. Incremental current density at the Pt electrode due to NO_x versus oxygen partial pressure for a constant NO concentration of 25 ppm. This behavior indicates that control of the oxygen partial pressure to a constant, non-zero value will be necessary to maintain good sensitivity.

could potentially affect the sensitivity of the sensor. Reaction (4) can be suppressed by controlling the oxygen partial pressure to values greater than the critical oxygen decomposition pressure for carbon monoxide. At an oxygen partial pressure of 100 ppm and carbon monoxide concentrations typical of lean diesel exhaust, reactions of nitric oxide and carbon monoxide could largely be suppressed over the platinum electrocatalyst.

Conclusions

A ceramic composite electrode has been identified for possible use as the oxygen roughing pump electrode. The composite is highly conductive, active for oxygen pumping, sufficiently refractory to be compatible with current sensor processing temperatures, and insensitive to the presence of NO_x. Non-noble metal-based, use of the material could help to lower the cost of sensor manufacture. Ceramic electrodes do not appear to be appropriate for use as the NO_x sensing electrode due to the tendency for partial reduction under oxygen partial pressures and applied potentials typical of that cell.

Cell currents due to NO_x were shown to be sensitive to the oxygen partial pressure. A mechanism consistent with observations involves the oxidation of nitric oxide to nitrogen dioxide on the surface of the electrocatalyst, followed by enhanced

electrochemical decomposition of the nitrogen dioxide to produce a cell current. These results suggest that control of oxygen in the NO_x sensing stage to a constant but non-zero value is essential in achieving high sensor sensitivity.

Under certain conditions, carbon monoxide will quantitatively reduce nitric oxide to nitrogen in the NO_x sensing stage, an effect that could significantly lower sensor sensitivity. Through control of the residual oxygen concentration in that portion of the sensor, reactions of carbon monoxide and NO_x can be suppressed.

References

1. Glass, Robert S., JoAnn Milliken, Ken Howden, and Rogelio Sullivan, "DOE Workshop on Sensor Needs and Requirements for Proton-Exchange Membrane Fuel Cell Systems and Direct-Injection Engines," USDOE Office of Energy Efficiency and Renewable Energy, 2000.

II.C.5 Advanced Portable Particulate Measurement System

Sreenath Gupta
Argonne National Laboratory
9700 So. Cass Ave.
Argonne, IL 60439

DOE Technology Development Manager: Kevin Stork

Industrial Collaborator:
Sensors Inc., Saline, MI

Objectives

- Evaluate Argonne's portable particulate measuring system for on-vehicle particulate matter (PM) measurements.
- Obtain feedback from an instrument manufacturer for potential improvements.
- Evaluate the instrument measurement sensitivity to the volatile organic fraction of PM.

Approach

- Reconfigure the existing instrument for on-vehicle demonstration on a 1999 Mercedes C-class vehicle.
- Perform measurements using a thermodenuder in the sample line to evaluate the measurement sensitivity to volatile organic fraction of PM.

Accomplishments

- Successfully demonstrated that the present instrument can be used as a portable emissions measurement system (PEMS) for typical vehicle operations on the highway.
- Obtained design goals from the instrument manufacturer for further improvement.

Future Directions

- Redesign and rebuild an improved version of the instrument per manufacturer suggestions.
- Complete the tests evaluating the sensitivity to the volatile organic fraction of PM.
- Explore the possibility to incorporate the capability to measure particle aggregate size and number density.

Introduction

Argonne National Laboratory (with funding from the DOE Office of FreedomCAR and Vehicle Technologies) has developed an instrument for diesel exhaust particulate characterization (Figure 1). This instrument (named TG-1), which is based on a technique called laser-induced incandescence (LII), is portable and facilitates real-time measurements especially during engine transients. Though the measurement of particulate mass concentration (mg/m^3) has been demonstrated so far, measurement of mean particle size and number density is also possible. Through tests conducted at Argonne, Caterpillar, and Cummins, this instrument was proven to exhibit excellent linearity, insensitivity to vibration, and excellent day-to-day repeatability [Ref. 1,2]. In FY 2004, it was decided to evaluate the instrument for on-vehicle PM measurements.

As diesel engine combustion has been improved to reduce PM emissions, the volatile organic fraction of PM has increased. It was our objective to evaluate the sensitivity of the present instrument to the volatile organic fraction of PM.

Figure 1. The Argonne TG-1 PM Measurement Device

Approach & Results

In FY 2004, Sensors Incorporated, an instrument manufacturer from Saline, Michigan, had shown interest in commercializing the present instrument. After two visits to Argonne, Sensors Inc.'s representative stated that their main interest was in the application of the present instrument to perform on-vehicle measurements, i.e., in adapting the present instrument as a portable emission measurement system (PEMS). Subsequently, the instrument was mounted on a 1999 Mercedes C-class vehicle as shown in Figure 2. The exhaust from the vehicle was partially sampled and diluted with air (in a ratio of 1 to 15) using Matter Engineering's rotating disk dilution system. Subsequently, the sample was passed through the sample cell of the TG-1 instrument, where instantaneous measurements were performed by the instrument. A small sample pump provided the suction necessary to draw in the sample through the system. While the data was collected by the passenger using a laptop computer, the vehicle was operated up to speeds of 60 mph on rural Michigan roads. Some of the photographs of these tests are shown in Figure 3, and Figure 4 shows sample data output.

As the volatile fraction of PM increases, it is possible that the TG-1 can be used to measure total PM. By passing the sample through a denuder, one can strip the volatiles and measure the solid carbon fraction using a TG-1. The difference of these values can give a measure of the volatile organic fraction. This concept is schematically shown in Figure 5. To

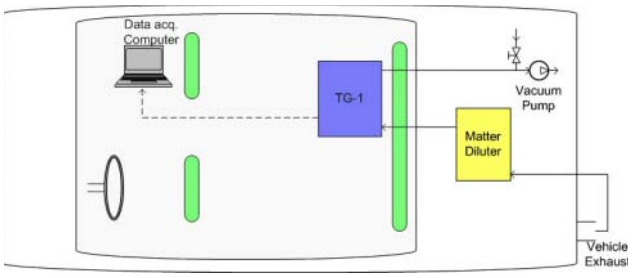

Figure 2. Schematic Layout for On-Vehicle Demonstration of the TG-1

Figure 3. The Instrumented 1999 Mercedes C-Class Vehicle (top) Sensors Inc. Personnel Taking On-Vehicle PM Data (bottom)

evaluate this concept, a thermodenuder from a German company was ordered and received after 3 months (Figure 6). Tests are underway to determine the efficacy of this unit in stripping the volatiles.

Conclusions

Though the use of TG-1 as a PEMS was successfully demonstrated, the following issues were raised by Sensors, Inc.

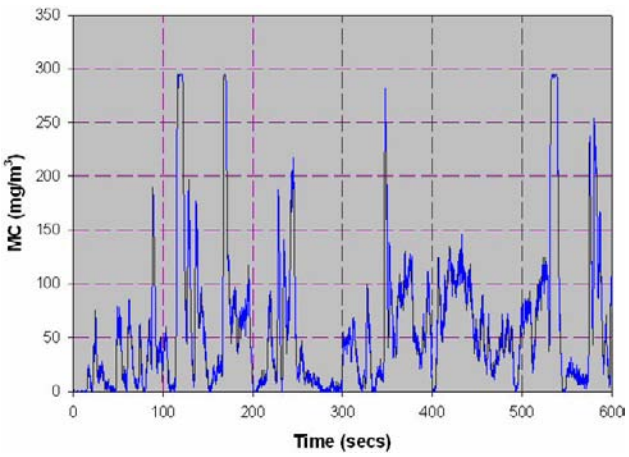

Figure 4. On-Vehicle PM Concentrations Measured Using the TG-1

- Footprint: Desirable to reduce by 50%.
- Weight: Currently at 40 lbs - needs to be reduced by half; in addition, the laser power supply needs to be integrated into the instrument.
- Power requirement: Currently at 1100 watts, which is well above power levels that can be supplied by a typical vehicle; desirable to be reduced to ~250 watts.

Considering the above issues, it was decided to use the recently developed diode pumped solid-state lasers that reduce the footprint, weight and power requirements by an order of magnitude. Additionally, the use of fiber optics for the delivery of both the laser as well the signals was considered. Such an arrangement allows placing the photo sensors away from the heated sample cell, thereby increasing their measurement sensitivity. Efforts are underway to finalize the blueprints of the next-generation version of this instrument.

Special Recognitions & Awards/Patents Issued

1. Portable LII Based Instrument and Method for Particulate Characterization in Combustion Exhaust; US patent No. 6,700,662.

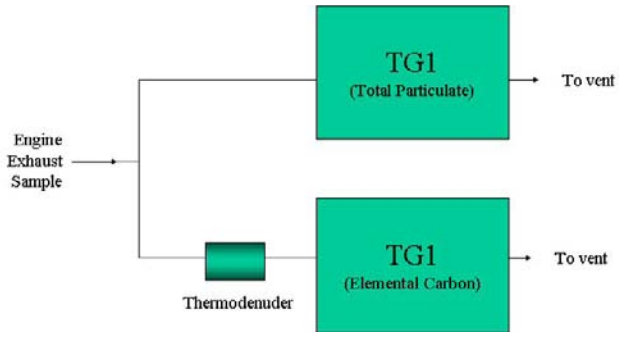

Figure 5. Schematic of the Concept to Measure Volatile Organic Fraction in Real Time

Figure 6. The Thermodenuder Heats the Sample to ~ 400°C and Absorbs the Volatiles Using Activated Carbon (The solid carbon aerosol is passed through.)

FY 2004 Publications/Presentations

1. Poster presentation at the Annual DOE Advanced Combustion Program Review, Argonne, IL.
2. Poster presentation at the DEER 2005 conference, San Diego, CA.

References

1. Sreenath Gupta, Gregory Hillman, Essam El-Hannouny and Raj R. Sekar, "Transient Particulate Emission Measurements in Diesel Engine Exhausts," SAE 2003-01-3155, Journal of Fuels and Lubricants.
2. Sreenath Gupta, "Transient, Real-time, Particulate Emission Measurements in Diesel Engines," 2003 DEER conference.

II.C.6 High-Energy, Pulsed Laser Diagnostics for the Measurement of Diesel Particulate Matter

Peter Witze
Sandia National Laboratories
PO Box 969, MS 9053
Livermore, CA 94551-0969

DOE Technology Development Manager: Kevin Stork

Objectives

- Develop real-time, engine-out particulate matter (PM) diagnostics for measuring size, number density volume fraction, aggregate characterization, volatile fraction, and metallic ash species and concentration.
- Transfer resulting technology to industry.

Approach

- A scanning mobility particle sizer (SMPS) is used as the reference standard for particle size distributions.
- Laser-induced incandescence (LII) is used to measure the soot volume fraction.
- Laser-induced desorption with elastic laser scattering (LIDELS) is used to measure the volatile fraction of the PM.
- Laser-induced breakdown spectroscopy (LIBS) is used to measure metallic ash species and concentration.
- Simultaneous measurements of elastic light scattering (ELS) and LII (ELSLII) are used to obtain the equivalent particle diameter.
- Simultaneous measurements of ELS and LII will be used to obtain the following PM aggregate parameters using the Rayleigh-Debye-Gans polydisperse fractal aggregate (RDG-PFA) approximation:
  - particle volume fraction
  - diameter of primary particles
  - number density of primary particles
  - geometric mean of the number of primary particles per aggregate
  - geometric standard deviation of the number of primary particles per aggregate
  - mass fractal dimension
  - radius of gyration of the aggregated primary particles
- Off-the-shelf components are used to build a measurement system that can be easily duplicated by industry partners.
- Artium Technologies Inc., in Sunnyvale, CA, is commercializing the resulting technology.

Accomplishments

- Time-resolved LII measurements of PM volume fraction have been obtained for engine startup/shutdown, exhaust gas recirculation (EGR) and throttle transients, and these measurements have been compared with SMPS measurements.
- Time-resolved LII measurements obtained for a variety of vehicles during FTP-75 have been compared with tapered element oscillating microbalance (TEOM) and electrical low pressure impactor (ELPI) measurements. LII was shown to be sensitive to better than 0.5 mg/mi.

- Real-time LIDELS measurements of the volatile fraction of diesel PM have been obtained for load and EGR sweeps.
- A collaborative LII investigation of the effects of EGR on PM was conducted with the Combustion Research Group at the National Research Council, Canada.
- Measurements of the calcium in lube-oil ash have been obtained using LIBS.
- A mobile, high-energy laser diagnostics (HELD) system has been built for use in other Sandia engine laboratories and off-site with industrial collaborators. The system was at Ford's Vehicle Emission Research Laboratory for two weeks in February, 2003; Cummins Technical Center for ten weeks in July-September, 2003; and Oak Ridge National Laboratory's National Transportation Research Center for ten weeks in April-June, 2004. All three collaborations resulted in technical papers.
- To demonstrate the ease of use of LII, operator-free measurements were obtained by Cummins for 7.5 weeks of 24/7 operation.
- Artium Technologies' prototype commercial LII instrument was successfully demonstrated on-board a diesel passenger car in November, 2003. The first commercial sales occurred in the spring of 2004.
- Time-resolved (4 Hz data rate) LIDELS measurements of the volatile fraction of diesel PM have been obtained for engine transients.

Future Directions

- Develop experimental capability to measure equivalent particle diameter using ELSLII.
- Extend the LIBS technique to enable time-resolved measurements using inexpensive analog detectors (rather than a spectrometer with an intensified camera).
- Develop experimental and modeling capability for RDG-PFA approximation for aggregate characterization.
- Continue the collaboration with Artium Technologies toward commercialization of HELD instrumentation for PM measurements.

Introduction

LII is a well-established technique for the measurement of PM volume fraction and primary particle size. Light from a high-energy pulsed laser is used to heat the PM to its vaporization point, resulting in thermal radiation that is proportional to the PM volume fraction. Simultaneous measurements of ELS from the particles at several discrete angles relative to the incident laser beam can be used to obtain additional information regarding the characteristics of PM aggregates using the RDG-PFA approximation.

LIDELS is a new technique we have developed for the real-time measurement of the volatile fraction of diesel PM. Laser energy is used to desorb the volatile matter from the diesel PM, and ELS measurements obtained before and after desorption give the volatile fraction. Conventional procedures require collection on filter paper, and subsequent analysis requires from several hours to several days to obtain a measurement. Our real-time LIDELS procedure uses a single laser to obtain a measurement in approximately one minute. Our time-resolved LIDELS procedure uses two lasers to obtain measurements at 4 Hz.

LIBS is a fairly well-established technique for measuring metallic ash. A focused laser beam is used to ionize the ash, resulting in atomic emissions that identify the species and their concentrations.

The ratio ELS/LII is routinely used in flame studies to measure the equivalent particle diameter of dry soot. Because diesel PM contains considerable volatile material, we are developing a new technique, ELSLII, that measures the elemental carbon diameter.

A single HELD system can perform all of the above tasks. Its main advantages over conventional

Figure 1. Mobile HELD System at the Cummins Technical Center in Columbus, IN

PM measurement techniques are that it can be applied in any environment (e.g., hot or cold, undiluted or diluted, etc.), it responds in real time and is very sensitive to low PM concentrations (e.g., the lower limit for LII is estimated to be one part per trillion, or about 0.5 mg/mi).

Approach

The complete HELD system has been assembled on a mobile cart of dimensions 2'x4', as shown in Figure 1, at the Cummins Technical Center in Columbus, Indiana. The only external connections required for use are the sample line for the diesel exhaust, a return vent line, and 110-volt power. The optical setups for LII, ELS, LIDELS, and ELSLII can coexist, whereas LIBS requires the installation of an additional focusing lens. The cabling connections to the data-acquisition oscilloscope are unique for each HELD technique. However, once properly connected, all HELD applications are totally PC controlled, providing essentially "hands-off" operation.

Each time we develop a new HELD technique or make a significant improvement or application of an existing one, we publish the procedures and results in an archived technical article. To further assist the transfer of HELD technologies to outside users, we are pursuing two parallel paths. Because off-the-shelf components are used whenever possible, the expedient approach is to "clone" the system from a shopping list of parts; the PC software and ancillary drawings and schematics are all in the public domain. The alternative is to purchase a commercial unit

Figure 2. 2002 Volkswagen Diesel Jetta with the Artium *LII-200*™ Instrument in the Trunk

provided by Artium Technologies, Inc., of Sunnyvale, CA. We are working directly with Artium on a no-fee basis to develop commercial products. At this time, Artium is marketing an LII instrument, but neither LIDELS nor LIBS are currently available other than by a development contract.

Results

LII is ideally suited for on-road PM measurements because neither dilution nor an operator is required. Shown in Figure 2 is a 2002 Volkswagen Jetta passenger vehicle with a turbocharged direct injection (TDI) diesel engine. The commercial LII instrument of Artium Technologies, *LII 200™*, was placed in the trunk along with a small generator and driven around the Livermore Valley for a day. Typical measurements are shown in Figure 3 for a freeway acceleration from a stop. In general, the spikes in PM emissions correspond to gear shifts by the automatic transmission.

The Sandia HELD system was taken to the Cummins Technical Center in the late summer of 2003 (Figure 1). Because Cummins runs the emissions test facility 24/7, the HELD system was configured with the LII output signal connected to the Center's analog data acquisition system. The system ran continuously for 7.5 weeks, logging 1078 individual tests. Among the tests logged were 363 Federal Test Procedure (FTP) steady-state mode tests

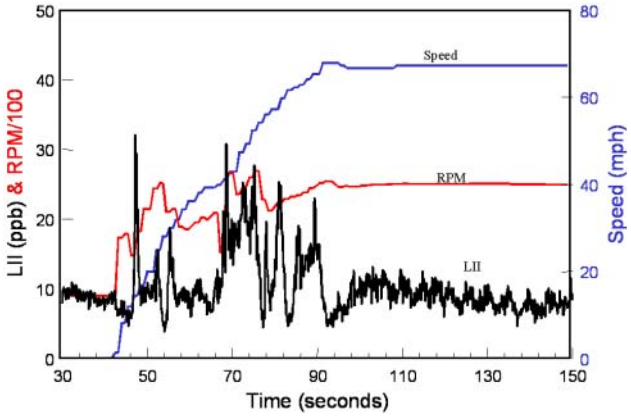

Figure 3. On-road LII Measurements for a Freeway Acceleration from a Stop

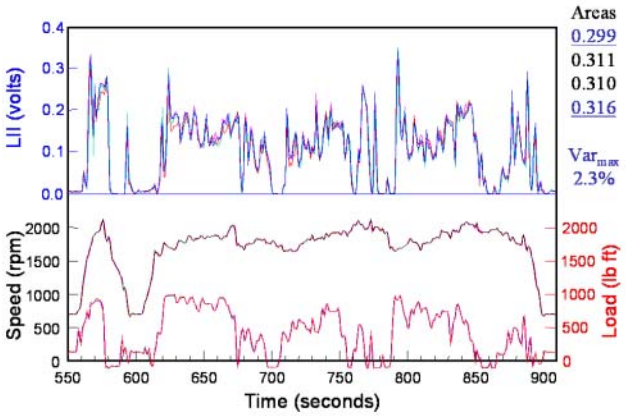

Figure 5. LII Measurements Obtained at Cummins for Four Repeats of a Segment of the Transient Heavy-Duty FTP

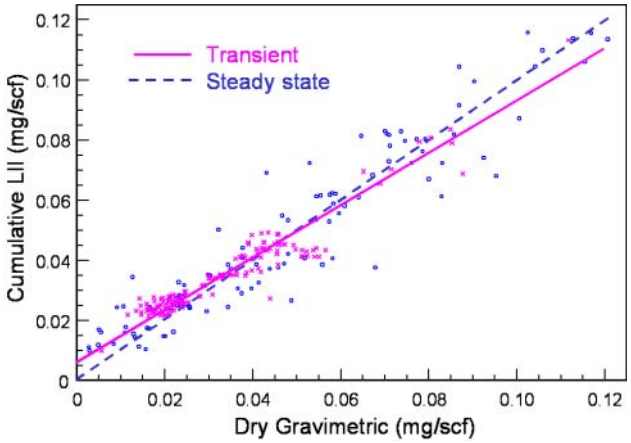

Figure 4. Correlation of LII and Gravimetric Measurements for Both Steady-State and Transient FTPs

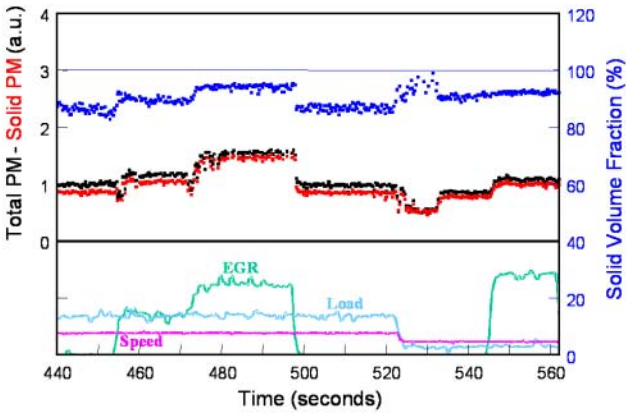

Figure 6. Time-Resolved LIDELS Measurements for Various Engine Transients

and 250 FTP transient tests for which gravimetric measurements of total particulate matter (TPM) were obtained. Of these tests, removal of the filter-based volatile matter using supercritical fluid extraction was performed on 142 and 147 of the tests, respectively. The correlation between the time-integrated LII signals and the dry gravimetric measurements for the steady-state mode tests was used to calibrate the LII measurements in mass units, as shown in Figure 4 (dashed line). This calibration was then used to evaluate the correlation between the LII and dry gravimetric measurements for the transient tests (solid line).

It is our belief that much of the scatter in the data of Figure 4 is due to artifacts in the dry gravimetric measurements. To support this contention, shown in Figure 5 are LII measurements for four repeat tests for a segment of the transient FTP. The test results are presented in four colors, and from the lower portion of the figure it is evident that the speed and load were precisely repeated. The LII results in the upper portion of the figure show very good reproducibility. The areas under the four LII curves are given to the right and reveal a variance of only 2.3%.

The time-resolved LIDELS technique is still undergoing refinement, but typical measurements for transients in load, EGR rate, and engine speed are presented in Figure 6. Two laser pulses separated by 120 ns are used. The first pulse measures the TPM and deposits the energy that desorbs the volatile material. The second pulse measures the remaining solid PM, i.e., elemental carbon, and the ratio of the two measurements gives the solid volume fraction.

Conclusions

- The LII technique has been demonstrated to run unattended for extended periods of time both at a heavy-duty diesel engine manufacturer's test facility and on-board a light-duty diesel passenger vehicle.
- LII measurements for the steady-state and transient FTP have been shown to correlate well with dry gravimetric measurements.
- Development of the LII technique for PM measurements is completed, and a robust, user-friendly instrument is being marketed by Artium Technologies, Inc.
- Time-resolved measurements of the solid volume fraction by the LIDELS technique have been successfully demonstrated. However, dynamic range, robustness, and cost remain as obstacles to commercialization.

Awards

1. SAE speaker award for Excellence in Oral Presentation at the SAE 2004 World Congress.

FY 2004 Presentations

1. "High-Energy, Pulsed Laser Diagnostics for Real-Time Measurements of Diesel PM Emissions," DOE/AEC Meeting, Livermore, January 27-28, 2004.
2. "Time-Resolved Measurements of Exhaust PM for FTP-75: Comparison of LII, ELPI, and TEOM Techniques," SAE International Congress & Exposition, Detroit, March 8-11, 2004.
3. "On-Board, Time-Resolved Diesel Particulate Measurements by Laser-Induced Incandescence," 14th CRC On-Road Vehicle Emissions Workshop, San Diego, March 29-31, 2004.
4. "Unattended, Around-the-Clock Particulate Measurements Using Laser-Induced Incandescence," 14th CRC On-Road Vehicle Emissions Workshop, San Diego, March 29-31, 2004.
5. "On-Board, Time-Resolved Diesel Particulate Measurements by Laser-Induced Incandescence," SAE Government/Industry Meeting, Washington, DC, May 10-11, 2004.
6. "High-Energy, Pulsed Laser Diagnostics for Real-Time Measurements of Diesel PM Emissions," DOE/AEC Merit Review and Peer Evaluation, Argonne, May 18-20, 2004.
7. "High-Energy, Pulsed Laser Diagnostics for Real-Time Measurements of Diesel PM Emissions," DOE/AEC Meeting, Detroit, June 22-23, 2004.
8. "High-Energy, Pulsed Laser Diagnostics for Real-Time Measurements of Diesel Particulate Matter Emissions," invited Keynote Lecture, 7th International Congress on Optical Particle Characterization (OPC2004), Kyoto, August 1-5, 2004.
9. "Time-Resolved Laser-Induced Incandescence Measurements for the EPA Heavy-Duty Federal Test Procedure," The Sixth International Symposium on Diagnostics and Modeling of Combustion in Internal Combustion Engines (COMODIA 2004), Yokohama, August 2-5, 2004.
10. "High-Energy, Pulsed Laser Diagnostics for Real-Time Measurements of Diesel PM Emissions," IEA Task Leaders Meeting, Helsinki, August 22-25, 2004.
11. "High-Energy Laser Diagnostics (HELD) for the Measurement of Diesel Particulate Matter," 10th Diesel Engine Emissions Reduction Conference (DEER 2004), San Diego, August 29-September 2, 2004.

FY 2004 Publications

1. Michelsen, H. A., Settersten, T. B., and Witze, P. O., "Development of Detection Techniques and Diagnostics for Airborne Carbon Nanoparticles," LDRD Final Report SAND2003-8666, November 2003.
2. Witze, P. O., Payne, G., Bachalo, W. D., and Smallwood, G. J., "Influence of Measurement Location on Transient Laser-Induced Incandescence Measurements of Particulate Matter in Raw Diesel Exhaust," *IEA Annual Report*, Fall 2003.
3. Michelsen, H. A., Witze, P. O., Hochgreb, S., and Kayes, D., "Time-Resolved Laser-Induced Incandescence of Soot: The Influence of Experimental Factors and Microphysical Mechanisms," *IEA Annual Report*, Fall 2003.
4. Witze, P. O., "High-Energy, Pulsed-Laser Diagnostics for the Measurement of Diesel Particulate Matter," *DOE/OFCVT Annual Report*, Fall 2003.
5. Witze, P. O., Chase, R. E., Maricq, M. M., Podsiadlik, D. H., and Xu, N., "Time-Resolved Measurements of Exhaust PM for FTP-75: Comparison of LII, ELPI, and TEOM Techniques," SAE Paper No. 2004-01-0964, March 2004.
6. Witze, P. O., Shimpi, S. A., Durrett, R. P., and Farrell, L. A., "Time-Resolved Laser-Induced Incandescence Measurements for the EPA Heavy-Duty Federal Test Procedure," Proceedings of The Sixth International Symposium on Diagnostics and Modeling of Combustion in Internal Combustion Engines (COMODIA 2004), August 2004.

II.C.7 Particulate Matter Sensor for Diesel Engine Soot Control

Michael Rhodes
Honeywell Inc.
MN65-2700
3660 Technology Drive
Minneapolis, MN 55418

DOE Technology Development Manager: Roland Gravel

Subcontractors:
University of Minnesota, Minneapolis, MN
Honeywell Control Products, Freeport, IL

Objectives

- To develop diesel engine exhaust particulate matter (PM) sensor prototypes that have low cost, high speed, reliability, and are capable of operating directly in the harsh exhaust of a diesel engine.
- Install and test the sensor prototypes and compare test results to results of other reference instrumentation.
- Use test results to improve sensor concepts and develop compatible sensor packages.
- Develop associated sensing electronics and signal processing hardware.
- Demonstrate prototype sensor by 4Q 2004.

Approach

The project has three main steps in order to accomplish the research:

- PM Sensor Development—Design and build several prototypes of PM sensors utilizing high-temperature materials for operation directly in the exhaust stream. Develop different readout electronic circuits to monitor the sensor and interface to data acquisition equipment and/or engine controllers.
- Sensor Testing—Establish a diesel engine test bed that will include reference particulate measuring instrumentation and potentially other gas sensing instrumentation. Establish a data acquisition system to record the testing results for further data analysis. These tests will be conducted at the University of Minnesota's Center for Diesel Research and will utilize equipment from their Particle Measurement Laboratory. Gas concentration and particle size distribution information will be recorded to compare to sensor test results.
- Sensor Packaging—Staff members of Honeywell Labs and Sensing and Controls Division will develop suitable sensor packages for the PM sensors. Packaging materials should provide protection to the sensor as well as the ability to withstand the harsh operational environment. Sensor packages will be exposed to high temperatures and corrosive and potentially condensing environments. Destructive and nondestructive testing of the sensor package will be completed.

Major Accomplishments to Date

- Established test facilities at the University of Minnesota using three commercial diesel engines. The first is a John Deere 4540T engine typical of medium-duty off-road applications, the second is a Caterpillar engine typical of heavy-duty on-road applications, and the third is a Volkswagen TDI (Euro IV) engine typical of passenger car applications.
- Established the feasibility of monitoring particulates directly in the exhaust manifold without pretreatment or dilution and without sensor fouling due to accumulation of particulate matter.

- Demonstrated the feasibility of monitoring particulates from each combustion event in real-time on a cylinder-by-cylinder basis.
- Correlated these cylinder-by-cylinder and cycle-by-cycle variations to engine operating parameters such as fuel injection variability and exhaust gas recirculation (EGR) behavior.
- Completed fabrication of concept prototype devices for testing in end-user facilities.

Future Directions

- Demonstrate prototype sensors and electronics in several end-user facilities. This will constitute the final deliverable on this project.

Introduction

Emission regulations worldwide emphasize reducing fine particulate matter emissions. Recent studies have shown that fine particles are more strongly linked with adverse health effects than are larger particles, and engines are an important source of fine particles.

Particles in the nucleation mode and in the accumulation appear to be formed by different mechanisms. Accumulation-mode particles are primarily carbonaceous and are associated with rich combustion and poor subsequent oxidation during the engine cycle. Most nucleation-mode particles are not even formed until the exhaust dilutes and cools. They consist of a complex, poorly understood mix of sulfuric acid and partially burned fuel and lubricating oil. Formation of these two types of particles likely occurs under different engine operating conditions, with heavy loads favoring carbonaceous accumulation-mode particles and light loads most likely favoring the formation of vapor-phase precursors of nucleation-mode particles. These precursors may not undergo gas-to-particle conversion until the exhaust cools and dilutes in the atmosphere.

In order to meet future emission standards, future diesel engines will have to be fitted with sophisticated combusion control systems and, almost certainly, an aftertreatment system including particle filters or traps. An effective exhaust particulate sensor would not only lead to a reduction of particulate emissions from the engine itself, but would also make traps and other aftertreatment devices more feasible. Particulate traps are now commercially available and are likely to be applied in high volume in the future. They are large, expensive and impose a significant fuel economy penalty. A particulate sensor would help reduce the amount of particulate matter created through better engine control. It could also be used to monitor particulate loading or breakthrough on downstream traps. Thus, the particulate trap could potentially be made smaller or be regenerated less often.

Approach

Solid particles present in diesel engine exhaust carry a significant electrical charge (Kittelson et al., 1986a; 1986b, Moon, 1984). We examined several types of sensors based on measurement of particle charge such as an ionization sensor, an image charge sensor, and sensors based on alternating current (AC) conductance and capacitance of the exhaust. Our preferred approach is an image charge sensor based on design simplicity, speed, and ruggedness.

The sensor probe is built on a commercial spark plug body as seen in Figure 1. This platform is ideal

Figure 1. Honeywell PM Sensor Probe Based on a "Spark Plug" Configuration

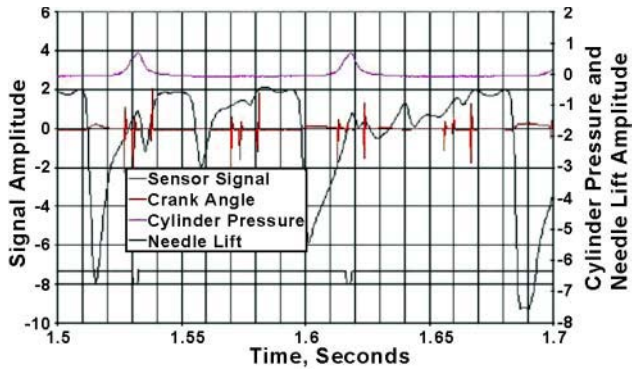

Figure 2. Typical real-time waveforms of sensor signal, cylinder pressure, crank angle, and needle lift. Data was taken on a John Deere 4540T test engine running at 1400 rpm, with no EGR and 90% load.

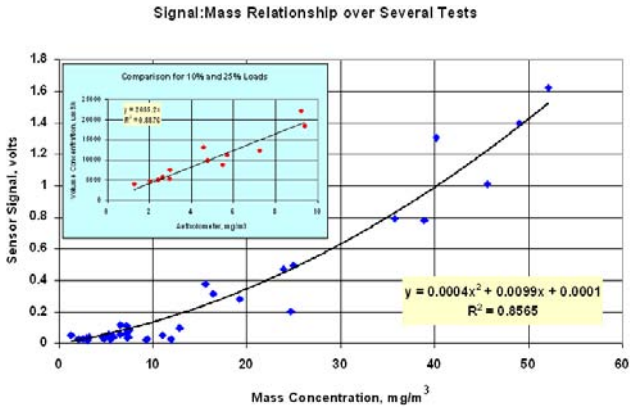

Figure 3. Correlation of Sensor Signal to Black Carbon Concentration as Measured with a Reference Fast-Response Aethelometer

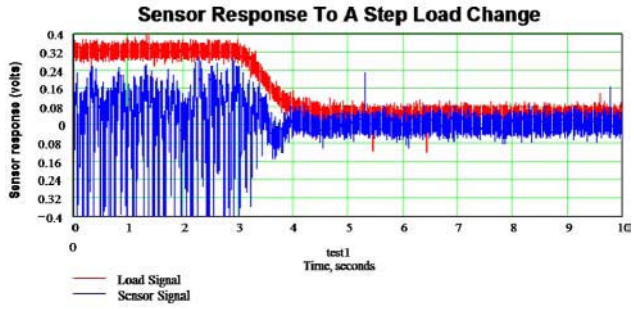

Figure 4. Response of the PM sensor to a step change in engine load. Note the overall effect on peak amplitude as well as changes in individual cylinder behavior.

for placement directly in the exhaust manifold as it withstands high pressures and temperatures and is stable towards vibration, gas composition and sooting found in that environment. Because of the extreme temperature of the probe—measured as high as 700°C—the electronics are remote from the sensor probe.

Results

The John Deere 4045T engine being used has one cylinder (cylinder number 4) that is instrumented with an in-cylinder pressure sensor. This pressure sensor is typically used to frame individual engine cycles for data analysis. Figure 2 shows the basic real-time sensor signal with corresponding traces of cylinder pressure, crank angle and fuel injector needle lift. A high degree of cycle-to-cycle and cylinder-to-cylinder variation is seen in the data. Similar effects, albeit smaller in magnitude on more modern, cleaner-burning engines, have been observed for the Caterpillar engine (showing 6 smoke peaks present for the 6 cylinders) and for the Volkswagen TDI engine. We suspect many of the variations in these more modern engines are due to the static and dynamic behavior of the EGR systems, although the effect is still under investigation.

The peak-to-peak amplitude of the individual smoke pulses and the average sensor output (RMS output) are well-correlated to smoke concentrations as measured with standard reference particulate instrumentation. Figure 3, for example, shows the correlation of sensor output (peak-to-peak) with a reference aethelometer measuring black carbon concentration. The sensor data were averaged over several engine cycles in order to correspond to the 1 second minimum response time of the aethelometer. The sensor output shows minimal correlation to temperature and pressure and has shown no fouling from accumulated particulate matter.

Figures 4 and 5 show the response of the sensor across operating loads—and hence smoke concentrations—of the John Deere test engine. One can see that the PM sensor easily tracks changes in smoke concentration resulting from engine load variations in real-time without sampling lags. This makes the sensor ideal as a feedback control element in engine control and/or EGR control applications.

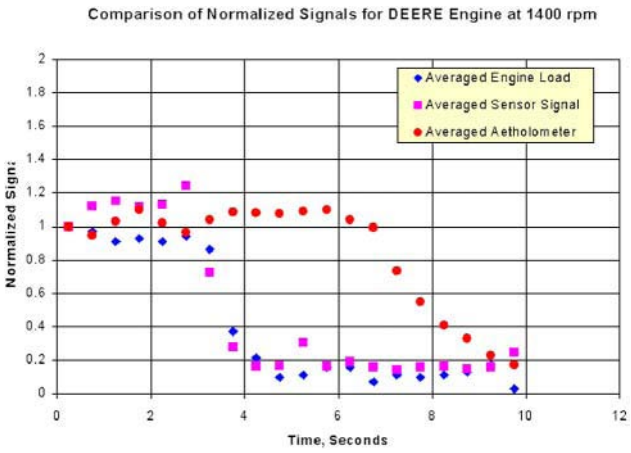

Figure 5. Correlation of the PM sensor signal and aethelometer to a step change in engine load. The time lag in the aethelometer signal corresponds to the residence time in the sampling and dilution tunnels. The PM sensor is running in real-time and shows no such time lag.

Conclusions

Considerable technical progress has been made during FY 2004. Namely, we achieved the following:

- Fabricated and tested several concept prototype sensor probes based on a very simple, manufacturable foundation.
- Developed an adequate test bed and data logging capabilities that allow examination of sensor behavior across multiple engine types and under varying engine conditions.
- Verified that the charge sensor approach gives us a reproducible signal that is well-correlated to exhaust smoke as characterized by several reference methods.
- Verified that the charge sensor responds in real-time (millisecond timescale) to instantaneous smoke concentrations from individual cylinder exhaust events.
- Observed that on our various test engines there is considerable variation in the sensor response from cylinder to cylinder and from cycle to cycle. This variability appears to be real variations in engine behavior and not artifacts of the sensor signal.
- Observed that in many cases, we can correlate this cylinder-to-cylinder or cycle-to-cycle variation to inconsistencies in fuel injection and/or EGR behavior.
- Observed that the sensor probe response does not degrade due to soot build-up or high temperature exposure over several hundred hours of operation.
- Developed prototype hardware and software in order to work with several engine/vehicle end-users to verify our findings in their facilities.

III Advanced Engine Designs for Improved Efficiency

III.A Heavy-Duty

III.A.1 Heavy Truck Engine Program

Brett Barnhart (Principal Investigator), Chris Nelson (Primary Contact)
Cummins, Inc.
1900 McKinley Ave.
Columbus, IN 47201

DOE Technology Development Manager: Roland Gravel

Objectives

- **Phase I** – Demonstration of 45% brake thermal efficiency (BTE) at cruise conditions while meeting 2002 Environmental Protection Agency (EPA) emissions regulations. Demonstration made in January of 2002.
- **Phase IIA** – Demonstration of 45% BTE at cruise conditions while meeting 2007 emissions regulations. Demonstration made in Q1 of 2004.
- **Phase IIB** – Demonstration of 50% BTE maximum while meeting 2010 emissions regulations. Demonstration due in 2006.

Approach

Phase I tasks are complete. Phase IIA tasks are complete. Phase IIB tasks are as follows:

- Engine Development
  - Advanced combustion systems for best NO_x/fuel economy trade-off for 2010
  - Analysis of data and sub-model development
  - Optimal combustion system design options
  - Controls architecture for an advanced combustion system
  - Air handling/exhaust gas recirculation (EGR) architecture
  - Advanced combustion single-cylinder testing
  - Definition and demonstration of subsystem architecture for 2010
  - Analysis and design of waste heat recovery techniques to support brake thermal efficiency targets
  - Design of waste heat recovery system hardware for test cell demonstration
  - Design of engine system controls to achieve optimal engine system efficiency
- Analysis/Development of NO_x & Particulate Matter (PM) Aftertreatment Systems
  - System architecture development
  - Engine procurement and test support
  - Model development and validation
  - Adsorber subsystem development
  - Soot filter subsystem development
  - Aftertreatment subsystem integration
  - Aftertreatment subsystem optimization
  - Aftertreatment subsystem integrity demonstration
- Exhaust Conditioning for NO_x and SO_x Regeneration
  - In-cylinder exhaust conditioning analysis and test

  - Evaluation of fuel and air handling systems
  - Development of engine management strategy for NO_x, SO_x, and diesel particulate filter (DPF) regeneration and exhaust stream conditioning
- Development and Integration of Control System
  - Controls architecture and modeling of engine, aftertreatment, and heat recovery systems
  - Aftertreatment sensor development
  - Control architecture definition for 2010
  - Control architecture demonstration for 2010
- Vehicle Demonstration
  - Engine and aftertreatment system demonstration in a heavy truck
  - Demonstration of 50% BTE maximum @ 2010 emissions in test cell
- Reporting
  - Implementation plan
  - Quarterly reports
  - Annual review & reports

Accomplishments

- Achieved and demonstrated 45% BTE while meeting 2007 emissions goals in test cell and in vehicle in support of Phase IIA deliverables.
- Demonstrated advanced recirculated exhaust gas cooling in support of Phase IIA efficiency goal.
- Developed a System Integration and Configuration Matrix to define potential engine architectures to support Phase IIB project goals.
- Developed a Pugh Matrix to define and identify optimal heat recovery techniques to achieve Phase IIB efficiency goals.
- Specified and procured a variable valve actuation (VVA) research tool to support advanced combustion research.
- Evaluated different forms of homogeneous charge compression ignition (HCCI) combustion and performed failure mode and effects analysis (FMEA) on each to identify and prioritize challenges.
- Developed engine-system models for HCCI and diffusion burn combustion techniques to help evaluate engine architectures and support system design.

Future Directions

- Evaluate different combustion types and refine hardware to achieve project deliverables. Follow analysis-led-design methods to maximize the return from research hardware expenses.
- Perform engine system modeling to predict engine, aftertreatment, and heat recovery system performance.
- Perform test cell testing to verify models and system performance.
- Define and acquire engine system components to support project goals.
- Develop model-based controls to support system performance.
- Perform bench-top component testing and system test cell testing.
- Define and acquire critical system components to verify model results and identify performance limits.
- Integrate the base engine into a heavy-duty vehicle for demonstration.
- Set up engine and heat recovery system demonstrations.

Introduction

Cummins Inc. is working to develop and demonstrate advanced diesel engine technologies to improve diesel engine thermal efficiency while meeting future emissions requirements. The effort meets the objectives outlined by the Department of Energy, which include two major phases. In Phase I (completed), Cummins worked to demonstrate by January, 2002, engine efficiency equal to or greater than 45% while complying with emissions regulations of 2.5 g/bhp-hr NO_x-hydrocarbon (HC) and 0.10 g/bhp-hr particulate matter, as defined in the EPA/Department of Justice Consent Decree with the diesel engine manufacturers. In Phase IIA, Cummins worked to demonstrate in early 2004, BTE of 45% in a multi-cylinder, heavy-duty diesel engine while complying with 2007 EPA emissions regulations of 1.2 g/bhp NO_x-HC and 0.01 g/bhp-hr particulate matter. In Phase IIB, Cummins shall work to demonstrate in 2006, BTE of 50% in a multi-cylinder, heavy-duty diesel engine while complying with the 2010 EPA emissions regulations of 0.2 g/bhp NO_x-HC and 0.01 g/bhp-hr particulate matter.

These project goals are challenging and require intensive research and development. Emissions reduction by traditional means will have a negative impact on BTE. The engine and emissions performance technologies advanced in this project will accelerate the development of high-efficiency, low-emission diesel engines.

Approach

Cummins' approach to these project objectives continues to emphasize analysis-led-design in nearly all aspects of the research. An emphasis is placed on modeling and simulation results to lead the way into feasible solutions.

For the deliverable in each phase, a configuration matrix study is planned to determine appropriate, feasible solutions. Engine system solutions include various air handling schemes, control system approaches, and aftertreatment system combinations. Based on extensive model/simulation data, previous testing experience, or verifiable supplier's information, a best-choice solution set of system components is selected. A variety of laboratory tests are conducted to verify performance and to tune system functions. Model predictions are verified, and models are refined as necessary. Often, different portions of the system are pre-tested independently to quantify their behavior, and their data is analyzed in a model-based simulation before combined test cell testing is conducted. Concurrent to laboratory testing and tuning are planning and preparation for a vehicle system demonstration. Once satisfactory test cell system performance is verified, the vehicle demonstration is conducted.

Data, experience, and information gained throughout the research exercise will be applied wherever possible to our final commercial products. Cummins continues to follow this cost-effective, analysis-led approach both in research agreements with agencies like the Department of Energy as well as in its commercial product development. Cummins feels this common approach to research effectively shares results as well as resources.

Results

During 2004, Cummins Inc. reached the Phase IIA project goals and moved on toward the Phase IIB portion of the project. A great deal of time was spent in modeling and analysis in preparation for the Phase IIB demonstration. Cummins' analysis-led-design methodology, which seeks to maximize the return from research expenses, resulted in an excellent foundation from which to reach the final project goals.

Achieved and demonstrated 45% BTE while meeting 2007 emissions goals (Phase IIA).

A Cummins ISX engine equipped with a high-capacity EGR system and prototype fuel system was operated in a test cell and was shown to be emissions compliant to 2007 emissions standards. This emissions-compliant engine also demonstrated achievement of a maximum BTE of 44% at a cruise condition when operated with a practical engine cooling system which included the heat rejection of recirculated and cooled exhaust gas.

An optimized cooled EGR method was developed which allowed further improvement in BTE to reach the project goal of 45%. This

System Selection Process (Pugh Matrix)

CONCEPT / CRITERIA	RANKINE CYCLE WITH REGENERATION	RANKINE CYCLE (REHEAT)	THERMO ELECTRIC SYSTEMS	ELECTRIC TURBO COMPOUND SYSTEMS	RANKINE CYCLE +THERMO ELECTRIC SYSTEM
	1	2	3	4	5
1. Power Generated	S	S	-	-	+
2. System Complexity.	S	-	+	-	-
3. Resistance to temperature.	S	S	-	S	S
4. Fuel economy increase obtained.	S	-	-	-	+
5. Compatibility with actual engines.	S	S	S	S	S
6. Number of components.	S	S	+	S	-
7. Effect over the emissions.	S	S	S	S	S
8. Weight of the system	S	S	+	+	-
9. Size of the system.	S	S	+	+	-
10. Durability of the system	S	S	S	S	S
11. Price	S	+	-	-	-
12. Ease of maintenance.	S	S	+	+	S
13. Ease of installation.	S	S	+	+	-
14. Power consumption	S	S	+	+	S
TOTAL +	0	1	7	5	2
TOTAL -	0	2	4	4	6
TOTAL S	14	11	3	5	6
Best possible choice...	14	10	6	6	2

*No direct effect over emissions. Decrease emissions due to fuel economy increase.

Figure 1. Pugh Matrix - Comparison of Selected Waste Heat Recovery Systems

optimized cooling method was test-cell operated only. Vehicle integration of this optimized technique would have imposed significant delay in the effort toward the Phase IIB goal.

Developed a System Integration and Configuration Matrix to define potential engine architectures to support Phase IIB project goals.

Architectural concepts consisting of engine and aftertreatment hardware were generated to deliver the Phase IIB performance targets. System-level technical requirement documents were also generated. Failure mode and effects analyses (FMEAs) were performed on several of the most promising architectures identified to achieve 2010 emissions requirements.

NO_x and PM aftertreatment system architecture for the Phase IIB deliverable began during the first quarter of 2004 in coordination with the overall System Integration Configuration Matrix (SICM).

The overall concept matrix was narrowed by assessing architectures against predicted performance measures (such as rated power levels and emissions compliance) and predicted costs (such as installed cost, development expenses and capital expenses). Promising architectures have been identified and are now being investigated by the engine and aftertreatment component teams to refine architectural definitions and improve performance expectations.

Developed a Pugh Matrix to identify optimal heat recovery techniques to achieve program efficiency goals.

Work performed at the University of Illinois in Urbana-Champaign produced the Pugh Matrix of energy recovery methods shown in Figure 1.

As shown, the method of Rankine Cycle with regeneration proved to be the most promising method as compared with the others listed. This evaluation is heavily based on previous research performed and documented in Society of Automotive Engineers (SAE) Papers 760343, 780686, 790646, and 830122.

Thermal electric systems which seek to use semi-conductors to generate electricity from a differential in temperature were considered for this project. However, they were not weighted favorably in the analysis as their level of development (high Figure of Merit semi-conductor materials) is not considered great enough yet for feasible application. These systems may eventually be incorporated if significant progress is made in the durability and manufacturability of newer, higher-performance materials.

The Organic Rankine Cycle (ORC) method was modeled to determine optimal performance and establish component specifications. Figure 2 shows the basic thermodynamic loops for this energy cycle.

Figure 3 presents a schematic diagram of this recovery technique as it could possibly be incorporated into an engine system.

A neural-network control system approach is being pursued for the waste heat recovery system. Critical adjustable parameters (CAPs) and critical functional responses (CFRs) were identified over the last quarter and are being used as the basis for control system development. The CAPs include engine speed, fueling, coolant temperature, air massflow, EGR massflow or charge mass percent, etc. CFRs include heat transfer to the turbine generator, ORC condenser cooling requirement, etc. These control system parameters will continue to be investigated and refined in the fourth quarter.

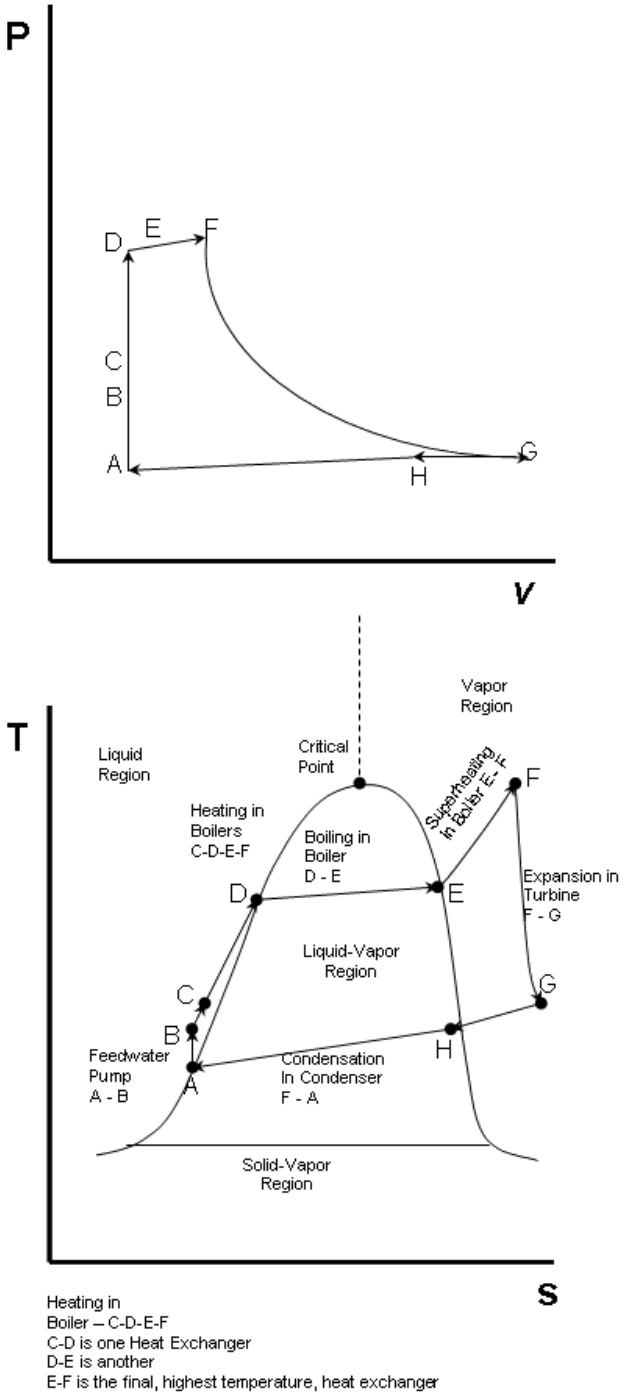

Figure 2. Rankine Cycle Pressure (P)-Specific Volume (*v*) and Temperature (T)- Entropy (s) Diagrams

Specified and procured a variable valve actuation research tool to support advanced combustion research.

Arrangements to purchase a variable valve actuation research tool were developed during the fourth quarter of 2003 and first quarter 2004. The acquisition lead-time for the tool was approximately 9 months. Delivery is expected to occur in mid-November, 2004.

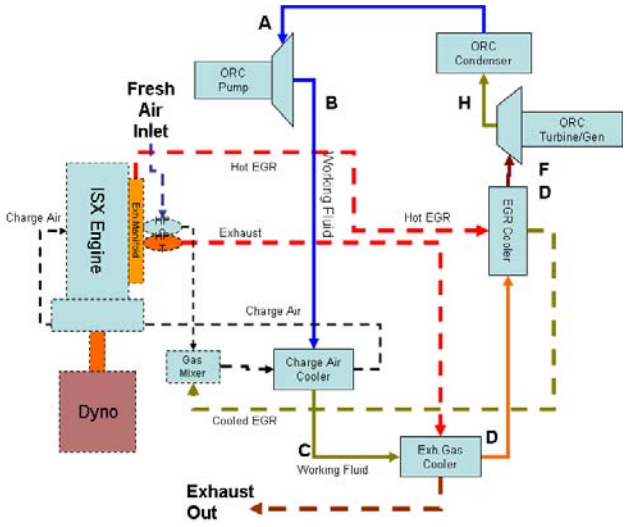

Figure 3. Organic Rankine Cycle Waste Heat Recovery Loop

The system will provide full-authority intake and exhaust valve motion control on a single-cylinder engine. This tool will support our research to identify the degree (if any) of valve control necessary to support combustion techniques capable of achieving emissions and thermal efficiency targets. This tool also offers us the ability to quickly test valve cam profiles without having to acquire hardware. This full-authority, electro-hydraulic valve actuation system is being acquired as a research tool only and is not expected to be considered as the Phase IIB demonstration engine system valve train design.

In relation to the acquisition of this variable valve actuation research tool, a single-cylinder ISX engine has been built. A test cell capable of handling the necessary controls, airflow, lubrication, and cooling requirements of a single-cylinder engine with a variety of combustion architecture possibilities has also been prepared.

The single-cylinder engine and variable valve train research tools are an investment in the future at Cummins. They are sure to be productive assets on this project and in future projects.

Evaluated different forms of HCCI combustion and performed an FMEA on each to identify and prioritize challenges.

Combustion modeling was focused on how to best implement pre-mixed charge compression ignition (PCCI)/lean quasi-homogeneous charge compression ignition (LQHCCI) combustion modes into a 6-cylinder engine. Ultra-low emissions have been demonstrated on a single-cylinder engine with fixed-time valve actuation. It is much more difficult to implement this combustion technique on a multi-cylinder engine. The FMEA identified several important items that require work or will continue to require work.

A code developed at Cummins for general fitting and optimization has now been integrated into the cycle simulation workflow. With this tool, cycle simulation results can be fitted with a surface and then used for any general optimization. This gives the ability to optimize with a minimum number of simulation runs.

Developed engine-system models for HCCI combustion and traditional diffusion burn combustion techniques to help evaluate engine architectures and support system design.

Detailed work has been ongoing to match our cycle simulation model to the most appropriate low-NO_x engine data. In this work, temperatures, pressures and flows throughout the system are matched to measured quantities. The details of the sub-models are tuned to achieve this. Very good agreement was achieved at several operating modes with a single-cylinder engine model. No "tweaking" of the model is required in order to match data at several different operating conditions. As has been typical for our engine cycle simulation, experimentally derived heat release is fed into the current model. This model has been used to select EGR and air handling equipment for engine testing. As a next step in the model development, work is currently ongoing to generate combustion models that will predict heat release as a function of crank angle from injection information. This will represent a significant improvement in our modeling capability. In addition to not requiring test data, the model will now include the impact that in-cylinder parameters have on the time history of in-cylinder heat release.

Conclusions

During the 2004 fiscal year, Cummins successfully completed the requirements of Phase IIA and made significant progress toward the Phase IIB project goals. In this effort we:

- Demonstrated 45% BTE in a 15L, heavy-duty diesel engine while achieving 2007 emissions compliance with an advanced engine cooling technique.
- Developed and refined a Systems Integration and Configuration Matrix to evaluate all possible engine system architectures for Phase IIB project goals.
- Performed advanced combustion modeling of ultra-low NO_x solutions including HCCI types of combustion.
- Performed refinement of diffusion burn combustion to achieve further reductions in NO_x production.
- Refined our control system development techniques with the incorporation of model-based controls.
- Defined, evaluated, and chose a waste heat recovery technique to use in the pursuit of the Phase IIB 50% BTE goal. Performed system analysis to initiate prototype procurement.

III.A.2 Heavy Truck Engine Project (Heavy Truck Clean Diesel, HTCD)

David Milam (Primary Contact), Eric Fluga, Jerry Coleman, Roger Rohlfing, Kevin Duffy, Tom Vachon
Caterpillar Inc.
Technical Center–F
Engine Research
PO 1875
Mossville, IL 61552-1875

DOE Technology Development Manager: Roland Gravel

Objectives

- Demonstrate the technologies required to improve fuel efficiency and comply with the 2007–2010 on-highway emission standards (0.2 g/bhp-hr NO_x, 0.01 g/bhp-hr PM) for heavy-duty trucks.
- Thermal efficiency improvement from a baseline of 43% to 50% is targeted.

Approach

- This project focuses on developing multiple paths for meeting 2007–2010 emissions while striving for 50% thermal efficiency. The procedure used is to conduct research on multiple paths and to develop multiple fuel economy building blocks to enable a down-select to the most promising path and building blocks for future production engines.
- Multiple emissions paths are being considered for meeting the 2010 emission requirements. Homogeneous charge compression ignition (HCCI) systems & NO_x aftertreatment systems are being explored to accomplish the 2010 emission requirements.
- HCCI development can be broken down into injector development, single-cylinder development, and multi-cylinder engine development. Injectors are being evaluated by using a variety of laser diagnostic techniques. A single-cylinder test engine (SCTE) is being used to evaluate different HCCI technologies. Engine simulation, combustion modeling, and optical studies are supporting the development of the SCTE. A multi-cylinder engine is also being used to evaluate different HCCI technologies and full engine system issues.
- Aftertreatment is being developed and evaluated to meet 2010 emission requirements. Technology areas that are being explored related to aftertreatment are aftertreatment system modeling, particulate matter (PM) aftertreatment, membrane technology, and NO_x aftertreatment.
- Thermal efficiency improvements are pursued using higher-risk, novel approaches in the areas of reduced engine friction, improved airflow through the engine and improved brake-specific fuel consumption (BSFC)/emissions trade-offs through developing advanced fuel systems.

Accomplishments

- Demonstrator truck with 2007 emissions technology developed and showcased at the 2003 Diesel Engine Emissions Reduction (DEER) conference and the 2004 SAE Government/Industry conference. This truck has provided key insight into system integration challenges and real driving cycle performance and is a key part of the development project.
- Demonstrated full-load and full-power HCCI operation on a single-cylinder test engine while achieving 2010 emissions levels. These are world record levels for operation of an engine in HCCI mode.

- Demonstrated the potential of NO_x aftertreatment to achieve 2010 emissions levels on a multiple-cylinder engine.

Future Directions

The Caterpillar team will utilize best-in-class design practices, advanced modeling techniques, single-cylinder engine testing and multi-cylinder engine testing to advance the technology to build on the major advances made in 2004. Technology development continues in the following key areas:

- Caterpillar will continue to focus on developing supporting engine systems to facilitate full-load HCCI on a multiple-cylinder engine. Fuel efficiency, cost and manufacturability will also be areas of focus.
- Caterpillar will continue to focus on developing methods and techniques to overcome NO_x aftertreatment durability challenges. The team will also focus on fuel efficiency, packaging and cost.
- Focus will continue on development of fuel economy building blocks.
- Focus will also continue on the development of transient simulation capabilities for enhancing the prediction of systems performance in "real-world" settings.

Introduction

Increasingly stringent air quality standards have driven the need for cleaner internal combustion engines. Many emissions reduction technologies adversely affect fuel consumption (and subsequently U.S. dependence on foreign oil). This project seeks to find technology paths and fuel economy building blocks which allow a more favorable trade-off between fuel economy and emissions. This favorable trade-off will reduce fuel used and its associated foreign dependency, lower owning and operating costs, and still allow compliance with the tighter emissions regulations. This heavy truck engine cooperative research agreement provides the framework to research, develop and demonstrate methods to provide better fuel economy.

Approach

The development team is utilizing a multi-discipline approach to address these complex technical challenges. The development team has a unique mix of technical experts from the fields of controls, combustion fundamentals, aftertreatment, engine design, engine development, and manufacturing. The team is concurrently developing the analytical tools to model and better understand the fundamentals of combustion and aftertreatment while delivering novel hardware to the test stand to validate models, improve our understanding, and advance the technology. This unique team is utilizing best-in-class design practices; advanced combustion, aftertreatment and engine system modeling techniques; rapid control strategy development tools; single-cylinder engine testing; multi-cylinder engine testing; and over 70 years of experience delivering successful compression ignition engine technology to the marketplace. In the initial stages of the project, the approach is to focus on many higher-risk technology developments. As additional information and knowledge is gained on the technologies, work then shifts to final development of chosen concepts and then, finally, to technology demonstrations. These new technologies will then be incorporated into Caterpillar's New Product Introduction programs.

Results

As stated above, Caterpillar has made significant progress in developing fuel-efficient solutions that are compliant with the emissions standards. Figure 1 shows technical data for the 2007 emissions technology demonstrator truck. This vehicle was put together to investigate and understand first-hand the challenges of integrating fuel-efficient technology that meets the 2007 emissions standards. The truck builds on ACERT® technology and brings together additional combustion systems, aftertreatment systems, air systems, and controls technology to meet 2007 emissions in a fuel-efficient manner. Figure 2 shows how the truck is also providing data for model validation. The validated models are then used in developing robust 2010 technology paths.

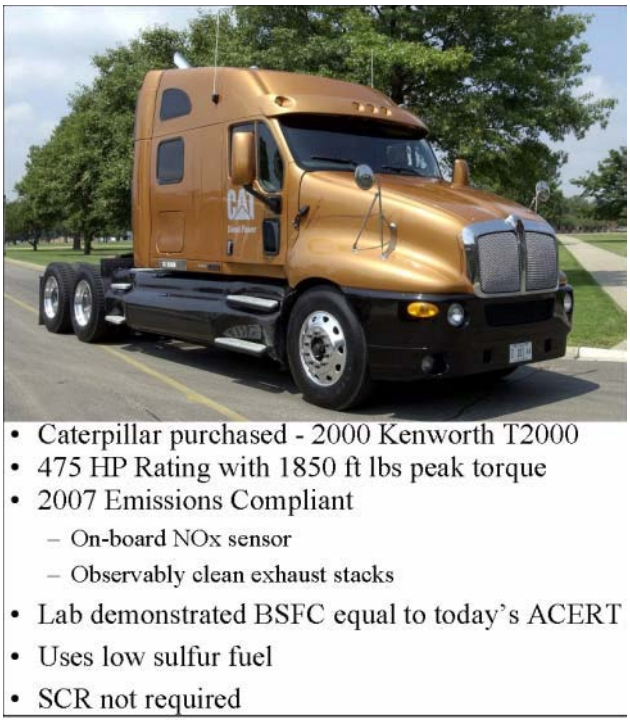

Figure 1. 2007 Emissions Demonstration Truck

In order to meet 2010 emissions in a fuel-efficient manner, HCCI is a key area of investigation within the HTCD program. Table 1 shows the multiple approaches that are used to develop HCCI under this project at Caterpillar Inc. The results showing the world-leading progress on HCCI are contained in the Diesel HCCI Development section submitted separately.

Another method or component to meet 2010 emissions is the use of NO_x aftertreatment. Figure 3 shows the elements of our NO_x aftertreatment system development at Caterpillar Inc. The figure shows that multiple aspects must be properly integrated to provide fuel-efficient operation of NO_x aftertreatment.

Conclusions

Through this Heavy Truck Engine Project cooperative research agreement, Caterpillar has developed and delivered a 2007 emissions technology demonstrator truck with fuel economy essentially equivalent to 2004 engines with ACERT technology. Caterpillar has aggressively developed multiple technology paths for efficiently meeting the

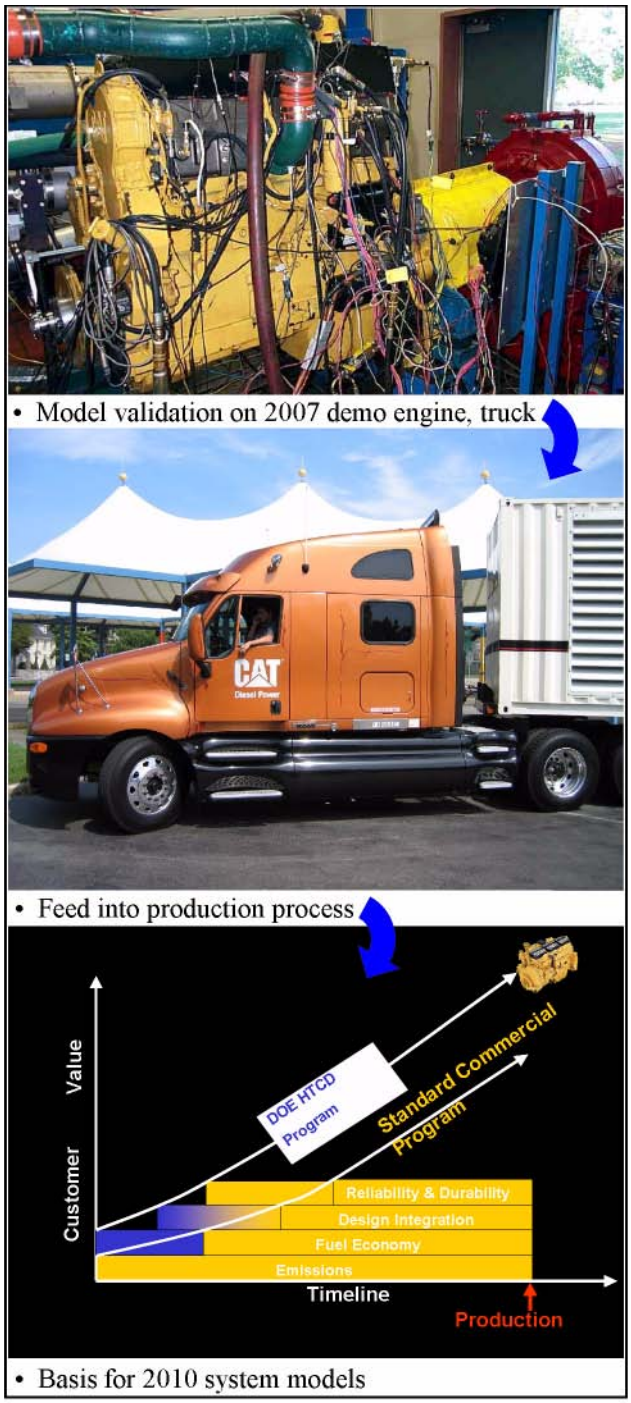

Figure 2. Simulation Process

challenges of 2010 emissions standards. HCCI development has resulted in world-class-leading power levels and significant technical progress against each of the key technical challenges. The progress has clearly positioned this advanced combustion technology as a potentially viable

Table 1. HCCI Development at Caterpillar

HCCI Fuels
Aftertreatment
Simulation
FEA
Single & Multi Cylinder Testing
Combustion Development
In-cylinder Diagnostics
Controls
Fuel Systems
Air Systems

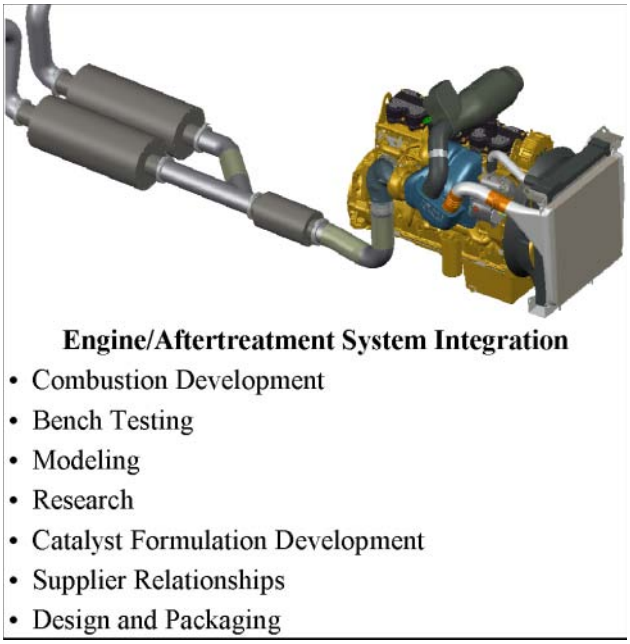

Figure 3. Diesel Aftertreatment System Development Process

approach to meeting the future regulatory and commercial requirements of the marketplace. The development on NO_x aftertreatment paths has shown the potential of this technology to help meet the 2010 emissions regulations. The system-level integration on which Caterpillar has focused is critical in developing this as a viable path. In summary, the technologies developed in this DOE/Caterpillar partnership have the potential to significantly reduce the nation's dependence on foreign oil and improve the trade balance.

FY 2004 Presentations

1. Duffy, K. "HCCI for Heavy Duty Engines," SAE Powertrain & Fluids Meeting, Pittsburgh, PA, October 2003.
2. Duffy, K. "HCCI for Heavy Duty Diesel Engines," SAE Government-Industry Meeting, Washington, DC, May 2004.
3. Duffy, K. "High Load Diesel HCCI Research," SAE Homogeneous Charge Compression Ignition Symposium, Berkeley, CA, August 2004.
4. Duffy, K., Fluga, E., Kieser, A. "Heavy Duty HCCI Development Activities," DOE DEER Conference, Coronado, CA, August 2004.
5. Verkiel, M., Driscoll, J. "Diesel Aftertreatment System Development," DOE DEER Conference, Coronado, CA, August 2004.
6. Rutan, K., Driscoll, J., Verkiel, M. "Transient Simulation of a 2007 Prototype Heavy Duty Diesel Engine," DOE DEER Conference, Coronado, CA, August 2004.
7. Duffy, K., Fluga, E., Faulkner, S., Heaton, D., Schleyer, C., and Sobotowski. "Latest Development in Heavy Duty Diesel HCCI," IFP International Conference on Which Fuels for Low CO_2?, Paris, France, September 2004.

FY 2004 Publications

1. Duffy, K., Fluga, E., Faulkner, S., Heaton, D., Schleyer, C., and Sobotowski. "Latest Development in Heavy Duty Diesel HCCI," IFP International Conference on Which Fuels for Low CO_2?, Paris, France, September 2004.

III.A.3 Improvement in Heavy-Duty Engine Thermal Efficiency While Meeting Mandated 2007 Exhaust Gas Emission Standards

Craig Savonen
Detroit Diesel Corporation
13400 Outer Drive, West
Detroit, MI 48239-4001

DOE Technology Development Manager: Roland Gravel

Objectives

- Quantify thermal efficiency degradation associated with reduction of engine-out NO_x emissions to the 2007 regulated level of ~1.1 g/hp-hr, starting from the Phase 1 project results achieved in calendar year 2002.
- Develop production-feasible technical solutions to achieve brake thermal efficiency of 45% while meeting 2007 regulated emissions.
- Develop roadmap of aftertreatment system requirements and related engine system technologies that can be effectively integrated while ultimately achieving 50% brake thermal efficiency and 2010 regulated emissions.

Approach

- Determine technical requirements for fuel injection, exhaust gas recirculation (EGR), and air mass systems.
- Utilize efficient combination of analytical and experimental tools to screen candidate engine subsystems and components.
- Determine precise and unique applications of multiple fuel injection events, advanced sensor or actuator hardware, and charge air/EGR management systems.
- Tune the integrated engine system for static and dynamic operation, using unique model-based controls approaches.
- Calibrate the integrated engine system across the engine speed-load range so that the engine can seamlessly navigate between local operating optimums.
- Strategize operation of the integrated engine system for best fuel economy while achieving low emissions and other engine system attributes such as driveability.

Accomplishments

- Achieved 43% brake thermal efficiency in a multi-cylinder engine configuration while demonstrating engine-out NO_x and particulate matter (PM) emissions of 1.1 g/hp-hr and 0.1 g/hp-hr, respectively, over the Environmental Protection Agency (EPA) hot cycle Federal Test Procedure (FTP).
- Produced subsequent tailpipe-out NO_x and PM emissions of ~1.0 g/hp-hr and <0.01 g/hp-hr, respectively, with integration of a diesel particulate filter (DPF).
- Completed 1st-order refinement of engine subsystems. By applying well-controlled multiple fuel injection events, the initial brake thermal efficiency penalty of ~3% relative to the production 2004 engine was eliminated. Subsequently, additional brake specific fuel consumption (BSFC) improvement potential was identified.

- Established a 1st-order technology roadmap to achieve the DOE thermal efficiency goal of 45% at 2007 regulated emissions level. These technologies are now being successively incorporated into a production-feasible engine testbed system and evaluated for their potential contribution.
- Developed model-based algorithms for future system controls, establishing a technology development platform and process for realizing advanced combustion characteristics that promise to reduce future emissions variability and provide opportunities for further fuel consumption reduction.

Future Directions

- Continue to incorporate promising technologies regarding high efficiency into pre-prototype engine testbeds while rationalizing production viability, driveability, reliability, and other desired attributes of the total engine system.
- Evaluate advanced fuel injection equipment, including hybrid systems, for the potential to enable combustion characteristics that will lead to over 45% thermal efficiency while meeting 2010 regulated emissions.
- Accelerate technology development regarding sensors and control algorithms required for a fully integrated multi-cylinder engine testbed.
- Solidify technology roadmap, demonstrating viability of key elements, while achieving 2010 emission levels with 50% brake thermal efficiency.

Introduction

This project (named Near Zero Emissions & 50% Thermal Efficiency, or NZ50) helps define conceptual engine configurations and advanced component technologies that can contribute to meeting DOE's thermal efficiency goals within stipulated future emission standards. Without ignoring 'real-world' considerations for commercialization, cost, and durability requirements, the technology concepts are pre-screened analytically. Each of the more promising approaches and subsystems influential to energy consumption, including those associated with fuel, charge air, EGR, combustion, sensing, and cooling, are then developed to a pre-prototype state so that tangible thermal efficiency potential can be quantified. Critical to this assessment, the concepts must be integrated, at least in a thermodynamic context, and then evaluated on a testbed representing prototype, multi-cylinder, future heavy truck engines. This technology evaluation process ensures that system solutions arising from the project that simultaneously exhibit potential for adequate emission control and fuel economy potential can be realistically earmarked for translation into future product development plans.

Approach

Major FY 2004 activities targeted the integration of engine subsystem technology in a pre-prototype configuration to achieve 2007 regulated emission standards while improving brake thermal efficiency. Analytical and experimental tools were used to tune advanced EGR cooler design, air/EGR delivery, and fuel injection control technologies. Unique multiple-input, multiple-output control techniques enabled more precise fuel, air, and EGR flow under diverse engine operating regimes. With 2007 regulated emission standards successfully demonstrated, the fuel and air/EGR management systems were rigorously exercised to forge thermal efficiency techniques that did not compromise emission reduction achievements. A major element of this activity involves novel application of multiple injection events with pre-prototype fuel injection systems.

Results

The basic test platforms used to march toward NZ50 goals include derivatives of 2004 production Series 60 engines, which were modified with advanced technology hardware and software. The

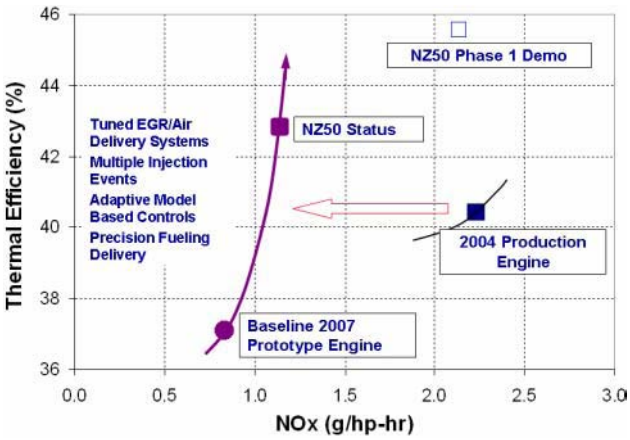

Figure 1. Thermal Efficiency vs. NO_x Emission Achievements

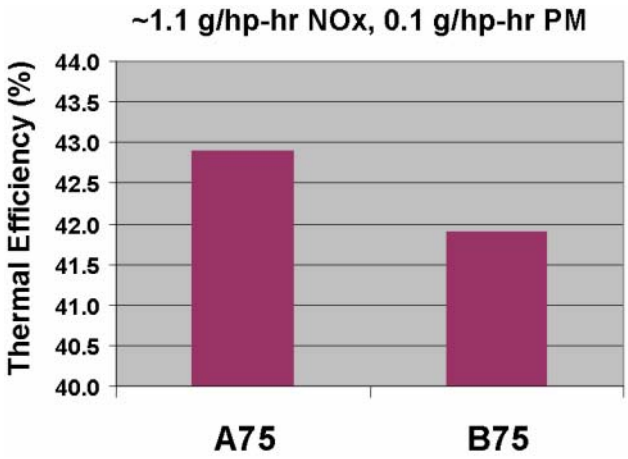

Figure 2. Thermal Efficiency Achievements at 2007 Emissions Levels

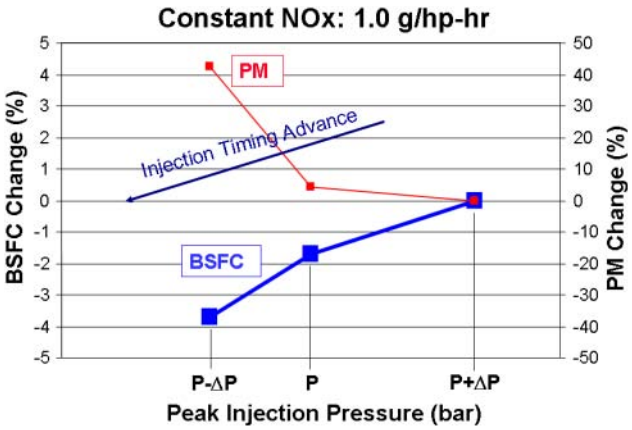

Figure 3. BSFC and PM Emissions Sensitivity to Injection Pressure

fuel injection and EGR subsystems were upgraded to provide prototype performance. Model-based controls within rapid prototyping software systems were integrated as the primary controller of the engine system. Supplementary electronic control units and actuators were used to drive the fuel injection system and other active subsystem hardware. Detroit Diesel Corporation's (DDC's) CLEAN Combustion© was applied to a limited degree under idle and low cycle power conditions. Preliminary calibration of the engine system produced engine-out emissions that are compatible with 2007 targets (NO_x = 1.0 g/hp-hr, PM emissions = 0.12 g/hp-hr) on both a steady-state (ESC) and transient (FTP) basis. Integration of the engine system with state-of-the-art DPF technology yielded demonstrated compliance with 2007 tailpipe-out emissions.

However, achievement of 2007 regulated emissions levels on the baseline 2007 prototype engine led to thermal efficiency degradation from the 2004 production baseline of ~40% to a level of ~37% (Figure 1). From this point, NZ50 project introduction of 2007 and later candidate technologies enabled recapture of lost efficiency. The application of advanced air/EGR delivery systems, multiple fuel injection strategies, more precise fueling delivery, and adaptive model-based control schemes improved thermal efficiency substantially. As illustrated in Figure 1, the current NZ50 status for demonstrated brake thermal efficiency is ~43%. Figure 2 expands the view of these experimental results at two key engine operating points, namely A75 (near peak torque speed and 75% engine load point of the ESC Test Procedure) and B75 (mid-speed and 75% engine load point of the ESC Test Procedure). Thus, the NZ50 achievements to date represent a 50% NO_x emissions reduction accompanied by nearly 6% improvement in absolute brake thermal efficiency relative to the prototype 2007 engine. It should be noted that the reference point for quoting thermal efficiency milestones corresponds to engine operation that is representative of over-the-road operation of a heavy-duty truck.

Application of multiple fuel injection event strategies to improve thermal efficiency is a critical technology being developed vigorously in the NZ50 project. For reference, as illustrated in Figure 3, with single fuel injection events, an injection pressure

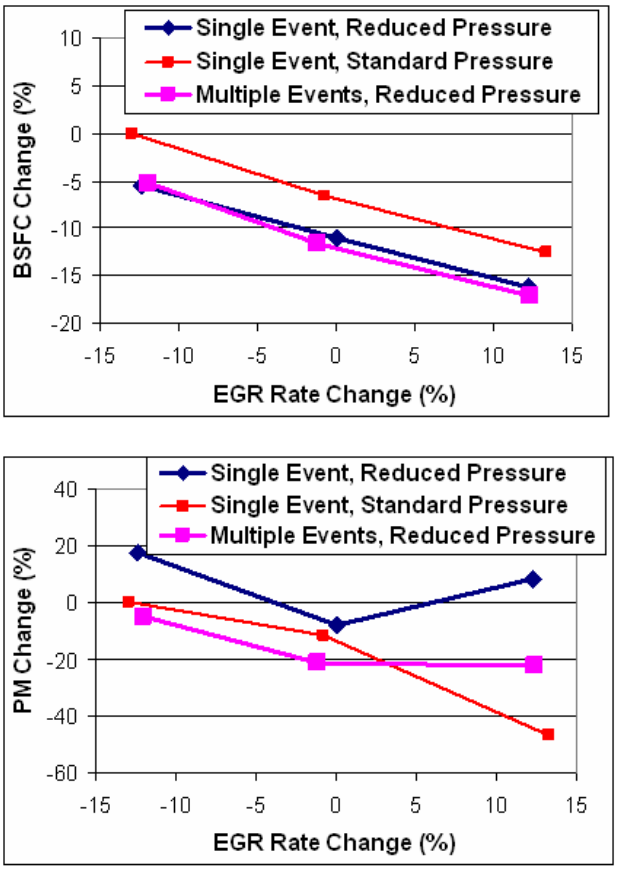

Figure 4. BSFC and PM Benefits from Multiple Injection Events at B100 (mid-speed and 100% engine load point of the ESC Test Procedure)

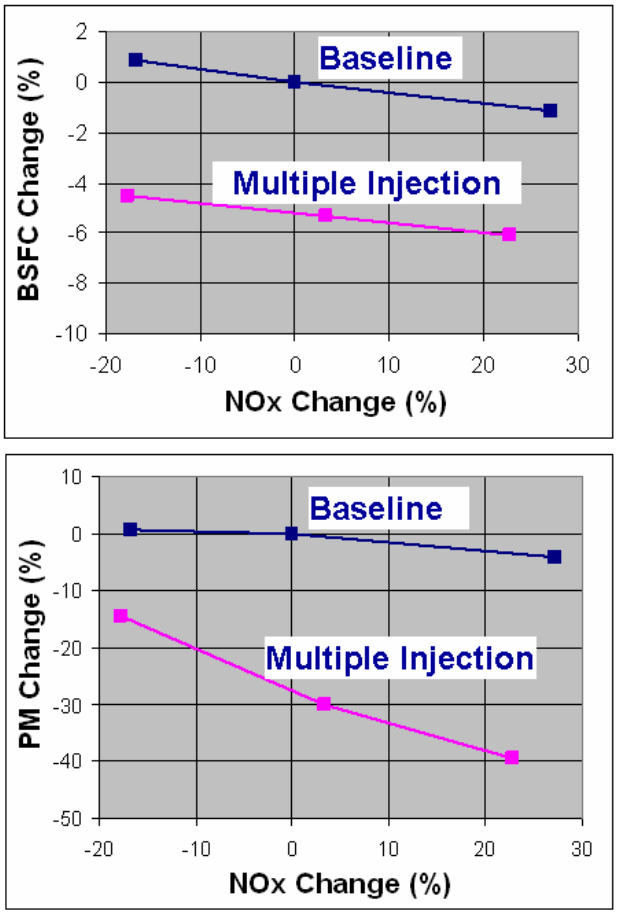

Figure 5. BSFC and Emissions Benefits from Multiple Injection Events at B25 (mid-speed and 25% engine load point of the ESC Test Procedure)

reduction may yield BSFC opportunities, but PM emissions will usually increase. This characteristic response is evidenced in Figure 3, whereby a 4% BSFC improvement is accompanied by 40% PM increase. Similarly, although not illustrated here, low NO_x emissions are achievable with high rates of EGR, but the resultant BSFC and PM and smoke emissions penalties can be prohibitively high.

To combat these characteristics, one angle of attack is the application of novel multiple injection strategies. Figures 4 and 5 show preliminary results for two distinctly different multiple injection strategies now being incubated in the NZ50 project. By careful development and strategic deployment of such strategies, improved thermal efficiency may be realized without detrimental impact on regulated emissions output.

Conclusions

Advanced development and integration of engine subsystems have led to the achievement of demonstrating 2007 EPA regulated emissions while improving thermal efficiency to 43%, representing a substantial improvement relative to the 2004 production engine baseline and to the baseline 2007 prototype engine. Model-based controls have been systematically proven as effective methodologies for exploiting benefits from the fueling, air, and EGR systems. The transition to more pervasive model-based controls with increased robustness and on-board optimizing functions is now underway. Active correction schemes are now being incorporated to widen the envelope within which low emissions and improved thermal efficiency can be attained.

III.B Light-Duty

III.B.1 Cummins/DOE Light Truck Clean Diesel Engine

John Stang (Primary Contact), David Koeberlein, Michael Ruth
Cummins Inc.
P.O. Box 3005
Columbus, IN 47201

DOE Technology Development Manager: John Fairbanks

Objectives

To develop a diesel engine system for light trucks and sport utility vehicles with the following attributes:

- Improved fuel economy
  - 50% improvement over the gasoline powered vehicle it replaces
- Emissions
  - Tier 2, Bin 5 full useful life emissions of 0.07 g/mi NO_x and 0.01 g/mi particulate matter (PM)
- Positive gasoline engine attributes
  - Noise
  - Acceleration
  - Cold start and warm up
  - Serviceability
  - Weight

Approach

- Fully analyze the overall combustion and performance of new smaller diesel engines using practical tools, including computational fluid dynamics, combustion kinetics, stress and heat transfer finite element analyses, and overall transient performance simulation.
- Establish bench tests to confirm the above models.
- Optimize the complete system design using the above models.
- Build and test complete system prototypes.

Accomplishments

- Improved engine-out emissions by 25% through variable nozzle turbocharger application.
- Completed improved air handling algorithm development to control the variable nozzle turbocharger and to provide air handling compensation at altitude.
- Completed evaluation of engine cold start and stable idle at -30 Centigrade.
- Achieved active aftertreatment regeneration with closed-loop lambda controls.
- Demonstrated power density of 48 HP/liter on a 4.2 liter V6.
- Demonstrated Tier 2 Bin 5 emissions capability through emission testing at sea level and at altitude with 150,000 mile thermally aged catalyst.
- Achieved engine-out emissions (EOE) of less than 0.3 g/mi NO_x and 0.1 g/mi PM using a steady-state transient test cycle approximation, using currently available diesel fuel.

Future Directions

Research and engineering work at Cummins over the past several years has focused on developing low-emission solutions and demonstrating those solutions in vehicle chassis testing. The project has emphasized realistic and cost-conscious solutions involving original equipment manufacturers and production intent suppliers. The project has been successful in demonstrating that light-duty diesel vehicles certified to Tier 2 Bin 5 tailpipe emissions standards are technically viable. However, there are several areas that the project has not addressed that are very suitable for future work to further the development of "Advanced Combustion Engine Enabling Technology". These areas include the following:

- Low-temperature combustion (LTC) zone expansion
  - Develop exhaust gas recirculation (EGR) cooling temperature and pressure targets versus speed and load required to maintain LTC-type combustion.
  - Develop calibration that will operate in LTC over the entire certification cycle.
  - Develop rich operation up to 10 bar brake mean effective pressure (BMEP).
  - Target:
    - 0.1 g/mi EOE NO_x
    - 23 mpg at 6500 lb inertia test weight (ETW) (steady-state approximation)
- Closed loop controls development
  - Build rapid prototype control systems with feedback capability on air/fuel ratio (both rich and lean), fueling correction and start of combustion or ignition timing.
  - Run transient operation on closed loop system.
  - Target:
    - Transient operation at Tier 2 Bin 5 emissions calibration
- Aftertreatment system optimization
  - Demonstrate low-cost, highly effective PM filter.
  - Demonstrate low-cost, highly effective NO_x control.
  - Demonstrate low-cost, highly effective 4-way catalyst.
  - Target:
    - PM filter effectiveness at 90%
    - NO_x-adsorbing catalyst (NAC) effectiveness at 60%
    - 4-way catalyst demonstration at Tier 2 Bin 5 emissions calibration
- System integration
  - Integrate advanced vehicle, transmission, engine and aftertreatment systems.
  - Tune advanced vehicle, transmission, engine and aftertreatment systems.
  - Tune vehicle for drivability and emissions performance.
  - Target:
    - Tier 2 Bin 5 emissions compliant
    - 23 mpg combined city/highway fuel economy
    - Good transient response

Introduction

Beginning in the mid 1980's, the light truck and sport utility vehicle (SUV) market share has steadily increased from 30 percent of all new light vehicles sold in the U.S. to what is now over 50 percent of a 14 million vehicle per year market. As this market has shifted from cars to trucks, the U.S. fleet-

averaged fuel economy has decreased. The increase in fuel consumption has driven the need to increase imported oil, affecting the overall trade balance and economy (and eventually, national security). This Department of Energy project is aimed at reducing America's dependence on foreign oil while not compromising America's choice of available vehicles.

Diesel engines have long been known for efficiency, reliability and durability. Unfortunately, due the nature of the physics involved, the emissions of oxides of nitrogen (NO_x) and particulates (PM) are significantly higher than legislated limits for light vehicles. America's limited knowledge of light vehicle diesels requires that a saleable product must not only meet the legislated parameters, but must exceed the positive attributes of gasoline-powered vehicles without exceeding the threshold market pricing. This Cummins project includes development of a diesel engine that will not require vehicle design changes or unrealistic fuel specifications, nor require the end user to modify driving or maintenance practices.

Approach

This diesel engine has been developed with a production design intent in mind since inception. This is evident in the use of high-volume, gasoline production accessories and components. Also notable in the design is the use of modern, design for manufacturing initiatives, such as integrated components and reduced bracketry.

The base architecture is designed specifically for light-duty use, as opposed to an adaptation of an industrial or medium-duty engine. This ensures the lightest design without compromise for varied applications. This also ensures the design can be optimized for the important customer attributes, including NVH (noise, vibration, and harshness), weight, and cost.

Development of this diesel engine has considered the use of the latest technology for emission controls. High-pressure, common rail diesel fuel injection systems used in high-volume European production engines are being utilized. Due to the U.S. emissions requirements, advanced aftertreatment devices are being used. Engine-out emissions (EOE) development continues to reduce the engine-out emission levels, thereby reducing the volume (displacement), total material needed and cost of the aftertreatment devices. Catalysts are typically loaded with expensive precious metals such as platinum, palladium and rhodium. The total cost for the aftertreatment system is targeted to be equivalent with that of an equal-emitting gasoline emission control system.

Results

The diesel engine developed by Cummins Inc. has demonstrated numerous objectives for this project (see Table 1). The basic design architecture of the engine lends itself to one overriding objective of a production intention program: low cost. The engine design utilizes integrated components that allow subassemblies to be assembled and tested prior to final engine assembly. These subassemblies, or modules, reduce final assembly times and material handling in a production environment.

Integration of the aftertreatment controls into the base engine and emission controls has been a major effort in this project. The NO_x aftertreatment device requires periodic conditions of fuel-rich exhaust stoichiometry in order to regenerate, or reduce, the stored emissions. This rich operation is not normal for diesel engines that typically only operate under lean conditions. Major emphasis was placed on being able to operate under rich conditions without adding additional hardware devices, such as an additional injector in the exhaust piping. Also, maintaining the original objectives set for this project, development had to focus on not inducing torque or noise fluctuations during these fuel-rich excursions. The successful integration of these controls, along with advanced catalysts, made possible achievement of Tier 2, Bin 5 emissions (see Figure 1).

Other significant accomplishments include the following:

Power Density

The Phase 2 V6 engine was targeted to have a peak power of 186 kW (250 bhp) at 4000 rpm. The best power achieved by July 2003 was 180 kW (241 bhp) @ 3600 rpm with a wastegated

Table 1. V Family Goals and Status

Description	Target		Actual (Status)	
	V6	V8	V6	V8
Emissions	EPA Tier 2 & CA LEV II		Tier 2 Bin 10 Interim Demonstrated, Tier 2 Bin 5 Final, Met in Vehicle	
Noise, dBa	69 Hood Open, Equal to Gas		72.7 db, Bare Engine in Test Cell	65.0 Interior, Cruise @ 65 mph, 1500 Pickup
Fuel Economy, MPG	50% Better than Gas		22.1 Combined, Durango (+60%)	21.7 Combined, BR1500 (+60%)
Quality/Reliability	Equal to Gas, <2 RPH First Year and <10 RPH Five Years		Focus in Phase 3	
Rated Speed	4000 rpm (5000 max.)		4000 rpm (5000 max.)	
Useful Life km(mi)	B10 > 325,000 (200,000)		Focus in Phase 3	
Performance	Gasoline-Like (9-10 sec 0-60 mph)		9.6 sec, 0-60 mph, 5940 lb PTW	8.8 sec, 0-60 mph, 6200 lb PTW
Displacement, Liter	4.2	5.6	4.2	5.6
Power, kW(hp) @ rpm	190 (250) @ 4000	260 (350) @ 4000	189 (254) @ 3600 WG 201 (270) @ 3800 VNT	224 (300) @ 4000 WG Interim Target Met
Torque Peak, Nm(ft-lb)	455(335), 569(420) max.	597(440), 760(560) max.	569 (420)	623 (460)
Warm Up	75 C(167 F) Coolant in 10 min. @ -30 C(-22 F)		49C in 10 min @ -30C	Focus in Phase 3
Serviceability	Equal to Gasoline		No Adjustments, Diesel Fuel Filter Added	
Cold Start	< 20 sec. @ -30 C (-22 F)		7.1 sec (1.2 sec Glow) @ -30C	Focus in Phase 3
Weight	295 (650)	340 (750)	301 (663)	357 (788)

turbocharger. The engine architecture has since been upgraded to include a variable geometry turbocharger, higher flow cylinder heads and new common rail fuel system equipment that allows for higher injection pressures. With the addition of this new hardware to the engine, the rated power moved from 180 kW (241 bhp) @ 3600 rpm to 205 kW (275 bhp) @ 3600 rpm, and 201 kW (270 bhp) @ 3800 rpm. Significant gains were also made to the torque curve below the torque peak. At 1600 rpm, torque output increased by 137 lb-ft (see Figure 2). The project goals were achieved while maintaining the mechanical limits of the engine.

Emissions Durability

In order to further the product demonstration, an altitude assessment was completed. The main purpose of the evaluation was to conduct emissions testing at altitude to demonstrate compliance with the Tier 2 Bin 5 emissions standards (see Table 3). Auxiliary objectives included evaluating vehicle driveability, measuring fuel consumption on a standard route, documenting cold start capabilities and assessing the aftertreatment system performance. Emissions testing at high altitude demonstrated that the vehicle is capable of operation at Tier 2 Bin 5 emissions levels with a thermally aged catalyst at 150,000 miles. Testing and documentation was performed on vehicle driveability, cold start performance and aftertreatment performance.

Cold Start

An engine calibration was developed that met many of the engine starting deliverables. Table 2 summarizes the results of this development.

Table 2. Summary of Optimized Calibration Test Results

VOC: Engine Must Start Well Cold			
Time to 1st Engine Fire	6.5 +/- 4.4 seconds	Target: Minimize	Development Target Achieved
Time to Engine Start:	7.1 +/- 4.8 seconds (0 sec glow plug preglow, newait start)	Target: 9 seconds	Development Target Achieved
VOC: Vehicle Must Warm Up Fast and Drive Well			
Coolant Tempera-ture @ 600 seconds	49.2 +/- 2.1 degC	Target: 75 degC	Development Result in Progress
Time to Exhaust Stack Temp > 275F	8.7 +/- 1.1 minutes	Target: Minimize	Development Target Achieved
1st Time UHC < 1000ppm	43 +/- 11.7 seconds	Target: Minimize	Development Target Achieved
1st Time UHC < 250ppm	75 +/- 32.4 seconds	Target: Minimize	Development Target Achieved
Idle RPM Std. Dev. < 30rpm	1.2 +/- 0.74 seconds	Target: Minimize	Development Target Achieved

Table 3. V6 Chassis Test Results

Test	CO [g/mi]	CO2 [g/mi]	NOx [g/mi]	NMHC [g/mi]	FE [mpg]	PM [g/mi]	
FTP-75 FUL limits	4.2	-	0.07	0.090	-	0.01	
FTP-75	0.399	480.27	0.033	0.089	21.12	0.006	•Start
FTP-75	0.367	491.67	0.038	0.056	20.32	-	•1600 mi
	0.241	519.18	0.074	0.043	19.16	-	•Aged & Alt. ~150,000 mi 5400 ft
bag 1	0.971	547.87	0.141	0.222	18.47	0.008	
	1.051	583.44	0.181	0.269	17.08	-	
	1.121	578.14	0.243	0.207	17.15	-	
bag 2	0.272	475.03	0.003	0.057	21.37	0.004	
	0.200	475.27	0.000	0.000	21.04	-	
	0.060	517.34	0.002	0.001	19.24	-	
bag 3	0.207	439.17	0.009	0.049	23.11	0.007	
	0.166	453.40	0.003	0.000	22.05	-	
	0.018	478.05	0.080	0.000	20.83	-	

V6 Bag Results @ 5000 lb. and 12.7 hp @50 mph

Reduced Engine-Out Emissions

Steady-state optimization work was performed which resulted in an early emissions demonstration of 0.64 g/mi NO_x and 0.11 g/mi PM over the FTP75 test cycle. This transient response and emissions

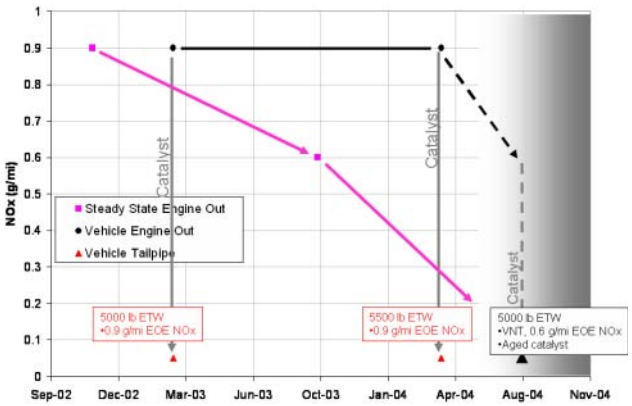

Figure 1. V6 Emissions Progression

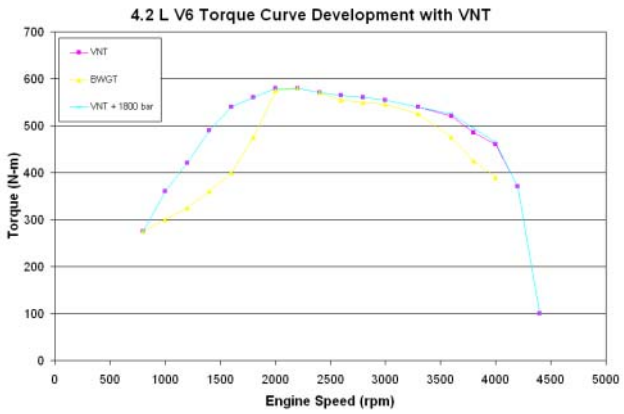

Figure 2. V6 Performance Results

testing indicated issues with the turbocharger vane position control method that was initially used on the engine. Boost pressure response was initially worse than that of the engine with a wastegated turbocharger. This work drove the need for improved algorithms in the engine control module (ECM) to control the turbocharger. During later development, a boost/fresh air flow control system demonstrated significantly better control. Transient emissions testing in-vehicle have also shown that the air handling system performs very well. Tailpipe emissions targets have been demonstrated at both sea level and altitude using this control system. Transient response data were repeated using the new air handling system with very good results. The steady-state boost stabilized much quicker and with less overshoot compared to the wastegated turbo. Further work needs to be done to optimize the transient response performance of the engine while balancing smoke emissions.

The demonstrations for this project have been done using Phillips 66 "DECSE" (Diesel Emission Controls Sulfur Effects, another DOE project) fuel and relatively fresh "degreened"-only catalyst systems. The "DECSE" fuel has very low sulfur content in solution (<4 ppm). Sulfur has tendency to poison the NO_x-adsorbing catalyst, resulting in poor performance as the catalyst ages. Fuel specifications for future diesel fuels include a maximum sulfur content of 15 ppm. While the low sulfur content of future fuels should aid in reducing catalyst poisoning, catalysts will eventually fail due to build-up of sulfur. Future work will include desulphation development and related catalyst durability work.

Conclusions

- Increased power density can be demonstrated with advanced air handling and fuel system technologies while achieving targeted emissions levels.
- NO_x adsorbers have the potential to meet the emissions durability target of 150,000 miles.
- Cold start and stable idle performance similar to gasoline engines can be achieved with advanced glow plug systems and high-pressure fuel injection equipment.
- Reduced engine-out emission levels can be attained which will balance both fuel consumption and driveability needs while having the potential to reduce the cost of the aftertreatment system.
- The advanced diesel engine can provide a viable business case for light trucks and sport utility vehicles.

Special Recognitions & Awards/Patents Issued

1. Air/oil coalescer with improved centrifugally assisted drainage, Patent No. 6,640,792.
2. Valve train with a single camshaft, Patent No. 6,390,046.

FY 2004 Publications/Presentations

1. CARB Global Climate Change Workshop, March 2004.
2. SAE Government and Industry Conference with DOE 21st Century Truck Display, May 2004.
3. DOE Diesel Engine Emission Reduction Workshop, San Diego, CA, August 2004.

III.B.2 Light-Duty CIDI Engine Technology Development

Houshun Zhang (Primary Contact) and Mike Balnaves
Detroit Diesel Corporation (DDC)
13400 Outer Drive, West
Detroit, MI 48239-4001

DOE Technology Development Manager: John Fairbanks

Objectives

- Demonstrate production-viable diesel engine technologies, specifically intended for North America.
- Demonstrate Tier 2 emissions compliance with significant fuel economy advantages.

Approach

- Apply advanced engine technology development methodology to concurrently develop the engine, vehicle powertrain and aftertreatment systems, as well as to systematically integrate and optimize these systems.
- Develop and use emerging combustion technologies in synergy with advanced aftertreatment technologies to pursue integrated engine, aftertreatment and vehicle system technical targets.
- Minimize development cycle time by leveraging technical findings from other government-sponsored and internally-funded programs at DDC.

Accomplishments

- Demonstrated Tier 2 Bin 3 emissions over the FTP75 cycle for a light-duty truck (LDT) equipped with a Diesel Engine for Light Truck Application (DELTA) engine using a diesel particulate filter plus selective catalytic reduction (DPF + SCR) system, while synergizing efforts with another DOE-DDC project. This aggressive reduction in emissions was obtained without ammonia slip and with a 41% fuel economy improvement, compared to the equivalent gasoline engine equipped vehicle. Demonstrated Tier 2 emissions compliance over the US06 cycle.
- Demonstrated engine-out Tier 2 Bin 10 emissions compliance. Demonstrated Tier 2 near-Bin 9 emissions compliance without active NO_x aftertreatment devices.
- Developed a fuel burner for DPF regeneration. Identified technical issues for a commercially-viable fuel burner that can potentially be utilized on a 2007 light-duty vehicle.
- Systematically characterized air system management options, including air bypass, post injection, and their combination, as part of developing a comprehensive commercially viable DPF regeneration strategy.
- Completed over 1540 hours of durability testing. Over time, a slight fuel consumption improvement was observed. Also, piston mechanical issues were identified and are being resolved.
- Conducted ash-loading tests of sintered metal diesel particulate filters. The objective of this study is to understand the effect of aging on aftertreatment performance, which is a key driver for commercialization potential. Over 1000 hours in ash-loading testing have been accumulated, and it is planned to continue these tests up to 3000 hours.
- Characterized DPF performance using a reactor bench. A key objective of this study is to provide fundamental performance data that will be utilized to calibrate DDC's state-of-the-art aftertreatment models. This integrated analytical and experimental approach to develop aftertreatment technology will benefit efforts to reduce the cost and complexity of aftertreatment devices, which is another key driver for light-duty commercialization potential for 2007 and beyond.

Future Directions

- Continue ash-loading tests up to 3000 hours.
- Complete DPF performance characterization utilizing a reactor bench.

Introduction

Detroit Diesel Corporation (DDC) is developing engine and aftertreatment technologies in support of the Department of Energy-sponsored Light-Duty Truck Diesel Engine development project. The objective of this effort is to demonstrate production-viable diesel engine technologies which are specifically tailored for the North American light truck market. Light-duty truck diesel engines are intended for a variety of vehicle applications, which range from small and mid-size sport utility vehicles (SUVs) and passenger vans to full-size pick-ups, SUVs and vans.

Approach

The DOE-DDC light-duty truck project has benefited substantially from DDC's integrated analytical and experimental approach to advanced engine technology development. This integrated development approach was utilized to concurrently develop the engine, vehicle powertrain and aftertreatment systems, as well as to systematically integrate and optimize these systems utilizing a robust control strategy. Figure 1 shows the key elements of this integrated approach. The focus of this project, however, is on the core engine system and those areas of the vehicle powertrain and aftertreatment systems that are closely coupled with core engine development. The project has also benefited from leveraging technical findings from other government-sponsored and internally-funded projects at DDC.

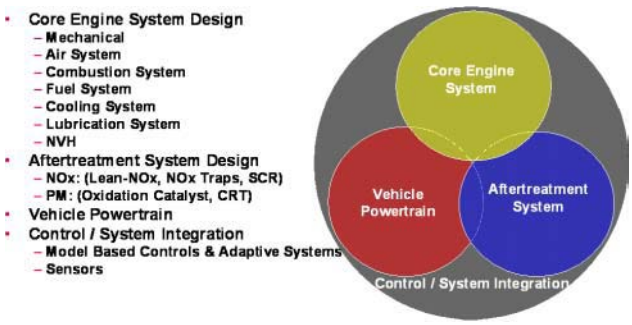

Figure 1. Integrated System Development Approach

Results

DDC successfully demonstrated Tier 2 Bin 3 emissions on a light passenger car platform as early as 2002 (Bolton, et al 2002[1]) as part of the DOE-DDC LEADER project. Building upon this technology demonstration and with increased emphasis on system integration, Tier 2 Bin 3 results were demonstrated on the light truck platform (Aneja, et al 2003[2]). Tier 2 compliance was also demonstrated over the US06 cycle on the light truck platform. In addition to the substantial emissions reduction, a 41% fuel economy improvement compared to the baseline gasoline engine equipped vehicle was obtained. Tier 2 Bin 10 emissions compliance was demonstrated without utilizing any aftertreatment, and Tier 2 near-Bin 9 emissions were demonstrated without the use of active NO_x aftertreatment. These accomplishments can be attributed to advanced combustion and aftertreatment technologies, synergistically integrated utilizing robust control strategies. Figures 2 and 3 present DDC's roadmap for LDT FTP75 emissions.

Having successfully demonstrated Tier 2 Bin 3 emissions compliance, the project's focus this year included increased emphasis on commercialization

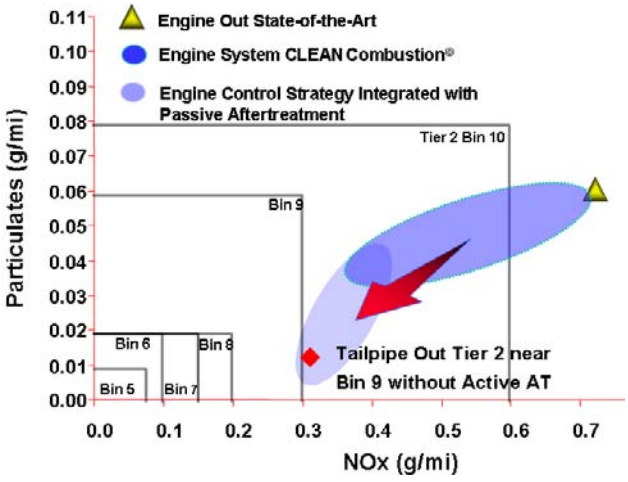

Figure 2. Passive Aftertreatment Emissions Reduction Roadmap; Light Truck Chassis Dynamometer Results

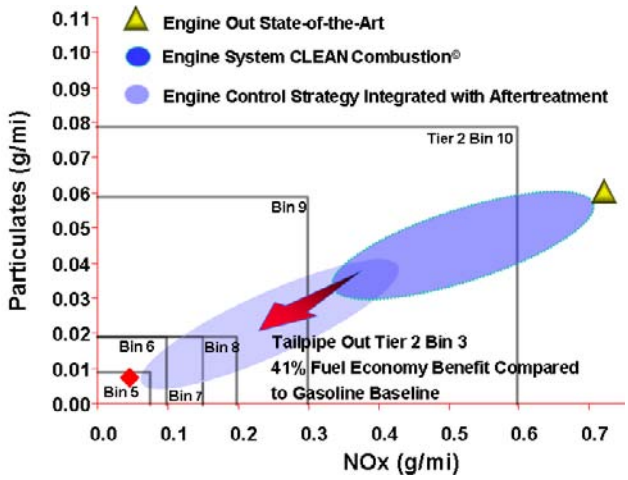

Figure 3. Tier 2 Bin 3 Emissions Roadmap; Light Truck Chassis Dynamometer Results

potential. Focus areas included durability testing, impact of aging of aftertreatment devices, development of a robust strategy for DPF regeneration, and reduced complexity and cost of aftertreatment devices.

A DELTA engine was installed in a durability test cell and has accumulated over 1540 hours of representative over-the-road durability testing. Component wear, fuel consumption and oil consumption were observed as a function of time. The fuel economy was observed to improve slightly over time, and the oil consumption was within acceptable limits, although slightly higher than GEN 0 version of the DELTA engine.

A fuel burner with emphasis on commercial viability was developed as part of a robust strategy for DPF regeneration. This fuel burner was demonstrated to ignite using exhaust gas without air assistance at a range of operating conditions. Figure 4 shows the temperatures at various spatial locations along the exhaust pipe during idle operation, which is a challenging operating condition with respect to exhaust temperature management. The fuel burner was ignited at 300 seconds in time as shown in Figure 4 and allowed the DPF inlet temperature to be raised from 100ºC to 650ºC.

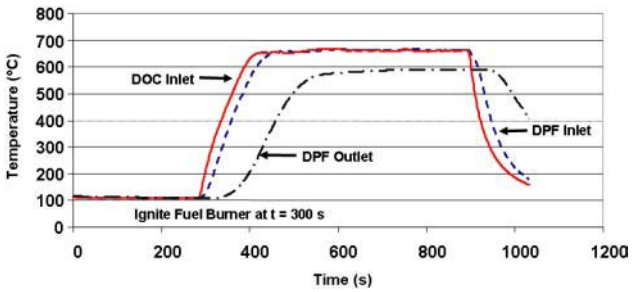

Figure 4. Exhaust System Temperatures at Idle; DPF Regeneration Utilizing Fuel Burner

Conclusions

Use of integrated combustion, aftertreatment and vehicle technologies allowed the DDC team to demonstrate state-of-the-art performance and emissions levels, meeting the project's emissions objectives. Specifically, Tier 2 Bin 3 emissions compliance was demonstrated along with a 41% fuel economy improvement over the gasoline engine baseline. Having successfully demonstrated Tier 2 Bin 3 emissions compliance, the project's focus this year included increased emphasis on commercialization potential. Focus areas included durability testing, impact of aging on aftertreatment device performance, development of a robust strategy for DPF regeneration, and reduced complexity and cost of aftertreatment devices.

FY 2004 Publications

1. Houshun Zhang, "Aftertreatment Modeling Status, Future Potential and Application Issues," 10th DEER Workshop, San Diego, August 29-September 3, 2004.

References

1. Brian Bolton, Nabil Hakim, and Houshun Zhang, "Demonstration of Integrated NO_x and PM Emissions for Advanced CIDI Engines," FY2002, Progress Reports for Combustion and Emission Control for Advanced CIDI Engines, U.S. Department of Energy, November, 2002.
2. Rakesh Aneja, Brian Bolton, Bukky Oladipo, Zornitza Pavlova-MacKinnon, and Amr Radwan, "Advanced Diesel Engine and Aftertreatment Technology Development for Tier 2 Emissions", 2003 Diesel Engine Emissions Reduction (DEER) Conference, August 24-28, 2003.

III.B.3 Variable Compression Ratio Engine

Charles Mendler
Envera LLC
7 Millside Lane
Mill Valley, California 94941

DOE Technology Development Manager: Roland Gravel

Objective

- Design and build a variable compression ratio (VCR) variant of the DaimlerChrysler 4-cylinder common-rail, turbo-compression direct injection (CDI) engine.
- Incorporate second-generation VCR subsystems into the 4-cylinder VCR DaimlerChrysler CDI engine.
- Demonstrate ability to integrate VCR into high-volume production inline and "V" configuration engine blocks.
- Provide VCR hardware that supports control of CDI and spark ignition (SI) homogeneous charge compression ignition (HCCI) combustion.
- Evaluate part-load efficiency potential for advanced SI engines having VCR and Atkinson-cycle cam timing.

Approach

- Design/build of VCR CDI engine applying design optimization computer models and prior hardware build analysis and data.
- Computer-aided design (CAD) modeling of a 90° V-8 engine VCR crankshaft cradle to establish fit within production engine block.
- GT-Power computer modeling of SI engine using prior dynamometer test data to tune the computer model.

Accomplishments

- The Envera VCR mechanism was successfully packaged into an inline 4-cylinder CDI engine, demonstrating feasibility of manufacturing VCR variants of production engines.
- The ability to package the Envera VCR mechanism into a production 90-degree V-engine block was successfully demonstrated using CAD modeling. Near-identical compression ratio was maintained on both cylinder banks.
- Second-generation VCR components have been successfully designed and are currently being built, including a small profile crankshaft cradle, lubrication system, oil sealing system, actuator mechanism, and chain drive.
- The spark-ignition VCR combustion system was tuned using GT Power modeling. Projected brake specific fuel consumption at the light load condition of 2 bar bmep and 2000 rpm is 330 g/kWh. The part-load efficiency of the SI-VCR engine is projected to be higher than that of the DaimlerChrysler A170 common-rail turbo-CDI current production engine.
- A patent has been allowed for intake ports designed by Envera LLC. The ports have industry-leading performance.

Future Directions

- A VCR variant of the DaimlerChrysler 1.7L 4-cylinder common-rail turbo-diesel will be operational in Spring 2005. The engine will be used to investigate CDI emissions, fuel economy, and advanced combustion benefits that can be attained with VCR.
- Demonstrate through hardware testing and computer modeling the ability to attain 25 percent improvement in SI fuel economy with HCCI combustion using VCR and adjustable valve settings for controlled combustion from idle to high load levels.
- Demonstrate through hardware testing and computer modeling the ability to attain 30 percent improvement in fuel economy with VCR, supercharging, and engine down-sizing at significantly lower production cost than hybrid electric vehicle (HEV) technology (dollars per percent increase in fuel economy) while meeting federal and state emission standards.

Introduction

Multiple project tasks were undertaken in 2004, including design/build of a VCR variant of the DaimlerChrysler 1.7L common-rail turbo-diesel, VCR packaging studies for a V-8 engine, and SI combustion system tuning using computer modeling.

The 4-cylinder CDI engine includes several all-new VCR components, including a small profile crankshaft cradle, lubrication system, oil sealing system, actuator mechanism, and chain drive. The VCR mechanism is compact and is packaged inside a modified stock engine block. One bay of the crankshaft cradle is shown in Figure 1, and Table 1 shows selected data for the engine. The engine will be operational in spring 2005.

A CAD model of a VCR crankshaft cradle for a V-8 engine was built to demonstrate that VCR can be packaged into stock V engine blocks and that the difference in compression ratio from bank to bank is minimal. Minimizing difference in compression ratio from bank to bank is needed for attaining high efficiency.

A finding of the V-8 design study is that the Envera VCR mechanism may facilitate use of aluminum engine blocks in diesel engines and provide weight reduction relative to cast iron block engines. The VCR crankshaft cradle is cast in ductile iron and provides significant bottom-end support.

Large gains in fuel economy can be attained by down-sizing in the V-engine market segment. For example, a 4.6-L V-8 engine could be replaced by a 50-percent smaller boosted 3.0-L V-6 engine to provide both efficiency and cost benefits.

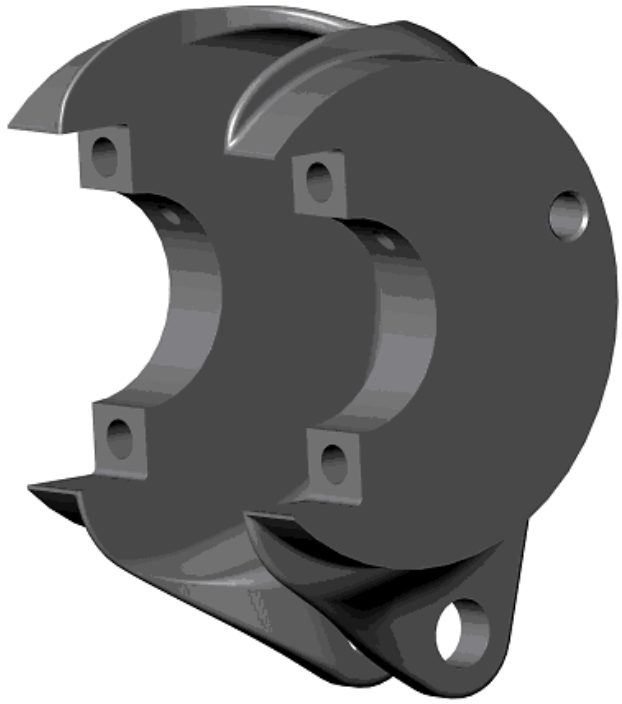

Figure 1. Single Bay of the Envera Crankshaft Cradle

In 2003, Envera LLC reported that indicated fuel efficiency values from dynamometer testing demonstrate potential for attaining a peak efficiency of over 38 percent using high-octane pump gasoline (93 octane) running at stoichiometric air/fuel ratio for effective reduction of emissions using proven 3-way catalytic converter technology.[1] In 2004, Envera used GT Power software to tune the engine for high efficiency at the part-load setting of 2 bar bmep and 2000 rpm. Brake specific fuel consumption was

Table 1. VCR 4-Cylinder Turbo-CDI Engine Specifications

Cylinders	4
Valves per cylinder	4
Valve actuation	DOHC
	Roller finger followers with hydraulic lash
Bore spacing	90 mm
Bore	80 mm
Stroke	84 mm
Bore/stroke ratio	0.95
Displacement	1.689 L
Compression ratio	18:1 maximum
	9:1 minimum
Fuel injection	Common-rail direct-injection
Cold-start	Glow plug
Boosting	Turbocharger

projected to be 330 g/kWh, and efficiency was projected to be 25.6% at the part-load condition. By comparison, the common-rail turbo-CDI currently sold in the DaimlerChrysler A170 has an efficiency of about 24% at 2 bar bmep and 2000 rpm.[2] This spark-ignited VCR engine is projected to be more efficient than the DaimlerChrysler CDI engine at part load. New camshafts have been made for dynamometer testing of the VCR engine to evaluate projected efficiency values.

Approach

The 4-cylinder VCR turbo-CDI engine is currently being designed and built. Design optimization computer models, prior analysis, and data are being used in the current project. The engine will be operational in spring 2005.

CAD modeling was used to evaluate packaging of the VCR crankshaft cradle in a 90° V-8 engine. The VCR crankshaft cradle fit within the production engine block, valuable for minimizing production cost and lead time.

GT-Power computer modeling was used to evaluate SI engine efficiency at part load.

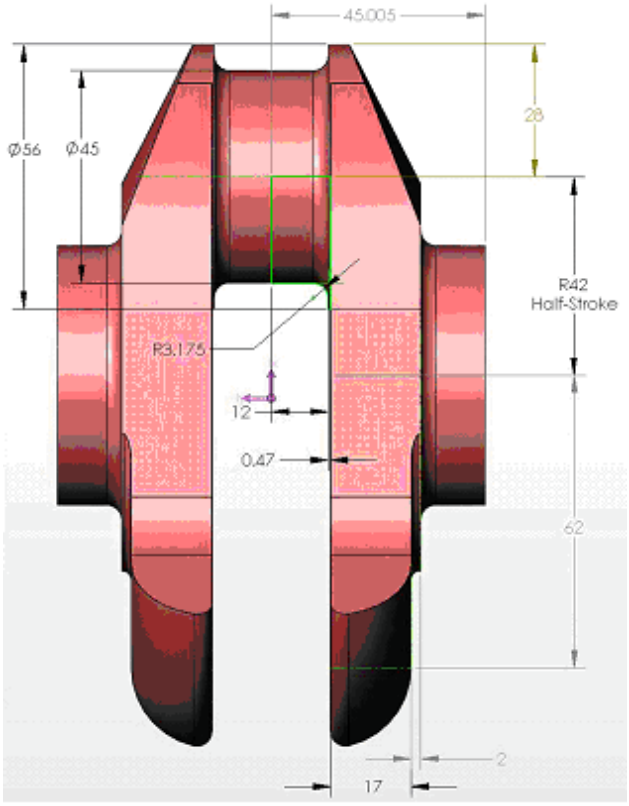

Figure 2. VCR crankshaft with rounded counterweight webs for tight packaging in the crankshaft cradle. The crankshaft has massive cheeks between the main journals and connecting rod journals to provide structure for highly boosted CDI operation.

Combustion burn rate values were assumed based on earlier dynamometer test data from the same engine.

Results

All-new VCR subsystems, including a small profile crankshaft cradle, lubrication system, oil sealing system, actuator mechanism, and chain drive, enhance commercial prospects of the Envera VCR mechanism.

To attain a small profile crankshaft cradle, crankshaft balance web size needed to be minimized. Figure 2 shows a portion of the VCR crankshaft which has rounded counterweight webs for tight packaging inside the crankshaft cradle. The crankshaft is internally balanced for each cylinder bay and features massive cheeks between main and rod journals to provide structure for highly boosted CDI operation.

Table 2. Efficiency Projections

General engine specifications SI-VCR 2-Cylinder	
Cylinders	2
Bore	81 mm
Stroke	90 mm
Displacement	928 cc
Bore off-set	15.5 mm
Valves per cylinder	4
Compression ratio	18:1 maximum
	8.5:1 minimum
Specific power output design limit	150 hp/L (139 hp)
Fuel	93 octane gasoline
Engine management	PFI Motec
Peak engine efficiency Results reported in 2003	
Engine Speed	2350 rpm
Fuel to air mixture ratio	Stoichiometric, lambda 1
Indicated mean effective pressure	10.7 bar
Projected friction mean effective pressure, fmep	1.10 bar
Brake mean effective pressure with assumed fmep	9.60 bar (imep - fmep)
Specific fuel consumption with assumed fmep	220.7 g/kWh (42.58 LHV)
Brake efficiency with assumed fmep	38.3%
Part-load engine efficiency 2004 Projection using GT Power computer modeling	
Engine speed	2000 rpm
Power at test condition	3.08 kW (4.13 hp)
Fuel to air mixture ratio	Stoichiometric, lambda 1
Fuel	93 octane gasoline
Indicated mean effective pressure	2.86 bar
Projected friction mean effective pressure, fmep	0.86 bar
Brake mean effective pressure with assumed fmep	2.0 bar (imep - fmep)
Specific fuel consumption with assumed fmep	330.0 g/kWh (42.58 LHV)
Brake efficiency with assumed fmep	25.6%

Table 3. SI-VCR and Turbo-CDI Efficiency Compared

Engine	SI-VCR	DaimlerChrysler A170 CDI[2]
Fuel	Gasoline	Diesel
Fuel System	PFI	Common-rail direct injection
Effiency Projections		
– 2 bar bmep 2000 rpm	25.6%	24.1% (interpolated)
– 3.09 kW (4.15 hp) at 2000 rpm	25.6%	16.7% (interpolated)
– Peak efficiency	38.3%	38.95%
Rated power with boosting	150 hp/L	56 hp/L (MY 2004)
Emission system	TWC	

The ability to fit the Envera VCR mechanism into modified production inline and V engine blocks was demonstrated. Compression ratio is almost identical on both sides of a 90° V engine, important for attaining high efficiency. CDI cast iron block engines may be lightened by using a ductile iron crankshaft cradle and an aluminum engine block.

Efficiency was projected for the gasoline-fueled Envera SI-VCR engine. At part-load of 2 bar bmep and 2000 rpm, brake specific fuel consumption of 330 g/kWh and brake thermal efficiency of 25.6 percent were predicted using GT Power software. The projected SI-VCR engine efficiency values are of particular interest because they are higher than the DaimlerChrysler A170 common-rail turbo-CDI efficiency values. Table 2 shows peak efficiency values reported by Envera in 2003 and new part-load efficiency projections from 2004. Table 3 provides a comparison of the SI-VCR engine efficiency and the DaimlerChrysler A170 CDI efficiency. The data indicates that the gasoline SI-VCR engine would return higher fuel economy than the diesel without the benefit of engine down-sizing. With down-sizing, the gasoline engine would provide better mileage than the diesel by a larger margin.

SI-VCR engines may have an advantage over smaller-displacement CDI engines (under roughly 200 horsepower). CDI engine efficiency improves with increase of engine displacement because turbocharger efficiency improves with increased

airflow. Larger CDI engines have higher efficiency than the DaimlerChrysler A170.

CDI engine efficiency can also be improved with VCR. The baseline for comparison is a moving target, and VCR is anticipated to advance CDI efficiency as well.

Conclusions

A second-generation Envera VCR engine will be operational in spring 2005. The CDI engine includes all-new VCR subsystems that enhance commercial prospects for the technology.

Efficiency projections conducted in 2004 suggest that gasoline-fueled SI-VCR engines may provide better fuel economy (without benefit of down-sizing) than some diesels, such as the DaimlerChrysler A170 common-rail direct-injection turbo-diesel engine. If down-sizing is allowed, fuel economy can be increased by a larger margin. The efficiency of CDI engines is improving and may remain higher than that of gasoline engines. Nevertheless, SI-VCR engine technology developed with funding from DOE has been a success and could play a significant role in reducing growth of national petroleum consumption.

Significant national oil savings could initially be realized by down-sizing large V-engines with smaller boosted V-engines having VCR (both CDI and SI). Saab and others estimate that VCR and down-sizing can improve SI fuel economy by about 30%.[3] The efficiency of the VCR engines could be further improved by HCCI combustion as that technology matures. GM and others estimate that HCCI combustion offers the potential for improving gasoline fuel economy by about 25%.[4] The VCR technology can be integrated into production engines and has significantly lower cost than HEV technology.

Patents

1. A patent has been allowed on a high-performance intake port invented by Charles Mendler. The port exhibits industry-leading flow values, which increases engine torque and reduces boost pressure requirements for engine down-sizing. The port was developed with funding from the U.S. Department of Energy. The publication number and date have not yet been issued.

References

1. Mendler, Charles: Variable Compression Ratio Engine Analysis, Advanced Combustion R&D, 2003 Annual Progress Report, FreedomCAR and Vehicle Technologies Program, U.S. Department of Energy, 2003.
2. Oak Ridge National Laboratory warm engine dynamometer test results for the DaimlerChrysler A170 common-rail turbo-CDI engine, undated test data provided to Envera by ORNL.
3. Automotive Engineering, page 36, December 2000.
4. Natj, Paul: The Wall Street Journal Online and on page B1, Autos: Car Makers Seek New Spark In Gas Engines, September 28, 2004.

IV Waste Heat Recovery

IV.1 Electric Boosting System (e-Turbo™) for SUV/ Light Truck Diesel Engine Applications

S. M. Shahed
Honeywell Turbo Technologies
3201 W. Lomita Blvd.
Torrance, CA 90505

DOE Technology Development Manager: John Fairbanks

Objectives

- Develop an electric boosting system suitable for 4- to 6-liter diesel engine SUV/light truck applications.
- Develop base electric machinery technology – motor/generator, power supply, rotor stability and temperature control.

Associated objectives consistent with ongoing R&D at Honeywell include:

- Develop an integrated control system for power, variable nozzle turbine (VNT), exhaust gas recirculation (EGR), and battery.
- Design and develop a low-inertia turbocharger to minimize power demand.
- Design and develop a variable geometry compressor to take full advantage of e-Turbo.

Approach

- Develop e-Turbo for a diesel engine (~2 liters) as a platform for technology development.
- Refine the design to meet duty cycle requirements and prove technology benefits.
- Using computer simulation, apply the small e-Turbo to each bank of a V-configuration engine (~4 liters) using baseline data from tests on the 2-liter engine.
- Conduct computer simulation of an integrated control system and assess benefits.
- Develop base electric machinery – motor/generator, power supply, rotor stability and temperature control.
- Develop an integrated control system for power, VNT, EGR, and battery.
- Design and develop a low-inertia turbocharger to minimize power demand.
- Design and develop a variable geometry compressor to take full advantage of e-Turbo.

Accomplishments

- A larger e-Turbo was designed and built for testing during Q4 2004. The design included duty cycle analysis to ensure proper cooling of electrical machinery under severe driving conditions and a bearing system that is stable under mechanical and electromagnetic forces at high speeds.
- Engine and vehicle tests using a 12-Volt e-Turbo system (with a second battery) were completed. Engine transient tests show significant improvement of torque and response. Steady-state torque with e-Turbo improved by 20-40% in the low speed range (see Figure 1). Transient response (time to 200 Nm of torque) was reduced from 6 to ~2.3 seconds at 1500 rpm (see Figure 2).
- Electric power generation with an e-Turbo was successfully demonstrated on bench and engine tests. At 3,000 rpm with EGR, 900 W of electrical power was generated with a 3.5% improvement in brake-specific fuel consumption (BSFC) (see Figure 3).
- Different cycles were tested to demonstrate the potential of e-Turbo as a partial substitute for the alternator. Impact on fuel consumption was measured.

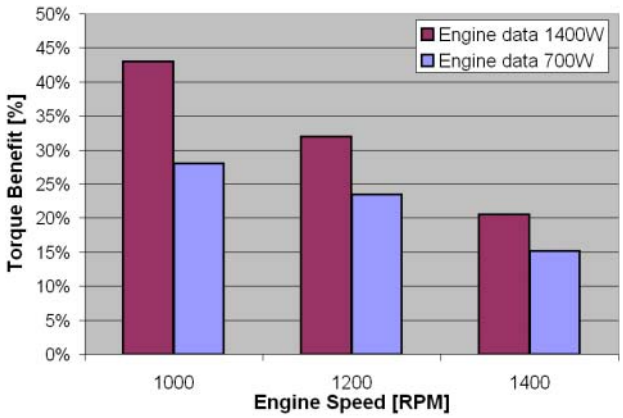

Figure 1. Steady-State Torque Improvement with e-Turbo in a 2-Liter Diesel Engine

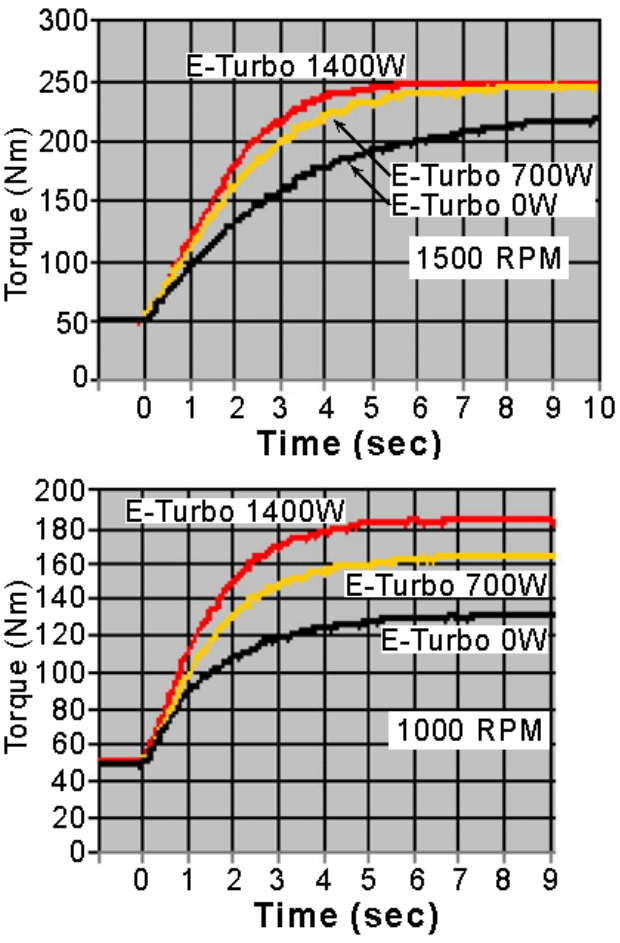

Figure 2. Transient Torque Response Improvement of a 2-Liter Diesel Engine with e-Turbo at 1000 and 1500 rpm

- Basic architecture for an integrated sensing and control system was developed, and preliminary control logic was tested using engine simulation (see Figures 4 and 5). It is too early in the project to quantify the benefits of an integrated control logic.
- A turbocharger with 40% reduced inertia (see Figure 6) was built and tested under an existing R&D program. For the e-Turbo, reduced inertia should improve transient response further and ease the demand on electrical machinery.
- A variable geometry compressor (VGC), which can be used to take full advantage of e-Turbo's capabilities, was built under existing R&D work. Tests demonstrated that at a pressure ratio of 2.8,

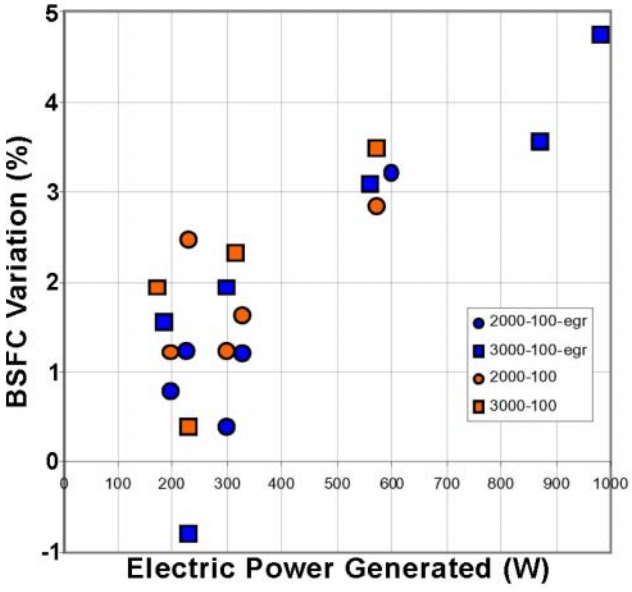

Figure 3. Electric Power Generation and BSFC Improvement with e-Turbo on a 2-Liter Diesel Engine

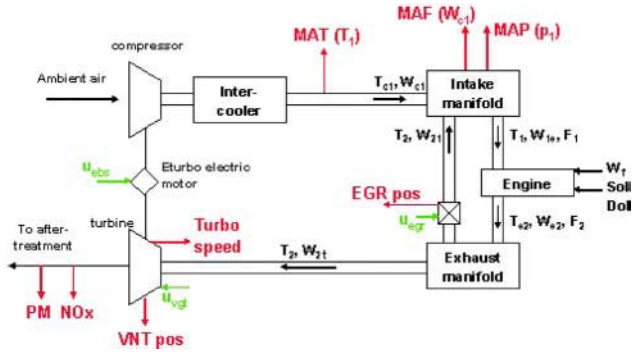

Figure 4. Basic Sensing and Control Parameters for e-Turbo

the VGC flow range was increased by 65% and compressor efficiency was increased by 3%. Engine tests demonstrate a 40% torque increase at 1500 rpm and 25% torque increase at 1200 rpm with a 2-liter, 110-kW diesel engine.

Future Directions

- Develop and demonstrate 3rd-generation improved prototype e-Turbo design.
- Begin simulation analysis of e-Turbo application to larger engine displacements of 4–6 liters, suitable for SUV/light truck applications. Initially focus on twin-turbo implementation of the 2nd-generation prototype design (one turbo on each bank of a V-configuration engine).
- Three other sub-tasks of the project consistent with ongoing R&D at Honeywell but also useful for e-Turbo include integrated control logic, low-inertia turbocharger and variable geometry compressor. Each of these projects was started before 2004 but became associated with this project earlier this year so far as they relate to e-Turbo. The tasks for the remainder of the project period include development of refined prototypes and testing to establish benefits that could then be suitability proven and incorporated into an e-Turbo system.

Introduction

The purpose of this project is to develop an electrical turbocharging/boosting system, e-Turbo™, for application to SUV and light truck classes of passenger vehicles. Earlier simulation work has shown the benefits of the e-Turbo™ system on increasing low-end torque and improving fuel economy. This technology improves the driveability/response of a turbo diesel in SUV/light truck applications. It also generates electrical power under conditions when there is excess exhaust energy available, thus improving fuel economy.

In addition, there is potential for diesel engine rightsizing by 10-30% to deliver a further 6-17% fuel economy improvement, in addition to the 30+% fuel economy benefit that a turbo diesel offers relative to conventional gasoline engines. In this rightsizing scenario, e-Turbo™ is even more critical to recover acceptable driving characteristics.

In parallel with the e-Turbo, the following technologies are being developed by Honeywell, each of which could be used independently or, as intended in this project, combined with e-Turbo to fully utilize the potential benefits of the e-Turbo system.

An integrated control system that controls EGR, fresh air, electrical power and battery charge in the most optimum way

A variable geometry compressor that increases the flow range of the compressor to avoid surge and make full use of high boost at low engine speeds

A low-inertia turbocharger to minimize power demands on the battery and electrical machinery

Approach

The approach is to develop a turbocharger in which a compact electric motor/generator is designed and mounted on the same shaft as the turbine and compressor wheels. It was decided to prove this technology on a small turbocharger first, identify all issues, assess the possible benefits and costs, and then scale it up as required.

Results

During 2000-2001, many electrical machinery concepts were evaluated. Work included extensive design and testing of permanent magnet motor/ generators and careful evaluation of switch reluctance motor technology. Trade-offs among cost, performance, temperature tolerance and control capability were evaluated. It was determined that induction motor technology was best suited for the e-Turbo application.

Early simulation was done to determine the benefits of electrical assist in increasing torque and response, as well as its ability to generate electrical power to improve fuel economy. The findings were

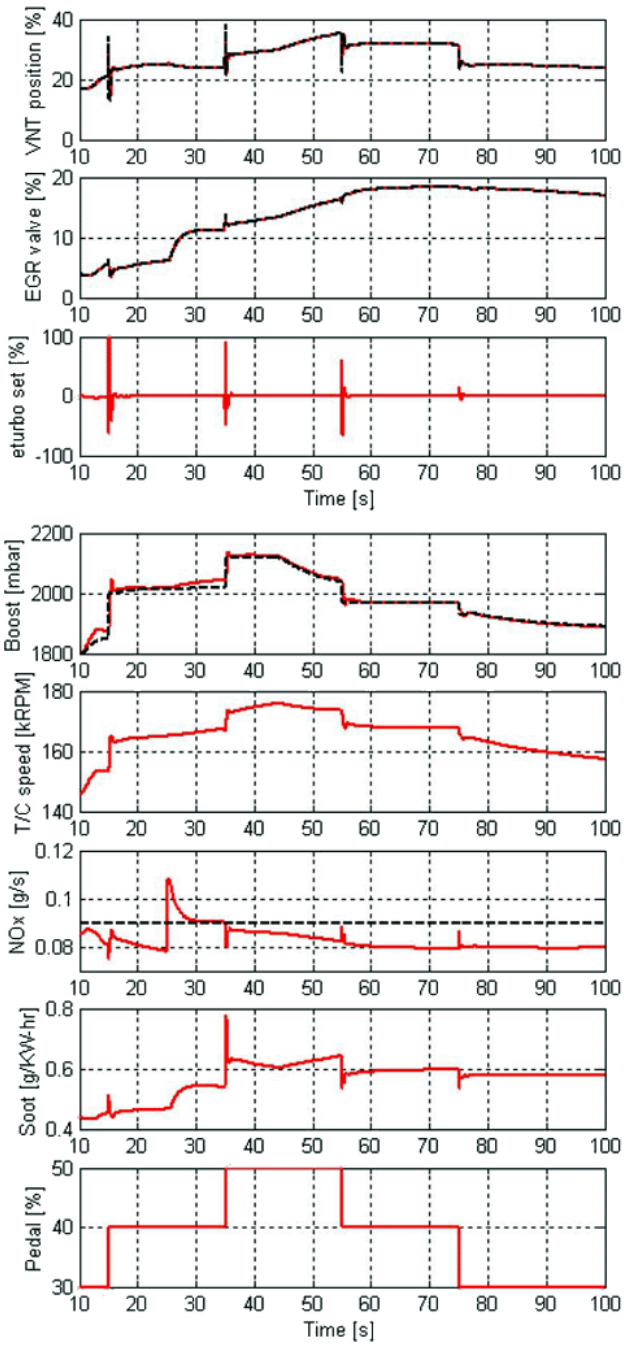

Figure 5. Preliminary Transient Simulation Results with Model-Based Control

reported at Diesel Engine Emissions Reduction (DEER) conferences. Design and development of an induction motor/generator system and an appropriate power electronics and control system were completed, and the systems were tested. Design iterations had to be carried out to make the system tolerant of high temperatures during hill-climbing

Figure 6. 40% Reduced Inertia Turbo

duty cycles. Adding a motor/generator to the turbocharger shaft adds mass and increases the length overhung beyond the bearing system. Design iterations had to be carried out to make the system stable at high rotational speeds and tolerant to electro-magnetic forces. The results of these iterations were reported at DEER conferences.

Early in 2004, the scope of work was expanded to bring critical considerations into the project. There were three additional design requirements that led to this expanded scope.

It was apparent that there was a need to develop an integrated control system to optimize control of EGR, boost, power generation and battery charge as an overall consistent system. This task was added to the scope, and the vast capability and know-how of Honeywell in control systems, both from industrial and aerospace applications, is being used to design an optimum control system.

Electric assist capability enables the turbocharger to operate at high pressure ratios even when engine speed is low. This increases the air supplied to the engine and enables more fuel to be burned and high torque to be generated. Unfortunately, state-of-the-art compressors without variable geometry were unable to fully use this capability because of an aerodynamic phenomenon known as surge, which can be very destructive to the turbocharger. One way to address this is to add variable geometry capability to the compressor. Considerable investment already made by Honeywell

in this technology for use with VNT (non-electric) passenger car turbos was brought into the project to help fully utilize the e-Turbo's capabilities.

The amount of power supplied to e-Turbo is limited by the size of electrical machinery, which necessarily has to be compact. Heat dissipation also becomes a problem under these conditions. Therefore, it was necessary to limit the power supplied. Reduction in turbocharger inertia makes it very responsive and reduces the amount of power required for a given response. Again, work done previously by Honeywell was brought into the project as an additional task to supply a low-inertia turbocharger to be later combined with e-Turbo technology.

Progress made on all these tasks is shown Figures 1-6. Figure 1 shows that steady-state torque is improved by more than 40% at low speeds. Figure 2 shows that transient response is greatly improved from 6 seconds to about 2 seconds to reach a given torque. Figure 3 shows that e-Turbo can be used to generate electrical power and improve fuel economy. Figures 4 through 6 are meant to be status reports on progress made to date and are not final results at this time.

Conclusions

e-Turbo technology improves low-speed torque of turbocharged diesel engines. In addition, turbo response is greatly improved. Both these benefits enable the use of diesel engines in SUV/light truck applications with vehicle performance exceeding the baseline gasoline engine performance. This can result in fuel economy savings of up to 30% compared to the baseline.

High torque at low speeds can possibly allow a 10-30% engine downsizing and a further 6-17% improvement in fuel economy while maintaining vehicle performance.

Electrical power generation by e-Turbo has further potential benefits. BSFC benefits of up to 6% at high loads and speeds have been shown. Fuel economy benefits over a representative duty cycle have yet to be determined.

In order to fully realize the benefits of e-Turbo, other technologies will be extremely useful. These include an integrated control system, variable geometry compressor and a low-inertia turbocharger.

FY 2004 Publications/Presentations

1. Steve Arnold, Craig Balis, Etienne Poix, Tariq Samad and S.M. Shahed, “Design & Development of e-Turbo™ for SUV and Light Truck Applications”, DEER Conference, August, 2004.

References

1. S. M. Shahed, John Allen and Jerry Artache, “The Development of Electrically Assisted Turbochargers for Diesel Engine Applications”, DEER Workshop, August 22, 2000.
2. S. M. Shahed, “Smart Boosting Systems – e-Turbo™ and e-Charger™ – New Frontier”, DEER Workshop, August 6, 2001.
3. S.M. Shahed, Chris Middlemass and Craig Balis, “Design & Development of e-Turbo™ for SUV and Light Truck Applications”, DEER Conference, August 2003.

IV.2 Diesel Engine Waste Heat Recovery Utilizing Electric Turbocompound Technology

Ulrich Hopmann
Caterpillar Inc.
PO Box 1875
Peoria, IL 61656-1875

DOE Technology Development Manager: John Fairbanks

Subcontractors:
Switched Reluctance Drives Ltd., Harrogate, UK
J.H. Benedict Co. Inc., Peoria, IL

Objectives

- Build laboratory engine that demonstrates technical feasibility
- Improve fuel economy by 5% with exhaust energy recovery

Approach

Caterpillar's experienced research team has chosen the following approach to develop an electric turbocompound (ETC) system:

- Develop turbocharger and system design from concept to preliminary and final design
- Analyze and test components
- Develop and test turbomachinery and electrical machinery
- Design, analyze and test control system
- Bench test complete ETC system on the engine

Accomplishments

- Turbocharger hardware has been procured and assembled
- The crankshaft and turboshaft motor/generator (M/G) have been designed, assembled and tested
- The control system has been developed and tested
- Turbocharger performance test on the gas stand has been completed (rotor dynamics test, compressor and turbine map)
- The turboshaft M/G characterization has been validated on the gas stand
- Determination of baseline performance and fuel consumption of the on-highway truck engine has been completed
- The ETC system has been installed on the engine in the test cell

Future Directions

Caterpillar will focus on engine testing of the complete ETC system.

- Commission engine and ETC control system in engine test cell
- Perform engine tests in turbocompound mode

Introduction

The principle of turbocompounding is a known technology for reducing fuel consumption. Research projects for truck-size diesel engines suggest a potential of 5% brake specific fuel consumption (bsfc) improvement [1]. Diesel engines for ship propulsion and stationary power generation have shown bsfc improvements on the same order. However, those systems consisted of a turbocharger plus an additional power turbine, which was mechanically connected to the crankshaft.

Research efforts at Caterpillar are now focusing on the development of an electric turbocompound (ETC) system for heavy-duty on-highway truck engines. The efforts cover concept, design and test. A cooperative project between the DOE Office of FreedomCAR and Vehicle Technologies and Caterpillar is aimed at demonstrating electric turbocompound technology on a Class 8 truck engine.

The goal is to demonstrate the technical feasibility and improve fuel economy. The system consists of a turbocharger with an electric M/G integrated into the turboshaft. The generator extracts surplus power at the turbine, and the electricity it produces is used to run a motor mounted on the engine crankshaft, recovering otherwise wasted energy in the exhaust gases. The electric turbocompound system also provides more control flexibility in that the amount of power extracted can be varied. This allows for control of engine boost and thus air/fuel ratio. The research work covered turbocharger design, system and component analysis, control system development, engine simulation, electrical machinery development and system and component testing.

Approach

A multi-disciplinary approach has been used in order to address the following key development areas: aero design, electrical machine design, engine performance, control system, structural analysis and testing.

The layout of the ETC turbocharger is a mid-mount configuration, i.e., the electrical machine is located between the compressor and turbine wheel.

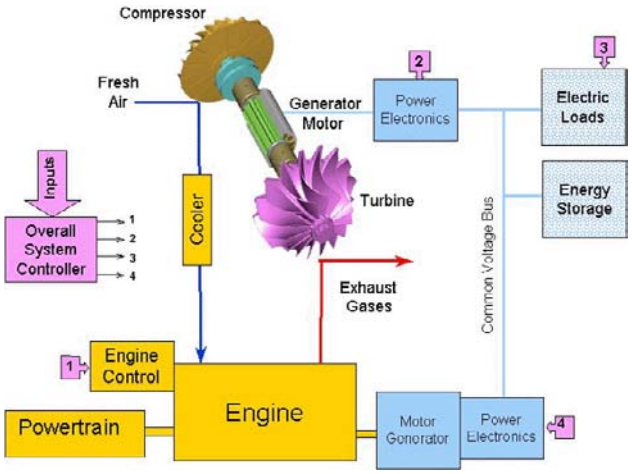

Figure 1. Electric Turbocompound Schematic

Four compressor and turbine stage high-performance machines were chosen.

The selection of the electrical machine was mainly driven by high shaft speeds and packaging constraints. Three basic machine types were compared: switched reluctance (SR), synchronous reluctance, and brushless permanent-magnet (PM). In a study, the constraints of shaft speed, rotor outside diameter, low centrifugal stresses, rotor inertia and cost led to the choice of an SR machine.

The control system manages power flux and communication between the engine and the ETC controller. Recovery of energy from the diesel engine exhaust is done electrically. A schematic of the system is shown in Figure 1. When the power produced by the turbocharger turbine exceeds the power requirement of the compressor, this surplus power is converted into electrical power by the electrical machine located on the turbocharger shaft. Surplus power at the turbine can be recovered by the ETC system through an electric motor mounted on the crankshaft, which assists the engine. The result of this process is an increase in system efficiency. Alternatively, the surplus power can be used to drive other electrical on-board devices or it can be stored. To improve vehicle driveability, the system can be run in turbo assist mode to accelerate the turboshaft.

Results

Having completed design and structural analysis of the turbo and electrical machinery, Caterpillar has

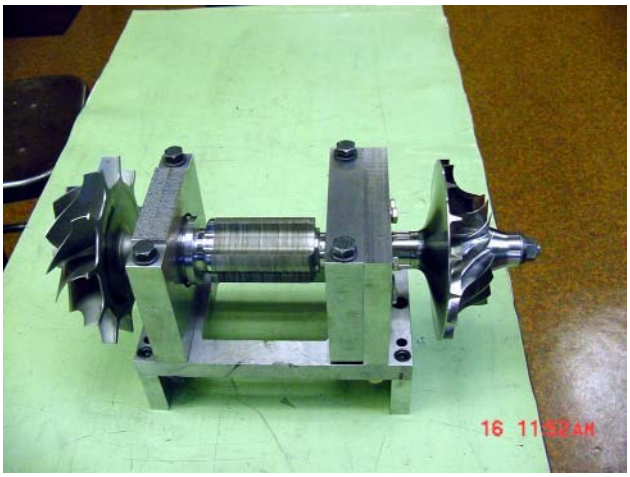

Figure 2. Turboshaft Rotor Assembly Balance

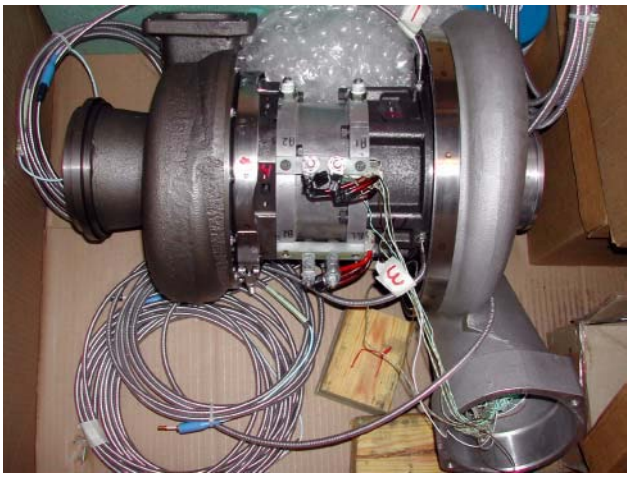

Figure 3. Assembled Turbocharger

finished design and procurement. A major task was the assembly and balancing of the turbocharger. Figure 2 shows the rotor assembly mounted onto the balancing fixture; Figure 3 shows the assembled turbocharger.

The crankshaft M/G has been tested in the motoring and generating modes up to 60 kW and 2400 rpm. The turboshaft M/G tests were carried out as a separate component test on a dynamometer and as part of the ETC turbocharger on the gas stand.

In order to manage the two electrical machines and to control the compound power, a new control system had to be developed. It has been successfully tested during the gas stand tests, where up to 46 kW were extracted from the turboshaft M/G.

The turbocharger gas stand tests have been completed (see Figure 4). Rotor dynamics measurements confirmed a stable shaft system; compressor and turbine performance data have been recorded.

Conclusions

A turbocharger and ETC system has been designed and built. Compared to a mechanical system, Caterpillar's novel ETC system offers more flexible engine operation, e.g., air/fuel ratio control and turbo assist mode. Performance predictions for the engine cycle indicate 3 to 5 percent improvement in fuel consumption. The system offers the potential for reduced emissions and improved driveability

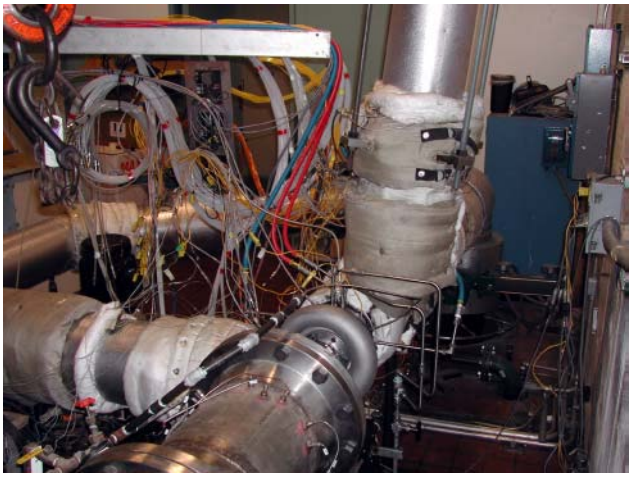

Figure 4. Turbocharger on Gas Stand

through improved air system response using the turbo assist capability.

FY 2004 Publications/Presentations

1. Hopmann, U.: "Diesel Engine Waste Heat Recovery Utilizing Electric Turbocompound Technology". DEER Conference, August 29-September 2, 2004, San Diego, CA.
2. Hopmann, U.: "Ein Elektrisches Turbocompound Konzept für NFZ Dieselmotoren". 9th Supercharging Conference, September 23-24, 2004, Dresden/ Germany.

References

1. Caterpillar Inc.: "LE55", internal research paper, 1982

IV.3 Clean Diesel Engine Component Improvement Program - Diesel Truck Thermoelectric Generator

N. B. Elsner, J. C. Bass, S. Ghamaty, D. Krommenhoek, A. Kushch, D. Snowden, S. Marchetti (Primary Contact)
Hi-Z Technology, Inc.
7606 Miramar Road, Suite 7400
San Diego, CA 92126

DOE Technology Development Manager: John Fairbanks

Subcontractors:
Rich Bergstrand, PACCAR Technical Center

Objectives

- The objective of the project is to develop a cost-effective thermoelectric generator (TEG) that will be powered by the diesel engine exhaust heat, in sizes from 1 kW to 10 kW.
- The thermoelectric generator, by generating required electrical power, will reduce fuel consumption and reduce corresponding emissions.
- Greater onboard generation of electricity could power any number of exhaust cleanup devices being developed to futher reduce emissions.
- Development of the next generation of thermoelectric technology called multi-layer quantum well films (MLQWF) should improve the thermoelectric conversion from the 5% to 6% available today to 20% to 30%.

Approach

- Design a 2½ W quantum well (QW) module as a building block leading ultimately to 80 W modules suitable for a 10-kW diesel truck thermoelectric generator (DTTEG) for the Tank Automotive Armaments Command (TACOM) Stryker Program.
- Continue development of sputtering and hot wall techniques for making QW films.
- Complete the design of the 10-kW DTTEG with QW modules.

Accomplishments

- Achieved >530,000 equivalent miles in road tests of the 1-kW DTTEG.
- Achieved successful laboratory and test cell tests on a 300-W automobile exhaust thermoelectric generator (AETEG).
- Specified and placed on order a 34" internal diameter (ID) sputtering machine.
- Designed, constructed, and operated a hot wall deposition apparatus for QW film.
- Obtained 14% efficiency on two QW couples.
- Developed QW couples with molybdenum (Mo) contacts for 500°C operation.

Future Directions

- Accelerate QW development with the installation and startup of the 34-inch ID machine.
- Continue to work with Pacific Northwest National Laboratory (PNNL) to produce QW film for QW modules.

- Test 2½-watt and larger QW modules (2005).
- Improve deposition rate for QW film to approach the predicted 25% efficiency.
- Develop the 10-kW TEG for the Army's Stryker program (2007-2008).

Introduction

Hi-Z Technology, Inc. (Hi-Z) is currently developing four different auxiliary generator designs that are used to convert waste heat from truck engines directly to electricity. The first project is the development of a 1-kW generator for heavy-duty diesel trucks. The second is a 300-W generator to be used on light-duty gasoline engine trucks or automobiles. The third is a 200-W generator to be used on a light-duty hybrid truck. The fourth is a 10-kW generator for Army Stryker trucks.

The 1-kW generator project [1] has been ongoing for several years and has completed testing for its response to over-the-road shock and vibration in a Class VIII Kenworth truck. Currently, the generator has logged in excess of 530,000 equivalent miles on PACCAR's test track and has completed the road test phase of the project.

The current focus of the 1-kW project has shifted from generator testing to the development of quantum well thermoelectric modules to replace the currently used bulk thermoelectric modules in the generator so that its output can be increased to about 4 kW, and ultimately to 10 kW under TACOM's Stryker program.

Approach

The 1-kW DTTEG is currently funded by DOE through December 31, 2004, with corporate participation from PACCAR and Hi-Z, and is shown mounted underneath the truck in Figure 1. The 300-W AETEG generator is being funded by the New York State Energy Research and Development Agency and DOE, and the work is being done for Clarkson University with corporate support from General Motors and Delphi. This generator is shown in Figure 2. The 200-W generator rework is being funded by DOE, and the work is being done for Ohio State University. The preliminary design 10-kW TEG for the Army's Stryker vehicle is shown in Figure 3.

Figure 1. 1-kW DTTEG on PACCAR Truck

Figure 2. Photograph of a 300-Watt Generator Mounted Beneath the Truck

Three of the above-mentioned generators (the exception being the 10-kW TEG for the Army's Stryker vehicle) currently use conventional Bi_2Te_3 alloy thermoelectric modules. The material in these modules has a value of ZT [figure of merit (Z) times its mean absolute operation temperature (T)] of about 1. The value of ZT has hovered around 1 since the mid-1950s, when semiconductor materials were introduced into thermoelectric conversion. In the late 1990s, new materials, including quantum well materials, started to increase the value of ZT to about 4 with some promise that even higher values can be

obtained as development continues. (See the 2003 Annual Report for an explanation.)

Results

Stryker 10-kW Generator. The Stryker 10-kW generator consists of two 5-kW thermoelectric generators arranged in series to fit in the underarmor space of the Stryker vehicle. One of the 5-kW generators occupies a region that is only 27 inches long and 10 inches in diameter. The location of the modules, compression band and cooling are as shown in Figure 3. The outside 10-inch dust cover is not shown on this figure. The hot side heat transfer is augmented with staggered arrays of fins and a small center displacement body to increase turbulence. The inside diameter (5.5 inches) and pressure drop are designed to closely match the engine exhaust muffler, which is replaced by the quantum well thermoelectric generators. Each of the quantum well modules are individually assembled, loaded in compression and then further side loaded to maintain excellent thermal contact on the hot side heat exchanger region. This hot side heat exchanger or exhaust tube is machined with octagonal flats to receive each of the 64 quantum well thermoelectric modules. At peak horsepower, each quantum well module is predicted to give ~80 watts. Thus, it is predicted that two 5-kW generators can be packaged with a CAT 3126 300-hp engine in a Stryker vehicle. Each 5-kW quantum well generator occupies slightly less space than the prior 1-kW generator made with Bi_2Te_3 thermoelectric materials.

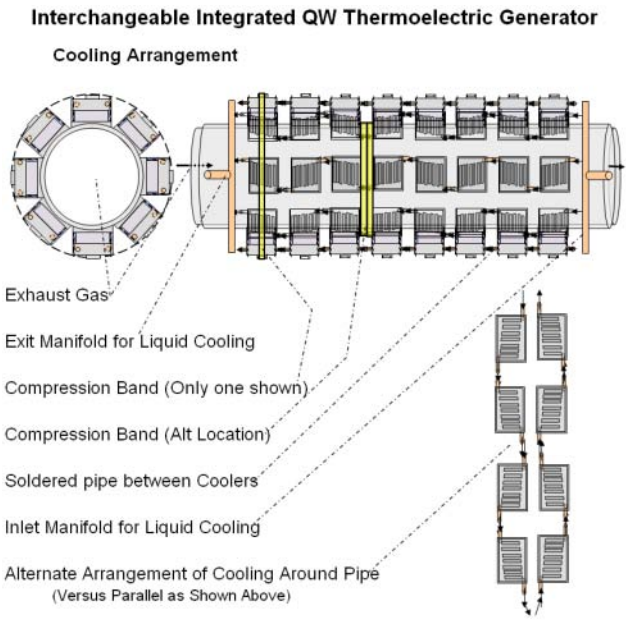

Figure 3. Preliminary Design of the 10-kW TEG for the Army's Stryker Program

DTTEG 1-kW Generator

TEG Mod 2 has completed its over-the-road testing with over 530,000 equivalent road miles at PACCAR's test facility.

The generator demonstrated capability of producing about 1 kW of electric power in the test cell when city water (+22°C) was used as a TEG cooling agent. The TEG produced 528 W of electric power during the road test at PACCAR's facility when engine coolant (+90°C) provided the TEG cooling. Future projects will address this need by including a separate coolant loop to lower the coolant temperature to the range of 30° to 50°C. Increasing the ΔT by 50°C almost doubles the power output. Bulk modules of Bismuth Telluride, as an interim solution while QW modules are being developed, may also be improved slightly to higher conversion efficiencies with optimized doped material. The total impact of both changes could produce over-the-road power in the 1 kW range with the Bi_2Te_3 alloy thermoelectric modules in the current TEG design (nominal 1 kW).

TEG Mod 2 post durability test inspection indicated that there was no evidence of any catastrophic failures. It was found that the TEG internal resistance increase (from 0.6 to 0.75 Ohms) could be partially attributable to electrical contacts corrosion. Further analysis is in progress. One hose that connects the cooling heat sinks was perforated and caused coolant leakage, the possible source of the corrosion. This can be easily cured by using higher-strength hoses.

Continued Development of Sputtering Techniques

DOE Oak Ridge Operations, DOE National Energy Technology Laboratory, the National Aeronautics and Space Administration and the Naval Sea Systems Command provided funding for the December 3, 2003 purchase of a $322,000 (34" ID) sputtering machine, which is due to be delivered to Hi-Z late in 2004. This machine is expected to increase Hi-Z's rate of sputtering by 100 to 200

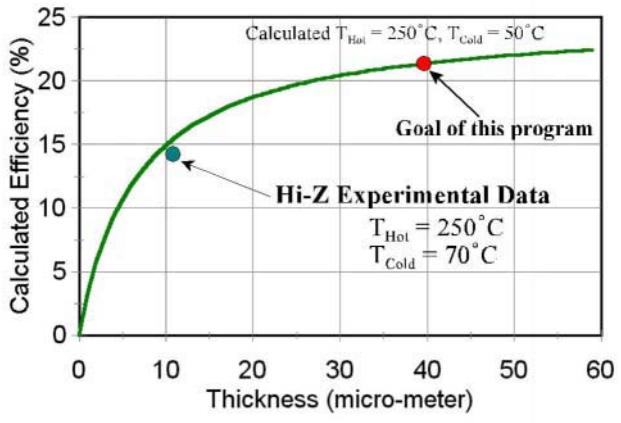

Figure 4. Efficiency of QW Couple *vs.* Film Thickness on a 5-μm Substrate

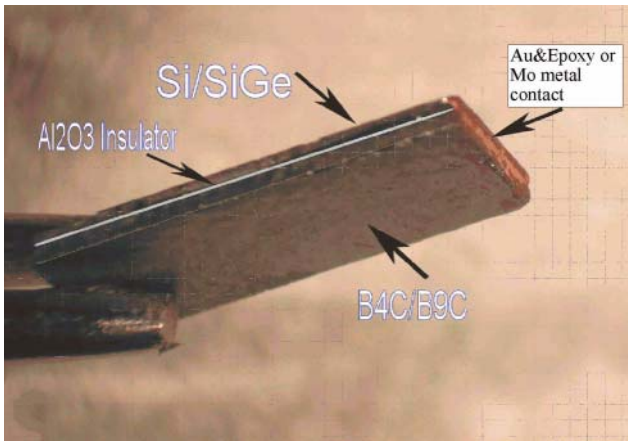

Figure 5. QW Si/SiGe-B_4C/B_9C Couple for Thermal Stability Test

times. In the interim, PNNL has been contracted to produce QW film. The first delivery of PNNL's QW film is scheduled in November.

QW Couple Efficiency Measurement

Hi-Z has assembled and tested two different single-couple modules. Both couples were made of B_4C/B_9C and N-type Si/SiGe, and the conversion efficiency from both tests was in excess of 14% at a temperature differential of 200°C.

The efficiency obtained was not corrected for any losses, but was based only on the power out of the couple divided by the power into the heater. The actual conversion efficiency of the couple was somewhat higher. The QW materials used in both couples were a total of 11 μm thick and were deposited on a 5-μm thick silicon substrate. The ratio of film thickness to substrate thickness can have a significant effect on the conversion efficiency because the substrate, which is both thermally and electrically in parallel with the QW, is essentially a parasitic heat loss. This can be seen in Figure 4, which presents a curve of the calculated B_4C/B_9C-Si/SiGe module efficiency as a function of QW thickness for films deposited on a 5-μm substrate for hot side temperatures of 200°C and 300°C.

Thermal Stability Mo Metal Contact

Figure 5 shows a new QW couple with B_4C/B_9C and Si/SiGe insulated with alumina. This couple was fabricated for a new thermal stability test for high temperatures. Laser-assisted sputtering was used to deposit the Mo metal contact.

Initial isothermal thermal stability testing of the Mo metal contact couple at 300°C for 300 hours exhibits very stable performance, as shown by the very slight increase in power with time. We will continue the thermal aging for longer times and at higher temperatures. More couples with metal contacts are being fabricated and will be life tested at several hot side temperatures.

Hot Deposition of QW Films

As an alternative to sputter deposition of quantum well films, electron-beam heating to effect vaporization and deposition is being investigated. A primary advantage of this technique is the possibility of attaining high deposition rates. A significant problem with electron-beam deposition is the possible decomposition of compounds during the deposition process, or at a minimum a serious change in stoichiometry of the deposited material. The hot-wall technique was developed to preclude such changes in stoichiometry by surrounding the evaporation space with a hot wall at higher temperature than the substrate on which the deposited film is formed. The hot-wall configuration has not previously been used with electron-beam-heated sources; we have begun evaluation of this approach with the goal of preparing layered QW films.

Figure 6. Hot Wall Deposition Apparatus

The equipment used for deposition consists of an electron-beam-heated, four-hearth source coupled with a hot-wall deposition region. The source is powered by an *Airco-Temescal*, 10-kW power supply (10 kV, 1 A) and is contained in an 18-inch diameter bell jar. Depositions are carried out in the 1^{-6} Torr pressure range. Typical deposition rates were 0.1 to 0.4 μm/min. Figure 6 shows the hot wall apparatus.

The primary emphasis of the project thus far is the deposition of SiC films using two different source materials obtained form *Cercom, Inc.* and *POCO Graphite*.

Conclusions

An advanced 10-kW TEG is achievable with 80-watt QW modules (which need to be developed), based on results with the 1-kW TEG.

QW test couples achieved 14% conversion efficiency to confirm a point on the theoretical curve.

QW modules with 20-25 micron film thicknesses on 5-micron thick Si should be capable of achieving 20% conversion efficiency, based on Hi-Z calculations.

QW couples are being fabricated with Mo contacts that exhibit stable performance.

Special Recognitions & Awards/Patents Issued

1. Hi-Z has been awarded 16 patents: five apply to QW material, two apply to TEGs

FY 2004 Publications/Presentations

1. Four (4) Quarterly Reports for DTTEG Program and presentations at the DEER ’04 Conference.
2. 20th IEEE SEMI-THERM Symposium, 2004, “New Technology for Thermoelectric Cooling”, John C. Bass, Daniel T. Allen, Saeid Ghamaty, and Norbert B. Elsner.
3. Chapter in The New Edition of Thermoelectric Energy Conversion Systems, published July 31, 2004 (in Japanese), “Thermoelectric Generators for Diesel Trucks”, J.C. Bass.
4. Chapter in The New Edition of Thermoelectric Energy Conversion Systems, published July 31, 2004 (in Japanese), “Fabrication of MilliWatt Modules”, N.B. Elsner.

References

1. Kushch, A.S., Bass, J.C., Ghamaty, S., Elsner, N.B., Bergstrand, R.A., Furrow, D. and Melvin, M., 2001, “Thermoelectric Development of Hi-Z Technology”, Proceedings, 7th DEER Conference, Office of Scientific and Technical Information, Portsmouth, VA.
2. “Proof-of-Principle Test for the Thermoelectric Generator for Diesel Engines”, 1991, Final Report, Hi-Z Technology, Inc., HZ 72691-1.
3. Elsner, N.B., Ghamaty, S., Normal, J.H., Farmer, J.C., Foreman, R.J., Summers, L.J., Olsen, M.L., Thompson, P.E. and Wang, K., 1994, “Thermoelectric Performance of $Si_{0.8}Ge_{0.2}$/Si Hetrostructures by MBE and Sputtering”, Proceedings, 13th International Conference on Thermoelectrics, AIP Press, Kansas City, MO.

IV.4 Thermoelectric Coating Process Scale-Up

Peter M. Martin (Primary Contact) and Larry C. Olsen
Pacific Northwest National Laboratory
902 Battelle Blvd.
MS K3-59
Richland, WA 99352

DOE Technology Development Manager: John Fairbanks

Objectives

- The overall objective of this project is to demonstrate a scaled-up batch process for the deposition of thin film thermoelectric (TE) coatings, namely, $Si/Si_{0.8}Ge_{0.2}$ and B_4C/B_9C multilayer material systems.
- Sputter deposit 1000-layer TE coatings onto 100 mm-diameter, 0.5 mm-thick silicon (Si) substrates.
- Determine an approach for depositing 1000-layer TE coatings onto 100 mm-diameter, 5 μm-thick Si substrates.
- Verify the thermoelectric properties of the deposited multilayer structures.
- Transfer the scaled-up process to Hi-Z Technology, Inc. for commercial production.

Approach

- Design and fabricate equipment required for depositing multilayer TE coatings.
- Define deposition process for thin film Si/Si_xGe_{1-x} and B_4C/B_9C TE multilayer coatings.
- Deposit test multilayer Si/Si_xGe_{1-x} and B_4C/B_9C TE coatings.
- Deposit p-type Si and $Si_{0.8}Ge_{0.2}$ TE coatings.
- Deposit 1000-layer n-type and p-type TE coatings on 6 inch 0.5 mm Si substrate.
- Deposit 1000-layer n-type and p-type TE coatings on 6 inch 10 μm Si substrate.
- Measure and verify all thermoelectric properties and performance.

Accomplishments

- Scaled up the deposition process for multilayer $Si/Si_{0.8}Ge_{0.2}$ and B_4C/B_9C TE structures to 0.5 m^2 substrate areas.
- Demonstrated prototype batch deposition of $Si/Si_{0.8}Ge_{0.2}$ and B_4C/B_9C TE structures.
- Demonstrated scaled-up $Si/Si_{0.8}Ge_{0.2}$ and B_4C/B_9C TE structures with TE properties good enough for use in a thermoelectric generator (TEG) module.
- Established measurements of TE properties of thin films at temperatures up to 800ºC.

Future Directions

- Develop $Si/Si_{0.8}Ge_{0.2}$ and B_4C/B_9C multilayer structures on non-crystalline substrates.
- Conduct TE performance measurements up to 800ºC.
- Develop methods to integrate $Si/Si_{0.8}Ge_{0.2}$ and B_4C/B_9C multilayer structures into TEG modules.
- Investigate new TE thin film materials.

Introduction

This project involves the development of methods to scale up production of multilayer thermoelectric coatings using sputtering processes. Molecular beam epitaxy (MBE) and magnetron sputtering processes are used to deposit $Si/Si_{0.8}Ge_{0.2}$ multilayer (quantum well) structures, and primarily magnetron sputtering is used to deposit B_4C/B_9C structures. Plasma-enhanced chemical vapor deposition is also used to deposit boron carbide thin films. Hi-Z Technology, Inc. now deposits these structures only on a small scale, with little evaluation of how deposition conditions affect the thermoelectric and electric properties. While the MBE process provides single crystalline structures (which may or may not be the most desirable), deposition rates are low and scale-up to large-area substrates is expensive and cumbersome.

Hi-Z develops and produces thermoelectric power-generating components. Their thermoelectric power modules are used for NASA's Mars mission, pellet stoves, self-powered appliances, space power generation, and diesel engines. The thermoelectric modules consist of multilayer $Si/Si_{0.8}Ge_{0.2}$ and B_4C/B_9C coatings on Si substrates. The ultimate power output of these modules, however, is limited by the current size of the module (1 cm^2). Power output can be increased significantly if the modules are stacked and increased in size. Pacific Northwest National Laboratory (PNNL) has the capabilities to scale up the Hi-Z deposition process and to deposit coatings on large areas and multiple substrates. Vacuum coating chambers are available at PNNL to coat substrates with diameters up to 2.5 m. This project has developed the process to deposit these multilayer thermoelectric coatings on Si substrates as large as 0.5 m^2 and has transferred this technology to Hi-Z.

Targeted coating designs are currently under development on a small scale at Hi-Z for use in their TEG devices that are attached to the exhausts of heavy-duty diesel vehicles. Use of PNNL's highly flexible coating facilities and knowledgeable staff has demonstrated the scale-up process. The ultimate goal of the project is to demonstrate production of 1000-or-more-layer coatings of $Si/Si_{0.8}Ge_{0.2}$ and B_4C/B_9C on batches of 100 mm-diameter Si substrates. Subsequent efforts will be aimed at extending the development of the process to include full-thickness coatings on 5 micrometer-thick Si and transfer of the technology to Hi-Z. Success of this project will allow commercial production of Hi-Z's multilayer thermoelectric coatings on the 100 mm-diameter or larger substrates.

Approach

This project is being carried out in PNNL's vapor-deposition coating facility. The overall approach is to develop and demonstrate the deposition process for multilayer thermoelectric films, scale up the process for prototype-scale deposition, verify thermoelectric properties of the films, fabricate thermoelectric films for devices testing, and transfer the scaled-up deposition technology to Hi-Z. Films will be deposited by the direct current and radio frequency magnetron sputtering processes. Multilayer coatings will be produced using an automated shuttering process. Important film properties such as conductivity (σ), Seebeck coefficient (S), power factor (σS^2T), thickness, mechanical stress and composition will be measured as part of the development effort.

Although the ultimate objective is to deposit multilayer film structures with each layer being on the order of 100 Å, initial process development will involve characterization of thicker layers. The project is structured into eight tasks. Tasks 1 through 4 involved development of preliminary coating parameters needed to produce individual layers having the required properties, and the production of multilayer coatings onto 0.5 mm-thick Si substrates. This includes n-type and p-type coatings. Phase II, undertaken in FY 2003 and FY 2004, involved development of methods required for production of full-thickness coatings on 100 mm-diameter by 5 µm-thick Si substrates. On completion of the development process, the technology will be transferred to Hi-Z.

Results

Single-layer Si and $Si_{0.8}Ge_{0.2}$ films and $Si/Si_{0.8}Ge_{0.2}$ multilayer structures were deposited by the PNNL scaled-up magnetron sputtering process onto Si substrates. Figure 1 shows the interior of the deposition chamber. The following chamber

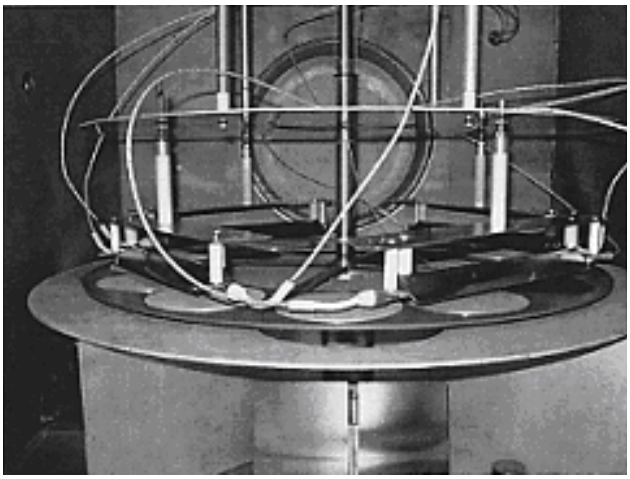

Figure 1. Scaled-Up Heater and Substrate Holder Assembly

modifications were made to scale up the deposition process:

- Four quartz heaters were placed above the substrate holder to achieve uniform heating over an area of 0.5 m^2.
- Shields were placed between the Si and $Si_{0.8}Ge_{0.2}$ or B_4C and B_9C cathodes to prevent cross talk.
- A precision stepper motor was attached to the substrate rotation assembly for precise thickness control.
- Both sputtering cathodes were in continuous operation.
- A third cathode was added for doping.

In this configuration, the substrate holder rotated continuously over the Si and $Si_{0.8}Ge_{0.2}$ sputtering targets with the rotation rate and deposition rate tuned for each target to obtain a layer thickness of 100 Å. Multilayer depositions were performed by moving the substrate sequentially from over the Si (or B_4C) target to over the $Si_{0.8}Ge_{0.2}$ (or B_9C) target. Batches of twelve 100 mm substrates, or areas of 0.5 m^2, could be covered. Before deposition, the substrate was heated to the required temperature by a resistive heater. The first layer deposited was Si, then a $Si_{0.8}Ge_{0.2}$ layer. Each layer was 100 Å thick. Thickness was determined simply by time of deposition. Structures with up to 3000 layers were deposited onto single-crystal Si substrates. B_4C/B_9C structures were heat-treated in vacuum at 1000ºC.

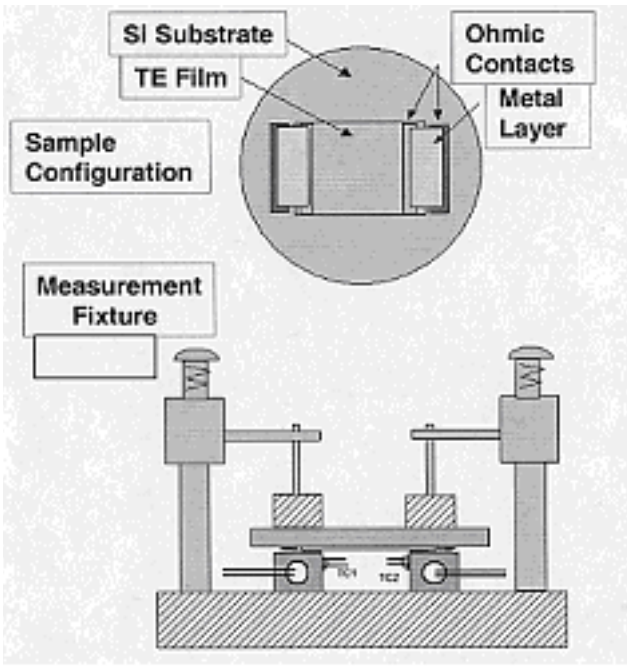

Figure 2. Diagram of Fixture Used to Make Thermoelectric Property Measurements

The electrical conductivity of the TE structures was measured by the four-point van der Pauw technique, and the Seebeck coefficient (thermopower) was measured by applying a temperature gradient across the sample and measuring the voltage generated. All measurements were done in-plane. The Seebeck coefficient and conductivity of the substrate were measured before and after deposition. The Seebeck coefficient and conductivity of the film were calculated using standard techniques. Figure 2 shows a diagram of the fixture used for TE measurements, and Figure 3 shows a fixture designed for high-temperature TE (up to 800ºC) measurements.

$Si/Si_{0.8}Ge_{0.2}$ films and multilayer structures with the highest electrical conductivity (σ), highest Seebeck coefficient and largest value of power factor (S^2T) were deposited at a substrate temperature of 400ºC. Single-layer B_4C and B_9C films had the highest electrical conductivity and Seebeck coefficient when deposited at 500ºC with Ge doping. B_4C/B_9C multilayer structures had high power factors near 0.06. Table 1 shows typical performance results for single and multilayer $Si/Si_{0.8}Ge_{0.2}$ structures on Si substrates. The values shown in Table 1 are comparable to or better than those

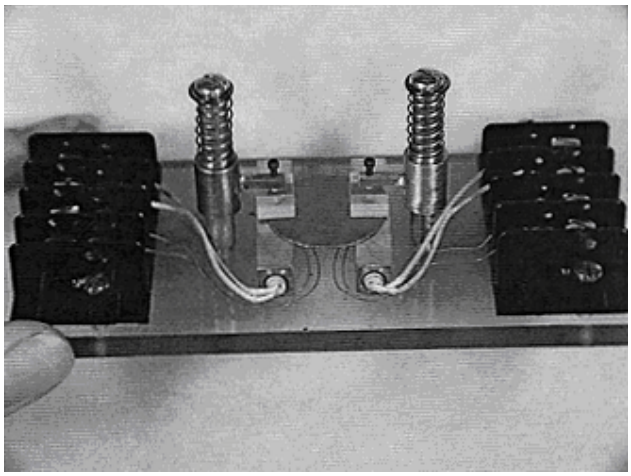

Figure 3. Fixture Used to Make High-Temperature Thermoelectric Property Measurements

Table 1. TE Properties of Thin Film Si/$Si_{0.8}Ge_{0.2}$ on Si (All films were doped with Ge)

Material	σ $(\Omega cm)^{-1}$	Seebeck Coefficient (μV/ºC)	Power Factor
n-Si	60	600	0.0065
n-$Si_{0.8}Ge_{0.2}$	35	800	0.0067
Si/ $Si_{0.8}Ge_{0.2}$ ML	300	750	0.051

previously reported for MBE-deposited and sputter-deposited multilayer structures [1,2,3,4]. We were able to deposit both n-type, and for the first time reported in the literature, p-type Si/$Si_{0.8}Ge_{0.2}$ multilayer structures. Table 2 summarizes typical performance results for single and multilayer B_4C/ B_9C structures on Si. In contrast to the literature, it was also possible to deposit n-type B_4C and B_9C films. Direct measurements, however, of ZT (thermoelectric figure of merit) are needed to unequivocally verify thermoelectric properties of the multilayer films and are in progress.

Tables 1 and 2 demonstrate two important results:

- The power factors of multilayers are much higher than for single layers (as predicted by Dresselhaus [5]).

Table 2. TE Properties of B_4C/B_9C Films on Si

Material	Heat treatment (ºC)	σ $(\Omega cm)^{-1}$	Seebeck Coefficient (μV/ºC)	Power Factor
B_9C	600	35	340	0.0012
B_9C	1000	1660	223	0.0025
B_4C/B_9C ML	600/1000	2560	201	0.031
B_4C/B_9C ML	600	4160	233	0.068

- Power factors near 0.05 can be realized on Si substrates. This would correspond to a ZT > 2 for thermal conductivity ~0.02 W/cmK.

Both tables demonstrate the effects of quantum confinement as predicted by Hicks and Dresselhaus [5]; i.e., the power factors of quantum well structures are significantly higher than those of single-layer films. Note that the power factor of single-layer B_4C and B_9C films are in the range of the Si/$Si_{0.8}Ge_{0.2}$ multilayer structures. Thus, with quantum confinement effects, B_4C/B_9C multilayer structures should have power factors significantly higher that those of the single-layer films.

Finally, 11 μm-thick B_4C/B_9C and Si/$Si_{0.8}Ge_{0.2}$ multilayer structures were deposited via prototype batch deposition onto 100 mm-diameter Si substrates and delivered to Hi-Z for use in TEG modules. These coatings contained over 1000 layers. Mechanical stress in the films was remarkably low, with virtually no observed substrate deformation.

Conclusions

- The deposition process for B_4C/B_9C and Si/$Si_{0.8}Ge_{0.2}$ multilayer thermoelectric films was successfully scaled up to prototype batch processing.
- Thermoelectric measurement capabilities up to 800ºC were established.
- Thermoelectric properties of B_4C/B_9C and Si/$Si_{0.8}Ge_{0.2}$ multilayer structures on Si are good enough for use in TEG modules.
- Batch production of B_4C/B_9C and Si/$Si_{0.8}Ge_{0.2}$ multilayer structures was demonstrated and materials delivered to Hi-Z Technology for use in TEG modules.

Patent Applications

1. Patent application: "Boron carbide films and quantum well structure with improved thermoelectric properties," P. M. Martin and L. C. Olsen.

FY 2004 Presentations

1. P. M. Martin and L. C. Olsen, "Recent Progress in Scale of Thermoelectric Quantum Well Films," High Efficiency Thermoelectrics Workshop, February 17-20, San Diego, CA.
2. L. C. Olsen and P. M .Martin, "Measurement of Thermoelectric Properties of Thin Films," High Efficiency Thermoelectrics Workshop, February 17-20, San Diego, CA.
3. P. M. Martin and L. C. Olsen, "Nanostructured Multilayer Films for Advanced Detector and Thermoelectric Applications," 2004 AIMCAL Conference, October 24-27, 2004, Charleston, SC. Invited.
4. P. M. Martin, L. C. Olsen and S. Baskaran, "Multilayer Thin Film Thermoelectric Materials for Vehicle Applications," 2004 DEER Conference, August 29-31, 2004, San Diego, CA.
5. P. M. Martin, "Advanced Thin Film Coatings at PNNL," PPG Research Center, July 12, 2004, Pittsburgh, PA. Invited.

FY 2004 Publications

1. P. M. Martin and L. C. Olsen, Nanostructured multilayer B_4C/B_9C and $Si/Si_{0.8}Ge_{0.2}$ films for advanced detector and thermoelectric applications, Proceedings of 2004 AIMCAL Conference. Invited.

References

1. T. Koga, A. Sun, S. B. Cronin and M. S. Dresselhaus, Applied Physics Letters, 73(20) (1998) 2950-2952.
2. S. Ghamaty and N. Elsner, Proceedings of the International Conference on Thermoelectrics (1999), 18th 485-488.
3. T. J. Hendricks, Proceedings of the Intersociety Energy Conversion Engineering Conference (1988), 23rd (Vol. 1), 339-45.
4. J. Farmer, T. Barbee, Jr., G. Chapline, Jr., M. Olsen, R. Foreman, L. Summers, M. Dresselhaus and L. Hicks, Lawrence Livermore Laboratory Report UCRL-ID-119652, January 20, 1995.
5. L. D. Hicks and M. S. Dresselhaus, Phys. Rev. B47 19 (1993) 12 727-731.

IV.5 High-Efficiency Thermoelectrics New Projects

Thermoelectrics is a promising technology to extract energy from the waste heat of advanced combustion engines. The electricity produced by thermoelectrics enables additional savings in engine parasitic losses through electric drive of components such as water and oil pumps that traditionally have been mechanically driven, using energy regardless of need. In March 2004, DOE issued a solicitation titled "Waste Heat Recovery and Utilization Research and Development for Passenger Vehicle and Light/Heavy Duty Truck Application". Based on this solicitation, DOE chose four new projects in thermoelectrics. The overall objective of each of these projects is to demonstrate a cost-effective way to improve fuel economy by 10% over the current level without increased emissions. Following are brief descriptions of what these projects intend to accomplish over their durations.

Prime Contractor: General Motors Corporation

Subcontractors:
General Electric Company
Research Triangle Institute
University of Michigan
University of South Florida
MIT - Lincoln Laboratory
Oak Ridge National Laboratory

Approach

The goal of this project is to demonstrate a 10% fuel economy improvement over the current level without increased emissions in a cost-effective way. This will be done by first verifying the performance of currently known bulk and thin-film materials with ZT>1. The materials will include those suitable for application to both exhaust and coolant waste heat, but will not necessarily be limited to these sources. Based on the results of materials performance validation, initial selection of the best materials for different waste heat temperatures will be made. Multiple materials may be needed to best match the conversion needs to the temperature of the waste heat energy sources. Conversion devices using these materials, the conversion subsystems, and an overall vehicle system will be modeled to enable initial calculation of energy recovery and conversion efficiency. The project will also determine packaging specifications for exhaust and radiator devices; develop functional and environmental standards; and determine cost targets for components, subsystems, and vehicle integration.

Prime Contractor: United Technologies Research Center

Subcontractors:
Pratt & Whitney
Hi-Z Technology
Pacific Northwest National Laboratory
Caterpillar, Inc.

Approach

The objective of this project is to develop thermoelectric technology that will improve diesel engine efficiency for heavy-duty on-highway trucks by 10%, thereby reducing fuel consumption by 9.3%. To meet this objective, the following methods will be employed: (a) development of cost-effective fabrication routes for the production of quantum well thermoelectric materials, enabling the commercialization of high-efficiency

thermoelectric modules; (b) demonstration of this technology in the form of an integrated ~500 Watt prototype thermoelectric generator on a Class 8 heavy-duty truck; and (c) delivery of a viable commercialization path for this technology to the automotive industry.

Prime Contractor: BSST LLC

Subcontractors:
Visteon Corporation
BMW NA
Teledyne Electronics Systems

Approach

The objective of this project is to improve the efficiency of internal combustion engines through technological advances in efficiency and cost-effectiveness of thermoelectric-based vehicle waste heat recovery systems. The tasks will include thermoelectric material fabrication (2 activities), subsystem design optimization (2 activities), and systems integration (4 activities). A complete system will be built and installed on a vehicle for testing.

Prime Contractor: Michigan State University

Subcontractors:
NASA Jet Propulsion Laboratory
Cummins Engine Company
Iowa State University
Marlow Industries
Tellurex Corporation

Approach

The objective of this project to construct a thermoelectric generator (TEG) couple of 20% efficiency, using newly developed Michigan State University (MSU) materials and demonstrated NASA Jet Propulsion Laboratory (JPL) thermoelectric technology. Cummins Engine Company will provide the major guidance in terms of the likely benefits from the application of TEGs and the tradeoffs of efficiency, cost and emissions requirements. Modeling of the system design parameters will be conducted by MSU, Iowa State University, and Cummins. Marlow Industries and Tellurex Corporation (leading U.S. manufacturers of thermoelectric devices) will provide guidance in evaluation of the thermoelectric materials and manufacturing methods.

V Off-Highway Vehicle Emission Control R&D

V.1 Off-Highway Heavy Vehicle Diesel Efficiency Improvement and Emissions Reduction

Jennifer Rumsey (Primary Contact), Wayne Eckerle, Donald Stanton, Lisa Farrell
Cummins Inc.
1900 McKinley Avenue
Columbus, IN 47201

DOE Technology Development Manager: John Fairbanks

Objectives

- Develop analytical tools to enable optimization of the combustion process for both emissions and low fuel consumption.
- Utilize combustion modeling capability to develop in-cylinder solutions to meet the Tier 3 emissions standards while maintaining fuel consumption levels.
- Verify that the Tier 3 engines meet emissions and fuel economy targets through single- and multi-cylinder engine testing.
- Investigate technology options to meet the Tier 4 emissions levels while maintaining fuel consumption levels.

Approach

- Develop analytical modeling capability to facilitate the design and optimization of in-cylinder combustion recipes to meet the Tier 3 emissions levels while maintaining fuel consumption levels.
- Utilize modeling tools to design combustion recipes on multiple engine platforms that meet the Tier 3 emissions targets while minimizing the impact on fuel consumption.
- Demonstrate the combustion recipes in single- or multi-cylinder engine tests and optimize the emissions and performance of the engines.

Accomplishments

- Combustion system design for Tier 3 completed on three engine platforms with fuel consumption close to Tier 2 values.
- Experimental engine validation and optimization completed for Tier 3 combustion system design.
- Improved combustion computational fluid dynamics (CFD) sub-models incorporated and validated.
- Calibration improvement model developed for transient calibrations.
- A new and improved CFD code is under development that will give improved combustion modeling capability for more complex combustion systems.
- Work has been initiated to develop engines to meet the Tier 4 emissions standards. This work has included an investigation into potential technologies to meet these standards as well as work to understand the customers' requirements.

Future Directions

- Complete the validation and optimization of the Tier 3 combustion recipes.
- Continue with combustion tool development.
- Continue with calibration tool development.

- Develop technologies including engine and aftertreatment solutions to meet the Tier 4 emissions levels at Tier 3 fuel consumption levels.
- Analyze the potential Tier 4 technologies' capability to meet the technical requirements of the project.

Introduction

Cummins is a world leader in the development and production of diesel engines for both on-highway and off-highway markets and is committed to the efforts to reduce the emissions of these products. The power range for this project includes 80-750 HP to achieve the Environmental Protection Agency's Tier 3 and 4 emissions levels shown in Figure 1. Cummins' anticipated product offerings regarding this topic include the following: B3.9, QSB6.7, QSC8.3, QSL9, QSM11, QSX15, and QSK19.

Off-highway emissions standards will result in reduced NO_x emissions for Tier 3 off-highway engines and an additional NO_x reduction as well as a reduction in PM for Tier 4 off-highway engines. While these emissions standards lag the on-highway standards, the unique requirements of the off-highway markets make it necessary to consider unique solutions that meet the requirements of these products.

Approach

Cummins' approach to developing next-generation engines to meet the reduced emissions requirements utilizes a customer-led focus as well as an emphasis on analysis-led design. Before the design of the new systems begins, work is completed to clearly understand the customers' requirements and how these impact the technical requirements of the products. An analysis of various technologies and their capabilities to meet these requirements is completed. An analysis-led approach is then utilized to design these future systems, followed by validation through single- and multi-cylinder engine testing and optimization. For Tier 3, an in-cylinder emissions solution was utilized to meet the emissions requirements with minimal impact on fuel consumption, performance, packaging, and cost.

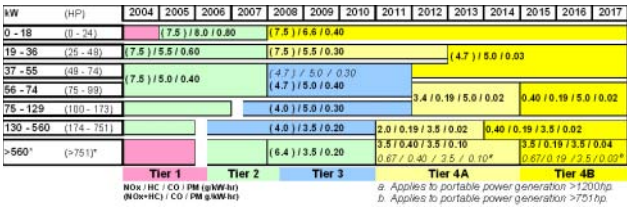

Figure 1. Summary of Tier 3 and 4 Emissions Standards

Results

In-cylinder solutions to achieve the Tier 3 emissions levels have been developed on the QSB6.7, QSC8.3, QSL8.9, QSM11, QSX15, and QSK19 with a minimal impact on fuel consumption. Fuel consumption varies from 2% better to 9 % worse compared to Tier 2, depending on the engine and application. The combustion recipe was first developed utilizing Cummins' combustion CFD modeling tool. This modeling tool has been improved by including new NO_x transport models, an improved spray model, and the ability to model multiple injection events. The combustion recipe was then validated and optimized using experimental single- or multi-cylinder engine testing.

A number of techniques have been employed to reduce the emissions levels while maintaining fuel consumption levels. A transient calibration technique (multivariable local regression, or MLR) has been developed which allows the calibration of the engine to be completed in one-half to one-third of the time needed for the conventional technique and results in a more optimized calibration. This technique improves the ability to prevent emissions overshoots and reduce fuel consumption during transient operation. Figure 2 shows a comparison of MLR's predicted NO_x and particulate emissions and actual emissions recorded over the first 900 seconds of the Federal Test Procedure (FTP) transient cycle.

Additional work is underway to further optimize the calibration of the Tier 3 engines and to complete mechanical verification of these engines.

As the Tier 3 work wraps up, the focus has shifted to meeting the Tier 4 emissions standards while continuing to maintain fuel economy and meet customer requirements. The Technology Development for Six Sigma approach will be utilized in developing technology for Tier 4. This consists of

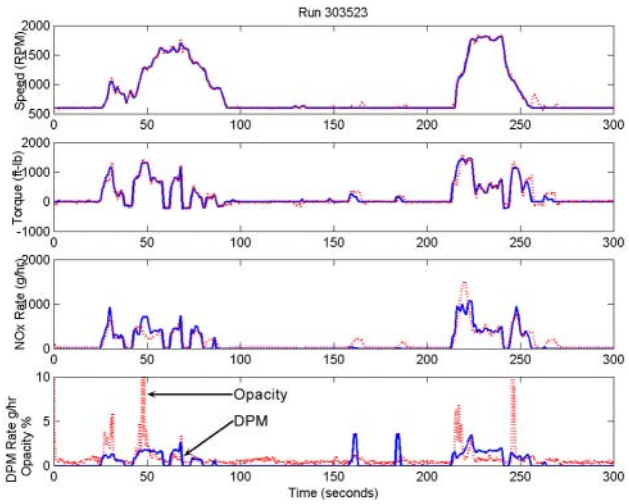

Figure 2. MLR Predicted Emissions for ISX '04 FTP Cycle Compared to Experimental Data

four phases of development as shown in Figure 3: Invent and Innovate, Develop, Optimize, and Certify. This process introduces a rigorous approach to technology development which emphasizes the relationship between the customer requirements and the technical solution and the development of a robust and tunable technology.

Currently, further improvements are being made to the combustion modeling tools to enable the design of these combustion systems. Work has been initiated to understand the customer requirements for Tier 4 products and to evaluate potential technologies, including in-cylinder and aftertreatment approaches, to meet these emissions standards.

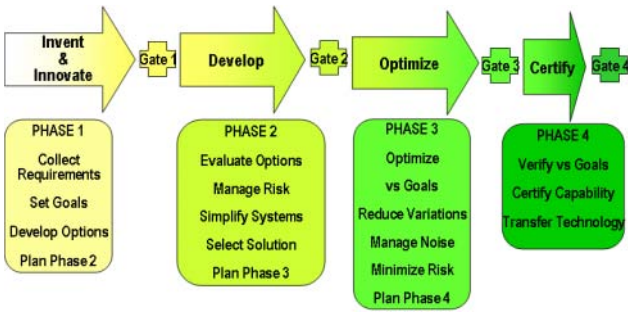

Figure 3. Tier 4 Technology Development Cycle

Conclusions

The design and optimization of Tier 3 compliant off-highway engines is nearing completion. Advances in the combustion CFD tool's capability to model and predict combustion recipe performance was a key enabler in the design of these solutions. An in-cylinder solution which does not require the use of cooled exhaust gas recirculation has been successfully employed across Cummins' off-highway engine product line (QSB6.7, QSC8.3, QSL8.9, QSM11, QSX15, and QSK19). A slight fuel consumption penalty has resulted for some engine platforms.

Work is now underway to develop the customer and technical requirements and understand the technology capabilities as we begin to investigate solutions to meet the Tier 4 emissions standards.

V.2 Exhaust Aftertreatment and Low-Pressure Loop EGR Applied to an Off-Highway Engine

Kirby J. Baumgard (Primary Contact), John H. Johnson (MTU), Antonio Triana (MTU)
John Deere Product Engineering Center
P.O. Box 8000
Waterloo, IA 50704

DOE Technology Development Manager: John Fairbanks

Subcontractors:
Michigan Technological University (MTU), Houghton, MI

Objectives

- Demonstrate that 4 g/kWh NO_x + HC (hydrocarbon) and 0.02 g/kWh particulate matter (PM) emission levels can be achieved over the ISO 8178 test cycle using cooled low-pressure loop exhaust gas recirculation (EGR) and a continuously regenerating diesel particle filter (CR-DPF). This will require optimizing the EGR strategy for NO_x reduction and also optimizing the engine for best brake specific fuel consumption (BSFC).
- Collect particle size distribution data and loading curve data for the CR-DPF that can then be used to verify the Michigan Technological University (MTU) aftertreatment model.
- Develop an aftertreatment model incorporating exhaust flow, filtration, heat transfer, reaction kinetics, and regeneration characteristics, including an NO_2-assisted oxidation sub-model and an "in the wall" sub-model to predict the regeneration behavior of a CR-DPF.

Approach

- Collect gaseous and particulate data over the ISO 8178 steady-state test cycle with and without exhaust aftertreatment.
- Measure the exhaust particle size distributions with and without the EGR/DPF emission control system over several engine-operating conditions.
- Determine DPF loading curves for various conditions.
- Modify the MTU aftertreatment model to include the NO-to-NO_2 conversion across the diesel oxidation catalyst and also the NO_2-assisted regeneration across the DPF.
- Use the engine and emission data collected to verify the MTU aftertreatment model.

Accomplishments

- The low-pressure loop EGR system has been optimized, and the goal of less than 4 g/kWh NO_x and less than 0.02 g/kWh PM over the ISO 8178 eight-mode test was achieved.
- All the engine emission data has been collected.
- The MTU aftertreatment model has been completed and calibrated with the collected data. The model determines the NO-to-NO_2 conversion across the diesel oxidation catalyst and predicts the NO_2-assisted and thermal regeneration across the CR-DPF as well as the pressure drop across the aftertreatment system.

Future Directions

- The plan is to switch to a 6.8-liter, more advanced diesel engine and reduce the NO_x from 4 to 2 g/kWh to meet the interim Tier 4 (2011) off-highway emission standards. The exhaust aftertreatment will be upgraded to the latest technology for better performance.
- MTU will add new subroutines to their computer code to model the new aftertreatment technology.

Introduction

This project evaluates the feasibility of using a low-pressure loop EGR system in combination with a high-efficiency CR-DPF to reduce both NO_x and PM. By removing the EGR downstream of the DPF, it can be routed to the upstream side of the turbocharger, and because the exhaust is free of particles, there is no abrasive wear on the turbo compressor wheel or fouling of the engine's intercooler. With this emission control strategy, the overall engine efficiency is greater than if a high-pressure loop EGR system was incorporated. A study by Moser et.al., 2001, indicated that the low-pressure loop EGR system with a DPF resulted in a BSFC that was 3.5% percent better than that of a high-pressure loop system with a DPF.

The major driving force for the research is to meet the future off-road diesel emission standards. The Off-Road Tier 3 standards take effect in 2006, and the Tier 4 standards begin in 2011. The technology gained from this project will contribute to meeting both the Tier 3 and Tier 4 standards with improved fuel economy.

Approach

A John Deere 6081H 175-kW engine has been used for this research. The engine's displacement is 8.1 liters and is turbocharged and intercooled. It incorporates a high-pressure common rail fuel injection system and is fully electronic. A CR-DPF was placed downstream of the turbocharger, and downstream of the CR-DPF a portion of the exhaust gas is routed back to the intake system. A cooler is incorporated to cool the EGR, which maximizes reduction of NO_x.

The test project consisted of obtaining baseline data with no aftertreatment or EGR over the ISO 8178 test cycle. An EGR strategy was determined, and additional tests were conducted with EGR and the CR-DPF. Several additional operating conditions were identified that were used for loading the DPF without regenerating. These conditions were necessary so that when the DPF was installed, the steady-state loading curves could be obtained. The data was used to validate the MTU model.

Results

The initial data was collected over the ISO 8178 eight-mode test cycle. Table 1 compares the results between the baseline data and the low-pressure loop EGR with the CR-DPF. The low-pressure loop EGR system reduced the NO_x emissions by an average of 28%. The CR-DPF reduced the PM and HC emissions by over 94%. The NO_x plus HC standard for Tier 3 is 4.0 g/kWh for this power engine, and the values obtained provide an acceptable margin for meeting the standards. The data also indicates that brake-specific fuel consumption (BSFC) improved slightly over the baseline data.

Table 1. Summary of the ISO 8178 Data

Data in g/kWh	NO_x	HC	NO_x + HC	PM	BSFC at FLRS[1]
Baseline, no EGR	5.22	.51	5.73	.132	211.9
With EGR/ CR-DPF	3.74	.03	3.77	.008	208.9

[1]Full Load Rated Speed

The DPF loading curve data was collected as shown in Figure 1. First, the data was collected with only the DPF portion of the exhaust aftertreatment. During this loading, the diesel oxidation catalyst was not installed and, therefore, there was no NO_2-assisted regeneration. This is evident because the pressure drop curves continue to increase as a function of time (see DPF 100%, DPF 75%, DPF 50% and DPF 25% curves). When the diesel oxidation catalyst was installed upstream of the DPF,

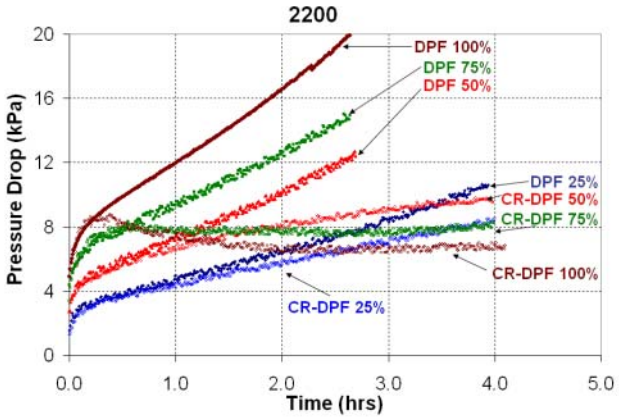

Figure 1. Pressure Drop Data Collected Over Time at 2,200 RPM and Various Percent Engine Loads for Both the DPF (diesel particle filter) and the CR-DPF (continuously regenerating diesel particle filter)

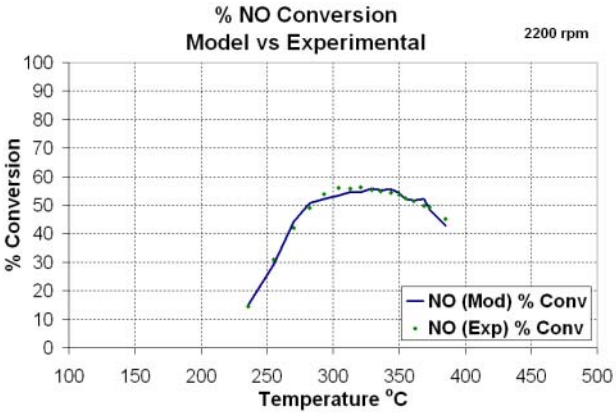

Figure 2. Oxides of Nitrogen Percent Conversion at 2,200 RPM, Model Versus Experimental

the pressure drop initially increased but then decreased and leveled off for the 100% and 75% load CR-DPF conditions. This indicates that the amount of soot being deposited within the DPF is equal to the amount being burned. For the CR-DPF 25% and 50% load conditions, the pressure drop continues to slowly build but at a much slower rate than with the DPF only. At these lower exhaust temperatures, there is NO_2-assisted regeneration occurring, but the amount of soot being deposited is greater than the amount being consumed. The amount of soot regenerated during these tests was determined by weighing the DPF before and after each loading test. By comparing the amount of mass collected within the DPF to the amount that entered, one can determine the amount that was regenerated. This information was used in the MTU model to verify the NO_2-assisted regeneration model.

The amount of NO_2-assisted regeneration is naturally dependent on the amount of NO_2 present. Therefore, it was necessary to determine the conversion rate of NO to NO_2 across the diesel oxidation catalyst. This data was obtained by operating the engine at several speeds and various loads to vary the exhaust temperatures. The data for 2200 rpm is shown in Figure 2 along with the MTU model results. The model results agree well with the experimental results. Similar results were obtained at 1400 rpm. Antonio (et.al.) reported these results in an earlier SAE publication.

In order to more accurately predict the pressure drop across the DPF, it is necessary to know the size distribution of the particles entering the DPF. Figure 3 shows the upstream and downstream distributions at 2200 rpm and 100% load. The solid line is the MTU model results and the open symbols are the experimental data. Similar results were obtained at 1400 rpm.

Figure 4 shows the modeled pressure drop results at 1400 rpm and 50% load. Again, the open symbols are the experimental results and the solid lines are the modeled results. The difference between the DPF and the CR-DPF pressure drop results is due to the NO_2-assisted regeneration. The slopes on the CR-DPF curves are still positive, indicating that there is still some soot being deposited. This is due to the fact that the NO_2-to-PM ratio is only 2.7:1. Theoretically, a ratio of 8:1 is needed to have sufficient NO_2 to react with all the soot.

The 8.1-liter engine was not designed for low-pressure loop EGR, and when the EGR was added, the NO_x emissions were reduced but the PM emissions increased. This corresponds to the well-known NO_x-to-PM relationship in which if the NO_x is reduced, the PM emissions increase. In order for this technology to be successful on this engine family, the engine-out PM emissions must be decreased. This could be done with an improved fuel injection system, optimized combustion system and a rematch on the turbo charger.

The next task of the project is to design a low-pressure loop EGR system to meet the interim Tier 4

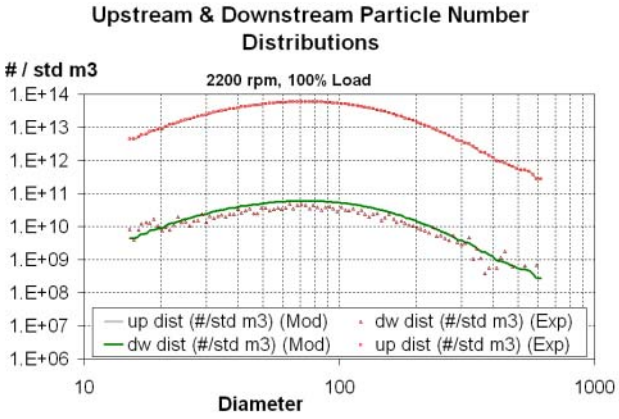

Figure 3. Particle Size Distributions Upstream and Downstream of the DPF at 100% Load and 2,200 RPM

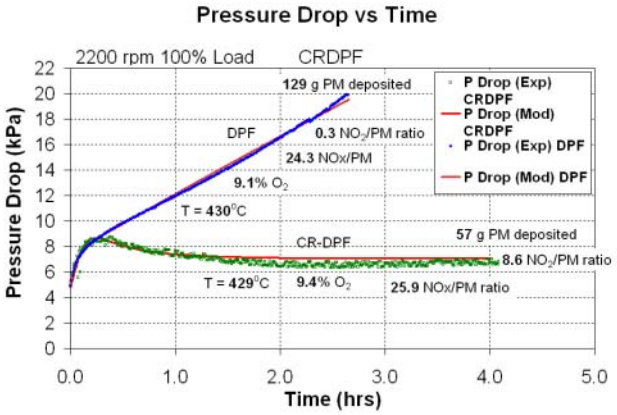

Figure 4. MTU Modeled Pressure Drop for Both the DPF and CR-DPF Conditions at 1,400 RPM and 50% Load

off-highway standards. This will require larger quantities of EGR and will require a more advanced engine. The engine will be 6.8 liters with a more advanced high-pressure common rail fuel system and a better-matched turbocharger. The exhaust aftertreatment will also be changed to the latest technology that incorporates a diesel oxidation catalyst and a catalyzed DPF. By adding catalytic material to both the diesel oxidation catalyst and the DPF, the theory is that more NO_2 will be available to react with the collected soot.

Conclusions

- The low-pressure loop EGR and CR-DPF system reduced NO_x emissions 28%, HC emissions 94% and PM emissions by 94%.
- The MTU model was able to incorporate the thermal and NO_2-assisted regeneration for the CR-DPF technology.
- The MTU model also properly predicted the pressure drop across the CR-DPF technology.

Presentations

1. Simulation of a Coupled Diesel Oxidation Catalyst and a Diesel Particulate Filter Model. Antonio Triana. Michigan Tech University. Presented at the June 16th, 2004 CLEERS Workshop in Detroit, Michigan.

References

1. Moser F., Sams T., Cartellieri W. Impact of Future Exhaust Gas Emission Legislation on the Heavy Duty Truck Engine. SAE 2001-01-0186.
2. Antonio P., Triana A.P., Johnson J.H., Yang S.L., Baumgard K.J. An Experimental and Numerical Study of the Performance Characteristics of the Diesel Oxidation Catalyst in a Continuously Regenerating Particulate Filter. SAE 2003-01-3176.

V.3 Advanced Fuel-Injection System Development to Meet EPA Emissions Standards for Locomotive Diesel Engines

Ramesh Poola
General Motors Corporation
Electro-Motive Division
9301 W. 55th Street
LaGrange, IL 60525

DOE Technology Development Manager: John Fairbanks

Subcontractors:
Argonne National Laboratory, Argonne, IL
Wayne State University, Detroit, MI

Major Technical Objectives of Phase I of the Project

- Demonstrate, via emissions modeling and engine testing, Tier 2 emissions-compliance potential utilizing an advanced fuel-injection system.
- Design and build a prototype advanced fuel-injection system suitable for a single-cylinder locomotive diesel engine.
- Conduct demonstration tests on a single-cylinder locomotive diesel engine to validate the new fuel-injection system design and injection strategies along with re-optimized engine hardware and operating conditions.

Approach

- Set up appropriate analytical (engine and combustion) models and conduct parametric studies to analyze the effects of various injection strategies.
- Develop conceptual designs of the injection system, system layout, and the electronic control strategy.
- Choose and build designs based on analytical predictions and structural and hydraulic analyses of selected hardware components.
- Test the new injection system along with various hardware engine upgrades in a single-cylinder locomotive diesel engine and obtain performance and emissions characteristics.
- Study fuel spray behavior and cavitation phenomena using appropriate analytical tools and optical methods.

Accomplishments

- Developed design concepts for key hardware components and system layout of the new fuel-injection system.
- Built prototype injectors and tested them in the hydraulic bench. The designs were iteratively improved based on the testing and operational observations.
- The final versions of the prototype injector and high-pressure pump (electric-motor driven) that were developed in this project were integrated with the single-cylinder test facility, and extensive engine testing was conducted. Performance and emissions data were gathered guided by the computational fluid dynamics (CFD) modeling results.

- Engine test results show that the new fuel-injection system has the potential to meet Tier 2 emissions goals with favorable NO_x-BSFC-PM (oxides of nitrogen – brake specific fuel consumption – particulate matter) tradeoff characteristics.

Future Directions

We plan to complete the remaining single-cylinder engine tests and spray imaging experiments at Argonne National Laboratory, and CFD studies on cavitation at Wayne State University during the first quarter of FY 2005. We plan to prepare a final report from our Phase I studies and submit to DOE during the second quarter of FY 2005. Further, the continuation of this collaborative work (Phase II, demonstration of the technology and hardware on a multi-cylinder locomotive diesel engine) will be explored in discussions with DOE.

Introduction

As a result of the railroad and locomotive technology roadmap workshop, a cooperative agreement was reached between the U.S. Department of Energy and the Electro-Motive Division (EMD) of General Motors Corporation in October 2002. The first phase of this cooperative R&D effort involves developing advanced fuel-injection technology and demonstrating its potential benefits towards meeting fuel savings goals and the EPA Tier 2 emissions standards using a single-cylinder research engine platform. The details of technical tasks involving engine modeling and parametric studies were reported in the FY 2003 annual report. The technical progress that we have made during FY 2004 (October 1, 2003 through September 31, 2004) is reported here.

Approach

The major activities pursued in FY 2004 include a series of single-cylinder engine tests with the new prototype fuel-injection system. Efforts were also directed at examining the fuel spray characteristics on the bench using a high-speed imaging technique. Our defined tasks to pursue in FY 2004 are as follows: (1) Task # 3 – bench-test component evaluations as well as an investigation of fuel spray characteristics using established optical diagnostic techniques, and (2) Task # 4 – implementation and testing of the prototype injection system in a single-cylinder engine. Analytical results that were previously obtained in FY 2003 were used to guide the engine testing. EMD's research facilities at Argonne National Laboratory were utilized in conducting single-cylinder engine testing and fuel spray imaging work. These efforts were carried out in close cooperation with our subcontractors, Argonne National Laboratory and Wayne State University. Our fuel-injection equipment supplier, Robert Bosch AG, supported the development of prototype injection hardware, testing on the hydraulic test bench, and development of control system software.

Features of Advanced Fuel-Injection System Applied for Locomotive Diesel Engines

Our advanced fuel-injection system, also known as Modular Common Rail System (MCRS), is a new and improved version of conventional Common Rail System (CRS). A system-level comparison between conventional CRS and MCRS is presented in Table 1;

Table 1. A System-Level Comparison between Common Rail Injection System (CRS) and Modular Common Rail Injection System (MCRS)

parameter/ system	CRS	MCRS
max. press. peaks	>+20 MPa	>+20 MPa
multiple injection	- limited (influence of pipe inner diameter/length)	- pilot/main/post injection lag > 0,4 ms (control valve/ nozzle dynamic)
retrofit	- problem area: rail(s) integration - system tests for different engine configuration (L6 - V18)	- simple retrofit - only components tests (no influence of engine configuration)
safety	- shielded rail(s)/ pipes	- shielded pipes (smaller pipe size needle than for CRS)
cost	- base	- ~ - 30 %

Table 2. A System-Level Comparison between Common Rail Injection System and Traditional Injection Systems, UIS/UPS

parameter	UIS/UPS	CRS
max. inj. pressure	< 200 MPa(cam size and driven limits)	< 180 MPa
max. press. peaks	< + 10 MPa	> 20 MPa
inj. press. control	- no	- yes
injection rate shaping	- triangle type shape - potential for press. modulated shaping w/ 2 stage closing of solenoid valve	- square type shape - limited potential by needle lift control
retrofit potential	- limited by original design	- limited by original design but w/ higher potential than cam driven systems
cost	- base	- higher espec with "double wall" rail and pipes

the advantages of MCRS over CRS are evident. A system-level comparison between existing cam-driven injection systems and CRS injection system is presented in Table 2 to illustrate the progression of injection system technology in locomotive diesel engines. The cam-driven injection systems include unit injector system (UIS) and unit pump system (UPS), which are currently being used in our 2-cycle and 4-cycle locomotive diesel engines, respectively. The conventional CRS system (with a rail-pipe injector) commonly used in passenger-car diesel engines has limited potential for use in large diesel engines because of high-pressure pulsations in the pipes and injectors. The higher costs of high-pressure piping further limit its use in large diesel engines. On the other hand, MCRS eliminates some of the technical shortcomings of conventional CRS. More importantly, MCRS minimizes the high-pressure pulsations that are generated on the pump

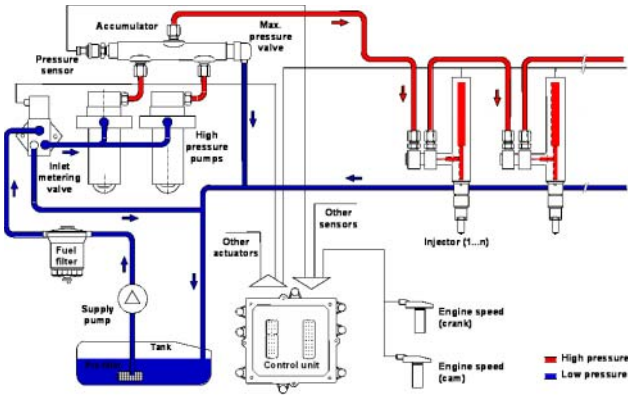

Figure 1. A Schematic Layout of Modular Common Rail Injection System for Large-Bore Medium-Speed Diesel Engines

side with two-stage damping volumes, a high-pressure accumulator (1) on the top of high-pressure pump and (2) integrated within the injector. Figure 1 shows the schematic layout of MCRS for large medium-speed diesel engines. The rail volume is split up and integrated both in the first-stage accumulator and second-stage accumulator within the injectors. This reduction of the distance between fuel accumulator and nozzle reduces the pressure pulsation in the injector significantly. High-pressure hard pipes with inner diameters between 3 and 4.5 mm connect the high-pressure pump, accumulator and injectors. An inlet orifice in the injector prevents any remaining pulsation from propagating through the fuel system. Each injector has a damping volume about 50 to 70 times larger than the maximum injection quantity. The minimized pressure pulsations in the connection pipe from the pump to the injectors permit the integration of the pressure relief valve and the pressure sensor in the accumulator of the high-pressure pump.

Figure 2 shows the cross-section of the MCRS injector design. The integration of control valves, which are currently being developed for future truck diesel engines, will allow the design and development of injectors with an integrated fuel accumulator. There are several advantages of having the control valve close to the needle. For example, it provides optimized packaging and fast response time, and it is pressure-balanced using hydraulic forces (rather than mechanical spring forces). It is fitted with close proximity to the nozzle to minimize

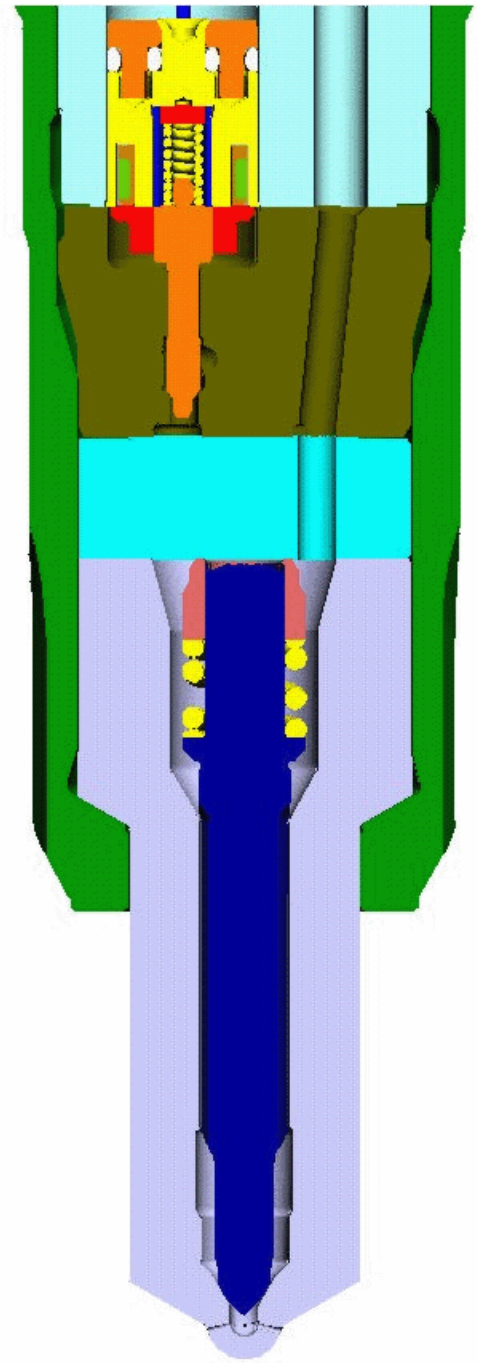

Figure 2. Cross-Section of MCRS Injector Design

the influence of hydraulic and pressure pulsations on the switching behavior of the nozzle. The opposite side of the needle seat is designed as a pressure-controlled chamber with inlet and outlet orifices integrated in the plate between solenoid valve and nozzle. The solenoid valve controls opening and closing of the needle and thus each injection event. The solenoid valve technology is currently being applied for three different sizes, from high-speed to medium-speed diesel engines with fuel injection quantities ranging from 500 to 3,000 mm^3 per stroke. The wider usage of this solenoid technology in different engine platforms helps to bring the cost down and improve component reliability.

Results

Component Evaluations – Needle Movement and Pressure Pulsations

The needle movement, nozzle and sac-hole injection pressure/injection rate characteristics were studied using a calibrated 1-D hydraulic model (a modified version of AMESim software). A comparison of injection rates and pressure pulsations between CRS and MCRS with single (main only) injection is shown in Figures 3 and 4, respectively. Similarly, the injection rates and pressure pulsation between CRS and MCRS were studied using a split injection (main and post injection). These results are presented in Figures 5 and 6. The advantages of MCRS, in particular pressure pulsations in the injector and injection rate, are quite evident from these results.

The shorter distance from the injector and integrated accumulator to the nozzle of the MCRS influences the injection rate in the first phase of the injection. The layout of inlet and outlet orifices allows an adaptation of the injection rate for reduced rate of cylinder pressure rise during the premixed phase of the combustion cycle. The MCRS also allows multiple injections for further reduced cylinder pressure gradients. In the case of CRS, the pipe inner diameter and pipe length strongly influence the injection rate and pressure pulsations. On the other hand, with MCRS the decrease in fuel pressure at the end of the injection depends primarily on the injector volume and the inlet orifice. Hydraulic analysis followed by bench tests (verification tests) show the excellent dynamic behavior of the MCRS for both single and multiple injection events, which results in great potential for engine optimizations with respect to performance, noise and emissions control.

Engine Tests

The prototype MCRS has been adopted for testing in the singe-cylinder locomotive diesel

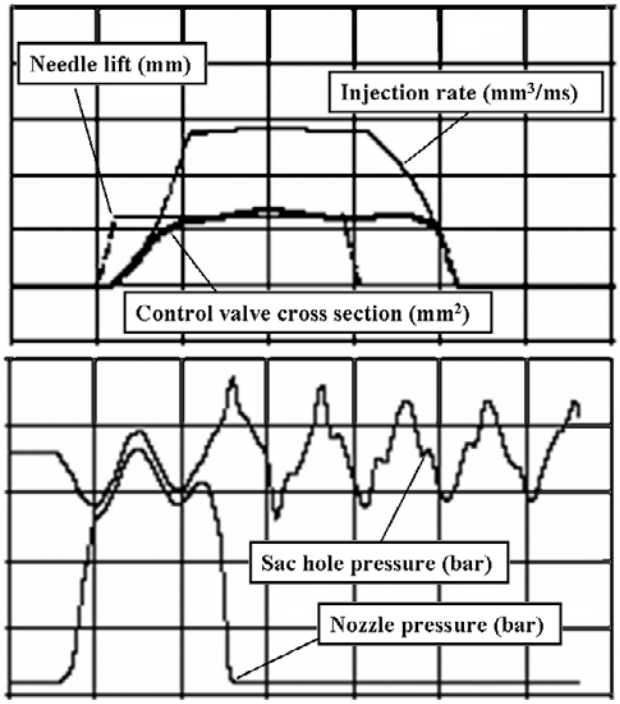

Figure 3. Needle and Injection Behavior Using CRS Single Injection

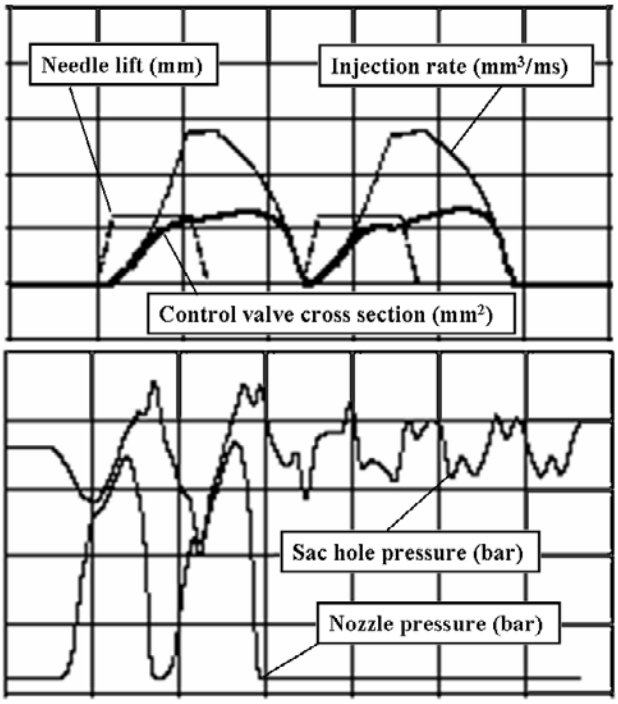

Figure 5. Needle and injection Behavior Using CRS Multiple Injections

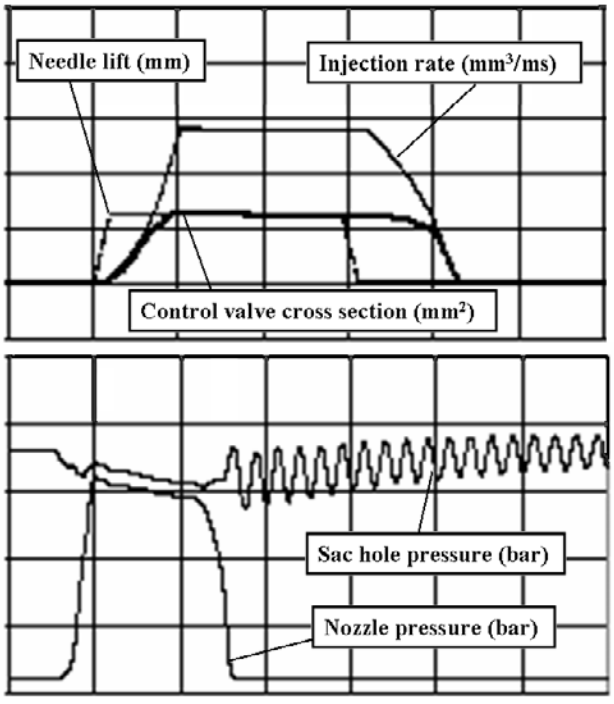

Figure 4. Needle and Injection Behavior Using MCRS Single Injection

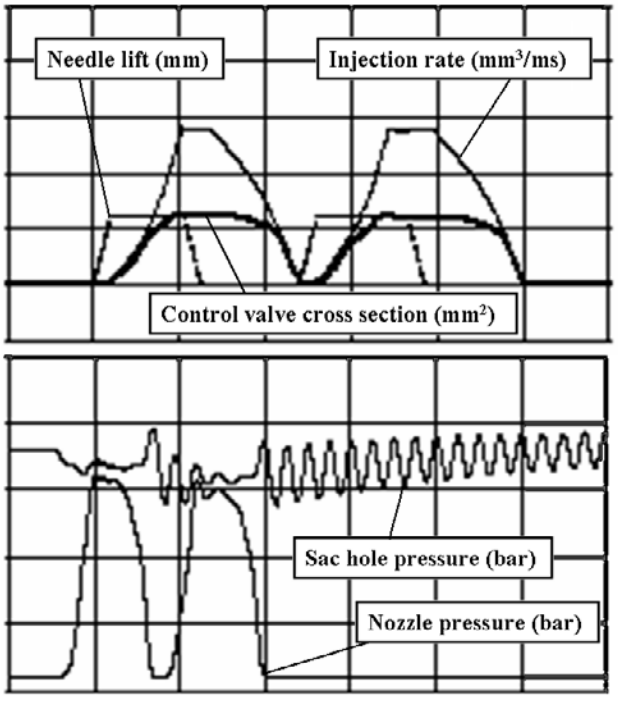

Figure 6. Needle and Injection Behavior Using MCRS Multiple Injections

engine. Figure 7 shows the top view of the engine with MCRS. For ease of operation and control, the high-pressure fuel pump was driven by an external electric motor. The injection profiles were selected

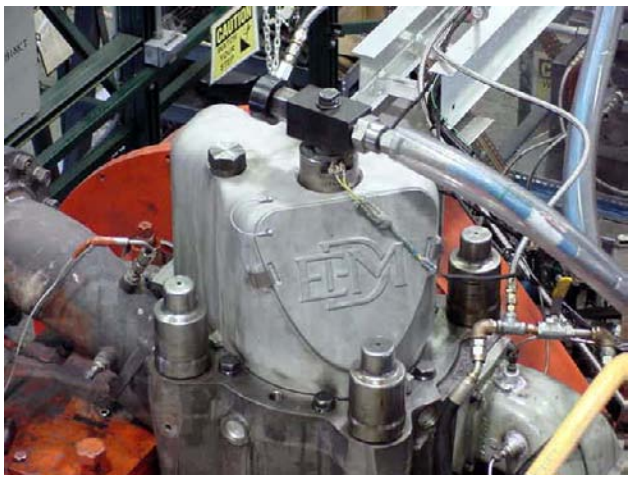

Figure 7. A Close-Up View of a Single-Cylinder Engine Integrated with MCRS Hardware

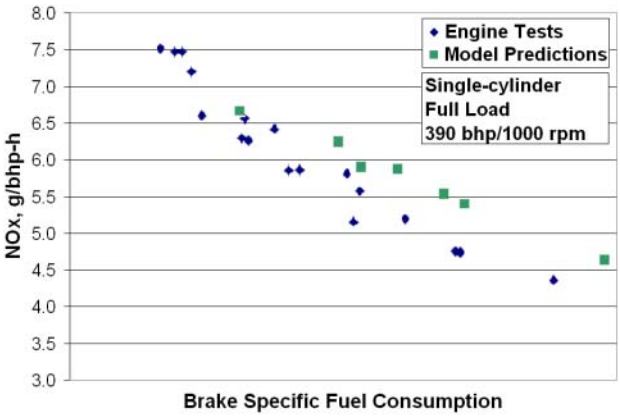

Figure 8. Performance and Emissions Tradeoff with MCRS (a comparison between experiments and CFD predictions)

from the CFD results for verification in the single-cylinder engine. Throughout our single-cylinder engine testing, inlet air density and exhaust backpressure were held constant. Figure 8 shows the key performance (BSFC) and target emissions (NO_x) tradeoff characteristics at full-load conditions using selected injection profiles. Each data point in this chart depicts a unique injection profile selected from a set of MCRS variables that include injection pressure, number of injections, injection timing of the first injection event, dwell time between the injection event(s), injection ramp-up rate, needle seat geometry, number of orifices, orifice aspect ratio, and spray included angle. The injection (duration) quantity was an output resulting from maintaining a constant engine full-load condition (constant engine output and engine speed.)

The salient results from engine testing with MCRS show a conventional NO_x and BSFC tradeoff. Despite wide differences in injection profiles that were generated using MCRS, the tradeoff trend was qualitatively similar to that of UPS when injection timing was altered. The test data show that the Tier 2 NO_x emission target of about 5 grams per bhp-hr can be met using MCRS with an optimized injection profile. For comparison purposes, CFD results were superimposed on the chart. Although our CFD model was not tuned for MCRS prior to the engine tests, the model predictions tracked quite well with engine test results, which shows the usefulness of the CFD model as a tool to (1) predict engine performance and emissions, (2) screen injection profiles, and (3) guide the future experiments. Using the single-cylinder engine test data, we plan to further improve our CFD model and its predictive capabilities, which can help to guide our future engine experiments.

To illustrate the potential of MCRS with respect to UPS, the engine performance and emissions data at engine full-load condition were compared and are shown in Figure 9. Unlike the case of MCRS, injection timing is the only variable when using UPS. The NO_x-BSFC data with UPS were obtained by simply changing the injection timing. This chart quantifies the differences between UPS and MCRS in terms of NO_x at a given BSFC and vice versa. First of all, a target NO_x of 5 grams was unattainable with UPS without relaxing limits on the exhaust gas temperature (~1200 deg F). Second, the BSFC was adversely affected by retarding the injection timing beyond 6 grams of NO_x. Without changing the cam profile and thus the injection profile, further optimization would be very difficult with the UPS. On the other hand, exhaust gas temperatures were well within the maximum limits when MCRS was used. The flexibility in altering the injection profile through control software allowed us to mitigate the peak cylinder pressure and exhaust gas temperature limits. Test results further demonstrate the superior NO_x-BSFC tradeoff characteristics with MCRS when compared to UPS. For example, at a constant BSFC, NO_x was reduced by about 15 to 20 percent. In addition to the reduction in NO_x emissions, engine

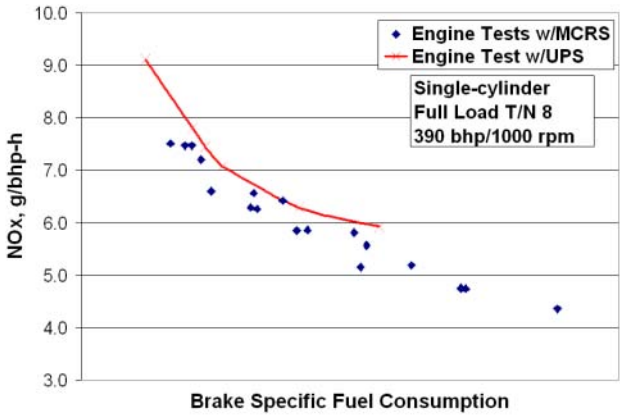

Figure 9. A NO_x-BSFC Comparison between UPS and MCRS at Full-Load Conditions

noise, and particulates, hydrocarbons and carbon monoxide emissions were also lower with MCRS (not shown). From the literature, it is obvious that the potential benefits of CRS can be fully captured when piston bowl shape is optimized with the fuel spray. Following trends in light-duty and heavy-duty diesel engines using advanced fuel-injection systems, the effects of piston bowl shape on emissions and performance are being studied along with various MCRS injection profiles; the ongoing engine tests are aimed to optimize the spray-bowl interactions.

Conclusions

- On the basis of single-cylinder engine tests, we demonstrated our Tier 2 internal NO_x goal of 5.0 grams per bhp-hr at engine full load with MCRS. Further, MCRS has better NO_x-BSFC tradeoff behavior when compared to UPS. Engine noise, visible smoke, and particulates were also lower with MCRS.
- To fully capture the potential of MCRS, spray-bowl optimization studies are being carried out using single-cylinder test engine facility. Studies aimed toward understanding the fuel spray behavior (using imaging techniques with high-pressure cold chamber) and cavitation behavior (using CFD tools) are ongoing in collaboration with our research partners.

Publications

1. "Comparing Cavitation in Diesel Injectors Based on Different Modeling Approaches," 2004, SAE Paper 2004-01-0027.

V.4 21st Century Locomotive Technology: Advanced Fuel Injection and Turbomachinery

Kent Cueman (Primary Contact), Anthony Furman, Farshad Ghasripoor, Roy Primus, and Jennifer Topinka
General Electric - Propulsion Systems Laboratory
One Research Circle
Niskayuna, NY 12309

DOE Technology Development Manager: John Fairbanks

Subcontractors:
Turbo Genset Inc.
University of Wisconsin - Madison, Madison, WI

Objectives

1. Develop and demonstrate an advanced fuel injection system to minimize fuel consumption while meeting Tier 2 emissions levels.

2a. Validate prototype electrically assisted turbocharger to full speed and power. Develop conceptual design for multi-cylinder engine.

2b. Demonstrate turbocharger efficiency improvement using abradable seals on the compressor and turbine housings.

Approach

Objective 1

- Develop combustion model for locomotive engine and verify model via test data.
- Use combustion model to optimize fuel injection strategy.
- Implement advanced fuel injection system on single-cylinder locomotive engine.
- Determine optimized fuel injection parameters via experiments, using model predictions as a guide.

Objective 2a

- Install electrically assisted turbocharger and test over operating range in motoring and generator modes.
- Measure performance and dynamic stability characteristics.
- Identify key areas of improvement.
- Develop conceptual design for multi-cylinder engine.

Objective 2b

- Perform clearance tests to determine efficiency improvement attributable to abradable seals.
- Specify and develop abradable seal material candidates.
- Perform rub tests to identify best choice(s).
- Implement abradable seals on full-scale turbocharger and characterize performance.

Accomplishments

Objective 1

- Calibrated and commissioned the computational fluid dynamics (CFD) combustion model at the University of Wisconsin-Madison to predict the performance of the locomotive engine.

- Developed CFD mesh to maximize usefulness for a given computation time and improved snapper routine.
- Exercised a genetic algorithm optimization process to identify the optimum high-pressure common rail (HPCR) design variables for N8. Design variables included fuel pressure, injection schedule, and fuel spray cone angle.
- Evaluated the HPCR hardware on a stand-alone functionality bench.
- Validated the CFD combustion model for the single-cylinder engine (SCE) with HPCR experimental data.
- Collected baseline engine performance data with the production unit pump system (UPS).
- Established a method to compare the brake performance of the single-cylinder engine operating with the UPS versus the HPCR.
- Installed the HPCR on the SCE and launched optimization study.

Objective 2a

- Obtained data on turbocharger system performance in generator and motoring modes from idle to maximum altitude speed.
- Successfully demonstrated high turbocharger acceleration rates under motor assist to N5 speed.
- Successfully demonstrated increasing levels of power recovery in generator mode from N6 to N8 maximum altitude speeds.
- Demonstrated stable rotor performance over full operating range.
- Identified key areas for improvement in scaling to current turbocharger platform.

Objective 2b

- Obtained cold and hot running clearance measurements on two turbocharger models (HDL, V12) to baseline clearance reduction potential.
- Developed spray parameters and prepared test specimens of candidate polymeric coatings for the turbocharger compressor application.
- Evaluated candidate samples in the GE Global Research Center (GRC) rub test facility for abradability and potential blade wear.
- Obtained air inlet and coated with candidate polymer for early evaluation in the electrically assisted turbocharger.
- Developed methodology to alloy the base polymer with metallic elements to improve durability while retaining compatibility with the aluminum compressor wheel.
- Performed hardness, bond strength and erosion tests on selected candidate coatings.
- Established coating thickness requirements as a function of compressor shroud line location. Developed programs for the robotic spray equipment to allow thermal spray coating of air inlets on both HDL and V12 turbochargers.
- Tested three polymeric-based coatings in the full-scale V12 turbocharger in the GRC turbocharger development test cell. Collected compressor performance data at multiple speed lines to assess efficiency gains at reduced clearance. Measured rotor dynamic response during coating rub.

Future Directions

Objective 1

- Continue optimization studies at N8.
- Expand testing and modeling at lower notches.
- Further optimize by changing fuel injection hardware.

Objective 2a

- Perform conceptual design, including packaging, for the larger Tier II turbocharger in preparation for multi-cylinder engine testing, pending resumption of funding.

Objective 2b

- Assess morphology of the as-sprayed coatings tested to date.
- Develop spray parameters and composition for improved polymeric coatings. Prepare rub test samples.
- Evaluate the coatings in the GRC rub rig. Downselect candidates for evaluation in the full-scale turbocharger.
- Coat and evaluate full-scale air inlet housing.
- Coat and test a metallic abradable on the turbine shroud.

Introduction

The goals and objectives of the Department of Energy and GE's 21st Century Locomotive Program are to develop freight locomotives that are 25% more efficient by 2010, while meeting Tier 2 emissions standards. Traditional methods to reduce fuel consumption typically come with a penalty of NO_x and PM emissions. GE is committed to bringing technology to the locomotive industry to achieve both low emissions and low fuel consumption. Over the past year, GE has worked to advance the technology at both the diesel engine and locomotive system levels. This document describes the technology at the diesel engine level, which involves improving the brake specific fuel consumption by development of advanced fuel injection and turbocharger systems.

Approach

The approach of the engine-related technology project varies by task. The methods by which GE will reach targets in the areas of advanced fuel injection, electrically assisted turbomachinery, and the turbocharger abradable seals are discussed below.

Advanced Fuel Injection

A Bosch high-pressure common rail (HPCR) system was implemented on a locomotive single-cylinder research engine. The system is capable of up to four injection events per cycle and produces injection pressures above 1800 bar. Parameters that must be optimized for best performance include rail pressure, injection schedule, and nozzle configuration. To better understand the combustion phenomena, CFD (KIVA) analysis was performed in collaboration with the University of Wisconsin – Madison. The KIVA modeling work provides input and guidance for the experimental study on the single-cylinder engine.

Electric Turbocharger

An electrically assisted turbocharger has been designed, built and evaluated. The advanced turbomachinery was tested at full scale in the GE GRC turbomachinery laboratory to identify performance potential. The opportunity to transfer energy between the electrical system and the flow stream provides an added degree of freedom for efficiency optimization. Modeling studies were used to predict performance gains given optimum airflow and pressure at the various locomotive notch settings (engine speed-torque combinations) of interest. Significantly improved transient engine response is expected in motoring mode at low notches, and up to 150 kW additional power recovery in generating mode at higher turbocharger speeds is expected.

Abradable Seals for Turbocharger

The application of abradable seals to the aluminum compressor wheel will be investigated in the literature. Materials that show potential for the temperature, speed, and blade material of the compressor will be selected and tested in a dedicated rub test facility. High-temperature metallic abradable seals will be selected for test on the turbine end of the turbocharger. Promising candidate materials will be downselected for test in a full-scale locomotive turbocharger. The turbocharger tests will be performed in the turbomachinery laboratory at GE GRC.

Results

Advanced Fuel Injection

The major accomplishments pertaining to the advanced fuel injection are the CFD model validation and the engine performance results with the HPCR. The CFD combustion model, which has the capability of multiple injections, predicts engine combustion very well. Previous reports showed that the model is well-calibrated for the UPS combustion event. The heat release curves were shown to match well, implying that the model is calibrated correctly and can be used for optimization studies. Figure 1 shows the common rail fuel system installed on the SCE. Experimental trends with the HPCR agree with the KIVA-based predictions. This allows us to build confidence in modeling capability for use on locomotive-scale engines, providing a foundation for further analysis. Results from the N8 optimization study were used to guide the experimental roadmap. Model optimization at N4 and N1 is now in progress.

Figure 1. Common Rail Fuel System Components Installed on the Single-Cylinder Locomotive Engine at GE GRC

Electric Turbocharger

The electrically assisted turbocharger has been designed, constructed, and successfully operated over a full range of conditions in both motoring and generator modes. The system has been run from idle to full speed with no issues encountered regarding structural integrity or rotor dynamics of the combined turbocharger, drive shaft and motor/ generator. The system has met the design rating of 150 kW in generator mode at maximum rated sea level turbocharger speed. Transient testing in motoring mode has indicated significant improvement in turbocharger load rate. Useful design data has been obtained regarding the vibration characteristics of the system, the efficiency of the compressor with and without the drive motor in place, and system surge limits. Optimization and characterization of the system control system were performed to maximize transient response of the turbocharger in motoring mode. Temporary damping was added to the inlet transition to correct a casing resonance in the middle of the speed range. An improved encoder was built and installed on the motor. Figure 2 shows the electrically assisted turbocharger installed on the test stand at GE GRC.

Additional modeling and simulations were performed to evaluate the potential improvement of the electrically assisted turbocharger on passenger locomotive station-to-station transit times under different scenarios of train size, turbocharger assist levels, engine idle rpm level, and station duty cycle.

Figure 2. Electric Turbocharger Installed on a Test Stand at GRC

Abradable Seals for Turbocharger

Candidate abradable seal materials have been identified for the turbocharger compressor and turbine shrouds. Polymeric samples for the compressor were prepared and evaluated in a dedicated rub rig under varying conditions of temperature, speed, and incursion rate. Four candidates were selected for application to the turbocharger based on rub test performance, tensile strength and bond strength. Two of the materials were pure polyester blends of varying particle size from alternate vendors. The remaining two were alloyed blends of polymeric and metallic components designed to provide additional strength and hardness to the coatings while still maintaining compatibility with the aluminum compressor wheel. Desired coating thickness profiles were developed for the compressor shroud through a series of measurements taken at cold, static conditions, and at full operating speed. The coatings were designed to permit near line-on-line contact at low N8 turbo physical speed and to rub at wheel speeds above this. Suitable programs were developed for the robotic thermal spray equipment to allow coating full-scale inlet housings for both the HDL and V12 turbochargers at the required varying thickness profile from inducer to exducer. A photograph of a coated air inlet before testing is shown in Figure 3.

Four coatings have been evaluated on the turbocharger test stand at conditions from idle to maximum rated speed. Results have varied depending on coating composition, with the pure polymeric blends exhibiting good abradability characteristics but somewhat low bond strength, and the alloyed blends exhibiting higher hardness but also some aggressiveness towards the aluminum compressor wheel. Performance gains measured at the tighter clearances are attractive. Real-time measurements of rotor shaft motion indicate no undesirable subsynchronous behavior during contact with the coating. Shaft motion and overall vibration remained within design limits. Contact with the coating is typically a one-time event at a given shaft speed. Once a rub has occurred at a given rpm, the wheel will run at or below that speed without continuing to contact the coating.

Two metallic-based coatings have been selected for application to the turbine shroud. The material is a NiCrFe-based alloy that is applied using the combustion spray process. Tests are planned to determine the hot running clearance between the turbine blades and stationary shroud for selection of initial coating thickness. A local vendor has been qualified under a separate program to spray the coating selected for initial trials.

Figure 3. Turbocharger Air Inlet after Application of Polymeric Abradable Coating

Conclusions

- The genetic algorithm approach is an appropriate tool to optimize injection parameters.
- SCE experimental trends agree with the KIVA-based predictions.
- Potential engine performance improvements with HPCR were identified and demonstrated.
- Additional experiments and hardware refinements are required to determine the optimum HPCR strategy over the range of locomotive operation.
- The prototype electrically assisted turbocharger met performance goals of acceleration, power recovery and rotor stability.
- Polymeric zero-clearance abradable coatings provide improved compressor efficiency with no loss in surge margin.
- Additional optimization is required to develop a coating that provides the desirable abradability characteristics while retaining sufficient durability for long-term locomotive service.

V.5 Off-Highway Emission Control with High System Efficiency (CRADA with John Deere)

Michael Kass (Primary Contact), Norberto Domingo, John Storey
Oak Ridge National Laboratory
NTRC
2360 Cherahala Blvd.
Knoxville, TN 37932

DOE Technology Development Manager: John Fairbanks

Objectives

- Evaluate the potential of NO_x-reducing aftertreatment technologies to achieve interim Tier 4 NO_x emission levels for off-highway heavy-duty diesel engines. The initial focus is to utilize urea-based selective catalytic reduction (SCR) to achieve brake-specific NO_x levels of 2 g/kWh over the ISO 8178 Off-Highway test cycle.
- Optimize key injection parameters to achieve improvements in fuel efficiency while meeting the 2011 Tier 4 emission levels for NO_x. The initial target value for brake-specific fuel consumption (BSFC) is 195 g/kWh.

Approach

- Install and set up a urea-SCR system in the exhaust system of a heavy-duty off-highway engine. The system consists of an oxidation catalyst, Bosch urea injector and dosing unit, and a Johnson-Matthey urea-SCR catalyst.
- Evaluate the performance of the urea-SCR system to reduce NO_x emissions for six modes of the ISO 8178 Off-Highway test cycle. Examine the slip of ammonia from the SCR catalyst during urea injection.
- Analyze the performance of the urea-SCR system to identify areas of further improvement.

Accomplishments

- Installed the urea-SCR system, including the dosing unit and catalysts. This included the fabrication of wiring harnesses and switches, and the setup of the software interface and drivers to operate the dosing system.
- Urea-SCR has been demonstrated to reduce NO_x emissions to interim Tier 4 levels over the ISO-8178 Off-Highway test cycle. Conversion efficiencies over 90% were observed for modes 1, 2, 3, 5, and 6 at near-stoichiometric delivery rates. Low exhaust temperatures for modes 4 and 8 prevented the application of the SCR system for these set points.
- Achieved apparent improvement in BSFC.

Future Directions

- Install and evaluate advanced engine control software. Initial focus will be to determine the influence of injection parameters on energy efficiency.
- Explore the potential for other NO_x reduction strategies to meet final Tier 4 NO_x and PM emissions.
- Conduct further urea-SCR studies to optimize NO_x conversion with selected injection control strategies to lower BSFC.

Introduction

Tier 3 Federal standards for new off-highway diesel engines require that NO_x and PM levels be regulated to 4 g/kWh and 0.2 g/kWh, respectively, for engines between 130 and 560 kW. The phase-in period for Tier 3 compliance is set to begin in 2006 and to be completed by 2008. Urea-SCR has been shown to effectively reduce NO_x emissions for on-highway applications but needs to be thoroughly evaluated for off-highway engines since both engine design and operating conditions are different. The utilization of advanced injection systems and controls is to be evaluated for improvements in both PM emissions and BSFC. This project seeks to develop and evaluate emission control methodologies with the goal of identifying pathways to meet interim Tier 4 and retrofit solutions.

Approach

The principal activity for FY 2004 was the installation and performance evaluation of a urea-SCR system for reducing NO_x emissions from a heavy-duty off-highway diesel engine. Upon receipt of the SCR system components, the system was installed. This required significant effort to make the urea dosing system operational. The urea-SCR evaluation was performed over a period of several weeks, and at the end of this period, the catalysts were sent to the manufacturer for refurbishment. The test protocol followed the ISO 8178 C1 test cycle for off-highway engines. Data were collected for a range of urea delivery rates, up to and exceeding the stoichiometric value. The level of ammonia slip was measured using a photoacoustic spectrometer and analyzed for each operating mode. In addition, the NO_x reduction performance was evaluated with and without use of a diesel oxidation catalyst (DOC) to condition the NO to equilibrium levels of NO_2.

A second activity for this FY was the installation of an advanced fuel injection system and evaluation of its effect on energy efficiency. The data was collected (for each mode) and compared to an earlier study using the original fuel injection system.

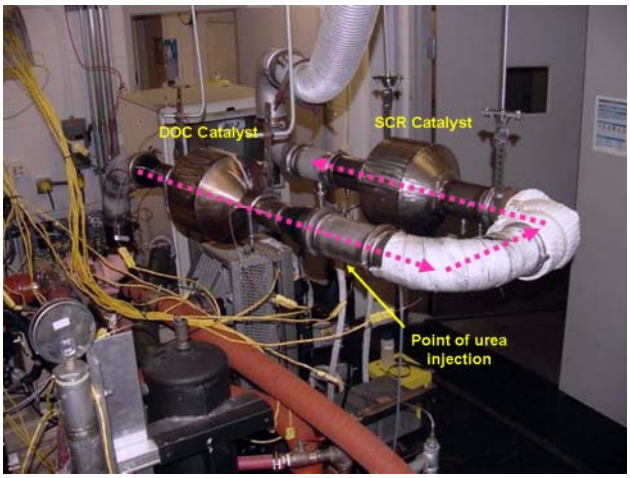

Figure 1. Urea-SCR System

Results

A photograph showing the arrangement of the catalysts in the engine exhaust line is shown in Figure 1. Installation of the urea-SCR system was completed by February. During the urea-SCR evaluation, it was necessary to closely monitor the temperature profile of the exhaust, especially that of the SCR catalyst since performance is closely related to temperature. The temperature profile for each mode is shown in Figure 2. As shown in this figure, the catalyst temperatures for modes 4 and 8 were too low to enable urea injection and were thus not considered during the evaluation.

For each mode, the baseline NO_x emissions were monitored before application of the urea. When steady state was reached, the urea was applied at a low level (usually around 500 g/h) and the temperature and emissions were allowed to stabilize. The engine-out, DOC-out, and tailpipe emissions of NO_x, hydrocarbons (HC), CO, CO_2, and O_2 were recorded for each setting. The urea level was gradually increased at selected values up to and slightly exceeding the stoichiometric level of urea required for theoretically complete conversion of the NO_x. This was performed with and without a DOC

ISO 8178 Mode	Turbo outlet	DOC inlet	DOC outlet	SCR Cat inlet	SCR Cat outlet
1	430	376	380	364	362
2	355	349	352	337	335
3	317	309	312	298	297
4	203	200	198	191	191
5	473	450	467	415	397
6	422	405	417	382	370
7	349	338	340	319	312
8	99	90	94	81	75

Figure 2. Key Exhaust Temperatures for Each Mode (degrees Celsius)

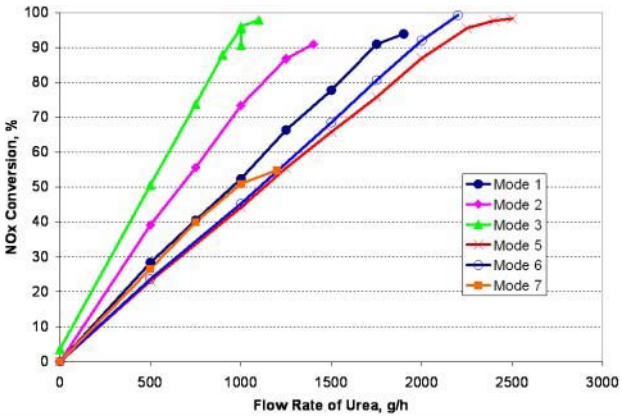

Figure 3. NO_x Reduction Performance of the Urea-SCR System for ISO 8178 Modes 1, 2, 3, 5, 6, and 7

placed in the exhaust upstream of the urea injector. In general, for modes 1, 2, 3, 5, and 6, the DOC improved the NO_x conversion significantly for urea delivery rates approaching the stroichiometric value, but it was less effective at improving the conversion during low applications of urea. The utilization of the DOC during mode 7, however, improved the NO_x conversion by 30% for all rates of urea injection. The NO_x conversion results (using the DOC) for each mode are shown in Figure 3. For modes 1, 2, 3, 5, and 6, the NO_x conversion increased to levels exceeding 90%. The urea delivery rate at which conversion passed 90% usually corresponded to the stoichiometric value. At urea levels at or exceeding stoichiometry, the conversion began to level and ammonia began to slip past the catalyst.

Unlike the other modes tested, the exhaust conditions during mode 7 did not allow for greater than 90% NO_x conversion. The highest value that could be attained was around 50%, which occurred significantly below the calculated stoichiometric value. As with the other modes, ammonia slip was observed for mode 7 once the rate of NO_x conversion with urea flow decreased. The total brake-specific NO_x level obtained using this system was determined to be around 1 g/kWh, which is well below the Tier 3 target level of 4 g/kWh and below the interim Tier 4 level of 2 g/kWh.

Conclusions

- Tier 3 NO_x emission levels were reached using a urea-SCR system. The addition of a DOC significantly improved the NO_x conversion efficiency of the system. However, the exhaust temperatures for modes 4 and 8 were too low to permit urea injection.
- The energy efficiency of the engine was improved through the application of an advanced fuel injection system. For all modes, except 4 and 8, the BSFC values were below the target level.

VI Acronyms and Abbreviations

°C	Degrees Celsius
°F	Degrees Fahrenheit
0-D	Zero-dimensional
1-D	One-dimensional
3-D	Three-dimensional
4Q	Fourth quarter
a.u.	Arbitrary units
A/cm^2	Amps per square centimeter
A/T	Aftertreatment
A75	Near peak torque speed & 75% engine load point of ESC Test Procedure
AC	Alternating current
AEC	Advanced Emission Controls Working Group
AETEG	Automobile exhaust thermoelectric generator
Ag	Silver
AHRR	Apparent heat release rate
Al	Aluminum
Al_2O_3	Aluminum oxide
ANL	Argonne National Laboratory
ANSI	American National Standards Institute
ASI	Time after the start of injection
ASME	American Society of Mechanical Engineers
AT	Aftertreatment
ATDC	After top dead center
atm	Atmosphere
Au	Gold
B	Boron
B100	Mid-speed & 100% engine load point of ESC Test Procedure
B25	Mid-speed & 25% engine load point of ESC Test Procedure
B75	Mid-speed & 75% engine load point of ESC Test Procedure
Ba	Barium
BaO	Barium oxide
BDC	Bottom dead center
BET	Named after Brunauer, Emmett and Teller, this method for determining the surface area of a solid involves monitoring the adsorption of nitrogen gas onto the solid at low temperature and, from the isotherm generated, deriving the volume of gas required to form one monolayer adsorbed on the surface. This volume, which corresponds to a known number of moles of gas, is converted into a surface area though knowledge of area occupied by each molecule of adsorbate.
bhp-hr	Brake horsepower hour
Bi_2Te_3	Bismuth Telluride
BMEP	Brake mean effective pressure
bmep	Brake mean effective pressure
BOI	Beginning of injection
BP	British Petroleum
BPF	Bandpass Filter
Bsfc	Brake specific fuel consumption
BSFC	Brake specific fuel consumption
btdc	Before top dead center
BTE	Brake thermal efficiency
C:N	Ratio of carbon to nitrogen
C_1	Carbon content in the exhaust or reformer in terms of carbon atoms
C_2H_6	Ethane
C_3H_6	Propylene
CA	Crank angle
CA50	Crank angle at which 50% of the combustion heat release has occurred
CAD	Computer-aided design
CAD	Crank angle degrees
CAI	Controlled autoignition
CAP	Critical adjustable parameter
cc	Cubic centimeter
CDI	Compression direct injection
CDPF	Catalytic diesel particulate filter
CeO_2	Cerium oxide
CFD	Computational fluid dynamics
CFR	Coordinating Fuel Research
CFR	Critical functional response
CHEMKIN	Name of chemical-kinetic code
CI	Compression ignition
CIDI	Compression ignition direct injection
CIMAC	International Council on Combustion Engines
CLEAN	Trademark for Detroit Diesel low-temperature combustion strategy
CLEERS	Cross-Cut Lean Exhaust Emissions Reduction Simulations

cm	Centimeter
cm^3	Cubic centimeters
CO	Carbon monoxide
CO_2	Carbon dioxide
COV	Coefficient of variation
CO_x	Oxides of carbon
CP	Chevron Phillips
cpi	Cells per inch
Cr	Chromium
CRADA	Cooperative Research and Development Agreement
CR-DPF	Continuously regenerating diesel particle filter
CRF	Combustion Research Facility
CRS	Common Rail System
Cu	Copper
CWLR	Constant weight loss rate
DC	Direct current
DCSF	Diesel combustion simulation facility
DDC	Detroit Diesel Corporation
DECSE	Diesel Emission Control Sulfur Effects
DEER	Diesel Engine Emissions Reduction
deg	Degrees
DELTA	Diesel Engine for Light Truck Application
DEM	Delayed and extended main
$DeNO_x$	Oxides of nitrogen reduction
DI	Direct injection
dm	Decimeter
DME	Dimethyl ether
DNS	Direct Numerical Simulation
DOC	Diesel oxidation catalyst
DoE	Design of experiment
DOE	U.S. Department of Energy
DOHC	Double overhead camshaft
DPF	Diesel particulate filter
DPNR	Diesel Particulate NO_x Reduction
DPV	Differential pulse voltammetry
DRIFT	Diffuse reflectance infrared Fourier transform
DRIFTS	Diffuse reflectance infrared Fourier-transform spectroscopy
DTTEG	Diesel truck thermoelectric generator
e^-	Electron
ECM	Electronic control module
EDS	Energy dispersive spectroscopy
EGR	Exhaust gas recirculation
$EINO_x$	Emissions index of NO_x
ELPI	Electrical low pressure impactor
ELS	Elastic light scattering
ELSLII	Elastic laser scattering with laser-induced incandescence
EMD	Electro-Motive Division of General Motors Corporation
EPA	U.S. Environmental Protection Agency
ESC	Steady-State Emission Test Procedure
ETC	Electric turbocompound
ϕ	Fuel/Air Equivalence Ratio
Fe	Iron
fFO	Fuel oxygen equivalence ratio
FLC	Federal Laboratory Consortium
FLRS	Full load rated speed engine condition
FMEA	Failure mode and effects analysis
fmep	Friction mean effective pressure
FSN	Filter smoke Number (AVL)
FTIR	Fourier transform infrared
ft-lb	Foot-pound
FTP	Federal Test Procedure
FTP	Federal Transient Protocol
FTP-75	Federal Test Procedure for LD vehicles
FWHM	The full width at half the maximum activity as a function of temperature
FY	Fiscal year
g	Gram
g/hp-hr	Grams per horsepower-hour
g/kWh	Grams/kilowatt-hour
g/mi	Grams per mile
GC-MS	Gas chromatography – mass spectrometry
GDI	Gasoline direct injection
GE	General Electric
Ge	Germanium
GHSV	Gas Hourly Space Velocity; a measure of gas flow rate through a reactor in units of liters of gas per liter of catalyst per hour, or L L-1 h-1, or h-1.
GRC	GE Global Research Center
GT-Power	Gamma Technologies engine modeling software
H_2	Diatomic (molecular) hydrogen
H_2O	Water
H_2O_2	Hydrogen peroxide

H_2-SpaciMS	Hydrogen-calibrated spatially resolved capillary inlet mass spectrometry
HC	Hydrocarbons
HCCI	Homogeneous charge compression ignition
HCN	Hydro-cyanic acid
HD	Heavy-duty
He	Helium
HECC	High-efficiency clean combustion
HELD	High-energy laser diagnostics
HEV	Hybrid electric vehicle
HMO	Hydrous metal oxide
hp	Horsepower
HPCR	High-pressure common rail
HR	Heat release
hr	Hour
HRR	Heat release rate
HTCD	Heavy truck clean diesel
HTML	High Temperature Materials Laboratory
Hz	Hertz
IC	Internal combustion
ICCD	Intensified Charge Coupled Device (camera)
ICE	Internal combustion engine
ID	Injection duration
ID	Internal diameter
IEA	International Energy Agency
IEEE	Institute of Electrical and Electronics Engineering
IMEP	Indicated mean effective pressure
imep	Indicated mean effective pressure
IR	Infrared
IVC	Intake valve camshaft
J	Joule
K	Kelvin
K	Potassium
K_2CO_3	Potassium Carbonate
K_2O	Potassium oxide
KeV	Kilo electron volts, a unit of energy
kg	Kilogram
kHz	Kilohertz
KIVA	a transient, three-dimensional, multiphase, multicomponent code for the analysis of chemically reacting flows with sprays developed at the Los Alamos National Laboratory
kJ	Kilojoule
kJ/L	Kilojoules per liter
kJ/m^3	Kilojoules per cubic meter
KL	Soot optical thickness
kPa	Kilopascal
kW	Kilowatt
L	Liter
L/D	Length-to-diameter ratio
La	Lanthanum
LANL	Los Alamos National Laboratory
lb ft	Pound foot
lb/mi	Pounds per minute
lbs	Pounds
lbs/sec	Pounds per second
LD	Light-duty
LDT	Light-duty truck
LEP	Low Emissions Technologies Research and Development Partnership (often abbreviated to Low Emissions Partnership); a consortium between Ford, General Motors and DaimlerChrysler
LES	Large eddy simulation
LHV	Lower heating value
LIBS	Laser-induced breakdown spectroscopy
LIDELS	Laser-induced desorption with elastic light scattering
LIF	Laser-induced fluorescence
LII	Laser-induced incandescence of soot
LLNL	Lawrence Livermore National Laboratory
LNT	Lean NO_x trap
LO	Light-off temperature – the minimum temperature at which half the maximum catalyst activity is identified
LQHCCI	Lean quasi-homogeneous charge compression ignition
LSC	Lanthanum strontium chromite
LTC	Low-temperature combustion
M/G	Motor/generator
m^2	Square meters
m^2/gm	Square meters per gram
m^3	Square meters
mA	Milliamps
mbar	Millibar
MBE	Molecular beam epitaxy
MCRS	Modular Common Rail System

MECA	Manufacturers of Emission Controls Association
MeOH	Methanol
mg/cm^2	Milligrams per square centimeter
mg/mi	Milligram per mile
mg/mm^2	Micrograms per square millimeter
mg/scf	Milligrams per standard cubic foot
min	Minute
MIT	Massachusetts Institute of Technology
MLQWF	Multi-layer quantum well films
MLR	Multivariable local regression
μm	Micrometer
mm	Millimeter
mmols	Micro-moles
Mn	Manganese
Mo	Molybdenum
mol	Mole
mol/s	Moles per second
MOU	Memorandum of Understanding
MPa	Megapascals
mph	Miles per hour
ms	Millisecond
MTU	Michigan Technological University
MY	Model year
N_2	Diatomic nitrogen
N_2O	Nitrous oxide
N_2O_3	Nitrogen trioxide
Na	Sodium
NEA	Nitrogen-enriched air
NH_3	Ammonia
NLCAT	National Laboratory Catalysis Conference
nm	Nanometer
Nm	Newton meter
NMHC	Non-methane hydrocarbon
NMOG	Non-methane organic gases
NMR	Nuclear magnetic resonance
NO	Nitric oxide
NO_2	Nitrogen dioxide
NO_x	Oxides of nitrogen (NO and NO_2)
ns	Nanosecond
NSR	Normalized stoichiometric ratio
NTE	Not-to-exceed
NTP	Non-thermal plasma
NTRC	National Transportation Research Center
O_2	Diatomic (molecular) oxygen
OEM	Original Equipment Manufacturer
OFCVT	Office of FreedomCAR and Vehicle Technologies
OH	Hydroxyl
OH PLIF	Planar laser-induced fluorescence of OH
OMS	Octahedral molecular sieve
ORC	Organic Rankine Cycle
ORNL	Oak Ridge National Laboratory
P	Pressure
P2P	Ratio of the peak activity of a new material to the peak activity of a reference material
PAC	Plasma-assisted catalyst
PC	Personal computer
PCCI	Premixed charge compression ignition
PD	Photodiode
PDF	Probability density function
PEMS	Portable emissions measurement system
PFI	Port fuel injection
PFI-DI	Port fuel injection/direct injection
PhosphorT	Phosphor thermography instrument
PLII	Planar laser-induced incandescence
PM	Particulate matter
PM	Permanent magnet
PMT	Photomultiplier tube
PNGV	Partnership for a New Generation of Vehicles
PNNL	Pacific Northwest National Laboratory
Post80	Late cycle injection after the main fuel pulse at 80° after top dead center
PO_x	Partial oxidation
ppb	Parts per billion
ppi	Pores per square inch
ppm	Parts per million
PRF	Primary Reference Fuels (iso-octane and n-heptane),
PRF80	PRF mixture with an octane number of 80 (i.e., 80% iso-octane and 20% n-heptane)
psi	Pounds per square inch
psig	Pounds per square inch gauge
Pt	Platinum
QSB5.9	Quantum System B Series 5.9Liter (Midrange Industrial Product)
QSC8.3/QSL9	Quantum System C Series 8.3 Liter, Quantum System L Series 9 Liter
QSK19	Quantum System K Series 19 Liter
QSX15	Quantum System X Series 15 Liter
QW	Quantum well
R&D	Research and development

RANS	Reynolds averaged navier stokes
RASP	Rotating arc spark plug
RCF	Rapid Compression Facility
RDG-PFA	Rayleigh-Debye-Gans polydisperse fractal aggregate
Rh	Rhodium
RIF	Representative interactive flamelet
ROI	Rate of injection
rpm	Revolutions per minute
RSM	Response surface method
s	Conductivity $(Wcm)^{-1}$
S	Seebeck coefficient
S	Sulfur
S/N	Signal-to-noise ratio
SAE	Society of Automotive Engineers
SBCE	Set-based concurrent engineering
sccm	Standard cubic centimeters
SCE	Single-cylinder engine
SCF/min	Standard cubic feet per minute
SCR	Selective catalytic reduction
SCTE	Single-cylinder test engine
sec	Second
SEM	Scanning electron microscopy
SGS	Subgrid-scale
Si	Silicon
SI	Spark ignition
SiC	Silicon carbide
SICM	System Integration Configuration Matrix
SIDI	Spark ignition direct injection
SINL	Spatially Integrated Natural Luminosity
SLPM	Standard liters per minute
SMPS	Scanning mobility particle scanner
SMR	Steam reformation
SNL	Sandia National Laboratories
SO_2	Sulfur dioxide
SOI	Start of injection
SO_x	Oxides of sulfur
SpaciMS	Spatially resolved capillary inlet mass spectrometer
Sr	Strontium
SR	Switched reluctance
sS^2T	Power factor (mV/ºC)
SU	Stanford University
SUV	Sports utility vehicle
SV	Space velocity
T	Temperature
T70	A fuel blend containing the oxygenate tetraethoxy-propane
TACOM	Tank Automotive Armaments Command
TCI	Turbulence/chemistry interactions
TDC	Top dead center
TDI	Turbocharged direct injection
TE	Thermoelectric
TEG	Thermoelectric generator
TEM	Transmission electron spectroscopy
TEOM	Tapered element oscillating microbalance
TGA	Thermal gravimetric analysis
THC	Total hydrocarbons
Ti:Si	Ratio of titanium to silicon
TPD	Temperature-programmed desorption
TPGME	Tri-propylene glycol monomethyl ether
TPM	Total particulate matter
TPR	Temperature-programmed reduction
TPRX	Temperature-programmed reaction
TRLC	Top-ring-land crevice
TWC	
UCB	University of California Berkeley
UEGO	Universal exhaust gas oxygen
UHC	Unburned hydrocarbons
UIS	Unit injector system
ULSD	Ultra-low sulfur diesel
UM	University of Michigan
UPS	Unit pump system
USCAR	U.S. Cooperative Automotive Research
V	Volt
VCO	Valve-covering orifice
VCR	Variable compression ratio
VDC	Voltage – direct current
VGC	Variable geometry compressor
VGS	Variable geometry spray
VNT	Variable nozzle turbine
VVA	Variable valve actuation
W	Watt
W/cmK	Watts per centimeter-Kelvin
wt%	Weight percent
XPS	X-ray photoelectron spectroscopy
XRD	X-ray diffraction
Y	Yttrium
yr	Year
Zn	Zinc
ZT	Dimensionless thermoelectric figure of merit; equal to: (electrical conductivity)(Seebeck coefficient)^2(temperature)/(thermal conductivity)

VII Author Index

A Strong Energy Portfolio for a Strong America

Energy efficiency and clean, renewable energy will mean a stronger economy, a cleaner environment, and greater energy independence for America. Working with a wide array of state, community, industry, and university partners, the U.S. Department of Energy's Office of Energy Efficiency and Renewable Energy invests in a diverse portfolio of energy technologies.

For more information contact:
EERE Information Center
1-877-EERE-INF (1-877-337-3463)
www.eere.energy.gov